

UNIVERSITY OF ILLINOIS
UNDERGRADUATE DIVISION
CHICAGO
LIBRARY



JOURNAL OF CELLULAR AND COMPARATIVE PHYSIOLOGY

BOARD OF EDITORS

ARTHUR K. PARPART, Managing Editor
Princeton University

W. R. AMBERSON
University of Maryland

D. W. BRONK
The Rockefeller Institute

M. H. JACOBS
University of Pennsylvania

H. F. BLUM
National Cancer Institute

L. B. FLEXNER
University of Pennsylvania

D. MARSLAND
New York University

F. BRINK
The Rockefeller Institute

E. N. HARVEY
Princeton University

D. MAZIA
University of California

VOLUME 48

AUGUST, OCTOBER, DECEMBER, 1956

PUBLISHED BY

THE WISTAR INSTITUTE OF ANATOMY AND BIOLOGY
PHILADELPHIA, PA.

U OF I
LIBRARY



Digitized by the Internet Archive
in 2024

CONTENTS

No. 1 AUGUST 1956

P. O. BISHOP AND W. R. LEVICK. Saltatory conduction in single isolated and non-isolated myelinated nerve fibers. Nine figures	1
PRESTON B. LOWRANCE, JAMES F. NICKEL, CHEVES MCC. SMYTHE AND STANLEY E. BRADLEY. Comparison of the effect of anoxic anoxia and apnea on renal function in the harbor seal (<i>Phoca vitulina</i> , L.). Two figures ..	35
EDWARD S. HODGSON AND KENNETH D. ROEDER. Electrophysiological studies of arthropod chemoreception. I. General properties of the labellar chemoreceptors of diptera. Six figures	51
A. R. SCHRANK. Several factors which influence the rate of <i>Avena</i> coleoptile respiration. Three figures	77
DEXTER M. EASTON. Some tensile properties of nerve. Five figures	87
MORGAN HARRIS. Occurrence of respiration deficient mutants in baker's yeast cultivated anaerobically. Two figures	95
A. S. V. BURGEN. The secretion of non-electrolytes in the parotid saliva	113
E. STREICHER. The entry of $P^{32}O_4$ into rat brain. One figure	139
KENNETH M. RICHTER. Studies on the individual and joint effects of histamine and an antihistaminic on growth, contractility and plasmocrine activity in cultures of embryonic chick heart. Eighteen figures	147

No. 2 OCTOBER 1956

BILL GAROUTTE AND ROBERT B. AIRD. Diffusion from brain slices in vitro. One figure	167
WILLIAM J. ADELMAN. The relation of accommodation to current distribution in single muscle fibers. Three figures	181
B. N. SMALLMAN AND L. S. WOLFE. Soluble and particulate cholinesterase in insects. Six figures	197
L. S. WOLFE AND B. N. SMALLMAN. The properties of cholinesterase from insects. Nine figures	215

CHANDLER McC. BROOKS, PAUL F. CRANFIELD, BRIAN F. HOFFMAN AND ARTHUR A. SIEBENS. Anodal effects during the refractory period of cardiac muscle. Two figures	237
GEORGE T. JOHNSON AND CARL MOOS. Succinoxidase activity of mitochondria from myxomycete plasmodia. Two figures	243
RALPH HOLT CHENEY. Comparative effect of methylated xanthines on the fertilization capacity and life span of <i>Arbacia</i> gametes. Three figures ..	253
T. C. NELSON. Sexual competence in <i>Escherichia coli</i>	271
JAMES H. GREGG AND RUTH D. BRONSWIEG. Biochemical events accompanying stalk formation in the slime mold, <i>Dictyostelium discoideum</i> . One figure	293
KATHERINE A. ZWORYKIN AND GEORGE B. CHAPMAN. Television microscopy of sporulation and spore germination of <i>Bacillus cereus</i> . Thirteen figures	301
A. A. ANDREASEN AND T. J. B. STIER. Anaerobic nutrition of <i>Saccharomyces cerevisiae</i> . III. An unidentified growth promoting factor and its relationship to the essential lipid requirements	317
SOCIETY OF GENERAL PHYSIOLOGISTS. Abstracts of papers presented at the eleventh Annual Meeting, held in conjunction with the meetings of the American Institute of Biological Sciences, at the University of Connecticut, Storrs, Connecticut, August 27-29, 1956	329

No. 3 DECEMBER 1956

JEROME J. WOLKEN. Photoreceptor structures. I. Pigment monolayers and molecular weight. Four figures	349
MARILYN L. ZIMNY. Metabolism of some carbohydrate and phosphate compounds during hibernation in the ground squirrel. Twelve figures	371
PAUL O. FROMM AND E. P. REINEKE. Some aspects of thyroid physiology in rainbow trout. Three figures	393
BETTY F. EDWARDS AND STEPHEN W. GRAY. Growth, work output and sensitivity to increased gravitational forces in wheat coleoptiles. Four figures	405
RITA GUTTMAN AND MILTON M. GROSS. Relationship between electrical and mechanical changes in muscle caused by cooling. Six figures	421
WALTER WELKOWITZ AND WILLIAM J. FRY. Effects of high intensity sound on electrical conduction in muscle. Twelve figures	435
W. R. SISTROM, MARY GRIFFITHS AND R. Y. STANIER. A note on the porphyrins excreted by the blue-green mutant of <i>Rhodospseudomonas spheroides</i> . Seven figures	459
W. R. SISTROM, MARY GRIFFITHS AND R. Y. STANIER. The biology of a photosynthetic bacterium which lacks colored carotenoids. Eleven figures ...	473
P. F. SCHOLANDER, L. VAN DAM AND THEODORE ENNS. The source of oxygen secreted into the swimbladder of cod. One figure	517
P. F. SCHOLANDER. Observations on the gas gland in living fish	523
P. F. SCHOLANDER AND L. VAN DAM. Micro gasometric determination of oxygen in fish blood. One figure	529

1121

SALTATORY CONDUCTION IN SINGLE ISOLATED AND NON-ISOLATED MYELINATED NERVE FIBRES¹

P. O. BISHOP AND W. R. LEVICK

*The Brain Research Unit, Departments of Surgery, Anatomy and
Physiology, University of Sydney, Australia*

NINE FIGURES

The hypothesis that conduction in myelinated nerve fibres is a discontinuous process is now firmly established and the evidence in favour of this saltatory hypothesis has recently been the subject of several critical reviews (Hodgkin, '51; Tasaki, '53; and Stämpfli, '54). Huxley and Stämpfli ('49) have drawn attention to the fact that the greater part of the evidence relates to the initiation or blocking of an impulse and very few experiments refer directly to transmission along a length of single fibre. Their experiments provided an account of conduction in terms of action currents along the length of the fibre. The experiments to be reported here are concerned with the recording of action potentials at a series of positions along the length of myelinated fibres both in the isolated and non-isolated state. It will be shown that the records may be satisfactorily interpreted in the light of the saltatory theory.

PART I

METHODS

The preparations used in these experiments were obtained from Queensland cane toads (*Bufo marinus*). Usually the segment of the tibial nerve which runs along the distal half

¹ Aided by grants from The National Health and Medical Research Council of Australia and I. Kahn Donation.

of the gastrocnemius muscle was selected and lengths of between 10–15 mm of single fibre were isolated. The Ringer solution used had the following composition: sodium chloride 111.5 mM; potassium chloride 2 mM; calcium chloride 1.1 mM; sodium bicarbonate 2.5 mM. Experiments were carried out in all seasons of the year at room temperatures which varied from 20 °C. to 30°C. In any one experiment the temperature would not have altered by more than 1°C.

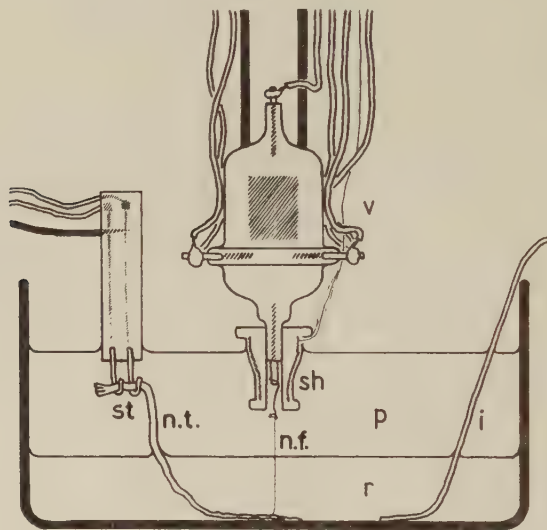


Fig. 1 Experimental arrangement for recording action potentials along a single nerve fibre. The stimulating electrodes (st) make contact with the sciatic nerve (n.t.) in the layer of paraffin (p) which floats on the layer of Ringer solution (r). The isolated nerve fibre (n.f.) is arranged vertically, its distal end making contact with the short grid lead of the input valve (v). A shield (sh), connected to the valve cathode, reduces the capacity of the grid to earth. The "indifferent" lead (i) is a silver wire.

The experimental arrangement is indicated in figure 1. The fibre was arranged vertically in a dish of Ringer solution, its distal end being caught by the hooked end of the fine (0.25 mm diameter) short (1 cm) grid lead of the input valve. Paraffin oil (B. P. grade) was layered on the surface of the Ringer and the interface thus produced was usually

moved down the fibre at 0.1 mm intervals by removing appropriate volumes of Ringer. This interface formed the mobile recording electrode, connection to which was obtained by means of a thick silver rod dipping into the Ringer solution. The stimulating leads were a pair of platinum wires (immersed in the paraffin) upon which the proximal nerve trunk lay. At all stages during the setting up and occasionally during the experiment the fibre was observed under the low power of a dissecting microscope. Fibres appeared to pass through the interface without difficulty, although visibility is poor through such great thickness of paraffin.

Amplifier input stage

Since the membrane action potential may have a rise time (10–90%) of about 100 μ sec and this may have to be recorded through a length of single fibre up to 15 mm in length having a resistance of 100 M Ω or more it is clear that the input impedance of the amplifier must be of a very high order. The input stage, using an acorn pentode (RCA 954), was similar to that described by Bishop ('49). The valve, which was normally operated without a grid leak, had a grid current of 3×10^{-11} A. measured with 1000 M Ω in the input circuit. The input capacity was reduced by means of a very small, carefully insulated shield, connected to the cathode, which closely surrounded the grid lead except below. The capacity of the 954 cathode to earth was reduced by using the output of the 954 to drive a second cathode follower with a lower output impedance. The output of the second cathode follower was connected to the insulated shielding surrounding the floating screen grid battery and the leads to the 954. The improvement in the frequency response could be demonstrated with the single fibre in place.

The calibration circuit shown at the bottom of figure 2 provided a ready means for testing the frequency response of the input stage at any time during an experiment. By this arrangement a rectangular step of voltage could be ap-

plied between the large pool of Ringer and earth. The voltage step response was always photographed at regular intervals throughout an experiment. This was only an approximate guide, however, because of the disposition of the stray capacities at the grid. The capacity of the grid to ground can be divided into two capacities: (a) the capacity of the grid to the large bulk of the Ringer, and (b) the capacity of the grid to the shield and the other valve electrodes. As far as potentials generated in the fibre are concerned, these two capacities are in parallel and blunt the response through the high resistance of the fibre. But with the voltage step applied to the bulk of the Ringer the capacity (a) shunts the high resistance of the fibre and improves the response at higher frequencies. With a very high resistance preparation (e.g. a single fibre left too long in paraffin), the response to the voltage step consists of a sharp jump, followed by an exponentially delayed rise to approximately the full height. The top of the jump divides the total voltage in the same ratio as the capacities (a) and (b), the amplitude of the jump being proportional to capacity (a). With the interface about 1 cm away from the hook on the grid lead, the jump is about half the total height indicating that under these circumstances the two capacities are about equal. The time constant of the input stage for potentials generated in the nerve fibre is given approximately by the time constant of the exponentially delayed rise measured from the top of the jump. Normally such a division between sharp step and exponentially delayed rise could not be distinguished even with 1 cm of single fibre between the grid lead and the Ringer. Under these conditions it was difficult to determine the true input time constant relating to potentials generated in the fibre and for any particular level of the paraffin-Ringer interface. However, the time constant of the second half of the rise of the voltage step response would not normally exceed about 30 μ sec with 1 cm of single fibre between the interface and the grid. In one fibre it was still less than 30 μ sec with 15 mm of single fibre

in the paraffin. This corresponds to a total input capacity at the grid under these conditions of less than $0.5 \mu\mu F$.

Attempts to determine the input capacity using a known series resistance to replace the single fibre gave little indication of the input capacity under working conditions because it introduced very much larger stray capacities than those present with the single fibre in place.

Other apparatus

The main amplifier and display were of conventional design. The frequency response of the whole apparatus (input effectively shorted) was flat from 100 c/s to at least 10 K c/s. The response to a rectangular step of voltage similarly applied had a time constant of rise of less than $10 \mu\text{sec}$. The output of the main amplifier also drove a differentiating circuit, incorporating feedback. It was estimated that the differentiating unit would respond to a step function of slope in the input circuit with a lag time constant of $0.5 \mu\text{sec}$. Normally the membrane action potential and its time differential were recorded successively, each as single sweeps, using the same beam of the oscilloscope. The fibre was stimulated by rectangular pulses applied to the nerve trunk through a small shielded air-cored transformer. While observations were being made the nerve was stimulated at a frequency of 30 to 40 shocks/min.

RESULTS

The potentials measured by the apparatus under these conditions (V_e , fig. 2) will be proportional to the membrane potential (V_m) at the level of the interface if two conditions hold, namely that (a) the external and internal longitudinal current paths are resistive and uniform, and (b) loops of current due to activity of the nerve fibre do not extend as far as the grid to any significant extent.

With regard to condition (a), it can be safely assumed that the conductors are resistive; it is more difficult to establish

that the non-uniformities which exist are not causing a significant distortion of the records. It is well known that the axis cylinder is markedly constricted at the node. Perhaps more serious are non-uniformities in the external conductor;

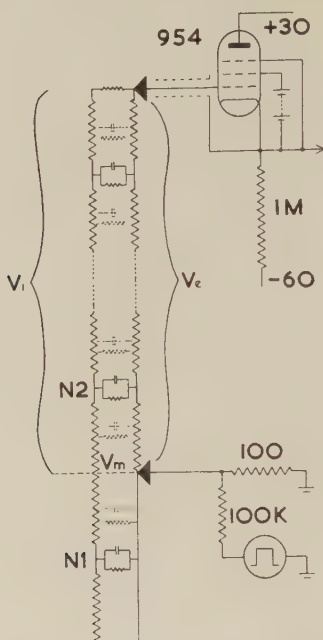


Fig. 2 Equivalent electrical circuit of the arrangement of figure 1. The resistive core of the fibre is shown at the extreme left. The other vertical strip is the external conductor of the fibre showing high resistance in paraffin (above) and negligible resistance in Ringer (below), the interface being shown by the short horizontal broken line. External and internal conductors are connected by various membrane elements: distributed capacitance and resistance along the internode, punctate capacitance and resistance at the nodes (N_1 , N_2). The input valve circuit is at the top right, the calibration circuit at the lower right.

e.g. small pieces of adhering connective tissue. Despite these non-uniformities in the external conductor along any one fibre and the fact that the pattern of the non-uniformities would vary from fibre to fibre the results obtained have been quite consistent in the one preparation and also from pre-

paration to preparation. It is probable, therefore, that the effects of such non-uniformities may be largely neglected.

Non-compliance with condition (b) gives rather more well-defined artefacts. In order that the records may not be complicated by activity affecting the grid it would be necessary to ensure that the impulse did not approach closer to the grid than a distance of about 3 mm. Lussier and Rushton ('51) have shown that the space constant of a group of large medullated fibres of frog sciatic is approximately 2.2 mm. When the fibre has an external resistance comparable to the internal resistance (i.e. immersed in paraffin) this space constant would be shortened to about 1.5 mm. Consequently, it is to be expected that at 5 mm from an active site in paraffin, loops of current would be very small; at 3 mm they could probably be neglected. When the activity is rather less than 3 mm from the grid, spurious potentials will be added on to the record. It is shown below that, on passing the interface into the paraffin, the conduction velocity of the impulse slows to between one-third and one-quarter of its former value, i.e. in one case from about 30 m/sec to 8 m/sec. This means that the rising phase of an action potential, with a foot to peak time of 250 μ sec, will have passed its peak when recorded at the interface before activity commences at a point 3 mm from the grid when the paraffin-Ringer interface is about 5 mm from the grid.

A great many of the records obtained in the various experiments were complicated to a greater or lesser degree by this artefact. This circumstance, however, was not wholly unwelcome in that it gave an indication of the state of the fibre in the paraffin and as to whether or not conduction was still taking place. However, the length of the single fibre from which the rising phase of an action potential can be relatively faithfully recorded was limited, on the one hand, by the appearance of diphasic artefact and, on the other, by a failing high frequency response when long lengths of single fibre separated the interface from the grid.

Typical examples of diphasic artefact are shown in figure 3. In column A the recorded action potentials (fundamentals) are shown together with, in column B, their corresponding time differentials. Each record corresponds to recording sites

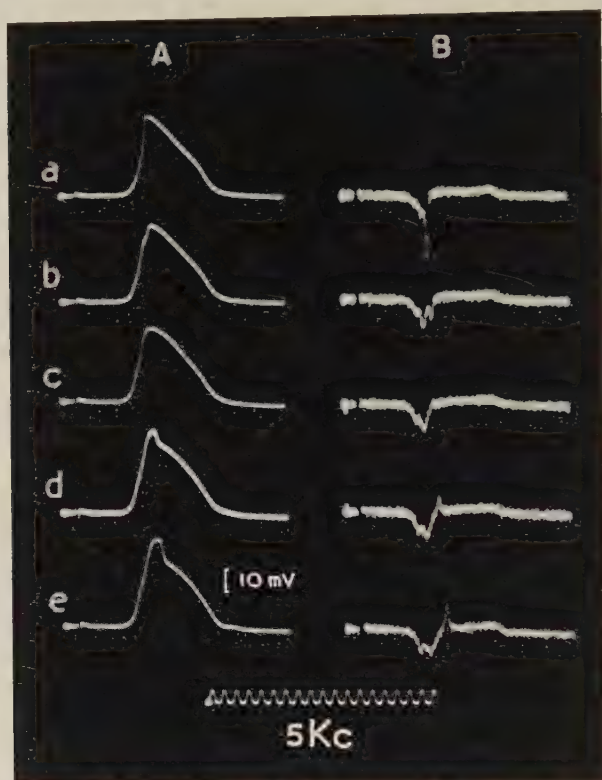


Fig. 3 "Diphasic artefact." Column A, fundamentals (waveforms actually recorded); column B, corresponding first differentials with respect to time; a to e, development of diphasic artefact. a, interface 2.5 mm from grid; in succeeding records, interface has been moved in 0.3 mm steps down the fibre. (At d, two records have been accidentally superimposed; the interface had been moved 0.1 mm between them.)

at 0.3 mm intervals along the fibre close to the end. In the fundamental series, the interesting feature as far as diphasic artefact is concerned is the last step on the rising phase, near the peak. Going down the series, this step becomes

smaller in height and slope and eventually becomes the flat top of the wave. Further down, it inverts to become the relatively fast first phase of the fall-away. In the last record it becomes larger and faster. These changes are reflected in the differentials; in the top record (b), it is represented by the very fast, tall downward spike. Proceeding down the series, this spike gets smaller, merges with the baseline, then inverts and becomes larger, now in the upward direction.

The interpretation is that there is a node on the stretch between interface and grid. In the upper records it is electrically closer to the interface and its contribution to the complete waveform is in the upward direction. When the interface moves down the fibre, a position is reached where this node is electrically half-way; its effect on the grid just balances the effect at the interface. When the interface is moved still lower, the grid alone is affected and the potential due to the node is added to the waveform in the reverse sense.

Effect of the paraffin

The immediate effects of the entry of the single fibre into the paraffin are reasonably clear but there are other and more slowly developing effects which have remained rather obscure.

As the single fibre goes into the paraffin, Ringer solution is stripped away from it so that only a very thin film of external conductor remains. In successful experiments the recorded action potential would normally be about 60 mV in amplitude. It is known that the amplitude of the membrane action potential is about 120 mV (Huxley and Stämpfli, '51). Consequently in paraffin the external resistance per unit length is approximately equal to the internal resistance per unit length; that is about 150 M Ω per cm. It is clear that an external resistance of this order would alter the electrical properties of the internode acting as a passive cable. The space constant is noticeably shortened and the time constant appreciably lengthened. These changes in the passive properties of the internode will

retard the spread of the action potential wave and attenuate it more strongly.

The records of the time differentials of the action potential enable the conduction velocity in paraffin to be measured. The maximum rate of rise of the action potential reaches a sharp peak as a node passes the interface (figures 5 and 6). This has always been recorded as a downward spike. The time at which this portion of the nodal waveform appears at the interface is therefore known with some precision. The appearance at the grid of the maximum slopes of the action potentials due to the activity of nodes in its vicinity was usually recorded in the differentials as smaller upward spikes appearing later in the trace. By recording arrival times for the point of maximum slope at the interface and the grid as successive nodes along the fibre pass the interface and knowing the corresponding conduction distances the conduction velocity in the paraffin may be calculated. Typical results are shown in graphical form in figure 4. As mentioned earlier the ratio of conduction velocity in paraffin to that in Ringer is approximately 0.3.

Apart from these immediate physical effects, paraffin has other more insidious effects. If a good preparation is left in oil for about an hour conduction suddenly fails and this was sometimes clearly associated with the development of a fairly localized high resistance patch at one part of the fibre presumably because of the complete interruption of the external conductor. In figure 4 it will be seen that between the 9th and 10th millimetre of single fibre (between node 4 and node 5) passing the interface there was a sharp increase in the degree of slowed conduction in the paraffin followed immediately by a failure of activity to reach the grid. Despite this marked change, however, the conduction time between N_1 and N_2 further up in the paraffin was relatively unaffected until conduction finally failed. That the effect was probably due to localized interruption of the external conductor is indicated by the fact that, between N_4 and N_5 passing the interface, the time constant of rise of the voltage step response

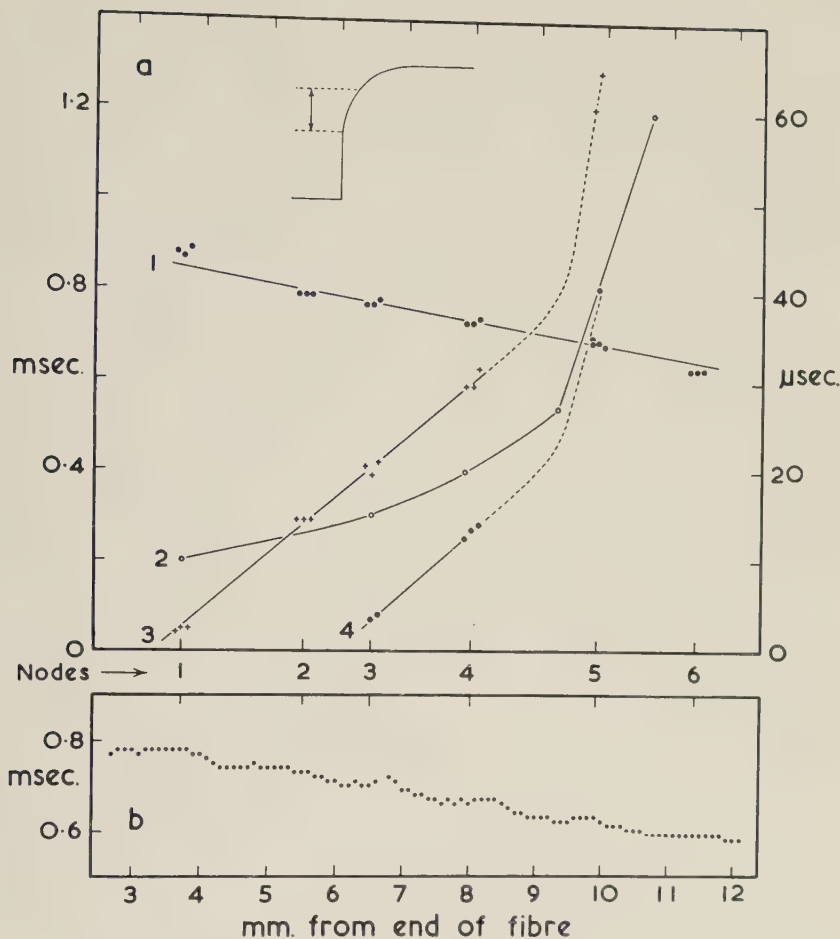


Fig. 4 (a) Conduction of the impulse in Ringer (1) and in paraffin (3,4). Graph (1) plots the time of arrival of the maximum slope of the action potential at the paraffin-Ringer interface (measured as each successive node passed the interface) against distance along the fibre. Graph (3) plots the time of arrival of the maximum slope of the action potential at node 1 [measured on the same record as for each point determining graph (1)] against distance along the fibre. Graph (4), corresponding plot for arrival time at node 2. Graph (2), time constant of rise of the response of the input circuit to a rectangular voltage step at various points along the fibre; time constant measured as shown in inset (see p. 4).

(b) Time for action potential to reach 10% of its peak height plotted against distance along fibre. Preparation used for (a) and (b) same as that for figure 6. The position of the nodes along fibre is indicated.

was slightly more than doubled in value. It was remarked above that, for some time at least, the external conductor and the core of the fibre have approximately equal resistance per unit length. For the input time constant to have doubled in the above instance indicates that the core had become the only effective conducting path from the interface to the grid. Full restoration of function was never achieved by resoaking the fibre in Ringer; the conduction velocity in the part of the fibre that had been exposed to paraffin remained permanently slowed.

If the fibre continues to be left in paraffin for some time after conduction has failed the resistance of the preparation may rapidly become inordinately high and values up to 2000 M Ω have been measured. Even if the paraffin had completely interrupted the external conductor, there would still remain the conductive core of the axis cylinder 1 cm of which has a resistance of only 150 M Ω . Apparently the core must eventually become involved and there is evidence that this effect is restricted to short lengths of the fibre. A similar high resistance effect was also obtained in a single experiment with silicone (Dow Corning 200/200). This circumstance suggests a mechanical explanation, namely that the fibre is being squashed or nipped. When the experiment is carried through rapidly only the initial reduction of the external conductor to a thin film need be considered as leading to distortion of the action potentials.

Action potentials recorded along single fibres

When a series of action potentials taken at small intervals along a stretch of nerve containing several nodes was examined, it was always found that the maximum rate of rise (as observed on the corresponding differential record) reached a maximum value periodically along the length of the fibre. The distances between these maximum value positions very rarely lay outside the range of the internodal distances to be expected in fibres of the size used. Hodler, Stämpfli and

Tasaki ('52), using rather a different experimental arrangement, were able to observe that a node was at the recording site when the action potential rose most rapidly. Unfortunately, in the present arrangement, it was not possible to observe the nodes while recordings were being made. In the description which follows it will be assumed that a node of Ranvier was present at the interface wherever the maximum slope of the action potential attained a maximum value.

Only 5 preparations were suitable for a detailed analysis similar to that described below though, in general, it was less extensive. One of these preparations (preparation A, figure 4 et seq.), considered to be the most suitable for the purpose, will form the main burden of the description. Figure 5 presents a representative sample of the records obtained along the length of the single fibre. It is to be noted that the scale on the left gives the actual length of the single fibre between the grid and the interface. However, potentials of sufficient amplitude to commence recording (cf. fig. 6, c) were not obtained until the interface had been lowered 2.4 mm from the grid. It is probable that the fibre had previously been damaged at some point in this interval so that the part above the damage formed a virtual extension of the grid. The effective length of the fibre is, therefore, probably about 2 mm less than that indicated by the scale on figure 5. Therefore, at the 7 mm position in figure 5, where the record in column A shows a diphasic artefact beginning just after the peak, the interface is effectively only 5 mm from the end of the fibre.

In column A of figure 5 is a series of action potential records (fundamentals) selected to correspond to positions at the nodes and to positions at one and two thirds of the internodal distance as indicated by the arrows. Column B contains records of the time differentials corresponding to each of the fundamentals. The main feature of interest in the fundamental series is the configuration of the rising phase including the peak. It is clear that the shape is not constant along the length of the fibre. At a node [record (a)] the main portion

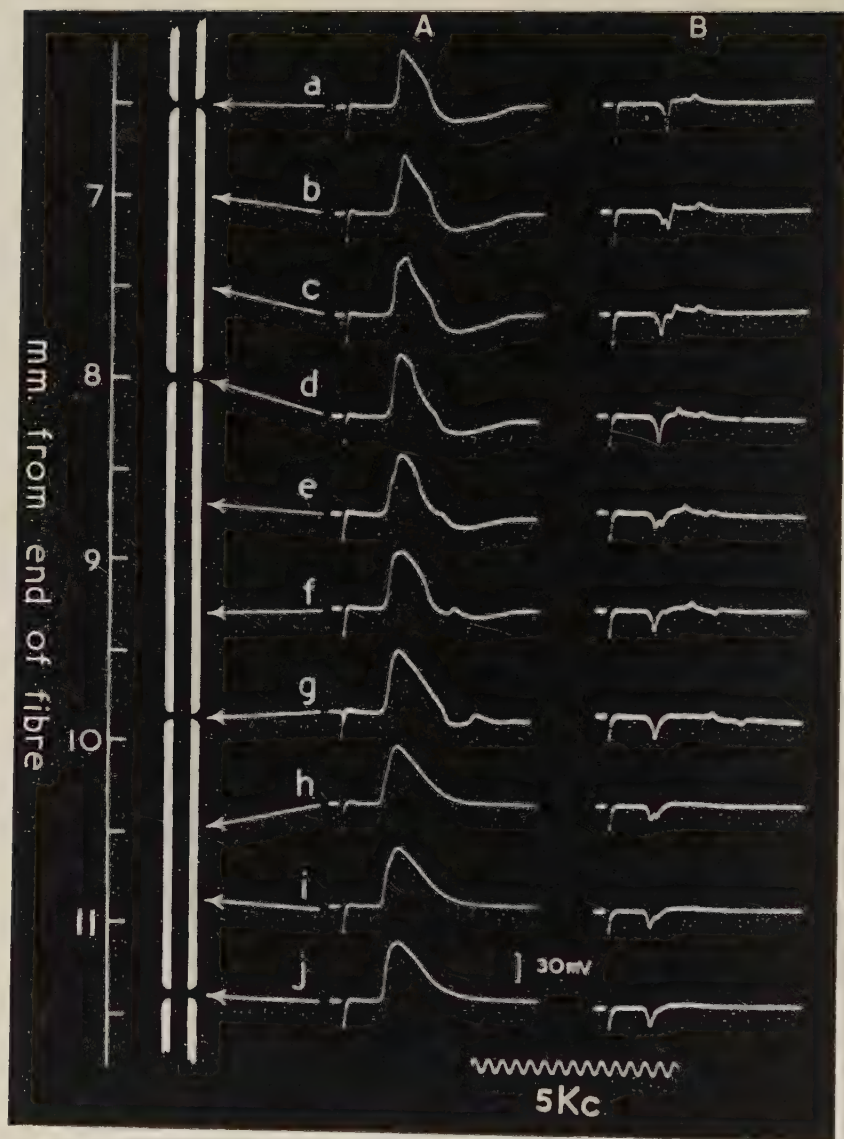


Fig. 5 Action potentials at indicated points along a single fibre. Column A, "fundamentals" (waveforms actually recorded); Column B, corresponding time differentials. For details, see text. Preparation was the same as that used for figure. 6.

of the rising phase of the action potential rises very rapidly. The portion of the rising phase of the action potential before this rapid phase is a smooth, rounded, relatively slow rise from the baseline. As the interface is lowered down the fibre this concave "foot" starts to "fill out" and "creep" steadily up the rising phase. Already in record (b) this discontinuity is more than half way up the rising phase of the action potential but the portion of the rising phase corresponding to it is still not very steep. In record (c) it constitutes almost the whole of the rising phase and has become much steeper while the part of the record corresponding to the steep-rising portion of record (a) has now become much less steep and appears only as a small late peak. In record (d) this peak is lost in the falling phase of the action potential and a new and earlier peak has been created by the fast rising portion which now constitutes the whole of the rising phase of the action potential. Thus the interesting *changes* occur along the internode rather than at the node. It can be seen that these changes are regularly repeated along each of the internodes.

The series of differential records shows the changes along the fibre rather more distinctly. In trace (a), column B, the differential record at the node shows an early, sharp, large-amplitude, downward spike which is followed by a longer, low-amplitude, upward hump. As the interface is lowered and the node goes into the paraffin, the differential spike rapidly gets smaller and later. Out of its "foot" (where it starts taking off from the baseline) a new spike gradually grows. Further down the fibre (c, column B), the new spike is much taller and the original spike is very late and very small, barely keeping below the baseline. In this record, the crossing of the baseline is just later than this small spike, corresponding to the late peak of the fundamental. It is clear that, as this late spike merges into the long, low, hump phase of the record, the crossing of the baseline will suddenly jump earlier, to a point just later than the peak of the new spike. This is what is seen in record (d) of column B and corresponds

to the sudden jump of the peak of the fundamental to its new earlier time. The new spike reaches its maximum amplitude in this record corresponding to the maximum rate of rise of the fundamental. In the other two internodes, these effects are repeated in a similar way. The small, late, upward peaks in the differential records correspond to the arrival at the grid of potential changes due to the activity of nodes 1 and 2 further up the fibre in the paraffin.

To bring out more clearly the changes that occur along the length of the fibre, several quantities have been plotted in the graphs of figure 6. The way in which the various measurements have been made is indicated in the tracings of internodal records inset on the lower right. The top graph of figure 6 indicates the maximum slope of the fundamental at each position along the fibre and it is clear that this value periodically reaches a maximum. It was assumed that each position where this occurred corresponded to the presence of a node. Although the length of most of the internodes falls into the range 1.5 to 2.0 mm which is to be expected for a fibre of this size, it can be seen that the internodes are only very roughly uniform in length. Huxley and Stämpfli ('49) report a $\pm 20\%$ variation. There is, however, a very short internode N_2 to N_3 , only 1 mm long and a similar observation was occasionally made in other preparations. Tasaki ('39) found that very short internodes are relatively common in the large motor fibres of the sciatic nerves in Japanese toads. The finding of both abnormally short and abnormally long internodes on otherwise regular normal fibres has been reported in a variety of animals (e.g. Vizoso and Young, '48).

The maximum rate of rise of the action potential recorded at N_3 is about 900V/sec which was the greatest slope that has been observed in this series of experiments. Since the experimental arrangement is such that only about one-half of the true action potential across the membrane is recorded, the actual rate of rise in this case must have been about 1800 V/sec. The figures for the other nodes in this prepa-

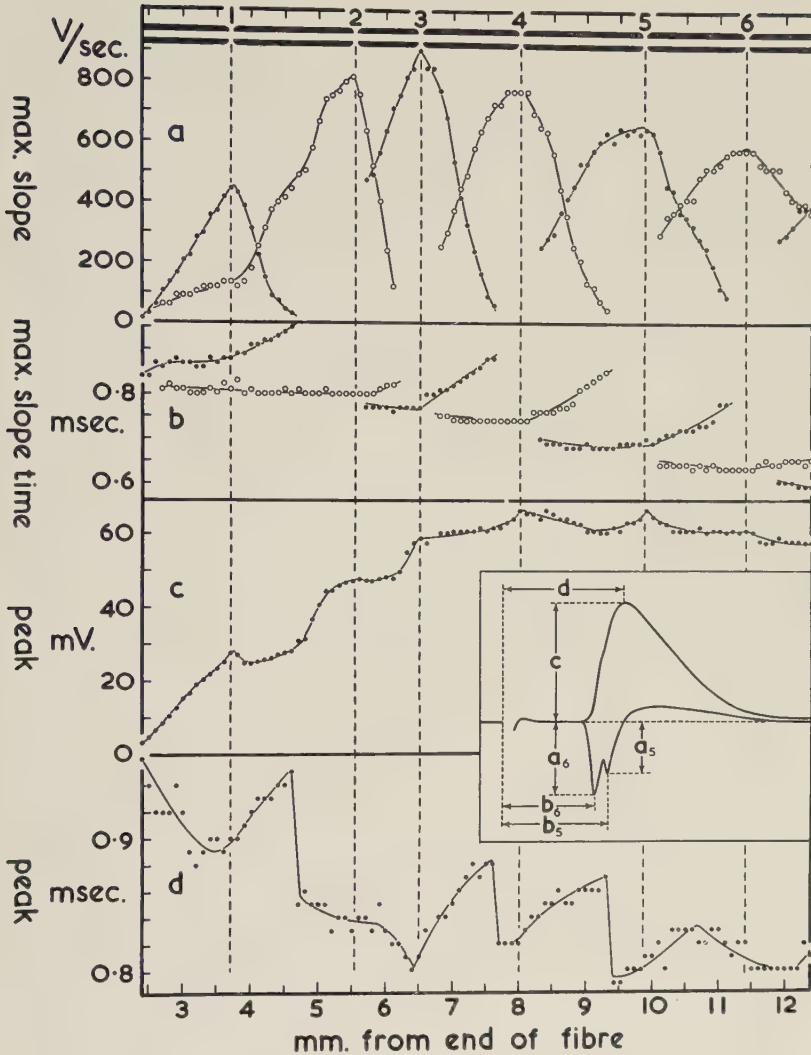


Fig. 6 Analysis of the variations of the action potential along a single fibre. The inset, lower right, shows how the parameters were measured. The tracings used for the inset were of records from an internodal point between N_5 and N_6 . Graph (a), maximum rate of rise of the fundamental; graph (b), conduction time of the maximum rate of rise; graph (c), peak amplitude of the fundamental; graph (d), conduction time of the peak of the fundamental; all plotted against distance from the end of the fibre. Position of the nodes (estimated) are indicated at the top of figure.

ration and the nodes of another preparation (B) are given in table 1.

The average rate of rise for all the nodes in table 1 is 630 V/sec, which would correspond to a value of 1260 V/sec for the action potential across the membrane. The largest rates of rise in both preparations were associated with very short internodes (1.0 and 0.7 mm respectively). The gradual decline in the maximum value of the maximum slope after node 4 in figure 6 is due to the increase in the external resistance that occurred while the interface was passing between

TABLE 1

PREPARATION	NODE	RISE RATE, V/sec.
A (30°C.)	N ₁	440
	N ₂	820
	N ₃	900
	N ₄	770
	N ₅	650
	N ₆	580
B (25°C.)	N ₁	590
	N ₂	530
	N ₃	530
	N ₄	480
	N ₅	610
	N ₆	690
	N ₇	640

the 9th and 10th millimetre of single fibre. The onset of this increased resistance is also suggested by the fairly sharp change in slope of the graph of the maximum slope of the 5th nodal waveform soon after the 9th millimetre had passed the interface.

An interesting feature of graph (a), in this and other preparations, is that the point on any one internode at which the components of the action potential recorded there, due to the separate activity of the adjacent nodes, have equal maximum slopes, is always approximately two-thirds of the internodal distance measured in the direction of impulse propagation.

Graph (b) of figure 6 plots the conduction time of the maximum rate of rise of the action potential at each position along the fibre. Each set of points yields a fairly characteristic graph in two phases. In the first stage, the graph is horizontal or directed very slightly downward (i.e. the time of the maximum slope gets slightly earlier). The second stage is a pronounced curve upward (i.e. gets later) which commences just as the peak value of the maximum slope [graph (a)] is passed, and therefore just as a node crosses the interface.

TABLE 2

PREPARATION	INTERNODE(S)	CONDUCTION TIME	CONDUCTION DISTANCE	CONDUCTION VELOCITY
		μsec	mm	m/sec
A (30°C.)	N ₂ -N ₁	80	1.8	22.5
	N ₃ -N ₂	30	1.0	33.3
	N ₄ -N ₃	30	1.5	50.0
	N ₅ -N ₄	40	1.9	47.5
	N ₆ -N ₅	70	1.5	21.4
	N ₆ -N ₁	250	7.7	30.8
B (25°C.)	N ₂ -N ₁	40	1.7	42.5
	N ₃ -N ₂	40	1.4	35.0
	N ₄ -N ₃	60	2.0	33.3
	N ₅ -N ₄	120	2.2	18.3
	N ₆ -N ₅	160	2.5	15.6
	N ₇ -N ₆	20	0.7	35.0
	N ₇ -N ₁	440	10.5	23.9

The internodal conduction time is here defined as the difference between the times of the maximum slopes of successive nodal waveforms estimated in each case just as the corresponding node crosses the interface, the velocity being then obtained by considering the internodal length. Internodal conduction times and velocities for two preparations are given in table 2.

The average conduction velocity in each preparation (30.8 and 23.9 m/sec respectively) is within the normal range (Erlanger and Gasser, '37; Tasaki, Ishii and Ito, '43). This would

be slightly greater if allowance is made for the decrement in conduction velocity as the impulse approaches the end of the fibre.

The findings presented in table 2 are largely independent of the presence of the paraffin. It is clear that internodal conduction times are by no means constant.

Graph (c) of figure 6 plots the maximum amplitude of the action potential (fundamental) at the various positions along the length of the fibre. The greatest amplitude recorded was 66 mV. As pointed out above, this is just over half the height of the action potential across the membrane reported by Huxley and Stämpfli ('51), indicating that in this experiment, the external resistance per unit length was a little greater than the core resistance per unit length. The curve shows small but reasonably well-defined peaks at the positions of the nodes (vertical broken lines). More correctly, the internodal points fall below straight lines joining the nodal points. The amplitude of the action potential at each end of the N_{4-5} internode is 66 mV while the minimum action potential along the internode (about two-thirds along from N_4 to N_5) is 60 mV, a 9% reduction. An internode in another experiment yielded a 6% reduction. This simple calculation cannot be satisfactorily applied to all internodes because the action potentials of the nodes at each end differ too much in height. Hence, although the reduction in amplitude in the internode is definite, its magnitude is a little uncertain but is of the order of 5–10%.

Graph (d) of figure 6 plots the conduction time of the peak of the action potential. The curves vary considerably from experiment to experiment and insufficient work has been done to describe a "normal" pattern. Two features are shown by graph (d). Firstly, the peak of the action potential becomes earlier as the interface approaches a node, and often, it is at its earliest just as the node crosses the interface. Secondly, as the interface leaves the node behind in the paraffin the peak gets progressively later and then suddenly jumps to an earlier time. The tracings shown in figure 7, c

are the peaks of the action potentials taken at 0.1 mm intervals in the portion of the N_3 - N_4 internode concerned. These sudden jumps occur at some point along the internode either near halfway or in the proximal one-third. They do not occur in every internode. From the results so far obtained, two factors appear to be associated with the absence of a jump; they are a short internode and a very short internodal conduction time.

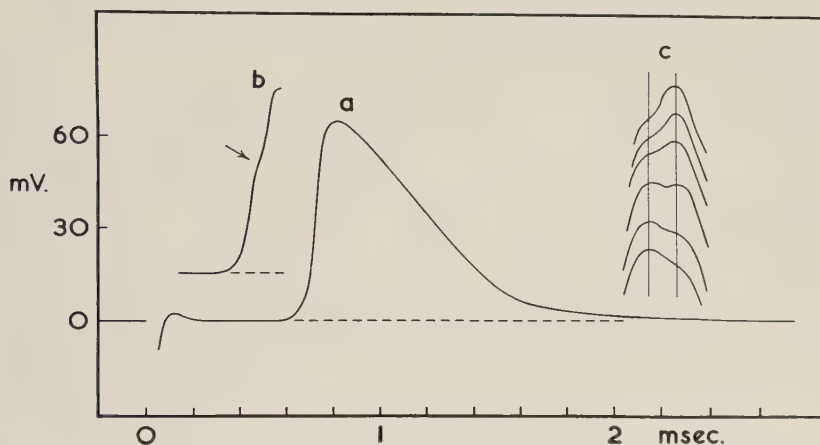


Fig. 7 Tracings of oscillograph records to show details of the action potential at different regions on the fibre (Preparation A): (a), nodal action potential (composite of records taken at N_4 and N_5); (b), rising phase of internodal record (N_3 - N_4) taken at 0.9 mm from the proximal node (N_4). Arrow indicates discontinuity on rising phase; (c), tracings of the peaks of the action potentials taken in the N_3 - N_4 internode to show the jump to an earlier time [not on the same scale as (a) and (b)]. The vertical lines are 60 μ sec apart. The abscissa and ordinate scales refer to (a) and (b) only.

In contradistinction to the peak, the foot of the action potential propagates with an approximately constant velocity. In figure 4, b the time at which the action potential attains 10% of its peak is plotted against distance along the fibre.

In the preparation of table 3 which details the nodal action potential, the nodes which were considered to have given the most normal response have been selected from the two experiments. These nodal records are free of the disturbing

artefacts discussed above with the exception of the distortion resulting from the sudden increase in the external resistance immediately distal to the node due to the effect of the paraffin. This would not seriously alter the rising phase of the action potential recorded at the node. In the case of preparation A the falling phase of N_5 was used instead of that of N_4 because the latter was still complicated by diphasic artefact. A tracing of the nodal action potential (N_4 and N_5 , preparation A) is shown in figure 7, a.

TABLE 3
Normal nodal action potential

	PREPARATION A (30°C.)	PREPARATION B (25°C.)
Rise time		
foot to peak	250 μ sec (N_4)	280 μ sec (N_5)
10% to peak	140 μ sec (N_4)	180 μ sec (N_5)
Maximum rate of rise (approx. half value)	770 V/sec (N_4)	610 V/sec (N_5)
Peak amplitude (approx. half value)	66 mV (N_4)	63 mV (N_5)
Fall time (peak to 10%)	780 μ sec (N_5)	640 μ sec (N_5)
Total duration (10% to peak + peak to 10%)	920 μ sec (N_4 and N_5)	820 μ sec (N_5)

The space distribution of the action potential

Each of the curves of figure 8 represents the distribution of the membrane potential along the length of the fibre at a given instant obtained by measuring the amplitude which each fundamental record had attained at that given time. The end of the nerve fibre is on the left and the impulse is invading the fibre from right to left. The positions of the nodes have been obtained from figure 6, a.

In order to ensure that the records of the action potentials can be directly related to one another, ideally, one would wish to record at all points on the fibre at the one time. This was obviously not possible and records had to be taken suc-

cessively along the fibre. The use of the paraffin, causing a sharp and successive increase in the external resistance, does introduce a serious error in that the action potential at any one position on the fibre is not the same before and after the passing of the interface. This seriously impairs the value of the space distributions obtained in this way (see discussion).

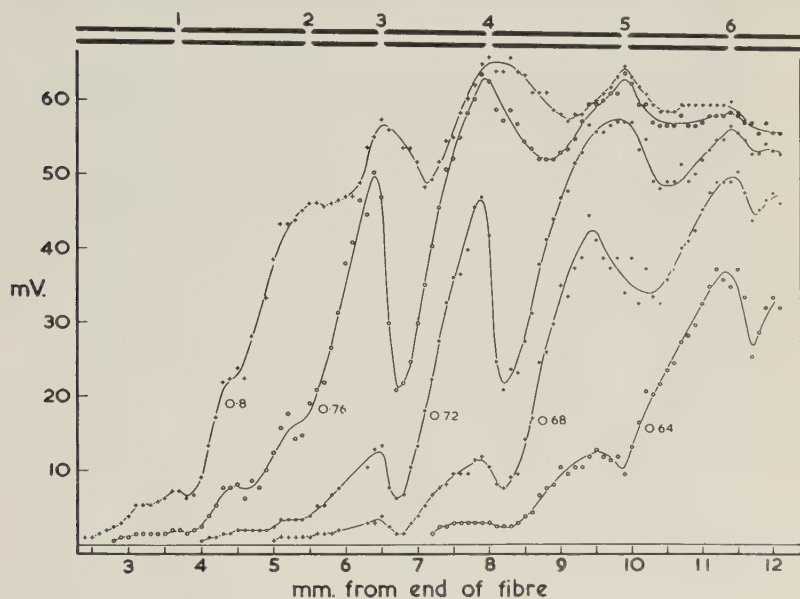


Fig. 8 Space distributions of the action potential at the indicated times after the stimulus artefact in msec, as the impulse invades the fibre from right to left. Same preparation as for figure 6. For details see text.

Considering any one space distribution, the most striking feature is that there is a number of maxima of potential along the part of the fibre occupied by the impulse, a maximum being here defined as a point, the amplitude of which is greater than that of nearby points on either side. Furthermore the positions of these maxima agree quite closely with the location of the nodes obtained from the consideration of the maximum slope of the action potential. It must be emphasised, however, that the use of paraffin in this way has the effect

of accentuating the maxima especially in respect to the proximal falling phases and the internodal "valleys."

PART II

Undissected single fibre inside a spinal root

METHODS

In preliminary experiments, the phalangeal preparation of Erlanger and Gasser ('37) was used. The main preparation, however, was the sciatic nerve and its ramifications down to the ankle together with the attached 8th and 9th spinal roots. The general arrangement was the same as that described in Part I, the spinal root (usually the 9th) taking the place of the single fibre. By dissecting out and stimulating separately each of the finer ramifications of the sciatic nerve, occasionally it is found that the threshold of one fibre in a twig is well below that of the others. The criterion of single fibre activity was that the response was strictly all-or-none. This was further supported by observing a bulk movement of the whole of the response in the play of stimulus-response latency variations with threshold stimulation.

RESULTS

In this experiment the external resistance is very low compared to the core resistance of the single fibre. Hence the recording arrangement will not appreciably alter the current distribution along the fibre. Furthermore, with the preparation resistance always low (less than $0.5\text{ M}\Omega$) the high frequency response of the input circuit of the amplifier is always adequate.

Records obtained in a typical experiment are shown in figure 9. These have been selected from the original series at regular positions along the fibre sufficiently apart (0.5 mm) to demonstrate a repeating pattern. Records in the original series were taken at 0.1 mm intervals. A fast time base was required for accurate observation of the changes. The long conduction distance and hence conduction time

meant that the stimulus artefact did not appear on the trace since it occurred some time before the start of the time base sweep.

The small discontinuities to be sought in the waveforms are of the same order of size as the random fluctuations due

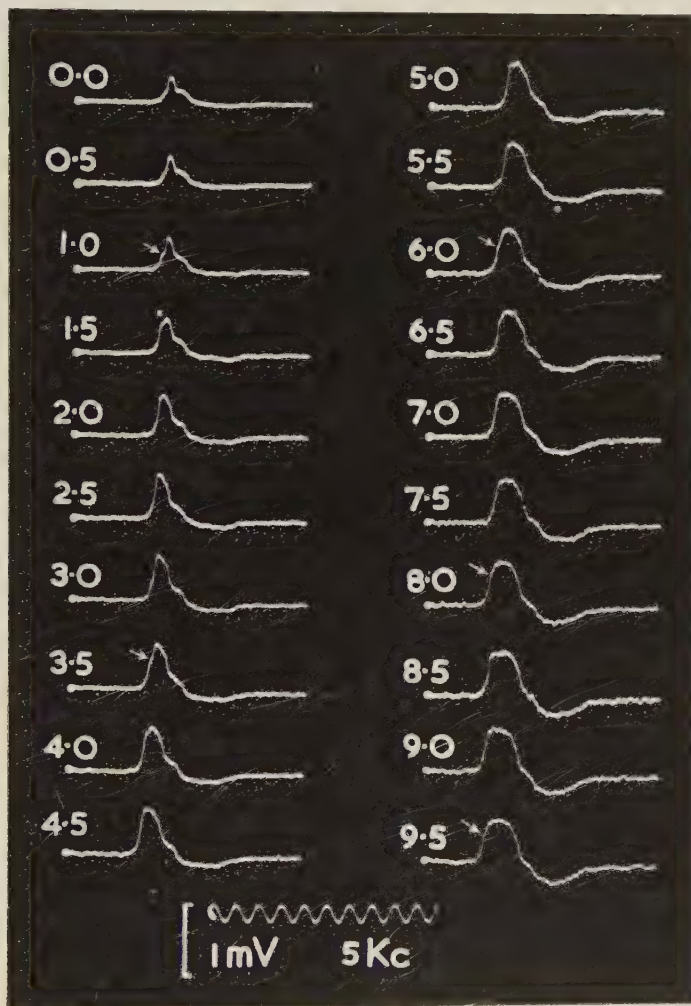


Fig. 9 Action potentials along an undissected single fibre inside a spinal nerve root. Record (0.0) was taken with the interface 1 mm from the grid. Thereafter records taken at 0.5 mm intervals as indicated. Arrows indicate discontinuities on the rising phase which appear in a recurring pattern.

to noise. Nevertheless alterations in the shape of the rising phase of the action potential as the interface is moved down the root can be made out reasonably clearly. In figure 9 arrows indicate the internodal waveforms in which the discontinuities are clearest. Without pressing comparisons too far, the records show similar changes in the rising phase to those shown by the isolated fibres described in Part I. In the series presented, 5 traces can be picked out as clear internodal (as contrasted to nodal) records with the convex or discontinuous rise. They are 1.0 mm, 3.5 mm, 6.0 mm, 8.0 mm, and 9.5 mm. The actual distances from the grid are these distances plus 1 mm, which is the approximate distance down the root at which the original series began. There were, therefore, 5 nodes along this fibre in a distance of about 10 mm giving an average internode of 2 mm. This is within the usual range for the fibres selected under these circumstances.

Unfortunately, the noise level of the records precludes the use of the electronic differentiator because the signal becomes lost in the noise of the differentiator output. Without this assistance, the quantitative appraisal of the records is very difficult.

DISCUSSION

There are two main difficulties associated with the interpretation of the results presented above. Firstly the nodes of Ranvier were not directly observed during the recording of the action potentials, their location being subsequently determined by measuring the amplitude of the time differential of the action potential. However, the fact that the action potential has its greatest maximum of slope at the node has been directly observed by Hodler, Stämpfli and Tasaki ('52). Secondly, the use of paraffin leads to an abrupt change in the external resistance of the fibre beyond the site of recording. This results in an attenuation of the passive spread of potential along the internode in paraffin and a delayed onset of the response at the node that has just passed into that phase. While records taken in the internode

may suffer distortion due to this effect, those obtained at the nodes before they go into the oil will have rising phases which are the least distorted.

Discontinuities in action potential records

While it is probable that the presence of the paraffin accentuates the discontinuities of the rising phase and peak of the action potential, the fact that they appear on the records obtained from undissected single fibres within spinal roots indicates that they are characteristic of the action potential under normal conditions. The external resistance per unit length of the spinal root in paraffin was far lower than that of the axis cylinder and the fact that the fibre had not been subjected to manipulative interference in any way comparable to that of the isolated preparation eliminates the effects of dissection. In all the experiments on spinal roots changes occurred on the rising phase of the action potentials recorded along the length of the fibre which closely resembled the changes more clearly seen, because of the better signal-noise ratio, in a dissected single fibre using the same technique. Furthermore, there was a similar recurrence of the sequence of changes with a periodicity appropriate to the expected internodal length.

A similar experiment was done by Stämpfli and Zottermann ('51) using the dorsal cutaneous nerve of the frog. Unfortunately none of the original records which were used for measurement were published. Despite the uncertainties of their method they observed that the action potential displayed periodic maxima of slope but did not observe the discontinuities of slope noted in the present investigation. A comparable experiment was subsequently performed on isolated fibres by Hodler, Stämpfli and Tasaki ('52). Periodic maxima of slope were again observed but no discontinuities of slope. A further variant of this experiment was performed by Laporte ('51) using medullated fibres in carps, frogs and bull-frogs. One of his conclusions was that "the shape and

magnitude of the spike are constant at all points of each internodal segment." This paper has already been criticised by several workers (Stämpfli and Zottermann, '51; Hodler, Stämpfli and Tasaki, '52; and Frankenhaeuser, '52) who have argued that Laporte's claim that the conduction time of the foot and of the peak of the action potential increases continuously with increasing conduction distance is not an argument against saltation but is, on the other hand, an expected consequence of the saltatory hypothesis. Frankenhaeuser's suggestion was not supported by any direct experimental evidence. The findings reported here (cf. fig. 6) make it probable that the stimulus-peak time of the action potential is, on the contrary, discontinuously related to conduction distance. Owing to the indefinite nature of the foot of the action potential it is difficult to make precise statements about its conduction time. However the conduction time of the foot, defined as 10% of the peak height at that site, is very much closer to a linear relationship with respect to distance (fig. 4, b). Although Laporte did not look for discontinuities on the rising phase of the action potential, the records he has published show no evidence of them, probably because of the restricted frequency response of his amplifier (cf. Frankenhaeuser, '52). It is interesting to note that Huxley and Stämpfli ('49) found two detectable maxima in the rate of rise of their calculated action potentials across the membrane.

The finding that internodal conduction time was not constant is contrary to Rushton's ('51) theory of the effects of fibre size in medullated nerve. However, Tasaki, Ishii and Ito ('43) have shown that, *in a statistical sense*, internodal conduction time is a constant (70 μ sec at 24°C.) and independent of fibre diameter. But they did not determine internodal conduction time directly and their graphs of conduction velocity against fibre diameter and internodal length against diameter showed a fairly wide scatter of points in each case. The data available in the present investigation is inadequate

to confirm that, in a statistical sense, internodal conduction time is a constant.

Analysis of the action potential records

At a node the shape of the record is largely determined by activity at that node with the earliest part of the rising phase being a portion of the potential wave which has spread along the internode from the next more proximal node. As the interface is moved proximally the forward spread from the proximal node, which forms the foot of the action potential, is recorded with increasing amplitude and slope. The effects due to the distal node are now recorded only after they have spread backwards to the recording site through the paraffin which adds to their attenuation and delay. In addition they are delayed by the increasing forward conduction time to the distal node due to the paraffin. As the interface continues to move proximally the discontinuity on the rising phase becomes still more marked because of the diminishing attenuation and increasing slope of the potential wave from the proximal node and the increasing attenuation and diminishing slope of the potential wave from the distal node. Thus the discontinuity moves gradually up the rising phase of the action potential towards the peak with the presence of the paraffin accentuating the effect.

In figure 6, a which graphs the periodic rise to a maximum of the maximum slope of the rising phase of the action potential along the fibre it will be seen that the rise to each peak is more gradual than the fall. This is largely due to the fact that the points determining the fall have been obtained with the particular node getting further away in the paraffin. Spread of the potential back from the node is thus more strongly attenuated and delayed under these conditions. The minimum value of the maximum rate of rise of the action potential occurs where the fall-away from one peak intersects the rise to the next peak. The actual position was found to be remarkably constant at a point two-thirds of the inter-

nodal distance from the proximal node. Under normal conditions this would be closer to the mid-internodal point. The estimated rate rise of the nodal action potential across the membrane of about 1300 V/sec is considerably faster than values given for non-medullated giant fibres (Hodgkin and Katz, '49; Weidmann, '51) and also for mammalian motor-neurones (Brock, Coombs and Eccles, '52).

The curves of figure 6, b call for some comment. It will be recalled that the points determining the curves give the timing of the maximum slope of the potential wave associated with each node at the various positions along the fibre. Each curve has a nearly horizontal portion which turns sharply upwards as the interface passes the node. It might be expected that the time of the maximum slope would occur progressively earlier as the interface moved down the internode towards the node concerned, but this change was found to be quite small. At the same time the points in figure 6, a indicate that there is a marked increase in the maximum slope. This suggests that the spread of the maximum slope is being largely determined by the resistive elements of the core, the sheath capacities causing little delay. No adequate explanation for this finding can be put forward although possibly the time of the maximum slope, measured in this way, may not be a very sensitive index of the expected slowing due to sheath capacities. The pronounced upward turn of the graphs in figure 6, b as the node enters the paraffin phase is readily explained by the fact that the potential wave is spreading back from the node through the paraffin. Furthermore, the node concerned is itself triggered with increasing delay.

The observation (fig. 6, c) that there is a diminution of the peak height of the action potential (5%–10%) agrees with a calculation of 10% by Huxley ('51) on the basis of the saltatory theory. A similar, though larger diminution was observed by Pfaffmann ('40). With regard to the sudden jumps to an earlier time displayed by the peak of the action potential (fig. 6, d), it is clear that, at any one position, the peak of a suitably placed nodal contribution will determine

the peak of the whole action potential. As the recording site is moved the amplitudes of the contributions alter and a position will be reached where the peak will be determined by another nodal contribution now more favourably situated. The timing of the peaks of the nodal contributions differs appreciably and hence there is the possibility of a sharp transition in time.

*Space distribution of action potential
across the membrane*

The presence of the paraffin has rather serious distorting effects on the form of the space distribution of the action potential across the membrane in that it tends to make the rising phase (distal slope) of the potential peaks convex upwards instead of concave upwards. This can be explained by changes in the longitudinal currents due to the progressive increase in the external resistance distal to the interface as the latter moves down towards the node concerned. In the original records the paraffin accentuates the increase in the slope of the rising phase of the action potential with respect to time at successive points down the internode. Similarly the fall-away from the potential peaks (proximal slope) in the space distribution is much sharper than normal because of the sudden slowing and attenuation of the action potential as the node enters the paraffin.

The troughs on the rising phase of the space distributions of figure 8 are, therefore, largely an artefact. Nevertheless, under normal circumstances, there must be at least one maximum of membrane potential on the rising phase of the space distribution of potential distal to the peak (maximum being defined as a point whose value is greater than that of nearby points on each side). Consider two adjacent nodes: there will be some point in time when membrane potentials at each node will be equal. In the internode between them there will be a dip in the space distribution of potential. Considering the state of affairs a moment earlier in time, the membrane

potential at the distal node will be less than that at the more proximal node of the pair. Hence the distal node can be considered to be on the rising phase of the space distribution at that slightly earlier time. Furthermore, it is possible to select the earlier time such that there is still some dip of potential between the two nodes. The conclusion then follows that there must be some time when the rising phase of the space distribution shows a maximum distal to the peak, or in other words, when a node on the rising phase has a dip of potential on its proximal side. This means that there must always be a phase of reversed longitudinal current during the rising phase of the action potential in the distal portion of an internode. Such a reversal of the external longitudinal current is seen in the published records of Huxley and Stämpfli ('49) and those of Hodler, Stämpfli and Tasaki ('52).

SUMMARY

1. A mobile paraffin-Ringer interface was used for obtaining records, which were proportional to the action potential across the membrane, at successive small intervals (0.1 mm or less) along the length of single isolated and non-isolated myelinated nerve fibres.

2. The limitations associated with the use of paraffin in this way have been investigated. The principal limitation results from the sudden increase in the external resistance of the fibre as it enters the paraffin phase.

3. The conduction velocity of the impulse in paraffin is about 0.3 of the conduction velocity in Ringer solution.

4. The following parameters of the action potential at each position on the fibre were studied: the maximum slopes of the rising phase, the conduction time of the maximum slope, the amplitude of the peak and the conduction time of the peak and of the foot.

5. The maximum slope of the rising phase of the action potential was measured directly from time differentials obtained by means of electronic differentiation. The maximum

slope achieved peak values at fairly regular intervals along the fibre. It was assumed that the positions of the peaks corresponded to the nodes of Ranvier.

6. The internodal action potential records showed evidence of a discontinuity on the rising phase due to the separate contributions of the nodes at each end of the internode. The discontinuity is clearly indicated by the two peaks in the time differential records. Conduction under these conditions is saltatory with respect to time as well as to space.

7. The peak amplitude of the action potential suffered a 5%–10% reduction in the internode.

8. The conduction time of the peak of the action potential was markedly discontinuous with respect to distance whereas that of the foot (10% peak height) was nearly continuous.

9. The internodal conduction time showed wide variations along the one fibre and from fibre to fibre.

10. The average nodal action potential had an observed maximum rate of rise of about 650 V/sec giving an estimated maximum slope of about 1300 V/sec for the total action potential across the membrane at the node.

11. Space distributions of the action potentials were prepared and discussed.

The authors are grateful for the help of various colleagues in the Brain Research Unit, particularly that of Dr. R. L. Manning, and for the technical assistance given by Mr. T. Jamieson and his staff. The figures were prepared for publication with the assistance of Mr. S. Woodward-Smith and Mr. K. Clifford of the Department of Illustration, University of Sydney.

LITERATURE CITED

- BISHOP, P. O. 1949 A high impedance input stage for a valve amplifier. *Electronic Engineering*, 21: 469–470.
- BROCK, L. G., J. S. COOMBS AND J. C. ECCLES 1952 The recording of potentials from motoneurons with an intracellular electrode. *J. Physiol.*, 117: 431–460.

- ERLANGER, J., AND H. S. GASSER 1937 Electrical signs of nervous activity, p. 29. University of Pennsylvania Press, Philadelphia.
- FRANKENHAEUSER, B. 1952 Saltatory conduction in myelinated nerve fibres. *J. Physiol.*, *118*: 107-112.
- HODGKIN, A. L. 1951 The ionic basis of electrical activity in nerve and muscle. *Biol. Rev.*, *26*: 339-409.
- HODGKIN, A. L., AND B. KATZ 1949 The effect of sodium ions on the electrical activity of the giant axon of the squid. *J. Physiol.*, *108*: 37-77.
- HODLER, J., R. STÄMPFLI AND I. TASAKI 1952 Role of potential wave spreading along myelinated nerve fiber in excitation and conduction. *Am. J. Physiol.*, *170*: 375-389.
- HUXLEY, A. F. 1951 Cited by Hodgkin, A. L. ('51), p. 396. *Biol. Rev.*, *26*: 339-409.
- HUXLEY, A. F., AND R. STÄMPFLI 1949 Evidence for saltatory conduction in peripheral myelinated nerve fibres. *J. Physiol.*, *108*: 315-339.
- 1951 Direct determination of membrane resting potential and action potential in single myelinated nerve fibres. *J. Physiol.*, *112*: 476-495.
- LAPORTE, Y. 1951 Continuous conduction of impulses in peripheral myelinated nerve fibers. *J. gen. Physiol.*, *35*: 343-360.
- LUSSIER, J. J., AND W. A. H. RUSHTON 1951 The relation between the space constant and conduction velocity in nerve fibres of the A group from the frog's sciatic. *J. Physiol.*, *114*: 399-409.
- PFAFFMANN, C. 1940 Potentials in the isolated medullated axon. *J. Cell. and Comp. Physiol.*, *16*: 407-410.
- RUSHTON, W. A. H. 1951 A theory of the effects of fibre size in medullated nerve. *J. Physiol.*, *115*: 101-122.
- STÄMPFLI, R. 1954 Saltatory conduction in nerve. *Physiol. Rev.*, *34*: 101-112.
- STÄMPFLI, R., AND Y. ZOTTERMANN 1951 Nachweis der saltatorischen Erregungsleitung am intakten Nervenstamm. *Helv. physiol. pharmacol. Acta*, *9*: 208-213.
- TASAKI, I. 1939 The electro-saltatory transmission of the nerve impulse and the effect of narcosis upon the nerve fiber. *Am. J. Physiol.*, *127*: 211-227.
- 1953 Nervous Transmission. Charles C Thomas, Springfield, Ill.
- TASAKI, I., K. ISHII AND H. ITO 1943 On the relation between the conduction-rate, the fibre-diameter and the internodal distance of the medullated nerve fibre. *Jap. J. med. Sci. Biophys.*, *9*: 189-199.
- VIZOSO, A. D., AND J. Z. YOUNG 1948 Internode length and fibre diameter in developing and regenerating nerves. *J. Anat., Lond.*, *82*: 110-134.
- WEIDMANN, S. 1951 Electrical characteristics of Sepia axons. *J. Physiol.*, *114*: 372-381.
- WOLFGRAM, F. J., AND A. VAN HARREVELD 1952 Modes of conduction in myelinated nerve. *Am. J. Physiol.*, *171*: 140-147.

COMPARISON OF THE
EFFECT OF ANOXIC ANOXIA AND APNEA ON
RENAL FUNCTION IN THE HARBOR SEAL
(PHOCA VITULINA, L.)¹

PRESTON B. LOWRANCE,² JAMES F. NICKEL,³ CHEVES McC. SMYTHE⁴
AND STANLEY E. BRADLEY

*The Mt. Desert Island Biological Laboratory, Salisbury Cove, Maine;
the Department of Medicine, College of Physicians and Surgeons,
Columbia University, and the Presbyterian Hospital,
New York, New York*

TWO FIGURES

The harbor seal (*Phoca vitulina*, L.) must tolerate repeated periods of asphyxia as a consequence of the apnea of diving. Irving, Scholander and Grinnell ('42) have shown that the hemodynamic responses to diving involve the development of bradycardia and diminution of blood flow through the muscles of the back. The renal circulation participates actively in this vasoconstrictive response to asphyxia (Bradley and Bing, '42). Sodium, potassium and water output decrease sharply in association with a fall in renal blood flow and glomerular filtration (Bradley, Mudge and Blake, '54). The mechanism of this response remains obscure. Anoxemia becomes evident shortly after apnea is induced, and may possibly play an important role in altering renal tubular function and urine for-

¹ Aided by the Edward N. Gibbs Prize Fund, New York Academy of Medicine, and the American Heart Association, New York, New York.

² John and Mary Markle Fellow in Medicine. Present address: Department of Medicine, University of Virginia School of Medicine, Charlottesville, Virginia.

³ Fellow of the New York Heart Association. Present address: Walter Reed Army Medical Center, Washington, D. C.

⁴ Research Fellow of the American College of Physicians. Present address: Boston City Hospital, Boston, Massachusetts.

mation. The present investigation was undertaken to determine whether the effects of asphyxia on renal function in the seal could be reproduced by anoxic anoxia.

METHODS

Young unanesthetized weanling female seals weighing 40 to 50 pounds were used throughout. When first obtained, these animals had to be force-fed by gavage with a mixture of pig liver and whole herring prepared in a Waring blender and diluted with water. In time, nearly all learned to take food voluntarily, though supplementary force-feedings were necessary to maintain body weight. Intramuscular administration of crystalline penicillin (600,000 units) at approximately weekly intervals proved effective in preventing the skin infections and subcutaneous abscesses to which young seals are peculiarly susceptible.

At the beginning of each experiment, the animal was strapped to a board and washed with running fresh water in order to remove all traces of sea water. Creatinine solution (5 gm in 300 cm³ of water) and herring-pig liver suspension (200–400 cm³) were then administered by stomach tube. Food was given in each experiment in order to insure the high glomerular filtration rate and plasma flow that have been shown to follow feeding in these animals (Hiatt and Hiatt, '42). No effort was made to impose a constant load of salt or water, because the comparison between anoxia and asphyxia was made in each experiment. Sodium p-aminohippurate (2.5 cm³ of a 20% solution) was injected subcutaneously into the hind flipper web. Urine samples were collected without wash-out through an indwelling catheter placed in the bladder, and blood samples were drawn from one of the flipper veins.

Protein-free plasma filtrates were prepared by precipitation with cadmium sulfate (Fujita and Iwatake, '31). P-aminohippurate was determined in this filtrate and in diluted urine by the method described by Goldring and Chasis ('44). Creatinine was determined in aliquots of the same specimens by the

method of Bonsnes-Taussky ('45). Clearance values were computed in the usual manner. Sodium and potassium in plasma and urine were determined with an internal standard flame photometer. Electrocardiograms were recorded with a Beck-Lee electrocardiograph. In one experiment, a strain gauge connected to the same instrument was used to record pressures obtained through an indwelling arterial needle.

Anoxia was induced by making the animals breathe a mixture of 10% oxygen and 90% nitrogen through a snugly fitting mask designed to fit the muzzle, with a cannister containing soda lime for absorption of carbon dioxide. The animals occasionally struggled free long enough to take several breaths of room air, but usually anoxia was severe enough to produce cyanosis of the visible mucous membranes. Apnea was produced by holding a closed funnel over the animal's nose and mouth, allowing it to breathe for only 10 to 15 seconds of each minute.

The sequence employed was three 10-minute periods of urine collection to serve as a control, followed by three 10-minute periods each during low oxygen breathing, recovery from anoxia, apnea, and recovery from apnea. Seven studies (1-7) were made in this manner, and in two (8, 9) anoxia only was imposed during water diuresis.

RESULTS

The results of these experiments are presented in table 1. Each datum therein is an average of three successive values obtained in the control and experimental phases of each study. The values are arranged by experiments collated during each study phase to permit comparison of individual experiments. Since these values are averages maximal changes have been obscured by inclusion of data from initial urine collection periods that fail to reveal immediately the effect of the stimulus (anoxia or apnea) owing to intra-renal delay. Thus in these data the changes are minimized and are not exaggerated by

TABLE 1
*Renal function in seals (Phoca vitulina, L.) during anoxia and apnea*¹

EXP. NO.	V cm ³ min.	C _{cr} cm ³ min.	C _{pa} h cm ³ min.	U _{Na} μEq cm ³	U _k μEq cm ³	U _{Na} V μEq min.	U _k V μEq min.	U _{Na} V C _{cr} μEq cm ³	U _k V C _{cr} μEq cm ³	U/P _{cr}	C _{Na} cm ³ min.	C _k cm ³ min.	C _{Na} C _{cr} %	C _k C _{cr} %
Control														
1	0.54	104	496	129	65	68	35	0.65	0.34	198	0.46	6.5	0.44	6.2
2	0.13	52	163	86	70	11	9	0.22	0.18	400	0.08	1.8	0.15	3.3
3	0.20	61	164	132	75	27	15	0.43	0.24	315	0.17	2.9	0.26	4.7
4	0.15	62	340	52	34	8	5	0.12	0.08	410	0.04	1.1	0.07	1.4
5	0.50	82	227	263	47	134	24	1.60	0.29	164	0.85	3.9	1.00	4.8
6	0.29	98	224	67	32	19	9	0.20	0.09	308	0.11	2.2	0.12	2.3
7	1.00	158	298	265	59	273	61	1.72	0.38	154	1.78	11.1	1.10	7.0
8	1.10	110	298	31	28	32	32	0.28	0.26	102	0.22	6.1	0.19	5.5
9	4.80	146	212	70	37	273	157	1.87	1.12	37	1.80	25.2	1.25	21.5
Anoxia														
1	0.20	35	106	67	61	13	12	0.41	0.41	173	0.09	2.5	0.27	8.7
2	0.15	51	106	66	57	10	8	0.20	0.17	342	0.06	1.7	0.12	3.4
3	0.31	74	166	113	72	24	15	0.32	0.21	355	0.14	3.4	0.19	4.6
4	0.08	30	71	51	48	3	3	0.15	0.14	365	0.01	0.8	0.08	3.2
5	0.17	30	45	138	37	25	10	0.78	0.21	171	0.16	1.3	0.22	4.6
6	0.31	71	151	74	45	22	14	0.34	0.31	221	0.12	3.2	0.19	4.6
7	0.30	24	39	161	52	9	11	1.45	0.47	110	0.25	1.9	0.92	7.6
8	0.23	10	22	24	18	0.24	0.26	0.51	0.39	47	0.03	0.5	0.35	6.7
9	0.93	18	18	25	33	14	25	0.86	1.14	36	0.12	4.2	0.63	16.3

1	0.17	55	166	251	87	61	23	1.25	0.43	203	0.38	5.4	0.85	9.9
2	0.18	54	103	91	68	16	12	0.30	0.22	309	0.11	3.2	0.21	4.1
3	0.28	84	179	160	92	49	24	0.54	0.30	302	0.28	5.4	0.31	6.9
4	0.12	26	103	59	34	6	4	0.29	0.16	212	0.04	0.4	0.17	3.5
5	0.49	76	155	173	51	86	24	1.14	0.33	156	0.56	5.6	0.74	7.4
6	0.36	80	236	69	57	26	20	0.31	0.26	225	0.14	4.8	0.17	6.1
7	1.60	111	253	238	86	372	137	3.36	1.22	71	2.30	23.9	2.09	21.4
8	1.80	94	222	30	26	50	46	0.55	0.49	53	0.35	7.7	0.39	8.3
9	2.50	125	185	86	80	215	199	1.70	1.57	51	1.40	23.2	1.11	30.2

Apnea

1	0.16	27	95	65	60	10	13	0.39	0.33	171	0.07	1.8	0.27	6.8
2	0.08	17	41	89	39	8	3	0.46	0.19	205	0.05	0.5	0.32	3.1
3	0.23	52	102	173	43	43	10	0.78	0.20	223	0.26	2.2	0.46	4.3
4	0.13	17	77	61	49	8	6	0.47	0.35	140	0.04	1.2	0.26	7.3
5	0.30	39	82	133	31	39	10	1.02	0.23	130	0.26	2.3	0.67	5.4
6	0.24	53	113	82	40	21	10	0.38	0.18	220	0.12	2.4	0.22	4.3
7	0.34	37	86	180	98	59	32	1.74	0.88	109	0.37	6.2	1.10	17.1
8														

Recovery from apnea

1	0.37	71	201	66	106	27	43	0.36	0.52	179	0.18	10.1	0.25	13.5
2	0.29	57	127	113	50	31	15	0.57	0.25	189	0.27	2.8	0.40	6.2
3	0.36	75	186	172	59	64	21	0.85	0.29	208	0.38	4.4	0.50	6.3
4	0.30	37	134	56	83	17	24	0.47	0.68	124	0.09	4.5	0.26	12.7
5	0.59	66	135	198	37	116	22	1.77	0.33	113	0.78	5.0	1.20	7.5
6	0.46	87	230	82	55	38	19	0.44	0.22	192	0.22	4.6	0.26	5.3
7	1.00	104	214	201	74	208	76	3.00	4.73	101	1.37	13.5	1.33	13.0

¹ Each datum is the average of values obtained in three successive urine collection periods in nine experiments, arranged according to experimental stage (control, anoxia-low oxygen breathing, recovery from anoxia, apnea, and recovery from apnea). Abbreviations: V = urine flow, C_{cr} = creatinine clearance, C_{pah} = p-aminohippurate clearance, U_{Na} = urinary sodium concentration, U_k = urinary potassium concentration, $U_{Na}V$ = urinary sodium output, U_kV = urinary potassium output, $U_{Na}V/C_{cr}$ = sodium excretion relative to glomerular filtration, U_kV/C_{cr} = potassium excretion relative to filtration, U/P_{cr} = urine-plasma creatinine concentration ratio, C_{Na} and C_k = sodium and potassium clearances, C_{Na}/C_{cr} and C_k/C_{cr} = sodium and potassium clearances relative to filtration or the percentage of filtered ion excreted in the urine.

the design of the experiment. The striking lack of agreement between control values for different animals (attributable to differences in hydration, food intake, and other less easily defined factors) diminishes the statistical significance of change. Nonetheless, distinct patterns of response to anoxia and apnea are evident.

Renal plasma flow and glomerular filtration rate

Renal plasma flow and glomerular filtration rate [sodium p-aminohippurate (PAH) and creatinine clearances respectively] decreased during both low oxygen breathing and apnea (table 1). It is likely that diminished renal extraction of PAH contributed to the change observed in PAH clearance since the filtration ($C_{in}/C_{p\ n}$) was unusually high in nearly every study during anoxia. This phenomenon was less obvious during apnea though the filtration fraction rose above 40% in 4 of the 7 experiments. In addition, the filtration fraction was high (more than 40%) in three experiments during the control periods, possibly because PAH plasma levels were too high. In any case, the extent of the decrement in PAH clearance and the parallel fall in filtration support the view that the major determinant was a fall in renal blood flow. Since arterial pressure probably tended to rise rather than fall during both anoxia and apnea (*infra vide*) it is evident that intra-renal vasoconstriction developed in both situations. Despite the large inter-individual differences (creatinine clearances ranging from 52 to 158, and PAH clearances from 163 to 496 $\text{cm}^3/\text{min.}$ during the control periods), and despite absence of an effect in one experiment (no. 3) anoxia produced a highly significant average reduction in both clearances (C_{cr} , $t=3.7$, $p<.01$; $C_{p\ n}$, $t=4.7$, $p<.01$). During apnea both renal plasma flow and glomerular filtration rate fell in every instance ($t=5.2$, $p<.01$ for both). No difference between these responses was noted although apnea appeared to produce more prompt and pronounced decrements in both clearances.

Urine flow

A fall in urine flow occurred in every study during anoxia and apnea but the averaged values in table 1 (V) fail to show it. Owing to the large variation from study to study the overall mean change observed was not statistically significant, but there is little doubt that it was physiologically significant. During diuresis as a result of preliminary water loading, both anoxia and apnea markedly reduced urine flow (nos. 7, 8, 9 — table 1). The diminution in urine flow tended to be relatively less than that in filtration, hence the creatinine urine-plasma concentration ratio (U/P_{cr} — table 1) decreased. This decrement was probably statistically significant for the data as a whole despite variation ($t=2.45$, $p < .05$ and $t=2.35$, $p < .05$ for anoxia and apnea respectively).

Hematuria was noted on several occasions during anoxia and apnea persisting throughout the recovery periods. Whether this was due to local trauma by the urethral catheter or to changes in glomerular capillary permeability could not be determined.

Sodium excretion

The urinary concentration and output of sodium (U_{Na} and $U_{Na}V$ — table 1) tended to fall during periods of anoxia and apnea. This effect was not regularly observed and appeared to be most apparent when urinary sodium concentration and excretion were high initially and a marked reduction in glomerular filtration occurred, as in the experiment presented in figure 1. Although considerable variation was observed (U_{Na} — 31 to 265 mEq/L, $U_{Na}V$ — 8 to 273 μ Eq/min.) during the control periods, the average changes were probably statistically significant during anoxia (U_{Na} — $t=2.78$, $p < .05$, $U_{Na}V$ — $t=2.35$, $p < .05$). The lack of statistical significance for the changes during apnea may be ascribed to the size of the series, persistence of low values during recovery from anoxia and inter-experimental variation. Examination of the data, as

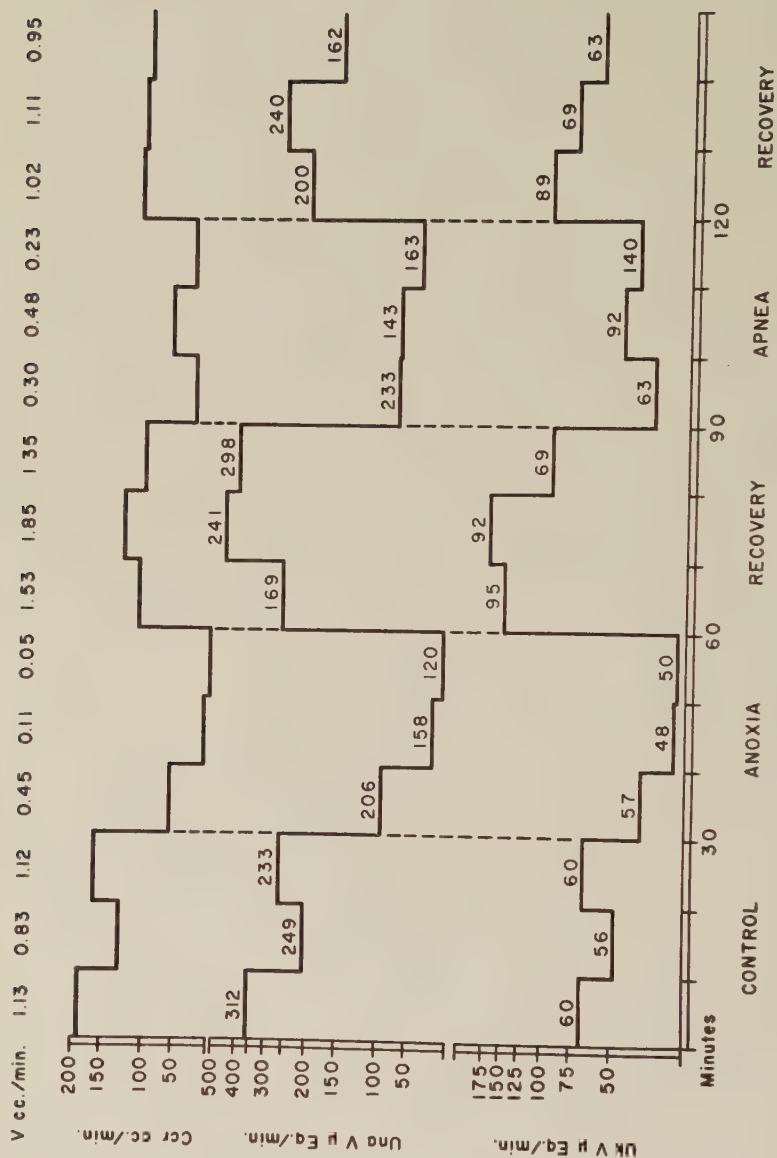


Fig. 1 Changes in the creatinine clearance (C_{cr}), water output (V), and electrolyte excretion ($U_{Na}V$ — sodium and U_KV — potassium) in the seal during anoxia and apnea. Numerical values for urinary sodium and potassium concentrations are inserted above $U_{Na}V$ and U_KV respectively.

in figure 1, indicates the physiologic significance of the changes in urinary sodium concentration and output during apnea. The sodium clearance changed similarly. The sodium output relative to filtration also decreased somewhat, of probable significance in anoxia ($t=2.40$, $p < .05$) and for the reasons mentioned above not statistically significant during apnea. The sodium-creatinine clearance ratio (C_{Na}/C_{cr} — the percentage of filtered sodium excreted in the urine) was not affected in any consistent manner. Thus, this ratio was reduced by anoxia in 4 instances but either rose or remained unchanged in 5. Although the value tended to fall on the average, the change was not significant.

Potassium excretion

Anoxia and apnea affected urinary potassium excretion in very much the same manner as sodium excretion though the changes were not as large nor as consistent. Potassium concentration and output in the urine (U_k and $U_k V$ — table 1) tended to fall but not significantly on the average except when control values were high (fig. 1). The average decrement in potassium clearance (C_k — table 1) was more marked, but the change was not above the 5% probability level ($t=2.34$ for anoxia, $t=2.19$ for apnea). Although it seems likely that potassium excretion was diminished during anoxia and apnea, the change appeared to be no greater than that occurring simultaneously in filtration. The ratio between potassium excretion or potassium clearance and filtration rate ($U_k V/C_{cr}$ or C_k/C_{cr} — table 1) did not change significantly, rising as often as it fell. In any event the responses to anoxia and apnea were indistinguishable.

Cardiovascular function

Since the heart rate usually slowed to palpation during anoxia as it does during apnea it seemed reasonable to believe that reflex bradycardia was also common to both responses. However, an attempt to confirm this impression by more exact

methods disclosed striking differences in the cardiac mechanism.

Electrocardiograms were recorded in three experiments and arterial pressure tracings were obtained in one. In one animal no change in cardiac rate occurred during 25 minutes of anoxia sufficiently severe to cause deep cyanosis. However, the QRS complex was altered by the development of a small Q, decreased amplitude of the R wave, and increased amplitude of the S wave. The amplitude of the P and T waves was diminished but no deviation of the ST segment was evident. In the second experiment, 10 minutes of anoxia resulted in slowing the heart to a rate of 22/min. accompanied by arrhythmia associated with respiratory movements. Asystole for periods as long as 4 to 5 seconds developed during expiration, followed by several rapid beats during inspiration. The P-R interval was increased, and the P and T waves became diphasic. In the third experiment, auricular fibrillation was induced, with ventricular responses again closely correlated with respiration (fig. 2, C, D, and E). Unfortunately, the inception of this rhythm was not recorded. After 10% oxygen was discontinued, the rhythm rapidly changed to auricular flutter with 2:1 conduction and then reverted to sinus rhythm.

Electrocardiograms obtained during asphyxia were similar to those described by Irving, Scholander and Grinnell ('42). Bradycardia usually occurred promptly, with the rate varying from 50 down to 12 beats per minute (fig. 2, A). When the rate was very slow, the P-R interval became longer, the P-Q segment was depressed, and the T-waves became sharply diphasic or inverted. These abnormalities disappeared instantly when apnea was terminated.

The arterial pressures (measured directly from the femoral artery in one animal) rose during both anoxia and apnea. From a control value of 80/56 mm Hg (mean measured by planimetric integration of the pressure pulse tracing — 70 mm Hg), the arterial pressure rose to 89/62 (mean 79) mm Hg during anoxia, and to 107/73 (mean 86) mm Hg during apnea.

DISCUSSION

The so-called "diving reflex" induced by apnea in seals and other aquatic mammals is presumed to serve as a means of enhancing resistance to protracted oxygen deficiency. In this view, the reduction in cardiac activity and the redistribution of blood flow to maintain oxygen supply to the heart and brain at the expense of more resistant tissues are primarily responses to apnea (probably mediated through neural pathways) which are antecedent to the development of anoxemia. Bradycardia undoubtedly develops almost immediately after breathing stops and is dependent upon vagal activity since it can be blocked by atropine (Irving, '39). However, renal vasoconstriction is not affected by atropine (Bradley and Bing, '42) and the results of the experiments reported here strongly suggest that anoxemia *per se* gives rise to the renal functional alterations during diving.

The changes in urine formation induced by apnea and anoxia are identical. With both, diminished output of sodium, potassium, and water are attributable chiefly to decreased glomerular filtration. Although sodium reabsorption by the tubules appears to increase relative to filtration, water reabsorption decreases significantly suggesting that the renal tubular mechanisms of water reabsorption may be more sensitive to oxygen lack. The tubular secretion of PAH also seems to be impaired by anoxemia. The potassium output remains relatively unchanged. Similar alterations occurred during apnea in the seal during these and earlier studies (Bradley, Mudge and Blake, 54).

Anoxia does not produce changes like these in dog or man (Smith, '51). Instead, increased urine flow and augmented excretion of electrolytes have been described. This difference is attributable perhaps to the absence of an intense intra-renal vasoconstriction like that usually observed in the seal. Such a vasoconstrictive response affects urine formation not only by reducing glomerular filtration but also by intensifying renal anoxia as a consequence of the fall in renal blood flow.

Whether vasoconstriction is directly attributable to anoxemia or to its secondary effects remains obscure. The abnormalities observed in cardiac function suggest that activation of the autonomic nervous system, of humoral defense mechanisms, or both may play an important role. Striking irregularities of rhythm ranging from ventricular premature contractions to auricular fibrillation and flutter (fig. 2) may develop. Similar arrhythmias may occur during infusion of epinephrine in dogs and man (Meek, '41). Moreover, severe anoxemia produces vagal inhibition of the heart in dogs (Greene and Gilbert, '22). Although bradycardia was not regularly caused by anoxia in these experiments, the close association between the pulse rate and respiratory movements may indicate a vagal influence. Apnea differs notably in this regard by its failure to evoke any change in rhythm other than reflex sinus bradycardia. This phenomenon may mean that the reflex change exerts a protective action or suppresses the secondary effects of anoxia, at least with respect to their influence upon the heart. It seems likely, however, that the renal vasoconstriction (and possibly vasoconstriction elsewhere in the body) during apnea is a result of anoxemia.

On the basis of the findings of this study a tentative outline of the sequence of events during diving or forced apnea may be set out as follows: The cessation of respiration appears to elicit changes in cardiac activity by reflex action that probably reduce the work and oxygen consumption of the heart and that may increase myocardial resistance to anoxemia. Independently the development of anoxemia evokes a widespread vasoconstrictive activity in which the renal circulation participates. In part as a result of intrarenal vasoconstriction, in part as a result of the direct action of oxygen lack, and possibly in part as a result of the extra-renal secondary effects of anoxemia (autonomic discharge, release of humoral agents), water and electrolyte excretion are greatly reduced. Further work is necessary to define more clearly (1) the role of reflex neurogenic control of the peripheral circulation, (2) the contribution of neuro-humeral influences upon the kidney and the cardiovas-

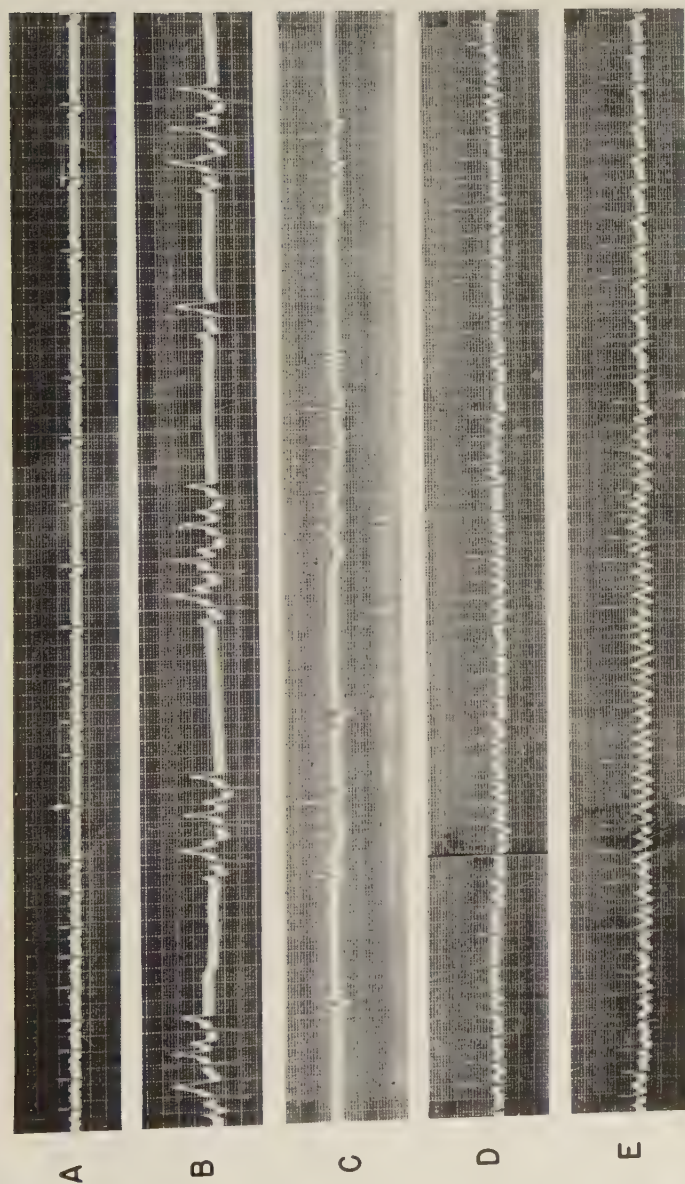


Fig. 2 Electrocardiograms recorded in the seal during apnea and anoxic anoxia.

A. Bradycardia during apnea.

B. Bradycardia developing after 10 minutes of anoxic anoxia, with multifocal premature contractions during inspiration.

C, D, E. Development of auricular fibrillation during anoxia and conversion to auricular flutter and sinus rhythm after termination of anoxia.

cular system, and (3) the changes in renal tubular function during apnea and anoxemia.

SUMMARY

Renal function in the harbor seal has been studied during the asphyxia of apnea, and during anoxic anoxia produced by inhalation of 10% oxygen in nitrogen. Both apnea and anoxia resulted in a diminution of glomerular filtration rate and renal plasma flow. The urine volume decreased, and the total output of sodium and potassium diminished. The urinary concentration of sodium tended to fall, whereas the urinary concentration of potassium usually remained unchanged. The tubular reabsorption of water decreased relative to filtration. The influence of vagal activity, respiratory movements, and cardiac rate and rhythm on renal function could be excluded. The conclusion was reached that in these experiments apnea and anoxia have comparable effects on renal function in the seal.

ACKNOWLEDGMENT

We should like to express our thanks to Miss Lottie Fogel and Miss Joan Hunt for valuable technical assistance.

LITERATURE CITED

- BONSNES, R. W., AND H. H. TAUSSKY 1945 On the colorimetric determination of creatinine by the Jaffe reaction. *J. Biol. Chem.*, 158: 581-591.
- BRADLEY, S. E., AND R. J. BING 1942 Renal function in the harbor seal (*Phoca vitulina*, L.) during asphyxial ischemia and pyrogenic hyperemia. *J. Cell. and Comp. Physiol.*, 19: 229-237.
- BRADLEY, S. E., G. H. MUDGE AND W. D. BLAKE 1954 The renal excretion of sodium, potassium, and water by the harbor seal (*Phoca vitulina*, L.): effect of apnea; sodium, potassium, and water loading; pitressin; and mercurial diuresis. *J. Cell. and Comp. Physiol.*, 43: 1-22.
- FUJITA, A., AND D. IWATAKE 1931 Bestimmung des echten Blutzuckers ohne Hefe. *Biochem. Z.*, 242: 43-60.
- GOLDRING, W., AND H. CHASIS 1944 Hypertension and Hypertensive Disease. The Commonwealth Fund.
- GREENE, C. W., AND N. C. GILBERT 1922 Studies on the responses of the circulation to low oxygen tension. VI. The cause of the changes observed in the heart during extreme anoxemia. *Am. J. Physiol.*, 60: 155-192.

- HIATT, E. P., AND R. B. HIATT 1942 The effect of food on the glomerular filtration rate and renal blood flow in the harbor seal (*Phoca vitulina*, L.). *J. Cell. and Comp. Physiol.*, 19: 221-227.
- IRVING, L. 1939 Respiration in diving mammals. *Physiol. Rev.*, 19: 112-133.
- IRVING, L., P. F. SCHOLANDER AND S. W. GRINNELL 1941 Significance of the heart rate to the diving ability of seals. *J. Cell. and Comp. Physiol.*, 18: 283-297.
- 1942 The regulation of arterial blood pressure in the seal during diving. *Am. J. Physiol.*, 135: 557-566.
- MEEK, W. J. 1941 Cardiac automaticity and response to blood pressure raising agents during inhalation anesthesia. *Physiol. Rev.*, 21: 324-356.
- SMITH, H. W. 1951 *The Kidney: Structure and Function in Health and Disease.* Oxford University Press.

ELECTROPHYSIOLOGICAL STUDIES OF ARTHROPOD CHEMORECEPTION

I. GENERAL PROPERTIES OF THE LABELLAR CHEMORECEPTORS OF DIPTERA

EDWARD S. HODGSON¹ AND KENNETH D. ROEDER
Barnard College and Columbia University, and Tufts University

SIX FIGURES

Chemoreception has long been recognized as a major sensory mechanism in the feeding, reproductive, and orientation activities of many animals. In most invertebrate animals the sensory endings of taste and olfaction are distributed, often quite widely, over the body surface. This experimental accessibility makes invertebrates especially suitable for experimentation on the physiology of chemoreception, particularly when, as in insects, the sensory surface lacks an aqueous or mucus coating and the responses to chemical stimulation are stereotyped, highly specific, and sensitive. Thus, more information on chemoreception is available for insects than for any other group of animals (Dethier and Chadwick, '48; Dethier, '53).

The chief difficulty encountered in all studies of chemoreception has been the lack of any means of directly measuring the activity of the primary sense cells. Criteria for the sensory effectiveness of chemical stimuli have generally been behavioral responses such as orientation of the whole organism, or movements of the mouthparts. However, even when these responses are highly stereotyped they do not necessarily provide a measure of the actual threshold of the primary sense

¹ Public Health Service Postdoctoral Research Fellow of National Institute of Neurological Diseases and Blindness.

cells, and can give little information regarding the coding of a chemical stimulus in terms of afferent nerve activity.

A number of attempts have been made to record the electrical activity in afferent nerve fibers from chemosensory cells. Barber ('51) has reported action potentials in the gnathobase nerves of *Limulus*, correlated with stimulation of the gnathobase spines by clam homogenates, temperature changes, or mechanical stimuli. Chapman and Craig ('53) were unable to detect any electrical potentials in nerve trunks connected to the legs and antennae of a variety of insects, following application of chemicals to those parts. They concluded that the electrophysiological techniques available at that time were incapable of recording activity in nerve fibers as small as those apparently concerned with chemoreception in insects. Roys ('54) noted an increase in the electrical activity recorded from nerves in appendages of the cockroach, following exposure of these parts to xylene, toluene, and benzene vapors. However, the same effect was observed upon exposure of isolated portions of the central nervous system to the same stimuli, so that the effect cannot be attributed to a specialized chemosensory mechanism, but rather illustrates the general irritability of nervous tissue when treated with many chemicals. In some work on vertebrates (Pumphrey, '35; von Euler, Liljestrand and Zotterman, '39; Pfaffmann, '41; Beidler, '53) it has been possible to record discharges in afferent fibers associated with the presumed receptor cells. However, these studies still leave in some doubt the nature of the response of the primary receptor surface to specific chemical stimuli.

Recent detailed histological studies of single chemosensory structures of insects suggested that it might be possible to apply electrophysiological methods to the study of single primary chemosensory neurons and achieve a much more precise analysis of unit chemoreceptor activity than has heretofore been possible. Grabowski and Dethier ('54) found that processes from two neurons extend to the tip of each sensory hair on the tarsus of the blowfly. Only the tips of the sensilla

were found to be sensitive to chemical stimulation. The localization of the receptor surface at the tip of the sensory hairs of insects is further supported by the fact that aqueous solutions of dyes penetrate only at the tips of sensilla basiconica on the antennae of the grasshopper (Slifer, '54).

While many of these sensory structures of insects are situated so that study of individual sensilla would be difficult, this is not true of many of the sensilla on the mouthparts of flies. Dethier ('55) has found that most of the hairs tested on the labellum of *Phormia* function as chemoreceptors, being sensitive to chemicals at their tips only. Silver staining of the sectioned hairs shows that two neurons have processes extending to a small localized sensory area at the tip of the hair (fig. 1). A third neuron near the base of the hair has no visible process extending within the hair. The relatively wide spacing of these hairs on the labellum suggested that electrodes might be positioned so that the electrical activity of the two neurons supplying a single receptor area on the tip of each hair could be recorded without other electrical potentials interfering. The object of the present paper is to report the successful results of this approach, which has been used to determine some of the general properties of chemosensory neurons of interest in understanding the basic physiology of chemoreception, and also the reactions of insects to chemical stimuli.

MATERIALS AND METHODS

The blowfly, *Phormia regina* Meigen, and the fleshfly, *Sarcophaga bullata* Parker, were used as the principal experimental animals. The former species has been extensively used in behavioral studies (Dethier, 53), and the histology of the labellar chemoreceptors, as described above, is known in detail (Dethier, '55). Most of the experiments were performed on both these species, which were reared in laboratory cultures. The responses of the chemoreceptors of both species were found to be essentially the same. Brief tests with other species are described later.

Preparations were set up as follows: a lightly-anesthetized fly was decapitated and its head crushed with forceps. This rendered the head electrically "silent," and the internal pressure resulting from the crushing process produced extension of the proboscis from the rest of the head. The crushed head and extended proboscis were fastened to a wax block with wire staples, and the preparation then positioned under a dissection microscope.

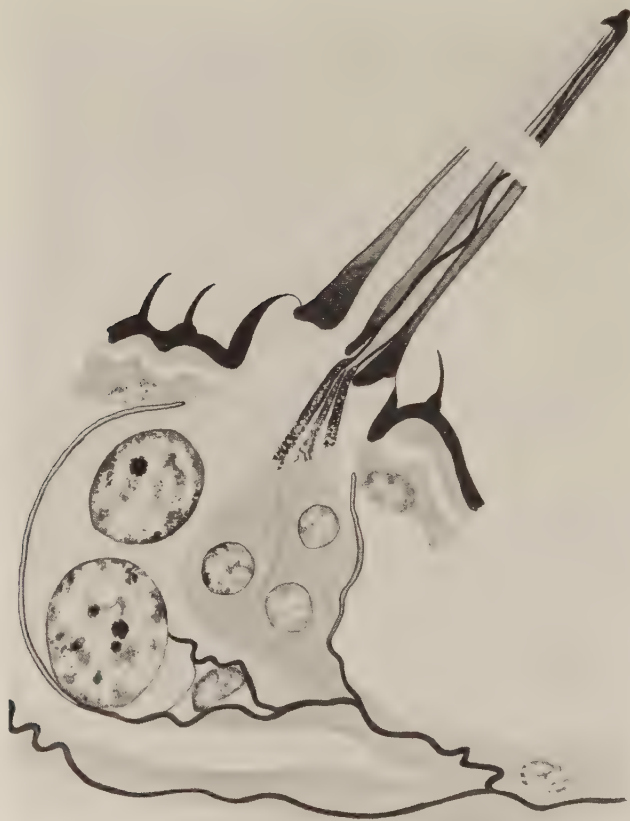


Fig. 1 Diagram showing histology of labellar hair and associated cells in *Phormia* (courtesy of V. G. Dethier). The large trichogen and tormogen cells are at left, and three neurons with silver-stained processes at right. Chemosensory area is confined to silver-stained tip of hair. The middle neuron, of the group of three, does not have any visible process extending to the chemosensory area.

The active electrode was designed to register potential differences between the sensory surface at the tip of a single hair and the crushed tissue of the head, as well as to serve as the vehicle for the chemical stimulus. It consisted of a piece of 1 mm (O.D.) glass tubing, 15 mm long and drawn out at one end to a diameter (approximately 0.1 mm) convenient to fit over the extreme tip of a single sensillum. Electrical contact with the sensory area was accomplished by means of a solution within the glass tube containing sodium chloride and the chemical under test. A Ag-AgCl wire dipped into this solution at the untapered end of the electrode. The assembled electrode was pushed through a small cork impaled on the rod of a semi-micro manipulator, an arrangement which permitted rapid and easy interchange of electrodes. The indifferent electrode consisted of a Ag-AgCl wire inserted into the crushed head of the fly.

The silver wires were connected to a push-pull cathode follower and r-c coupled Grass P-4 amplifier, followed by a cathode-ray oscilloscope. Activity was monitored from a loud speaker. In some cases potential changes were photographed direct from the oscilloscope by means of a Grass camera, although in most cases it was more convenient to record each experiment complete on a Magnacord PT6-J tape recorder at 7.5 inches per second. Tapes were subsequently replayed into the oscilloscope for inspection or photographic recording. A comparison of photographic records taken before and after the same spike sequence had been recorded on tape (fig. 2, C and D) shows that the fast spikes characteristic of chemical stimulation suffered only minor distortion, although slower electrical changes underwent both diminution and phase-shift during the taping process. A microphone was used to cue experimental conditions and other data on the same tape. Spike counts were made by visual inspection from long sections of photographic record.

An observation was begun by lowering the electrode so that the sensory area at the tip of a single hair made contact with the surface film of the solution in the electrode tip. This

completed the input circuit through the hair, and applied the test chemical at the same instant. This instant was signalled by a large and troublesome artifact (see below), followed by a succession of spike potentials when the electrode solution contained a stimulating substance. The small size of the sensory area (no more than $1.5\ \mu$ diameter; Dethier, '55) was

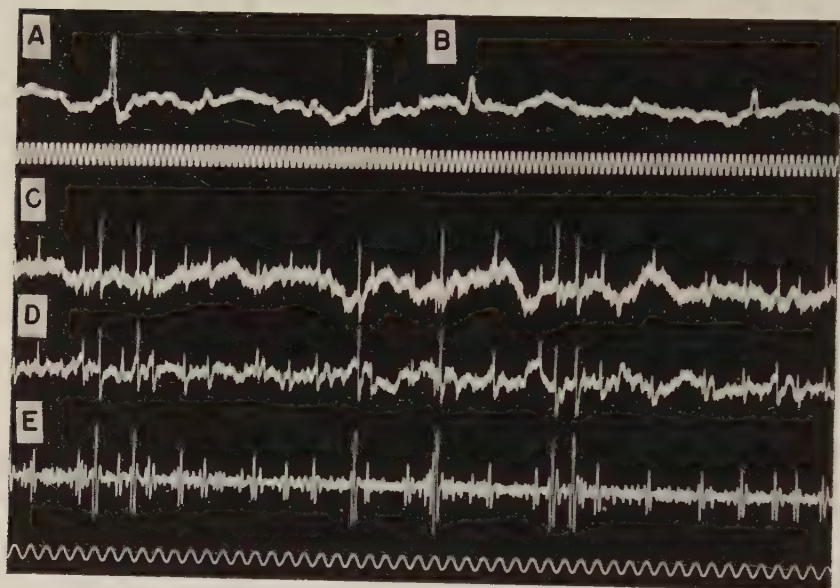


Fig. 2 Effects of recording methods on form of chemoreceptor potentials. (A) Unfiltered *L* spikes, photographed directly from oscilloscope. (B) Unfiltered *S* spikes, same hair as (A), photographed directly from oscilloscope. (C) Unfiltered record showing *L* and *S* spikes photographed directly from oscilloscope. (D) Same as (C) except taken from tape recorder replay. (E) Same as (D) except filtered to pass frequencies between 600 and 1,000 cycles/second. Time signals: (A) and (B), millisecond oscillations; (C) — (E), 10 msec oscillations.

responsible for high resistance in the electrical path through the sensillum. This necessitated some electrolyte in the electrode solution, and it was not possible to test the response with distilled water in the electrode.

The complex artifact produced when the "open-circuit" condition of the cathode follower was terminated by bringing the electrode into contact with the tip of the hair, was fre-

quently sufficient to block the pre-amplifier for 0.1 second. Since that portion of the receptor activity which brings about the response of the animal was believed to take place within 0.1 second after the stimulus was applied, various methods were used to reduce amplifier block during this important interval. In a few favorable cases, it was possible to eliminate the cathode follower. This reduced block due to the artifact but usually decreased the signal-to-noise ratio to an unacceptable level. Capacitance of 5-micro-microfarads in series with the active electrode reduced the artifact sufficiently to prevent amplifier block in most cases. Drift of the input grids could also be controlled by shorting the cathode follower input until the instant of electrode contact.

Even with the artifact reduced to the point where the amplifier did not block, troublesome baseline fluctuation immediately following the artifact made recording and counting of spike potentials difficult during the first few milliseconds of the response. In order to meet this difficulty the amplified spike potentials were passed through a Krohn-Hite ultra low frequency variable band-pass filter, adjusted to pass frequencies between 600 and 1,000 cycles per second. Narrow filtering of this type caused considerable distortion of the spike potentials (fig. 2, C and E), but the spikes could readily be distinguished and counted. The tape recorder made it possible to examine the unfiltered and filtered versions of the same impulse sequence, so that it was felt that narrow filtering introduced no serious errors into the observations.

Since the technique is being reported in detail here for the first time, it seems appropriate to note some of its advantages and limitations. Among the advantages are the fact that it makes possible the easy study of the responses of the actual chemosensory cells to stimuli within the normal physiological range, and does so without injury to the receptor cells. Most preparations will give completely normal and reproducible responses for 30 to 60 minutes after originally set up. Compared with the technically difficult micro-electrode methods which the authors previously reported (Hodgson and Roeder,

'54), this method is far superior and has replaced the former method entirely. Among the disadvantages of the method are the necessity to have a conducting solution in the stimulating electrode, and the presence of a solution in contact with the receptor surface during all observations. The former difficulty can be largely overcome by using merely a trace of electrolyte in the electrode during tests of chemicals which are non-electrolytes, but it precludes the possibility of studying pure hygroreception. The necessity for a fluid contact with the receptor surface would produce a physiologically abnormal condition if this method were used to study some kinds of olfactory receptors. However, this difficulty could be avoided by use of animals having olfactory receptors which are normally immersed, such as aquatic water beetles (Hodgson, '53), and experiments on a variety of marine and freshwater arthropods are underway.

RESULTS

The two fiber response from a single sensillum

Since this is believed to be the first instance in which it has been possible to study the unit activity of primary chemoreceptor neurons, most of the experiments reported here were designed to demonstrate some of the basic characteristics of the receptor activity.

Two types of spike potentials were obtained (fig. 2, A and B). From any one hair on the labellum, relatively large spike potentials (record A) are obtained when the stimulating electrode contains 0.03 to 1.0 molar sodium chloride. When the electrode contains a sucrose solution with only a trace of electrolyte, smaller spikes (record B) predominate. Both of these spikes are monophasic and represent an increase in negativity at the tip of the chemosensory hair, with respect to the indifferent electrode in the head of the fly. The large spikes will be here designated the *L* spikes; they range in size from 150 μ V to 0.5 mV. The small spikes, designated the *S* spikes, are about one-half the voltage of the *L* spikes. The

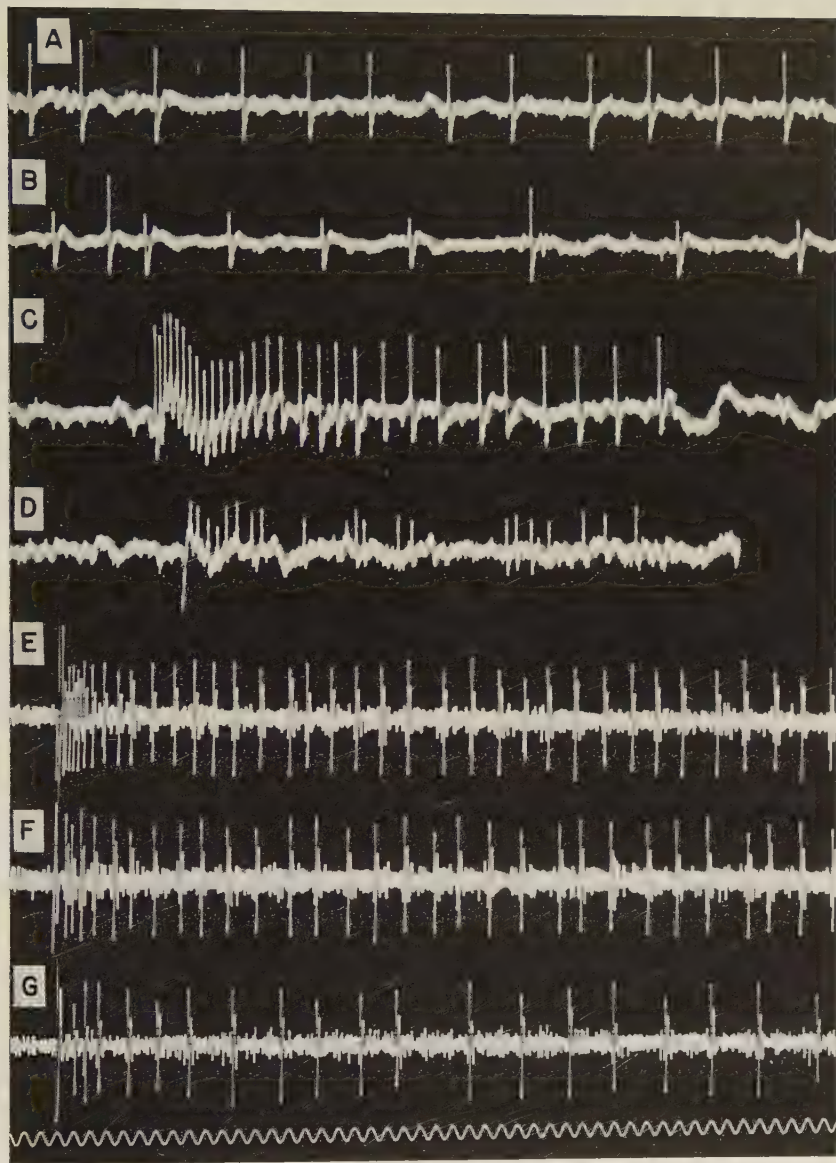


Fig. 3 (A) Portion of response to 0.5 molar NaCl. (B) Portion of response to 0.25 molar sucrose mixed in 0.1 molar NaCl; same hair as (A). (C) Response of *L* fiber to mechanical stimulation. (D) Response of *S* fiber to mechanical stimulation; same hair as (C). (E) Initial response to 0.5 molar NaCl. (F) Initial response to 0.25 molar NaCl. (G) Initial response to 0.1 molar NaCl. (E) (F) and (G) recorded from same hair; large stimulus artifact at left marks instant of stimulus application in each. Time base all records, 10 msec oscillations.

major parts of both *L* and *S* spikes have a duration of about 1 msec, but in most cases this portion of the spike is clearly preceded by a slower increase in negativity resembling a prepotential. Because of the size of the spike, the slowly rising phase is most easily observed in an *L* spike (fig. 2, A). Although absolute spike height varied somewhat with different electrolyte concentrations in the electrode, when both *L* and *S* spikes were obtained from the same hair, as was usually the case, they preserved their relative heights without intergradation. There seems to be no doubt that each represents the response of a separate neural unit.

Longer records of activity from one chemosensory hair are shown in records A and B of figure 3. Record A is part of a response to 0.5 molar NaCl, while B is part of a response recorded from the same hair after application of a mixture of 0.25 molar sucrose and 0.1 molar NaCl. In record B, the *S* spikes predominate, only two *L* spikes occurring in this sequence. It seems certain that the *L* and *S* spikes must represent impulses arising in the two neurons which have been shown (Dethier, '55) to send processes to the receptor area at the tip of each labellar hair. In this paper, the *L* and *S* designation will be applied not only to both the "large" and "small" spikes, but also to the two neurons from which the spikes originate. Reference to *L* and *S* fibers is not meant to imply that the two neurons themselves are different in size, for they are not (Dethier, '55), but is merely a convenient way of avoiding duplication of terms when referring to the receptor neurons rather than the spike potentials associated with their activity.

If the tip of a labellar hair is cut off, no response to chemical stimulation can thereafter be obtained. However, mechanical movement of the hair, within one to three minutes after the tip has been removed, can often still evoke typical *L* and *S* spikes (see below). This must mean that the neurons do not immediately die if their distal processes are severed, although that part of the neuron which controls the initiation of responses to chemicals is localized near the tip of the labellar

hair. This correlates well with the results of behavioral studies (Dethier, '55), and indicates that the processes of chemical stimulation being studied depend upon the operation of specialized receptor mechanisms, and are definitely not simply the result of less specific effects of the chemicals upon nerve tissue.

Of the more than 80 preparations studied in this manner (usually a number of chemosensory hairs in each preparation), five records have shown evidence of a third spike potential. The third spike has been barely above the amplifier noise level, and occurs infrequently in all the records in which it can be recognized. The frequency of the third spike has never been observed to change during chemical or mechanical stimulation of the labellar hair. It is possible, but by no means certain, that this spike originated in the third neuron which is associated with each labellar hair, but which does not have a process connected to the chemosensory area on the tip of the hair. The functional significance of the third neuron associated with each hair therefore remains unknown.

Responses to mechanical stimulation

Proboscis extension, part of the normal feeding behavior of the flies, can sometimes be obtained by mechanical stimulation of the labellar hairs. The responses of the *L* and *S* fibers to movement of a labellar hair were studied by moving the electrode after the hair had been inserted into it. The results were analyzed in detail in 12 preparations manipulated in this way.

The frequency of both *L* and *S* spikes can be affected by mechanical movement of the labellar hair, although in 28 cases photographed only 7 showed responses of the *L* spike to mechanical movement. Responses of the *S* fiber to movement of the hair are relatively easy to obtain. There appeared to be no differential effect upon the two neurons when a hair was bent in different directions, but the *L* fibers seemed to respond only to larger displacements of the hair. Record C

of figure 3 shows a typical *L* fiber response to bending. Record D of figure 3 shows an *S* fiber response to bending the same hair. Comparison of these two records shows another characteristic of the two sensory neurons which may be symptomatic of an important physiological difference between them. Although the duration of firing after bending of the hair is approximately the same for both neurons, the *L* fiber shows a much more regular pattern of response, and a much more even pattern of adaptation. The irregular grouping of the *S* fiber response seems to be characteristic of the activity of this neuron, for the same thing can be observed in comparing the responses of the two neurons to chemical stimulation. This difference undoubtedly contributes to the greater variability of *S* fiber responses during repeated tests with the same stimulus (see fig. 5), and it is not unlike the irregularities observed in the firing of neurons which innervate taste receptors in vertebrates (Pumphrey, '35; Pfaffmann, '41).

It is difficult to estimate the extent to which responses to mechanical stimulation of the labellar hairs may enter into the normal feeding behavior of the flies. However, control of mechanical movement of the electrode by the manipulator used made it possible to determine how far the end of a labellar hair would have to be bent in order to produce a mechanical response in the neurons. With the outer fringe of hairs, each of which measures about 300 μ in length, no mechanical responses of either the *L* or *S* fibers were detected following any displacement of less than 100 μ at the hair tip. Two cases of *S* fiber response were observed during bending of the hair by that amount. Observations of feeding behavior of flies indicate that this amount of displacement of the tip of the labellar hair may be fairly frequent when the labellum is thrust into cracks and depressions in certain food materials. Consequently, it seems possible that mechanical stimulation of the *S* fibers may play some role in the normal feeding behavior. *L* fiber responses were observed only after approximately twice this amount of bending of the hair, so whether

the *L* fiber response to mechanical stimulation is of any behavioral significance in normal conditions might be doubted. When testing the effects of chemicals, it was necessary to move the fluid filled electrode directly down over a labellar hair, using a movement in line with the slope of the hair, in order to avoid any purely mechanical stimulation of either the *L* or *S* fibers. When this precaution was taken, it was not difficult to avoid mechanical responses mixed in with the chemical responses of the two neurons.

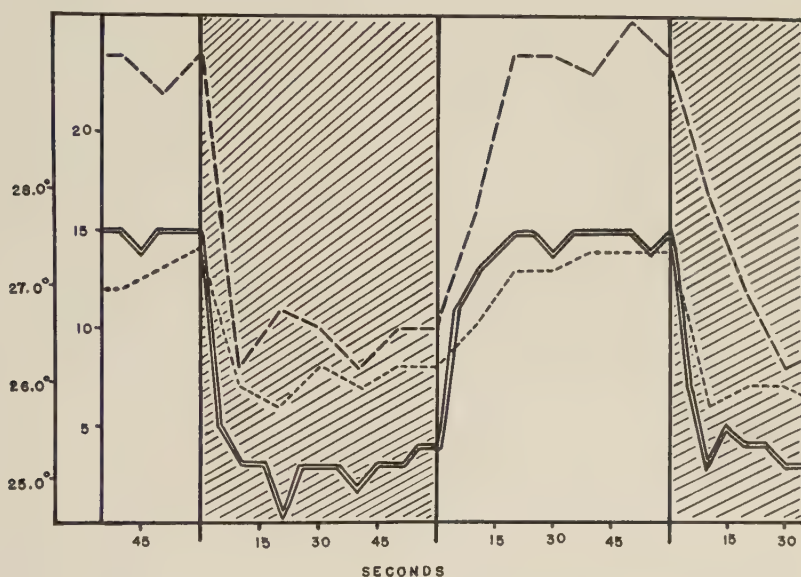


Fig. 4 Effect of temperature on response frequency of two *L* fibers. Double line, temperature; broken lines, frequency of firing recorded from two hairs on same preparation, during constant stimulation with 0.5 molar NaCl. Ordinate scales (left) temperature (C), and (right) number of nerve impulses/second. Shaded areas, microscope light off; unshaded areas, light on.

Temperature effects

The preparation was found to be quite sensitive to temperature changes. Typical data are presented in figure 4. Temperature was varied by switching the microscope light on and off, and the actual temperature just under the surface

of the labellum was measured with a thermistor inserted into the tissue. When the light was switched off (shaded area in fig. 4), the temperature dropped within 15 seconds to a relatively stable low level. When the light was turned on, the temperature rose within 15 seconds to a relatively steady high level. The broken lines in figure 4 show the number of impulses during one second intervals in *L* fibers continuously stimulated by 0.5 molar NaCl. Although the level of activity of the two *L* fibers was quite different, it is clear that their discharge frequency changed significantly with the temperature change. The temperature effect has been studied in 8 preparations. In one preparation, the frequency of *L* spikes decreased significantly when the labellum was cooled by as little as 0.1°C. In two preparations, fibers which appeared to be completely inactive could be stimulated to a low frequency discharge with temperature increases of less than 1.0°C. Failure of the *S* fiber to maintain a steady adapted level of discharge precluded any clear-cut conclusion concerning the *S* fiber response to temperature changes. Since the temperature obviously could be an important variable, all of the experiments were performed on preparations which had been warmed to $27.5^{\circ} \pm 0.2^{\circ}\text{C}$. for at least one minute before administration of any stimulus.

Adaptation and disadaptation

When the response of the *L* fiber is measured during application of a constant chemical stimulus, considerable adaptation occurs during the first second, followed by a less rapid decline in activity for the next few seconds (fig. 2, E, F, G). Subsequently, the discharge frequency remains steady or declines very slowly. In some preparations exposed to constant stimulation the ultimate frequency, reached after early adaptation, has remained constant for as long as one hour. Adaptation curves for *L* and *S* spikes are shown in figure 5, where the solid circles represent the average values obtained with 6 repetitions of an experiment in which 0.5 molar NaCl was

applied to the tip of the same labellar hair. The variation is plotted as twice the standard error of the mean. The differences in activity during the first three seconds are statistically significant, while the subsequent variations are not. With the *S* fiber (open circles) in any one test the data tend to follow the same pattern, although at a much lower frequency and with considerable grouping of spikes. The data

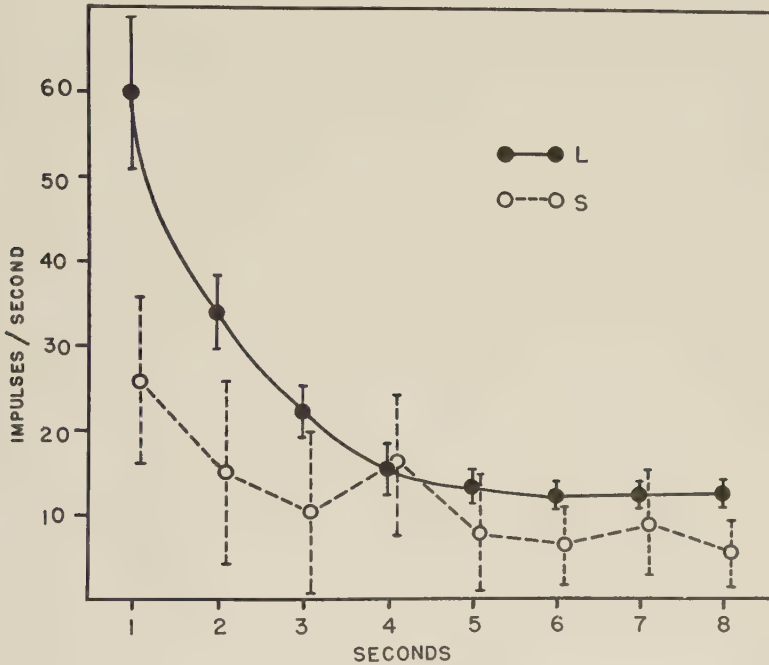


Fig. 5 Adaptation in *L* and *S* fibers during first 8 seconds after stimulus applied. Variations are 2X standard errors of means.

for *S* fibers, shown in figure 5, are based on 6 repetitions of an experiment in which 0.5 molar sucrose was applied to the tip of the same hair from which the *L* fiber data were obtained. The considerable variations (again shown as twice the standard errors of the means) are largely due to grouping of the *S* fiber spikes. The *S* fiber tends to cease firing altogether after one or two minutes. These facts made the *S* fiber gen-

erally the more difficult of the two fibers to study experimentally, and these differences may be symptomatic of a basic difference in the physiology of the two chemosensory neurons.

In planning experiments, it was necessary to know also the conditions under which the fully adapted receptor is restored to a condition in which it will respond to a subsequent stimulus at the initial frequency of discharge. The situation was complicated by the fact that the technique precluded information on the completely unstimulated (no fluid on the sensory area) sensillum. Roeder ('55) has termed the process signalled by increasing sensitivity following withdrawal of a constant stimulus "disadaptation," and the term will be used here in that sense.

The first attempts to measure the time course of disadaptation in *L* and *S* fibers were made by rinsing the tips of the labellar hairs with distilled water after each test. The results were surprising, and varied enormously with different flies. In 8 of 16 preparations studied in this connection, all activity of both *L* and *S* fibers ceased after a distilled water rinse, and responses could not be detected in any salt concentration until five minutes after the rinse. In these cases, the response did not reach the initial frequency until 25–40 minutes after the rinse. In the other 8 preparations to which a distilled water rinse was applied, the results ranged from no effects to varying degrees of reduction of receptor activity. Some additional evidence suggested that the large differences from preparation to preparation might result from differences in the general nutritional state of the flies, and a separate study is planned on this problem. However, to minimize any discrepancies which might be introduced from nutritional differences in the flies, all the preparations were made from flies removed from rearing cages containing abundant food and water.

It was found that in order to restore the *L* receptor activity to its initial level no rinse was needed following application of salt to a chemosensory hair, providing only that an interval of four minutes or more was allowed to elapse between with-

drawal of the stimulus and its application in the next test. With shorter rest intervals, the initial frequency of receptor firing varied between the low, fully adapted frequency and the initial frequency, depending upon the duration of the rest interval. The *S* fibers gave their most reproducible responses during the first few seconds after application of a stimulus if the sugar solution was rinsed off with Hoyle's insect Ringer solution and the next test applied four minutes later. The *S* fiber response appeared to be completely disadapted by such treatment, although it is characteristically more variable than the *L* fiber response during the first few seconds, as has been noted above. All of the experiments reported in this paper were carried out with this treatment of the hairs between tests.

*Relationship between stimulus strength and
frequency of chemoreceptor firing*

The initial discharge frequency of both the *L* and *S* fibers can be correlated with the concentrations of the stimulating chemicals. Typical data are shown in figure 6, where the response of an *L* fiber to NaCl and the response of the *S* fiber (of the same hair) to sucrose are plotted. The number of impulses was counted during the first second after the stimulus was applied, because the principal differences with varying concentrations appear during that time. This can be seen in the photographs of actual experimental records, of which records E, F, and G of figure 3 are typical. Stimulus concentrations higher than those shown in figure 5 do not produce any further increase in the frequency of receptor discharge, so the higher frequencies shown actually represent maximal or "saturation" frequencies of the receptor responses. There is considerable variation in the general level of activity of receptors in different preparations, and between different hairs of the same preparation, but the shapes of the concentration/frequency curves are generally similar to those illustrated in figure 6.

One additional finding will be mentioned because of its possible bearing upon the behavioral significance of the 2-fiber chemoreceptor system. In records of two hairs, out of a group of 12 hairs studied with a wide range of sodium chloride concentration, it was found that at concentrations of 0.062 and 0.031 molar NaCl, the response occurred predominantly in

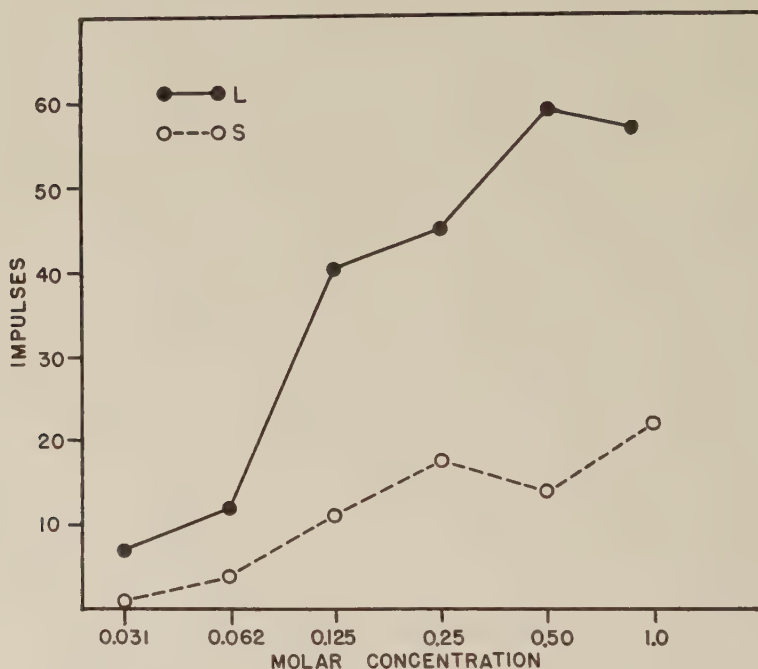


Fig. 6 Relationship between stimulus strength and frequency of receptor discharge. *L* fiber stimulated by NaCl, and *S* fiber of some hair stimulated by sucrose. Ordinate, number of impulses during first second after application of stimulus.

the *S* fibers, the *L* spikes appearing infrequently and then only in groups of two or three spikes. Higher concentrations of NaCl caused typical *L* fiber responses in these same hairs so that this result could not be attributed to a failing preparation. It is interesting to note that at about these low concentrations of NaCl solutions, an occasional fly, out of a large

group being tested behaviorally, will give a positive feeding response to a very weak salt solution, although higher salt concentrations are rejected in the usual manner (T. Smyth, personal communication). These observations would seem to lend some support to the idea that stimulation of the *S* fiber mediates an "acceptance" or feeding response, while stimulation of the *L* fiber mediates a "rejection" or avoidance reaction.

Tests with other chemicals

The hypothesis that the *L* and *S* fibers might mediate avoidance and feeding behavior, respectively, could be tested by using other chemicals to which the flies are known to give clear-cut behavioral responses. The following chemicals were tested as stimuli for the labellar chemoreceptors, using the molar concentrations indicated: KCl (0.50; 0.20); NaBr (0.50; 0.20); citric acid (0.20; 0.10); HCl (0.05; 0.01); l-propanol (1.0; 0.25); l-pentanol (0.05; 0.01); d-glucose (0.5; 0.10); d-arabinose (0.5; 0.10). Of these chemicals, only the two sugars stimulated the *S* fiber, and only the two sugars evoked the normal feeding reaction of the intact animal. All the salts, acids, and alcohols, at the concentrations tested, stimulated only the *L* fiber. The nature of the responses from both the *L* and *S* fibers appeared to be much the same as with stimulation by NaCl or sucrose, although there were considerable differences in the initial frequencies of response following stimulation. The highest concentrations of propanol and pentanol caused irreversible effects within a few seconds after application. In these cases the spikes showed marked grouping, and when 0.05 molar pentanol was applied, all receptor activity ceased six minutes later. These were the only instances of pathological effects which were observed. Each of the chemicals in the group was tested on four different hairs, located on four different preparations, and gave consistent results.

Tests with other species

To determine whether the results obtained with *Phormia* and *Sarcophaga* applied to other flies, two other species, *Musca domestica* and *Drosophila melanogaster*, were briefly tested. (The latter species was kindly supplied by Dr. Richard Miller of Harvard University.) Four preparations of each of these additional species were studied. The labellar hairs of *Musca* and *Drosophila* show *L* fiber responses when treated with NaCl, and a predominance of *S* fiber responses when treated with sucrose containing only a trace of NaCl. This was interpreted as evidence that the two fiber chemoreceptor system of the labellar hairs operates in essentially the same way in many Diptera. However, because of difficulties associated with the smaller size of the *Musca* and *Drosophila* preparations, the experiments on these forms were not carried further.

DISCUSSION

So far as the authors are aware, the present experiments are the first in which it has been possible to make a direct study of the activity of known single primary chemoreceptor neurons. Consequently, a comparison of these findings with those previously reported from other studies might be expected to show any characteristics originating in the junction between the presumed receptor cell and the neuron associated with it, the latter being the closest analytical approach to the actual receptor in previously reported studies.

By and large, the resemblances of these findings to the previous descriptions based on second order nerve activity or activity of nerves associated with the primary receptor outweigh the differences. The relationship between chemical stimulus concentration and spike frequency in the excited afferent fibers is essentially the same relationship as that found in studies of the sense of taste in mammals (Pfaffmann, '41; Beidler, '53). In both insects and mammals, there is a rapid increase in frequency of firing as the concentration of stimulant is raised above threshold. Above a certain concen-

tration of stimulant, however, there is no further increase in the frequency of receptor discharge. It is interesting to note that the stimulus concentration at saturation may be the same order of magnitude (about 0.5 molar NaCl, for example) both for insects and mammals.

As might be expected, the latent period between application of a stimulus and the initial response of the receptor is considerably shorter when the actual receptor cell is studied, as with the present methods, than when recordings are made some distance from the primary receptor. Pfaffmann ('41) has recorded responses within approximately 25 to 75 msec after stimuli were applied to taste receptors of the cat. Beidler ('53) states that the latency with 0.2 molar NaCl applied to taste receptors of the rat is of the order of 45 to 55 msec. The same concentration of NaCl applied to a labellar chemoreceptor of a fly commonly initiates receptor discharge with a latency of 5 to 10 msec. Therefore, the mechanism of activation of the receptor cell must occupy an even shorter time than it was previously necessary to take into account. The receptor adaptation curves reported for mammals are essentially the same as those found here. In each case, the frequency of receptor discharge declines rapidly during the first second and reaches a relatively steady level within a few seconds (Pfaffmann, '41; Beidler, '53). What part the relatively low base level of receptor discharge may play in the behavioral responses remains to be shown.

An interesting difference between the insect and mammalian chemoreceptor preparations lies in the effects of temperature. The magnitude of response of rat chemoreceptors to salt stimulation has been found to vary little with change in temperature, and this has been invoked as evidence that enzymatic reactions are not directly involved in the initial steps of taste receptor stimulation by sodium salts (Beidler, '54). It has been shown above that the frequency of impulses from insect chemoreceptors does vary markedly with temperature changes, while Frings and Cox ('54) have shown that temperature influences the thresholds of behavioral re-

sponses of flies to stimulation of tarsal chemoreceptors. It will be interesting to note whether further work bears out a fundamental difference in the processes operative during stimulation by salts in mammalian and insect chemoreceptors.

With regard to the implications of the data more strictly limited to insects, the outstanding features is the specialization of different neurons which respond either to sugars or non-sugars, and the close correlation of feeding or non-feeding responses with this dichotomy of afferent nerve impulses. The hypothesis that sugars stimulate chemoreceptors by processes different from those occurring during stimulation by other chemicals has already been suggested on the basis of behavioral studies on insect chemoreception (Dethier, '53). Such a physiological difference might provide an explanation for the stereotyped character of many feeding responses of insects. The two fiber, acceptance or avoidance, concept is supported also by the fact that it is at the concentrations where dilute NaCl solutions sometimes stimulate the *S* fiber that some flies will occasionally drink dilute NaCl solutions. In most field situations, with complex mixtures of chemicals contracting the chemoreceptors, the response, or lack of response, may depend upon a precise ratio of impulses from each of the two chemoreceptor neurons, as well as upon factors still unknown. The problem of correlating behavioral and receptor thresholds, and the neural mechanisms underlying the whole feeding reaction, cover such a wide scope that they have been intentionally avoided in experiments conducted to date. Additional experiments which are necessary prerequisites for such a study are now underway.

Since the frequency of afferent discharge from both *L* and *S* fibers can be influenced by temperature and by mechanical displacement of a labellar hair, information about several properties of the environment can be conveyed to the central nervous system through a single afferent fiber. It is possible that some temperature effects might be mediated through changes in the responses of insect sense receptors which are not sensitive exclusively to temperature changes. The re-

sponses of the *S* fiber to mechanical stimulation, which are more easily obtained than similar responses of the *L* fiber, presumably would reinforce the sensory input which produces feeding responses, and would be another example of an economy of nervous pathways for transmission of various types of information. These observations are consistent with the generally held idea that the smaller number of neurons in Arthropods, as compared to Vertebrates, is partially compensated by the greater variety of tasks which they may perform (Wiersma, '52).

An unexpected result during these experiments was the effect which distilled water rinses applied to the tips of the labellar hairs had upon the discharges of the chemoreceptor neurons, especially those cases in which all receptor discharge ceased for considerable periods after the rinse. Water rinses are commonly used in studying the gustatory receptors of vertebrates, and the afferent nerve activity is quickly restored to a low basal level following a rinse of the receptor area (e.g. Beidler, '53). The exact reason for the various degrees of block which result from similar treatment of insect chemoreceptors is not known, and in view of the fact that behavioral tests on flies are customarily made after they drink water to repletion (Dethier and Chadwick, '48) this is one of the problems which will have to be studied more extensively before attempts to correlate receptor and behavioral thresholds can be made on a sound basis.

Successful preliminary tests with other insects, diplopods, and crabs indicate that the technique used here can be applied to the study of chemoreception in many arthropods. Ability to study chemoreceptor activity apart from the reactions of whole animals offers a means of analyzing the mechanisms which underly many patterns of behavior that are of ecological significance (Hodgson, '55) as well as providing a tool for studying the fundamental physiology of this sensory system. High impedance input devices, designed to extend this method to new preparations and problems are now under construction.

ACKNOWLEDGMENTS

A preliminary note on this technique has been published elsewhere (Hodgson, Lettvin and Roeder, '55), and the present authors take pleasure in acknowledging the valuable suggestions of Dr. J. Y. Lettvin, of the Electronics Research Laboratory of Massachusetts Institute of Technology, which have continued to contribute greatly to this work. Dr. V. G. Dethier, of the Johns Hopkins University, has kindly made available to us unpublished findings on the histology of the labellar chemosensory hairs, and also made numerous helpful suggestions during the course of the experiments and preparation of the manuscript.

SUMMARY

Electrophysiological techniques were used to record impulses from labellar chemosensory neurons of various *Diptera*. The responses of the primary chemoreceptor cells to salts, sugars, acids, and alcohols were studied. The two neurons which innervate the chemoreceptor area on the tip of a labellar hair have different modes of sensitivity. The receptor neuron with the smaller voltage spike potentials (designated the *S* fiber) responds only to sugars, of the chemicals tested. The receptor neuron with the larger spike potentials (designated the *L* fiber) responds to salts, acids, and alcohols. Very low concentrations of NaCl sometimes stimulate the *S* fiber.

These findings are consistent with the hypothesis that the *S* fiber mediates responses which lead to ingestion of the stimulus, and the *L* fiber mediates responses which result in avoidance of the stimulus. It is postulated that this type of peripheral discrimination mechanism is partly responsible for the stereotyped nature of insect feeding reactions. The chemoreceptor neurons are sensitive to mechanical stimulation and to temperature changes as small as 0.1°C. This is believed to be the first time that the activity of a single primary chemoreceptor neuron has been directly studied. The results are compared with those obtained in studies of neurons supplying chemoreceptors in Vertebrates.

LITERATURE CITED

- BARBER, S. B. 1951 Contact chemoreception in *Limulus*. Anat. Rec., 111: 561. (Abstract.)
- BEIDLER, L. M. 1953 Properties of chemoreceptors of tongue of rat. J. Neurophysiol., 16: 595.
- 1954 A theory of taste stimulation. J. Gen. Physiol., 38: 133.
- CHAPMAN, J. A., AND R. CRAIG 1953 An electrophysiological approach to the study of chemical sensory reception in certain insects. Canadian Ent., 85: 182.
- DETHIER, V. G. 1953 Chemoreception. Chap. 21 in "Insect Physiology," ed. K. D. Roeder. New York, Wiley.
- 1955 The physiology and histology of the contact chemoreceptors of the blowfly. Quart. Rev. Biol., 30: 348.
- DETHIER, V. G., AND L. E. CHADWICK 1948 Chemoreception in insects. Physiol. Rev., 28: 220.
- EULER, U. S. VON, G. LILJESTRAND AND Y. ZOTTERMAN 1939 The excitation mechanism of the chemoreceptors of the carotid body. Skand. Arch. Physiol., 83: 132.
- FRINGS, H., AND B. L. COX 1954 The effects of temperature on the sucrose thresholds of the tarsal chemoreceptors of the flesh fly, *Sarcophaga bullata*. Biol. Bull., 107: 360.
- GRABOWSKI, C. T., AND V. G. DETHIER 1954 The structure of the tarsal chemoreceptors of the blowfly, *Phormia regina* Meigen. J. Morph., 94: 1.
- HODGSON, E. S. 1953 A study of chemoreception in aqueous and gas phases. Biol. Bull., 105: 115.
- 1955 Problems in invertebrate chemoreception. Quart. Rev. Biol., 30: 331.
- HODGSON, E. S., AND K. D. ROEDER 1954 Electrical response of insect chemosensory neurons to normal stimuli. Anat. Rec., 120: 718. (Abstract.)
- HODGSON, E. S., J. Y. LETTVIN AND K. D. ROEDER 1955 The physiology of a primary chemoreceptor unit. Science, 417.
- ROEDER, K. D. 1955 Spontaneous activity and behavior. Sci. Monthly, 80: 362.
- SLIFER, E. H. 1954 The permeability of the sensory pegs on the antenna of the grasshopper (Orthoptera, Acrididae). Biol. Bull., 106: 122.
- PFAFFMANN, C. 1941 Gustatory afferent impulses. J. Cell. and Comp. Physiol., 17: 243.
- PUMPHREY, R. J. 1935 Nerve impulses from the receptors in the mouth of the frog. J. Cell. and Comp. Physiol., 6: 457.
- ROYS, C. 1954 Olfactory nerve potentials a direct measure of chemoreception in insects. Ann. N. Y. Acad. Sci., 58: 250.
- WIERSMA, C. A. G. 1952 Neurons of arthropods. Cold Spring Harbor Symp., 17: 155.

SEVERAL FACTORS WHICH INFLUENCE THE RATE OF AVENA COLEOPTILE RESPIRATION¹

A. R. SCHRANK

Department of Zoology, University of Texas, Austin

THREE FIGURES

INTRODUCTION

Extensive variations in the rates of O₂ consumption by the *Avena* coleoptile have been reported in the literature. Bonner ('33), using Warburg flasks containing 89 to 120 sections 3.1 mm long, obtained a rate as low as 17 mm³ of O₂/100 mg of fresh weight/hour. Probably the highest rate was reported by Thimann and Commoner ('40), who used a single 3 mm coleoptile section in a microrespirometer. They observed a rate of about 60 mm³ O₂/100 mg/hour. Other investigators (Bonner, '36; duBuy, '40; Commoner and Thimann, '41; Berger, Smith and Avery, '46; Bonner, '49) have reported values between the above extremes. Numerous experimental variables apparently account for these deviant results. These variables include such things as the age of the coleoptile, method of growing, variety of seed, temperature at which measurements were made, pH of the medium, specific pretreatment of sections, number of sections per lot, measuring technique and possibly others. The present paper treats the effects of decapitation, geotropic stimulation and gamma irradiation of the seeds on *Avena* coleoptile respiration.

MATERIALS AND METHODS

Coleoptiles of *Avena sativa*, grown from seeds of the Victory Strain (U. S. Department of Agriculture, C. I. 2020),²

¹ Supported in part by the Atomic Energy Commission.

² Generously supplied by the U. S. Department of Agriculture.

were used. The method of growing the seedlings and the laboratory conditions were the same as previously described (Schrank, '44). The coleoptiles were pulled off the top of the primary leaf and then placed in the respirometer with the cut ends submerged in Shive's solution. They were left undisturbed for one hour before the measurements were started.

Exposure to the radioactive source was accomplished in the following manner. The selected seeds were allowed to reach constant weight at a relative humidity of 86%. Then

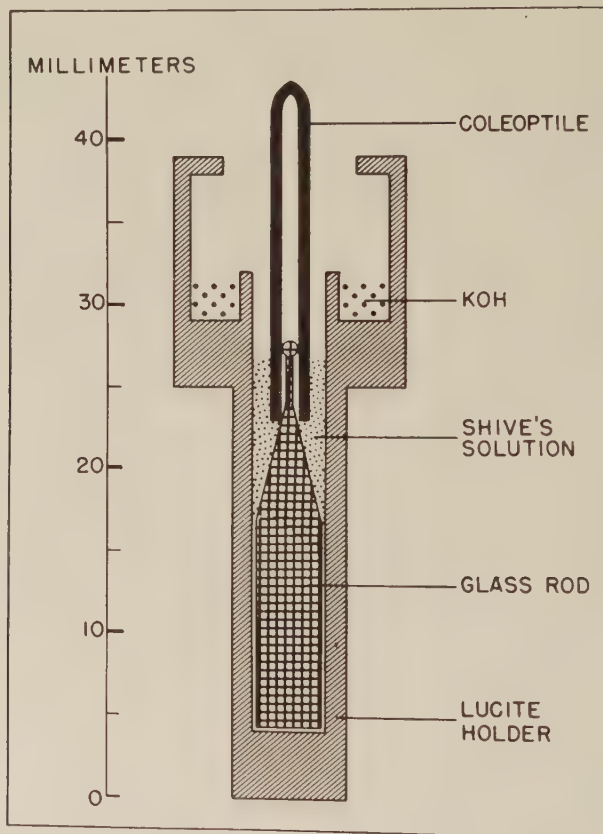


Fig. 1 A longitudinal section of the lucite respirometer insert showing the position of the coleoptile.

they were placed in a chamber 2 cm from 86.5 millicuries of Co^{60} , which delivered 288 r/hour at this distance. The gamma rays emitted were at 1.16 and 1.31 mev. After irradiation the seeds were stored at 86% relative humidity until they were used.

All respiration measurements were made at 22° C. (± 0.5) in aluminum microrespirometers constructed somewhat like the model designed by Stern and Kirk ('48). The CO_2 was absorbed by 10% KOH. Figure 1 shows a diagram of a longitudinal section of the lucite insert, which was designed to keep the coleoptile in the upright position. Each respirometer chamber had a volume of 1.4 cm³. A purified kerosene oil droplet was used as the indicator in the capillary with an inside diameter of 0.5 mm.

EXPERIMENTAL RESULTS

Endogenous respiration

Curve I in figure 2 shows the O_2 consumed by a coleoptile from a 20 mm plant. Since all the points fall very close to a straight line, the rate of respiration remained unchanged for at least two hours. This rate is maintained without organic substrates in the medium. In an average curve, representing the O_2 consumption of 10 coleoptiles, the points fall more nearly on a straight line. Coleoptiles of this length yield an average Q_{O_2} (mm³ of O_2 at STP/100 gm dry weight/hour) of 630 with a standard deviation of 54 which is within the range of previously reported values.

Factors affecting the respiration rate

Changing the coleoptile from the vertical to the horizontal position. Since the respirometers were designed so that they could rest on their backs, it was possible to observe the effect of changing the coleoptiles from the vertical to the horizontal position. Curve II in figure 2 represents typical results. When the coleoptiles were rotated to the horizontal position at the end of the first hour, an immediate increase in the

rate of O_2 consumption was observed in every experiment. The increased rate, of 28% shown by the curve, persisted for 20 minutes. After that the respiration almost always resumed the original rate. Similar effects were observed for once-decapitated coleoptiles. Controls indicated that the observed increase in the rate of oxygen utilization was not due to the manipulation of the respirometer. The fact that a net gain of O_2 consumed was evident at the end of the second hour shows that the increased rate could not be caused by merely altering the steady condition of the CO_2 absorption.

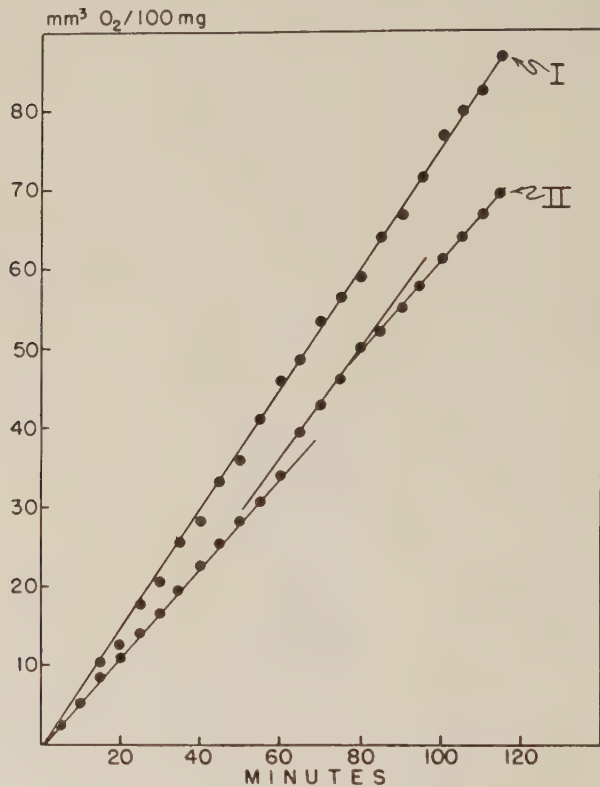


Fig. 2 Oxygen consumption of individual coleoptiles expressed on the basis of fresh weight. Curve I shows the rate for a coleoptile from a 20 mm plant. Curve II shows the rate for a coleoptile from a 30 mm plant which was changed from the vertical to the horizontal position at the end of the first hour.

Removal of the apical three millimeters. In these experiments the coleoptiles were decapitated, and then allowed to remain undisturbed in the respirometer for one hour before the measurements were started. The average rates of respiration are presented in table 1. Decapitated coleoptiles maintain higher rates of respiration than comparable intact coleoptiles. The difference in the rates is not large, but it is statistically significant. Application of the "t" test yields a probability of

TABLE 1

Oxygen consumption per 100 mg of fresh weight of intact and decapitated coleoptiles. Each value is the average for 10 coleoptiles

COLEOPTILES FROM 30 MM PLANTS	MM ³ OF OXYGEN/100 MG/HOUR	
	First hour	Second hour
Intact	29.7	29.4
Decapitated	34.2	34.0

TABLE 2

Oxygen consumption per 100 mg fresh weight of the apical 10 mm from coleoptiles of various lengths. Each value is the average for 10 coleoptiles

APICAL 10 MM FROM COLEOPTILES OF VARIOUS LENGTHS	MM ³ OF OXYGEN/100 MG/HOUR	
	First hour	Second hour
10 mm	65.4	61.0
20 mm	54.7	54.5
30 mm	47.3	47.8
40 mm	44.4	43.2

less than 0.01. Although it was not experimentally tested, the higher rate of respiration of the decapitated coleoptiles could be caused either by the increased metabolism required for the regeneration of a functional apex or by the injury of decapitation.

Length of the coleoptiles. The average volumes of O₂ consumed per hour by the apical 10 mm from coleoptiles of various lengths are shown in table 2. When the results are expressed on the basis of fresh weight, it appears that the rate of respiration decreases as the coleoptiles increase in

length or age (See introduction). The same relationship holds when a unit of length is the standard of comparison. Data of this type are frequently expressed on the basis of dry weight. The average dry weight of 10 mm coleoptiles is 0.52 mg, but the apical 10 mm of a 40 mm coleoptile weighs only 0.34 mg when dry. On the basis of dry weights the rates of respiration of the apical segments from plants of different lengths are approximately the same. The values, within the limits of experimental error, are from 625 to 654 mm³ of O₂/100 mg dry weight/hour and show no relationship to coleoptile length. The use of dry as well as fresh

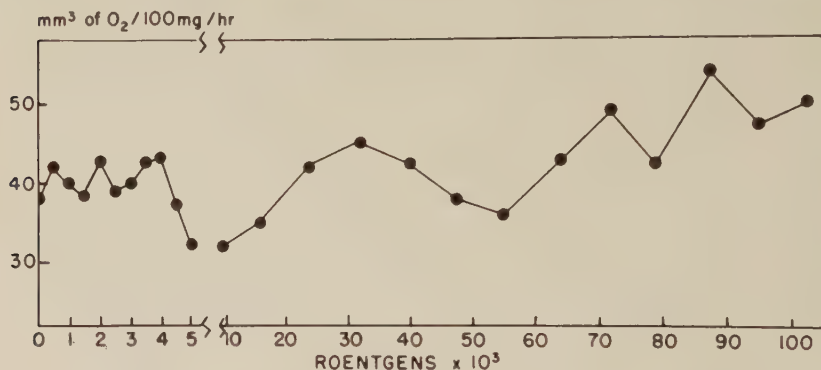


Fig. 3 Rates of oxygen consumption by coleoptiles grown from seeds which have been exposed to various dosages of irradiation from Co⁶⁰. Each point is the average of 10 measurements.

weights is involved in the interpretation of experiments on the effects of gamma irradiation which follow.

Exposure of the seeds to radioactive cobalt. A series of respiration measurements were made on the apical 10 mm segments of coleoptiles grown from seeds which had been exposed to Co⁶⁰. The curve in figure 3 shows the effects of various dosages of irradiation. As the dosage is increased from 0 to 4,000 r, there are minor variations (when the points at 1,500 and 2,000 r were compared by the "t" test a probability of 0.2 was obtained) and a general increase in the rate of O₂ consumption. This increase is small (14%) but

significant ($p=0.05$). Dosages from 4,000 to 5,000 r cause the respiration rate to drop abruptly to a minimum rate ($p=\text{less than } 0.01$) which is maintained by dosages up to 10,000 r. From 10,000 to 100,000 r two cycles of increased and decreased respiration rates result in a second gradual overall increase. The rate of O_2 consumption for coleoptiles grown from seeds exposed to 100,000 r is 39% higher than for normal coleoptiles.

Coleoptiles, from seeds exposed to 100,000 r grown until they are 96 hours old, reach an average maximum length of 12 mm. For control coleoptiles the maximum length is about 45 mm. The data in table 2 reveal a higher rate of respiration for shorter coleoptiles when expressed on the fresh weight basis. This fact might appear to indicate that gamma irradiation causes the increase in O_2 consumption indirectly by inhibiting growth. The average dry weight of the apical 10 mm of control coleoptiles was 0.34 mg, while the dry weight of the corresponding segments of coleoptiles grown from seeds receiving 80,000 r was essentially the same. Thus the ordinate in figure 3 could be changed to mm^3 of O_2 /100 mg dry weight/hour by multiplying the values on the ordinate by 17. This means that the effects of gamma rays on respiration are equally apparent when the results are expressed on the basis of dry weight.

DISCUSSION

The numerous papers, which have been published on the effects of ionizing radiations on respiration and metabolism of tissues, contain many incompatibilities and contradictions. Frequently, some form of inhibitory effect was observed, although the respiration of individual cells appears to be remarkably resistant to X-rays (Barron, '54). Stimulatory effects have been reported in a few instances (Redfield and Bright, '22; Stoklasa, '30; Williams and Sheard, '32; Frankenthal and Back, '44). Redfield and Bright ('22) exposed dry radish seeds to radium rays and observed increased CO_2

liberation, but they found no direct relationship between CO_2 metabolism and growth.

Effects of gamma irradiation on seeds of *Avena* apparently have not been reported. Both X-rays and gamma rays applied to the seeds will inhibit the subsequent growth of roots and coleoptiles (unpublished results). The threshold for gamma rays appears to be about 10,000 r for root inhibition and somewhat lower for coleoptile inhibition. Coleoptiles grown from seeds receiving 100,000 r from Co^{60} will attain only about $\frac{1}{4}$ their normal length, but they will consume 39% more O_2 than the controls. From this it appears that the inhibition of growth by gamma rays is not dependent on the effects of the irradiation on O_2 consumption.

SUMMARY

1. The endogenous respiration of individual *Avena* coleoptiles taken from seedlings 96 hours old was measured in aluminum microrespirometers. Uniform rates were maintained for at least two hours.

2. Geotropic stimulation and decapitation cause slight increases in the rate of oxygen consumption.

3. The rates of oxygen utilization of coleoptiles grown from seeds exposed to gamma rays from Co^{60} are dependent on the radiation dosage. Doses from 5,000 to 10,000 r inhibit the rate of oxygen consumption. From 0 to 5,000 r there is a slight increase in the respiration rate, and from 10,000 to 100,000 r there are several cycles of increased and decreased rates which result in a net increase of 39%.

4. Since coleoptiles grown from seeds exposed to 100,000 r manifest an increased rate of respiration but grow only one-fourth as long as controls, the inhibition of growth by gamma rays apparently is not dependent on the effects of irradiation on O_2 consumption.

LITERATURE CITED

- BARRON, E., S. GUZMAN 1954 The effect of X-rays on systems of biological importance. Ed. by Alexander Hollaender. McGraw-Hill Book Co., Inc., New York. Chap. V: 283-314.

- BERGER, J., B. SMITH AND G. S. AVERY 1946 The influence of auxins on the respiration of the *Avena* coleoptile. *Amer. J. Bot.*, *33*: 601-604.
- BONNER, J. 1933 The action of the plant growth hormone. *J. Gen. Physiol.*, *17*: 63-76.
- 1936 The growth and respiration of the *Avena* coleoptile. *J. Gen. Physiol.*, *20*: 1-11.
- 1949 Relations of respiration and growth in the *Avena* coleoptile. *Amer. J. Bot.*, *36*: 429-436.
- COMMONER, B., AND K. V. THIMANN 1941 On the relation between growth and respiration in the *Avena* coleoptile. *J. Gen. Physiol.*, *24*: 279-296.
- DUBUY, H. G., AND R. A. OLSON 1940 On the relation between respiration, protoplasmic streaming and auxin transport in the *Avena* coleoptile. *Amer. J. Bot.*, *27*: 401-413.
- FRANKENTHAL, L., AND A. BACK 1934 The effect of X-rays on the respiration of fowl erythrocytes. *Biochem. J.*, *33*: 351-354.
- REDFIELD, A. C., AND E. H. BRIGHT 1922 The effect of radium on metabolism and growth in seeds. *J. Gen. Physiol.*, *4*: 297-301.
- SCHRANK, A. R. 1944 Relation between electrical and curvature responses in the *Avena* coleoptile to mechanical stimuli. *Plant Physiol.*, *19*: 198-211.
- STERN, H., AND P. L. KIRK 1948 A versatile microrespirometer for routine use. *J. Gen. Physiol.*, *31*: 239-242.
- STOKLASA, J. 1930 Die physiologischen Wirkungen der Strahlen des Radiums auf die Dynamik und Energetik der Kohlensäure Assimilation. *Biochem. Z.*, *218*: 361-396.
- THIMANN, K. V., AND B. COMMONER 1940 A differential volumeter for micro-respiration measurements. *J. Gen. Physiol.*, *23*: 333-341.
- WILLIAMS, M. M. D., AND C. SHEARD 1932 The effect of X-ray on the electric potential and the rate of oxidation of frog's skin. *Protoplasma*, *15*: 396-414.

SOME TENSILE PROPERTIES OF NERVE¹

DEXTER M. EASTON²

Department of Zoology, University of Washington, Seattle

FIVE FIGURES

INTRODUCTION

Measurements of the elastic properties of muscle have been applied to the problem of muscle contraction (Buchta and Kaiser, '51). Tensile characteristics in nerve are also important, because distortion is an effective means of generating impulses in tension receptors and isolated nerve; and because of the normal changes in nerve length during bodily movement. Effects of stretch upon the membrane potentials of nerve and muscle have been described (Ling and Gerard, '49; Turner, '51). The present report shows that in nerve, as in muscle, the form of the stress-strain curve depends upon the interval between measurements and upon the prevailing tension.

METHODS

Bundles of nerve fibers were obtained from the walking legs of the common edible crab of the Northwest, *Cancer majister*, and from *C. productus*. Successive segments were detached from the proximal part of the leg until only the fibers attached to the dactyl (most distal segment) remained. Although the excitability was not tested, the method of preparation does not ordinarily impair the conduction of impulses. A small, glass, double hook was tied to each end of a nerve bundle by a bowline knot in the nerve or, in the early experiments, with silk or nylon thread. One hook was suspended from the arm of a Roller-Smith precision balance (fig. 1 A). The other

¹ This investigation was supported (in part) by a grant-in-aid from the Agnes Anderson Fund, University of Washington.

² Present address: Department of Physiology, Florida State University, Tallahassee, Florida.

was looped on the end of a glass rod driven by a caliper (B). The nerve was immersed in a sea water bath (C) through the double wall of which water at 10° was usually circulated. A Vernier slide caliper was used in the early experiments. In either case, the caliper was adjusted to zero tension at the beginning of each experiment.

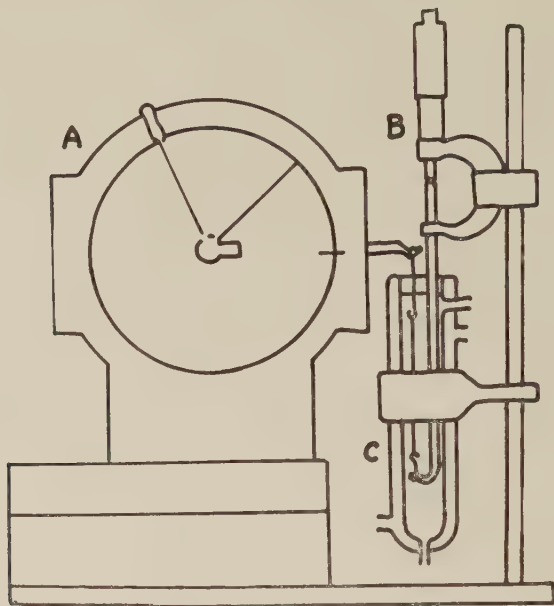


Fig. 1 Apparatus for observing tensile properties of crab nerves, as described in text.

OBSERVATIONS

When tension applied to the nerve was increased by successive standard increments and maintained at each level, a sigmoid length-tension curve was obtained (fig. 2). Release of internal stress followed each application of external strain, and the tension was kept constant by adjusting the length with the caliper. Each point on the graph includes the initial and final length during one minute under the prevailing tension. For the lower curve, tension was increased by 20-mg steps, and for the upper one, by 40-mg steps. Curves representing other determinations on this nerve at increments of 20,

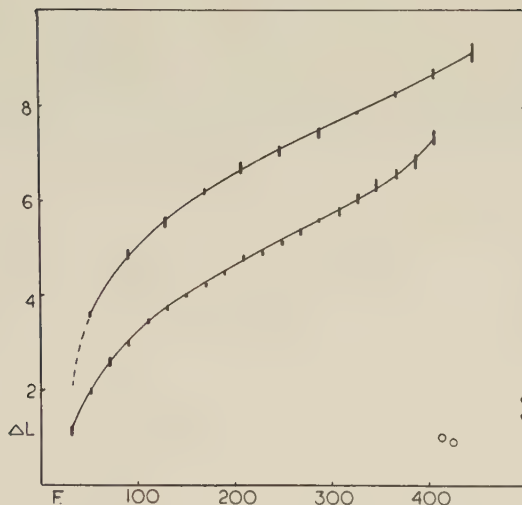


Fig. 2 Stress-strain curve of crab nerve bundle. Abscissa: cumulative force (mg on balance) stretching nerve. Ordinate: cumulative length increment (mm) of nerve at each tension. Vertical lines include initial and final lengths during one minute. Tension applied continuously without release. Lower curve, 20 mg increments; upper curve, 40 mg. Open circles, lower curve after release of tension; filled circles, upper curve after release of tension.

30, and 60 mg were parallel in the region of their inflection points. Successive curves were displaced upward, the amount depending upon the tension increments.

For a number of nerve bundles, stretched with a slide vernier caliper, stress-strain curves were constructed and the modulus of elasticity was calculated from the stress-strain formula

$$H = (\Delta F/A)/(\Delta l/l)$$

$\Delta F/\Delta l$ was obtained from the flattest part of the curve for each bundle (see fig. 2). The results are shown in table 1, in the legend of which the meanings of the symbols are given. Irregular cross-sections and twisting caused considerable variation in apparent diameter measured with an ocular micrometer. The tabulated values are the averages of 6 or more measurements of each bundle.

For the experiment graphed in figure 3, the tension was released between determinations, and immediately reapplied

at the increased length. Increments of 1 mm were used and the tension required to keep the nerve at the set length during three minutes was determined. As the tension stretched the nerve, the balance was adjusted to keep the length constant. The exponential curves from each initial point on the over-all

TABLE 1
Modulus of elasticity of crab nerve bundles. Calculated from flat regions of curves as in figure 2

	NERVE	l (mm)	Δl (mm)	ΔF (mg)	d (mm)	H
C. maj.	B ₂	61	2	255	.44	5,600
	B ₃	32	5	1000	.36	6,250
	B ₄	27	4.5	600	.36	3,480
	B ₆	51	3	720	.42	8,800
	C ₁	59	3	450	.44	5,400
	C ₂	57	0.2	770	.72	5,500
	C ₃	64	3	300	.21	19,600
	C ₄	62	3	450	.28	14,800
	D ₁	29	1	700	.60	7,150
	D ₂	49	4	475	.44	3,740
	D ₃	58	2	275	.31	10,700
	D ₄	60	3	430	.38	11,200
C. prod.	E ₂	60	2	375	.34	3,000
	E ₃	57	4	300	.24	2,300
	E ₆	51	2	475	.26	3,420
	E ₅	42	2	475	.26	4,800
		42	2	625	.51	6,350

l (mm) = initial length of nerve.

Δl (mm) = increment in length from flat part of stress-strain curve.

ΔF (mg) = increment in force required to produce Δl .

d (mm) = average diameter of nerve fiber bundle (average of 6 or more measurements along the bundle).

$$H = (\Delta F/A)/(\Delta l/l) \text{ where } A = \pi \left(\frac{d}{2} \right)^2.$$

curve represent the temporal decay of tension at given lengths. Thus, these curves correspond to the converse of the situation in figure 2, where the straight lines show the changes in length at constant tension.

Figure 4 demonstrates the linear relation between tension and elongation at small extension when the tension was ap-

plied from zero and immediately restored to zero after measurement of the tension. The micrometer setting was increased by 0.2 mm increments, and 5 minutes elapsed between each point so determined. The curve represents the spread in

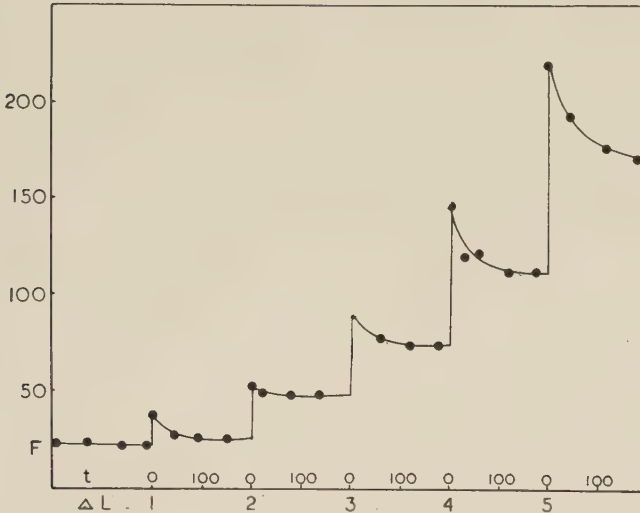


Fig. 3 Stress-strain curve of nerve bundle. Abseissa: Lower line, cumulative length increment; upper line, time (sec.) nerve was left at each length. Ordinate: Tension (mg) in nerve at each length. After three minutes at each length, tension released only long enough to readjust micrometer to new length reading.

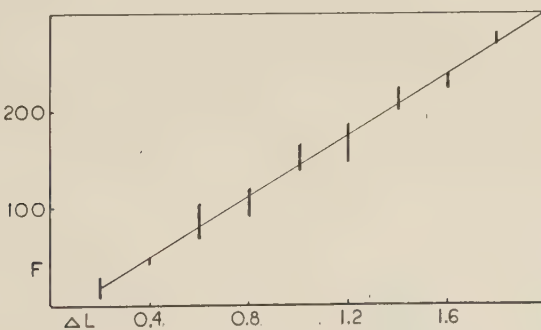


Fig. 4 Stress-strain curve of crab nerve. Abseissa: Cumulative length increment. Ordinate: Tension (mg) at each length. Vertical lines: spread for three successive measurements on one nerve. Tension released immediately after measurement; 5-minute recovery allowed between each measurement.

three successive complete determinations of these data in one nerve bundle. The tension was higher than in nerves not allowed to recover between measurements. The points are reproducible. The line appears straight because it corresponds to the foot of the previous curves.

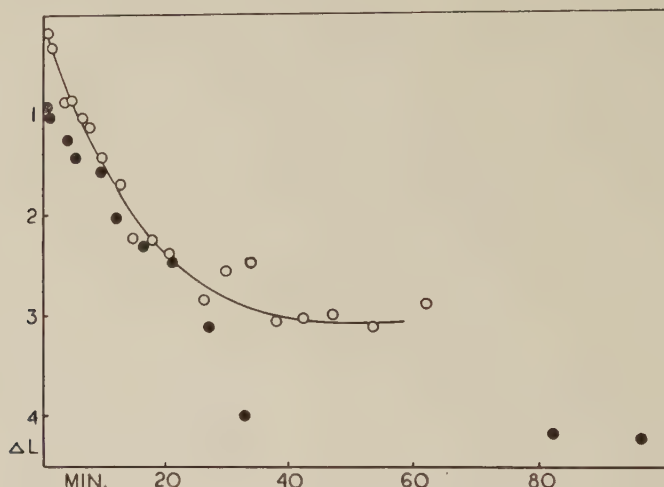


Fig. 5 Recovery of nerve from stretch. Abscissa: time after release of initial tension. Ordinate: cumulative decrease in nerve length at zero tension. Filled circles, initial tension 400 mg for 25 sec.; open circles, initial tension 500 mg for 60 sec.

The recovery from stretch is shown in figure 5. The length of the nerve at zero tension was determined at intervals after the release of initial tension. The nerve was then allowed to hang free until the next measurement. Somewhat more shortening occurred after 400 mg tension for 25 sec. than after the next application of 500 mg for 60 sec.

DISCUSSION

Blix (1892) demonstrated that time is an important factor in determining the form of the stress-strain curve of muscle. It is now clear that for nerve the form of the curve depends upon the method of measurement. The nerves were elastic because under certain conditions stress was directly propor-

tional to strain (especially fig. 4). They were quasiplastic in dissipating applied tension even though they had already been stretched considerably during dissection.

If the elastic property measured by H is primarily due to the connective tissue, then the range of values for this modulus may be accounted for in terms of differences in the relative amount of connective tissue in different nerves. Consistent with this idea, the range of H values is particularly great for small bundles. Brisbin and Allen show approximately straight lines in plots of extension vs. applied weight in crab muscle. Insufficient data is presented to calculate an H value, but a replot of the data as extension vs. weight shows a suitable flat region and a displacement of successive curves similar to those shown in figure 2.

In describing stress-strain curves for single resting muscle fibers, Buchtal and Kaiser ('51) remark that the first of a series of curves is considerably different from those following. They ascribe this difference to "a large alteration in the minute structural pattern of the fiber, which required about an hour for restitution." This slow process is probably similar to the slow shortening observed in the present experiments. Whether this restitution may depend upon metabolic processes is an interesting problem for further research. Further simultaneous measurement of the recovery from rapid stretch and the resulting trains of impulses may provide an understanding of the process of mechanical excitation of nerve and the mechanism of mechanoreceptors.

SUMMARY

Stress-strain curves were constructed for nerve bundles pulled from the walking legs of *Cancer majister* and *C. productus* and stretched in sea water at 10°. Development of tension was greatest when each increment of elongation was applied from zero tension after 5-minutes rests between determinations. The stress-strain relation was a straight line at small extensions (up to about 5%). Release of tension (creep) occurred when the length was maintained at each elongation,

and the stress-strain curve became sigmoid at high extensions (beyond about 15%). Calculated from the flat part of such curves, the modulus of elasticity ranged between 3,000–20,000 mg/mm². Nerves placed under several hundred milligrams tension for several seconds shortened for half an hour after release of tension.

LITERATURE CITED

- BLIX, M. 1893 Die Länge und die Spannung des Muskels. *Skand. Arch. Physiol.*, 4: 339–409.
- BRISBIN, G. W. F., AND F. ALLEN 1939 The elastic extensibility of muscle. *Canad. J. Res.*, 17: 33–48.
- BUCHTAL, F., AND E. KAISER 1951 The rheology of the cross-striated muscle fiber. *Biol. Medd. Kbh.*, 21(7).
- LING, G., AND R. W. GERARD 1949 The influence of stretch on the membrane potential of frog muscle fibers. *J. Cell. Comp. Physiol.*, 34: 397–405.
- TURNER, R. S. 1951 The rate of conduction in stretched and unstretched nerve fibers. *Physiol. Zool.*, 24: 323–329.

OCCURRENCE OF RESPIRATION DEFICIENT MUTANTS IN BAKER'S YEAST CULTIVATED ANAEROBICALLY

MORGAN HARRIS ¹

*Laboratoire de Génétique, Faculté des Sciences
Université de Paris, Paris, France*

TWO FIGURES

INTRODUCTION

The analysis of respiratory function in yeast by Ephrussi and co-workers (see general reviews by Ephrussi, '52; Slonimski, '53) indicates that the formation of respiratory enzymes is mediated by a complex involving genes, cytoplasmic particles, and environmental factors. This picture stems largely from the study of respiration-deficient mutants which occur spontaneously or may be induced in populations of *Saccharomyces cerevisiae*. Such mutants are easily detected by small colony size in the presence of limiting concentrations of sugar, and by characteristic differences in the cytochrome spectrum. The variants constitute approximately 1% of the cell population in the majority of yeast strains studied. Respiration in mutant cells is essentially lacking owing to the loss of cytochrome oxidase and other associated enzymes although fermentation is unimpaired. Mutants of this type arise continuously during vegetative reproduction of either haploid or diploid stains and have accordingly been termed *vegetative littles*.

¹ Merck Senior Postdoctoral Fellow in the Natural Sciences of the National Research Council, 1953-54. Present address: Department of Zoology, University of California, Berkeley 4, California.

The origin of vegetative littles is not readily accounted for in mendelian terms as a gene mutation. The character in question disappears in the progeny of hybrids between normal and mutant cells, and is not recovered despite repeated backcrosses to the mutant strain. These facts suggest the occurrence of a cytoplasmic rather than a nuclear mutation. The explanation advanced by Ephrussi postulates the existence of cytoplasmic units endowed with genetic continuity and essential for the synthesis of respiratory enzymes in normal cells. On this basis the origin of vegetative littles would represent an irreversible loss or inactivation of the particles concerned.

The mechanism through which mutant littles are produced from normal cells is still obscure. The present investigation is concerned with one aspect of this problem, viz. whether production of vegetative littles occurs in anaerobic as well as aerobic cultures. If an aerobic process is essential to the cytoplasmic change, mutation should cease in the absence of oxygen. On the other hand, if production of littles is independent of the presence of oxygen, no difference would be expected under anaerobic conditions. In practice an experimental answer to this question is complicated by the fact that normal cells and vegetative littles do not grow at the same rate (Ephrussi, L'Héritier et Hottinguer, '49), so that selection as well as mutation must be considered in population analyses.

The experiments to be described deal with cultures of normal yeast growing for long periods in rigorous anaerobiosis. For this work the apparatus of Stier, Scalf and Brockmann ('50) has been used, which permits continuous cultivation of yeast under nitrogen for weeks or months. The incidence of vegetative littles has been determined in these cultures and the results interpreted on the basis of growth rates measured on normal strains of yeast, mutant strains, and mixtures of the two.

MATERIAL AND METHODS

All experiments were performed with *Saccharomyces cerevisiae*, strain "Yeast Foam," obtained originally from Professor O. Winge in Copenhagen. Aerobic cultures were grown at 25° C. under conditions of maximum aeration (10 ml medium in 100 ml Erlenmeyer flask with continuous agitation on a reciprocal shaker: 110 complete strokes/min with an amplitude of 4–6 cm). Anaerobic cultures were grown at 28° C. with continuous stirring in an all-glass apparatus constructed according to the specifications of Stier et al. ('50). Slight modifications were made for convenient removal of daily yeast crops. The gas phase was high purity dry nitrogen furnished by the Société "Air Liquide," Paris, with an oxygen content, according to the producer, of less than 0.005%. The standard medium utilized in the present experiments contained 7% yeast extract and 15% glucose (Scalf and Stier, '50), and was fortified with ergosterol and Tween 80 following the observation of Andreasen and Stier ('53) that yeast cells in anaerobiosis may require sterols and unsaturated fatty acids for optimal growth. The exact composition of the medium used was as follows:

Yeast extract (Difco)	70	gm
(control no. 413224)		
Glucose	150	gm
KH ₂ PO ₄	5	gm
Ergosterol	0.05	gm
Tween 80	8.0	ml
Ethanol	12.0	ml
Distilled water to	1000	ml

To facilitate preparation of the medium a stock solution was first prepared by dissolving ergosterol in a boiling mixture of ethanol and Tween 80. The yeast extract and phosphate were then dissolved in water and the resulting preparation appropriately supplemented with the stock solution of ergosterol. Glucose was dissolved separately in a second solution and both sterilized at 120° C. for 20 minutes.

Growth was estimated principally from measurements of optical density made with a Meunier electrophotometer. Tav-

litzki ('49) and Slonimski ('53) have demonstrated that cell number and dry weight are proportional within limits to the opacity of yeast cell suspensions. In addition, cells were enumerated directly with a Levy counting chamber, and protein determinations were performed by a biuret method based on the procedure of Stickland ('51).

The percentage of vegetative littles in the populations studied was estimated by plating diluted aliquots in Petri dishes containing agar with 0.5% yeast extract and 0.5% glucose. The proportion of small colonies was determined by counting after 6 days incubation at 25°C. Mutant strains were obtained by subculture of small colonies and in all cases the characteristic deficiency in the cytochrome system verified by examination with a Hartridge reversion spectro-scope (Slonimski, '53).

For manometric work standard Warburg techniques were employed. Measurements of oxygen consumption, fermentation, and cytochrome oxidase were performed according to procedures outlined by Slonimski ('53, '54). Details will be described in the appropriate experimental sections.

RESULTS

Characteristics of cultures growing in continuous anaerobiosis

In a typical operation, the Stier apparatus was assembled in a sterile room with 5 l of medium in the reservoir flask and 30 ml inoculum in the culture flask. The inoculum contained cells in the stationary phase after two previous aerobic transfers in the medium to be used. The culture was diluted to 230 ml by addition of medium from the reservoir, giving an estimated initial optical density of 1800 (approximately 28×10^6 cells/ml). Flushing with nitrogen was then initiated to establish anaerobic conditions in the entire apparatus. The flow rate was maintained at 50 ml/minute for the first two days and reduced to approximately 2 ml/minute thereafter. The culture was maintained in an even suspension at all

times by the continuous operation of a magnetic stirrer (Stier et al., '50).

As a routine the progress of anaerobic cultures was followed by draining the culture flask every 24 hours. Each sample was removed under positive pressure to maintain anaerobiosis in the apparatus. A fresh growth cycle was then initiated by diluting the residue in the culture flask to a final volume of 230 ml. With this schedule daily samples consistently showed an optical density of about 25,000 units (approximately 380×10^6 cells/ml). This limiting population was maintained through successive growth cycles for many weeks without change. No infections were observed at any time in the Stier apparatus.

The degree of anaerobiosis actually obtained in these cultures was studied in several experiments inasmuch as this point is clearly critical for the question of mutation in anaerobic cells. Anaerobic yeast is characterized by an inability to respire, owing to the rapid loss of cytochromes a, b, and c as well as cytochrome oxidase. An adaptive synthesis of these enzymes occurs, however, if the cells are exposed to oxygen and this process may be followed by measurements of oxygen uptake (Ephrussi and Slonimski, '50; Slonimski, '53). Following these observations, therefore, cytochrome oxidase was determined in several samples from a Stier culture over a 28 day period. The cells were removed from the apparatus, washed immediately in ice-cold M/5 phosphate buffer, pH 6.5, and exposed to ultrasonic treatment for 40 minutes in air. An apparatus manufactured by the Société de Condensation et d'Applications Mécaniques, Paris, was used for this purpose, giving a frequency of 960 kilocycles/sec. with an output of 10 watts/cm² at the surface of the crystal. The extract obtained after treatment, still iced, was centrifuged twice for 10 minutes each time at 3000 RPM in a refrigerated International Centrifuge. The pellets were discarded and the final supernatant dialyzed overnight against M/50 phosphate buffer pH 7.3, before assay. The results (table 1) indicate that cytochrome oxidase falls to a low

level by 4 days and remains without significant change during subsequent culture. It may be pointed out that the concentration of cytochrome *c* used in the assay was saturating for the enzyme in anaerobic preparations but not for extracts from the initial aerobic inoculum. The actual differences between aerobic and anaerobic values are therefore greater than shown in the table (Slonimski, '53).

TABLE 1
Cytochrome oxidase activity in ultrasonic extracts made from yeast cultivated anaerobically

DAYS IN CULTURE	R $\frac{\text{cyt. } c}{\text{O}_2}$ (d.w.)	Q $\frac{\text{cyt. } c}{\text{O}_2}$ (protein)
Aerobic inoculum	16.1	57.4
4	0.9	4.3
8	0.5	4.4
14	0.1	..
20	0.3	..

Standard conditions for determinations:

Cytochrome *c* = 6.0×10^{-5} M, ascorbate = 0.017 M, phosphate = 0.064 M,
NaCl = 0.011 M, pH = 6.9, *t* = 28°C.

$Q_{\text{O}_2}^{\text{cyt. } c}$ (protein) = $\mu\text{l O}_2$ consumed/hr/mg protein in ultrasonic extract

$R_{\text{O}_2}^{\text{cyt. } c}$ (d.w.) = $\mu\text{l O}_2$ consumed/hr/mg dry weight of original cell suspension before ultrasonic treatment.

In a second group of experiments, adaptation to oxygen was measured on cell suspensions taken from the Stier apparatus at various intervals, using the procedures of Slonimski ('54). Measurements over an 8-hour period were used to determine initial and final rates of oxygen consumption ($\frac{d \text{O}_2}{dt}$) as well as the acceleration of oxygen uptake ($-\frac{d^2 \text{O}_2}{dt^2}$) during this interval. The values obtained are summarized in table 2. A marked decrease in initial oxygen consumption is apparent for samples of 4 days incubation or more, with a prominent adaptive rise over the 8-hour period of measurement. The data of tables 1 and 2 are thus in agreement with the typical picture for anaerobic yeast as outlined by Slonimski ('54). It is interesting to find that

the characteristics of adaptation to oxygen are substantially similar in the two investigations in spite of differences in media, growth rates, and duration of anaerobiosis. On the other hand, the spectral changes observed for anaerobic yeast in the present experiments showed certain differences from those observed previously (Ephrussi and Slonimski, '50; Slonimski, '53), in particular the persistence of a very weak cytochrome c α -band and the absence of a strong cytochrome b_1 component. It may be emphasized, however, that the

TABLE 2

Respiratory adaptation of yeast taken from an anaerobic culture

DAYS IN CULTURE	$\frac{d O_2}{dt}$ ($\mu l O_2 \times h^{-1} \times mg d.w.^{-1}$)		$\frac{d^2 O_2}{dt^2}$ ($\mu l O_2 \times h^{-2} \times mg d.w.^{-1}$)	
	at 0 hours	at 7 hours	initial (between 1-3 hrs.)	mean (between 1-7 hrs.)
Aerobic inoculum	85.3	122.4	9.1	4.5
1	18.5	66.5	12.0	5.8
4	8.3	57.9	11.1	6.4
8	10.9	62.6	11.3	6.6
15	2.3	67.5	13.5	8.6

Standard conditions for determinations:

90 mg glucose and 0.5 dry weight yeast in each flask. KOH in center well.

0.2 M phosphate, pH = 6.5, t = 28°C.

Glucose added 30 min. before zero time; $\frac{d O_2}{dt}$ value at 0 hour obtained by extrapolation (Slonimski, '54).

cytochrome oxidase values obtained here are of the same order of magnitude as those found in the earlier investigations. The spectral differences in question thus do not connote a lesser degree of anaerobiosis in the present experiments.

Incidence of vegetative littles in anaerobic cultures

The proportion of vegetative littles in yeast populations under aerobic conditions represents a balance between uni-directional (or irreversible) mutation and selection since the mutants grow more slowly than normal cells (Ephrussi, L'Héritier and Hottinguer, '49). If under anaerobiosis the

action of either factor is increased or decreased relative to the other, a change in proportion of mutants should result. This possibility has been examined by plating samples taken from an anaerobic culture over a period of 32 days. Table 3 gives the results of this experiment, which show clearly that the percentage of vegetative littles remains constant under anaerobiosis and does not differ significantly from the value for aerobic cultures (e.g. the original inoculum). The data also suggest that the proportion of mutants remains the same whether transfer is made from stationary phase or log phase to successive growth cycles.

TABLE 3

Incidence of vegetative littles in yeast cultured anaerobically in Stier apparatus

DAYS IN CULTURE	OPTICAL DENSITY	ELAPSED GENERATIONS	TOTAL COLONIES COUNTED	NO. OF LITTLES	% LITTLES
Aerobic inoculum	0	789	7	0.9
4	25,200 ¹	15	942	4	0.4
8	24,800 ¹	31	2248	5	0.2
15	25,600 ¹	59	1177	10	0.9
22	25,000 ¹	87	1486	8	0.5
28	19,200 ²	135	1511	4	0.3
32	16,800 ²	173	684	7	1.0

¹ Sample taken from stationary growth phase.

² Sample removed before stationary growth phase was reached.

These results permit alternative interpretations: either (1) mutation and selection are both unchanged under anaerobic as compared to aerobic conditions, or (2) both are altered in the same direction and to the same degree. Stating the same problem in a somewhat more useful form, if one factor (e.g. selection) can be demonstrated to occur anaerobically, it follows that the other (mutation) must take place under the same conditions to maintain the constant proportion of mutants as documented in table 3. These considerations led to a study of growth rates in normal and mutant strains of yeast, under both aerobic and anaerobic conditions, and to the examination of population changes in synthetic mixtures of

the two. The results obtained will be outlined in the following sections.

Growth rates of strains derived from normal cells and vegetative littles

A primary group of experiments was performed to compare growth rates under aerobic conditions of strains recently

TABLE 4

Aerobic generation times of normal and mutant strains of yeast in second fluid transfer from colonies on agar plates

TYPE	HOURS IN FIRST TRANSFER	STRAIN NO.	GENERATION TIMES (IN HOURS) IN SECOND FLUID TRANSFER			
			Successive determinations			Average
Normal	24	G 1	1.68	1.49	1.62	1.6
		G 2	1.56	1.53	1.56	1.6
		G 3	1.73	1.42	1.40	1.5
		G 4	1.72	1.45	1.50	1.6
Little	120	P 1	4.51	4.02	...	4.3
		P 2	4.10	4.45	...	4.3
		P 3	2.81	2.67	...	2.7
		P 4	4.60	5.78	...	5.2
Little	48	P 11	11.00	10.43	...	10.7
		P 12	11.22	8.67	...	10.0
		P 13	9.83	9.77	...	9.8
		P 14	5.13	5.54	...	5.3
Little	24	P 31	16.84	16.08	...	16.5
Little	17	P 101	32.01	15.45	...	23.7
		P 102	27.65	19.77	...	23.7
		P 103	16.11	15.77	...	15.9

isolated from colonies on solid media. Accordingly normal or mutant colonies were selected from agar plates after 6 days of incubation and inoculated into 10 ml standard medium in a 100 ml Erlenmeyer flask. After a variable interval (see table 4) but before the stationary phase was reached, subtures of each strain were established in a second flask of the same medium for growth measurements. The initial optical density was adjusted to 50-200 units and changes determined

over a period varying from 12 hours to 5 days. In order to compare the results obtained, mean generation times over successive intervals were calculated from the formula:

$$\text{M.G.T.} = \frac{\text{Time in hours}}{\log_2 \text{ O.D.}_2 - \log_2 \text{ O.D.}_1}$$

Table 4 summarizes these findings. It is apparent that strains established from normal colonies are more rapid in growth than any of the mutant strains, with little variability between individual normal strains studied. On the other hand, a wide spectrum in generation time is observed for the vegetative littles. A clear correlation appears to exist between the duration of the initial culture and the mean generation time as measured in the succeeding transfer. These facts suggest that growth begins at a very slow rate following the initial isolation of vegetative littles in the standard fluid medium. The phase of acceleration is greatly extended and a logarithmic growth phase is reached only after a considerable period in culture. The irregularity of acceleration between individual strains similarly incubated suggests the selection of rapidly-growing variants rather than adaptive changes in the population as a whole, but the existing data are not adequate for a decision on this point. It may also be pointed out that the growth rates of recently isolated mutants were more rapid when measured in a medium containing 0.5% yeast extract and 3% glucose rather than in the more complex standard medium used generally in the present experiments, but did not in any case approach the low generation times of normal cell strains.

A more general comparison of mutant and normal strains was also carried out using a single little, P_3 , stabilized by 5 transfers under aerobic conditions in the standard experimental medium, and the stock strain "Yeast Foam." An anaerobic P_3 culture was established in the Stier apparatus and after 7 days a growth curve was obtained for the mutant strain by withdrawing samples at intervals during a single growth cycle. Simultaneous measurements were carried out

on an aerobic P_3 culture. Cell counts and protein determinations were made in addition to measurements of optical density. The data obtained are shown in table 5 and can be compared with similar information derived for anaerobic and aerobic Yeast Foam cultures. These data show that even after repeated transfers in the standard medium the mutant strain has a higher generation time and lower maximal population than the normal strain of origin. Secondly, the results indicate that Yeast Foam can grow at the same rate aerobically and anaerobically, whereas a considerable decrease in growth rate of normal strains under anaerobic conditions was observed by Tavlitzki ('49) and Slonimski ('53). It may be emphasized, however, that the medium used in the present investigation was markedly different from those of the earlier experiments mentioned, and contained in particular ergosterol and Tween 80, shown by Andreasen and Stier ('53) to be growth factors for yeast under anaerobic conditions. Table 5 on the other hand indicates that the mutant P_3 grew more slowly under anaerobiosis. The metabolic studies listed suggest that aerobic cultures of vegetative littles may have a higher rate of fermentation than the corresponding anaerobic cultures although the data on this point are restricted to the stationary phase and do not cover an entire growth cycle.

Population changes in mixtures of normal and mutant strains

On the basis of the growth studies outlined above, two experiments were carried out to follow population changes in known mixtures of normal cells and vegetative littles. The first experiment was performed under anaerobic conditions in the Stier apparatus with an inoculum consisting of 90% P_3 vegetative littles and 10% G_2 normal cells. Anaerobiosis was established as usual and samples withdrawn daily for plating to determine the proportion of littles in the population. Subsequent counts showed that the percentage of littles remained close to the initial level for two or three days in

TABLE 5

Characteristics of P₃ vegetative little after repeated aerobic transfers in standard experimental medium, and comparison with parent "Yeast Foam" strain

STRAIN	CULTURES USED FOR GROWTH MEASUREMENTS	LIMITING POPULATION		GENERATION TIME IN LOGARITHMIC GROWTH PHASE			MEASUREMENTS ON CELLS FROM STATIONARY GROWTH PHASE			
		No. cells per ml	Total protein per cell, mg	Successive determinations		Average	Q _{O₂}	Q _{CO₂}	N ₂	Q CO ₂
P ₃ little	Aerobic	465 × 10 ⁶	1.5 × 10 ⁻³	1.93	2.24	1.92	2.0	< 5.0	383	361
	Anaerobic	305 × 10 ⁶	1.3 × 10 ⁻³	2.51	2.67	2.52	2.6	< 5.0	172	195
Yeast Foam	Aerobic	566 × 10 ⁶	1.4 × 10 ⁻³	1.68	1.49	1.62	1.6
	Anaerobic	378 × 10 ⁶	1.3 × 10 ⁻³	1.58	1.74	...	1.7

Q_{O₂} = rate of respiration in μl O₂/hr/mg dry wt., measured at pH 6.5, t = 28°C., 0.2 M phosphate, 90 mg glucose and 0.5 mg dry weight yeast per flask.

Q_{CO₂} and Q_{N₂} = aerobic and anaerobic fermentation in μl CO₂/hr/mg dry wt., measured at pH 4.5, 0.05 M phosphate-succinate buffer, 90 mg glucose and 0.7 mg dry weight yeast per flask.

culture and then declined rapidly. Figure 1 compares the observed population shifts with a curve of expected changes based on relative growth rates and maximal populations for the two strains respectively. The two curves are approximately parallel in their latter parts but differ with respect to the initial phase. The simplest interpretation of these facts is that population shifts in the mixture are governed by relative growth rates but normal cells do not grow at a maximal rate for the first two or three days in anaerobiosis.

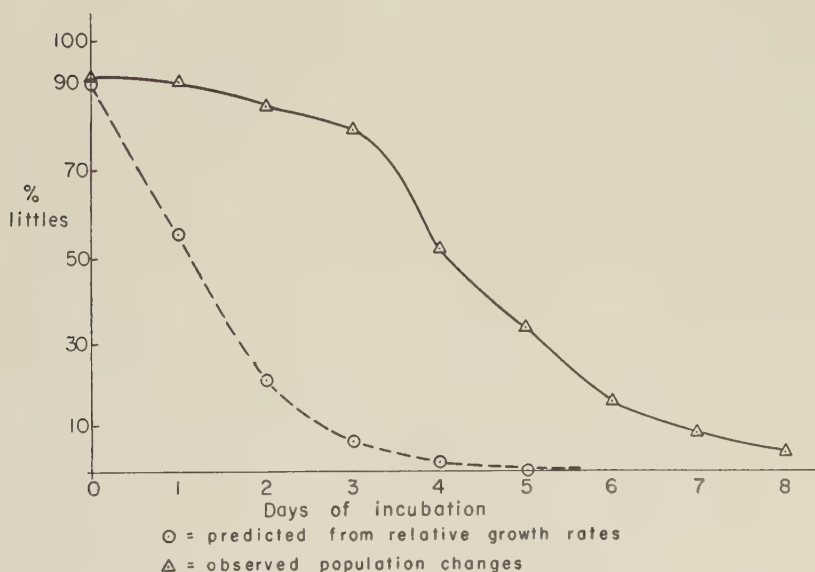


Fig. 1 Population changes in mixtures of G_2 normal cells and P_3 littles, under anaerobic culture.

The possibility remained, however, that growth of the P_3 littles was stimulated by the presence of normal cells in the mixture, if only temporarily. An interaction of this type, if present, should be more clearly evident in mixtures with a higher disparity in growth rates of the two components. A second experiment was therefore carried out using a freshly isolated vegetative little instead of the P_3 strain described above.

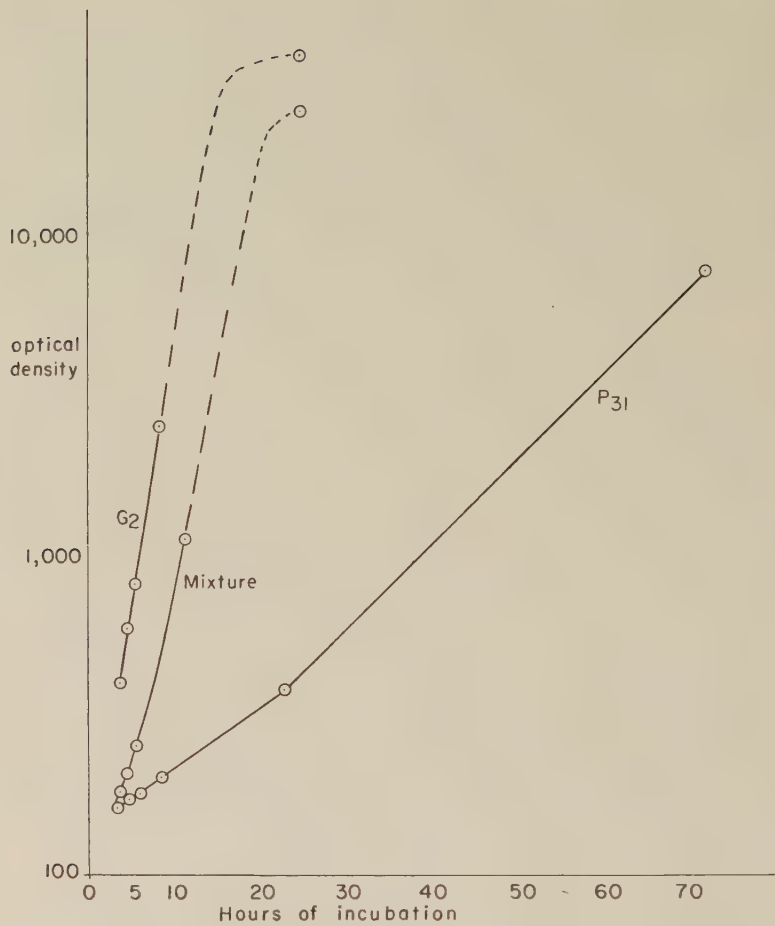


Fig. 2 Aerobic growth rates of P₃₁, G₂ and mixture (19% P₃₁ : 21% G₂).

TABLE 6

Population changes in mixtures of G₂ normal cells with P₃₁ vegetative littles recently isolated from colony on agar plate

TYPE OF CULTURE	HOURS OF INCUBATION	TOTAL COLONIES COUNTED	VEGETATIVE LITTLES		NORMAL COLONIES	
			No.	%	No.	%
Initial mixture	0	586	438	78.8	118	21.2
Anaerobic	24	870	7	0.8	863	99.2
Aerobic	24	956	6	0.6	950	99.4

The mutant selected (P_{31} , table 4) was removed from an agar plate after 6 days of incubation, suspended in 10 ml standard medium, and incubated aerobically on a shaker for 24 hours. A culture of G_2 normal cells was simultaneously inoculated from an agar slant and incubated similarly. From these cultures a mixture was prepared consisting of 79% P_{31} littles and 21% G_2 normal cells as determined subsequently by plate counts. An aliquot of the mixture was placed in the Stier apparatus and incubation begun immediately with a rapid flow of nitrogen. A second aliquot of the mixture was incubated aerobically, along with cultures of the two components in separate flasks. Changes in the aerobic cultures were followed by measurements of optical density at appropriate intervals and the growth curves obtained are shown in figure 2. The wide difference in growth rates of normal and mutant cells is evident, and the net growth rate of the mixture shows a rapid acceleration to parallel that of the G_2 normal culture. These facts suggest the essential elimination of added P_{31} littles in a single aerobic growth cycle, and the results from plating (table 6) verify this conclusion. While the growth curve of the anaerobic mixture was not followed in detail, the facts available indicate a similar disappearance of the P_{31} mutants in the first 24 hours of incubation. The limiting optical density observed at this time was typical of normal rather than mutant strains, and plate counts (table 6) confirmed the absence of added littles in the cell population. The experiments described thus provide no evidence for growth stimulation of vegetative littles by normal cells present in the same population.

DISCUSSION

The significance of the data from mixture experiments is based on the assumption that the growth rates measured are typical of mutant and normal cells in natural populations. On technical grounds this might be questioned since in the present investigation mutants were isolated on a solid medium of simple composition, and could conceivably require more

adaptation than normal cells when subsequently introduced into the complex standard medium for growth measurement. That this objection is not valid, however, is indicated by the original experiments of Ephrussi, Hottinguer and Chimenes ('49). In this investigation the solid and liquid media used were identical in composition except for the presence of agar. Nevertheless freshly isolated mutants grew more slowly than normal colonies and accelerated in subsequent transfers. Similar observations have been made by Prevost ('53).

It thus seems apparent that for the standard medium used in the present experiments, selection operates against vegetative littles and is active in anaerobic as well as aerobic conditions. Since the proportion of spontaneous mutants remains constant in normal strains cultivated anaerobically, it appears that the production of vegetative littles must continue in the absence of oxygen to balance the observed process of selection. The fact that the incidence of vegetative littles is the same under both aerobic and anaerobic conditions (table 3) suggests that (1) selection in either case is essentially complete under the conditions described so that practically all the littles present in these populations at any one time are recently produced, and (2) the mechanics of the mutation process are independent of the presence of oxygen.

A further point of interest stems from the observation that littles and normal cells do not necessarily grow at the same rate in anaerobiosis (table 5); whereas the previous data of Slonimski ('53) appeared to show that no difference exists under these conditions. The evolution of growth rates here observed provides a simple explanation for this discrepancy, for it is apparent that a similar growth rate for mutant and normal cells is only to be expected after many serial passages of the mutant strain. The vegetative little studied by Slonimski had in fact been stabilized in this way by over 450 transfers before the measurements in question were made. In any event the fact that recently isolated littles do not grow as rapidly as normal cells even anaerobically suggests that the mutation process involves a broader defi-

ciency than the respiratory changes previously described. The nature of the additional deficiency remains as an interesting future problem.

ACKNOWLEDGMENTS

The author wishes to thank Professor Boris Ephrussi for suggesting the present problem and for the many courtesies received as a guest in his laboratory. The daily counsel and assistance of Dr. Piotr Slonimski as well as that of Professor Ephrussi was indispensable to the progress of the investigation and is gratefully acknowledged.

SUMMARY

1. Cultures of *Saccharomyces cerevisiae*, strain Yeast Foam, were established in the apparatus devised by Stier, Scalf, and Brockmann for the continuous cultivation of yeast under anaerobic conditions. In these cultures the proportion of respiration-deficient mutants (vegetative littles) remains constant over several weeks, and does not differ from values observed in aerobic cultures.

2. Comparison of normal and mutant strains indicates that vegetative littles are characterized by a low initial growth rate in the standard experimental medium, accelerating over successive transfers but remaining well below the growth rate typical for normal strains of yeast.

3. Normal and mutant strains were used to construct synthetic populations and the subsequent changes were followed under both aerobic and anaerobic conditions. In either case the percentage of vegetative littles declines to the spontaneous level, over a period proportional to the difference in growth rates of the two components.

4. The occurrence of selective processes in anaerobic cultures implies the continued production of vegetative littles to account for the constant percentage of spontaneous mutants observed in these populations. It is concluded that mutation of normal cells to vegetative littles is independent of the presence of oxygen under the conditions of the present study.

LITERATURE CITED

- ANDREASEN, A. A., AND T. J. B. STIER 1953 Anaerobic nutrition of *Saccharomyces cerevisiae*. I. Ergosterol requirement for growth in a defined medium. *J. Cell. and Comp. Physiol.*, **41**: 23-36.
- EPHRUSSI, B. 1952 The interplay of heredity and environment in the synthesis of respiratory enzymes in yeast. The Harvey Lectures, Series XLVI: 45-67.
- EPHRUSSI, B., PH. L'HÉRITIER AND H. HOTTINGUER 1949 Action de l'acriflavine sur les levures. VI. Analyse quantitative de la transformation des populations. *Ann. Inst. Past.*, **77**: 64-83.
- EPHRUSSI, B., H. HOTTINGUER, AND A. CHIMENES 1949 Action de l'acriflavine sur les levures. I. La mutation "petite colonie." *Ann. Inst. Past.*, **76**: 351-367.
- EPHRUSSI, B., AND P. P. SLONIMSKI 1950 La synthèse adaptative des cytochromes chez le levure de boulangerie. *Biochim. et Biophys. Acta*, **6**: 256-267.
- PREVOST, G. 1953 Unpublished observations.
- SCALF, R. E., AND T. J. B. STIER 1950 Effect of commercial malt sprouts on the anaerobic growth of distillers' yeast. *Transact. Kentucky Acad. Sci.*, **13**: 69-77.
- SLONIMSKI, P. P. 1953 La formation des enzymes respiratoires chez la levure. *Actualities Biochimiques* No. 17, Masson, Paris, 204 pp.
- 1956 Mécanisme de l'adaptation respiratoire chez le levure. I. Conditions et cinétique de la synthèse induite de la cytochrome oxidase en absence d'azote exogène. (In preparation.)
- STICKLAND, L. H. 1951 The determination of small quantities of bacteria by means of the biuret reaction. *J. Gen. Microbiol.*, **5**: 698-703.
- STIER, T. J. S., R. E. SCALF AND M. C. BROCKMANN 1950 An all-glass apparatus for the continuous cultivation of yeast under anaerobic conditions. *J. Bact.*, **59**: 45-49.
- TAVLITZKI, J. 1949 Action de l'acriflavine sur les levures. III. Etude de la croissance des mutants "petite colonie." *Ann. Inst. Past.*, **76**: 497-509.

THE SECRETION OF NON-ELECTROLYTES IN THE PAROTID SALIVA ¹

A. S. V. BURGEN

Department of Physiology, McGill University, Montreal, P. Q., Canada

INTRODUCTION

In the elaboration of a glandular secretion many processes are probably at work. In the case of some constituents active transfer is certainly involved, in others a passive equilibration under an osmotic gradient will account satisfactorily for the concentration of the substances in question. Now while there has been extensive investigation of the substances presumed to be actively transferred both in the salivary and other secretions, there has been little investigation of passively moving substances.

The outstanding study of the secretion of non-electrolytes in the saliva is that of Amberson and Hober ('32) and these workers were able to show in the cat submaxillary gland that non-electrolytes of small molecular volume and relatively high lipid solubility penetrated into the saliva with ease. Increase of molecular volume or decreased lipid solubility greatly decreased the amount entering the saliva. Similar results were reported by Jeangros ('28).

Amberson and Hober also found that glycine and alanine either did not penetrate at all or only in very small amounts. Recent work (Woldring, '55) has shown that small amounts of a number of amino acids do appear in saliva. The poor penetration of amino acids was attributed to their low lipid solubility and relatively large molecular volume, but their zwitterionic character might also decrease their ability to cross cell membranes.

¹ Aided by a grant from the National Research Council of Canada.

These studies were designed to show the order of permeability of the secreting cell; they were not designed to demonstrate any change in the cell characteristics *as a result of the secretory process*. In the papers so far quoted in no case was the rate of secretion of saliva considered as a parameter of permeability and indeed only Araki ('51) seems to have attempted this approach. He found an inverse relationship between the urea in human parotid saliva and the rate of secretion. Unfortunately his saliva samples contained an urease, probably of bacterial origin, and the saliva samples low in urea had a high ammonia content. Araki concluded that the changes in urea concentration were largely due to the action of the urease.

In the present work a detailed analysis of the secretion of 10 non-electrolytes in the parotid saliva of the dog has been undertaken. It will be shown that there are characteristic relationships between the rate of secretion and the concentration of non-electrolytes in the saliva.

A mathematical analysis of these curves permits us to follow the permeability of the salivary cells as a function of the rate at which they are secreting and thus gives information about the change in properties of the cell membrane during the secretory process. Our results confirm Amberson and Hober's deduction that the cell membrane is pored, but in addition demonstrate that the pores change their character when the cell is activated.

METHODS

Dogs weighing 8–16 kg were anaesthetised by the intravenous injection of 5–6 ml/kg of a solution of 1 gm chloralose and 10 gm urethane in 100 ml of warm 0.9% NaCl. The auriculotemporal nerve was dissected and prepared for stimulation as described previously (Burgen, '55). The parotid duct was exposed in the cheek and cannulated for collection of saliva. In all cases the nerve was stimulated by supra-maximal rectangular pulses of 0.5–2 msec. duration. The rate of secretion was varied by changing the rate of stimulation

in the range of 0.5–50 per second, and a period of 4 minutes rest was allowed between each collection. The rates of stimulation were applied in random order. After discarding the first 4–5 drops the saliva was collected in weighed screw cap bottles. One-half to one and one-half milliliters were required depending on the nature of the analyses to be performed.

In all cases an attempt was made to produce a steady plasma level of the test substance throughout the experiment by giving a loading dose followed by maintenance doses. In the earlier experiments the loading dose was given intravenously and the maintenance doses were given through a fine polythene tube inserted into the peritoneal cavity. Maintenance doses were given every 10 minutes, the delay in absorption smoothing out variations in the plasma concentration. In the later experiments the maintenance dose was given by continuous intravenous infusion through a polythene tube inserted into the lateral saphenous vein and pushed up into the femoral vein. A motor-driven syringe was used to deliver the infusion at a suitable constant rate that was between 15–40% of the loading dose per hour. If the maintenance dose had been correctly estimated the plasma level settled down to either a steady or a very slow changing level at 2–2½ hours after administration of the loading dose. Collection of arterial blood from the femoral artery into heparinised tubes and of saliva samples could then commence.

In all the experiments a plot of the rate of secretion against frequency of stimulation was made in order to check any deterioration of the preparation.

Samples of plasma were dried to constant weight in a hot air oven to determine the total plasma solids. The solids of saliva were assumed to be 1%. This involves an error of less than 1% in estimation of saliva water in the case of dog parotid saliva. Concentrations of solutes were expressed as millimols/kg plasma or saliva water (i.e. millimolal). The parotid gland was dissected out at the end of the experiment and weighed. The rate of secretion could then be expressed as mg saliva/gm gland/minute. In order to compare different

•

experiments the rate of secretion is expressed as a *percentage of the maximum rate* in all except figures 1 and 2. This percentage secretion rate is used in all the calculations. The mean maximum secretion rate was 551 ± 81 (SE of mean) mg/gm/min.

In some cases the concentration of solute in the gland water was determined in the minced gland.

Rigid tests of the passive nature of the transfer of any given non-electrolyte were not ordinarily carried out, if the saliva/plasma ratio for a given rate of secretion remained constant over a 2-3-fold range of plasma concentration. In the case of creatinine it is important to work with high blood levels as the endogenous Jaffe reacting substances have a higher permeation rate than exogenous creatinine.

In the case of mannitol high plasma levels (15-35 mmol/l) were necessary because of the very slow rate of transfer into saliva. In order to avoid dehydration of the animal by osmotic diuresis and to reduce the amount of mannitol required for maintenance of the blood level, both renal pedicles were tied by a paravertebral approach.

When the passive behaviour of a substance has been demonstrated it is a convenience to express saliva concentrations as a percentage of the plasma concentration, i.e. plasma concentration is set to 100.

Of the substances used only urea and chloramphenicol are appreciably bound to plasma proteins. The binding of urea is given by Kennedy, Hilton and Berliner ('52) as 5.3%. Chloramphenicol binding was measured by centrifuging a solution of chloramphenicol in plasma in a cellophane sac and then measuring the concentration in the plasma and ultrafiltrate. The mean binding was found to be 32.3%. Corrections for binding were applied to the results for these two substances.

ANALYTICAL METHODS

In several cases standard methods of analysis gave trouble owing to the fact that salivas secreted at different rates differ

in pH, concentrations of buffer substances and proteins. Modification to deal with these problems are described below. All the colorimetric determinations were carried out in the Beckman DU Spectrophotometer.

Creatinine. An alkaline picrate reagent buffered to pH 12 with borate gave better results than the usual reagent and should be useful in other applications, e.g., urine creatinines.

The reagent was made up as follows: 24 gm of Boric acid (buffer reagent quality) was dissolved in 325 ml of 10% NaOH and made up to 500 ml with distilled water. The alkaline picrate solution was made up freshly by adding 4 ml of this solution to 5 ml of saturated aqueous picric acid. Saliva was deproteinised with half the amounts of sodium tungstate and sulphuric acid used by Folin and Wu ('19) for plasma. Two milliliters of the filtrate were mixed with 1 ml of the alkaline picrate reagent and the colour read after 15–30 minutes at 520 m μ .

Thiourea. The method of Chesley ('44) is very sensitive to slight variations of final pH; dilution of the Grote's reagent 1:20 with M/5 phosphate buffer pH 6.3 made it quite insensitive to the pH of the protein free filtrate. The colour was read at 600 m μ .

Glycerol. Holst's ('44) anthrone method was used with slight modifications. The anthrone reagent is stable if made up in 90% V/V H₂SO₄ instead of concentrated H₂SO₄. In addition the tendency of the solution to char was much reduced by heating at 150°C. instead of 170–5°C. The colour was read at 504 m μ .

Mannitol. Mannitol was oxidised by the method of Corcoran and Page ('47). The formaldehyde formed was estimated by the chromotropic acid reagent recommended by O'Dea and Gibbons ('53). Care was taken to carry out the colour development in the dark. The colour was read at 570 m μ .

Methenamine. Methenamine was hydrolysed by heating 0.2 ml of a zinc filtrate with 0.2 ml 0.5 N HCl in a boiling water bath for 20 minutes — the tube mouth being covered with aluminum foil. The liberated formaldehyde was then

estimated with the O'Dea and Gibbons chromotropic acid reagent from which the SnCl_2 had been omitted. (The SnCl_2 precipitates in the presence of the ammonia produced in methenamine hydrolysis.)

N-Acetyl 4-amino antipyrine (NAAP). After trials of several methods NAAP was estimated by a modification of the Bratton and Marshall ('39) method for sulphonamides.

Four milliliters of a zinc filtrate were placed in a test tube, 1 ml of 2.5 N HCl added, and after covering with foil the tube was heated in a boiling water bath for 30 minutes. After cooling in the refrigerator 0.5 ml of fresh 0.1% NaNO_2 was added and 10–15 minutes later 0.5 ml of 0.5% ammonium sulphamate. Twenty minutes later 0.5 ml of 1% N-(1 naphthyl) ethylene diamine hydrochloride was added and the tubes left in the refrigerator overnight (the coupling occurs very slowly) and the blue colour read at 590 m μ .

Chloramphenicol. Chloramphenicol was estimated by the method of Glazko, Wolf and Dill ('49).

Urea, N-methyl urea, N-ethylurea. Urea was estimated by the method of Archibald ('45). Methyl urea and ethyl urea were estimated by the same method after removal of urea with a suspension of urease powder before deproteinisation.

The possibility that salivary urea was being hydrolysed by a bacterial urease was excluded by following the urea concentrations during storage. There was no appreciable change. However, to guard against occasional contamination the samples were subjected to protein precipitation immediately after collection.

Oil/water distribution coefficients were determined in the usual way at room temperature between olive oil which had been washed thoroughly, first with dilute sodium bicarbonate, then water, and finally with M/20 phosphate buffer pH 7.0. The test substance was dissolved in a measured volume of the phosphate buffer.

RESULTS

The relationship between concentration of non-electrolyte in the saliva and the rate at which the saliva was secreted has been studied on the 10 substances listed in table I. In these experiments all other variables have been controlled so that the rate of secretion is the sole variable and the effect of this has been followed up to the maximum rate of secretion attainable. The results obtained with these substances fall into two well defined patterns which are illustrated in figures 1 and 2.

TABLE 1

SUBSTANCE	M.W.	O/W COEFF. = B	CURVE NO.
Urea	60	0.00016	4
N-Methylurea	74	0.00046	3
Thiourea	76	0.0012	1
N-Ethylurea	88	0.0018	2
Glycerol	92	0.000069	5
Creatinine	113	0.00014	8
Methenamine	140	0.00021	9
Mannitol	182	0.00001	10
4-Acetamino antipyrine	245	0.0035	7
Chloramphenicol	325	2.5	6

In the first type, illustrated in figure 1 by methenamine, the concentration in the saliva is an inverse function of the rate of secretion.

The second type is illustrated in figure 2 by N-methylurea, in this the concentration at first falls with increase in rate of secretion, passes through a minimum and then rises with further increase in rate of secretion, the curve is thus U-shaped.

Since the maximum rate of secretion of the glands we have studied has varied rather little it is possible to plot all the 10 substances on the same abscissa if the rates of secretion are expressed as a percentage of the maximal rate. In order to accommodate the wide range of salivary concentrations found, a logarithmic concentration scale has been used. In

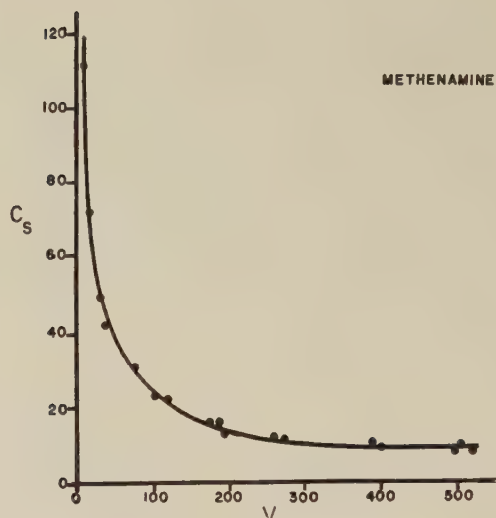


Fig. 1 Secretion of methenamine in parotid saliva. Ordinate: concentration of methenamine in the saliva as per cent of plasma concentration. Abscissa: rate of saliva secretion in mg/gm gland/ minute.

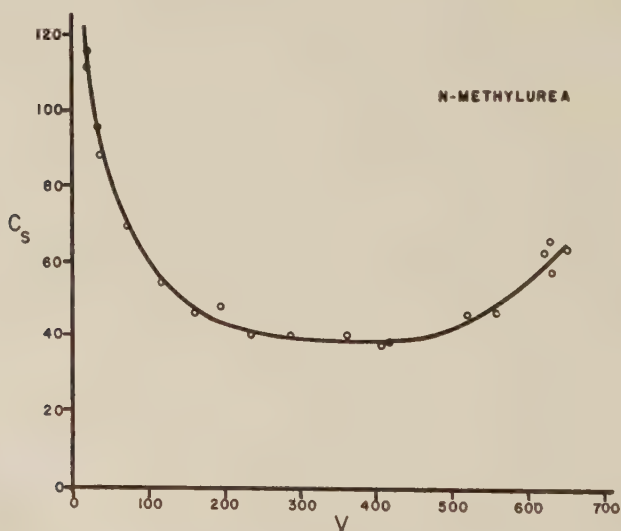


Fig. 2 Secretion of N-methylurea in parotid saliva. Scales as in figure 1.

figure 3 curves for all the 10 substances are plotted. Four substances, N-ethylurea (2), chloramphenicol (6), 4-acetamido antipyrine (7) and methenamine (9) give curves of the first type; the other 6 substances thiourea (1), N-methylurea (3),

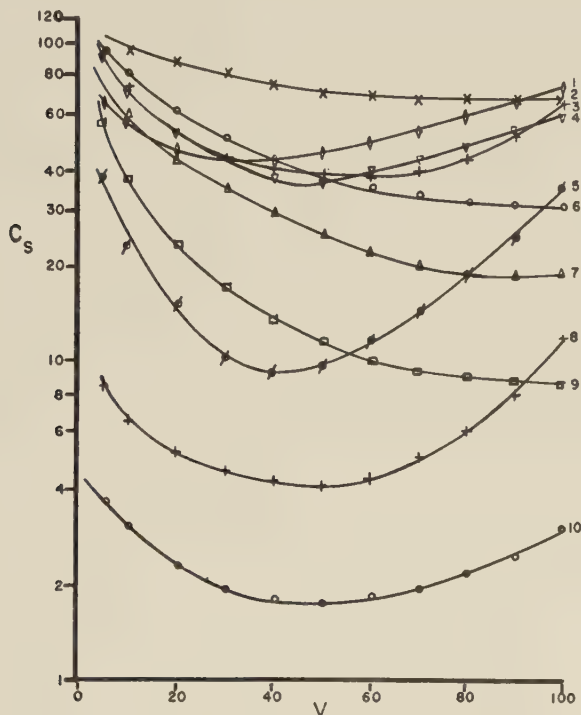


Fig. 3 Secretion of 10 substances in parotid saliva. Ordinate: concentration of substance as per cent of plasma concentration. Abscissa: rates of secretion as percentage of maximum. 1 = thiourea; 2 = N-ethylurea; 3 = N-methylurea; 4 = urea; 5 = glycerol; 6 = chloramphenicol; 7 = 4-acetamidoantipyrine; 8 = creatinine; 9 = methenamine; 10 = mannitol.

urea (4), glycerol (5), creatinine (8) and mannitol (10) give curves of the second type.

These curves are reproducible in different animals within quite small tolerances. In particular a great many experiments have been carried out with creatinine with little variation and a few experiments with these substances have been carried

out on the cat parotid and the dog submaxillary. The general form of the curves in these glands is very similar to those obtained with the dog parotid but the absolute concentrations are slightly different.

It is important to know whether the concentration of a substance in the saliva represents a steady state or a transient secretion. This has been tested by prolonged stimulation of the auriculotemporal nerve and collection of several samples of saliva. It was found that the concentration of solute remained constant during the course of a prolonged period of secretion if the rate of secretion was unchanged; if the rate of secretion decreased then the concentration changed only to that extent predicted by the curves given in figure 2. In these tests the total amount of secretion was equal to 2-3 times the water content of the gland and 20-150% of the initial gland content of the test solute. We are therefore confident that within the limits of accuracy of our procedures we are dealing with a steady state.

In order to proceed with the analysis of these curves we also need to know where the concentration drop between the plasma and the saliva occurs. This may occur between extracellular fluids and the cytoplasm (across what we will call the *outer cell face*), between the cytoplasm and the saliva (across the *inner cell face*) or across both faces. We can settle this problem by analysis of the concentration of the solutes in the gland. Such estimations for thiourea, creatinine, NAAP, mannitol, and methenamine showed that in all cases the concentration in the gland water was within 10% of the concentration in the plasma water. This difference is probably not significant because of the difficulty of obtaining uniform samples of the parotid gland owing to fat inclusions.

In some respects these findings were surprising — for instance, mannitol is known to penetrate most cells extremely slowly (Hober, '45; Davson, '51) and has consequently been used as a measure of extracellular fluid space. It is metabolised by the liver, however, and so presumably can enter

liver cells without too much difficulty. It is curious that another substance CNS^- that is used to measure extracellular space can also readily penetrate salivary gland cells and indeed is considerably concentrated in the saliva. These facts point to a higher permeability for the *external* face of the salivary gland cells than is usual for other cells.

It should be noted that this situation applies to substances that yield both types of concentration curves thus showing that the difference in curves is not due to the imposition of an additional barrier at the outer cell boundary in one case and not in the other.

For our present purposes it is clear that for substances of both Type I and Type II the gland cytoplasm is in equilibrium with the blood and that for analytical purposes we need to deal with a dynamic concentration gradient solely across the inner cell membrane. This is a fortunate circumstance as it leads to a very simple kinetic treatment.

Let us consider the concentration-flow relationship in saliva that would be expected if the solute moves by diffusion through a membrane of constant geometry and permeability into a *secreted fluid initially free from the substance in question*.

In view of the equilibrium between the gland cytoplasm and the plasma we can regard the cytoplasm as an extension of the plasma and treat the inner cell membrane as a unique discontinuity of infinitely small thickness. In general the barrier to diffusion of molecules of the kind we are concerned with produced by a cell membrane is of such a magnitude that the effective diffusibility is less than one ten thousandth (Davson and Danielli, '43) of the diffusibility in free solution. It will be shown later that these conditions are valid for the parotid gland. In this case the concentration gradients in the cytoplasm and saliva will be negligibly small compared to that occurring in the membrane and the error introduced by assuming that the *whole* of the gradient will occur in the membrane is trivial (see also Keynes, '51). We have already demonstrated that the concentration of non-electrolyte is not

time dependent and we may therefore apply the Fick equation for the steady state to diffusion in the gland.

$$Q = P (c_p - c_s) \quad (1)$$

(c_p = plasma molal concentration; c_s = saliva molal concentration; P = permeation coefficient; Q = transfer of solute per unit time.)

Under our conditions $Q = V \cdot c_s$ where V = rate of secretion. We have decided for convenience to call $c_p = 100$ and express c_s as a percentage denoted by C_s . Equation (1) may therefore be rewritten

$$V \cdot C_s = P (100 - C_s) \quad (2)$$

$$\text{or} \quad P = \frac{V \cdot C_s}{100 - C_s} \quad (2a)$$

$$\text{or} \quad C_s = \frac{100 P}{V + P} \quad (2b)$$

$$\text{or} \quad Q = \frac{100 V \cdot P}{V + P} \quad (1a)$$

The relationship between C_s and V predicted by equation 2b for various values of P is shown in figure 4 a. Figure 4 b shows the relationship of Q to V — it will be noticed that Q tends to a constant level as the rate of flow increases provided that the value of P is not above 10.

The curves of figure 4 a seem quite similar to the Type I curves seen in figures 1 and 3, but are not like the Type II curves. We may test more rigidly how well the experimental points fit the theoretical curves by calculating a presumptive permeation constant P' from these values by the use of equation 2a. Naturally if the agreement with theory was perfect the values of P' when plotted against V should give a straight line parallel with the abscissa, i.e. P' should be independent of V .

In figure 5 the values for the 4 Type I substances are re-plotted in this way. All 4 curves are slightly convex with respect to the abscissa but the rise is not large. The ratio between minimum and maximum values of P' is 1:1.5 for

chloramphenicol, 1:1.6 for NAAP, 1:1.6 for methenamine and a little higher 1:2.0 for ethylurea. These deviations from ideal behaviour are quite small, but if we examine the Type II substrates in the same way (fig. 6) the position is very different. For mannitol $P' = 0.3$ at $V = 10$ and $P' = 3.0$ at $V = 100$ — a 10-fold increase; for creatinine the corre-

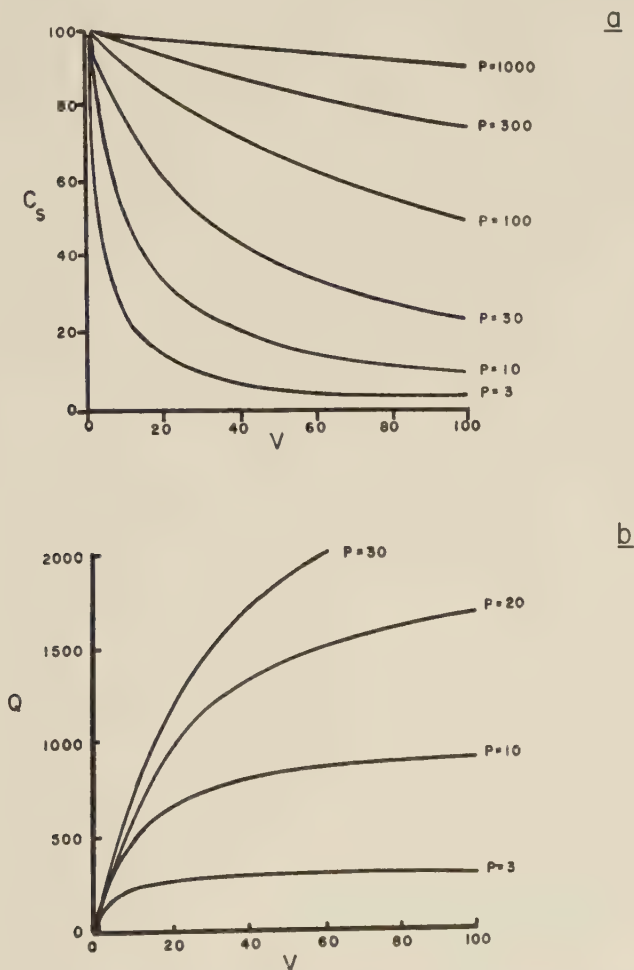


Fig. 4 (a) Theoretical curves for C_s as a function of V for various values of P . Calculated from equation (2b). (b) Theoretical curves for Q as a function of V for various values of P . Calculated from equation (1a).

sponding figures are 0.7 and 13.5—a 20-fold increase; for glycerol 3.0 and 44—a 15-fold increase; thiourea 14-fold; urea 8-fold; N-methylurea 7-fold. For these substances the deviations from the constant permeability hypothesis are gross and systematic.

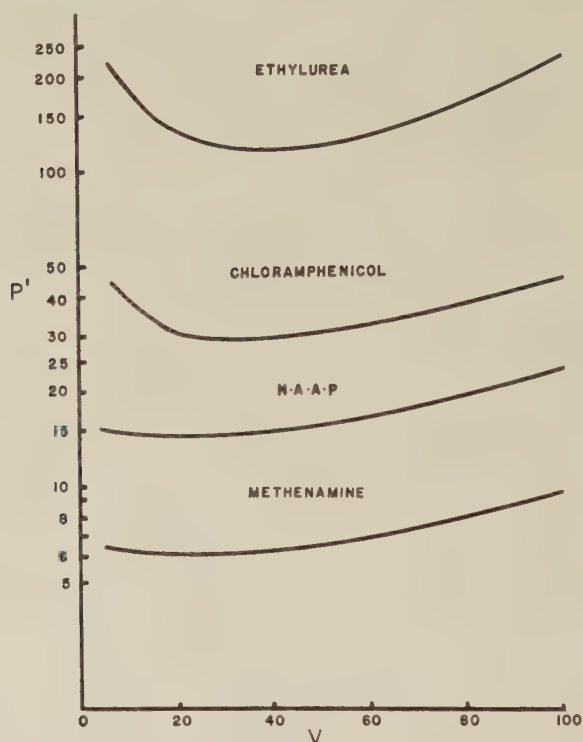


Fig. 5 Values of P' for the 4 Type I substances calculated from equation (2a).

It appears then that with increasing rate of saliva secretion the permeability increases very strikingly in the case of mannitol, creatinine and glycerol, to a somewhat lesser degree with urea, thiourea and methylurea and on a much smaller scale with ethylurea, NAAP, chloramphenicol and methenamine. Since the gland is in equilibrium with the extracellular space as far as the test molecules are concerned this increase in permeability must be in the same membrane as the per-

meability at low flow rates. For purposes of analysis we may regard the inner cell membrane as having two permeabilities in parallel.

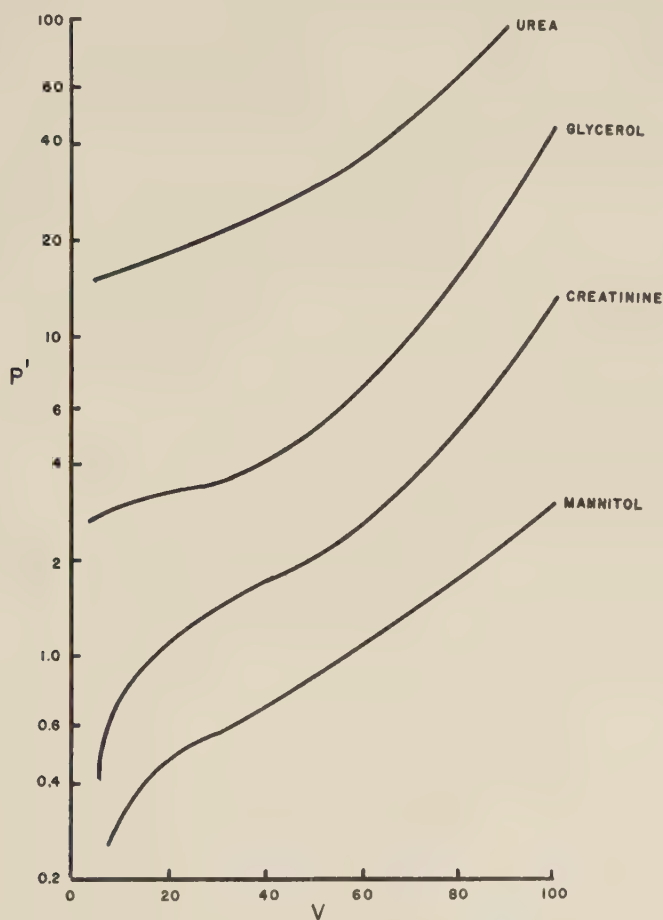


Fig. 6 Values of P' for 4 Type II substances calculated from equation (2a).

The increase in cell permeability may be visualized as occurring in one of two ways, either (a) the resting cell membrane is uniformly permeable to the test solutes, and with cell activation an overall increase in permeability occurs without change of the membrane selectivity; (b) in the resting

cell the solute penetrates mainly through the membrane lipid, perhaps also through sparsely distributed pores in the lipid, with cell activation the lipid is unchanged, but the pores increase in size and number.

In the first case both the resting and active permeabilities will be related mainly to the lipid solubilities of the molecules and only to a minor extent to molecular size. In the second case the resting permeability will be mainly related to lipid solubility and the active permeability to molecular size.

The properties of two permeabilities in parallel can be best understood by using the formal identity of Fick's equation with Ohm's law.

$$\frac{dQ}{dt} = P(C_1 - C_2)$$

is identical with

$$\frac{dQ}{dt} = I = G(E_1 - E_2)$$

where G is the electrical conductivity.

Now G and P are dimensionally equivalent and the same network properties will apply to both.

Parallel conductivities are additive, thus

$$G_{\text{total}} = G_1 + G_2 + \dots G_n$$

similarly

$$P_{\text{total}} = P_1 + P_2 + \dots P_n$$

We may therefore obtain the value of P' for zero flow — that is the resting state and subtract this from the value of P' for any flow rate to find the parallel permeability added to the resting permeability at this flow. We may call the resting permeability at $V=0$, P''_0 and obtain it by extrapolating the plot of P' to the ordinate after correcting for osmotic reabsorption (see below). The second partial permeability is designated P'' and is obtained by the relationship

$$P''_v = P'_v - P''_0$$

For simplicity P''_{100} (i.e. $V=100$) is used for the second

function. We can now examine P''_0 and P''_{100} as a correlate of the molecular size and oil-water distribution coefficients of our test substances, listed in table 1.

In figure 7 a and b are plots of P''_0 and P''_{100} against molecular weight. While there is some tendency for P''_0 to decrease with increase in molecular weight (chloramphenicol—No 6 being the main exception) the correlation is poor. However

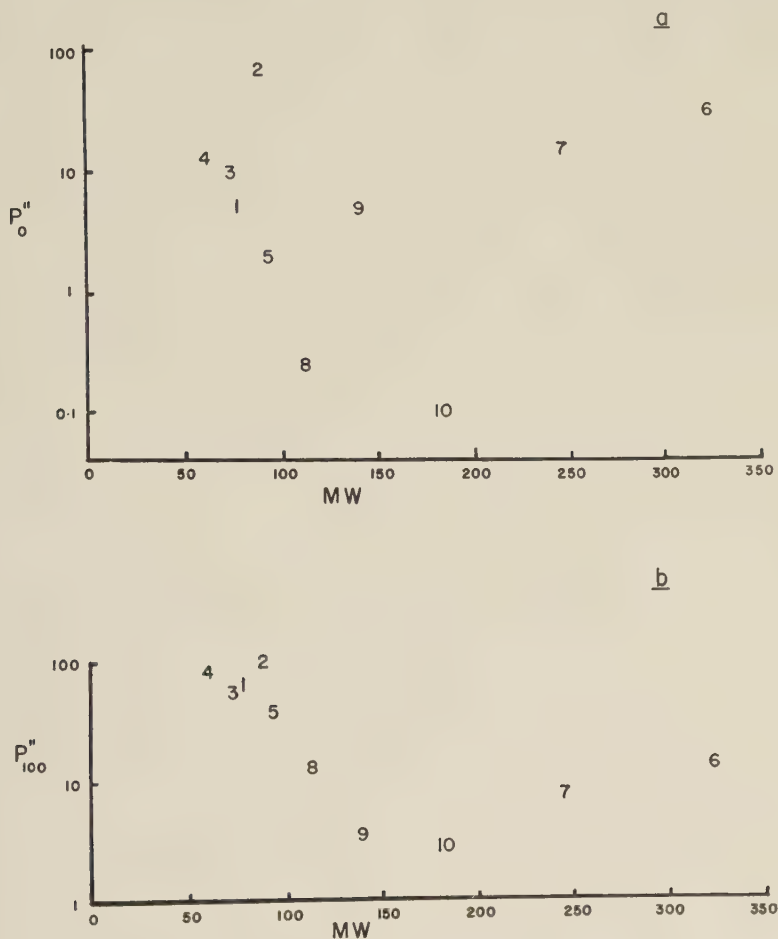


Fig. 7 Dependence of the permeation constant on molecular weight. Ordinate (a): P''_0 ; ordinate (b): P''_{100} . Abscissa: molecular weight.

the correlation of molecular weight with P''_{100} is better — with a steep decline in permeation for substances with $MW > 100$ ($\sim 3.2 \text{ \AA}$ molecular radius). Both chloramphenicol and NAAP give values higher than expected, the deviation for chloramphenicol being due in all probability to its exceptionally high lipid solubility (cf. table 2). The existence of some dependence of P''_o on molecular size can be shown more clearly by plotting $\frac{P''_o}{B}$ against MW (fig. 8), where B is the

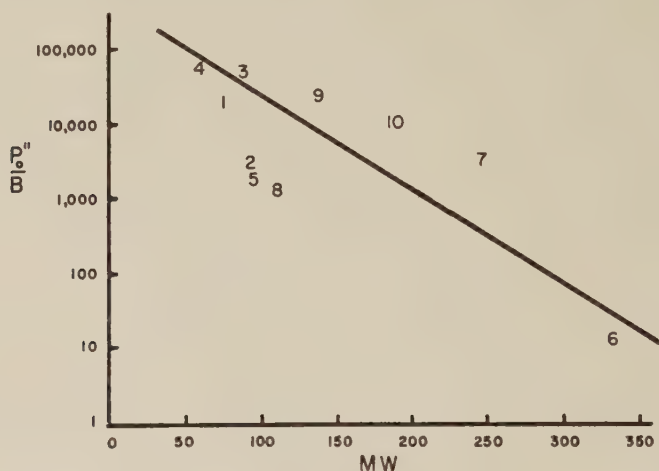


Fig. 8 Relationship of P''_o to molecular weight/oil-water distribution coefficient.

oil/water distribution coefficient), the anomalous positions of chloramphenicol and NAAP are now eliminated. The dependence is unusual however as $\frac{P''_o}{B} \propto MW^{-3}$ (approximately) instead of the proportionality to $MW^{-\frac{1}{2}}$ expected for free diffusion in solution and through non-porous membranes.

Figure 9a and b shows the plot P''_o and P''_{100} against the oil/water distribution coefficient B . In this case P''_o shows quite a significant correlation with B but P''_{100} shows very little. The value of P''_o for chloramphenicol is considerably lower than might be expected for a substance of such high lipid solubility. The plotting of $P''_o \sqrt{MW}$ or $P''_{100} \sqrt{MW}$ instead of P''_o and P''_{100} does not improve the correlation.

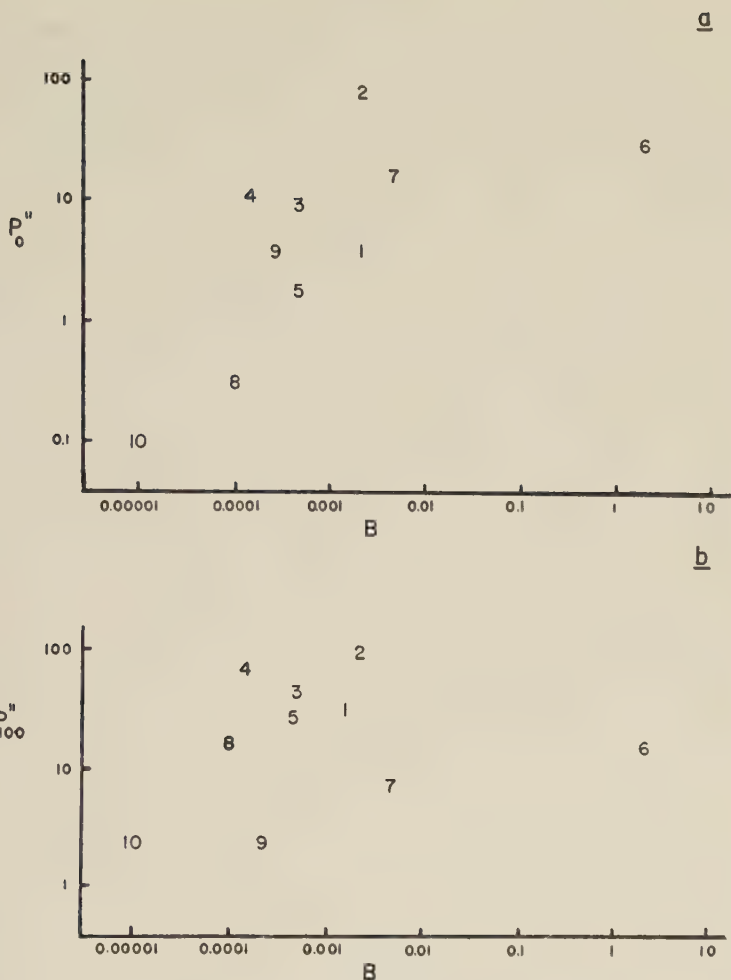


Fig. 9 Dependence of the permeation constant on the oil water distribution coefficient. Ordinate (a): P_o'' ; ordinate (b): P_{100}'' . Abscissa: olive oil-water distribution coefficient.

Davies ('50) has shown that most of the depression of permeability at a cell membrane may be attributed to the energy hump that must be surmounted in order that the transition of the molecule from lipoid to water phase (or vice versa) may occur. An oil/water coefficient greater than *one* will therefore impose the same order of hindrance to perme-

ation that will be imposed by a lipoid solubility below *one*. The minimum energy barrier exists when the oil/water solubility is unity. The anomalous position of chloramphenicol is thus due to the oil/water solubility being greater than unity — its correct position would be for an O/W coefficient of ~ 0.4 (i.e. the W/O coefficient).

These results may be summarised as follows: P''_0 shows a strong dependence on the lipoid solubility of the molecules and little dependence on their size, whereas P''_{100} shows a strong dependence on molecular size but practically none on lipoid solubility.

The dependence of both P''_0 and P''_{100} on molecular size is related to the power of the molecular weight in the manner to be expected for permeation through a membrane containing pores rather than a dependence on the square root of molecular weight expected for a membrane without an organized structure.

It is instructive to convert the permeation constant found in this work to approximate values in c.g.s. units. This may be done by converting flow rates to $\text{cm}^3/\text{g}./\text{sec.}$ and by making an estimate of (a) the area of membrane through which the solute is diffusing, and (b) the thickness of the cell membrane. The area of membrane calculated from histological measurements is $7.5 \times 10^3 \text{ cm}^2/\text{g.}$; the thickness of the membrane has been assumed to be 100 \AA (cf. Davson, '51). The use of these values will only give an approximate value for D' , the restricted diffusion coefficient, but the order of difference from the free diffusion coefficient is so great that they are adequate.

$$D' = P' \times 1.2 \times 10^{-14} \text{ cm}^2/\text{sec.}$$

Table 3 shows that the diffusion of the solutes through the cell membrane was at least a million times slower than for free diffusion — this is the order of difference found for other cells and justifies the assumption made earlier that the inner cell membrane could be treated as a sharp discontinuity with no appreciable diffusion gradient in the adjoining solvent.

It will have been noticed in figures 1 and 2 that at very low rates of secretion we may see saliva concentrations that are higher than the concurrent plasma concentration and corresponding with these we often see a rise in P' at low flow rates. These phenomena are only seen with substances that penetrate into the saliva relatively easily (especially with urea, thiourea, methylurea). Since all these substances appear to behave passively with respect to saliva/plasma ratio, it seems reasonable to look for a common mechanism which could concentrate them, without acting directly upon them. The most likely explanation is solvent (i.e. water) reabsorption. Water reabsorption in the acini would produce no change in the system of transfer by diffusion that appears to operate for Type I compounds and hence could produce no concentration of solute; such water uptake in the acini must be regarded simply as a fraction of the total water influx which is taken into account in measuring the rate of water secretion, i.e., net water flux. To account for the concentration of solute the water reabsorption must be occurring in the duct system. A water reabsorption in the ducts is to be expected in view of the relatively large osmotic gradient between the saliva and blood at low flow rates (0.20–0.25 Osmols) (Burgen, '55) and the improbability that the duct system could be completely impermeable to water molecules.

It is simple to make a rough calculation of the magnitude of the water reabsorption in the ducts by finding the minimum water loss correction required to prevent the P' curve rising at the low end. When C_s rises above 100 this can be made with reasonable accuracy. Equation 2a then becomes

$$P' = \frac{(V + \Delta V) \cdot \frac{C_s V}{(V + \Delta V)}}{100 - \frac{C_s V}{V + \Delta V}} \quad 3a$$

where ΔV is the amount of water reabsorbed/gm/minute which reduces to

$$\Delta V = \frac{V(100P' - [P' + V] C_s)}{V \cdot C_s - 100P'} \quad 3b$$

If the osmotic pressure of saliva and plasma is known for these samples then the water permeability may be calculated thus

$$P_{\pi \text{ water}} = \frac{\Delta V}{\Delta \pi} = \text{mg water/g./Osmol/min.}$$

(where $\Delta \pi$ = plasma — saliva osmotic difference in Osmols). The osmotic pressure of saliva and plasma was measured cryoscopically in many of these experiments (Burgen, '55) and can therefore be used in these calculations. Table 2 shows the results of such calculations in 8 experiments — the value of P_{π} ranged from 5–40 m/g./Osmol/min. with a mean water permeability of 21 ± 4 (SE of mean). It would be expected that the order of absorption obtained would be the same for all substances if the mechanism was a common passive concentration and the results in the table despite their low order of accuracy seem to bear this out.

TABLE 2
Magnitude of osmotic water reabsorption in salivary duct system

TEST NON-ELECTROLYTES	OSMOTIC REABSORPTION COEFFICIENT (mg H ₂ O/g./Osmol/min.)
Urea (a)	18
Urea (b)	5
Methylurea (a)	23
Methylurea (b)	40
Ethylurea (a)	30
Ethylurea (b)	15
Methenamine	18
Chloramphenicol	17
	<hr/> 21 \pm 4 <hr/>

TABLE 3

	D' 37°C.		D 37°C.	D/D' V = O
	V = O	V = 100 cm ² /sec.		
Urea	1.4×10^{-13}	1.2×10^{-12}	1.7×10^{-5}	1.2×10^8
Ethylurea	1.2×10^{-12}	2.3×10^{-12}	1.2×10^{-5}	1×10^7
Glycerol	1.6×10^{-14}	5×10^{-13}	1.1×10^{-5}	6.6×10^8
Mannitol	1.2×10^{-15}	3.7×10^{-14}	0.84×10^{-5}	7.2×10^9
Chloramphenicol	3.7×10^{-13}	5.3×10^{-13}	0.62×10^{-5}	1.7×10^7

It is interesting that the plots of P' for substances which penetrate into the saliva with difficulty (fig. 6) such as mannitol and creatinine do not show this upswing at low flow rates. The reason is seen by a consideration of equation 3a. For these substances because C_s is small the denominator

$$100 - \frac{C_s V}{V + \Delta V} \div 100$$

Equation 3a therefore may be written approximately as

$$P' = \frac{C_s V}{100} \quad 3c$$

which is independent of ΔV .

The permeability properties of the salivary gland suggest that the inner cell membrane consists of a lipid layer interrupted by water-filled pores. At rest, molecules are able to penetrate through the lipid matrix and only to a limited extent through the pores, and with activity the increase in permeability is due to an increase in permeability through the pores. The results in figure 7 show that the diameter of these pores is such that molecules with a radius greater than 3.2 Å pass only with considerable difficulty. The marked increase in permeability shown for mannitol and creatinine on cell activation presumably means that the *mean pore diameter increases*. It is not possible to decide whether this accounts for the whole of the increase in permeability or whether an increase in the number of pores also occurs.

Now our working hypothesis postulated that the increase of permeability with activity was due to an increased diffusion of the solutes owing to a change in membrane characteristics. But we must clearly try to distinguish between *increased diffusion* and *ultrafiltration* through water-filled pores. Thus while the results for some of the larger molecules indicate that these pass almost wholly through cell membrane lipid and not in solution in the secreted water, this does not settle the matter, it merely tells us that the membrane pores through which either diffusion or ultrafiltration is taking place are too small to admit more than a small fraction of these molecules.

While there may be little qualitative difference between the treatment of solutes by these two processes there may be large quantitative differences as Prescott and Zeuthen ('53) have found for water permeation into various eggs, where filtration was always a more rapid process than diffusion. Another factor may be that owing to the characteristics of molecular filtration, with a constant pore size, the concentration of solute in the ultrafiltrate decreases as the flow rate increases (Pappenheimer, '53). This would mean that to account for an increased permeability the pore size would have to increase somewhat more if it were due to filtration than if it were due to diffusion. Renkin ('54) has given a theoretical treatment of the problem of pore size in diffusion and filtration.

Work on the transfer of potassium ions across salivary cells (Burgen, '56) may throw some light upon this problem. When the gland is activated the outward permeability of the cell to potassium may increase up to 30-fold. This increase in permeability occurs at *both* the inner *and* outer face of the cell. The outflux of potassium at the outerface is running counter to the net *influx of water* so that in this case at least the increased solute transfer is due to increased diffusibility and not to filtration.

The distinction between filtration and diffusion through pores will probably remain uncertain until some procedure is devised that permits the dissociation of permeability to non-electrolytes from the rate of saliva secretion. Up to the present time no such procedure has been discovered.

SUMMARY

1. The secretion of 10 non-electrolytes in the dog's parotid saliva have been studied as a function of the rate of saliva secretion.
2. The secretion of these substances is passive.
3. The concentration of non-electrolytes in the saliva for a given rate of secretion is not time dependent.

4. Except at very low rates of secretion the concentration in saliva is lower than in the plasma; however, the concentration in the gland is the same as in the plasma.

5. Two types of concentration curves are found: (a) the concentration decreases with increase in rate of secretion, (b) the concentration decreases, passes through a minimum and then rises with further increase in rate of secretion.

6. Analysis of the concentration curves shows that penetration through the resting membrane is largely through the membrane lipid, but the increase in permeability with nerve stimulation is largely due to opening of water-filled pores in the membrane.

ACKNOWLEDGMENTS

I am indebted to Miss Norah Pedley for invaluable assistance and to Dr. K. G. Terroux and Mr. P. Seeman for help with some of the experiments. A generous supply of chloramphenicol (chloromycetin) was donated by Parke Davis and Co.

LITERATURE CITED

- AMBERSON, W. R., AND R. HOBER 1932 The permeability of mammalian salivary glands for organic non-electrolytes. *J. Cell. and Comp. Physiol.*, **2**: 201-121.
- ARAKI, Y. 1951 Nitrogenous substances in saliva. *2. Urea and rhodan*. *Jap. J. Physiol.*, **2**: 255-259.
- ARCHIBALD, R. M. 1945 Colorimetric determination of urea. *J. Biol. Chem.*, **157**: 507-518.
- BRATTON, A. C., AND E. K. MARSHALL 1939 A new coupling component for sulphonamide determination. *J. Biol. Chem.*, **128**: 537-550.
- BURGEN, A. S. V. 1955 The osmotic work of saliva secretion in the dog. *J. Cell. and Comp. Physiol.*, **45**: 465-478.
- 1956 The secretion of potassium in the saliva. *J. Physiol.*, **132**: 20-39.
- CHESLEY, L. C. 1944 A method for the determination of thiourea. *J. Biol. Chem.*, **152**: 571-578.
- CORCORAN, A. C., AND I. H. PAGE 1947 A method for the determination of mannitol in plasma and urine. *J. Biol. Chem.*, **170**: 165-171.
- DAVIES, J. T. 1950 The mechanism of diffusion of ions across a phase boundary and through cell walls. *J. Phys. Chem.*, **54**: 185-204.
- DAVSON, H. 1951 A textbook of general physiology. Churchill, London.

- DAVSON, H., AND J. F. DANIELLI 1943 The permeability of natural membranes. Cambridge University Press, Cambridge.
- FOLIN, O., H. WU 1919 A system of blood analysis. *J. Biol. Chem.*, *33*: 81-110.
- GLAZKO, A. J., L. M. WOLF AND W. A. DILL 1949 Biochemical studies on Chloramphenicol (Chloromycetin). I. Colorimetric methods for the determination of Chloramphenicol and related nitro compounds. *Arch. Biochem.*, *23*: 411-418.
- HOBER, R., ED. 1945 Physical chemistry of cells and tissues. Blakiston, Philadelphia.
- HOLST, E. J. 1944 Glycerol oxydation in the animal organism. *Acta Physiol. Scand.*, *7*: 69-79.
- JEANGROS, J. 1928 Untersuchungen über die Permeabilität der Zellen. XIV. Zur Frage der Ausscheidung der Zuckerarten durch die Speicheldrüsen. *Biochem. Z.*, *200*: 367-378.
- KENNEDY, T. J., J. G. HILTON AND R. W. BERLINER 1952 Comparison of inulin and creatinine clearance in the normal dog. *Am. J. Physiol.*, *171*: 164-168.
- KEYNES, R. D. 1951 The ionic movements during nervous activity. *J. Physiol.*, *114*: 119-150.
- O'DEA, J. F., AND R. A. GIBBONS 1953 The estimation of small amounts of formaldehyde liberated during the oxidation of carbohydrates and other substances with periodate. *Biochem. J.*, *55*: 580-586.
- PAPPENHEIMER, J. R. 1953 Passage of molecules through capillary walls. *Physiol. Rev.*, *33*: 387-423.
- PRESCOTT, D. M., AND E. ZEUTHEN 1953 Comparison of water diffusion and water filtration across cells surfaces. *Acta Physiol. Scand.*, *23*: 77-94.
- RENKIN, E. M. 1954 Filtration, diffusion and molecular sieving through porous cellulose membranes. *J. Gen. Physiol.*, *33*: 225-244.
- WOLDRING, M. G. 1955 Free amino acids of human saliva; a chromatographic investigation. *J. Dent. Res.*, *34*: 248-256.

THE ENTRY OF $P^{32}O_4$ INTO RAT BRAIN

E. STREICHER¹

Department of Physiology, University of Chicago, Chicago, Illinois

ONE FIGURE

While the mode of entry of $P^{32}O_4$ into the brain is still a matter of some conjecture, it has generally been assumed that the rate of phosphate penetration is quite low due to the relative impermeability of the blood-brain barrier and/or the blood-cerebrospinal fluid barrier to this ion. However, if the movement of phosphate from blood to brain were slow in relation to the rates of intracellular phosphorylations, the specific activities of the various phosphorylated compounds should change temporally at approximately the same rate. Under these circumstances, the specific activities of the different brain constituents would remain unaffected by an increase or moderate decrease in phosphate turnover, since all fractions will have attained radioactive equilibrium with each other. Also, the total radioactivity of the brain could then be used as an index of barrier permeability to $P^{32}O_4$. To ascertain the validity of these assumptions and the constraints which would be imposed upon the method of measuring cerebral metabolism *in vivo* with P^{32} , specific activity-time curves were obtained for several phosphorylated moieties of rat brain.

METHODS

Male Sprague-Dawley rats weighing approximately 250 gm (± 15 gm) were employed in these studies. Each animal was injected intraperitoneally with 200 μ c of hydrolyzed P^{32} in the form of $Na_2HP^{32}O_4$. After various time intervals rang-

¹ Present address: Section on Aging, National Institute of Mental Health, Bethesda, Md.

ing from 20 minutes to 20 hours, the animals were sacrificed by decapitation. The heads were frozen immediately in dry ice and acetone, and a sample of mixed blood was obtained from each carcass. The blood was centrifuged at 4°C., the acid-insoluble compounds of the plasma were precipitated with cold 10% trichloroacetic acid (TCA), and the inorganic phosphate of the plasma was precipitated as MgNH_4PO_4 . The frozen brains were chipped out of the skulls with a hammer and chisel, and the brain tissue was homogenized in cold 10% TCA. The acid-soluble compounds were separated into inorganic phosphate, delta 7 phosphate and organic acid-soluble fractions, the last mentioned comprising, for the most part, the phosphate of the glycolytic intermediates. The delta 7 fraction consisted of labile phosphate derived from adenosine triphosphate and phosphocreatine by hydrolysis in 1 N hydrochloric acid at 100°C. for 7 minutes. The acid-insoluble compounds were separated by the method of Schneider ('45). The phosphorus of the following crude fractions was obtained by precipitation as MgNH_4PO_4 , or by ashing in 10 N sulphuric acid for 12 hours at 110°C.: inorganic phosphate, delta 7 phosphate, organic acid-soluble (OAS), phospholipid (PL), phosphoprotein (PP), and total nucleic acid (NA). A 1 ml aliquot of each fraction was counted in liquid form and analyzed for phosphate by the method of Fiske and Subbarow ('25) as modified by Gomori ('42). The material was counted by means of an Eck and Krebs-type Geiger-Mueller counting tube, Model 10-A, manufactured by the Radiation Counter Laboratories. The coefficient of variation of the counts ($\frac{\sqrt{N}}{N} \times 100$) and was less than 4%.

The values obtained for the specific activities of the inorganic phosphate fractions have been omitted from the results because of the contamination of these samples with phosphate derived from blood, bone, and the breakdown of labile compounds. However, when reasonable values for inorganic phosphorus were obtained (about 20 mg %) the specific activities of these fractions were approximately equal

to those of the delta 7 fractions. This is in accordance with the findings of Sacks and Culbreth ('51).

In these experiments, the results which were obtained in each fraction have been expressed in terms of (1) absolute specific activities (counts/minute)/(microgram of phosphorus) and (2) as relative to the maximum specific activity that was observed. The magnitude of the absolute specific activity reflects the turnover rate of a fraction, while the use of relative specific activities affords a convenient method of comparing curves independent of amplitude.

RESULTS AND DISCUSSION

It was observed that the absolute specific activities of most fractions increased continuously for 20 hours, while the specific activity of the delta 7 fraction attained its maximum after one hour (table 1, fig. 1).

At the 20 minute interval, the absolute and relative specific activities of all compounds are dissimilar and are logically arranged in the descending order: delta 7, OAS, PP, NA, and PL, according to expectation. Starting at the one hour mark, the relative specific activities of the OAS, PP, and NA fractions are almost identical, indicating that by this time the availability of inorganic phosphate for subsequent incorporation had become limiting, except for the slowly exchanging PL component.

The rate of phosphate entry into the brain is at least partially determined by the concentration gradient of $P^{32}O_4$ between blood and brain. If the differential is sufficiently large, the rate of penetration of the ion is not limiting with respect to intracellular phosphorylation. Under the experimental conditions described above, this situation was in effect for most fractions for less than 60 minutes after the administration of the tracer. Temporally, this coincided with a precipitous rise and decline in the plasma specific activity and with the rising phase of the delta 7 specific activity-time curve. At the one hour mark, when the rate of entry had become limiting, the specific activity of the inorganic phos-

TABLE 1

The specific activities of various fractions of normal rat brain at various times after the intraperitoneal injection of 200 μ c of P^{32} per animal

FRACTION	20 MINUTES	1 HOUR	4 HOURS	20 HOURS
Inorganic phosphate of plasma (± 1 S.D.) ¹	1278 (± 382)	752 (± 247)	219 (± 117)	110 (± 2.2)
% Maximum sp. ac. measured	100	58.8	17.1	8.6
Delta 7 (± 1 S.D.)	21.0 (± 4.3)	39.3 (± 7.1)	34.6 (± 4.0)	29.8 (± 2.6)
% Maximum sp. ac. measured	53.4	100	88.0	75.8
Organic acid-soluble (± 1 S.D.)	3.3 (± 0.82)	7.3 (± 1.3)	11.2 (± 1.4)	16.6 (± 2.6)
% Maximum sp. ac. measured	19.9	44.0	67.5	100
Phosphoprotein (± 1 S.D.)	1.4 (± 0.26)	4.3 (± 0.23)	7.1 (± 0.55)	11.0 (± 2.0)
% Maximum sp. ac. measured	12.7	39.1	64.5	100
Total nucleic acid (± 1 S.D.)	0.39 (± 0.10)	1.6 (± 0.16)	2.5 (± 0.12)	4.0 (± 0.22)
% Maximum sp. ac. measured	9.8	40.0	62.5	100
Phospholipid (± 1 S.D.)	0.057 (± 0.018)	0.24 (± 0.16)	0.95 (± 0.26)	3.0 (± 0.0)
% Maximum sp. ac. measured	1.9	8.0	31.7	100
Number of animals	3	3	3	2

$$^1 \text{S.D.} = \sqrt{\frac{\sum x^2}{N-1}}$$

phate of the plasma was approximately 19 times that of the delta 7 fraction. There appears to be little doubt however, that the ion can traverse the blood-brain barrier, as well as the blood-cerebrospinal fluid barrier (Bakay, '54). In fact, the slow descent of the rapidly exchanging delta 7 fraction

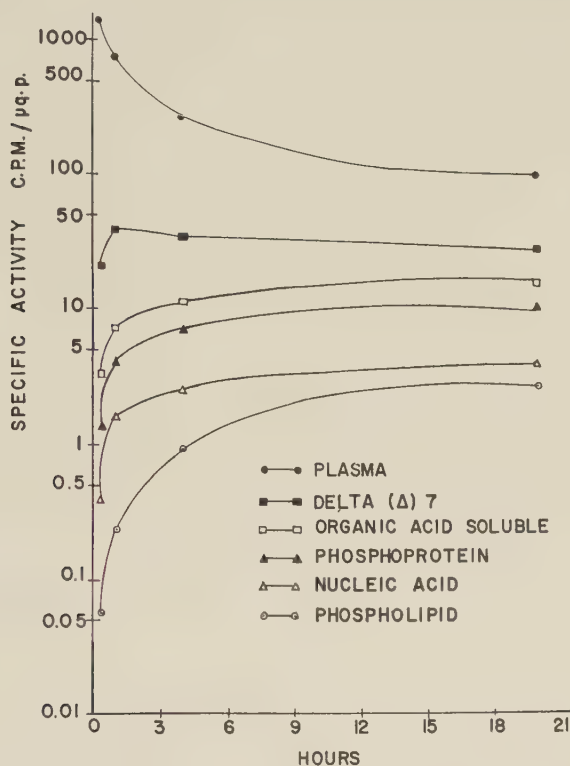


Fig. 1 Specific activity-time curves of various phosphate-containing fractions of rat brain.

after one hour suggests that the cerebrospinal fluid may provide a secondary source of the tracer, although the shape of this portion of the delta 7 specific activity-time curve may well represent a damped reflection of the plasma specific activity-time curve.

In cerebral metabolic studies where the tracer is employed to measure comparative rates of phosphate exchange under

various physiological conditions, the animals must be sacrificed some time before the rate of entry of the ion becomes limiting relative to rates of intracellular phosphorylations. Under the present experimental conditions the duration of the experiment would preferably be limited to 20 minutes or less to ascertain the effects of altered turnover on the specific activities of most fractions. This time interval would be significantly prolonged if the specific activity of the plasma inorganic phosphate were maintained at a constant level for the duration of the experiment, i.e., maximizing the concentration gradient of $P^{32}O_4$ between blood and brain. Also because of its very low rate of phosphate exchange, metabolic fluctuations would be reflected in the phospholipid fraction for at least several hours after the administration of a single dose of the tracer. Of course specific activity-time curves should be obtained under any set of experimental conditions to ascertain the optimal duration of the experimental period and to evaluate the restrictions imposed by the blood-brain barrier. For example, using mice, Dawson and Richter ('50) observed a 15% decrease in the relative specific activity of the phospholipid and nucleoprotein fractions after three hours of pentobarbital anesthesia, while in a 20 minute experiment employing rats, decrements of 30 to 40% were observed in the phosphoglyceric acid, phosphoprotein, and phospholipid fractions (Streicher, '54).

Since exchange in the phospholipid fraction is not restricted to the same extent as in the PP, OAS, and NA fractions by the availability of P^{32} , the specific activity or total counts recovered from brain tissue can be used only as a rough measure of barrier permeability several hours after the administration of a single dose of the tracer. The PL fraction contributes less than 0.5% of the total number of counts 20 minutes after P^{32} is injected, but accounts for approximately 15% of the total radioactivity of the brain 20 hours later.

Aside from the existence of blood-extracellular fluid barriers, the apparent movement of $P^{32}O_4$ into tissues may be influenced by several other factors. An unknown fraction of

the tissue inorganic phosphate may be unavailable ("isolated") (Juni et al., '48) or only slowly available for exchange. The tracer may not freely permeate the cell membrane or cytoplasm. Also, it should be noted that the specific activity of a relatively small pool of tissue inorganic phosphate is constantly modified not only by exchange with the plasma or extracellular fluid, but in addition by exchange with a relatively enormous amount of acid-insoluble phosphate of low specific activity.

The possible influence of these factors may be illustrated in the observations of Hevesy and Hahn ('40). By intermittent injections of $P^{32}O_4$, the specific activity of the inorganic phosphate of the plasma of rabbits was maintained at a constant level from 100 minutes to 50 days. They reported that the inorganic phosphate of the kidney was virtually at radioactive equilibrium with the plasma after 100 minutes, while the specific activity of the inorganic phosphate of the brain, as well as muscle, increased continuously for 50 days, and at the end of this period was found to be 56 and 88% respectively that of the plasma. Eleven and one-half hours after the start of the experiment, the specific activity of the inorganic phosphate of muscle was only 17.6% of the 50 day value, despite the absence of a blood-muscle barrier to $P^{32}O_4$.

SUMMARY

Analysis of specific activity-time curves for several phosphorylated moieties of rat brain indicates that, with the exception of the phospholipid fraction, the rate of $P^{32}O_4$ entry into rat brain becomes limiting relative to intracellular phosphorylation within one hour after the administration of a relatively large dose of the tracer. The significance of these observations to cerebral metabolic studies conducted *in vivo* with P^{32} has been discussed.

LITERATURE CITED

- BAKAY, L. 1954 Studies on the blood-brain barrier with radioactive phosphorus. IV. Spatial aspects of phosphate exchange between plasma and brain. Arch. Neurol. Psychiat., 71: 673.

- DAWSON, R. M. C., AND D. RICHTER 1950 The phosphorus metabolism of the brain. *Proc. Roy. Soc. B.*, *137*: 252.
- FISKE, C. H., AND Y. SUBBAROW 1925 The colorimetric determination of phosphorus. *J. Biol. Chem.*, *66*: 375.
- GOMORI, G. 1942 A modification of the colorimetric phosphorus determination for use with the photoelectric colorimeter. *J. Lab. and Clin. Med.*, *27*: 955.
- HEVESY, G., AND L. HAHN 1940 Rate of renewal of the acid soluble organic compounds in the organs and the blood of the rabbit. *Klg. Danske Vidensk. Selskab. Biol. Medd.*, *15*: No. 7.
- JUNI, E., M. D. RAMAN, J. M. REINER AND S. SPIEGELMAN 1948 Turnover and distribution of phosphate compounds in yeast metabolism. *Arch. Biochem.*, *18*: 387.
- SACKS, J., AND G. G. CULBRETH 1951 Phosphate transport and turnover in the brain. *Am. J. Physiol.*, *165*: 251.
- SCHNEIDER, W. C. 1945 Phosphorus compounds in animal tissues. I. Extraction and estimation of desoxypentose nucleic acid and of pentose nucleic acid. *J. Biol. Chem.*, *161*: 293.
- STREICHER, E. 1954 Effect of anesthetic and convulsant drugs on P^{32} exchange in rat brain. *Fed. Proc.*, *13*: 146.

STUDIES ON THE INDIVIDUAL AND JOINT EFFECTS
OF HISTAMINE AND AN ANTIHISTAMINIC
ON GROWTH, CONTRACTILITY AND
PLASMOCRINE ACTIVITY IN
CULTURES OF EMBRY-
ONIC CHICK
HEART¹

KENNETH M. RICHTER

*Department of Anatomy and the Tissue Culture and Experimental Cell Study
Laboratory, University of Oklahoma School of Medicine, Oklahoma City*

EIGHTEEN FIGURES

INTRODUCTION

Although not in uniform agreement as to details, numerous "in vivo" studies indicate that histamine and antihistaminics influence such general fundamental processes as contraction, growth and secretion (Goodman and Gilman, '41; Feinberg, Malkiel and Feinberg, '50). In contrast, relatively few studies on the effects of these drugs on tissues grown "in vitro" have been made. At the time the present study was initiated, all previous work had been limited to the influence only of histamine on growth and general cytomorphology and the observations were not in uniform agreement (Funayama, '38; Heubner and Schreiber, '40; Lettré and Albrecht, '41, '43; Pomerat and Emerson, '44). The present study concerns the individual and joint effects of histamine and an antihistaminic on the growth, contractility, plasmocrine activity and special cytomorphology of heart tissues grown in culture.²

¹ Supported by Grants-in-Aid from the Helen Hay Whitney Foundation.

² Portions of this study were presented at the 1954 Tissue Culture Association Meeting in Galveston.

MATERIALS AND METHODS

To obtain comparative data on the individual and joint effects of histamine (histamine-di-hydrochloride, Hoffman-La-Roche) and an antihistamine (chlor-trimeton Maleate, Schering), 4 general groups of cultures were set up from pooled ventricular heart fragments of 8-12 day old chick embryos. The same nutrient medium was used in all the groups and was varied from the control group (I) only by the addition of 10 or 100 μ of histamine/cc (group II), of 10 or 100 μ g of antihistamine/cc (group III), and of 10 or 100 μ g each of histamine and antihistamine/cc (group IV). The basic nutrient consisted of 5% 8-day chick embryo extract, 45% human ascitic fluid, and 50% Tyrode. In some series, the conventional chicken plasma clot was used in addition to this fluid nutrient, but the drug concentrations were kept the same as those above.

The heart fragments were cultured by roller tube, hanging drop or special perfusion chamber techniques for two days at 37.5 C. All cultures were checked twice daily to obtain data on pulsatile activity, growth and general cytomorphology. In addition, representative live cultures were examined after 24 hours with the phase microscope for data on mitochondria, golgi complex, plasmocrine material, nucleoli etc. The latter structures were again studied in detail by phase contrast at the end of two days after fixation in 1% osmic acid.

For phase contrast time-lapse motion picture data, the cultures were set up in special perfusion chambers in control media and grown for 24-48 hours. The activities of selected cell groups in the growth zone were then recorded for 2-4 hours before and 6-8 hours after starting a nutrient containing 100 μ g histamine/cc through the chamber.

The recommended therapeutic blood level of several different antihistamines currently used is approximately 10-30 μ g/cc blood/4-5 hours. The experimental drug concentrations used in this study approximate closely the general minimal therapeutic (10 μ g/cc) and toxic concentrations (100 μ g/cc).

The level of 10 μg of histamine/cc of medium was selected arbitrarily on the basis (1) that total blood histamine may range from .1 to 18.3 $\mu\text{g}/\text{cc}$ (Valentine, Pearse and Lawrence, '50) and (2) that heart tissue of cattle, dog, and rabbit contains an average of 8.48 $\mu\text{g}/\text{gm}$ of tissue (Ishihara and Iwao, '38). The concentration of 100 $\mu\text{g}/\text{cc}$ was selected arbitrarily and in keeping with the 10-fold concentration of antihistamine used.

RESULTS

The relative effects individually and jointly of histamine and antihistamine at 10 and 100 $\mu\text{g}/\text{cc}$ on the pulsatile contraction of cardiac muscle tissue of the explants are summarized respectively in tables 1 and 2. The data so presented is based on hanging drop cultures grown in a fluid medium. The statistical reliability of the data is as indicated (tables 1, 2). Daily observations on contraction were in general accord with the tabulated data and showed further that pulsatile contraction was lacking in the majority of cultures 8–12 hours after starting treatment with (a) 10 or 100 μg of antihistamine/cc (III), (b) with 100 μg of histamine/cc (II), and (c) with 100 μg each of histamine and antihistamine/cc (IV).

The comparative effects individually and jointly of histamine and antihistamine at 10 and 100 $\mu\text{g}/\text{cc}$ on fibroblast growth in the explants are summarized respectively in tables 1 and 2. Fibroblast growth when it occurred, was uniformly dense and extensive in both the control (I) and experimental groups (II, III, IV) when the drug levels used were 10 $\mu\text{g}/\text{cc}$. At drug levels of 100 $\mu\text{g}/\text{cc}$, fibroblast growth was dense in the control group but uniformly thin in the experimental groups (II, III, IV) when it occurred.

Phase contrast studies of the osmic fixed fibroblasts revealed that irrespective (1) of whether the cells were treated with histamine or antihistamine or jointly with them, or (2) whether the drug level was 10 or 100 $\mu\text{g}/\text{cc}$, there were no apparent changes from normal in the structural appearance

TABLE 1

Data relative to individual and joint effects of 10 $\mu\text{g}/\text{cm}^3$ of histamine-HCl and antihistamine on the end-points, contractility and growth

EXPERIMENTAL GROUP	NUMBER OF CULTURES	NUMBER OF CULTURES CONTRACTING AFTER 24 HRS.			NUMBER OF CULTURES GROWING AFTER 24 HRS.		
		Actual number	Actual value in	Relative value in	Actual number	Actual value in	Relative value in
			%	%		%	%
I Controls	84	25	30	100	56	67	100
II Histamine	91	25	28	93	63	69	103
III Antihistamine	97	10	10	33	48	50	73
IV Histamine and antihistamine	104	17	16	53	95	91	136
Totals	376	77			262		
Statistical treatment:		χ^2 sig P less than .01			χ^2 sig P less than .001		

TABLE 2

Data relative to individual and joint effects of 100 $\mu\text{g}/\text{cm}^3$ of histamine-HCl and antihistamine on the end-points, contractility and growth

EXPERIMENTAL GROUP	NUMBER OF CULTURES	NUMBER OF CULTURES CONTRACTING AFTER 24 HRS.			NUMBER OF CULTURES GROWING AFTER 24 HRS.		
		Actual number	Actual value in	Relative value in	Actual number	Actual value in	Relative value in
			%	%		%	%
I Controls	66	30	46	100	47	71	100
II Histamine	39	3	8	17	10	26	37
III Antihistamine	50	0	0	0	30	60	85
IV Histamine and antihistamine	48	0	0	0	23	48	68
Totals	203	33			110		
Statistical treatment:		χ^2 sig P less than .001			χ^2 sig P less than .001		

of the nuclei, nucleoli, or mitochondria of these cells (figs. 1-10). However, significant differences between the various groups (I, II, III, IV) were noted relative to the golgi bodies and associated vacuolar or plasmocrine droplets of these cells. Further, these group differences varied according to whether the drug concentration was 10 $\mu\text{g}/\text{cc}$ (figs. 1-4) or 100 $\mu\text{g}/\text{cc}$ (figs. 5-10). In control group fibroblasts, the golgi bodies consisted of reduced numbers of small, dark granules which were intimately associated with the surfaces of a few but prominent vacuolar droplets with the whole being definitely oriented at the nuclear pole (fig. 1) (Pfuhl, '33; Porter, Claude and Fullam, '45). At general drug concentrations of 10 $\mu\text{g}/\text{cc}$, the histamine treated (II) and antihistamine treated (III) fibroblasts showed increased numbers of vacuolar or plasmocrine droplets and associated golgi bodies (figs. 2, 3), while the jointly treated fibroblasts (IV) showed only golgi bodies and plasmocrine droplets (fig. 4) which were in size, number and distribution identical to those of the control group cells (fig. 1). At general drug concentrations of 100 $\mu\text{g}/\text{cc}$, the histamine treated fibroblasts (II) showed relative to the control cells an extensive increase in the amount and number of plasmocrine droplets and golgi bodies (figs. 6, 7). In antihistamine treated cells (III) the plasmocrine droplets and golgi granules were in excess of those in control cells (I) and less abundant than those in the histamine treated ones (II) (compare figs. 6, 7, 8). Fibroblasts treated jointly with 100 μg each/cc of histamine and antihistamine (IV) contained much more plasmocrine material than the controls (compare figs. 1, 5, 9, 10) and somewhat less than the histamine treated cells (II) (compare figs. 6, 7, 9, 10).

Time-lapse motion picture records (one frame/15 seconds) showed that fibroblasts in cultures treated with histamine at 100 $\mu\text{g}/\text{cc}$ showed almost immediate increases in the amount of intracellular plasmocrine material and in the degree and rate of cell surface activity. The latter was characterized by numerous, short, rounded and blunt-tipped ectoplasmic processes which were asynchronously formed and retracted. This

type of surface activity ceased in certain cells of the fibroblast growth zone after approximately two hours. These cells became ovoid in shape (figs. 11-14) and then began to pulsate slowly in regular fashion (figs. 15-18) for several hours. Frame-by-frame analysis of the pictures revealed that the average duration of each pulsatile contraction was about 45 seconds. The relaxation phase (figs. 16, 17, cells A, B) averaged 30 seconds and the contraction phase (figs. 15, 18, cells A, B) averaged 15 seconds, although there were minor variations in the duration of these phases in each cell analyzed. In the relaxation phase the cells increased notably in length (figs. 16, 17) and during the contraction phase shortened and acquired repeatedly a characterizing form and size (figs. 15, 18). The gross configuration of the cells in the contraction phase is practically identical to that possessed by them prior to active pulsatile contraction (figs. 11-14, 15, 18) and suggests that the initial rounding up may possibly represent a kind of contracture. The other, non-pulsating, cells in the growth zone continued to show much surface activity for several hours when the ectoplasm of many appeared to localize as or become the sites of large fluid blisters. Eventually, all surface activity ceased and the cells became quiescent.

DISCUSSION

It appears to be generally assumed concerning the antagonistic action of histamine and antihistamine (1) that the biologic response to either of these substances should be reversible by the other (Jahn and Danforth, '52) and (2) that antihistamines exert prominent antihistaminic effects only in presence of histamine (Feinberg, Malkiel and Feinberg, '50).

The individual and joint effects of histamine and antihistamine on the contraction of cardiac muscle. It is generally accepted that high concentrations of histamine and prolonged treatment with relatively small amounts effect functional disturbances and a general weakening of cardiac muscle "in vivo" and that small amounts have little or no effect on heart

action (Goodman and Gilman, '41; Wright and Montag, '51; Feinberg, Malkiel and Feinberg, '50). The results of the present study are in general agreement with these "in vivo" findings, in that spontaneous contraction of cardiac muscle in culture is not altered by low concentrations ($10\text{ }\mu\text{g/cc}$) but is markedly inhibited by high concentrations ($100\text{ }\mu\text{g/cc}$, tables 1, 2). Although there seems to be no positive evidence that histamine stimulates the contraction of cardiac muscle "in vivo"; it is well-known that it does stimulate smooth muscle contraction (Barsoum and Gaddum, '35; Code, '37; Feinberg, Malkiel and Feinberg, '50). Nevertheless, the data recorded here indicate that while the over-all terminal effect of high concentrations of histamine is an inhibition of cardiac muscle contraction; it would seem, on the basis of the time-lapse data, that this terminal inhibitory effect may be preceded by a period in which histamine at high concentrations initiates slow, regular pulsatile contractions in certain cells of the fibroblast growth zone. It is suggested that these cells so responding are incompletely differentiated cardiac muscle cells (figs. 11-18).

While antihistamines are thought to be spasmolytic, little appears to be known specifically of their effects on cardiac muscle (Levitan and Scott, '49). My studies indicate that at both concentrations used here, antihistamine had a marked inhibitory effect on the contraction of cardiac muscle (tables 1, 2). Concentrations of less than $10\text{ }\mu\text{g/cc}$ are without effect although this was erroneously recorded in an abstracted note (Richter, '54).

Relative to the joint effect of these substances on cardiac contraction, it can only be said (1) in view of the individual effects of these drugs at $10\text{ }\mu\text{g/cc}$ that the inhibitory action of antihistamine was partially suppressed (reversed?) in the presence of histamine (table 1) and (2) that there appeared to be no antagonistic action between these substances at toxic concentrations when pulsatile contraction was completely inhibited (table 2).

The individual and joint effects of histamine and antihistamine on fibroblast growth. With reference to the effect of histamine on growth, there is general agreement on only one point, namely, that fibroblast growth is inhibited by high concentrations (Heubner and Schreiber, '40; Funayama, '38; Richter, '54). Heubner and Schreiber place the effective inhibitory concentration at 1 mg/cc, although in my studies growth was notably inhibited at one-tenth this amount (table 2). Except for the report of Funayama that low concentrations stimulate fibroblast growth, the remainder of the evidence indicates that they are without effect (table 1) (Richter, '54; Heubner and Schreiber, '40). Nothing appears to be known of the effect of antihistamine on the growth of fibroblasts. The present studies indicate that antihistamine mildly inhibits their growth at both 10 and 100 μ g/cc (tables 1, 2). Relative to their joint effects on the growth of these cells, it would appear that simultaneous administration at 10 μ g each/cc stimulated their growth; while at 100 μ g each/cc, fibroblast growth was partially inhibited but not to the extent histamine alone did so at this concentration (table 2). It would seem, therefore, that the more pronounced growth inhibiting effect of histamine was partially suppressed (reversed ?) in the presence of antihistamine at the high concentration.

The individual and joint effect of histamine and antihistamine on secretory activity. Lettré and Albrecht ('41, '43), Pomerat and Emerson ('44) and Richter ('54) have reported that one of the effects of histamine on cells grown in culture is to cause the formation of numerous cytoplasmic vacuolar droplets. Because of this circumstance and because of the generally unsettled and incompletely understood status of vacuolar droplets in many cell types grown in culture, it seems essential to emphasize certain features concerning them which seem generally to have escaped critical attention for many years. While these droplets are well-known to tissue culturists, it generally seems to go unappreciated that two types of droplets exist, that both may be present simultaneously in the

same cell, and that each represents a distinctly different kind of protoplasmic activity. Both types of droplet on general appearance alone are most similar, if not indistinguishable. The one type results directly from the phenomenon of pinocytosis or the ingestion of discrete droplets of fluid medium (Lewis, '42; Pomerat, '51). This type seems not to be involved in these studies as time-lapse records showed no evidence of pinocytosis. However, the other type and the one which is involved in these studies is a specific "de novo" product elaborated by the living cell (Lewis, '19; Renaut, '07; Dubreuil, '13; Richter, '55 and others). This type according to adequate accounts arises in association with the golgi complex (Hirsch, '39; Bowen, '29a, b; Dawson, '42; Richter, '55) whether the cells be typical glandular ones or otherwise. It is the general practice of tissue culturists, and without reference to the type of droplet involved, to consider their presence as a sign of cellular degeneration (Lewis, '19; Cameron, '50). It is certain that the second type of droplet is of common occurrence both "in vivo" and "in vitro" (Heilbrunn, '40; Renaut, '07; Dubreuil, '13; Pfuhl, '33) and in the majority of exocrine and endocrine glands where they represent specific secretory manifestations (Bowen, '29a, b; Dawson, '42; Hirsch, '39; Richter, '55). It should be pointed out that Renaut ('07) in studies aimed at systematizing secretory activities of cells and at the characterization of secretory products, recognized this type of vacuolar droplet in connective tissue fibroblasts as a specific secretion product characteristic of a type of secretory activity which he designated by the term, plasmocrine. These droplets are regarded in this study as plasmocrine droplets in accord with the term and interpretation placed on them originally by Renaut ('07) and supported by the great bulk of evidence concerning them. The observations made in this study in no way detract from this interpretation, because the histamine- and antihistamine-induced changes in plasmocrine activity noted here parallel

the generally known effects of these substances on glandular secretion "in vivo" (Feinberg, Malkiel and Feinberg, '50).

In typical glandular cells, the level of secretory activity most generally may be gauged roughly by the amount of secretion product present (Bowen, '29a, b; Hirsch, '39). However, such a direct relationship may be of variable reliability simply as a consequence of the fact that a secretory cycle includes a phase of extrusion of some kind (Richter, '55), so that in all situations the amount of product present may (1) reflect simply a retention of the product or (2) an actual level of secretory activity. A distinction may be made if the amount of product is correlated with cytomorphic changes in other associated protoplasmic organelles (Dawson, '42; Bowen, '29a, b; Hirsch, '39; Richter, '55).

It seems quite clear from the work of others (Lettré and Albrecht, '41, '43; Pomerat and Emerson, '44) and that reported here (figs. 1, 2), that histamine stimulates the plasmocrine activity of chick heart fibroblasts and that the degree of stimulation varies directly with its concentration. This response accords well with general "in vivo" findings that histamine stimulates gastric, lachrymal and salivary secretion (Feinberg, Malkiel and Feinberg, '50). According to my data, antihistamine, also, stimulates plasmocrine activity and this effect varies with its concentration (figs. 1, 3, 5, 8). In contrast though, arginine, one of the first agents found to have antihistaminic properties, was reported by Lettré and Albrecht ('43) not to stimulate this activity in the chick heart fibroblasts. However, the results obtained here are in accord with the finding of Halpern ('42) and Emmelin and Ruren ('49) that secretory activity "in vivo" is stimulated by certain antihistamines. As to the joint effect of histamine and antihistamine on plasmocrine activity, it seems that the stimulatory effect of each of these substances was either completely suppressed (figs. 1-4) or partially so (figs. 5-10) when these substances were administered simultaneously at the low and high concentrations respectively. These results agree with

the same finding of others "in vivo" (Yonkman, Oppenheimer, Rennick and Pellet, '47; Emmelin and Muren, '49).

ACKNOWLEDGMENTS

I would like to express my thanks to Professor C. R. Doering for the statistical treatment of my data, Professor H. A. Shoemaker and Professor A. Kurtz for certain technical information on the chemistry of the antihistamines.

SUMMARY

Data bearing on the individual and joint effects of histamine-dihydrochloride and an antihistamine (chlor-trimeton) on the growth, contractility and plasmocrine activity of chick heart tissues in culture are presented.

1. Antihistamine strongly inhibits the contraction of cardiac muscle at concentrations of 10 and 100 $\mu\text{g}/\text{cc}$ while histamine strongly inhibits only at 100 $\mu\text{g}/\text{cc}$. The more pronounced inhibitory effect of antihistamine is partially suppressed when these substances are used simultaneously at 10 μg each/cc. There is no apparent antagonistic action when used jointly at the toxic concentration (100 μg each/cc).

2. Antihistamine at both 10 and 100 $\mu\text{g}/\text{cc}$ mildly inhibits fibroblast growth; while histamine at 10 $\mu\text{g}/\text{cc}$ has no effect and strongly inhibits at 100 $\mu\text{g}/\text{cc}$. Their joint administration at 10 μg each/cc stimulates fibroblast growth, while at 100 μg each/cc the more pronounced inhibitory effect of histamine is partially suppressed.

3. Histamine and antihistamine each stimulates plasmocrine activity in fibroblasts at 10 and 100 $\mu\text{g}/\text{cc}$; but histamine is the more stimulatory of the two. Jointly administered, their stimulatory effect is completely suppressed at 10 μg each/cc and partially so at 100 μg each/cc.

4. Histamine at 100 $\mu\text{g}/\text{cc}$, shown by time-lapse records, initiates slow, regular pulsatile contractions in certain cells of the fibroblast growth zone which may be incompletely differentiated cardiac muscle cells.

LITERATURE CITED

- BARSOUM, G. S., AND J. H. GADDUM 1935 The pharmacological estimation of adenosine and histamine in blood. *J. Physiol.*, *85*: 1-14.
- BOWEN, R. H. 1929a The cytology of glandular secretion. *Quart. Rev. Biol.*, *4*: 299-234.
- 1929b *Ibid.*, *4*: 484-519.
- CAMERON, G. 1950 *Tissue Culture Technique*. Acad. Press, Inc., New York. 2nd Ed.
- CODE, C. F. 1937 The quantitative estimation of histamine in blood. *J. Physiol.*, *89*: 257-268.
- DAWSON, A. B. 1942 Some morphological aspects of the secretion process. *Fed. Proc.*, *1*: 233-240.
- DUBREUIL, G. 1913 Le chondriome et le dispositif de l'activite secreteoire aux differentes stades du developpement des elements cellulaires de la ligne connective, descendants du lymphocyte (globules blanc de la lymphe et du sang, cellules connectives cartilagineuse et osseuses). *Arch. d'anat. microscop.*, *15*: 53-151.
- EMMELIN, N., AND A. MUREN 1949 Effects of antihistamine compounds on the adrenaline liberation from the suprarenals. *Acta Physiol. Scandinav.*, *17*: 345-355.
- FEINBERG, S. M., S. MALKIEL AND A. R. FEINBERG 1950 *The antihistamines*. Yearbook Publishers, Inc., Chicago, pp. 5-291.
- FUNAYAMA, M. 1938 Über den Einfluss einiger aromatischen Amine auf die in vitro-Kultures von Fibroblasten. *Chem. Abstr.*, *32*: 1355.
- GOODMAN, L., AND A. GILMAN 1941 *The pharmacologic basis of therapeutics*. Macmillan Company, New York.
- HALPERN, B. N. 1942 Les antihistaminiques des synthese. Essais de chimio-therapie des états allergiques. *Arch. internat. de pharmacodyn. et de therap.*, *68*: 339-408.
- HEILBRUNN, L. V. 1940 *Protoplasm and colloids*. The Cell and Protoplasm. Science Press, Lancaster, Pa., p. 188-198.
- HEUBNER, W., AND E. SCHREIBER 1940 Versuche über chemische Zellreizung an Fibroblastkulturen. III. Mitteilung: Histamin. *Naunyn-Schmiedeberg's Arch. exper. Path. u. Pharmak.*, *194*: 105-108.
- HIRSCH, G. C. 1939 Form and Stoffwechsel der Golgi-Körper. *Protoplasma Monogr.*, *18*: 1-394.
- ISHIHARA, M., AND T. IWA0 1938 Über den Histamingehalt des Herzens. *Naunyn-Schmiedeberg's Arch. exper. Path. u. Pharmak.*, *108*: 110-113.
- JAHN, T. L., AND W. DANFORTH 1952 Inhibition of growth of a green flagellate by the antihistamine, B-dimethylaminoethyl (Benadryl). *Proc. Soc. Exp. Biol. and Med.*, *80*: 13-15.
- LETTRE, H., AND M. ALBRECHT 1941 Zur Wirkung von B-phenyläthylaminen auf in vitro gezuchtete Zellen. *Ztschr. f. Physiol.*, *271*: 200-207.
- 1943 Zur Wirkung von Aminen auf in vitro gezuchtete Zellen. *Ztschr. f. physiol. Chem.*, *279*: 206-208.
- LEVITAN, B. A., AND H. J. SCOTT 1949 Inhibition of chloroform-adrenaline fibrillation by antihistamines. *Canad. M. A. J.*, *61*: 303-306.

- LEWIS, W. H. 1919 Degeneration granules and vacuoles in the fibroblasts of chick embryos cultivated in vitro. *Johns Hopkins Hosp. Bull.*, 30: 81-91.
- 1942 The relation of the viscosity changes of protoplasm to ameboid locomotion and cell division. A symposium on the structure of protoplasm. Iowa State College Press, pp. 163-197.
- PFUHL, W. 1933 Golgi apparatus of plasma of clasmatocytes and fibrocytes in normal loose connective tissue; metabolic inclusions, chondriome and golgi apparatus. *Ztschr. f. anat. u. Entweklngsgesch.*, 99: 649-668.
- POMERAT, C. M., AND G. A. EMERSON 1944 Induction of aqueous vacuolization in cells grown in tissue culture by various agents. *Proc. and Trans. Tex. Acad. Sci.*, 28: 91.
- PORTER, K. R., A. CLAUDE AND E. F. FULLAM 1945 A study of tissue culture cells by electron microscopy. *J. Exp. Med.*, 81: 233-245.
- RENAUT, J. 1907 Les cellules connectives rhagiocrine. *Arch. Anat. Microscop.*, 9: 495-606.
- RICHTER, K. M. 1954 Studies on the individual and joint effects of histamine-hydrochloride and chlor-trimeton on cultures of embryonic chick heart. *Anat. Rec.*, 118: 453-454.
- 1955 Studies on leukocytic secretory activity. *Ann. N. Y. Acad. Sci.*, Art. 5, 863-895.
- VALENTINE, W. N., M. L. PEARCE AND J. S. LAWRENCE 1950 Studies on the histamine content of blood, with special reference to leukemia, leukemoid reactions and leukocytoses. *Blood*, 5: 623-647.
- WRIGHT, H. N., AND M. MONTAG 1951 A textbook of pharmacology and therapeutics. W. B. Saunders Co., Phila., 5th Ed.
- YONKMAN, E. F., E. OPPENHEIMER, B. RENNICK AND E. PELLET 1947 Pharmacodynamic studies of a new antihistaminic agent, Pyribenzamine (N,N-dimethyl-N-benzyl-N-[α -pyridyl]-ethylenediamine hydrochloride): II. Effects on smooth muscle of the guinea pig and dog lung. *J. Pharmacol. and Exp. Therap.*, 89: 31.

PLATES

All figures are unretouched photomicrographs or copies of selected frames from cinematographs. Cultures shown in figures 1-10 were fixed in osmic acid and photographed in water under the 4 mm objective of the dark-medium phase contrast microscope with a 35 mm Leica in combination with the Micro-Ibso attachment. The initial magnification at film was $143\times$ and enlarged in printing to $656\times$.

Figures 11-18 are copies of selected frames from 16 mm time-lapse motion pictures of a living culture made with the Cine Special camera operating at 1 frame/15 seconds in combination with the dark-medium phase contrast microscope using the 8 mm objective. The magnification at film was $67\times$ and they were enlarged in printing to $375\times$.

Abbreviations

F, extracellular fat droplet
GB, golgi body
N, nucleus
Nu, nucleolus
PD, plasmocrine droplet

PLATE 1

EXPLANATION OF FIGURES

- 1 Fibroblasts in the growth zone of a control culture in the $10\text{ }\mu\text{g/cc}$ series (table 1, I) after 48 hours of cultivation showing the normal nuclei and nucleoli and the normal complement of golgi bodies and plasmocrine droplets.
- 2 Fibroblasts in the growth zone of a culture after 48 hours treated with $10\text{ }\mu\text{g}$ histamine/cc (table 1, II) showing normal nuclei, and nucleoli, and increased numbers of golgi bodies and plasmocrine droplets.
- 3 Fibroblasts in the growth zone of a culture after 48 hours treated with $10\text{ }\mu\text{g}$ antihistamine/cc (table 1, III) showing normal nuclei and nucleoli and slightly increased numbers of golgi bodies and plasmocrine droplets.
- 4 Fibroblasts in the growth zone of a culture after 48 hours treated jointly with $10\text{ }\mu\text{g/cc}$ each of histamine and antihistamine. (table 1, IV) showing normal nuclei and nucleoli and a normal complement of golgi bodies and plasmocrine droplets.

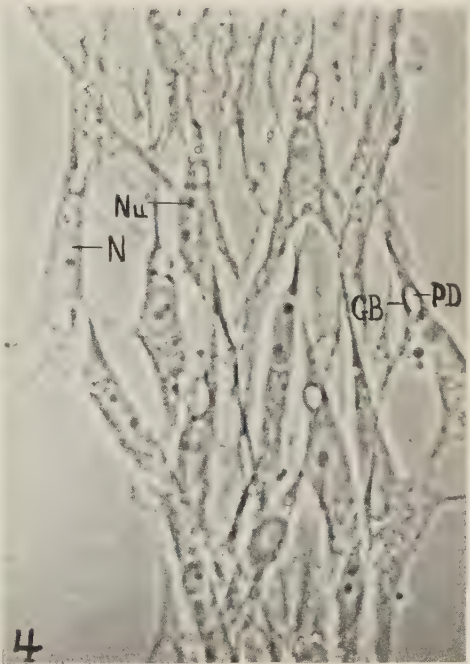
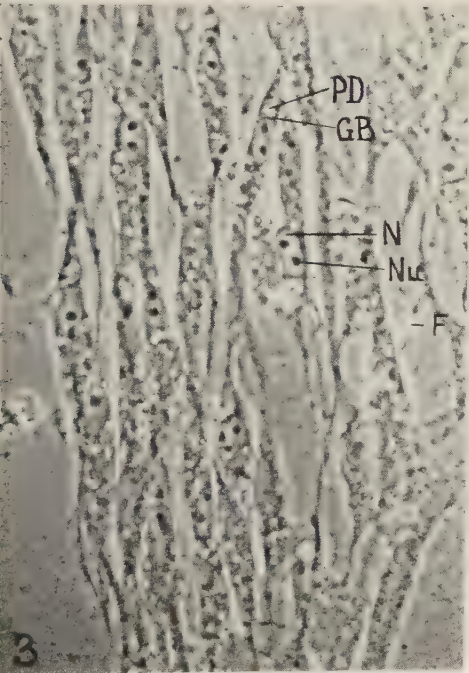
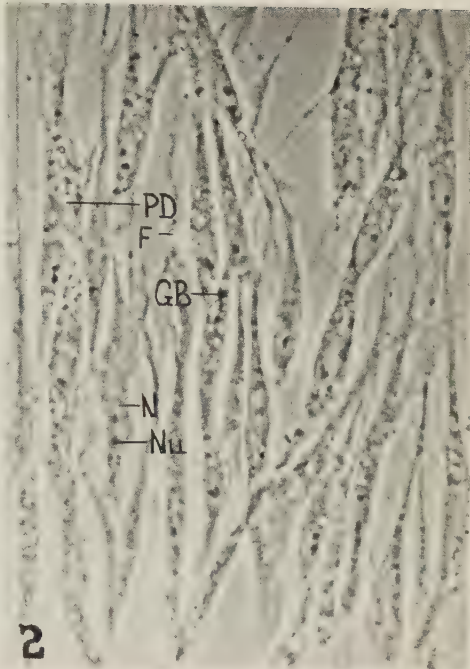
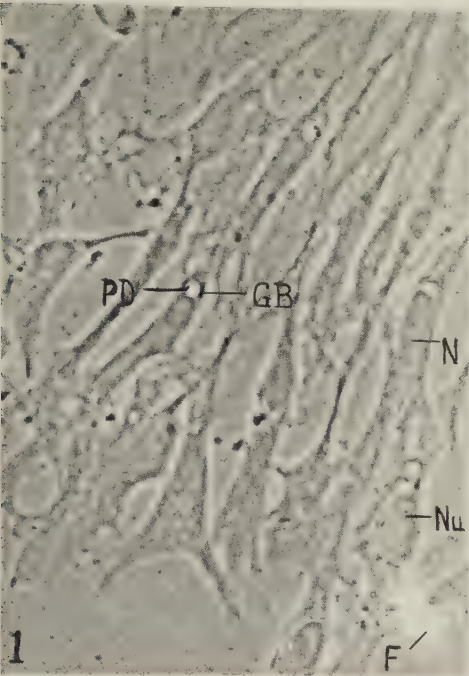


PLATE 2

EXPLANATION OF FIGURES

- 5 Fibroblasts in the growth zone of a control culture in the 100 $\mu\text{g}/\text{cc}$ series (table 2, I) after 48 hours showing the normal nuclei, nucleoli and normal complement of golgi bodies and plasmocrine droplets.
- 6, 7 Fibroblasts in the growth zone of a culture after 48 hours treated with 100 μg histamine/cc (table 2, II) showing normal nuclei and nucleoli and markedly increased numbers of golgi bodies and plasmocrine droplets.
- 8 Fibroblasts in the growth zone of culture after 48 hours treated with 100 μg antihistamine/cc (table 2, III) showing normal nuclei and nucleoli and slightly increased numbers of golgi bodies and plasmocrine droplets.
- 9, 10 Fibroblasts in the growth zones of two different cultures after 48 hours treated jointly with histamine and antihistamine at 100 $\mu\text{g}/\text{cc}$ (table 2, IV) showing normal nuclei and nucleoli, and a complement of golgi bodies and plasmocrine droplets which is somewhat less in amount than that of the histamine treated cells (figs. 6, 7).

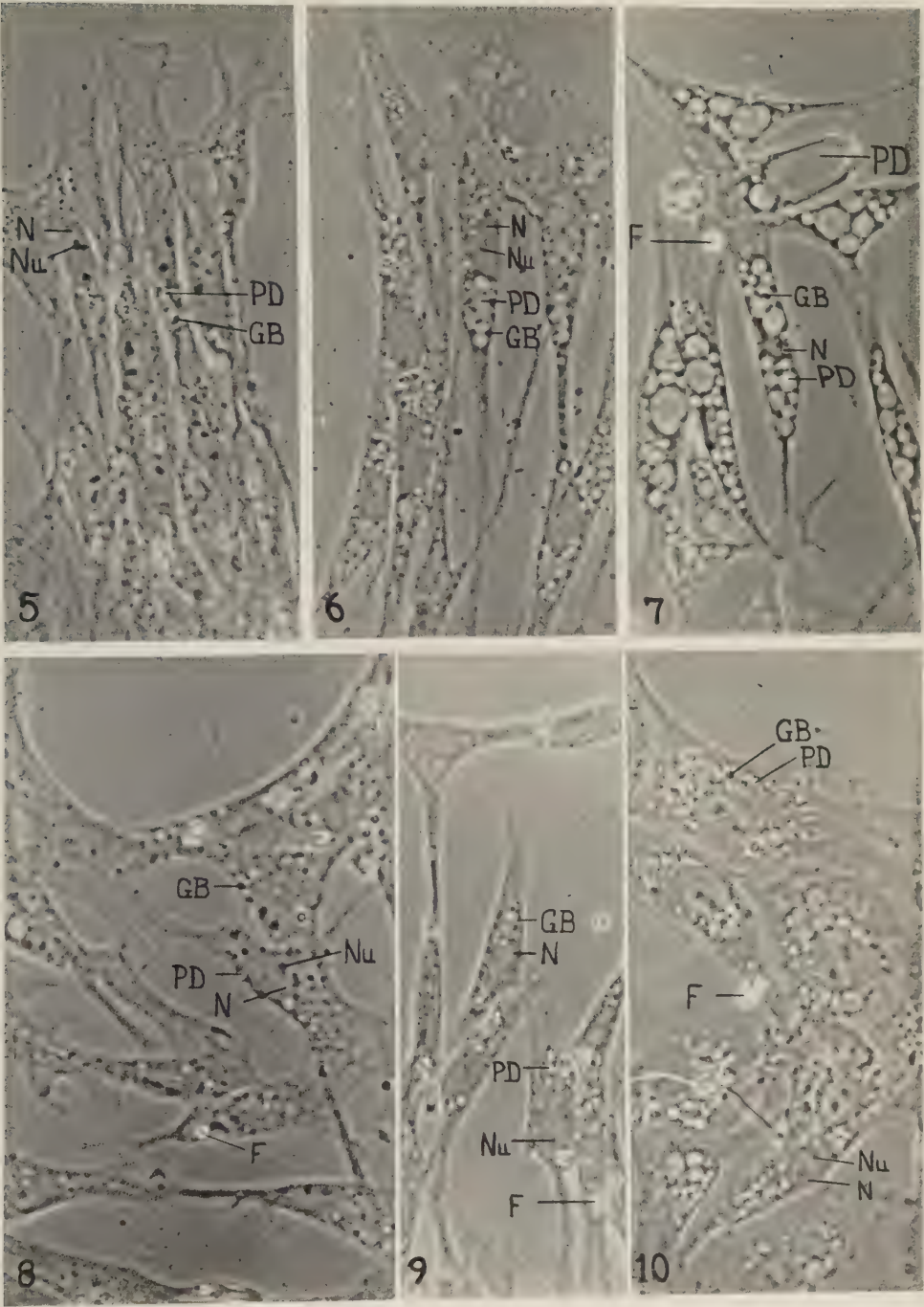
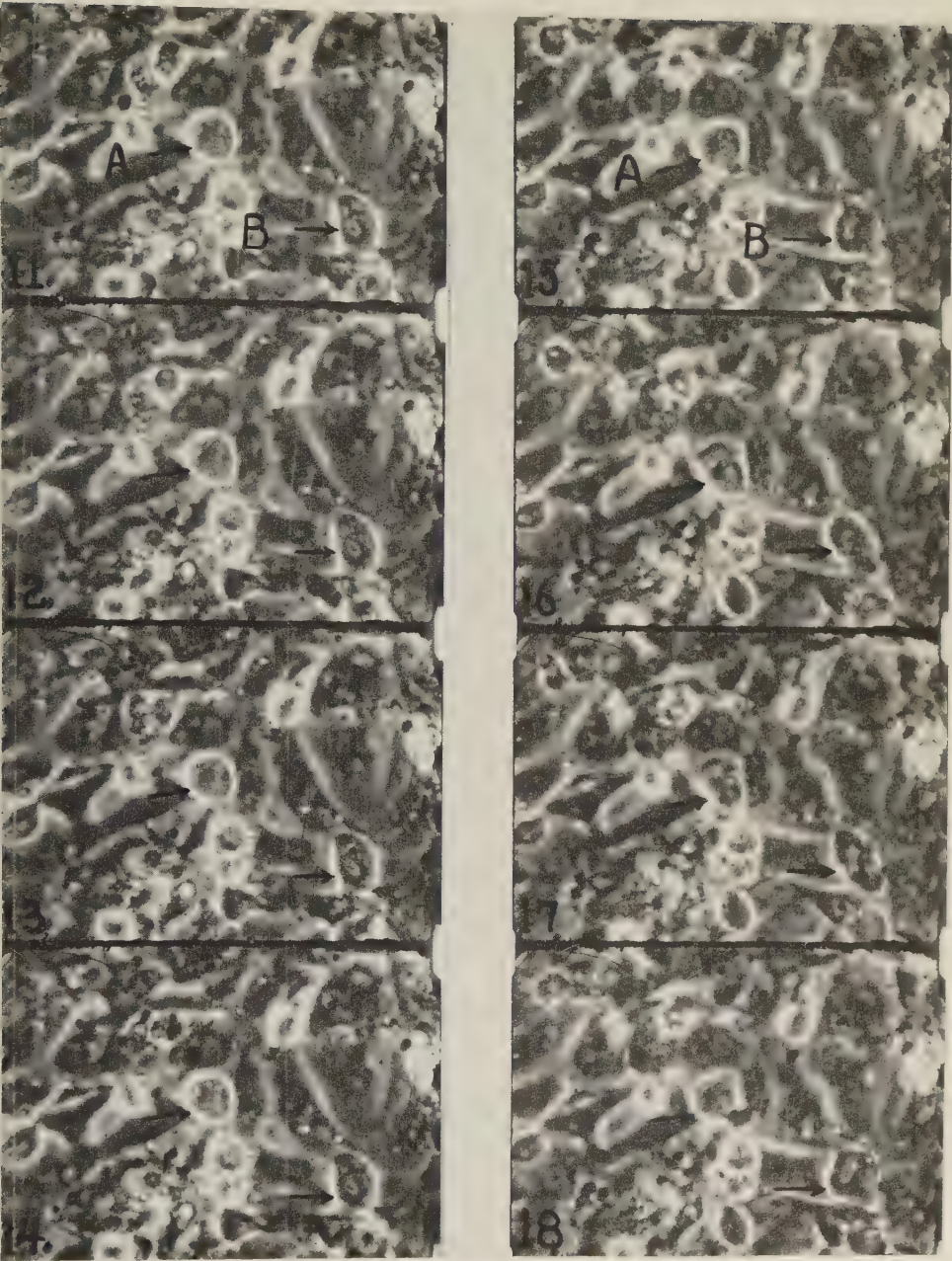


PLATE 3

EXPLANATION OF FIGURES

- 11-14 Consecutive frames from a time-lapse motion picture of a group of fibroblasts in the growth zone of a culture after about 4 hours of treatment with 100 μ g histamine/cc showing the differentially-rounded up cells, A and B and others not designated before they began regular pulsatile contractions. Note especially the absence of any change in shape or size of these two cells during the 1 minute (4 frames) sequence shown.
- 15-18 Consecutive frames from the same film sequence and of the same cells shown in figures 11-14 but approximately 10-20 minutes later showing cells A and B passing through one complete pulsatile contraction. Cells A and B happen to be contracting synchronously. In figure 15 both are in a phase of contraction and in figures 16 and 17 both are in a phase of relaxation. In figure 18 a new contraction cycle is starting and both cells are in a phase of contraction.



DIFFUSION FROM BRAIN SLICES *IN VITRO*¹

BILL GAROUTTE AND ROBERT B. AIRD

*Departments of Neurology and Anatomy, University of California School of
Medicine, San Francisco, California*

ONE FIGURE

For some time the double exponential curve has been accepted as describing the diffusion of radioactive molecules out of or into tissue slices *in vitro*. Levi and Ussing ('48) appear to have been the earliest to report such curves, using radioactive sodium and the isolated frog sartorius. A number of investigators (Harris and Burn, '49; Wesson et al., '49; Abelson and Duryee, '49; Edelman, '52; Mudge, '53; Shanes, '54; Shanes and Berman, '53 and '55; Demis and Rothstein, '55; Garoutte and Aird, '55) have confirmed the form of these diffusion curves, using different tissues and different tracer materials.

Many of the workers mentioned have concluded that double exponential diffusion curves arise partially or entirely because of different rates of diffusion from extracellular and intracellular fluid spaces, although some have indicated the likelihood of ion binding as an additional or alternative mechanism. Harris and Burn ('49) and Shanes and Berman ('55) also mentioned the probable importance of diffusion processes *in se*. We have recently ('55) published a brief report containing strong presumptive evidence that such curves are not related to tissue compartmentation or to ion binding, at least under the experimental conditions described. The present paper is an extension of this thesis to additional tracer materials, with additional experimental confirmation.

¹ This investigation was supported by the Cox Fund for Medical Research and by the Lucie Stern Fund for Research in Epilepsy.

Such a presentation should be of particular interest in view of the recent publication in this journal (Shanes and Berman, '55) of an extensive set of experiments based upon such diffusion curves.

In an earlier publication, we (Adams, Aird, and Garoutte, '52) based conclusions regarding the accessibility of electrolytes to diffusion on the assumption that the double exponential curve of diffusion was due to tissue compartmentation. These conclusions have not been confirmed in detail after extensive repetition of the experiments.

In an attempt to explain this apparent error, a more thorough review of the literature on diffusion was undertaken. The most extensive and mathematically rigorous treatment of the problem of diffusion through and out of solids is contained in Barrer's monograph ('51). Barrer's comprehensive presentation, the theoretical analysis of diffusion processes by Danckwerts ('51), and the experimental and theoretical study of March and Weaver ('28) made it apparent that curves of diffusion, identical with those obtained with living tissues, could be obtained with homogeneous solid materials. March and Weaver, for example, studied the diffusion of ions out of solidified gelatin, obtaining a double exponential form indistinguishable from the curves described above which have been obtained by biologists. The practical application of physical diffusion theory, therefore, supplies one possible explanation for the diffusion curves obtained with biological tissues. This has been discussed at some length by previous workers, especially Harris and Burn ('49) and Shanes and Berman ('55).

Another explanation for the double exponential curve of diffusion, likewise unrelated to tissue compartmentation, was suggested to us by Dr. A. A. Koneff of the Department of Anatomy. He pointed out that when tissue slices are prepared, the surface layer is almost invariably fractured and otherwise damaged to a depth of a fraction of a millimeter — a fact easily demonstrated histologically. This partial disruption of the tissue structure at the surface would be ex-

pected to decrease the surface resistance to diffusion and should result in increasing the rate of diffusion out of this layer.

Since these two mechanisms can account for the double exponential curve of diffusion without recourse to differing availabilities related to tissue compartmentation, it immediately becomes imperative to apply this information to the existing biological literature and to check it experimentally, if possible.

Two types of experiment have been performed. The first set of experiments was done with three tracer materials which are generally accepted to be distributed differently in tissue, e.g. sodium, potassium, and water. Such tracers with different tissue distributions (cellular versus interstitial) should give double exponential curves which are quantitatively distinct, providing tissue compartmentation is important in the determination of the form of the curves. As will be seen later, this was found not to be the case.

The second type of experimental approach was based on the postulate that radioactive sodium in the vascular tree *in vivo* must enter the extracellular spaces of the tissue before it enters cells. This extracellular fraction of sodium should have a higher specific activity at the beginning than at the end of its uptake in the intact animal. On this basis, if the double exponential curves are related to extracellular-intracellular compartmentation, the first, rapid sodium diffusion fraction should have a higher specific activity than the later portion. This also was not found to be the case.

METHODS AND MATERIALS

Blocks or slices of brain tissue of known surface-to-volume ratio were removed from animals — hamsters or guinea pigs — which had received a single intraperitoneal injection of radioactive sodium or potassium. Surface-to-volume ratio for the slices was determined by direct measurement and calculation of surface area, volume being taken as determined by weight. Each tissue block was individually placed in a

50 ml separatory funnel in a 3 cm³ aliquot of aqueous 50% sucrose, or standard Ringer's solution, and agitated by compressed air admitted from below. The aqueous medium was thereafter washed into metal cups, dried, and the amount of radioactivity which had diffused was measured by means of a shielded scintillation counter.² In the experiments where 50% sucrose was used as the diffusion medium, the loss of water by diffusion was also measured, on the assumption that loss of weight of the tissue was principally due to loss of water.

Diffusion from blocks of 20% gelatin of similar dimensions into 50% sucrose solution was also studied.

Diffusion was not carried beyond 10 or 12 minutes because of gross maceration of the tissue which usually appeared after this period of agitation.

In a single series of experiments, the uptake of radioactive sodium by diffusion into brain slices was quantitated.

RESULTS

The results of these experiments are displayed graphically in figure 1 (A-F), while numerical data obtained in the same experiments are tabulated in table 1.

In table 2 are listed the results of the specific activity experiments mentioned in an earlier paragraph. The diffusion technique for these experiments was the same as for the experiments listed in table 1. The preliminary steps differed slightly, however. In the experiments of table 1, guinea pigs were given radio-isotopes intraperitoneally, and the brain slices were removed after equilibration had occurred (more than 7 hours in the case of sodium, and about 24 hours in the case of potassium). On the other hand, in the experiments of table 2, where only radio-sodium was used, some of the animals were sacrificed one-half or 4 hours after intraperitoneal injection and others after intervals greater than 7 hours, so that the specific activity before and after equilibration *in vivo* could be compared.

² Counters were provided by the Radioactivity Research Center, University of California Medical Center, San Francisco; Dr. K. G. Scott, Director.

TABLE 1

Summary of experimental data illustrated in figure 1

TISSUE	CURVE OF FIG. 1	TRACER	DIFFUSION MEDIUM	(A) (ESTI- MATED) SUB- FACE- TO- VOLUME RATIO	(B) FRACTION LOST RAPIDLY	QUOTIENT (B)/(A)
<i>mm²/mm³</i>						
Hamster	(A) — a	Na ²⁴	50% Sucrose	0.97	.08	.083
Brain	(A) — b	Na ²⁴	50% Sucrose	1.04	.10	.096
Brain	(A) — c	Na ²⁴	50% Sucrose	1.83	.16	.088
Brain	(B)	K ⁴²	50% Sucrose	1.69	.13	.082
Brain	(C)	Water	50% Sucrose	1.04	.11	.106
Brain	(D) — a	Na ²⁴	Ringer	1.05	.13	.124
Brain	(D) — b	K ⁴²	Ringer	1.22	.10	.082
Brain	(D) — c	K ⁴²	Ringer	1.82	.19	.104
AVERAGE						.096 ± .014
Guinea pig	(E) — a	Water	50% Sucrose	0.82	.055	.067
Brain	(E) — b	Water	50% Sucrose	1.71	.12	.071
Brain	(E) — c	Na ²⁴ uptake	50% Sucrose	1.43	.07	.049
AVERAGE						.062
20% Gelatin	(F) — a	Na ²⁴	50% Sucrose	1.02	.28	.277
20% Gelatin	(F) — b	K ⁴²	50% Sucrose	0.86	.23	.268
AVERAGE						.272

TABLE 2

Interval between intraperitoneal injection and sacrifice	FIVE MINUTES' DIFFUSION				TWO MINUTES' DIFFUSION
	12-20 hr.	8-12 hr.	4-8 hr.	Less than 4 hr.	$\frac{1}{2}$ hr.
No. of guinea pigs	15	5	12	11	8
Ratio of Na ²⁴ specific activities. Extract/brain	0.73	0.75	0.81	0.85	0.78
Standard deviation	± 0.22	± 0.13	± 0.24	± 0.39	± 0.17

Also in table 2 are presented the specific activities of diffusible sodium after different periods of diffusion. As seen from figure 1, two minutes of diffusion included most of the rapid phase, while 5 minutes included a significant fraction of the slower phase. The specific activities after these two diffusion intervals are given in table 2.

For the specific activity experiments, the total brain sodium was determined after homogenization and dilution by means of a Beckman DU spectrophotometer with flame attachment.

DISCUSSION

Consideration of results obtained in present study

Each curve of figure 1 consists of an initial steep branch which represents rapid diffusion for the first $1\frac{1}{2}$ to $2\frac{1}{2}$ minutes of immersion, followed by a slower phase which continued for at least 10 more minutes. As is graphically demonstrated in figure 1, the form of the diffusion curves did not depend on type of tissue, on surrounding medium, or on tracer used.

The single curve (E-c) of passive uptake of radio-sodium by brain slices was also of this form.

Fig. 1 Semi-logarithmic diffusion curves of Na^{24} , K^{42} , or H_2O from hamster brain (curves A, B, C, D), guinea pig brain (curves E), or gelatin slices (curves F).

(A) Hamster brain in 50% sucrose solution, with radio-sodium as tracer agent. Curves 'a', 'b', and 'c' are of different surface-to-volume ratios. (See table 1.) Each point is the average of 10-18 experimental determinations.

(B) Hamster brain in 50% sucrose with radio-potassium as tracer agent. Each point is the average of 8-12 experiments.

(C) Hamster brain in 50% sucrose solution. Curve of water loss (i.e. weight loss). Each point is the average of 10-16 experiments.

(D) Hamster brain in standard Ringer's solution. Radio-sodium in curve 'a' (8-12 experiments per point), and radio-potassium in curves 'b' and 'c' (3-5 experiments per point). Surface-to-volume ratios were different for the three curves.

(E) Guinea pig brain in 50% sucrose solution. Curves 'a' and 'b' represent loss of water; curve 'c' represents the passive uptake of radio-sodium, calculated as $100 \left(1 - \frac{\text{Na}^{24}\text{-Brain}}{\text{Na}^{24}\text{-Medium}} \right) \%$. (3-7 experiments per point).

(F) Solidified 20% gelatin slices in 50% sucrose solution, with radioactive sodium 'a' or potassium 'b' as tracer. (Each point is the average of 6-12 experiments.)

From table 1 the percentage of rapid loss of tracer can be seen to vary with the surface-to-volume ratio. This is also apparent graphically in figure 1 where the amount of rapid diffusion, using respectively radio-sodium (A-abc), radio-potassium (D-be), or water (E-ab) as tracers, was related directly to the surface-to-volume ratio when other experimental variables were held constant.

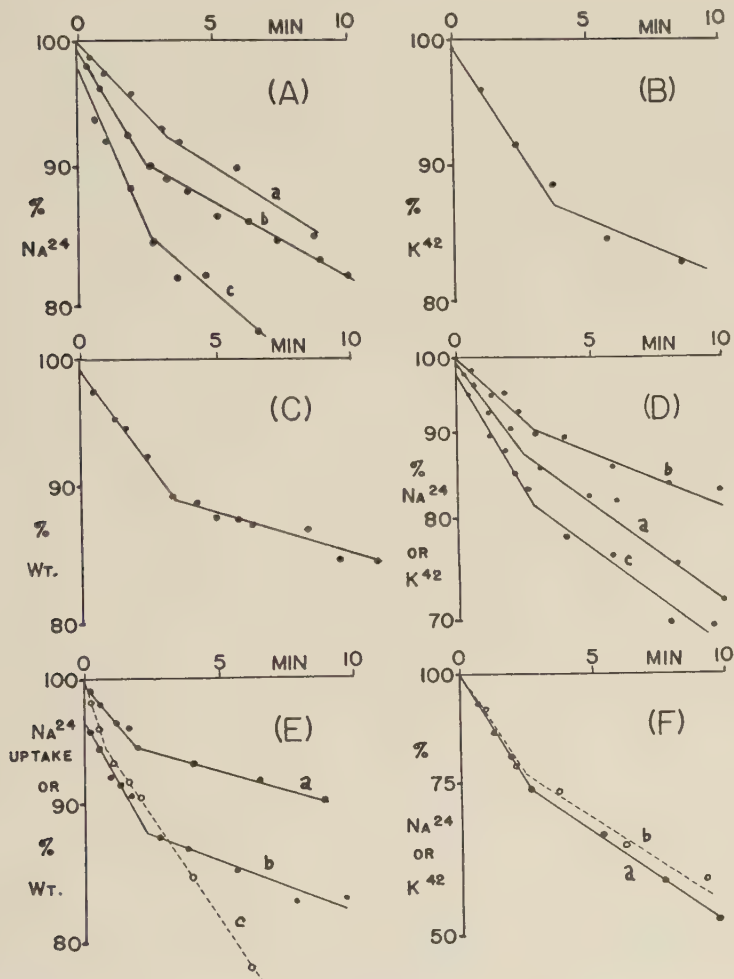


Figure 1

In order to make the relationship clearer, the quotient obtained by dividing "Fraction Lost Rapidly" by "Estimated Surface-to-Volume ratio are seen to be approximately equal for the various experiments with a given tissue, thus demonstrating analytically the direct relation between surface area and percentage of rapid diffusion. This relation does not appear to be significantly altered by changing diffusate or diffusion medium.

As suggested in an earlier paragraph, one of the strongest arguments against the form of the diffusion curves' being determined by tissue compartmentation is the fact that the initial fractions of diffusion for different tracers are equal. The relative amounts of sodium, of potassium, and of water in the first, rapid component of diffusion are seen from figure 1 (A, B, C) to be practically identical. Had the surface-to-volume ratios been more nearly the same, these rapid components would undoubtedly have been equal within the limits of experimental error (this is a graphic way of looking at the data of the last column in table 1, as discussed above). If tissue compartmentation were of great importance to these curves, one would have to assume that the extracellular proportions of sodium, potassium, and water are identical, which is, of course, not acceptable. A possible alternative explanation has been proposed by Shanes and Berman ('55), namely, that a portion of one or more of the tracer materials may be "bound" in some way to myelin or other component of nervous tissue. However, as they have demonstrated in their series of diffusion curves with different diffusates, binding, if present, causes deviation from the theoretical form of the curves only as the concentrations approach diffusion equilibrium. The present curves do not involve the necessity of this consideration, since equilibrium is not approached.

On the basis of the data of figure 1 and table 1, it is clear that the quantitative characteristics of these curves cannot be resolved on the basis of tissue compartmentation, or binding. They are, however, readily accounted for by surface effects:

fracturing of the surface layer and the process postulated by physical diffusion theory.

In view of the points made above, it would appear that the superficial layer of the tissue slices must be involved in the rapid phase of diffusion. Accordingly, it would be of interest to know what thickness of tissue could account for this rapid phase, assuming total or near-total loss of tracer from the surface layer.

From the experimental data of figure 1 (A-a), taken as a specific example, the thickness of this surface layer may be calculated as follows:

$$0.08 \times 1 \text{ mm}^3 = 0.08 \text{ mm}^3$$

since .08 of the radio-sodium is lost in the rapid phase. Thus, the rapid radio-sodium loss is the equivalent of that contained in 0.08 mm^3 out of every 1.0 mm^3 of tissue. Since the surface area is 0.97 mm^2 per cubic millimeter, the thickness of the hypothetical depleted surface layer can be calculated:

$$0.08 \text{ mm}^3 \div 0.97 \text{ mm}^2 = 0.82 \text{ mm or } 82 \mu$$

Similar calculations were used to obtain the last column of table 1.

The thickness of the depleted layer is thus seen to be less than 100μ or $\frac{1}{10} \text{ mm}$ (average for hamster brain, $96 \pm 14 \mu$; guinea pig, 62μ) which is of the order of magnitude of the known histological disruption of the surface layer of tissue.

Another interesting observation based on the curves of figure 1 may be made. Several of the curves do not pass through the point of origin. This intercept at zero time represents the loss of tracer that occurs in the first few seconds of immersion in diffusion medium. These essentially instantaneous losses are also roughly related to the surface-to-volume ratio as seen from figure 1 (A-abc, D-be), and are also probably functions of surface area and can be interpreted as due to a very thin film of dissolved tracer material which is loosely adherent to the surface and which washes off mechanically in the first few seconds of immersion. Calculations similar to those of the previous paragraph give an average thickness of about 10μ , not unreasonable for such a film.

The data of table 2, derived from the specific activity experiments described under *Methods*, indicate that the specific activity of sodium diffusing out of pieces of brain is essentially the same both before and after *in vivo* equilibration between plasma and brain. The specific activity is also shown to be the same whether diffusion was of short or longer duration.

To account for the double exponential curves of diffusion, then, it may be postulated that the first phase of diffusion is rapid because of surface effects — surface fracturing and/or the processes of physical diffusion theory — while the later, less rapid phase is probably due to diffusion through the undamaged tissue in the depths of the slice.

Because the effects both of superficial fracturing and of classical diffusion processes depend upon the surface area exposed, it is not possible with the present experiments to distinguish between them, or to decide with any certainty the relative importance of the two mechanisms.

CONSIDERATION OF RESULTS OBTAINED BY OTHERS

These data throw a new light on some of the experimental observations of previous workers. The work of Hill ('28) contains the germ of the present interpretation, inasmuch as he emphasized the "extraordinary effect of thickness upon the speed of attaining equilibrium by diffusion," observing that in frog muscle exposed on one side only, a piece 0.5 mm thick reaches equilibrium in one and one-quarter minutes, while a piece 5.0 mm thick requires two hours. On the other hand, he emphasized that equilibration by diffusion between the inside and outside of a muscle cell takes only about 6 seconds. These two facts by themselves strongly suggest that cellular-interstitial compartmentation cannot significantly affect the rate, which will be determined by the slowest process in the series, in this case, diffusion out of the tissue.

Some of the interesting observations recently reported by Shanes and Berman ('55) can also be interpreted in the light of the present data. They used the stripped sciatic nerves of

toads, with a diameter, in one experiment, of 0.82 ml. Since the nerve is, for practical purposes, cylindrical, the surface-to-volume ratio is very easily calculated to be about 4.9 mm^2 per mm^3 . This surface-to-volume ratio is nearly three times as high as any that we have studied, accounting quite readily for their large initial rapid phase of diffusion. Also, considering the important variable effect of tissue traumatization, secondary to handling, there may be some justifications for suspecting that the small dimensions of the tissue pieces used may account for the fact that their curves are less accurately double exponential than others that have been reported in the literature.

The decreasing slope of diffusion in the later portions of their curves must be related to equilibration between nerve and surrounding fluid, as was originally discussed by Hill ('28) and as Shanes and Berman have reiterated. Shanes and Berman have also stressed the importance of binding of ions or molecules in this later portion of the diffusion curve. By another experimental approach we have recently confirmed their demonstration of such binding. These experiments will be the subject of a later publication.

The present data similarly offer some additional clarification for the findings of Edelman ('52) on the diffusion of deuterium oxide out of dog muscle. He studied diffusion out of undamaged muscle and out of muscle which had first been frozen and thawed in order to rupture the cell membranes. The first, rapid branch of the double exponential curve (see his fig. 9) was the same in both situations — as would be expected on the basis of the present hypotheses, since this part of the curve depends primarily upon surface effects and the degree of surface damage produced by the preparation and handling of the specimen would not be greatly altered by the process of freezing-thawing. The slope of the second part of his double exponential curves was increased after freezing-thawing. This probably occurs, as he concluded, because the

rate of diffusion through the depths was increased by the disruption of cellular membranes produced by the process of freezing and thawing and consequent diminution of diffusion resistance.

The present hypothesis also simplifies the assumptions necessary to explain the double exponential curves found by Abelson and Duryee ('49) for diffusion of radio-sodium out of frog eggs. Their radio-autographic observation of ring patterns early in the course of diffusion supplies a direct confirmation of the importance of surface diffusion. Sodium binding, to which they ascribed the double exponential curves, appears to be unrelated under the given experimental conditions, although it is, of course, not ruled out as a metabolic mechanism.

The present experimental observations are also of interest in relation to the earlier studies of Shanes ('54) on the diffusion of sodium through the epineurium of the bullfrog. He found, in a series of exceedingly delicate experiments, that diffusion through the epineurium alone gave the same curves as diffusion out of the undisturbed nerve with epineurium in place. He concluded that the two branches of the curve of diffusion out of intact nerve were due to the epineurium alone. The present experiments give additional support to Shanes' conclusions, supplying an explanation for his obtaining the double exponential curve from epineurium alone.

Creese ('54) has recently published a series of experiments with viable rat diaphragm indicating that if tissue pieces are thin enough, the ordinary physical processes of diffusion occur more rapidly than the rate of active metabolic exchange, and the latter determines the resultant curve.

We should like to re-emphasize that the converse is also true, namely, if time required for diffusion from the depths of the tissue is longer than that required for metabolic exchange, even in viable tissue, the physical processes of diffusion become of considerable or even predominant importance. Actually, both processes must be effective under most conditions, and it may be difficult from consideration of

diffusion-exchange curves alone to determine the contribution of each.

The tissue in the present experiments was largely non-viable, so that primarily physical processes of diffusion — as opposed to metabolic exchange processes — were involved.

SUMMARY

Experimental evidence is presented which indicates that the double exponential curves of diffusion of various diffusates from brain tissue slices *in vitro* into a surrounding agitated aqueous medium can be related to exposed surface area rather than to intracellular-extracellular tissue compartmentation or to ion binding. (The undoubted importance of either or both of these latter mechanisms in certain other experimental situations is not questioned.)

The first, rapid phase of the double exponential curve probably can be explained adequately on the basis of two characteristics of tissue slices. Fracturing of the surface of the slice, incident to its cutting and handling, increases the effective diffusion area and, therefore, the initial rate of diffusion. The physical laws of diffusion from solids would account for similar effects. The contributions of these two mechanisms under actual experimental conditions are indistinguishable.

The later, slower portion of the double exponential diffusion curve represents diffusion through deeper, undamaged tissue.

As stressed by Shanes and Berman ('55), binding of one sort or another probably determines the form of the curves as equilibrium is approached.

ACKNOWLEDGMENTS

We are grateful to Dr. Kenneth G. Scott and to Dr. Ernest L. Dobson, through whose kind cooperation the radioactive isotopes used in this study were obtained and prepared, and also to Dr. I. S. Edelman and Dr. Louis A. Strait for their helpful comments and suggestions.

LITERATURE CITED

- ABELSON, P. H., AND W. R. DURYEE 1949 Radioactive sodium permeability and exchange in frog eggs. *Biol. Bull.*, 96 (3): 205-217. (Abstracted in: *Biol. Abstr.*, 1950, 24 (1): 33, no. 270.)
- ADAMS, J. E., R. B. AIRD AND B. GAROUTTE 1952 Fluid and electrolyte exchange in the brain in experimental convulsions. *Tr. Am. Neurol. A.*, 77: 34-38.
- BARRER, R. M. 1952 Diffusion in and through solids. Cambridge University Press, London.
- CREESE, R. 1954 Measurement of cation fluxes in rat diaphragm. *Proc. Roy. Soc., London*, s. B, 142: 497-513.
- DANCKWERTS, P. V. 1951 Absorption by simultaneous diffusion and chemical reaction into particles of various shapes and into falling drops. *Tr. Faraday Soc.*, 47: 1014-1023.
- DEMIS, D. J., AND A. ROTHSTEIN 1955 Relationship of the cell surface to metabolism. XII. Effect of mercury and copper on glucose uptake and respiration of rat diaphragm. *Am. J. Physiol.*, 180 (3): 566-574.
- EDELMAN, I. S. 1952 Exchange of water between blood and tissues. Characteristics of deuterium oxide equilibration in body water. *Am. J. Physiol.*, 171: 279-296.
- GAROUTTE, B., AND R. B. AIRD 1955 Diffusion of sodium ions from cerebral tissue in vitro. *Science*, 122: 333-334.
- HARRIS, E. J., AND G. P. BURN 1949 The transfer of sodium and potassium ions between muscle and the surrounding medium. *Tr. Faraday Soc.*, 45: 508-528.
- HILL, A. V. 1928 The diffusion of oxygen and lactic acid through tissues. *Proc. Roy. Soc., London*, s. B, 104: 39-96, December 1.
- KONEFF, A. A. 1954 Personal communication.
- LEVI, H., AND H. H. USSING 1948 The exchange of sodium and chloride ions across the fiber membrane of the isolated frog sartorius. *Acta Physiol. Scand.*, 16: 232-249.
- MARCH, H. W., AND W. WEAVER 1928 The diffusion problem for a solid in contact with a stirred liquid. *Physical Rev.*, 31: 1072-1082, June.
- MUDGE, G. H. 1953 Electrolyte metabolism of rabbit-kidney slices studies with radioactive potassium and sodium. *Am. J. Physiol.*, 173: 511-522, June.
- SHANES, A. M., AND M. D. BERMAN 1953 Penetration of intact frog nerve by ions and sucrose. *Fed. Proc.*, 12: 130-131, No. 426.
- 1955 Penetration of the desheathed toad sciatic nerve by ions and molecules. II. Kinetics. *J. Cell. and Comp. Physiol.*, 45: 199-240, April.
- SHANES, A. M. 1954 Effects of sheath removal on the sciatic of the toad, *Bufo marinus*. *J. Cell. and Comp. Physiol.*, 43: 87-98, February.
- 1954 Sodium exchange through the epineurium of the bullfrog sciatic. *J. Cell. and Comp. Physiol.*, 43: 99-105, February.
- WESSON, L. G. JR., W. E. COHN AND A. M. BRUES 1949 The effect of temperature on potassium equilibria in chick embryo muscle. *J. Gen. Physiol.*, 32 (4): 511-523, March 20.

THE RELATION OF ACCOMMODATION TO CURRENT DISTRIBUTION IN SINGLE MUSCLE FIBERS

WILLIAM J. ADELMAN¹

*Department of Physiology and Biophysics, College of Medicine,
University of Vermont, Burlington, Vermont*

THREE FIGURES

The aim of these investigations was to determine the degree of applicability to single muscle fibers of certain concepts derived primarily from the study of nerve. In addition, it was desired to see whether the appearance of repetitive cathodal closing responses and anodal opening responses in muscle were related to the area of membrane depolarized, particularly considering the role of the "accommodative" process.

That sciatic nerves of "citratated" frogs possess little or no accommodation at large and indefinitely localized cathodal areas and considerable accommodation at sharply localized small cathodal areas has been noted previously (Benoit and Benoit, '37). Similarly, Suzuki ('38) reported that the value of the time constant of accommodation, λ , was greater at a large fluid electrode than it was at a punctate cathode. Benoit ('49), working on frog *sartorii*, was able to show that diffuse cathodal stimulation favors repetitive responses, while stigmatic cathodal stimulation favors simple twitch responses.

Thus it was decided to test the basic contention that prolonged convergent current flow in an excitable tissue favors accommodation. The use of the single muscle fiber prepara-

¹ Present address: Department of Physiology, School of Medicine, University of Buffalo, Buffalo, New York.

tion eliminates the possibility that the effect lies in some structure external to the fiber itself (such as the sheath).

PREPARATION

The retrolingual membrane of the frog has been described by Fischl and Kahn ('28), Gelfan ('30), Pratt ('30), and Grundfest ('32) as being an excellent preparation for the study of single skeletal muscle fibers. These fibers are widely separated from one another thus facilitating individual stimulation. Generally, it has been found that with ordinary care preparations can be made that will remain in excellent condition for many hours. In addition to these aspects the membrane provides an *in vivo* circulated environment which is difficult to duplicate in studies on single muscle fibers in other preparations. While the fibers in the retrolingual membrane show some branching and anastomosing, areas of activity are strictly limited and no fully conducting continuum exists. Responses of the fibers can be easily seen by microscopic observation at relatively low powers.

Rana pipiens was used throughout these experiments.

METHOD

The method employed in the preparation of the retrolingual membrane was essentially that of Pratt and Reid ('30) as modified by Grundfest ('32). A Lucite block was cemented to a large Petri dish and the dish was then filled with a 50/50 mixture of paraffin and beeswax up to the level of the top of the Lucite block.

A frog which was decerebrated by pithing was then placed supine on the surface of the dish and the tongue laid out so that it covered the Lucite block. A longitudinal slit was then made on the ventral surface of the tongue and the musculature and other tissues retracted so that the retrolingual membrane remained excellent for many hours after the initial preparation.

Following the dissection to expose the membrane, the frog was inverted and the tongue fastened over the Lucite block by means of pins so that the membrane could be trans-illuminated and the Petri dish was filled with Ringer's solution so that the tongue was completely immersed. The entire preparation was then placed on the stage of a Bausch and Lomb stereoscopic wide field microscope and illuminated by means of a substage lamp. The beam of light passed through a heat filter previous to passing through the membrane.

In early experiments stimuli were applied through large calomel half-cells connected by agar-Ringer bridges to a diffuse electrode and a localized capillary electrode. The capillary electrodes were made from glass tubing (4 mm inside diameter) pulled out in a micro-flame to a capillary having an opening of about 50 to 100 μ in diameter. These were filled with Ringer's solution. The relatively large opening of the capillary insured that responses elicited by stimulation were always conducted and not local. In later experiments stimuli were applied through the calomel half-cells to two capillary electrodes which had openings about 10 to 60 μ in diameter.

Two stimulators were employed in the experimental procedure. The first stimulator supplied a rectangular direct current pulse, the "make" of which was manually controlled by means of a switch operated by a thyratron tube key. The "break" was effected directly from a manual switch. Current direction could be reversed by means of a commutator. This stimulator was used primarily to compare cathodal closing and anodal opening responses in the single muscle fibers.

The second stimulator supplied direct current shocks in either direction, with supplementary very brief condenser-discharge test shocks ($RC = 0.08$ msec) at either anode or cathode, and exponentially blunted shocks. Shocks were repeated automatically at a set frequency. It was desired to minimize polarization or any long term accumulative change that might occur in the excitable system of the fibers due to repeated current flow in the same direction. This was accomplished by means of a double-pole double-throw relay trig-

gered by the break of the constant pulse so that the current direction of alternate shocks was automatically reversed. The test shock was directed either anodally or cathodally by means of a switch. The magnitudes of the D.C. and of the test shock were independently controlled by Beckman Helipot potentiometers equipped with Duodials. These potentiometers were helix wound and were linear to $\pm 0.1\%$. Therefore, by direct reading of the Duodial the relative potentials could be precisely determined.

The performance of both stimulators was checked frequently by direct observation of the pulse forms on an oscilloscope. This method was also used to calibrate the controls governing the timing of the test shocks. The pulses of both stimulators ascended and descended as if capacitor-shunted with RCs of 0.05 and 0.10 msec respectively. The make and break of the constant pulse of both stimulators were free of any disturbing transients.

Within the limits of error of the method there appeared to be perfect physical summation between the constant current and the condenser discharges (whether they were similarly or oppositely directed) in the second stimulator. Also noted in the second stimulator was the complete independence of the magnitude of the test shock and its timing with respect to the make of the constant pulse.

The second stimulator permitted measurement of accommodation by the test shock method (Erlanger and Blair, '31; LeFevre, '50) and by the exponentially blunted shock method of Solandt ('36). The stimulator was usually set to deliver a test stimulus (of whatever form was in use) every 4 seconds. The duration of the constant pulse was about 40 msec when the test shock method was employed; this was increased to about 120 msec when exponentially blunted shocks were used. Blunting of the D.C. pulse was accomplished by means of Cornell-Dubilier Decade Capacitors. The timing of the test shock was similarly controlled by a 2,000 ohm helipot.

Thresholds to the various stimuli were approached from above, and the last conducted response was taken as the

index. Those responses in which the contraction occurred over the entire length of the fiber in question were taken as conducted responses. Where branching was evident, the contraction could be seen to traverse the branches as well as the portion of the fiber on which the electrodes were applied. Even with relatively small capillary openings there seemed to be little doubt that the responses measured were conducted and not local.

Assurance was desired that the response would be due to direct stimulation of the muscle, and not due to stimulation of the muscle through the nerve. Therefore previous to preparation of the retrolingual membrane all frogs were completely curarized. The dosage used was about 8 mg/kg of frog and was injected into the dorsal lymph sac. This usually resulted in complete paralysis in 10 to 20 minutes. Abbott Laboratories d-Tubocurarine-Cl was used throughout. The response to this dosage may be compared to Wright and Taylor's data ('49). They noted that 4.4 mg of d-Tubocurarine-Cl/kg of frog injected into the dorsal lymph sac resulted in complete paralysis in 20 to 30 minutes.

RESULTS

Effects of direct current stimulation

A. Electrodes: one diffuse, one punctate. Whenever a single muscle fiber in the retrolingual membrane was stimulated with direct current it was noted that the responses at both cathode and anode changed markedly on reversing the direction of the current flow.

Table 1 shows the results of determinations on 36 single muscle fibers. Whenever the capillary electrode was the cathode and the diffuse electrode was the anode, anodal opening responses were elicited. In many cases these were repetitive. Cathodal closing responses were never repetitive. Whenever the pore electrode was the anode and the diffuse electrode was the cathode, repetitive cathodal closing responses were elicited. No anodal opening responses could be detected. This pattern

of responses would imply that accommodation (at both electrodes) occurred only when the more punctate electrode was made cathode. This was borne out by direct measurements of the accommodation.

These determinations, usually of the exponentially blunted shock type, were made either immediately before, or immediately after direct current stimulation. A few determinations of accommodation by the test shock method were also made at the diffuse electrode. In order for the very rapid test shock to stimulate diffusely over such a large area, very high voltages were necessary, and these generally exceeded the limits of the stimulator. However the test shock method

TABLE 1

TYPE OF ELECTRODE		CATHODAL CLOSING RESPONSE ¹	ANODAL OPENING RESPONSE
Anode	Cathode		
Diffuse	Punctate	Non-repetitive	Always present (sometimes repetitive)
Punctate	Diffuse	Repetitive	Always absent or indeterminate

¹ Thresholds were lower at the punctate electrodes.

gave additional evidence for the absence of anodal accommodation when the anode was punctate.

With the exponentially blunted shocks it was found there was considerable accommodation at the cathode whenever the cathode was punctate, whereas at the diffuse cathode little or no accommodation could be seen.

In figure 1 may be seen a typical result of the exponentially blunted shock type of accommodation measurement. With the punctate cathode, considerable accommodation is shown, with a λ value of about 2.4 msec. The mean λ value for 10 such determinations was 6 msec. At the diffuse cathode, the record in figure 1 shows little or no accommodation. While there was no direct determination of accommodation at the diffuse an-

ode, the appearance of the anodal opening response is a good indication that accommodation had occurred here also.

Thus, it was seen that the accommodation to the direct current pulse became quite different when the current direction was changed. In order to determine whether distortion of the wave form of the constant pulse might be the cause of the change in response, the output of the stimulator was checked frequently on the oscilloscope screen during stimulation of a fiber. No distortions or apparent transients could be seen

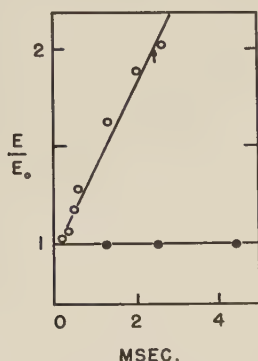


Fig. 1 Effect of current direction on "accommodation" in a single muscle fiber. Exponentially blunted shocks applied through a large diffuse electrode and a punctate microelectrode. Threshold in rheobase multiples (ordinate) plotted against time constant of rise (RC) of current strength (abscissa). λ estimated as reciprocal slope at $E/E_0 = 2$. Open circles: with anode diffuse and cathode punctate. Closed circles: with cathode diffuse and anode punctate.

with current flow in either direction. Interchanging the calomel half-cells did not alter the results in any manner. Replacing the electrodes with different sets of electrodes had no effect on the results. As far as could be seen the only determining factor for the type of accommodative response seen was whether the cathode or anode was either diffuse or punctate.

The results of this work suggested that stimulation with two punctate electrodes might give further information. Such a series of experiments, in which two capillary electrodes were

used, is considered in the next section. One of these electrodes usually had a larger capillary opening than the other; but in a few experiments the two capillary electrodes were of virtually the same size.

B. Electrodes: both punctate. Whenever a single muscle fiber in the retrolingual membrane was stimulated with direct current through two capillary electrodes it was noted that repetitive cathodal closing responses always occurred when the cathode had the larger capillary opening. Whenever the

TABLE 2

TYPE OF ELECTRODE		CATHODAL CLOSING RESPONSE ¹	ANODAL OPENING RESPONSE
Anode	Cathode		
Larger	Smaller	Non-repetitive	Always present (sometimes repetitive)
Smaller	Larger	Repetitive	Always absent or indeterminate

¹ Thresholds were lower at the smaller electrodes.

TABLE 3

TYPE OF ELECTRODE		CATHODAL ACCOMMODATION	ANODAL ACCOMMODATION
Anode	Cathode		
Larger	Smaller	Considerable	No determinations
Smaller	Larger	Negligible	Negligible

cathode had the smaller capillary opening (the anode having the larger capillary opening) anodal opening responses were noted. In many cases these were repetitive. Table 2 shows the results of determinations on 43 different muscle fibers.

Accommodation measurements taken either immediately after or immediately before direct current stimulation showed a matching of the response with the recorded accommodation. Both the exponentially blunted shock method and the test shock method were used in these determinations. Table 3 summarizes the type of accommodation found at the particular electrodes.

The test shock method could not be used to determine the accommodation at the anode when this was at the larger electrode. This was due primarily to the fact that the threshold at the more punctate of the two electrodes was invariably lower than that at the more diffuse of the two electrodes, as would be expected. Therefore any sub-threshold conditioning shock of appropriate magnitude for determining diffuse anodal accommodation would be above the threshold at the more punctate cathode and would make this method invalid.

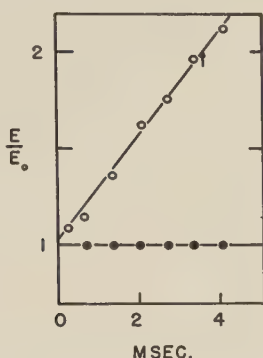


Fig. 2 Effect of current direction on "accommodation" in a single muscle fiber. Exponentially blunted shocks applied through two microelectrodes of differing pore size. Threshold in rheobase multiples (ordinate) plotted against time constant of delay rise (RC) of current strength (abscissa). λ estimated as reciprocal slope at $E/E_0 = 2$. Open circles: cathode at smaller electrode. Closed circles: cathode at larger electrode.

Figure 2 represents a typical result of accommodation determination by means of exponentially blunted shocks. The curve for accommodation at the more punctate cathode shows a λ of about 3.6 msec. The average of 10 such determinations was 7 msec. However the curve at the more diffuse cathode shows virtually no accommodation.

In figure 3 may be seen typical results of accommodation determinations by the test shock method. Curve A represents the actual threshold changes at a more punctate cathode when a sub-threshold D.C. shock is applied. As can be seen from the curve, accommodation was considerable and even resulted

in a slight cathodal depression. This confirms the less direct findings obtained by means of exponentially blunted shocks. Curve B represents the threshold changes at the more punctate anode and indicates that accommodation is negligible.

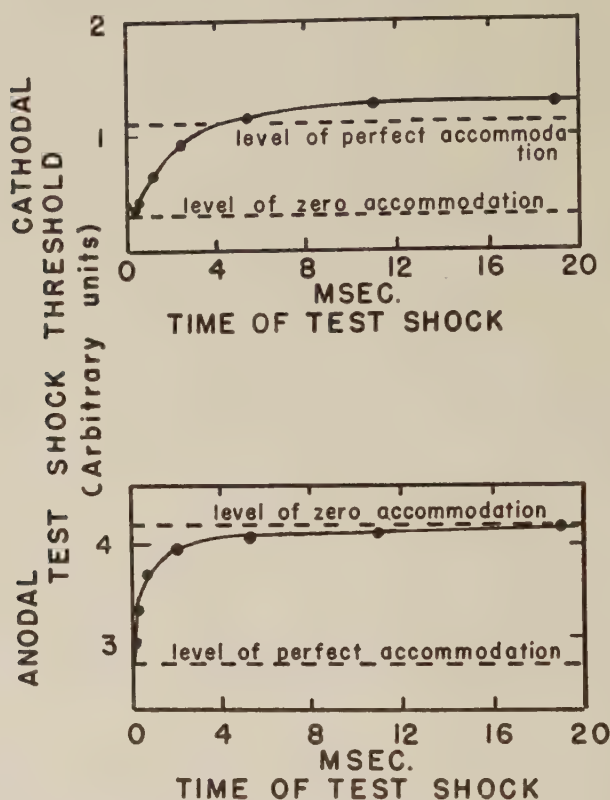


Fig. 3 Threshold changes at localized electrode at "make" of D.C. shock in a single muscle fiber. Test shock amplitude plotted against interval between "make" of D.C. and test shock. Ordinate: test shock threshold (arbitrary units). (A) Upper curve: test shock at smaller cathode. Amplitude of D.C. is 81% of rheobase. (B) Lower curve: test shock at smaller anode. Amplitude of D.C. is 88% of rheobase. Curves are representative of six complete determinations.

This type of electrode arrangement allowed for the investigation of whether or not specifically excitable regions were responsible for the accommodation changes noted. In these experiments the two electrodes were placed on the muscle

fiber and a series of determinations were made. Then the electrodes were replaced on the fiber so that each occupied the opposite position and the determinations were repeated. In 10 determinations of this kind the responses that were specific for more punctate electrode did not change when the electrodes were reversed. The same was true for the more diffuse electrode. Varying the interelectrode distance did not affect the specificity of the responses; nor did moving the pair of electrodes from one position on a fiber to another position on the same fiber. Likewise the pattern of responses remained the same on shifting the electrodes from one fiber to another. In all, about 30 determinations of this kind were completed. Thus it seemed that the cause of the type of accommodative responses seem lies in some portion of the external circuit. Again the stimulators were checked and the calomel cells were interchanged. Nothing other than the electrodes themselves could be determined as contributing to the pattern of responses recorded.

The electrodes were replaced frequently with new electrodes. Even with varying size pore openings the pattern of response remained the same; i.e., with the cathode more diffuse than the anode, accommodation was absent or negligible; but when the anode was the more diffuse, accommodation was favored.

In experiments using electrodes of approximately the same size pore openings no definitive results were obtained. Difficulty was encountered in producing electrodes with identical pore openings; however the general problem is more complex than the production of electrodes with identical diameters. Current distribution would also depend upon the distance of the pore opening from the fiber proper.

DISCUSSION

From the results it would seem that the theoretical considerations of Hill ('36) with respect to the manner of involvement of accommodation in the excitation system are partially valid for the fibers in the retrolingual membrane.

Whenever repetitive cathodal closing responses are seen, no accommodation is measured; whenever anodal opening responses are seen, considerable accommodation is indicated. However in Hill's analysis the threshold changes at the anode and the cathode are considered to be "mirror images" of each other. In the development of his analysis Hill considers only the case where accommodation is "normal" or perfect; in the fully accommodated state the threshold is the same as in the resting state. However this seems to be hardly ever the case. (For example, figure 3, A shows considerable accommodation appearing at about 6 msec; figure 3, B shows complete lack of accommodation at the anode.)

The impracticability of direct measurement of accommodation at the diffuse anode is regrettable. While the threshold changes at cathode and anode are not "mirror images," the cathodal accommodation picture does indicate to some extent what is occurring at the anode. The recording of opening responses at the diffuse anode, and the occurrence of considerable cathodal accommodation are strong indications that accommodation is occurring at the diffuse anode. For many years it has been common practice of investigators to measure accommodation at the cathode and to infer from this the state of accommodation at the anode.

In terms of the geometry of current flow through the fiber membrane, the results reported here would indicate that accommodation occurs only when the current is decidedly convergent in its flow through the fiber.

In terms of the recent theory proposed by Hodgkin and Huxley ('52) for the activity of the squid giant axon, increased accommodation at the cathode implies an increased potassium conductance and an increased degree of sodium inactivation, while increased accommodation at the anode implies the converse. This situation results in a continually rising threshold at the cathode during current flow, while developing the conditions at the anode for anodal opening responses to appear when current flow ceases. On turning the anodal polarizing current off, the membrane potential returns to its resting level

with a reduced outward potassium current and an increased sodium current inward. The net ionic current is inward and the membrane depolarizes giving rise to an anodal opening response.

Since increasing the area of the membrane depolarized at the cathode or decreasing the area polarized at the anode both increase accommodation as the results in this communication indicate, it is possible to speculate that the ionic conductance and the degree of inactivation are functions of the area of membrane altered in potential. If the Hodgkin and Huxley theory is to be applied to muscle the addition of a space factor seems somewhat necessary. Indeed, Hodgkin and Huxley suggest that the oscillations seen in membrane potential upon current application to the squid axon may be damped out by stimulation through punctate electrodes. This suggestion is based on the reasoning that adjacent regions on the membrane will have different membrane potentials giving rise to currents which increase damping. Generally, neural systems which are highly oscillatory such as opener motor nerve fibers in the walking legs of crustacea show little accommodation and possess only slightly damped excitatory states (Wright and Adelman, '54). Consequently, by again leading back through the phenomenon of accommodation we may state that these systems show a less pronounced potassium conductance and sodium inactivation.

SUMMARY

1. Cathodal closing excitation and anodal opening excitation of the single muscle fibers in the retrolingual membrane of the frog were investigated with prolonged constant currents applied through different electrode arrangements.

(a) Repetitive cathodal closing excitation was favored by having the cathode more diffuse than the anode.

(b) Anodal opening excitation was favored by having the anode more diffuse than the cathode.

2. Accommodation has been measured with exponentially blunted D.C. shocks and with brief condenser-discharge test

shocks superimposed at either electrode at controlled intervals following the closing of a constant current.

(a) Accommodation was found negligible when a diffuse cathode and punctate anode were used; when a punctate cathode and diffuse anode were used accommodation was favored.

3. Accommodation seems to be favored by convergent current flow through the single muscle fibers of the retrolingual membrane.

4. The applicability of modern excitation theory to retrolingual membrane muscle fibers has been discussed. It has been found that certain assumptions made in the derivation of this theory are invalid for this tissue:

(a) "Normal" or perfect accommodation was rarely seen.

(b) Anodal threshold behavior did not parallel that at the cathode.

5. Applications of the results to the recent theories of Hodgkin and Huxley have been discussed.

The writer wishes to express his sincere thanks and appreciation to Dr. Paul G. LeFevre for his constructive guidance and warm-hearted encouragement throughout this investigation and to Dr. F. J. M. Sichel for his advice and for the use of many pieces of essential equipment.

Expenses in part were defrayed by the United States Public Health Service Grant RG-2681 B-46.

LITERATURE CITED

- BENOIT, P. H., AND M. BENOIT 1937 Action des courants progressifs sur le nerf myélinisé "decalcifié." Influence de la dimension des électrodes. *Comp. rend. Soc. Biol.*, 125: 49-52.
- BENOIT, P. H. 1949 Les constants du temps de la fibre musculaire striée et la problème de la transmission synaptique. *Arch. des Sci. Physiol.*, 3: 259-284.
- ERLANGER, J., AND E. A. BLAIR 1931 The irritability changes in nerve in response to subthreshold constant currents, and related phenomena. *Am. J. Physiol.*, 99: 129-155.
- FISCHL, E., AND R. H. KAHN 1928 Untersuchungen an einem Nerv-Muskelpräparate zur Beobachtung einzelner querqestreifter Muskelfasern. *Arch. ges. Physiol.*, 219: 33-46.

- GELFAN, S. 1930 Studies of single muscle fibers. I. The all-or-none principle. *Am. J. Physiol.*, *39*: 1-8.
- GRUNDFEST, H. 1932 Excitability of the single fibre nerve-muscle complex. *J. Physiol.*, *76*: 95-115.
- HILL, A. V. 1936 Excitation and accommodation in nerve. *Proc. Roy. Soc. London, B*, *119*: 305-355.
- HODGKIN, A. L., AND A. F. HUXLEY 1952 A quantitative description of membrane current and its application to conduction and excitation in nerve. *J. Physiol.*, *117*: 500-544.
- LEFEVRE, P. G. 1950 Excitation characteristics of the squid giant axon: A test of excitation theory in a case of rapid accommodation. *J. Gen. Physiol.*, *34*: 19-46.
- PRATT, F. H. 1930 On the grading mechanism of muscle. *Am. J. Physiol.*, *93*: 9-18.
- PRATT, F. H., AND M. A. REID 1930 A method for working on the terminal nerve-muscle unit. *Science*, *72*: 431-433.
- SOLANDT, D. Y. 1936 The measurement of "accommodation" in nerve. *Proc. Roy. Soc. London, B*, *119*: 355-379.
- SUZUKI, M. 1938 Zur Frage des Einschleichens des Stromes. *Arch. ges. Physiol.*, *239*: 81-96.
- WRIGHT, E. B., AND W. J. ADELMAN 1954 Accommodation in three single motor axons of the crayfish claw. *J. Cell. and Comp. Physiol.*, *43*: 119-132.
- WRIGHT, E. B., AND R. E. TAYLOR 1949 The comparative actions of Dihydro-beta-erythroiden and d-tubocurarine in the frog. *J. Cell. and Comp. Physiol.*, *34*: 327-350.

SOLUBLE AND PARTICULATE CHOLINESTERASE IN INSECTS ¹

B. N. SMALLMAN AND L. S. WOLFE

*Science Service Laboratory, Canada Department of Agriculture,
London, Ontario*

SIX FIGURES

In a study of cholinesterase in insects, Babers and Pratt ('51) observed a difference in the distribution of the enzyme in homogenates of houseflies and bees. They found that when a homogenate of fly heads was centrifuged, most of the cholinesterase activity was in the supernatant; but when a homogenate of bee heads was treated in the same way, most of the activity was in the precipitate. This observation suggested to us that cholinesterase in insects may exist in two states — soluble and particulate; and further, that the properties of the enzyme might differ with its state. Certain enzymes have been demonstrated both in solution and associated with cell particles, and it has been shown that the same enzyme in these different states may exhibit different properties, including the response to inhibitors (Green, '52; Peters, '52). If this phenomenon could be demonstrated for cholinesterase in insects, it would have interesting implications for the mode of action of the organophosphorus insecticides.

This study is concerned with the demonstration that the cholinesterase activity of homogenates of insect nervous tissue is, in fact, distributed between a soluble and a particulate fraction, and with an examination of the conditions affecting this distribution *in vitro*. A subsequent study (Wolfe and Smallman, '54) examines the properties of the enzyme in the two states.

¹ Contribution No. 33.

MATERIALS AND METHODS

Homogenates were prepared from heads of the housefly, *Musca domestica*, heads of the worker honeybee, *Apis mellifera*, brains of the honeybee, and nerve cords of the roach, *Periplaneta americana*. Heads or excised tissues were homogenized immediately in the desired suspension medium, using a Potter-Elvehjem glass homogenizer. Tissue concentrations were as follows: fly heads, 30 mg (15–18 heads) per milliliter; bee heads, 100 mg (10 heads) per milliliter; bee brains, 8 brains per milliliter; roach cords, 4 cords per milliliter. The pH of homogenates was determined immediately and adjusted to neutrality when necessary. Homogenates were centrifuged in an MSE Hi-speed centrifuge at 10,000 g for 10 minutes, unless stated otherwise.

Cholinesterase activity was determined by the manometric or the titrimetric method at 25°C. The manometric method was used for most of the work. The conditions of assay were: 0.5 ml enzyme preparation; 2.0 ml NaHCO₃ (0.025 M, final); 0.2 ml ACh Br (0.01 M, final). All determinations were made in duplicate, and activities were calculated as b₃₀'s by the method of Aldridge, Berry and Davies ('49). The titrimetric method has been shown to be more appropriate than the manometric method for estimating the effects of salts on cholinesterase activity (Smallman and Wolfe, '55). Therefore, the titrimetric method was used for certain parts of this study concerned with the effect of salts on the distribution and activity of fly head cholinesterase. The basic procedure was the same as that described previously (Smallman and Wolfe, '55). The conditions of assay were: enzyme preparation, equivalent to one fly head per milliliter; ACh Br, 0.015 M; suspension medium de-ionized water or salt solutions as indicated; pH, 8.0 maintained with 0.1 N NaOH. Corrections for non-enzymic hydrolysis were made by carrying out the same procedure with the same enzyme preparation after treatment with TEPP, 1×10^{-5} M, for three hours.

RESULTS

Demonstration of activity in the supernatant and centrifugate from insect homogenates

Several different insect tissues were examined to determine whether the cholinesterase activity could be separated into two fractions by centrifugation. Fly heads, bee heads, bee brains, and roach cords were homogenized, each in three suspension media: water, sucrose (0.25 M), and KCl (0.5 N) and adjusted to pH 7.0. The homogenates were centrifuged at 10,000 g for 10 minutes. The supernatant was decanted and the particulate material was resuspended in the same volume of the suspension medium and centrifuged again, as before. The supernatant (washing) was again decanted and the washed particulate again taken up in the same volume of suspension medium. This procedure yielded three fractions for the determination of cholinesterase activity: the washed particulate material, the initial supernatant, and the washings from the particulate fraction.

Figure 1 shows the relative activities of these three fractions calculated as percentages of the total activity. The following points are made:

1. All 4 preparations, whether suspended in water, sucrose, or KCl, showed activity in both the particulate and supernatant (soluble) fractions.
2. The particulate fraction loses some activity on washing; in every case, the washings show activity.
3. The amount of activity lost by the particulate fraction during washing is uniformly smaller when KCl is used as the suspension medium.
4. In any one preparation the distribution of activities follows the same pattern in water and sucrose, but changes in KCl to give a higher proportion of the activity in the particulate.
5. In apparent contrast to the observation of Babers and Pratt ('51), the distribution of activities between the super-

natant and particulate fractions, when separated in water, was the same with fly heads and bee heads.

In the following sections, these findings are examined further.

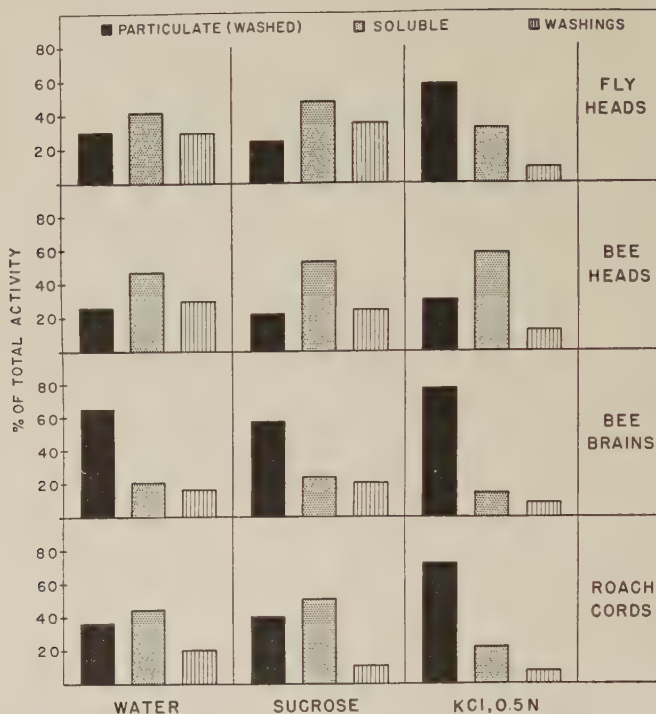


Fig. 1 Distribution of cholinesterase activity in fractions separated by centrifugation of insect homogenates suspended in various media.

Examination of the state of the two fractions

The finding that one washing removes considerable activity from the particulate fraction (fig. 1) raises the possibility that the enzyme may be adsorbed on the particles so lightly that further washings would remove all of it. Accordingly, the particulate fraction from fly heads was separated and washed repeatedly by successive re-suspensions and centrifugations in fresh suspension medium. This procedure was carried out in the three suspension media: water, sucrose (0.25 M), and KCl (0.5 N).

Figure 2 shows the results. Repeated washing in water and sucrose reduced the cholinesterase activity of the particulate fraction until after 5 washings it stabilized at about 20% of the total activity. With KCl as the suspension medium, much less activity was lost during washing; after three washings the activity stabilized at 35% of the total activity.

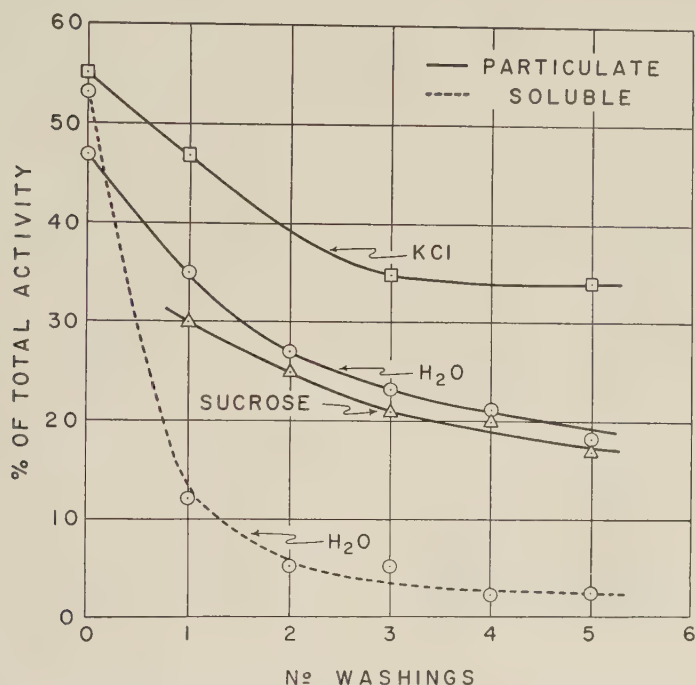


Fig. 2 Effect of washing on the cholinesterase activity of the precipitate obtained by centrifuging fly head homogenates in various media. The dotted line shows the activity remaining in the supernatant after washings with water.

A proportion of the enzyme therefore seems to be firmly bound to the particulate matter.

We then sought to determine whether the cholinesterase demonstrated in the supernatant is, in fact, in the soluble state. The possibility exists that the enzyme in the supernatant may still be attached to small particles which remain suspended after centrifugation at 10,000 g for 10 minutes. To

test this possibility, fly-head homogenates were centrifuged in sucrose (0.25 M) for one hour at centrifugal forces from 500 g to 15,000 g.

Figure 3 shows the results. The upper half of the figure shows that centrifugation for one hour at gravities from 0 to 5,000 precipitates nearly all the enzyme that can be

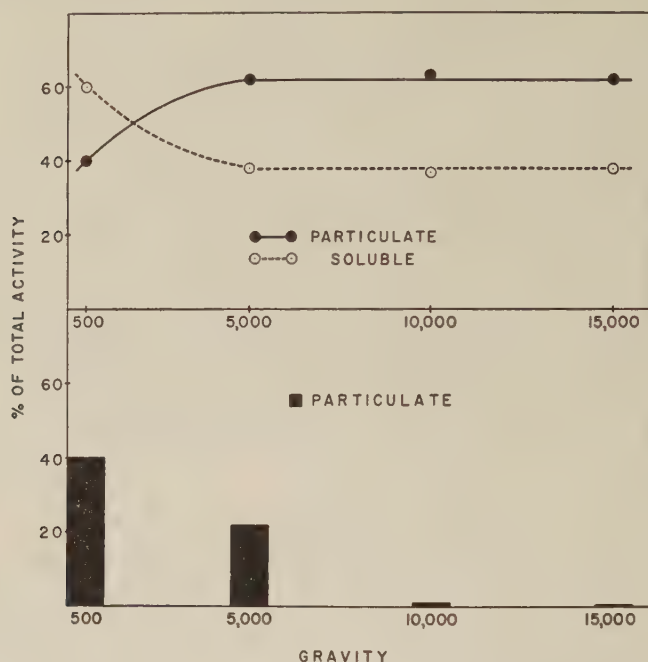


Fig. 3 Upper half: effect of centrifugal force on the distribution of cholinesterase activity between the two fractions from fly head homogenates suspended in 0.25 M sucrose. Lower half: increments in the proportion of activity precipitated at increasing centrifugal forces.

removed from the supernatant under these conditions; at gravities from 5,000 to 15,000 little further enzyme is precipitated from the supernatant and the activity of both fractions remains almost constant.

However, this evidence does not preclude the possibility that the enzyme in the supernatant may be attached to microsomes remaining suspended after centrifugation for one

hour at 15,000 g. Subsequent to above experiment, fly-head homogenates in 0.25 M sucrose were centrifuged for one hour in a Spinco Preparative centrifuge at 26,000 g, 35,000 g, 43,000 g, and 50,000 g. At all 4 gravities, the activities of the centrifugates were the same, and accounted for 79% of the total activity. At 5,000 g to 15,000 g, the activities of the centrifugates were also the same, but accounted for only 63% of the total activity (fig. 3). This difference suggests that a microsomal fraction is present and is precipitated between 15,000 g and 26,000 g. However, on the original point of this experiment, the evidence shows that part of the cholinesterase activity remains in the supernatant after centrifugation at gravities well above those required to sediment all particulate matter from 0.25 M sucrose solutions (Schneider '48). This evidence indicates that the enzyme does indeed exist in the soluble state.

Figure 3 also affords information on the nature of the particulate fraction. As shown in the lower half of the figure, two-thirds of the particulate enzyme is precipitated by centrifugation for one hour at 500 g; the remainder is precipitated between 500 g and 5000 g. Only large cell fragments and nuclei would be expected to sediment at 500 g from 0.25 M sucrose (Schneider, '48). It seems, therefore, that most of the particulate enzyme is associated with large cell fragments and nuclei.

*Effect of salt concentration on the distribution
of activity between the two fractions*

The presence of an electrolyte clearly affects the distribution of cholinesterase between the two fractions. This is apparent from figure 1 which shows that the particulate fraction had a higher proportion of the total activity when the tissues were suspended in KCl than when the suspension medium was water or sucrose. The relatively higher activity in the particulate fraction seems to result from the smaller loss during washing and, except in the preparation of bee heads,

from the lower proportion of the activity in the soluble fraction.

To obtain further information on the effect of KCl, fly heads were homogenized and centrifuged in several different concentrations of the salt. The cholinesterase activity of the supernatant and centrifugate was measured by the titrimetric method. Figure 4 shows the striking shift in activity from the soluble to the particulate fraction under the influence of low concentrations of KCl. As compared to the distribution

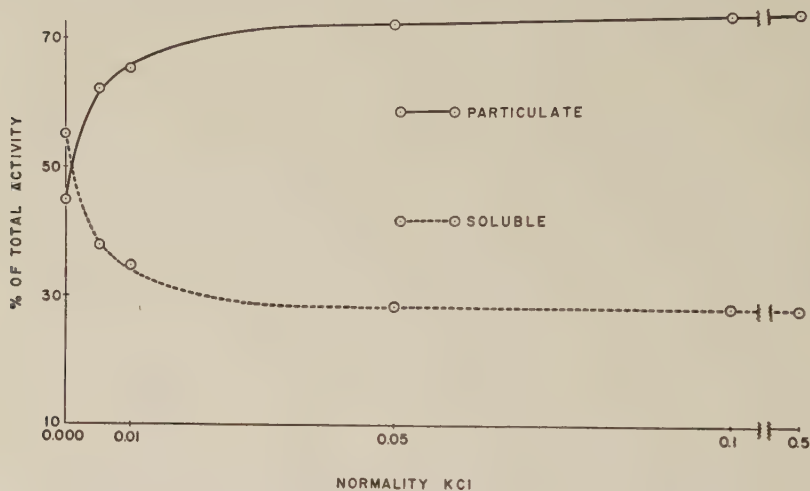


Fig. 4 Effect of KCl concentration on the distribution of cholinesterase activity between the two fractions.

in de-ionized water, 20% of the total activity was shifted from the soluble to the particulate fraction by KCl, 0.01 N. This shift continues until, between 0.05 N and 0.1 N KCl, an equilibrium is established and no further change in distribution occurs up to 0.5 N KCl. The form of these curves suggests an adsorption phenomenon. Tiselius ('48) has shown that salts at moderately low concentrations strongly promote the adsorption of proteins on particulate matter. His data for the adsorption of egg albumin on silica gel under the influence of various concentrations of ammonium sulphate yield a curve similar to that shown in figure 4. We suggest

that salting out adsorption is also responsible for the transfer of cholinesterase from the soluble state to the particulate matter in fly homogenates suspended in KCl. The effect of KCl therefore is to promote an adsorption of soluble enzyme on the particulate matter, and for this adsorption to be stronger, and less subject to washing out, than in the presence of water alone. These effects appear to account for the observed differences in the distribution of the enzyme when the various insect preparations were separated in water and KCl.

Besides its effect on the relative distribution of cholinesterase between the two fractions, KCl was found to increase the absolute activity of the enzyme. In all experiments using KCl as suspension medium, the total activity of the two fractions was considerably higher than when the suspension medium was de-ionized in water. This activation of the enzyme by KCl was examined further to determine whether the two fractions were equally susceptible to activation by KCl. Accordingly, homogenates of fly heads were centrifuged and suspended in various concentrations in KCl. At each concentration, the activities of both fractions were determined, and compared as percentages with the activity of the corresponding fraction separated and suspended in de-ionized water. The results are shown in figure 5.

As compared to its activity in water, the activity of the particulate enzyme increased linearly from 50% in 0.005 N KCl to almost 300% in 0.5 N KCl. On the other hand, the activity of the soluble enzyme in the lower salt concentrations was lower than its activity when separated and measured in water, but between 0.05 N and 0.1 N KCl the activity reached the same level as that in water; from 0.1 N to 0.5 N KCl the activity increased sharply above the activity in water. When the activities of both fractions were added together ($P + S$), the values fell between the values for the separate fractions, and increased linearly from 12% activation in 0.005 N KCl to 150% activation in 0.5 N KCl. For comparison, the values of Chadwick et al. ('53) for the activation of whole homoge-

nates of fly heads by KCl were plotted on the same line. The figure shows that good agreement was obtained between the two sets of values, and indicates that salt activation of whole homogenates may be accounted for in terms of the two fractions.

The data of figure 5 might be thought to indicate that the two fractions respond differently to the presence of KCl;

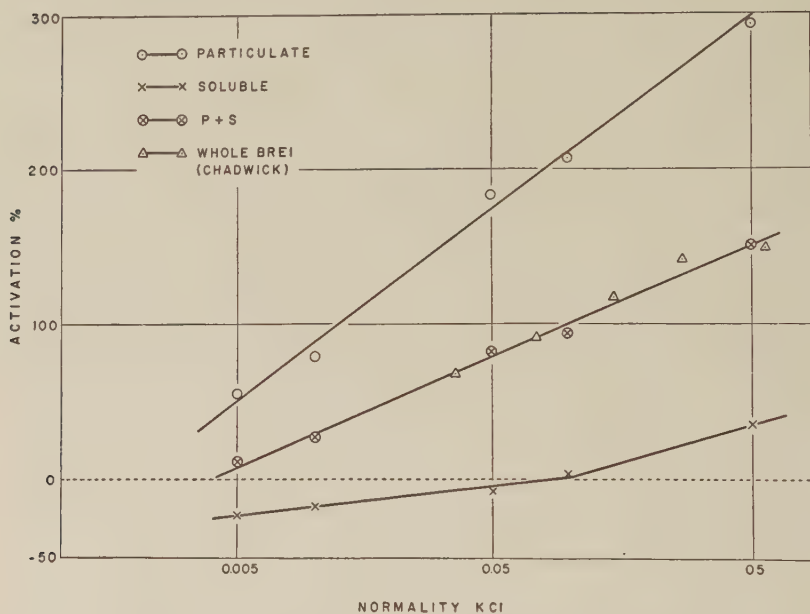


Fig. 5 Effect of KCl concentration on the cholinesterase activity of the fractions separated from fly head homogenates suspended in KCl solutions, as compared to the activity when separated in de-ionised water.

the activity of the soluble fraction appears to be depressed or only slightly higher than its activity in water, in contrast to the marked activation of the particulate fraction. However, this difference may be explained as the result of the shift of activity from the soluble to the particulate fraction when the fractions are separated in KCl (fig. 4). At low concentrations of KCl, this shift is large and the activation is small so that the activity of the soluble fraction is lower

than its activity when separated and measured in water. Above 0.1 N KCl, however, an equilibrium is established between the two fractions (fig. 4), and no further transfer of enzyme from the soluble to the particulate enzyme occurs; at this same normality, the activation of the soluble fraction becomes apparent (fig. 5).

To eliminate the effect of this shift, the two fractions were first separated in de-ionized water and then made 0.5 N by addition of KCl. For comparison, the fractions were separated in the presence of KCl (0.5 N) as before. Table 1 shows the results. When the separation medium was 0.5 N KCl, the activation of the particulate fraction was high and the activation of the soluble fraction was much less, as before.

TABLE 1
Activation (%) of Fly ChE Fractions by 0.5 N KCl

FRACTION	SEPARATION MEDIUM		
	KCl, pH 7.7	KCl, pH 6.8	H ₂ O pH 6.8
Particulate	293	172	149
Soluble	34	73	153
P + S	150	144	150

However, when the separation was made in water, both fractions were activated equally by additions of KCl (0.5 N). The activation of the whole system (P + S) by 0.5 N KCl was the same whether the separation was made in water or KCl. Both fractions therefore respond equally to the activating effect of KCl. In addition to its activating effect, KCl also affects the distribution of the enzyme between the two fractions. Regardless of the distribution, however, the sum of the activities of both fractions remains the same.

These effects are not specific for KCl. NaCl was found to affect the distribution and activity of the enzyme in the same way as shown with KCl in table 1. Moreover, a number of other salts have been shown to activate the cholinesterase of fly heads (Chadwick et al., '53; Smallman and Wolfe, '55).

Table 1 also shows that the pH of the separation medium alters the degree of activation of the two fractions. The difference results from the effect of pH on the distribution of activity between the two fractions. This effect is examined in the following section.

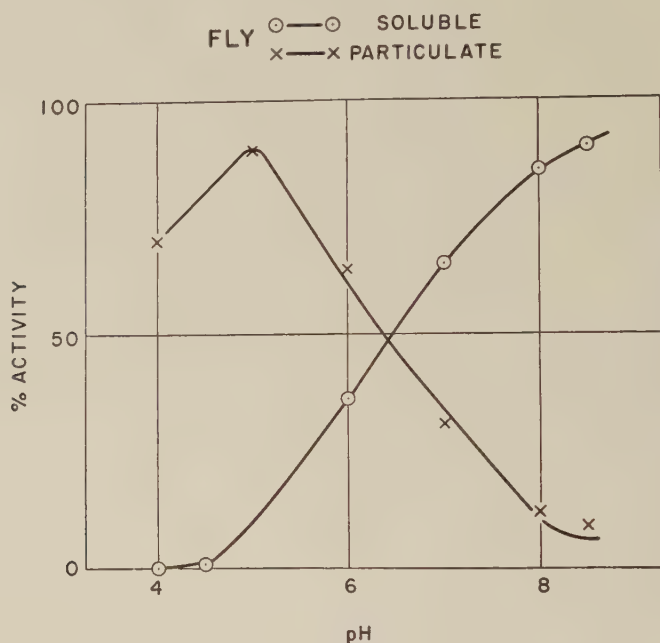


Fig. 6 Effect of pH on the distribution of cholinesterase activity between the two fractions.

*Effect of pH on the distribution of activity
between the two fractions*

Homogenates of fly heads were prepared in water and the pH adjusted to various values between pH 4.0 and 8.5. The homogenates were then centrifuged and the activity of the two fractions determined by the manometric method.

The results are shown in figure 6. At pH 8.0 to 8.5, 90% of the total activity was in the soluble fraction. As the pH of the homogenates was reduced, the proportion of the activity in the soluble fraction fell, until at pH 6.5 the activity

was about equally distributed between both fractions. Below pH 6.5, the proportion of the activity in the particulate fraction increased about 90% at pH 5.0. At lower pH, the enzyme showed some inactivation.

This effect seems to account for the difference between fly and bee head preparations reported by Babers and Pratt ('51). Our early work confirmed their observation that in the fly most of the activity is in the supernatant but in the bee most of the activity is in the precipitate. Later we found that homogenates of bee heads are acid (pH, 5.0-5.5), presumably because of release of the secretion of the pharyngeal glands; homogenates of fly heads are nearly neutral. When homogenates of bee heads were neutralized, the distribution of activity between the two fractions was the same as in the fly head preparation in water (fig. 1).

DISCUSSION

Various authors have considered the physical state of true cholinesterase *in vitro*. There is general agreement that the cholinesterase of erythrocytes is bound to the stroma (Augustinsson, '48; Mounter and Whittaker, '50). However, no such agreement exists on the state of cholinesterase in homogenates of nervous tissue. Centrifugation of such homogenates has yielded results indicating that the enzyme is almost all in the soluble state, or that it is all bound to particulate matter, or that a portion exists in both states. Our results obtained with homogenates of fly heads show that all these types of distribution may be found, depending on the conditions of separation.

In insects, Chadwick et al. ('53) found that more than 90% of the cholinesterase activity of fly head homogenates was contained in the supernatant after centrifugation. However, these authors worked with homogenates brought to pH 8.0, and at this pH we have shown (fig. 6) that about 90% of the activity is, in fact, in the supernatant. Babers and Pratt ('51) found the cholinesterase of fly head and bee head homogenates distributed between the precipitate and the supernatant after

centrifugation. We have already suggested that the difference in distribution they observed between the fly and the bee is not generic but results from the low pH of bee head homogenates.

In vertebrates, Little ('48) has shown that the true cholinesterase in mouse brain homogenates may be separated into two fractions by centrifugation at 900 to 2000 g. Centrifugation of water homogenates at pH 6.8 yielded 90% of the activity in the supernatant, but in the presence of a salt (NaCl, 0.075 M), the distribution was reversed yielding 65% of the activity in the precipitate. Little's figure showing these results is similar to our figure 4 which shows that fly head homogenates when separated in water yielded 60% of the activity in the supernatant, but when separated in KCl, 0.05 M, yielded 70% of the activity in the precipitate. However, Little's finding that increasing the pH above neutrality increased the proportion of the activity in the precipitate, is in contrast to our finding with fly head homogenates, and to the findings of others with erythrocyte cholinesterase (Augustinsson, '48; Mounter and Whittaker, '50).

Whittaker ('53) has re-examined Little's findings and shown that if the supernatant obtained by centrifugation at 2000 g was centrifuged at 16,000 g, about 75% of the "supernatant" activity was precipitated. He assumes that the application of higher centrifugal force would precipitate still more of the enzyme, and concludes that the acetylcholinesterase of brain must be regarded as attached to particulate material. This conclusion does not seem to be supported in the case of fly head homogenates, for we have shown that an appreciable proportion of the activity still remains in the supernatant after centrifugation at 50,000 g for one hour. Moreover, Hagen ('54) has found that centrifugation of homogenates of adrenal medulla at 100,000 g for 30 minutes fails to remove all cholinesterase activity from the supernatant.

On the whole therefore, the evidence from other work, coupled with our findings in insects, favours the generalization

that the cholinesterase of nervous tissue is distributed between a soluble and a particulate fraction *in vitro*.

The effect of salts on this distribution, which we attribute to salting out adsorption on the particulate matter of homogenates, seems well defined. Both Little ('48) and Whittaker ('53) have found with mouse brain, as we have with fly heads, that the addition of relatively low concentrations of salts to water homogenates results in a shift of cholinesterase activity from the supernatant to the precipitate. Little ('48) has drawn attention to the possibility that some apparent discrepancies may result from differences in the endogenous salt content of homogenates of different concentration. We have shown elsewhere (Smallman and Wolfe, '55) that the marked effect of homogenate concentration on the activation of cholinesterase by added salts may be attributed to the endogenous salt concentration. For the same reason, an effect of homogenate concentration on the distribution of activity between the two fractions seems likely, especially since the distribution is strongly affected by small changes in salt concentration at low salt molarities (fig. 4).

Most of the particulate cholinesterase in fly head homogenates is sedimented by low centrifugal forces at which only large cell fragments and nuclei would be expected to sediment. If the enzyme is attached to the cell membrane, as Nachmanshon ('46) has demonstrated with squid axon, then the activity of the particulate fraction might be attributed to the enzyme adsorbed on fragments of cell membranes. However, nuclei isolated from brain homogenates have been shown to retain a high proportion of the true cholinesterase of whole homogenates (Richter and Hullin, '51). The enzyme contained in nuclei may therefore also contribute to the activity of the particulate fraction obtained by low-speed centrifugation. In contrast to these findings, Burgen ('54) has reported that histochemical localization of true cholinesterase in the dog central nervous system has shown no enzyme in the nucleus, no specific concentration at the cell surface, and the highest concentration in the somatic cytoplasm. Part of this cytoplasmic cholinesterase may be

particulate, for Hagen ('54) has shown that a large part of the cholinesterase of the adrenal medulla is sedimented from sucrose suspensions in the microsome fraction. Our finding that additional enzyme is precipitated from fly head homogenates between 15,00 g and 26,000 g suggests that a microsomal fraction exists here too.

That care must be taken in extrapolating from such *in vitro* studies to the intracellular distribution of enzymes *in vivo* is emphasized by our finding that cholinesterase may become adsorbed on or desorbed from the particulate material in tissue homogenates depending upon the conditions of preparation.

SUMMARY

1. When homogenates of fly heads, bee heads, bee brains, and roach nerve cords were centrifuged, the cholinesterase activity was found to be distributed between the supernatant and the precipitate.

2. Repeated washing of the precipitate from fly head homogenates removed some of the enzyme but a proportion remained fixed.

3. After centrifugation of fly head homogenates at forces up to 50,000 g for one hour, a proportion of the enzyme remained in the supernatant.

4. Most of the particulate enzyme was sedimented from sucrose suspensions at 500 g for one hour, but additional enzyme was precipitated between 15,000 g and 26,000 g.

5. The distribution of activity between the two fractions was markedly affected by low concentrations of KCl. When separated in the presence of KCl, the distribution was altered in favor of the particulate fraction, as compared to the distribution when fractions were separated in de-ionized water.

6. The distribution was strongly affected also by pH. At low pH most of the activity was in the particulate fraction, but at high pH the distribution was reversed.

ACKNOWLEDGMENT

The authors wish to thank Mr. J. B. Edwards for technical assistance throughout this work.

LITERATURE CITED

- ALDRIDGE, W. N., W. K. BERRY AND D. R. DAVIES 1949 Simplified calculations suitable for routine use of linear regression. *Nature*, 164: 925.
- AUGUSTINSSON, K. B. 1948 Cholinesterases. *Acta Physiol. Scand.*, 15: Supplement 52.
- BABERS, F. H., AND J. J. PRATT 1951 Comparison of cholinesterases in heads of house fly, cockroach, and honey bee. *Physiol. Zool.*, 24: 127.
- BURGEN, A. S. V. 1954 Central and sensory transmission. *Pharmacol. Rev.*, 6: 95.
- CHADWICK, L. E., J. B. LOVELL AND V. E. EGNER 1953 The effect of various suspension media on the activity of cholinesterase from flies. *Biol. Bull.*, 104: 323.
- GREEN, D. E. 1952 Organized enzyme systems. *J. Cell. and Comp. Physiol.*, 39, Supplement 2: 75.
- HAGEN, P. 1954 The concentration of the cholinesterase activity of adrenal medulla in the microsome fraction. *Biochem. J.*, 57: XXXIV.
- LITTLE, J. M. 1948 Two fractions of specific cholinesterase present in homogenized normal mouse brain. *Am. J. Physiol.*, 153: 436.
- MOUNTER, L. A., AND V. P. WHITTAKER 1950 The esterases of horse blood. 2. The specificity of horse blood erythrocyte cholinesterase. *Biochem. J.*, 47: 525.
- NACHMANSON, D. 1946 In: *Currents in Biochemical Research*. New York (p. 335).
- PETERS, R. A. 1952 Lethal synthesis. *Proc. Roy. Soc. B.*, 139: 143.
- RICHTER, D., AND R. P. HULLIN 1951 Isolated nuclei from cells of the cerebral cortex. Preparation and enzyme content. *Biochem. J.*, 48: 406.
- SCHNEIDER, W. C. 1948 Intracellular distribution of enzymes. *J. Biol. Chem.*, 176: 259.
- SMALLMAN, B. N., AND L. S. WOLFE 1954 The effect of salts on the estimation of cholinesterase activity. *Enzymologia*, 17 (3): 133.
- TISELIUS, A. 1948 Adsorption separation by salting out. *Arkiv. fur Kemi, Mineralogi och Geologi*, 26B No. 1: 5 pp.
- WHITTAKER, V. P. 1953 Specificity of pigeon brain aceto-cholinesterase. *Biochem. J.*, 54: 660.
- WOLFE, L. S., AND B. N. SMALLMAN 1956 The properties of cholinesterase from insects. *J. Cell. and Comp. Physiol.*, 48: 215.

THE PROPERTIES OF CHOLINESTERASE FROM INSECTS ¹

L. S. WOLFE AND B. N. SMALLMAN

*Science Service Laboratory, Canada Department
of Agriculture, London, Ontario*

NINE FIGURES

INTRODUCTION

Knowledge of the properties of insect cholinesterase is of fundamental importance to the hypothesis of the mode of action of the organophosphate insecticides. In a previous paper (Smallman and Wolfe, '54) we have shown that the cholinesterase activity of homogenates of insect nervous tissue can be separated into a soluble and a particulate fraction by centrifugation. The conditions affecting the distribution of activity between the two fractions were studied. The present paper considers some of the properties of the enzyme in the soluble and particulate fractions and compares these findings with the properties reported for the ChE of insects and other animals.

MATERIALS AND METHODS

Houseflies were reared under standard conditions. Worker bees were obtained from the local apiaries. The heads were homogenized in a glass or Teflon Potter-Elvehjem type homogenizer and separated into fractions by centrifugation as described previously (Smallman and Wolfe, '54). Large cuticle fragments were removed before centrifuging by straining the homogenate through two layers of muslin. Cholinesterase activity was determined either by the manometric or the titrimetric method at 25° C. unless otherwise stated. The

¹ Contribution No. 39.

detailed conditions of measurement are given with the appropriate tables and figures in the text. In the manometric method the b_{30} 's were calculated from the data by the method of Aldridge, Berry and Davies ('49).

TABLE 1

Hydrolysis of esters by the soluble and particulate fractions of fly and bee head cholinesterase.¹ Activity expressed in μ l CO_2 /mg head tissue/hour

SUBSTRATE		HOUSE FLY		BEE	
		Soluble	Particulate	Soluble	Particulate
Acetyl choline	0.1 M	11.0	3.0	2.8	1.0
Acetyl choline	0.01 M	26.6	8.4	6.4	2.0
Acetyl B methyl choline	0.1 M	4.2	1.5	9.6	3.2
Acetyl B methyl choline	0.01 M	7.8	2.0	5.2	1.7
Butyryl choline	0.1 M	10.0	3.0	1.8	0.4
Butyryl choline	0.01 M	14.0	5.0	2.9	1.1
Benzoyl choline	0.1 M	1	0	0	0
Benzoyl choline	0.01 M	1	0	0	0
Triacetin	0.1 M	19	6
Triacetin	0.01 M	13	4
Tributyryl	0.1 M	3	1
Tributyryl	0.01 M	1	0

¹ Manometric method, pH 7.4, 25°C., Augustinsson's bicarbonate - Ringer's solution (R_{30}). Determinations in triplicate.

RESULTS

Substrate specificity

Fly or bee heads were homogenized in distilled water and the pH carefully adjusted to pH 7.0. The homogenate was then centrifuged at 10,000 g for 10 minutes and the centrifugate washed twice with distilled water at pH 7.0. This procedure yielded approximately 70% of the total cholinesterase activity in the supernatant, and 30 % in the centrifugate. Table I summarized the results of experiments on the rate of hydrolysis of different substrates by these two fractions. The housefly preparation showed the highest rate of hydrolysis with acetyl choline, 0.01 M, for both fractions. The bee preparation hydrolysed acetyl choline faster at 0.01 M than at 0.1 M; but acetyl β methyl choline was hydrolysed

almost twice as rapidly at 0.1 M as at 0.01 M final concentration. Butyryl choline was hydrolysed at about half the rate of acetyl choline by either fraction in both preparations at the low concentrations. Benzoyl choline was not hydrolysed. Non-choline esters such as triacetin, ethyl acetate, tributyrin and ethyl butyrate were hydrolysed but in the latter two esters at an insignificant rate at low concentrations. The non-choline esters have low water solubilities and relatively high vapour pressures which limit the accuracy with which their hydrolysis rates can be determined. Inhibition by excess substrate was found only with the choline esters.

The substrate specificity of the soluble and particulate cholinesterase of fly heads is similar to that of acetyl cholinesterase of Augustinsson and Nachmansohn ('49) from the erythrocytes and conductive tissue of vertebrates. The cholinesterase of bee heads differs from that of fly heads in the relative rate of hydrolysis of acetyl β methyl choline at high substrate concentrations; but at low substrate concentrations both fractions show the same specificity pattern as found for fly head ChE. Metcalf and March ('50) and Metcalf, March and Maxon ('55) showed that fly head and bee head homogenates could be differentiated into two types with regard to their behaviour towards acetyl choline and acetyl β methyl choline. The absence of inhibition by excess substrate for acetyl β methyl choline and butyryl choline as well as the greater rate of hydrolysis of these substrates at high concentrations were ascribed to the presence of non-specific aromatic esterases. Roen and Maeda ('53) obtained similar results for the oriental fruit fly but their data indicates excess substrate inhibition for the hydrolysis of acetyl β methyl choline. Babers and Pratt ('50) found that fly brain cholinesterase was more effective in hydrolyzing acetyl choline than acetyl β methyl choline but for the bee brain acetyl β methyl choline was the preferred substrate. Our results also show marked differences between bee and fly head cholinesterases at high substrate concentrations but these differences were much less in the 0.001 M to 0.01 M substrate concentration

range. It is in this concentration range that acetyl choline is hydrolysed at a higher rate than all other choline esters by fly and bee heads.

Substrate concentration — activity relationships

Enzyme activity was determined over a wide range of substrate concentrations with both the particulate and soluble fractions of fly and bee heads. Acetyl choline and acetyl β methyl choline were used as substrates. In figure 1 are shown the pS-activity plots for fly head cholinesterase. The following features are noted:

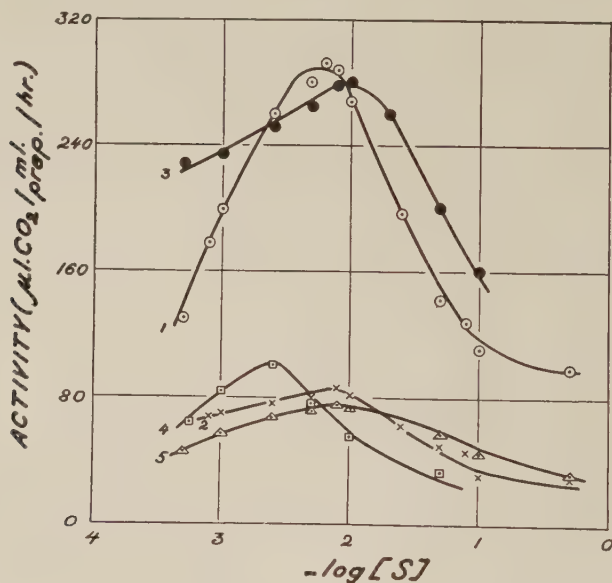


Fig. 1 The hydrolysis of acetyl choline and acetyl β methyl choline by fly head particulate and soluble cholinesterase. Manometric method and conditions as given in table 1.

1. Soluble fraction, ACh as substrate.
2. Particulate fraction, ACh as substrate.
3. Particulate fraction, three times the tissue concentration of 2.
4. Soluble fraction, three times dilution of 1.
5. Soluble fraction, acetyl β methyl choline as substrate. (Particulate fraction similar to soluble.)

1. The optimal substrate concentration was 0.0075 M for the particulate fraction, 0.006 M for the soluble fraction with acetyl choline as substrate; with acetyl β methyl choline 0.01 M for the particulate and 0.0075 M for the soluble fraction. These figures refer only to the experimental conditions given in the figure legend.

2. The bell-shaped curve predicted by Haldane ('30) for inhibition by excess substrate was approximated only by the soluble fraction. The particulate fraction showed a peculiar assymetry. The fall-off in rate of hydrolysis at low substrate concentrations was much smaller for the particulate enzyme.

3. A three times increase in tissue concentration did not alter the shape of the pS-curve for the particulate fraction. There was a shift, however, in optimal substrate concentration from 0.0075 M to 0.01 M but this could have been due to chance as indicated by the scatter of points about the curves in figure 1.

4. A three times dilution of the soluble fraction caused a shift in optimum substrate concentration from 0.006 M to 0.0025 M.

In figure 2 the pS-curve for the soluble and particulate fractions separated from bee heads are shown. The optimum substrate concentration in both fractions was 0.1 M for acetyl β methyl choline whereas for acetyl choline the optima were 0.005 M for the particulate and 0.0025 M for the soluble fractions. Although the rate of hydrolysis of acetyl β methyl choline at high substrate concentrations was 4 to 5 times that of acetyl choline, at low substrate concentrations this was reversed. Richards and Cutkomp ('45) and Babers and Pratt ('51) and Kooistra ('50) reported this difference and believed it indicated specific differences among insect cholinesterases. Babers and Pratt found no optimum for acetyl β methyl choline probably because they did not work at high enough substrate concentrations. Kooistra found optimal substrate concentrations of 0.0056 M with acetyl choline and 0.03 M acetyl β methyl choline. Comparison of bee head with fly head cholinesterase (figs. 1 and 2) reveals two significant

points. First, that at the pS optimum for acetyl choline, acetyl β methyl choline is hydrolysed at a slower rate, regardless of enzyme source (fly or bee) or state (soluble or particulate) and, secondly, that the pS at which excess substrate inhibition by acetyl β methyl choline occurs for the

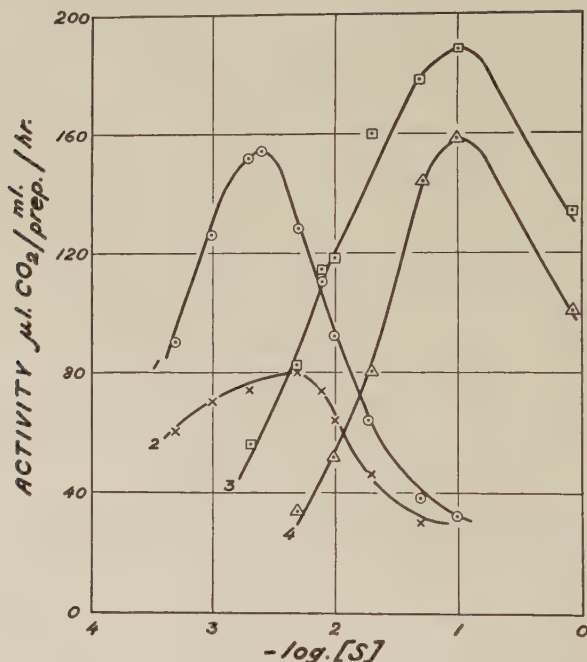


Fig. 2 The hydrolysis of acetyl choline and acetyl β methyl choline by bee head particulate and soluble cholinesterase. Experimental conditions same as figure 1.

1. Soluble fraction, ACh as substrate.
2. Particulate fraction, ACh as substrate.
3. Soluble fraction, A β MeCh as substrate.
4. Particulate fraction, A β MeCh as substrate.

enzyme from bee heads is very much lower than for the enzyme from fly heads. Also the lower values of the pS optima of the bee head enzyme with acetyl choline as substrate compared to the fly enzyme may result from the lower enzyme concentration in the bee head tissue as reflected in the lower b_{30} 's.

Dilution of the fly head soluble fraction lowers the pS optimum as shown in figure 1.

The Michaelis constants (K_s) and the dissociation constants (K^1_s) for the formation of the inactive complex (ESS) were evaluated by the method of Lineweaver and Burk ('34). The values for the soluble fraction are shown in table 2. Lineweaver and Burk plots for the particulate fractions deviated considerably from linearity and were unsuitable for calculation of Michaelis constants.

It will be shown below that the values of K_s and pS optimum depend on the concentration of salts in the suspension medium (Myers, '52; Smallman and Wolfe, '54) and on the pH of measurement. The importance of the concentration of the

TABLE 2

*Constants for the cholinesterase of the fly and the bee. Soluble fraction only.
(Experimental methods same as table 1)*

	HOUSE FLY		BEE	
	ACh	A β MeCh	ACh	A β MeCh
K_s	6.3×10^{-4}	4×10^{-4}	6.5×10^{-4}	8.5×10^{-3}
K^1_s	8.0×10^{-2}	2×10^{-2}	8.7×10^{-3}	1.06
pS optima	2.25-2.6	2.1	2.6	1.0

enzyme preparation has been shown already. Because of the variability of conditions and methods used by different workers in the estimation of cholinesterase activities over a range of substrate concentrations, direct comparisons of enzyme constants are difficult.

Chadwick et al. ('53), using the titrimetric method (de-ionized water as suspension medium; house fly head tissue conc. approx. 2 mg/ml; activity measured at pH 8.0), obtained a pS optimum with acetyl choline as substrate of 2.8 which shifted to 2.6 when the suspension medium was 0.5 M NaCl. Babers and Pratt ('51), using the manometric method (modified Ringer's suspension medium, approx. 0.025 M total salts; final tissue conc. approx. 3.5 mg/ml; measured at pH 7.2), obtained a pS optimum of 2.0- 2.1. The values obtained in

the present study were 2.25–2.6, and 2.1 for the soluble and particulate fractions respectively. However, when the pS optima were determined by the titrimetric method (see fig. 5) over a range of salt concentrations much lower values were obtained. Even when the titrimetric method was used with salt concentrations equivalent to Ringer solutions, the pS optima remained lower than the values obtained by the manometric method. These differences may arise from the method of determination. Smallman and Wolfe ('54) have demonstrated that the sodium bicarbonate used in the manometric procedure alters the enzyme activity as compared to the activity in other sodium salts.

pH — activity relationships

The activity-pH curve for the cholinesterase of fly heads was determined by the titrimetric method and found to be flat between 8.5–9.0. At pH 8.5 the cholinesterase in the particulate fraction is almost completely solubilized (Smallman and Wolfe, '54) and consequently it was not possible to obtain a pH optimum for the enzyme in the particulate state. Chadwick et al. ('54) stated that the pH optimum for fly head cholinesterase was at least as high as 8.0 and probably 9.0. Both they and we found no shift in the pH optimum on changing the substrate concentration. In these respects fly head cholinesterase is similar to "specific cholinesterase" (Augustinsson, '48).

The variation of pS-activity with pH was investigated with the results given in figure 3. A shift in the pS optimum occurs as the pH is altered. The Michaelis dissociation constants from each set of experimental data were calculated. Figure 4 shows the plot of pK_s against pH. At acid pH values, a straight line of approximately +1 slope was obtained which curved to a straight line of zero slope at alkaline pH values. Applying the theoretical interpretations of Dixon ('53), and Friedenwald and Maengwyn-Davies ('54), the changes in slope of the pK_s against pH plots result from changes in ionization of the active centers on the enzyme surface.

Results similar to these were obtained by Hase ('52) for horse serum cholinesterase. He ascribed the bend in the curve to the ionization of the functional groups in the active surface of the enzyme. The pK value for house fly cholinesterase was 7.6 which compares very well with the pK of 7.7

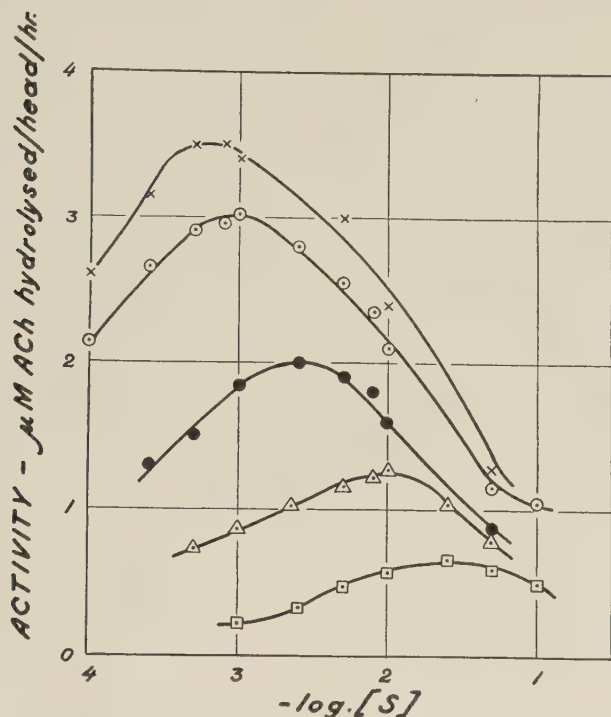


Fig. 3 The effect of pH on the hydrolysis of fly head cholinesterase at various substrate concentrations (ACh). Titrimetric method, no added salts.

×—× pH 9.0; ○—○ pH 8.0; ●—● pH 7.0
 Δ—Δ pH 6.0; □—□ pH 5.5.

obtained by Hase. The enzyme from fly head tissue possesses an anionic site of similar ionization constant to cholinesterase from other sources.

It is interesting to note that the isoelectric point of human serum cholinesterase protein is close to, if not identical, with that of a globulin which is about pH 4.8 (Cohn et al., '46). Chadwick et al. ('54) reported precipitation of housefly cholin-

esterase at pH 5.0–5.1. This in itself is indicative of the presence of strongly ionizing acid groups (see Johnson, Eyring and Polissar, '54). Maximum stability occurs at alkaline pH's for most cholinesterases.

Salt-concentration — activity relationships

The manometric method of estimating cholinesterase activity presents difficulties for studies on pH dependence,

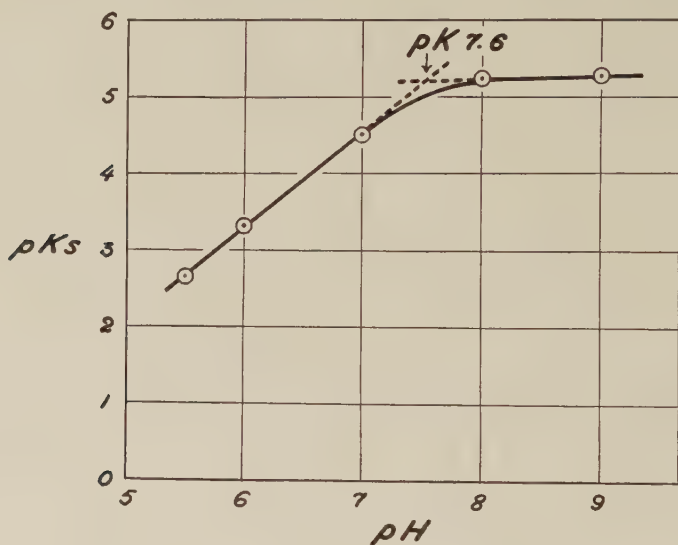


Fig. 4 Relationship between pH and pK_s for fly head cholinesterase. Calculated from experimental results of figure 3.

salt activation and measurement of reaction rates at very low substrate concentrations. Therefore the titrimetric method was used to study the effect of NaCl on enzymatic activity at various concentrations of substrate and salt. The results are shown in figure 5. A shift in pS optimum towards lower values at high salt concentration was found. Myers ('52) and Smallman and Wolfe ('54) found similar shifts for human erythrocyte cholinesterase. Table 3 summarizes the characteristics of the curves shown in figure 5.

Table 3 shows that while sodium chloride leads to an increase in the rate of hydrolysis, at the same time there is a reduction in affinity of enzyme for substrate as reflected by the increasing values of K_s and the shift in the pS optimum.

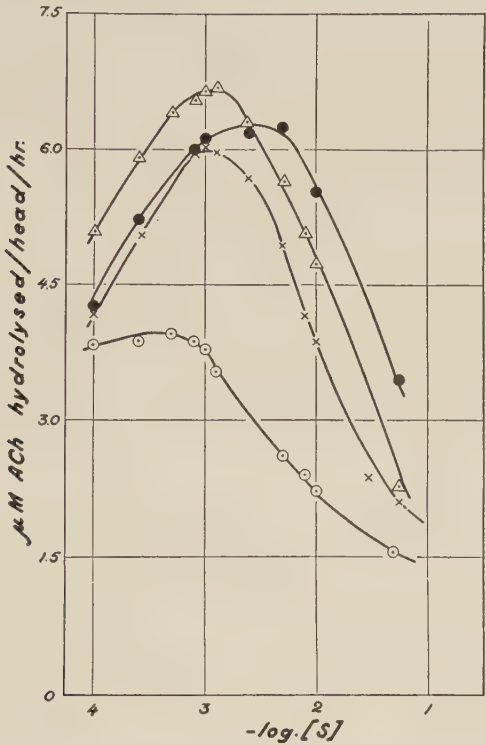


Fig. 5 The effect of NaCl on the hydrolysis of acetyl choline at varying concentrations by fly head cholinesterase. Titrimetric method, pH 8.0. \circ — \circ No salts; \times — \times 0.005 M NaCl; \triangle — \triangle 0.1 M NaCl; \bullet — \bullet 0.5 M NaCl.

TABLE 3
Constants for fly head cholinesterase suspended in various concentrations of salts.
(Conditions as for fig. 5)

SALT CONCENTRATION	K_s (ACh)	VOPT. μM ACh/head/hr.	pS OPT.
No salts	ca. 8×10^{-7}	4.0	3.3
0.005 M NaCl	3.5×10^{-6}	6.0	3.0
0.1 M NaCl	7.3×10^{-6}	6.7	2.8
0.5 M NaCl	1.3×10^{-5}	6.3	2.6

The results shown in figure 5 emphasize the importance of studying salt effects over a wide range of substrate concentration to a maximum around 0.5 M NaCl at 0.01 M substrate concentration. Chadwick et al. ('54) also found the rate of hydrolysis maximal at 0.5 M NaCl with acetyl choline 0.015 M. However, if the rate at optimum substrate concentration is taken, the hydrolysis rate reaches a maximum in the presence of 0.1 M NaCl. At salt concentrations above 0.1 M ionic interference with the hydrolysis of substrate may be responsible for this effect. It is suggested that the velocities at optimum substrate concentrations, rather than an arbitrarily chosen substrate concentration, should be used to determine the magnitude of rate activation by salts.

The pS-plots in the absence of salts are asymmetrical. The optimum for fly head cholinesterase is 0.0005 M in the absence of salts but the rate at the lowest substrate concentration for which a reaction rate could be determined (0.0001 M) differed little from the optimum.

Temperature — activity relationships

Activation. The rate of hydrolysis of acetyl choline by the soluble and particulate fractions from fly heads as a function of temperature was investigated (fig. 6). Below 30° the inactivation of the enzyme protein by heat is negligibly small and therefore the temperature-activity plots represent the effect of temperature on the catalysed reaction only. Figure 6 shows distinct differences between the soluble and particulate fractions. Optimum temperatures of 30° and 35° were found for the soluble and particulate fractions respectively.

The temperature-activity plots for the range 15°–30° C. were linear for the soluble fraction and slightly convex upwards for the particulate fraction. Both sets of data would therefore yield significantly curved Arrhenius plots making the calculation of μ values impossible. The temperature activity relationships of human erythrocyte cholinesterase adsorbed on the red cell membranes was determined for a

comparison with the particulate fraction of fly heads. The preparation was made from packed red cells freed from serum cholinesterase by repeated washings in isotonic saline, haemolysing, and further washing in slightly acid conditions (pH 6.0) until most of the haemoglobin was removed. It was found that in this preparation the activity was directly

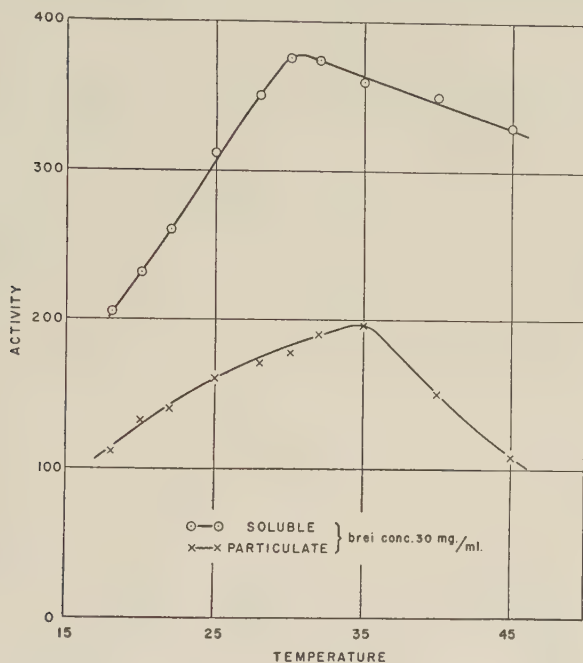


Fig. 6 Hydrolysis of acetyl choline by fly head soluble and particulate cholinesterase as a function of temperature. Activity measured manometrically, 0.025 M NaHCO_3 , no additional salts, ACh 0.01 M.

proportional to temperature from 0°–30° C. and that this was not altered by changes in salt concentration. Glick ('41) recorded a μ value of 5,100 cal./mole for true cholinesterase from mammalian erythrocytes but his data could equally well accommodate a linear plot of rate against temperature. Roen and Maeda ('53) did obtain a curved plot (concave upwards) for the effect of temperature on the activity of the cholinesterase from the oriental fruit fly but did not calculate μ

values. A satisfactory explanation for the curved Arrhenius plots obtained must await further study.

Inactivation. Most enzymes at or near their pH optima possess high activation energies for the denaturation process. Studies of the inactivation by heat are of some importance in indicating stability differences. It was thought that a study of the inactivation of the soluble and particulate cholinesterase

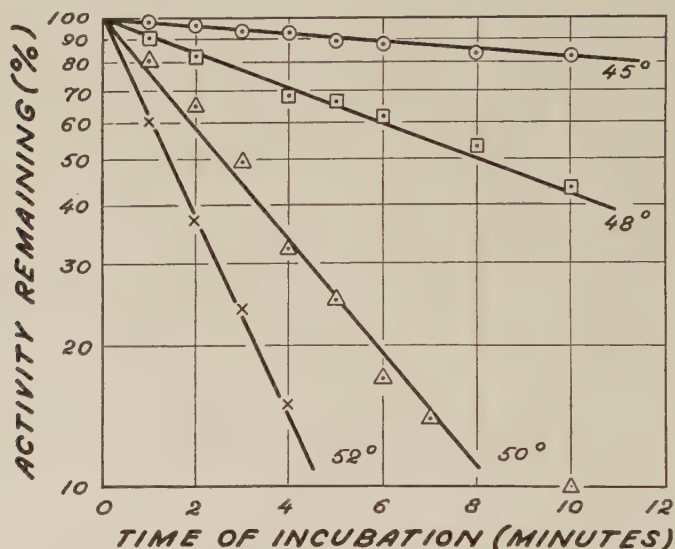


Fig. 7 The rate of inactivation of fly head soluble cholinesterase at different temperature. Activity measured manometrically, 0.025 M NaHCO_3 , no additional salts, ACh 0.01 M.

might reveal such differences. Unfolding of the enzyme protein molecule by breaking cross linkages, mainly of the hydrogen bond type, is now thought to occur during heat inactivation of proteins. The activation energies for this process when the enzyme is absorbed on cellular particles therefore should differ from those when it is in the completely soluble state.

The rate constants for inactivation were determined for both fractions by measuring the decrease in activity as a

function of time for temperatures between 45° and 55°. From Arrhenius plots of these results the activation energies were calculated. The experimental results are shown in figures 7 and 8. The following features are noted:

1. The plots for the soluble cholinesterase conformed to a first order reaction, but those for the particulate cholinesterase showed that after an initial period which conformed to a first order reaction, marked deviations occurred.

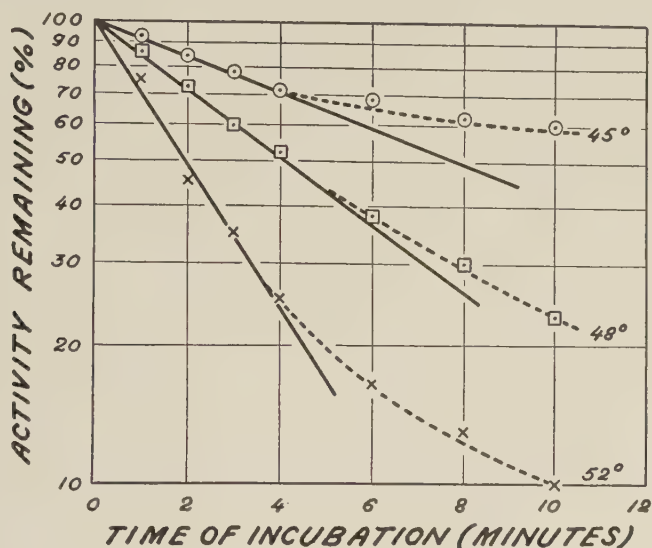


Fig. 8 The rate of inactivation of fly head particulate cholinesterase. Conditions same as figure 7.

2. The ΔH^\ddagger value, calculated using the Transition State Equation from the plots of $\log k$ vs. $1/T$, was 79,000 cal./mole for the soluble cholinesterase. Using the first order section of the curve for the particulate cholinesterase, a ΔH^\ddagger of 37,000 cal./mole was obtained. From these results it is seen that there are considerable differences in the energy required to inactivate the soluble and particulate cholinesterase. The magnitude of these differences suggests a definite difference in the physical state of the enzyme.

Protection by NaCl. Figure 9 shows the effect of various concentrations of NaCl on the rate of inactivation of the enzyme. In the absence of salts, the soluble cholinesterase is rapidly inactivated at 50°. In the presence of NaCl 0.5 M the enzyme is almost completely protected at 50°. Only when the temperature is raised to 60° is the rate of inactivation equivalent to that obtained in the absence of salts.

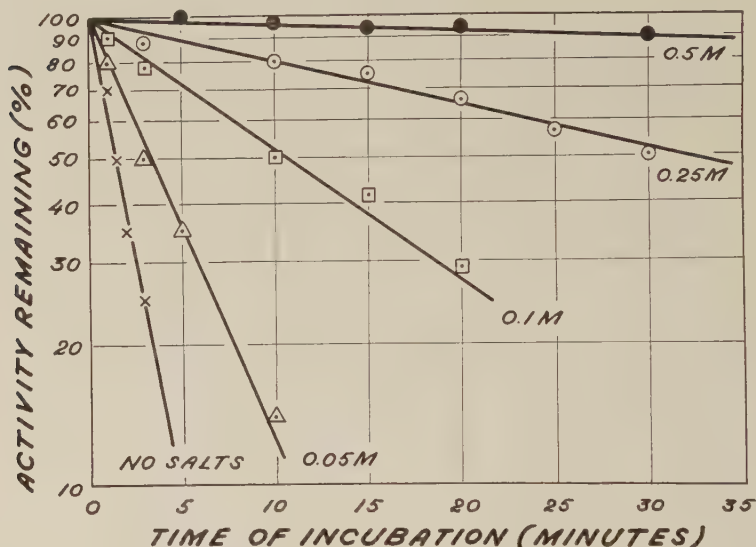


Fig. 9 The effect of salts on the rate of inactivation of fly head soluble cholinesterase at 50° C. Titrimetric method, pH 7.5, ACh 0.01 M.

DISCUSSION

The properties of the cholinesterase of fly heads are similar to those of the "specific" or acetyl cholinesterase from mammalian sources. Although non-specific esterases cannot be entirely excluded, the pattern of activity to various substrates suggests that these esterases are either absent or present in very small amounts. The substrate specificities of the soluble and particulate cholinesterase are identical, and therefore differences of the cholinesterase in these two states can be ascribed to differences in the environmental and physical state

of the enzyme protein *in vitro*. Little ('48) studied the factors controlling the distribution of cholinesterase activity in soluble and particulate fractions of homogenates of mouse brain and found (1) the substrate specificity pattern was the same for both fractions and the same as that for "true" cholinesterase, (2) the particulate fraction was more heat labile and (3) the two fractions had the same pH optimum. Our results agree with Little's work. However, his pH optimum of 7.5 is low. This probably resulted from the method of varying the pH by adjusting the bicarbonate concentration in the manometric procedure. There is considerable retention of CO₂ at bicarbonate concentrations giving pH's above 7.5 (see Birmingham and Elliott, '52).

It is well known that many cations affect the activity of cholinesterases. Myers ('51, '52) showed that NaCl has two distinct actions. First, it acts as a reversible competitive inhibitor causing an increase in the values of K_s and consequently a shift to higher values in the optimal substrate concentration and, secondly, it activates the enzyme. In other words, NaCl decreases the affinity for substrate while at the same time increasing the hydrolysis rate. The results obtained in the present investigation are similar to Myers' and we have extended his experiments to include the condition in the absence of salts. The affinity for acetyl choline in the absence of salts is very high (extremely low K_s) and it is thought that if it were possible to determine hydrolysis rates at lower substrate concentrations the hydrolysis rate might also prove to be faster than when salts were present, i.e., the pS curves in the presence of salts would cross the pS curve in the absence of salts (fig. 5).

Three factors, among others, are important in determining the rate of hydrolysis of substrate by an enzyme: first, the rate of diffusion of substrate molecules to the specific sites on the enzyme protein; second, the affinity of these sites for the specific substrate; and, third, the rate of diffusion of the hydrolysis products away from the sites. Any explanation of the effect of salts on enzyme activity must be related in some

way to these factors. The researches of Myers ('50), Wilson and Bergmann ('50) and Adams and Whittaker ('50) have produced convincing evidence for the presence of an anionic active centre in the cholinesterase protein.

Myers ('50, '51) has suggested that the decrease in affinity of cholinesterase for acetyl choline in the presence of salts is a result of electrostatic interactions between the anionic active centers and the metal cations. Besides this interaction, salts may also change profoundly the shape and size of anionic proteins by altering the intramolecular bonding (Kirkwood, '54). A possible explanation of the activation of cholinesterase by salts is that the general opening up and expansion of the protein structure in the presence of salts facilitates the diffusion of substrate molecules to the active centers as well as revealing further centers within the protein molecule. The products of hydrolysis are also able to diffuse away more quickly and consequently the turnover of substrate molecules is increased.

At NaCl concentrations below 0.1 M, fly head cholinesterase is extremely sensitive to changes in salt concentration and in this region the effect of salts on the size and shape of the enzyme protein is possibly the major factor producing the increase in hydrolysis rate. However, if the salt concentration is increased above 0.1 M the hydrolysis rate at optimal pS decreases. In this region the cationic interactions with the active sites may be dominant and may reach a level that is not compensated by the increased availability of the active sites to substrate molecules. Myers ('52) found for erythrocyte cholinesterase a similar decrease in optimal hydrolysis rate when the salt concentration reached 0.5 M.

Smallman and Wolfe ('54) using the human red blood cell preparations found that the hydrolysis rate at optimal pS continued to increase with increasing salt concentrations up to 0.5 M. The titrimetric method was used in the latter experiments and consequently sodium bicarbonate interference was eliminated. The level of salt concentration at which

a decrease in hydrolysis rate occurs is approximately 0.5 M for erythrocyte cholinesterase.

The large ΔH^\ddagger values for the inactivation of proteins are explained in terms of the energy required to break large numbers of weak secondary intramolecular bonds. When these bonds are broken the protein molecule is disorganized and opens out into a flexible chain structure (see Johnson et al., '54). Proteins adsorbed on surfaces are in a more unfolded state than when in solution (Davies, '53), suggesting that less energy would be required to disorganize a portion adsorbed on particulate matter. The finding that the ΔH^\ddagger value for particulate cholinesterase is significantly lower than the value for the soluble enzyme may be interpreted this way.

Finally we have shown that salts protect the soluble cholinesterase from inactivation by heat. This again is thought to result from electrostatic associations of the alkali metal cations with the protein. Although cations lead to a certain degree of opening up of the protein structure they also protect the protein from complete disorganization. Considerably more energy would be required to inactivate the proteins in the presence of cations.

ACKNOWLEDGMENTS

We wish to thank Dr. D. M. Miller and Dr. R. D. O'Brien for their excellent advice and criticism and Mr. J. B. Edwards for technical assistance.

SUMMARY

1. Properties of the cholinesterase of the soluble and particulate fractions of homogenates of fly and bee heads were investigated. The enzyme in both fractions showed similar substrate specificities and pS relations. Differences in kinetic and thermodynamic properties could be explained on the basis of the different physical environment of the enzyme in the soluble and particulate states.

2. The fly head cholinesterase possesses substrate specificities similar to the specific cholinesterase from mammals.

The values for pS optima were found to vary with salt concentration, pH and tissue concentration. The pS curves for the particulate enzyme were asymmetrical.

3. The variation of pS-activity relationships with pH was investigated. The enzyme in the soluble fraction was found to contain dissociable anionic groups with pK value of 7.6.

The pS-activity curves in the absence and presence of salts were obtained, and the enzyme constants calculated from the experimental data were compared and discussed.

5. The temperature optimum for the enzyme from the soluble and particulate fractions was 30° and 35° respectively. The Arrhenius plots from 0 to 30° C. are curved.

6. The ΔH^\ddagger values for the inactivation by heat were determined. A value of 79,000 cal./mole was obtained for the enzyme in the soluble state and 37,000 cal./mole when in the particulate state. A probable explanation for these differences is presented. NaCl markedly protects the enzyme from heat inactivation.

7. A possible explanation of the effect of salts on enzyme activity and affinity is discussed.

LITERATURE CITED

- ADAMS, D. H., AND V. P. WHITTAKER 1950 Cholinesterases of human blood. *Biochim. Biophys. Acta*, **4**: 543.
- ALDRIDGE, W. N., W. K. BERRY AND D. R. DAVIES 1949 Simplified calculation suitable for routine use of linear regression. *Nature*, **164**: 925.
- AUGUSTINSSON, K. B. 1948 Cholinesterase. *Acta Physiol. Scand.*, **15**: Supplement 52.
- AUGUSTINSSON, K. B., AND D. NACHMANSOHN 1949 Distribution between acetyl cholinesterase and other choline ester splitting enzymes. *Science*, **110**: 98.
- BABERS, F. H., AND J. J. PRATT 1950 Cholinesterase of house flies resistant to DDT. *Physiol. Zool.*, **23**: 58.
- 1951 Comparison of cholinesterase in heads of house fly, cockroach and honey bee. *Physiol. Zool.*, **24**: 127.
- BIRMINGHAM, M. K., AND K. A. C. ELLIOT 1952 Application of Henderson-Hasselbach equations to single and mixed buffer solutions. *Can. J. Med. Sc.*, **30**: 403.
- CHADWICK, L. E., J. B. LOVELL AND V. E. EGNER 1953 Effect of suspension media on activity of cholinesterase from flies. *Biol. Bull.*, **104**: 323.

- CHADWICK, L. E., J. B. LOVELL AND V. E. EGNER 1954 Relationship between pH and activity of cholinesterase from flies. Biol. Bull., 106: 189.
- COHN, E. J., AND OTHERS 1946 Preparation and Properties of Serum and Plasma Proteins. J. Amer. Chem. Soc., 68: 459.
- DAVIES, J. T. 1953 Shapes of molecules of poly-amino acids and proteins at interfaces. p. 4. Biochim. Biophys. Acta, 11: 165.
- DIXON, M. 1953 pH and enzyme affinities. Biochem. J., 55: 161.
- FRIEDENWALD, J. S., AND G. D. MAENGWYN-DAVIES 1954 Kinetic theory of enzymatic activity. p. 191. See Johnson et al.
- GLICK, D. 1941 Nature and significance of cholinesterase. Biol. Symposia, 5: 213.
- HALDANE, J. B. S. 1930 Enzymes. Longman, Green, London.
- HASE, E. 1952 Mechanism of action of cholinesterases. J. Biochem. Tokio, 39: 259.
- JOHNSON, F. H., H. EYRYNG AND M. J. POLISSAR 1954 Kinetic basis of molecular biology. Wiley, New York.
- KOOISTRA, G. 1950 Action of acetyl choline in intestine of *Periplaneta americana* L. Physiol. Comp. et Oecol., 2: 75.
- LINEWEAVER, H., AND D. BURK 1934 Determination of enzyme dissociation constants. J. Amer. Chem. Soc., 56: 658.
- LITTLE, I. M. 1948 Two fractions of specific cholinesterase present in homogenized normal mouse brain. Amer. J. Physiol., 153: 436.
- METCALF, R. L., AND R. B. MARCH 1950 Properties of acetyl cholinesterase from bee, fly and mouse. J. Econ. Ent., 43: 670.
- MYERS, D. K. 1950 Effect of electrolytes on cholinesterase inhibition. Arch. Biochem. and Biophys., 27: 341.
- 1951 Differentiation of three types of competitive inhibitors. Arch. Biochem. and Biophys., 31: 29.
- 1952 Effect of salt on the hydrolysis of acetyl choline by cholinesterases. Arch. Biochem. and Biophys., 37: 469.
- RICHARDS, A. G., AND L. CUTCOMP 1945 Cholinesterase of insect nerves. J. Cell. and Comp. Physiol., 26: 57-61.
- ROAN, C. C., AND S. MAEDA 1953 The cholinesterase of the Oriental Fruit Fly and its *in vitro* reactions with various insecticidal compounds. J. Econ. Ent., 46: 775.
- SMALLMAN, B. N., AND L. S. WOLFE 1954 Effect of salts on the estimation of cholinesterase activity. Enzymologia, 17 (3): 133.
- 1956 Soluble and particulate cholinesterase from insects. J. Cell. and Comp. Physiol., 48: 197.
- WILSON, J. B., AND F. BERGMANN 1950 Active surface of acetyl cholinesterase. J. Biol. Chem., 185: 479.

ANODAL EFFECTS DURING THE REFRACTORY PERIOD OF CARDIAC MUSCLE ¹

CHANDLER McC. BROOKS, PAUL F. CRANEFIELD, BRIAN F. HOFFMAN AND ARTHUR A. SIEBENS

Department of Physiology, State University of New York, College of Medicine at New York City, Brooklyn, N. Y.

TWO FIGURES

INTRODUCTION

Studies of the excitability cycle of the heart and of single cardiac fibers have shown that during diastole and in the late phases of the refractory period the propagated response is initiated at the cathode prior to break of the test shock. Earlier in the relative refractory period excitation occurs at the anode following the break. This anodal break excitation has several peculiarities: in particular a weaker or shorter stimulus may excite when a stronger or longer one will not (the "no-response" phenomenon). This communication presents recent studies of the action of the anode during the relative refractory period of ventricular muscle.

METHODS

These studies have been restricted to dog ventricle. Transmembrane resting and action potentials were recorded from single fibers of isolated specialized conducting tissue by means of an intracellular microelectrode and single-ended cathode follower. Stimulation of the same fiber was accomplished by passing current pulses of known polarity through a 100 Meg Ohm series resistor and a second microelectrode inserted 0.5–1.5 mm from the recording site. In studies of

¹Supported in part by a grant from the Life Insurance Medical Research Fund.

the intact heart in situ monophasic electrograms were obtained by means of a suction electrode. The heart was driven at a fixed rate and its excitability at various intervals of the cycle tested by stimuli applied through electrodes attached to the heart's surface. Pairs of electrodes or single stigmatic electrodes were used as described in previous publications (see Brooks et al., '55) to obtain the strength-interval and strength-duration curves.

RESULTS

As found in earlier experiments excitation is anodal in origin during a portion of the cardiac excitability cycle. This portion lies within the refractory period, coinciding with the initial limb of the local electrogram T-wave and with the major dip of the strength-interval curve (Orias et al., '50). When the surface electrogram is recorded from bipolar electrodes placed between the stimulating electrodes and the stimulus is positioned at different intervals of the cycle the major deflection of the action potential during the dip reverses in direction (turnover) indicating that the direction of propagation has reversed and that the site of excitation has moved.

Latencies recorded by bipolar electrodes near the anode suddenly shorten (e.g. from 70 to 30 msec.) coincidentally with the turnover, whereas those recorded by electrodes near the cathode abruptly lengthen (e.g. from 30 to 60 msec.).

The most striking feature of anodal break excitation during the dip is that an effective stimulating pulse may become ineffective if it is increased in either strength or duration (fig. 1). This phenomenon has been referred to as the "nothing" or "no-response" effect. A stimulus is said to give a "no-response" (as distinguished from a subthreshold stimulus) only if a weaker or shorter stimulus is effective. It can be seen from figure 1 that further strengthening or lengthening may again cause the stimulus to be effective in producing a propagated response.

The "no-response" phenomenon has been observed with transmembrane recording and stimulation of single fibers of the cardiac conduction system by B. F. Hoffman (Hoffman, '56). It can be seen in figure 2 that a repolarizing (anodal) pulse of greater magnitude fails to stimulate at a moment

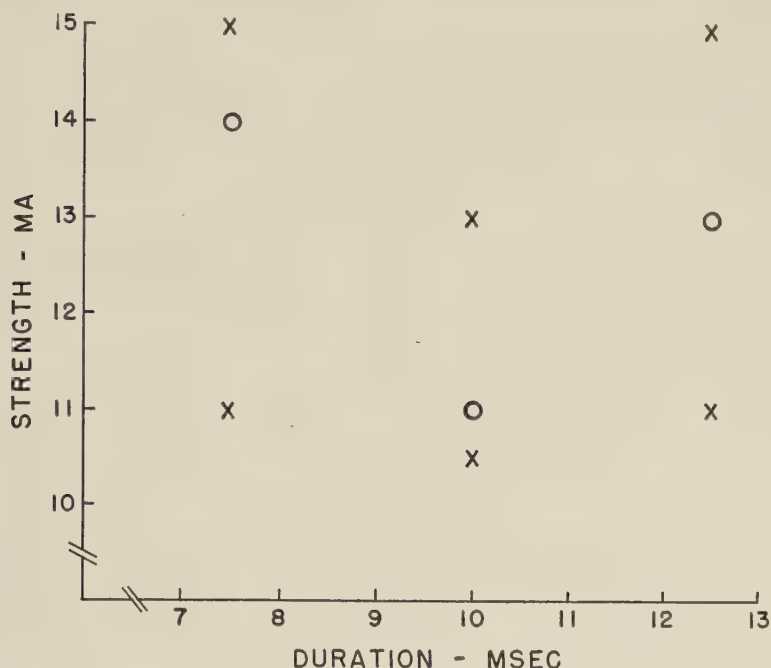


Fig. 1 The result of a stimulus of variable duration (fixed make time, variable break time). X—indicates excitation, O—indicates "no-response." The cycle was 450 msec. long, the make time of the stimulus was 175 msec. after the preceding R wave. In this cycle the major dip area extended from the 190 to 210 msec. interval. All "effective" stimuli (X) were suprathreshold.

when a weaker pulse of the same duration does stimulate. This appears to be exactly similar to the "no-response" observed in the whole heart. The "dip" has also been observed in single fibers, i.e., anodal pulses which fail to excite either earlier or later in the cycle do excite, on the break, at a certain part of the repolarization phase.

DISCUSSION

Anodal break excitation is a familiar feature of classic excitability theory. It is probable that the low threshold to anodal break excitation during this portion of the cardiac cycle is related to the fact that the closure of the anode aids repolarization.

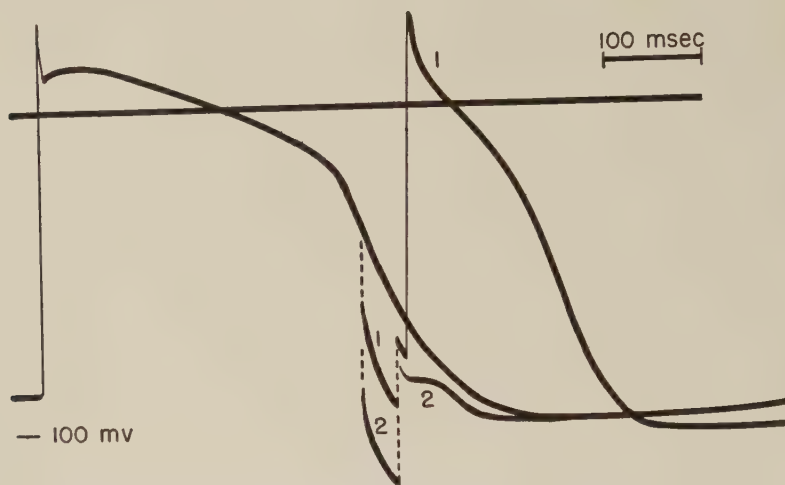


Fig. 2 Transmembrane action potential recorded by one intracellular electrode from a single specialized conducting fiber of the dog ventricle. Driven action potential (on left of figure) and effects of two anodal pulses of 40 msec. duration applied during repolarization through a second intracellular microelectrode. Weaker pulse (1) elicits an action potential following the break; stronger pulse (2) gives rise to no propagated response.

An interpretation of the “no-response” phenomenon is that during the dip the effectiveness of anodal break excitation is critically dependent on the preceding effect of anodal closure, e.g. a pulse strong enough to induce all-or-nothing repolarization (Weidmann, '56) might fail to excite at the break, whereas a weaker pulse which brings the membrane to an intermediate meta-stable state might do so. Another, basically distinct, mechanism for the “no-response” could be the initiation of local activity which fails to propagate. Records obtained with suction electrodes demonstrate the first mechanism and suggest the presence of the second.

LITERATURE CITED

- BROOKS, C. McC., B. F. HOFFMAN, E. E. SUCKLING AND O. ORIAS 1955 Excitability of the Heart. Grune and Stratton, New York.
- HOFFMAN, B. F. 1956 In preparation.
- ORIAS, O., C. McC. BROOKS, E. E. SUCKLING, J. L. GILBERT AND A. A. SIEBENS 1950 Excitability of the mammalian ventricle throughout the cardiac cycle. *Am. J. Physiol.*, 163: 272-282.
- WEIDMANN, S. 1956 *Elektrophysiologie Der Herzmuskelfaser*. Medizinischer Verlag Hans Huber, Bern und Stuttgart.

SUCCINOXIDASE ACTIVITY OF MITOCHONDRIA FROM MYXOMYCETE PLASMODIA ¹

GEORGE T. JOHNSON AND CARL MOOS

*Department of Botany and Bacteriology, University of Arkansas, Fayetteville,
and The Department of Biophysics, Columbia University, New York*

TWO FIGURES

Cowdry ('18) investigated the cytology of 10 slime molds, primarily on the basis of stained slides prepared by the paraffin method. This work provided the first clear demonstration that mitochondria are present in myxomycetes; some attention was also devoted to the vacuoles, nuclei, and general protoplasmic structure. Howard ('31, '32) added cytological information concerning *Physarum polycephalum*, especially with reference to nuclear structure in both resting and dividing stages. Andresen and Pollock ('52) presented detailed data concerning the percentage volume of nuclei, vacuoles, mitochondria and pigment granules in the plasmodium of this same species. They also attempted to separate the cytoplasmic inclusions by centrifugation *in vivo*, but found it difficult to obtain reproducible stratification of particulates within the intact organism. Sponsler and Bath ('53) obtained electron micrographs from plasmodial material of *P. polycephalum* which show some particles 6000 Å in diameter, some 1500 Å, some 300 Å, and some of other sizes, suggesting that a wide variety of submicroscopic particle types may eventually be disclosed.

Despite the reputation slime molds have long held as classical examples of "protoplasm" the functional aspects of their protoplasmic particulates have been poorly investigated.

¹ This study was initiated in the Department of Biology, Massachusetts Institute of Technology, Cambridge, Massachusetts.

Holter and Pollock ('52) compared the dipeptidase and succinic dehydrogenase activity of intact plasmodia, of plasmodia stratified by centrifugation *in vivo*, and of homogenates. Succinic dehydrogenase activity appeared to follow the distribution of granular components of stratified plasmodia and it was suggested that this enzyme is localized in the mitochondria. Dipeptidase activity, on the other hand, was diffusely distributed in the cytoplasm. In the present study differential centrifugation techniques have been used to fractionate the particulates from homogenates of slime mold plasmodia. Cytological examinations have been made to identify the separations achieved. Data concerning the occurrence of succinoxidase activity in *P. polycephalum* and its distribution in various fractions of the plasmodial homogenates have been obtained. The data provide additional information concerning the function of slime mold particulates and hence are recorded below.

MATERIALS AND METHODS

The strain of *P. polycephalum* used in this work was obtained from Dr. W. Seifriz of the University of Pennsylvania, to whom we express our thanks. Plasmodia were grown in culture dishes, with rolled oats as a nutrient following the method described by Camp ('36). The homogenates were prepared by means of a Potter-Elvehjem type stainless steel homogenizer (see Potter, '49) at temperatures near 0°C. with all solutions previously chilled. Homogenate fractions were separated under similar conditions in a refrigerated centrifuge.

Oxygen uptake measurements were made using conventional manometric techniques. Unless otherwise indicated each Warburg vessel contained 1.6 ml of myxomycete homogenate or homogenate fraction in the suspending medium indicated; 0.2 ml 0.2 M phosphate buffer at pH 7.2; and 0.4 ml 1×10^{-4} M cytochrome *c* (Nutritional Biochemicals Corporation). The side arm contained 0.3 ml of 0.5 M sodium succinate pH 7.0 (or equivalent of other substrate used) and the center well

0.5 ml 6N NaOH. Readings were also made on control vessels without substrate (volume replaced by 0.3 ml distilled water) and corrections made for the endogenous values obtained. Cups were oxygenated for two minutes and then equilibrated for 6 minutes at 25°C. before the substrate was tipped from the side arm into the center well. Aliquots of homogenates or homogenate fractions were introduced into tared containers and dried in an oven at 55°C. for determination of dry weight, corrections being made, where necessary, for the sugar or other solutes in the suspending medium.

EXPERIMENTAL RESULTS

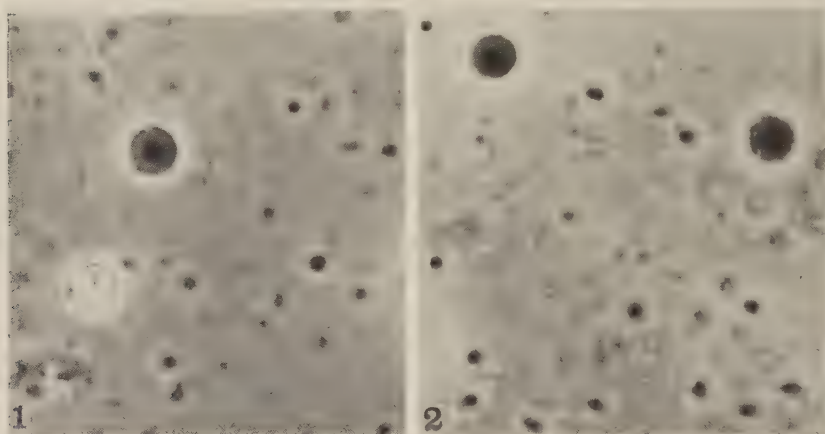
Identification of protoplasmic particulates. Four types of particulates are easily recognized both in living material and in homogenates: (1) pigment granules — so called because they contain the characteristic yellow pigment of the plasmodium. They are highly refractile, irregular in shape, and vary considerably in size (from 1–9 μ in diameter); (2) nuclei — colorless, spherical bodies, about 4–7 μ in diameter, containing one or more nucleoli; (3) mitochondria — small, colorless bodies 0.5 to 1.0 μ in diameter; (4) smaller particulates — objects near the limit of resolution of the optical microscope, hence too small to measure accurately with this instrument. Their nature has not been determined.

Staining reactions indicate that the mitochondria identified in *P. polycephalum* are identical with the structures described as mitochondria by Cowdry ('18) in other myxomycetes. With iron-alum hematoxylin, they appear black (as do the nuclei) against a light grey background. After aniline acid fuchsin and methyl green (Bensley's method) the mitochondria are seen as red dots against a blue-green background. When stained by Altman's method (aniline acid fuchsin and picric acid) the mitochondria appear red, the background yellow. Following Benda's method the mitochondria stain dark-blue, the background red.

All 4 particulate types can be observed in fresh material with the ordinary microscope; however critical adjustment

of the illumination is required. With phase contrast the pigment granules appear as very bright refractile bodies; the nuclei and mitochondria both appear dark but are clearly distinguished by their size (figs. 1 and 2). Hence phase contrast observations are much more satisfactory for accurate analysis of the types of particulates present in homogenates or homogenate fractions.

Separation of particles by centrifugation. The relative sedimentation properties of the various particulates were



Figs. 1 and 2 Homogenates of *Physarum polycephalum*. Phase contrast photographs showing a pigment granule (fig. 1), nuclei, and mitochondria. \times approx. 880.

investigated by centrifuging a homogenate at various speeds for a given time and examining sediment and supernatant with the phase contrast microscope. Smears were also prepared and stained with iron-alum hemotoxylin as a further check on the type of particulate present. Sometimes all nuclei and pigment granules appear in the sediment after centrifugation and washing in distilled water at forces as low as $1000\text{--}3000 \times g$ within 10 to 30 minutes. The supernatant resulting contains most of the mitochondria and is designated the "mitochondrial fraction." While free of nuclei and pigment granules this fraction is not pure; smaller particulates

are also present. Fractions containing nuclei only, or pigment granules only, are difficult to prepare. Mitochondria are so abundant and of such density that a considerable number remain in the sediment, even after repeated washing followed by centrifugation at relatively low forces ($600 \times g$). However, fractions containing a much greater number of pigment granules and nuclei and far fewer mitochondria than are present in the original homogenate are easily obtained. These are called "nuclear fractions" in the present paper, though pigment granules also occur and some mitochondria are still present.

Identification of succinoxidase activity. Preliminary succinoxidase assays were made on unfractionated homogenates prepared in three different suspending media: (1) a salt solution described by Chambers ('43) as more compatible with the plasmodium of *P. polycephalum* than other salt mixtures he had studied²; (2) a sucrose solution of the same tonicity (0.275 M) as Chambers' solution brought to pH 7.0 with phosphate buffer; (3) distilled water.

The succinoxidase activity (endogenous subtracted) of these three homogenates (based on a two hour assay at 25°C.) was as follows: Chambers' solution 2.51 $\mu\text{l}/\text{mg}/\text{hr}$; 0.275 M sucrose, 2.52 $\mu\text{l}/\text{mg}/\text{hr}$; distilled water, 2.93 $\mu\text{l}/\text{mg}/\text{hr}$. The succinoxidase system was thus shown to be relatively stable. Not only did it seem to make little difference which of these three suspending media was used to prepare the homogenate, homogenates prepared in any of the media retained most of this activity even after standing for several hours.

Cultures grown by Camp's method may be kept fairly clean, but they are rarely bacteria-free. Standard dilution plate assays made on nutrient agar indicated that 1 ml of the homogenate prepared under our conditions contained $1,350,000 \pm 250,000$ bacteria. To test the contribution of bacterial activity to the activity obtained oxygen uptake measurements were

² This solution contained KCl (0.120 M), NaCl (0.013 M), and CaCl_2 (0.003 M). It was brought to pH 7.0 by the addition of a small amount of KHCO_3 , and is hereafter referred to as Chambers' solution.

next made using heavy suspensions of bacteria obtained from the assay plates. The mixture presumably included all the types of bacteria normally found in plasmodial homogenates. The heaviest suspension prepared contained approximately 487,500,000 bacteria in each Warburg cup (determined by dilution assay). The data (table 1) indicate that negligible succinoxidase activity is obtained with more than 200 times the bacterial mass normally present in the homogenates. Hence the strong activity of the homogenate is due to plasmodial enzymes and not to bacterial metabolism of succinate.

Further tests on the identification of the system were made by determining the effect of inhibitors (malonate and cyanide)

TABLE 1

Analysis of the contribution of bacteria to homogenate succinoxidase activity

MATERIALS TESTED	OXYGEN UPTAKE			
	30 min.	60 min.	90 min.	120 min.
Homogenate ¹	410	720	1120	1514
487,500,000 bacteria	15	35	40	66
48,750,000 bacteria	0	0	6	9

Endogenous subtracted. Final volume 3.0 ml. Temp. 25°C. All values in μ l oxygen uptake for the period indicated.

¹ Contains $1,350,000 \pm 250,000$ bacteria.

on oxygen uptake under the assay conditions (table 2). The data indicate that malonate is a strong inhibitor, with the effective concentrations near the substrate concentration, suggesting a competitive inhibition by malonate such as occurs with mammalian succinic dehydrogenase. KCN added to active homogenates strongly inhibited oxygen uptake in concentrations as low as 0.001 M suggesting that the succinoxidase system is a typical one and that cytochrome oxidase may be the terminal oxidase involved. In other experiments, under conditions that gave high oxygen uptake with succinate as substrate, no appreciable uptake resulted with similar concentrations of pyruvate, lactate, citrate, glutamate, glycerol, mannitol or glucose. Extensive tests for sparking effects or possible co-factor requirements of homogenates have not yet

been made, but under the conditions of these experiments a striking specificity for succinate as a substrate was clearly demonstrated.

Succinoxidase activity of homogenate fractions. Experiments were next designed to ascertain the relative succinoxidase activity of mitochondrial fractions obtained by differential centrifugation compared to nuclear fractions. Eight grams wet weight of plasmodium were homogenized in 0.275 M sucrose solution (adjusted to pH 7.0 with phosphate buffer)

TABLE 2

Effect of inhibitors on succinoxidase activity of Physarum homogenates

INHIBITOR	OXYGEN UPTAKE		
	20 min.	40 min.	60 min.
None ¹	298	531	768
0.1 ml 0.5 M malonate	89	242	395
0.2 ml 0.5 M malonate	65	167	286
0.3 ml 0.5 M malonate	40	133	227
0.1 ml 0.03 M KCN	58	114	152
0.2 ml 0.03 M KCN	39	71	103

Endogenous subtracted. Suspending medium 0.275 M sucrose. Final volume 3.0 ml. Temp. 25°C. All values in μ l oxygen uptake for the period indicated.

¹ Cup contents: 1.4 ml homogenate; 0.3 ml 10^{-4} M cytochrome *c*; 0.2 ml 0.2 M PO_4 buffer at pH 7.2; 0.3 ml 0.5 M sodium succinate; 0.3 ml water; 0.5 ml 6 N NaOH in the center well. In cups containing inhibitors distilled water was replaced to the extent indicated in the table.

to make a total volume of 40 ml. This was filtered through cheese cloth and centrifuged 5 times at $1400 \times g$ for 20 minutes, resuspending the sediment each time in 40 ml fresh sucrose solution. The sediment remaining after the last washing constituted the nuclear fraction. The supernatants from the 5 washings were combined and centrifuged at $18000 \times g$ for 20 minutes. A sediment resulted which was resuspended twice more in fresh sucrose solution and recentrifuged, leaving a final sediment which formed the mitochondrial fraction. Each fraction was resuspended in 10 ml 0.275 M sucrose solution for assay purposes (table 3).

The succinate QO_2 of the mitochondrial fraction was almost 10 times greater on a dry weight basis than that of the nuclear fraction. This suggests that the mitochondria are the primary centers of succinoxidase activity and that the activity of the nuclear fraction may be due to the mitochondria found therein. The addition of cytochrome *c* stimulated oxygen uptake in both fractions and a much greater response occurred with the mitochondrial fraction than with the nuclei. This is further evidence that cytochrome oxidase may function as a terminal oxidase in this system.

Fractionation experiments were next extended to attempts to quantitate the percent of total homogenate activity that could be recovered in the fractions. Eight grams wet weight

TABLE 3
Comparative oxygen uptake of homogenate fractions

SUBSTRATE	NUCLEAR FRACTION	MITOCHONDRIAL FRACTION
Succinate (with cytochrome)	3.11	33.6
Succinate (no cytochrome)	2.3	15.6

Endogenous subtracted. Suspending medium 0.275 M sucrose. Final volume 3.0 ml. Time 120 min. Temp. 25°C. All values in $\mu\text{l}/\text{mg}/\text{hr}$.

of plasmodium were homogenized as described above (0.275 M sucrose solution, pH 7.0). This homogenate was centrifuged for 20 minutes at $1400 \times g$. The sediment was resuspended and washed twice in sucrose solution, recentrifuging each time for 20 minutes at $1400 \times g$. The final sediment is designated the nuclear fraction; the three supernatants were saved for recentrifugation at higher speeds. The first of the three supernatants was centrifuged at $18000 \times g$ for 20 minutes resulting in a higher speed precipitate. This precipitate was resuspended in sequence in the second and third low speed supernatants and centrifuged at $18000 \times g$ so that any particulate matter separated from the nuclear fractions in the low speed washings ($1400 \times g$) could be added to the high speed sediment. The final high speed sediment is designated as the mitochondrial fraction. The nuclear and mitochondrial frac-

tions were taken up in 10 ml fresh sucrose solution for assay purposes. All supernatants from the high speed washings were pooled forming a "supernatant"; at this point it was 320 ml. Succinoxidase assays on an aliquot of the homogenate and on the three fractions isolated are reported in table 4.

The activity of the fractions did not account for all the activity of the homogenate; however it did account for over 73%. In this experiment a mitochondrial fraction was also obtained that, on a dry weight basis, had a higher rate of oxygen uptake in the presence of succinate than did the nuclear fraction. The activity of the mitochondrial fraction was

TABLE 4

Distribution of homogenate succinoxidase activity in homogenate fractions

SUBSTANCE TESTED	SUCCINATE QO ₂ μl/hr	SUCCINATE QO ₂ μl/mg/hr
Unfractionated homogenate	1888.2	7.76
Nuclear fraction	939.4	7.4
Mitochondrial fraction	314.0	22.4
Supernatant fraction	133.1	1.95
Total recovered in fractions	1386.5	...
% Activity recovered in fractions	73.4%	...

Endogenous subtracted. Suspending medium 0.275 M sucrose. Final volume 3.0 ml. Time 120 min. Temp. 25°C.

only three times greater than that of the nuclear fraction (rather than ten times as large) nevertheless this difference is believed to be accounted for by the fact that in this experiment more emphasis was placed on the complete recovery of particulates than on a complete separation of nuclei and mitochondria. For this reason the nuclei were washed only three times instead of five. Microscopic examination disclosed many more mitochondria in the nuclear fraction than in the previous case. Hence the data in table 4 are taken as confirmation of the data reported in table 3, and as additional evidence that most, if not all, of the succinoxidase activity in *P. polycephalum* is localized in the mitochondria.

SUMMARY

1. Myxomycete mitochondria have been separated from the larger protoplasmic constituents by differential centrifugation techniques.

2. Myxomycete homogenates show strong succinoxidase activity. Evidence presented indicates that most, if not all, of this activity is localized in the mitochondria and that cytochrome oxidase may function as a terminal oxidase for this system.

LITERATURE CITED

- ANDRESEN, N., AND B. M. POLLOCK 1952 A comparison between the cytoplasmic components in the myxomycete, *Physarum polycephalum*, and in the amoeba, *Chaos chaos*. Compt. Rend. Trav. Lab. Carlsberg. Sér. Chim., 28 (6): 247-264.
- CAMP, W. G. 1936 A method of cultivating myxomycete plasmodia. Bull. Torr. Bot. Club, 63: 205-210.
- CHAMBERS, R. 1943 Electrolytic solutions compatible with the maintenance of protoplasmic structures. Biol. Symp., 10: 91-109.
- COWDRY, N. H. 1918 The cytology of the myxomycetes with special reference to mitochondria. Biol. Bull., 35: 71-94.
- HOLTER, H., AND B. M. POLLOCK 1952 Distribution of some enzymes in the cytoplasm of the myxomycete, *Physarum polycephalum*. Compt. Rend. Trav. Lab. Carlsberg. Sér. Chim., 28 (5): 221-245.
- HOWARD, F. L. 1931 The life history of *Physarum polycephalum*. Am. J. Bot., 18: 116-133.
- 1932 Nuclear division in plasmodia of *Physarum*. Ann. Bot., 46: 461-477.
- POTTER, V. R. 1949 The Homogenate Technique. In: Manometric Techniques and Tissue Metabolism by Umbreit, Burris and Stauffer. Burgess Publishing Company, Minneapolis.
- SPONSLER, O. L., AND J. D. BATH 1953 A view of submicroscopic components of protoplasm as revealed by the electron microscope. Protoplasma, 42: 69-76.

COMPARATIVE EFFECT OF METHYLATED XANTHINES ON THE FERTILIZATION CAPACITY AND LIFE SPAN OF ARBACIA GAMETES

RALPH HOLT CHENEY

*Biology Department, Brooklyn College, Brooklyn, New York
and The Marine Biological Laboratory,
Woods Hole, Massachusetts*

THREE FIGURES

While investigating the effect of caffeine (1:3:7 trimethylxanthine) upon reproductive processes and growth, the writer (Cheney, '45) demonstrated that concentrations below M/200 (0.10%) were variable in effect but above m/200 caffeine was clearly inhibitory, reducing O₂ uptake of the fertilized Arbacia egg and the cellular respiration of the developing organism. That study did not include observations on the unfertilized egg nor on spermatozoa. The previous investigation was limited to the trimethylxanthine.

The current paper presents evidence for the effect upon insemination, the cortical changes, fertilization, and the life span of separately pretreated Arbacia eggs and sperm for different periods in different concentrations of the tri(1:3:7) and two dimethyl (1:3 and 3:7) xanthines, namely — caffeine, theophylline and theobromine. This study is a part of a general investigation of the effect of methylated xanthines upon the cellular physiology of plants and animals. These test compounds differ chemically only in the number and position of the CH₃ groups.

MATERIALS AND PROCEDURE

Eggs and sperm of *Arbacia punctulata* were used and the experiments were performed at 22°C. Gametes were discarded

unless immediate mixing of controls resulted in 98 to 100% fertilization. Eggs possessed their normal jelly coat. Gametes were shed directly into filtered sea water (SW) or into the desired molarity of caffeine-in-sea-water (CSW), theophylline (TpSW), or theobromine (TbSW), for stated periods varying from zero to 60 hours for pretreatment prior to mixing. Gametes were mixed in SW only and the sequence of events associated with insemination and fertilization were observed. Examination was made generally at a magnification of $1100\times$ with depression-slide-hanging drop preparations. Photomicrographs were taken also at $440\times$, $950\times$, and $1250\times$, using dry, water, and oil immersion lenses under light and dark field illumination. The formation of the fertilization membrane (FM) was followed and special attention was given to changes in the cortical area of the egg following insemination as well as to the time factor and physical characteristics of the FM.

E. B. Harvey ('43) in comparing photomicrographs of sperm and the fertilization membrane of *Arbacia*, as revealed by the light microscope at $1000\times$ and by the electron microscope at $15,000\times$, described the sperm head as arrow-shaped with a short, slightly narrower, middle piece possessing a pair of spherical bodies, and a long filamentous tail. The head with the middle piece measured $4\text{ m}\mu$ long \times $2\text{ m}\mu$ across the base. The tail is approximately $45\text{ m}\mu$ long. She described the FM at $1000\times$ as an uniformly thin, transparent membrane 3 to $5\text{ m}\mu$ from the surface of the egg. It is elastic at first and stretches with centrifugation from a sphere of $80\text{ m}\mu$ in diameter to a spheroid having a length of $140\text{ m}\mu$ (E. B. Harvey, '33). Five minutes after fertilization, the FM thickens and resists stretching. E. N. Harvey ('11) noted that the cortical granules of the *Arbacia* egg were not displaced by ordinary centrifugation. These granules are maintained in the cortex even in the clear halves and quarters of eggs broken by centrifugation (E. B. Harvey, '46). In my present study, these characteristics of the sperm and egg and the FM were accepted as a part of the criteria for normalcy.

Both non-centrifuged and centrifuged eggs were employed because eggs, centrifuged to produce the five-layer stratification stage (E. B. Harvey, '32), show the nearly colorless, cortical granules best when examined under ordinary bright light illumination. Under these conditions, the wave of cortical granule change was accompanied by a slight crenation of the egg surface, and as described by Moser ('39), it could be followed accurately with a Stop Watch. When the sperm were added via a micropipette under the cover slip, the eggs were observed continuously. The time factors for normalcy in *Arbacia* for the sequence of cortical changes and FM elevation were in general agreement with Moser ('39) as follows:

1. Time to beginning of cortical granule change (dissolution) after insemination was 10 to 20 seconds. It is quite possible that a non-visible alteration may occur in the surface of the egg in a fraction of a second, a process which may prevent polyspermy before optical changes in the cortex are discernible.

2. Cortical reaction is completed in an average of 10 seconds.

3. Time between cortical reaction completion and the beginning of the FM elevation is 3 to 5 seconds.

4. FM completely smooth, rounded, and separated fully and free from all "blisters" occurs in 3 to 5 seconds.

In practice, there was a variation in the total time factor from 25 to 50 seconds, the entire range of which I interpreted as normalcy.

Since it is known (Glaser, '15; Lillie, '14, '15a, b; Gray, '28; Rothschild, '48) that diluting a sperm suspension increases the fertilizability power of the sperm and also that the life span of sperm in SW decreases with increasing dilution of the suspension; and, that survival is a function of the concentration of sperm and of the oxidative respiration, attention was given to standardizing the amounts of gametes and solutions employed. The stock volume of eggs and sperm utilized per experiment was reasonably constant. To assure an equivalent physiological state, all eggs and all sperm were

shed from one female and one male respectively into separate stender dishes. Forty ml volumes of solutions (SW, CSW, TpSW, TbSW) were added to each dish of 45 ml total capacity. Then each control or experimental dish received 1 ml of concentrated eggs plus three drops of wet sperm from the proper dish (SW, CSW, TpSW, TbSW). In a brief, separate series, one drop of "dry" sperm was used. Results were the same. For the bulk FM experiments, the dish with mixed gametes was rotated and test samples removed within 15 to 30 seconds for immediate examination continuously for several minutes until the FM was formed fully. A few experiments were run in which an approximate standardization of the concentration of eggs was obtained by low centrifugation to give a 35% suspension but the deletion of this step simplified the procedure and was more satisfactory for the purpose.

Experiments giving critical attention to cortical changes were done by placing a drop of egg suspension, non-centrifuged or centrifuged in different experiments, on the cover slip of a depression-slide-hanging-drop preparation. The sperm were introduced via a hand micropipette inserted under the cover slip through a groove in the slide. Continuous observation at $1100\times$ was made under light or dark field illumination until all visible changes had occurred in the cortex and the FM had developed completely.

In the stender dish bulk experiments, frequent examination at $500\times$ were made and followed through the 4-celled stage. At first, only M/400 concentrations of these three methylated xanthines were employed because M/400 is the maximum solubility of theobromine, the least soluble of the three compounds. Effects of lower molarities down to M/10,000 were inert or gave insignificant variations. Higher concentrations were used in so far as solubility permitted. The effect of a fifteen minute and longer periods of pretreatment of gametes in M/400, and also in M/200, M/40, and M/10 of the drugs prior to mixing in SW, upon the fertilization and the FM

development was determined particularly by the appearance in time and the physical characteristics of the FM. See table 1.

RESULTS

The rapid cortical changes and the time of appearance, the physical characteristics, and the full development of the FM to a smooth, entirely freed structure from the egg surface were the criteria for normalcy. The cellular (physical) structure through the 4-celled stage was observed to ascertain any delayed abnormalities.

TABLE 1

Effect of 15-minute pretreatment molarities on formation of fertilization membrane

AGENT ↓	MOLARITIES →			
	M/400	M/200	M/40	M/10
TbSW	F.M.		(Solubility exceeded)	
TpSW	F.M.	F.M.	F.M. delayed	Solubility exceeded
CSW	F.M.	F.M. delayed	F.M. delayed	No F.M. RC.

These data, see table 2, parallel (within the time limits 12 hours for eggs and 30 hours for sperm) the normal Viability Time Table (Cheney, '50), for behavior in SW alone, the natural environment. The results of exposure to the experimental solutions for longer periods than 12 to 30 hours as stated above, do not parallel the time effects seen in the controls in SW. The writer, however, to be well within the limits of safety, has suggested (Cheney, '50) for experimental purposes, the utilization of eggs not exceeding 8 hours and sperm not over 24 hours post-shedding age.

Reference to the accompanying graph, figure 1, illustrates the experimental data. Photomicrographs were taken to show the phenomenon of the general orientation and motility of viable sperm to the egg,—see figure 2; and, to show the absence of such an orientation and the lack of motility of non-viable sperm, see figure 3. This observation of the mass

TABLE 2
Viability time table for Arbacia gametes

SHED AGE OF	Shedding medium is SW or M/400 TbsW, TpsW, CSW																							
	Post-shedding AGE of egg in hours												---											
SPERM IN HOURS	IMMEDIATELY MIXED IN SW AFTER SHED INTO:						MIXED IN SW AFTER 4 HOURS IN:						MIXED IN SW AFTER 16 HOURS IN:						MIXED IN SW AFTER 24 HOURS IN:					
	SW	Tb	Tp	C	SW	Tb	Tp	C	SW	Tb	Tp	C	SW	Tb	Tp	C	SW	Tb	Tp	C	SW	Tb	Tp	C
↓ FRESH	100% F.M.*	100% F.M.*	100% F.M.	100% F.M.	100% F.M.	100% F.M.	100% F.M.	100% F.M.	100% F.M.	100% F.M.	100% F.M.	100% F.M.	90 to 100%	90 to 100%	90 to 100%	90 to 100%	0 to 1%	0 to 1%	0 to 1%	0 to 1%	0 to 1%	0 to 1%	0 to 1%	0 to 1%
4 hrs	"	"	"	"	"	"	"	"	"	"	"	"	"	"	"	"	"	"	"	"	"	"	"	"
16 hrs	"	"	"	"	"	"	"	"	"	"	"	"	"	"	"	"	"	"	"	"	"	"	"	"
24 hrs	"	"	"	"	"	"	"	"	"	"	"	"	"	"	"	"	"	"	"	"	"	"	"	"
36 hrs	75% 0%FM	90% "	90% "	90% "	90% "	90% "	90% "	90% "	90% "	90% "	90% "	90% "	65% 0%FM	80% "	80% "	80% "	80% "	80% "	80% "	80% "	80% "	80% "	80% "	80% "
48 hrs	"	"	"	"	"	"	"	"	"	"	"	"	"	"	"	"	0%	0%	0%	0%	0%	0%	0%	0%
50 hrs	"	"	"	"	"	"	"	"	"	"	"	"	"	"	"	"	"	"	"	"	"	"	"	"
54 hrs	"	"	"	"	"	"	"	"	"	"	"	"	"	"	"	"	"	"	"	"	"	"	"	"
60 hrs	"	"	"	"	"	"	"	"	"	"	"	"	"	"	"	"	"	"	"	"	"	"	"	"

tendency towards concentric rings of sperm or at least towards a general directional position of sperm towards the egg, is of interest here in view of the report by Rothschild ('49) that a particular orientation at the molecular level between the egg surface and the sperm is essential for successful fertilization.

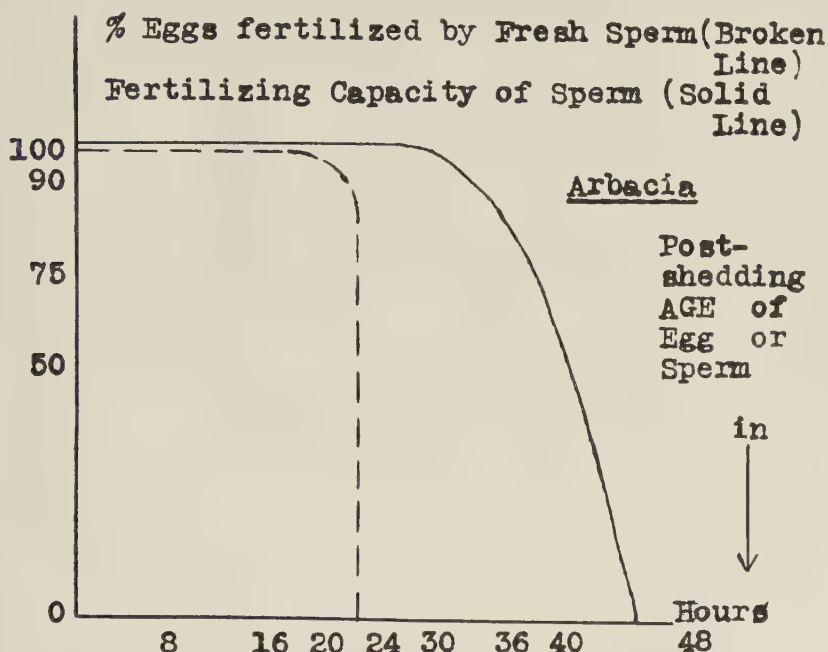


Fig. 1 Viability age graph.

The Viability Time Table for *Arbacia* gametes in M/400 CSW, TpSW, or TbSW, indicates clearly that this concentration did not shorten the life span. To a degree, there is evidence of an extension of the functional life span in some cases, — see table 1. In all cases wherein the concentration of methylated xanthines was sufficient to prevent the fertilization or in which the pretreatment period was prolonged enough to result in no FM formation, the colloidal cortical granules did not disappear optically following insemination as always occurred when fertilization was successful. In

contrast, whenever eggs proven by test to be non-fertilizable, the uniform, fine network type of distribution of the cortical granules appeared to be disorganized and grouped irregularly. Dissolution occurred in only a few granules.

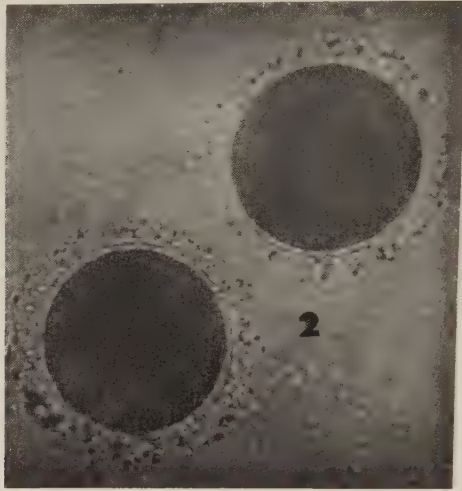


Fig. 2 Photomicrographs @ 440 \times of two fresh eggs with viable sperm oriented to them in concentric rings.

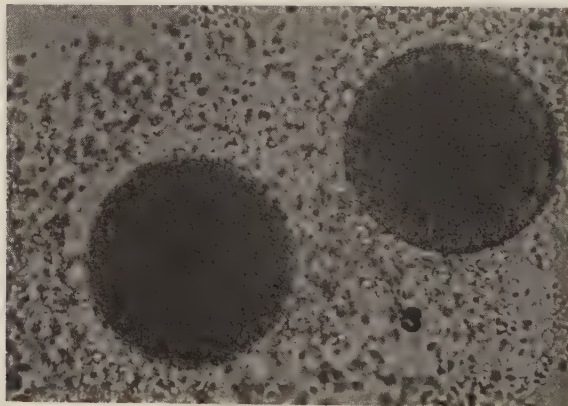


Fig. 3 Photomicrographs @ 440 \times of two fresh eggs with non-viable sperm showing absence of the orientation to the eggs and no concentric ring formation.

DISCUSSION

Lillie ('15-a) noted a positive chemotaxia of the sperm towards the egg and the cessation of motility with mass coagulation but he did not associate the mass orientation phenomenon directly with the fertilization capacity of the sperm. Although sperm velocity is not a critical measure of the fertilizing potency, a complete loss of motility and lack of mass orientation towards the egg is indicative of impotency. According to my observations, any sperm age period or immersion time in any concentration of methylated xanthines resulting in such an effect on the sperm, coincided with their incapability of fertilizing the egg. The metabolism involved in the physical and vital phenomena observed may not have any direct relationship to each other. This similarity in time may be merely a coincidence.

Although a concentration of M/400 of any one of these three compounds does not shorten the life span of *Arbacia* gametes, higher concentrations (when solubility permitted) do indicate a reduction effect and an inhibitory effect upon the functional ability of the egg to become fertilized. Danesio ('49) and Maxia ('50) reported in agreement with the general results of my earlier experiments (Cheney, '48) of the caffeine effects upon *Arbacia* fertilization and development. They stated, however, that similar results were obtained with much lower concentrations of caffeine, and that even with M/10,000 an antimutagenic influence was noted on the sea urchin, *Paracentrotus lividus*. I have no explanation of the surprising effectiveness of these low concentrations unless *P. lividus* is more sensitive than *Arbacia* to caffeine. This may well be the case as the egg of this species is quite different from the *Arbacia* egg. A temperature difference in the sea water tanks at Woods Hole and at Naples might be a significant factor. The critically effective molarity of a drug on a cell sometimes varies several-fold with slight temperature differences.

Judging the sensitivity of gamete longevity to each compound by its ability to fertilize or to be fertilized, demonstrated

the egg to be more sensitive than the sperm to injury by all three compounds. This is in agreement with an earlier observation (Cheney, '48) with the trimethylxanthine alone. There is some evidence that the order of decreasing effectiveness of the two dimethylxanthines, theophylline and theobromine, on the functional life span is $Tb > Tp$. This becomes apparent at least with the aged *Arbacia* gametes. This indication agrees with a previous record (Cheney, '49a) in a study dealing with the relative effect of these dimethylxanthines on *Arbacia* developmental sequences.

The effects of these compounds is apparently not related primarily to their molecular weight as a factor in their penetration and permeability, since aged gametes were affected in the order of $C > Tb > Tp$, whereas their molecular weight sequence is $C > Tp > Tb$. It can be noted that their inhibitory effectiveness increases with the number of methyl groups substituted for nitrogen-bound hydrogen in the xanthine nucleus.

Fol ('77) noted the progressive elevation of the FM following insemination; and, changes in the egg surface with insemination and fertilization have been reported by many investigators including Just ('19), Runnström ('28), Moser ('39), Ohman ('45), Rothschild and Swann ('49), and by Parpart and Laris ('55). These changes show considerable variation in their details in the several species used. For example, Rothschild and Swann ('49) described a relatively clear, wide cortical band of the unfertilized egg which was reduced appreciably in the fertilized egg in the case of *Psammechinus miliaris* (the sea urchin at the Scottish Marine Biological Station, Millport, Scotland); whereas, Moser ('39) described a narrow cortical picture of nearly colorless granules which dissolve after insemination. The cortical band brightness is also reduced in the fertilized egg. All investigators, regardless of individual variations in fact and interpretation, agree that cortical changes are associated critically with the initiation of the fertilization process and the elevation of the FM. Recently Parpart and Laris ('55) from

observations made on their television microscope, propose a new and plausible theory for the lifting of the FM. They assume that water is liberated from the exploded cortical granules of their colloidal material (presumable protein). These colloids are highly active osmotically for about 30 seconds. They reason that it is this water passage from the cortical granules and surrounding medium into the perivitelline space which lifts the vitelline membrane which becomes transformed into the FM.

My observations are in conformity with this idea of the generality of the cortical change. Specifically, with reference to methylated xanthines, it was clear that as long as the pretreatment (immersion time) period did not result in preventing fertilization, the cortical granules remained normal in distribution and appearance until insemination. In eggs, pretreated in such concentrations of these compounds as to destroy fertilizable potentiality, or for a time (in lower concentrations) sufficient to prevent the fertilization, the cortical granules had undergone some sort of physical change causing the cortex to appear darker and the uniform, fine network pattern of the granules to be broken and the granules are grouped irregularly. That a significant physical change does occur in the cortex together with a loss of surface papillation when the egg is rendered non-fertilizable specifically by one of the methylated xanthines, caffeine, has been demonstrated by Cheney and Lansing ('55) via electron microscopy. Whether this alteration in cortical granules is the only necessary phenomenon to post-insemination events or whether certain gelation changes occur as a result of cortical granule change or constitute an independently essential phenomenon is impossible to state at this time in spite of a careful study of optical sections and surface views under $1250\times$ magnifications of both non-centrifuged and centrifuged material wherein the eggs had been centrifuged to a degree which produced stratification but still allowed fertilization. Caffeine concentrations sufficient to delay the fertilization process and cleavage time observably but not to arrest it

completely, also delay cortical gelation changes (Cheney, '48 and '49b). It is difficult to compare the extent of the physical differences, other than the time factor, in the gelation of the cytoplasmic matrix of a normal egg with an egg in which fertilization is delayed (but does occur) due to a chemically inhibitory agent such as caffeine. It is of interest here to note that by pressure-centrifugation measurements of the displacement of the red pigment bodies in the cortical cytoplasmic plasmagel layer of *Arbacia*, Marsland and Zimmerman ('55) offer physical data to show that normal fertilization initiates a complex series of extensive, rapid changes in the gelation state of the cortical cytoplasm. By this one red-pigment criterion, they demonstrated the necessity and extent of one type of physical cytoplasmic behavior accompanying the post-fertilization process. If applied to drug-treated eggs, their technique might reveal some significant differences from the normal, non-treated egg in the sol-gel sequences and/or degree.

My observation of the apparently synchronous occurrence between the favorable transformations of the physical uniformity pattern of the cortical granules and the ability to be fertilized; or conversely, the similar correlation between the unfavorable physical change of the cortical colloids and the inability of the egg to become fertilized, tempts one to speculate that these cortical granules constitute some sort of a physico-chemical block to some essential enzyme-substrate system which must be activated to allow fertilization sequences. This concept might also account for the sudden and multifold increase in respiration known to accompany the metabolism of the *Arbacia* as it undergoes its transition from the unfertilized to the fertilized condition.

It was observed in the study of every aged sperm, although only a very few are viable, those few often succeed in fertilizing eggs but cause only a very poor lifting of the FM. Delayed examination does reveal cleavage in a few eggs of such cultures. Tyler ('50) noted a similar effect with the action of aged sperm in his study of the influence of amino-acids and

peptids on the life span of *Arbacia* sperm. It is of interest here that Runnström, at the September 1950 Meeting of the International Congress of Cell Biology at Yale University, reporting on the discovery of a sperm surface enzyme (probably hyaluronidase) which depolymerizes the jelly coat substance, assumed that this essential enzyme was more abundant in the young than in the aged sperm.

Although the trimethylxanthine, caffeine, is known to inhibit certain enzyme activity, as reported by Torda and Wolff ('48) for muscle adenosinetriphosphatase; and, by Nachmansohn and Scheemann ('45) for cholinesterase in nerve tissue, this type of inhibition may not be the mechanism of critical action on the life span of the *Arbacia* gametes. Angustinsson and Gustafson ('49) have reported little or no ChE exists in the sea urchin egg, at least in *Paracentrotus lividus*. Methylated xanthines in higher concentrations cause a reduction in the life span but in lower concentrations, even in the M/400, they are ineffective or with a slight suggestion of life extension. This extension effect is not due to the utilization of these compounds as nutrients. There is no evidence from any cellular research of which I am aware, that indicates methylated xanthines can be so utilized. Kidder and Dewey ('49) have shown that di- and trimethylxanthines specifically are not employed as nutrients in the protozoan, *Tetrahymena geleii*. They reported all naturally occurring methylated xanthines are nutritively ineffective except the monomethylxanthine with the CH_3 group at position One.

On the other hand, a slight prolongation of the functional life span of the gametes might be explained by the possibility of a surface effect which may precede an intra-cellular enzymatic inhibition. In a study of centrifugation effects on eggs in caffeine, the author (Cheney, '49b) demonstrated a surface action. Runnström ('50) reported that amino-acids prolong the fertilizing life of sea urchin sperm. Tyler ('50) and Tyler and Atkinson ('50) have attributed the extension of the life span by amino-acids as due to a surface reaction by suggesting that these substances oppose the dissolution of a surface

constituent, the antifertilizin, of the sperm; and, thereby retard the liberation of this substance which is essential to fertilization. Any extension, however, in the apparent viability due to methylated xanthines should be regarded at present as probably not significant. The data in tables 1 and 2 are based primarily upon the capacity to be fertilized or to fertilize. Observations were founded upon cortical changes and their time relationships to the appearance of the FM and its physical characteristics; whereas, the work-sheet details of the time rate for the development in SW of the cleavage stages through the blastula- gastrula- pluteus sequence *after* an initial pretreatment in methylated xanthines, present variable evidence, — namely, of slight retardation with M/400 TbSW or CSW and a slight acceleration with M/400 TpSW. Such variations were not consistent and in order of magnitude, they were not greater than the variation in O₂ consumption occurring with low concentrations of caffeine (Cheney, '45). These variations (less than 10%) were considered not to be significant for this material. Faced with a difference in the degree of effectiveness of M/400 concentrations of these three compounds upon diversified plant and animal cell types as reported in the literature, it suggests that M/400 of C, Tp, Tb, is a border line molarity for cellular response. Hence, it may be effective for some cell types and not for others. Kihlman and Levan ('49) have shown that M/400 caffeine produces binuclear and later multinucleated cells with failure of the cell wall to form in *Allium* root tips. Such variability in the action of methylated xanthines in M/400 on sex cells, development, and growth, challenges an interpretation of their significance to cell life in general metabolism; and, in higher concentrations, these experiments offer specific evidence for the inhibitory influence of these compounds upon reproductive physiology.

SUMMARY

1. Pretreatment of *Arbacia punctulata* eggs and sperm in M/400 CSW, TbSW or TpSW, does not alter significantly

the functional life span of either gamete. Immersion in M/400 concentrations for time periods which do not prevent fertilization, does not affect the appearance nor the distribution of the clear, vacuolar-like, cortical granules.

2. Higher concentrations than M/400 tend to reduce the life span of both gametes.

3. When eggs are rendered non-fertilizable, either by their post-shedding age or by high concentrations of methylated xanthines, the uniformity of the fine, colloidal pattern of cortical granules is interrupted. The granules become grouped into irregular masses, a portion of which may undergo dissolution.

4. The inhibitory effect of methylated xanthines on the fertilization process in *Arbacia* increases with the number of CH_3 groups replacing nitrogen-bound hydrogen in the xanthine nucleus.

5. The comparative intensity of the inhibitory effect of these compounds is one of degree. The nature of the physical effect is identical.

6. Theoretical explanations are discussed and the possibility of a surface action preceding an intra-cellular enzymatic reaction is presented for the effect of di- and trimethylxanthines on the life span of *Arbacia* gametes.

7. Evidence is given that the visible mass orientation in the form of concentric layers of sperm towards the egg is maintained, irrespective of the individual sperm pathway, as long as the sperm retain their normal motility and viability.

8. There is a direct relationship between the fertilizing capacity of sperm and their orientation and motility since, in the absence of these characteristics, the spermatozoa are impotent.

LITERATURE CITED

- ANGUSTINSSON, K., AND U. T. GUSTAFSON 1949 Cholinesterase in developing sea urchin eggs. *J. Comp. and Cell. Physiol.*, *34*: 311-321.
- CHENEY, R. H. 1945 The effects of caffeine on oxygen consumption and cell division in the fertilized egg of the sea urchin, *Arbacia punctulata*. *J. Gen. Physiol.*, *29*: 63-72.

- CHENEY, R. H. 1948 Caffeine effects on fertilization and development in *Arbacia punctulata*. *Biol. Bull.*, 94: 16-24.
- 1949a *Arbacia* sensitivity to methylated dioxypurines. *Anat. Record*, 105: 44-45.
- 1949b Stratification and deformation of *Arbacia punctulata* eggs centrifuged in caffeine solutions. *Biol. Bull.*, 96: 70-73.
- 1950 Viability of *Arbacia* gametes in relation to time. *Biol. Bull.*, 99: 354-355.
- CHENEY, R. H., AND A. I. LANSING 1955 Caffeine inhibition of fertilization in *Arbacia*: Electron Microscopy. *Exptl. Cell Research*, 8: 173-180.
- DANESIO, V. 1949 Sull' Azione antimitotica della caffeina in *Paracentrotus lividus*. *Boll. d'Soc. Ital. d'Biol. Sperm.*, 25: 1014-1016.
- FOL, H. 1877 Sur le commencement d'henogenie chez divers animaux. *Arch. Sci. Nat. and Phys. Geneve.*, 58: 439-472.
- GLASER, O. 1915 Can a single spermatozoon initiate development in *Arbacia*? *Biol. Bull.*, 28: 149-153.
- GRAY, J. 1928 The effect of dilution on the activtiy of spermatozoa. *Brit. J. Exp. Biol.*, 5: 337-334.
- HARVEY, E. B. 1932 The development of half and quarter eggs of *Arbacia punctulata* and of strongly centrifuged whole eggs. *Biol. Bull.*, 62: 155-167.
- 1933 Effects of centrifugal force on eggs of *Arbacia punctulata* as observed with the centrifuge-microscope. *Biol. Bull.*, 65: 389-396.
- 1943 The spermatozoon and fertilization membrane of *Arbacia punctulata* as shown by the electron microscope. *Biol. Bull.*, 85: 151-156.
- 1946 Structure and development of the clear quarter of the *Arbacia punctulata* egg. *J. Exp. Zool.*, 102: 253-276.
- HARVEY, E. N. 1911 Studies in permeability of cells. *J. Exp. Zool.*, 10: 507-556.
- KIDDER, G. W., AND V. C. DEWEY The biological activity of substituted purines. *J. Biol. Chem.*, 179: 181-187.
- KIHLMAN, B., AND A. LEVAN 1949 The cytological effect of caffeine. *Hereditas*, 35: 109-111.
- LILLIE, F. R. 1914 Studies in fertilization VI. The mechanism of fertilization in *Arbacia*. *J. Exp. Zool.*, 16: 523-588.
- 1915a Sperm agglutination and fertilization. *Biol. Bull.*, 28: 18-33.
- 1915b Studies in fertilization. VII. Analysis of variations in the fertilizing power of sperm suspensions of *Arbacia*. *Biol. Bull.*, 28: 229-251.
- MARSLAND, D. A., AND A. ZIMMERMAN 1955 The energetics of cell division: fluctuations in the structural state of the cortical plasmagel layer of the *Arbacia* egg in relation to the first and second cleavage divisions. *Biol. Bull.*, 109: 364.
- MAXIA, C. 1950 Nuove osservazioni sull'azione antimitotica della caffeina. *Boll. d'Soc. Ital. d'Biol. Sperm.*, 26: 556-557.

- MOSER, F. 1939 Studies on a cortical layer response to stimulating agents in the Arbacia egg. I. Response to insemination. *J. Exp. Zool.*, *80*: 423-446.
- NACHMANSOHN, D., AND H. SCHEEMANN 1945 On the effects of drugs on cholinesterase. *J. Biol. Chem.*, *159*: 239-240.
- OHMAN, L. 1945 On the lipids of the sea urchin egg. *Arkiv. för Zoologi*, *36A*: 1-95.
- PARPART, A. K., AND P. C. LARIS 1955 A theory for the lifting of the fertilization membrane of the egg of Arbacia punctulata. *Biol. Bull.*, *109*: 350.
- RUNNSTRÖM, J. 1928 Die Veränderungen der Plasmakolloide bei der entwicklungsregung des Seeigeleies. *Protoplasma*, *4*: 338-514.
- 1950 Respirative and fertilizing capacity of sea urchin sperm in the presence of sperm albumin and jelly coat solution. *Biol. Bull.*, *99*: 324.
- ROTHSCHILD, L. 1948 The physiology of the sea urchin spermatozoa (Senescence and dilution effect). *J. Exp. Biol.*, *25*: 353-368.
- ROTHSCHILD, L., AND M. M. SWANN 1949 A propagated response to sperm attachment. *J. Exp. Biol.*, *26*: 164-176.
- TORDA, C., AND H. G. WOLFF 1948 Effect of acetylcholine, caffeine and alkaloids on activity of muscle adenosinetriphosphatase. *Amer. J. Physiol.*, *152*: 86-92.
- TYLER, A. 1950 Extension of the functional life span of spermatozoa by amino-acids and peptides. *Biol. Bull.*, *99*: 324.
- TYLER, A., AND E. ATKINSON 1950 Prolongation of fertilizing capacity of sea urchin spermatozoa by amino-acids on sea urchins *Lytechinus pictus* and *Strongylocentrotus purpuratus*. *Science*, *112*: 783-785.

SEXUAL COMPETENCE IN *ESCHERICHIA COLI*¹

T. C. NELSON²

Department of Genetics, University of Wisconsin

INTRODUCTION

Most studies of recombination in bacteria have emphasized genetics rather than physiology (discussion by M. Westergaard in Lederberg et al., '51). The modification of the phenotypic expression of mating type by aerobic cultivation of parental cells (Cavalli et al., '53) and the effects of streptomycin and ultraviolet irradiation (Haas et al., '48; Hayes, '53) on fertility have been investigated. The action of certain chemical compounds on the recovery of progeny has also been demonstrated (Clark, '53). A previous kinetic analysis (Nelson, '51) gave results which agreed with modified second order kinetics, that is, with a theoretical model of random collisions of two species of particles, the parent cells.

The usual technique of crossing (Lederberg et al., '51) is inadequate for physiological purposes. Parental cells from compatible strains genetically labelled to allow selective recovery of recombinants are mixed in agar or spread on the surface of agar media. Under these conditions no estimation of kinetic constants is possible since the opportunities for intercellular contact cannot be determined. This study is concerned with the rates and extents of recombinant formation under conditions which allow calculation of kinetic constants. It is an attempt to determine the physiological mechanism of the cellular interaction on which gene recombination is based.

¹ Contribution No. 596 from the Department of Genetics, University of Wisconsin, Madison 6, Wisconsin. This work has been supported in part by a research grant (C-2157) from the National Cancer Institute, National Institutes of Health, Public Health Service.

² Postdoctoral Research Fellow, National Cancer Institute, National Institutes of Health, Public Health Service.

METHODS

The techniques previously described (Nelson, '51) have been used. Parental cells of appropriate mating type were grown separately, washed by centrifugation, and resuspended in buffer. Mating was initiated by mixing the resuspended parental cells. Aliquots were periodically plated in media selective for progeny to determine the time course of syngamy. In these experiments the mating types used were Hfr (high frequency of recombination) and F⁻. The use of the ambivalent F⁺ was avoided to allow a greater range of measurement and to avoid side reactions such as plate recombination and compatibility state infection (Cavalli et al., '53).

Auxotrophic parental strains carrying the following arrays of genetic markers were used: W 1895 (methionine- Hfr [Cavalli et al., '53]), W 2323 (methionine- Hfr [Hayes, '53]), W 2057 and W 2060 (threonine- leucine- thiamine- Hfr, isolated as a segregant from a persistent diploid from the cross of W 1895 by threonine- leucine - thiamine- F⁻), W 1607 and W 2207 (methionine- F⁻), and W 1956 (threonine- leucine- F⁻). Derivatives of these strains carrying unselected markers were also used (ability to ferment lactose or xylose, resistance to bacteriophages T1 or T6, and resistance to streptomycin or furadroxyl). All of the stocks were lysogenic for the temperate bacteriophage lambda. Thus induction of phage development during mating was avoided (Jacob, '54; Wollman, '54).

Reciprocal crosses, W 1895 by W 1956, and W 1607 by W 2057 (or W 2060), uncovered no effect of the nutritional markers except a variation in yield of selected prototrophic and other recombinants. The *recombinant ratio R*, the ratio of zygotes to recombinants, might be expected to differ for reciprocal crosses due to linkage of elimination segments to selected loci (Nelson and Lederberg, '54). In this paper the term "prototroph" will be used to designate the following selected recombinant classes: true thiamine independent prototrophs and thiamine dependent but otherwise nutritionally

non-exacting recombinants. The recombinant ratios for "prototrophs" approximate 10 for the cross W 1895 by W 1956 and 100 for the cross W 1607 by W 2057 (or W 2060). Zygotes were determined in these crosses by a technique devised by J. Lederberg (personal communication). The parental strains were Hfr lactose-fermenting and F- lactose non-fermenting. Colonies sectoring for ability to ferment lactose on eosin-methylene blue lactose agar were considered to arise from zygotes. Nutritional deficiencies do not interfere with fertility as shown by the recovery of zygotes from homoauxotrophic crosses (crosses of parental cells containing similar nutritional deficiencies) of proliferating cells.

Cultures were grown from small inocula in 10 ml of un-aerated Penassay Broth (Difco) in a 37°C. water bath for 18-24 hours. Cultures were washed twice by centrifugation and resuspension in cold sterile 1.0% saline and finally resuspended at the desired cell density in basal salts buffer lacking any carbon or energy source (Lederberg, '50). The washing procedure and composition of the buffer were varied for individual experiments.

Crosses were performed by mixing suspensions of the parental strains and incubating in a 37°C. water bath without agitation or aeration. The time yield of "prototrophs" was determined by plating varying volumes of parental cells diluted 1:100 in cold saline or buffer. "Prototrophs" were selected by plating in a synthetic medium consisting of mineral salts + 0.5% glucose + 1.6% unwashed agar (Difco) + 0.02 gamma/ml thiamine (Lederberg, '50). Selection for thiamine independence was relaxed by addition of thiamine to the medium to eliminate errors due to trace contamination of the medium and reversion. The plates were incubated at 37°C. for 48 hours and then counted. The yield of "prototrophs" is assumed to be a relative measure of the syngamic events. The total number of parental cells was determined by plating in nutrient agar or surface spreading on eosin-methylene blue lactose agar.

Reconstruction experiments excluded the following sources of error within the range of concentrations of parental and recombinant cells used in these experiments: (i) mutual suppression of crowded recombinant colonies, (ii) competitive suppression of recombinant colonies by excess of either parent (Jinks, '52; Ryan, '53), (iii) plate reversion, and (iv) plate recombination. Plate recombination did occur with more than 10^7 cells of either type per milliliter of unwashed agar medium. The densities used for assay plates were well within this limit. A plot of log "prototrophs" versus log parental cells gave the expected slope of 2 (Nelson, '51). Addition of only 0.08 gamma dehydrated nutrient broth (Difco) per milliliter of plating agar, representing a 1% contamination, increased the recombinant yield by 10^4 at lowest frequency of "prototrophs" (equivalent to one "prototroph" per 100 parental cells) and gave a slope of 1 corresponding to plate recombination.

RESULTS

Saturation. Crosses were made with parental cells mixed in varying ratios, the less numerous parent varying from a concentration almost equal to the more numerous parent, about 10^9 cells/ml, to 10^5 cells/ml. If syngamy proceeds to completion, that is, every parental cell undergoes syngamy, then all of the parental cells of the less frequent class should yield zygotes. Actually the reaction reaches a limit, saturates, at about 1/100th of this expected value as shown in figure 1. This saturation could be explained if the medium changed or if only a limited fraction of the parental cells were competent to undergo syngamy. Since changing the medium after saturation did not reinitiate syngamy it is assumed that only a fraction of the parent cells is competent.

Either or both parents might be heterogeneous with respect to competence. If both are then reinitiation of syngamy should follow the addition of fresh competent cells of mating type complementary to the type still in excess. If only one type possesses limited competence then addition of this mating

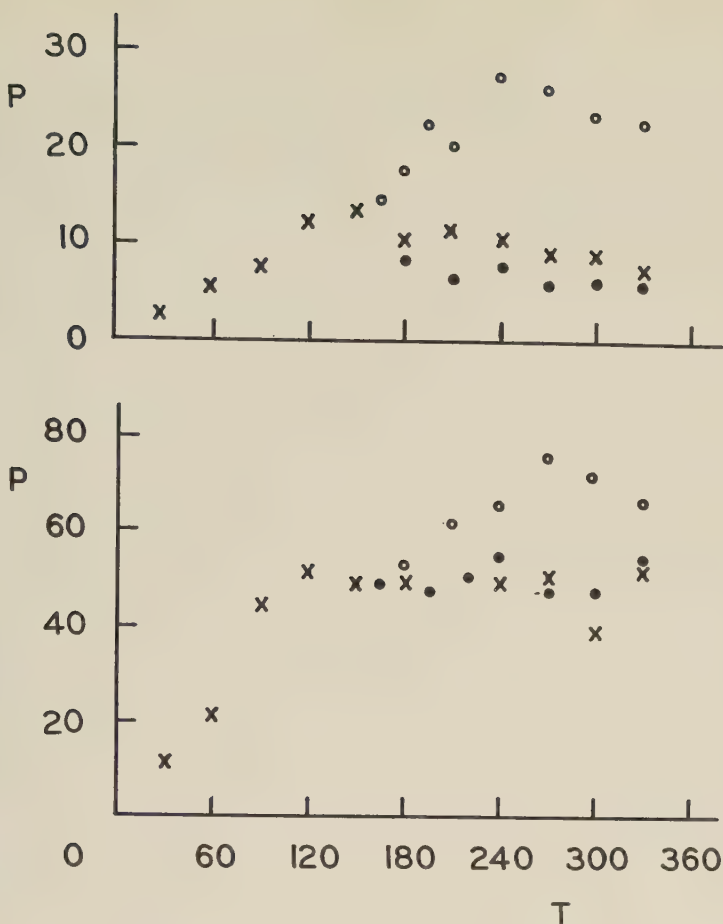


Fig. 1 *Addition of fresh parental cells following saturation.*

F⁻ cells were originally present in excess in the upper figure. The initial concentration was 2.4×10^9 F⁻ and 2.2×10^8 Hfr cells/ml. 3.0 ml aliquots of the cross tube (10.0 ml total volume) were distributed into three tubes at 150 minutes. 0.3 ml of buffer was added to one tube (crosses). Fresh F⁻ cells (0.3 ml) were added to a second tube to a final concentration of 3.5×10^9 F⁻ cells/ml (solid circles). Fresh differentially marked Hfr cells (0.3 ml) were added to a third tube to a final concentration of 3.0×10^8 Hfr cells/ml (open circles).

Hfr cells were originally in excess in the lower figure. The initial concentration was 1.5×10^9 Hfr and 2.9×10^8 F⁻ cells/ml. The same procedure was used; fresh buffer added to one tube (crosses), fresh F⁻ cells added to a second tube to a final concentration of 3.3×10^9 cells/ml (solid circles), and fresh Hfr cells added to a third tube to a final concentration of 2.7×10^9 Hfr cells/ml (open circles).

The concentration of "prototrophs" per milliliter in each cross tube was determined as a function of time. The ordinate must be multiplied by 10^3 to obtain the number of "prototrophs"/ml.

type should reinitiate syngamy regardless of the initial ratios of cells provided that unreacted cells of the opposite mating type are still available. To test this point freshly prepared cells of mating types Hfr and F⁻ were added to aliquots of crosses which had saturated. As shown in figure 1 only the addition of freshly prepared cells of mating type Hfr reinitiated syngamy regardless of which parent was initially present in excess. Only about 1% of the Hfr cells possess competence. All F⁻ cells are competent in the sense that they can undergo syngamy with a competent Hfr cell.

In these reinitiation experiments a second level of saturation was obtained. If the first and second batches of cells were genetically differentiated by an unselected marker, the ability to ferment lactose, the expected ratio of markers was recovered among the "prototrophs." The average levels of saturation with and without addition of fresh Hfr cells were calculated for the experiment given in figure 1. Forty-six per cent of the final "prototroph" colonies from platings at 330 minutes were expected to derive from matings of F⁻ cells with the second batch of Hfr cells. On the basis of control crosses, 26% of these, or 54 of the 459 "prototroph" colonies isolated, purified, and tested, should carry the differential marker. Sixty isolates were found to carry this marker. This shows that newly added competent Hfr cells are incapable of potentiating incompetent Hfr cells.

Decay of competence. Hfr cells stored in buffer at 37°C. for two or more hours were found to be inactive in reinitiating syngamy. Only freshly prepared Hfr cells or Hfr cells stored in buffer at 0°C. were active. F⁻ cells, either freshly prepared or stored at 0 or 37°C., yielded "prototrophs" when mixed with freshly prepared Hfr cells. This decay of competence of Hfr cells might be due to matings among the Hfr cells, if mating complexes or their immediate progeny are assumed to be incompetent. Matings of Hfr by Hfr cells were shown by "prototroph" recovery from the crosses W 1895 by W 2060 and the recovery of colonies sectorized for ability to ferment lactose from the cross W 1895 by W 2057.

The time rate of decay of competence was measured by storing Hfr cells in buffer at 37°C. for varying periods of time. Aliquots were withdrawn, mixed with an excess of F⁻ cells, and the time yield of "prototrophs" determined. The ratio of "prototrophs" at saturation without storage to "prototrophs" at saturation following storage was used as a measure of competence. If loss of competence is to be accounted for by Hfr by Hfr matings the rate of decay of competence should depend upon the concentration of Hfr cells. The effect of concentration was found only at high cell densities. The rate of decay of competence is not decreased as rapidly with dilution of the Hfr cells as would be expected if it were due solely to Hfr by Hfr matings (the ratio of the rates would be proportional to the square of the dilutions). Figure 2 demonstrates the decay of competence of stored Hfr cells. The reaction is approximately first order with a reaction rate constant of about 10^{-2} minute⁻¹.

Decay of competence occurred in Hfr strains W 2057 and W 2060 as well as W 1895 but not in F⁻ strains W 1607 or W 1956. However strains from Hfr cultures selected for increase in motility did show spontaneous loss of competence although the strains had the compatibility reaction of F⁻ cells. These cultures did not show conversion to the F⁺ mating type upon contact with F⁺ cells (personal communication from P. D. Skaar and Esther M. Lederberg).

Three reactions therefore occur in suspensions of cells of Hfr and F⁻ mating types in buffer: heterogamy of F⁻ and competent Hfr cells, intratype matings of Hfr cells, and a first order decay of the competence of Hfr cells. The first two reactions were dependent upon the concentration of cells and the last reaction was independent.

Effect of medium. Lederberg (personal communication) found no increase in yield of prototrophs when parental cells were densely packed in saline by centrifugation. Increased yields were obtained if magnesium ion was present in the plating medium. The low rate of syngamy in distilled water, saline, and buffers of low ionic strength was confirmed. Both

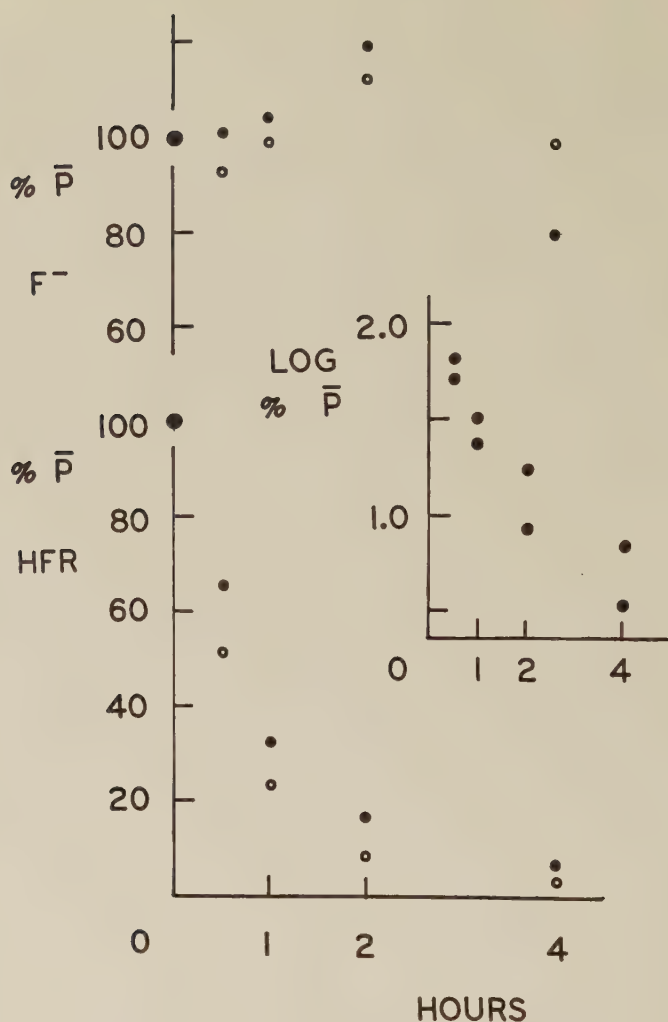


Fig. 2 First and second order decay of competence of Hfr cells.

Hfr and F⁻ cells were held in buffer at 37°C. Samples were withdrawn at the indicated times and mixed with an excess of freshly prepared cells of opposite compatibility to determine the saturation level of "prototrophs." A value of 100% corresponds to 4.0×10^5 "prototrophs" per 1.5×10^8 Hfr cells/ml and 8.3×10^4 "prototrophs" per 1.3×10^8 F⁻ cells/ml. Approximation to a first order reaction is shown by the log plot of "prototrophs." The reaction rate constant for first order decay of competence, K_h , was 1.4×10^{-2} /minute for the Hfr cells. The reaction rate constant for 'intratype matings' of Hfr cells (second order decay), K_{HH} , was 2.6×10^{-2} ml/minute. Closed circles refer to cultures of diluted cells, 1.5×10^8 Hfr cells/ml or 1.3×10^8 F⁻ cells/ml. Open circles refer to cultures of concentrated cells, 1.5×10^9 Hfr cells/ml or 1.3×10^9 F⁻ cells/ml.

the rate and extent of syngamy were found to depend on the ionic strength and cation concentration and composition of the medium. Univalent ions were additive in effect while divalent ions were not additive as shown in table 1. Syngamy occurred only in the pH range 6 to 8.

The results of kinetic experiments may be trivial if the non-specific formation of clumps of parental cells in which mating later occurs is being measured (Lederberg et al., '51). Decay of competence would then be due to the formation of homogeneous clumps of cells, be experienced by both Hfr and F⁻ cells, be dependent upon cell density, and reversed upon mechanical disruption of the clumps. However, syngamy should then be potentiated by incubation of mixtures of parental cells at low temperatures since salt agglutination is independent of temperature. As shown in table 1 few "prototrophs" were recovered from crosses incubated at 0°C. and pre-incubation of the mixed parental cells at 0°C. did not increase the rate of "prototroph" formation when the cells were transferred to a water bath at 37°C.

The initial attachment of Hfr and F⁻ cells was not reversible on dilution. However syngamy could be prevented and mating complexes previously formed could be disrupted by agitation by an oscillating table as well as by more violent means (Jacob, '55; Wollman, '55). Neither aeration, glucose, cyclic amino acids, or filtrates of previous crosses affected the rate of syngamy in buffer. Reduction of the fluidity of the medium with the non-toxic (70 to 80% of the parental cells were recoverable after 150 minutes in the highest concentrations of Metho-Cel) methylated cellulose Metho-Cel was accompanied by a reduction in the rate and extent of syngamy as shown in table 1 (Anderson, '53).

Syngamy in suspensions of multiplying cells. Crosses were performed with cells growing in broth in order to achieve maximal frequencies of zygotes. Inocula of 0.01 to 1.0 ml of lactose fermenting streptocycin sensitive Hfr and lactose non-fermenting streptomycin resistant F⁻ cells from the exponential phase of growth were made into 10 ml of fresh

TABLE 1

Effect of medium on rate of syngamy

A Rates in buffer with different cations

CATION OF SALT		CONCENTRATION OF PARENTAL CELLS		RATE OF SYNGAMY
Univalent	Divalent	Hfr	F-	"Prototrophs" ml minute parental cell (Hfr) × parental cell (F-) ×
K ⁺	none	2.4 × 10 ⁸ /ml	2.5 × 10 ⁸ /ml	9.5 × 10 ⁻¹⁵
Na ⁺	none	(experiment 1)		11. × 10 ⁻¹⁵
1/2 K ⁺ + 1/2 Na ⁺	none			12. × 10 ⁻¹⁵
K ⁺	none	7.4 × 10 ⁸ /ml	9.1 × 10 ⁸ /ml	.55 × 10 ⁻¹⁵
K ⁺	Mg ⁺⁺	(experiment 2)		1.3 × 10 ⁻¹⁵
K ⁺	Ca ⁺⁺			1.3 × 10 ⁻¹⁵
K ⁺	1/2 Mg ⁺⁺ + 1/2 Ca ⁺⁺			.62 × 10 ⁻¹⁵
Basal buffer:		K ₂ HPO ₄ or Na ₂ HPO ₄	4.02 mM/L	
		KH ₂ PO ₄ or NaH ₂ PO ₄	.734 mM/L	
		MgSO ₄ or CaCl ₂	.406 mM/L	

CONCENTRATION OF MgSO ₄ M/L	CONCENTRATION OF PARENTAL CELLS		RATE OF SYNGAMY	SATURATION LEVEL "PROTOTROPHS"/ML
	Hfr	F-		
0	8.7 × 10 ⁸ /ml	5.8 × 10 ⁸ /ml	2.9 × 10 ⁻¹⁵	2.3 × 10 ⁴
10 ⁻⁴	(experiment 3)		4.0 × 10 ⁻¹⁵	5.9 × 10 ⁴
10 ⁻³			5.5 × 10 ⁻¹⁵	11. × 10 ⁴
10 ⁻²			5.6 × 10 ⁻¹⁵	13. × 10 ⁴
10 ⁻¹			3.4 × 10 ⁻¹⁵	9.0 × 10 ⁴

Basal buffer of potassium phosphates

B Rates in buffer at different temperatures

TEMPERATURE OF WATER BATH °C.		TIME OF PLATING	"PROTOTROPHS" OBTAINED PER ML OF 10 ⁻² DILUTION		RATE OF SYNGAMY
0-120 minutes	120-240 minutes				
0	..	120	6, 10	1.0 ml	.05 × 10 ⁻¹⁶
0	0	240	22, 14	1.0 ml	.06 × 10 ⁻¹⁶
0	37	240	1600 472	1.0 ml 0.3 ml	9.1 × 10 ⁻¹⁶
37	..	120	2240 1210	1.0 ml 0.5 ml	13. × 10 ⁻¹⁶

Concentration of Hfr cells = 1.1 × 10⁹/mlConcentration of F- cells = 1.3 × 10⁹/ml

C Rates in buffer with Metho-Cel

CONCENTRATION OF METHO-CEL	RELATIVE VISCOSITY	RATE OF SYNGAMY
% (wt/vol)		
0	1	21. × 10 ⁻¹⁵
0.70	8.55	6.4 × 10 ⁻¹⁵
0.90	18.0	3.3 × 10 ⁻¹⁵
1.00	35.3	2.0 × 10 ⁻¹⁵
1.20	67.9	1.0 × 10 ⁻¹⁵

Concentration of Hfr cells = 3.7 × 10⁸/mlConcentration of F- cells = 5.1 × 10⁸/ml

Penassay broth at 37°C. Zygotes were detected as colonies sectoring for lactose fermentation on eosin-methylene blue lactose agar containing 200 gamma/ml dihydrostreptomycin. The lowest number of zygotes that could be detected by this method was 0.1% of the number of F⁻ cells. The rate of formation of zygotes was greater than the rate of growth of parental cells until the maximum frequency of zygotes was obtained. Growth and zygote formation ceased simultaneously. The maximum frequency of zygotes, about 10% of the total number of cells, was thus obtained immediately prior to the cessation of growth.

Four methods were used to attempt to increase this frequency: (i) The initial mixture of parental cells, resuspended in fresh broth, was made at cell densities equal to or greater than those obtained at the cessation of growth, 3×10^8 cells/ml in unaerated and 1×10^9 cells/ml in aerated broth, to 10^{10} cells/ml. No growth was detectable and the maximum frequency of zygotes was less than 1% of the total number of cells.

(ii) An excess number of parental cells of one or both types was added during or at the end of growth. Growth ceased and no additional zygotes were formed.

(iii) The initial ratio of Hfr to F⁻ parent cells was varied from 100 to 1 to 1 to 100. At the ratios 100 to 1 and 20 to 1 the number of zygotes reached a frequency of one-half the number of F⁻ cells.

(iv) The exponential phase of growth was prolonged by addition of fresh medium just prior to cessation of growth. The frequency of zygotes did not increase.

These results show that growth is necessary for the production of maximum frequencies of zygotes. The failure to obtain increased frequencies of zygotes by continuous cultivation of cells in the exponential phase of growth at high cell densities indicates that only a fraction of the cells are capable of mating at any given moment. This populational discontinuity is physiological rather than hereditary since

repetition of these crosses using unreacted parent cells from a previous cross gave similar results.

Hfr by Hfr matings and second order decay of competence. Three methods were used to estimate the rate of Hfr by Hfr interactions: (i) Mating of Hfr by Hfr: "Prototrophs" were recovered from the cross W 1895 \times W 2057 (or W 2060). Here two crosses are actually occurring; competent cells of strain W 1895 mating with incompetent (or possibly competent cells as well) cells of strain W 2057 and vice versa. This was confirmed by the distribution of unselected markers among the "prototrophs" in both Hfr \times Hfr and F+ \times F+ crosses. 'Intratype matings' of cells of the same strain would not be detected. Table 2 gives the adjusted rates of "prototroph" formation (= "prototrophs" formed per minute per parental cell per parental cell). These rates are uncorrectable for 'intratype matings' of cells of the same strain and for decay of competence. The rate of Hfr \times Hfr mating was considerably less than the sum of the two comparable Hfr \times F- cross rates, suggesting that not all Hfr \times Hfr complexes are fruitful. No "prototrophs" were recovered from F- \times F- crosses.

(ii) Effect of concentration of Hfr cells on rate of loss of competence: In buffer suspensions of Hfr cells first order decay of competence and 'intratype mating' remove competent cells. The rate of disappearance of competent Hfr cells was measured indirectly by the maximal yield of "prototrophs" obtained by crossing the residual competent Hfr cells in aliquots of the suspension with an excess of F- cells. The difference in rates of decay at high and low cell densities is a measure of the second order reaction, presumably 'intratype mating' of Hfr cells, as shown in figure 2. Where K_{hH} and K_h are the rate constants of 'intratype Hfr mating' and first order decay of competence, H and F are the concentrations of all Hfr and F- cells initially, \bar{P}_0 and \bar{P} are the saturation levels of "prototrophs" determined in an excess of F- cells at time zero and t:

$$\ln \frac{\bar{P}_0}{\bar{P}_0 - \bar{P}} = (K_{hH} H + K_h) t$$

The values given in the legend of figure 2 were calculated by this method.

(iii) Second order decay of Hfr cells in cross mixtures: By changing the ratio of Hfr to F⁻ cells the frequencies of cell collisions resulting in detectable zygotes, Z, should be varied. Thus, in the experiment given in table 3, the ratio of undetectable complexes, M, resulting from matings of Hfr by Hfr cells, to detectable zygotes, Z, resulting from matings of Hfr to F⁻ cells, should be proportional to H^2/HF for any one tube. In tubes W and Y where the concentrations of F⁻ cells, F, were similar, the expected ratio of the rates of formation of detectable zygotes should be proportional to H_W/H_Y or 3.33, if 'intratype matings' of Hfr cells do not occur. The

TABLE 2
Rate of intratype mating of Hfr cells

STRAINS CROSSED AND COMPATIBILITY			CONCENTRATION OF PARENTAL CELLS		RATE OF SYNGAMY	
			methionine —	threonine — leucine — thiamine —	"prototrophs" ml	
					minute parental cell	parental cell
<i>cells/ml</i>						
W 1895 Hfr	×	W 1956 F —	5.2×10^8	6.3×10^8	1.4×10^{-14}	
W 1895 Hfr	×	W 2057 Hfr	5.2×10^8	3.0×10^8	$.21 \times 10^{-14}$	
W 1607 F —	×	W 2057 Hfr	5.5×10^8	3.0×10^8	$.11 \times 10^{-14}$	

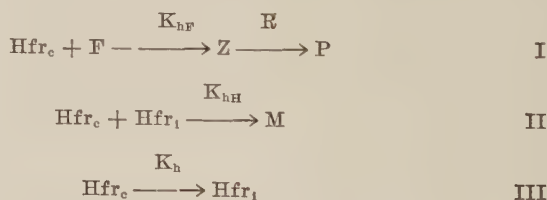
TABLE 3
Rates of syngamy in crosses with varying ratios of parental cells

TUBE	CONCENTRATION OF PARENTAL CELLS		RATE OF SYNGAMY		RATE OF DISAPPEARANCE OF Hfr CELLS DUE TO INTRATYPE MATING B — A
			observed	expected (for no intratype mating of Hfr)	
	Hfr	F —	A	B	
	<i>cells/ml</i>		<i>"prototrophs"/ml minute</i>		
W	1.8 × 10 ⁸	1.2 × 10 ⁸	5.6 × 10 ²	11. × 10 ²	5.4 × 10 ²
X	1.8 × 10 ⁸	.36 × 10 ⁸	2.2 × 10 ²	4.0 × 10 ²	1.8 × 10 ²
Y	.54 × 10 ⁸	1.2 × 10 ⁸	3.3 × 10 ²		
Z	.54 × 10 ⁸	.36 × 10 ⁸	1.2 × 10 ²		

same value, 3.33, applies to tubes X and Z. Assuming no 'intratype matings' in tubes Y and Z the expected rates of "prototroph" formation in W would be $3.33 \times 3.3 \times 10^2/\text{ml minute}$ and equal to $11. \times 10^2/\text{ml minute}$, and in X would be $4.0 \times 10^2/\text{ml minute}$. The difference between the expected and experimental values is a measure of the rate of 'intratype mating' of Hfr cells and is about equal to the rate of heterogamy.

Comparison of i, ii, and iii indicates that, since productive mating of Hfr by Hfr is less rapid than heterogamy ($\text{Hfr} \times \text{F}^-$) and the second order decay of competence of Hfr cells is about as rapid as heterogamy, it is possible that $\text{Hfr} \times \text{Hfr}$ complexes are formed which lead to loss of competence without fruitful mating. The rate constant K_{hH} is then an overall measure of second order processes leading to loss of competence for which the term 'intratype mating' will be used for brevity.

Collision efficiency. Let the *collision efficiency of heterogamy* be defined as the probability of zygote formation between a competent Hfr cell and a F^- cell per collision. Let the *competent fraction C* be defined as the ratio of competent Hfr cells to total Hfr cells at the time of initiation of syngamy by addition of F^- cells. The calculation of collision efficiency must then take into account heterogamy (reaction I), 'intratype mating' of Hfr cells (reaction II), and first order decay of competence (reaction III):



The zygote M formed by the mating of competent Hfr cells (Hfr_c) and incompetent Hfr cells (Hfr_i), or possibly with other competent Hfr cells as well, is not detectable in the usual cross. The concentration of zygotes Z is then a function of time t , where H and F are the initial concentrations of Hfr

and F- cells regardless of their state of competence, h is the concentration of competent Hfr cells at time t , and the K 's are reaction rate constants. Integration of the differential kinetic equations for these simultaneous reactions between the given boundary conditions yields:

$$\begin{aligned}\frac{dz}{dt} &= K_{hF} h F \\ -\frac{dh}{dt} &= K_{hF} h F + K_{hH} h H + K_h h \\ Z &= \frac{K_{hF} C H F}{K_{hF} F + K_{hH} H + K_h} \left\{ 1 - \exp [- (K_{hF} F + K_{hH} H + K_h) t] \right\}\end{aligned}$$

The initial rate of formation of zygotes is then approximately (compare Nelson, '51):

$$\frac{dz}{dt} = K_{hF} C H F$$

The concentration of zygotes at saturation \bar{Z} if $\bar{Z} \ll F$ is then:

$$\bar{Z} = \frac{K_{hF} C H F}{K_{hF} F + K_{hH} H + K_h}$$

The theoretical rate constant for collisions, K_T , may be calculated from the von Schmoluchowski coagulation equation and the Sutherland-Einstein diffusion equation. Substituting numerical values for the temperature (37°C.) and viscosity of the buffer (0.7 centipoise) a value of 2.4×10^{-10} ml/minute is obtained. This value must be corrected in each experiment for the fraction of collisions, f , occurring between crossable bacteria (that is, bacteria capable of yielding a detectable zygote). Where p is the ratio of Hfr to total cells, q is the ratio of F- to total cells, and $p + q = 1$, $f = 2pq$. The collision efficiency of heterogamy is then equal to K_{hF}/fK_T .

Calculations from the cross W 1895 \times W 1956 in buffer (table 2) where $H = 5.2 \times 10^8$ /ml, $F = 6.3 \times 10^8$ /ml, $\bar{P} = 1.6 \times 10^5$ /ml, $dP/dt = 4.5 \times 10^3$ /ml minute, $K_h = 1.54 \times 10^{-2}$ /minute, and K_{hH} is assumed equal to K_{hF} , give $C = 0.012$ and $K_{hF} = 1.1 \times 10^{-11}$ ml/minute. In this experiment $f = 0.5$ and the collision efficiency of heterogamy = 0.1.

Calculations for a cross run in broth when the rate of formation of zygotes is most rapid, average $H = 2.8 \times 10^8/\text{ml}$, average $F = 3.9 \times 10^8/\text{ml}$, and $dZ/dt = 7.4 \times 10^5/\text{ml minute}$, gives $K_{hF} C = 6.8 \times 10^{-12} \text{ ml/minute}$. Since saturation does not occur during growth C is calculated as the ratio of zygotes ($3.7 \times 10^7/\text{ml}$) to parental cells (average H plus average F) and is equal to 0.055. Then K_{hF} is equal to $1.2 \times 10^{-10} \text{ ml/minute}$, $f = 0.49$, and the collision efficiency of heterogamy is equal to 1.

The rates of synagamy reported in this paper have been reduced to a per cell (Hfr) per cell (F^-) basis. Thus the experimental value $\frac{dP}{dt} \frac{1}{H F}$ with the units "prototrophs" ml/minute parental cell (Hfr) parental cell (F^-) and the experimental value $\frac{dZ}{dt} \frac{1}{H F}$ with the units zygotes ml/minute parental cell (Hfr) parental cell (F^-) are theoretically equal to $K_{hF} C/R$ and $K_{hF} C$ respectively.

Level of saturation of "prototrophs" in excess of one parental type

Experiments were performed in which the level of saturation of "prototrophs" \bar{P} was measured in varying concentrations of one parent type, the other parent type being present in excess. The concentration of zygotes at saturation, \bar{Z} , in excess of F^- parental cells, is then defined by the saturation formula given previously. 'Intratyping mating' and first order decay of competence may be neglected under these conditions, hence:

$$\begin{aligned}\bar{Z} &= C H \\ \bar{P} &= R^{-1} C H\end{aligned}$$

Where $\bar{P} = 1$ the intercept value $\log H = -(\log 1/R + \log C)$. As shown in figure 3 the intercept value obtained was consistent with independently measured values of R (10^1) and C (10^{-2}).

The kinetic formula previously derived does not apply with an excess of competent Hfr cells since the concentration of F^- cells cannot be assumed constant. An excess of competent

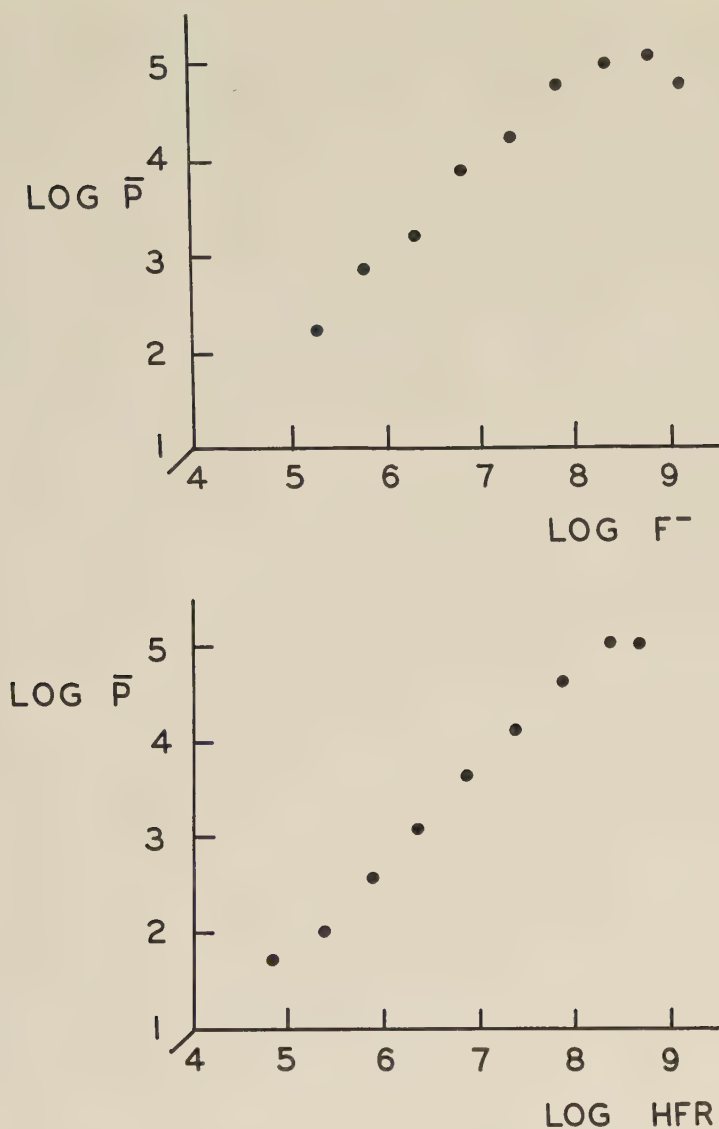


Fig. 3 Saturation levels with excess of one parent type.

Variable numbers of Hfr and F^- cells suspended in buffer were mixed at 37°C . "Prototrophs" were determined when saturation had occurred at 120, 150, and 180 minutes following mixing. 6.4×10^8 Hfr cells/ml were used in the experiment varying the concentration of F^- cells. 2.3×10^8 F^- cells/ml were used in the other experiment varying the concentration of Hfr cells.

Hfr cells could not be obtained experimentally for a sufficient length of time, due to intratype mating and first order decay of competence, to titrate all F⁻ cells.

DISCUSSION

The collision efficiencies for heterogamy, 0.1 for crosses in buffer and 1 for crosses in broth, are typical. Obviously lower values are obtained in buffers of varied composition and in broth after cessation of growth. The calculations of collision efficiency of heterogamy and of 'intratype mating' of Hfr cells are only approximate. The experimental rate constants are functions of several colony counts subject to dilution and plating errors. A standard error at least equal to the determined value is probable. That the determined values are close to the expected values may be happily fortuitous.

Values for collision efficiencies greater than 1, up to 5, have been occasionally obtained in broth. The calculation of the theoretical collision frequency K_T assumes that the motion of the bacteria is solely Brownian. Active motility of the bacteria occurs in broth but not in buffer. The "diffusion coefficient" of bacteria can be determined experimentally by measuring the mean displacement of a cell per unit time in a ruled chamber (Wilkie, '54). The "diffusion coefficient" calculated from the Sutherland-Einstein equation (3.2×10^{-9} cm²/second) and used in the calculation of the theoretical rate constant K_T agrees with measured values for bacteria that are not recognized as being intrinsically motile (7×10^{-9} cm²/second). Motile bacteria from broth cultures show non-random displacements per unit time 100 to 500 fold greater than non-motile bacteria. The variation in motility between bacteria in broth cultures is large.

A discontinuous distribution for the collision efficiency occurs since only a fraction of the Hfr bacteria are capable of undergoing syngamy; 1% in buffer suspensions, and less than 10% of the Hfr and F⁻ bacteria in broth. The determined collision efficiencies of 0.1 and 1 refer to these competent cells. Competence is one element in the determination of fertility.

The mechanism responsible for competence and its loss is unknown. Possibly competent cells represent the fraction of the population in a given phase of the division cycle. The collision efficiency of 'intratype mating' of Hfr cells in buffer is also 0.1 if it is assumed that incompetent Hfr cells act as F⁻ phenocopies. The heterogeneity in diffusion rates of motile bacteria raises the problem of preferential involvement of motile cells as one partner in the cross. Crosses with non-motile strains should provide an answer.

Some properties of the attachment reaction, or conjugation stage (Jacob and Wollman, '55), can be derived. The requirements for buffer of adequate ionic strength would indicate that the primary effect of cations is the neutralization of the repulsive electrostatic forces among suspended bacteria, as in agglutination. This effect would be non-specific and would operate between bacteria of any mating type (Maccacaro, '55). The temperature dependence, absence of potentiation of syngamy by pre-incubation at low temperature, and irreversibility of the attachment on dilution obviate non-specific agglutination as the rate limiting step. The non-additive effect of divalent cations indicates that specific surface groups may be involved. The fragility of mating complexes to mechanical disruption suggests that they may be two or many-celled complexes at this stage (Lederberg, '55). These conclusions about the attachment reaction of bacterial syngamy are similar to current thought concerning the mechanism of virus penetration. Unfortunately the low frequency of syngamy in defined media, the side reactions, and the requirement for viable issue hinder an analysis similar to the studies of Puck's group (Puck and Lee, '55).

SUMMARY

The kinetics of syngamy in *Escherichia coli* K 12 was measured with washed non-proliferating bacteria in buffer suspensions and with bacteria growing in broth. Heterogamy occurred between bacteria of different mating type about once per ten (calculated) collisions in buffer and at every collision

in broth. Second order decay of competence of Hfr cells in buffer occurred with a collision efficiency approximately equal to that of heterogamy. The Hfr bacteria exist in buffer in a labile competent state decaying to inactivity at a rate of 10^{-2} /minute. The initial frequency of competent Hfr cells prepared from growing cultures was 10^{-2} and the maximal frequency of zygotes in growing cultures was 0.1. The effective attachment of Hfr and F⁻ bacteria is irreversible to dilution, not accelerated by previous non-specific agglutination, and affected by ionic strength, concentration and type of cation, and viscosity of the medium.

ACKNOWLEDGMENTS

The author wishes to thank Drs. Esther M. and J. Lederberg and M. L. Morse for many helpful discussions. Samples of Metho-Cel were kindly supplied by Dow Corning Corporation, Midland, Michigan.

LITERATURE CITED

- ANDERSON, T. F. 1953 The morphology and osmotic properties of bacteriophage systems. Cold Spring Harbor. Symp. Quant. Biol., 18: 197-203.
- CAVALLI, L. L., J. LEDERBERG AND ESTHER M. LEDERBERG 1953 An infective factor controlling sex compatibility in *Bacterium coli*. J. Gen. Microbiol., 8: 89-103.
- CLARK, J. BENNETT 1953 Effect of chemicals on the recombination rate in *Escherichia coli*. J. Gen. Microbiol., 8: 45-49.
- HAAS, F., O. WYSS AND W. S. STONE 1948 The effect of irradiation on recombination in *Escherichia coli*. Proc. Nat. Acad. Sci., 34: 229-232.
- HAYES, W. 1953 The mechanism of genetic recombination in *Escherichia coli*. Cold Spring Harbor Symp. Quant. Biol., 18: 75-93.
- JACOB, FRANÇOIS AND ÉLIE WOLLMAN 1954 Induction spontanée du développement du bacteriophage lambda au cours de la récombinaison génétique chez *Escherichia coli* K 12, C. r. Soc. Biol., 233: 317-319.
- 1955 Étapes de la récombinaison génétique chez *Escherichia coli*. C. r. Soc. Biol., 240: 2566-2568.
- JINKS, J. L. 1952 Competitive suppression and determination of linkage in microorganisms. Nature, 170: 106-108.
- LEDERBERG, J. 1950 Isolation and characterization of biochemical mutants of bacteria. Methods in Medical Research, 3: 5-22.
- LEDERBERG, J., E. M. LEDERBERG, N. D. ZINDER AND E. R. LIVELY 1951 Recombination analysis of bacterial heredity. Cold Spring Harbor Symp. Quant. Biol., 16: 413-443.

- LEDERBERG, J., in S. WAKSMAN (editor) 1955 Perspectives and Horizons in Microbiology. Rutgers University Press, New Brunswick, New Jersey, 24-29.
- MACCACARO, G. A. 1955 Cell surface and fertility in *Escherichia coli*. *Nature*, 176: 125.
- NELSON, T. C. 1951 Kinetics of genetic recombination in *Escherichia coli*. *Genetics*, 36: 162-175.
- NELSON, T. C., AND J. LEDERBERG 1954 Postzygotic elimination of genetic factors in *Escherichia coli*. *Proc. Nat. Acad. Sci.*, 40: 415-419.
- PUCK, T. T., AND H. H. LEE 1955 Mechanism of cell wall penetration by viruses. II. Demonstration of cyclic permeability change accompanying virus infection in *Escherichia coli* B cells. *J. Exp. Med.*, 101: 151-176.
- RYAN, FRANCIS J. 1953 Competitive suppression of prototrophs. *Nature*, 171: 400-401.
- WILKIE, D. 1954 The movements of spermatozoa of bracken *Pteridium aquilinum*. *Exp. Cell Res.*, 6: 384-391.
- WOLLMAN, ÉLIE L., AND FRANÇOIS JACOB 1954 Lysogénie et la récombinaison génétique chez *Escherichia coli* K 12. *C. r. Soc. Biol.*, 239: 455-456.
- 1955 Sur le mécanisme du transfert de matériel génétique au cours de la récombinaison chez *Escherichia coli*. *C. r. Soc. Biol.*, 240: 2449-2451.

BIOCHEMICAL EVENTS ACCOMPANYING STALK FORMATION IN THE SLIME MOLD, *DICTYOSTELIUM DISCOIDEUM*¹

JAMES H. GREGG AND RUTH D. BRONSWIEG

*Department of Biology, University of Florida, Gainesville and Marine Biological
Laboratory, Woods Hole, Massachusetts*

ONE FIGURE

The life cycle of the slime mold, *Dictyostelium discoideum*, has been described by several authors among them being Raper ('41) and Bonner ('44). During the vegetative stage, the independent amoebae feed upon bacteria and reproduce by binary fission. However, from the onset of aggregation to the cessation of fruiting an exogenous food supply is unnecessary and possibly unavailable. Therefore, during this period, all energy-requiring developmental phenomena depend upon an endogenous food source.

Raper and Fennell ('52) have shown that during the culmination period the stalk cells build a cellulose sheath around themselves and cellulose is deposited in the walls of the spore cells. The slime molds must produce this polysaccharide from endogenous materials which also must satisfy energy requirements. In view of this it was of interest to investigate the role of the carbohydrates (total reducing substances) during this period. Previous work by Gregg, Hackney and Krivanek ('54) has shown that various nitrogenous components in *D. discoideum* are utilized during the transition of the migrating pseudoplasmodia to mature sorocarps. Such studies which attempt to correlate biochemical changes with their resulting morphological expression should prove fruitful in studies of differentiation of the slime mold.

¹ This investigation was supported in part by a research grant G-3616 (C) from the National Institutes of Health, Public Health Service.

MATERIALS AND METHODS

The procedure followed in culturing the slime mold *D. discoideum* was identical with that reported by Bonner ('47). In order to determine the quantity of slime molds involved in the analyses, the material was first placed upon tared discs of collodion film. They were dried in an oven at 60°C. for 24 hours and then weighed on a quartz helical balance to the nearest microgram. The analyses of total carbohydrate (total reducing substances) were made by modifications of the method of Gregg ('48) and Nelson's colorimetric procedure (Nelson, '44) (table 1).

TABLE 1
Analyses of total reducing substances

SLIME MOLD TISSUES
Hydrolyze in 1.0 ml of 2.2% HCl for 3 hours.
↓
Homogenize slime molds with a glass rod and precipitate proteins with 20 μ l of 10% NaWO ₄ .
↓
Dilute to 2.25 ml with distilled H ₂ O and centrifuge at 1000 \times g for 10 minutes.
↓
Transfer 1.0 ml of supernatant to 10 mm \times 150 mm test tube.
↓
Neutralize with 60% KOH to a phenol red end point with the aid of a micro buret.
↓
Add 1.0 ml of Somogyi reagent (Somogyi, '45) and heat at 100°C. in a water bath for 15 minutes.
↓
Cool, add 1.0 ml of arsenomolybdate reagent (Nelson, '44) and dilute to 3.25 ml with distilled H ₂ O.
↓
Read in Beckman spectrophotometer at 250 m μ .

PREPARATION OF SLIME MOLDS

Vegetative amoebae. The vegetative amoebae were harvested from two to four plates, filtered through cotton and centrifuged in distilled water at 500 g for 10 minutes. The supernatant was discarded and the washing process was repeated until the amoebae were relatively free of bacteria.

The amoebae were placed upon tared collodion discs with a fine-tipped pipette, dried and weighed prior to the analyses of total reducing substances.

Migrating pseudoplasmodia. The collecting surface was prepared by cutting discs approximately 20 mm in diameter (with the aid of a test tube) from nutrient agar plates which had been inoculated about 48 hours previously. These discs were inserted into similar sized spaces in plates prepared from Bonner's solution made 2% in agar (Bonner, '47). The pseudoplasmodia migrated from the nutrient agar onto the

TABLE 2

Ranges of total dry weight and total reducing substances in the slime mold analyses. The ranges of reducing substances were obtained by analyzing 1.0 ml of the 2.25 ml digest

STAGE	μ G DRY WEIGHT	μ G REDUCING SUBSTANCES/ML
Vegetative amoebae	120.9 - 760.1	2.97 - 33.1
Migrating pseudoplasmodia	270.2 - 1012.5	10.5 - 45.7
Mature sorocarps	143.6 - 549.6	7.04 - 38.2
Spores	126.6 - 492.7	4.91 - 26.3
Stalks	50.5 - 168.5	3.00 - 10.4

non-nutrient surface which decreased the possibility of contamination from bacteria and nutrient (glucose). The migrating pseudoplasmodia were collected using a hair loop, placed upon the collodion discs and weighed.

Mature sorocarps. A collecting surface similar to that described for use in the preparation of migrating pseudoplasmodia was employed. The pseudoplasmodia were allowed to fruit and then collected by the same technique as described previously. The spores and stalks were separated by fine-tipped forceps, placed on tared collodion discs, dried and weighed.

The ranges of total dry weight and total reducing substances of the various stages are presented in table 2.

RESULTS

From the data listed in table 3, it is obvious that an increase in reducing substances/dry weight occurs during the development of the slime mold. During the transition from the vegetative amoebae to the migrating pseudoplasmodia an 18.8% increase in total reducing substances/dry weight occurred. By the end of fruiting, however, a 44.2% increase in total reducing substances/dry weight occurred relative to the initial amount in the vegetative amoebae.

By separating the spores from the stalks it was possible to analyze each for total reducing substances/dry weight. The spores exhibited a 24.6% increase while the stalks increased by 40.7% as compared to the vegetative amoebae. Although

TABLE 3

*The μg reducing substances/ μg dry weight of the various stages of *D. discoideum* $\times 10^2$. ("σ" abbreviates "standard deviation")*

	μG REDUCING SUBSTANCES	NO. OF EXP.	σ
Vegetative amoebae	8.67	31	4.14
Migrating pseudoplasmodia	10.30	17	1.53
Mature sorocarps	12.50	19	2.12
Spores	10.80	20	1.83
Stalks	12.20	21	3.96

the stalks appear to have the greatest increase the difference between the spores and stalks is not statistically significant ($P = > 0.05$)².

It was difficult to determine whether the method of analyzing total reducing substances included polysaccharides such as cellulose which is deposited in the walls of the spore and stalk cells. However, unhydrolyzed spores and stalks treated with periodic acid followed by Schiff's reagent revealed an intense purplish-red coloration (Gomori, '52). This is indicative of the presence of polysaccharides in spores and stalks. If the same histochemical procedure is conducted upon spores and stalks hydrolyzed in 2.2% HCl, a reddish color of con-

² Statistical analysis of difference determined by Student's t-test.

siderably less intensity remained as compared to the unhydrolyzed slime molds. Therefore, it appears that while probably the major part of the carbohydrates are included in the analyses for total reducing substances they are not included in their entirety.

DISCUSSION

These data indicate that a consistent increase in total reducing substances/dry weight occurs in *D. discoideum* during the transition from the vegetative stage to the mature sorocarp (table 3). Since the analyses of total reducing substances probably do not include the entire polysaccharide content of the mature sorocarps, it is reasonable to assume that the values of total carbohydrates may actually be even greater than the determined values.

From the initiation of aggregation until the end of fruiting the slime mold depends upon the materials which were obtained during the vegetative stage. Although a consistent increase in total reducing substances/dry weight occurs during morphogenesis it is unlikely that they can increase except at the expense of other metabolic components such as the proteins. It has been demonstrated by Gregg, Hackney and Krivanek ('54) that certain protein nitrogen components are utilized during culmination. It seems reasonable to suggest that a relationship exists between the amount of protein utilized and the total reducing substances formed during morphogenesis (fig. 1). Possibly the carbohydrates obtained during the vegetative stage are insufficient in quantity to provide for the morphogenetic needs of the organism; but this does not indicate, however, that the slime mold fails to utilize carbohydrate during development. In the event that proteins provide intermediates from which carbohydrates may be synthesized, the extent to which the carbohydrates are being utilized would be masked.

It is suggested, then, since all morphogenetic processes in the slime mold must continue without an exogenous source of food, that the necessary intermediates are provided to

a large extent by the proteins. These intermediates could be transformed into cellulose which is deposited extracellularly by the stalk and spore cells. It seems probable also that these intermediates serve as an energy source for processes related to morphogenetic movements in *D. discoideum*.

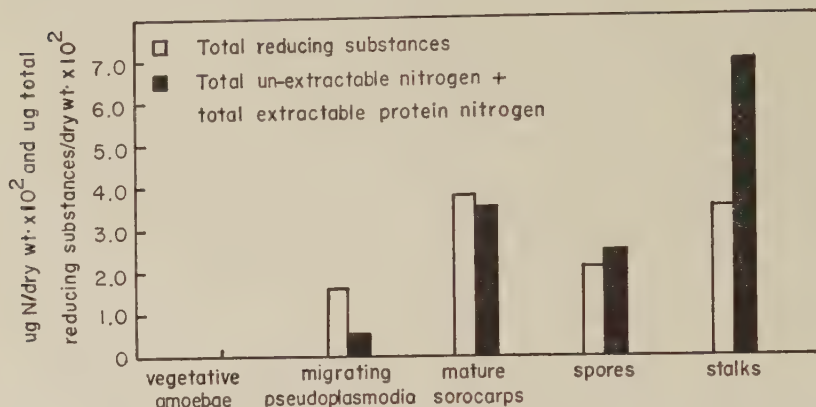


Fig. 1 The relationship between the accumulated increase in total reducing substances and the accumulated loss in total un-extractable nitrogen + total extractable protein nitrogen. The nitrogen component data was calculated from Gregg, Hackney and Krivanek ('54).

SUMMARY

1. The procedures necessary in determining total reducing substances /dry weight of the slime mold *Dictyostelium discoideum* were described.
2. The total reducing substances/dry weight show a consistent increase from the vegetative stage to the formation of the mature sorocarp.
3. The possibility is discussed that proteins provide intermediates which the slime molds utilize to obtain energy and to synthesize the polysaccharides necessary in stalk formation.

LITERATURE CITED

- BONNER, J. T. 1944 A descriptive study of the development of the slime mold *Dictyostelium discoideum*. *Am. J. Bot.*, 31: 175-182.
- BONNER, J. T., AND D. ELDRIDGE, JR. 1945 A note on the rate of morphogenetic movement in the slime mold, *Dictyostelium discoideum*. *Growth*, 9: 287-297.

- BONNER, J. T. 1947 Evidence for the formation of cell aggregates by chemotaxis in the development of the slime mold *Dictyostelium discoideum*. J. Exp. Zool., 106: 1-26.
- GOMORI, G. 1952 Microscopic histochemistry. University of Chicago Press, Chicago, Illinois.
- GREGG, J. R. 1948 Carbohydrate metabolism of normal and hybrid amphibian embryos. J. Exp. Zool., 109: 119-134.
- GREGG, J. H., A. L. HACKNEY AND J. O. KRIVANEK 1954 Nitrogen metabolism of the slime mold *Dictyostelium discoideum* during growth and morphogenesis. Biol. Bull., 107: 226-235.
- NELSON, N. 1944 A photometric adaptation of the Somogyi method for the determination of glucose. J. Biol. Chem., 153: 375-380.
- RAPER, K. B. 1941 Developmental patterns in simple slime molds. Growth (Symposium), 5: 41-76.
- RAPER, K. B., AND D. I. FENNELL 1952 Stalk formation in *Dictyostelium*. Bull. Torrey Bot. Club, 79: 25-51.
- SOMOGYI, M. 1945 A new reagent for the determination of sugars. J. Biol. Chem., 160: 61-68.

TELEVISION MICROSCOPY OF SPORULATION AND SPORE GERMINATION OF BACILLUS CEREUS

KATHERINE A. ZWORYKIN AND GEORGE B. CHAPMAN¹

*RCA Laboratories, Princeton, New Jersey, and Department
of Biology, Princeton University,
Princeton, New Jersey*

THIRTEEN FIGURES

An extensive review of the literature has revealed only a few papers which present the results of observations of living sporulating and germinating bacteria. Of these papers, the most informative have been those by Wyckoff and Ter Louw ('31), who used ultraviolet microscopy, Bayne-Jones and Petrilli ('33), who used cinematography and Knaysi ('46, '52), who employed light and phase microscopy.

A new method, that of television microscopy, facilitates continuous observation of living cells, and provides a means for controlling the optical contrast of cells and their components, (Parpart, '51; Flory, '51; Zworykin and Flory, '52). The present study has found this method useful in determining the fate of certain cytoplasmic inclusions. In addition, some new observations on the processes of sporulation and germination are described.

MATERIALS AND METHODS

The culture used in this work was the A.T.C.C. strain no. 7064 of *Bacillus cereus*. Following 24 hours of growth at 30°C. in nutrient broth, a 3 mm loop of the culture was transferred to the surface of a nutrient agar slant and incubated at 30°C. for 24 hours. Such a slant provided cells

¹ Present address: Department of Biology, Harvard University.

in various stages of sporulation. A moderately heavy suspension of the sporulating cells was made in brain heart infusion (Difco) broth and a 2 mm loop of the suspension was inoculated into a "well" made in a previously prepared thin layer of yeast extract brain heart infusion agar—0.5% yeast extract (Difco), brain heart infusion (Difco), 1.5% agar (Difco)—on a no. 1 cover glass. The "well"—simply a hollowed-out area in the agar—made it possible, when properly formed, to obtain a satisfactory compromise of optical conditions, oxygen supply, nutrient medium and restraint of

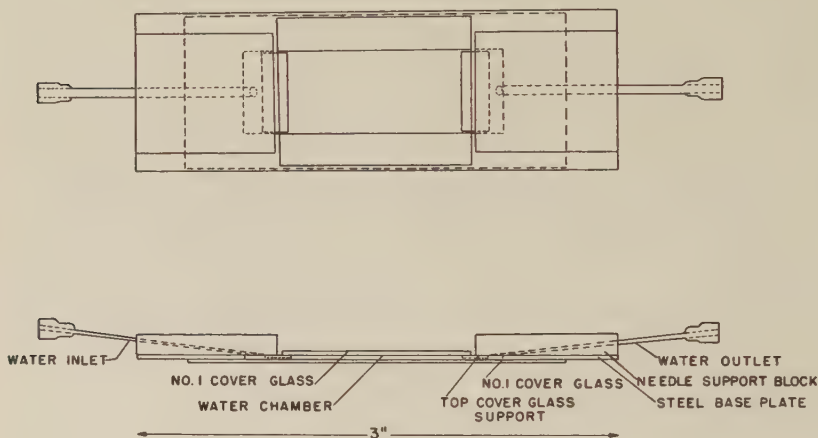


Fig. 1 Constant temperature slide.

cell motion. The preparation was then sealed with "vaspar," agar down, onto the top glass of a constant temperature slide (See fig. 1). All glass to metal seals were made with de Khotinsky cement. Distilled water, from a constant temperature water bath, was passed through the slide at a rate of about one drop per second during the period of observation of all preparations. The temperature of the input water was usually about 37°C.

The slide (Text fig. 1) was placed on the stage of a Bausch and Lomb light microscope, and the specimen was studied using a 90 \times , 2 mm, N.A. 1.30, apochromatic, oil-

immersed objective and a $7.5\times$ compensating ocular. Illumination was provided by a Bausch and Lomb microscope illuminator Type 31-33-85. The light was passed through distilled water in the container provided with the illuminator, but no other filters were used.

A Vidicon television camera was mounted over the microscope ocular and was cable-connected to a monitor and control unit. Permanent records of the images produced on the monitor viewing screen were obtained by photographing the screen with a Graphic View camera, equipped with Supermatic (X) lens, operated at $f/4.5$. An exposure time of one-half second was used with Kodak Super-XX film pack. Following development, contact prints were made using Kodak Azo No. 5 paper. Final magnification of the figures is approximately $7,000\times$.

RESULTS AND DISCUSSION

Figures 2 to 9 are photographs of the same field taken at various intervals over a $25\frac{1}{2}$ hour period. Four cells which are of particular interest have been designated "a," "b," "c," and "d" on each of the 8 figures.

In figures 2 to 4, sporangium "d" is seen to disintegrate and thereby to set free its endospore. Such disintegration of the sporangium is the classical picture of endospore release as described by Knaysi ('52). Incidentally, two additional cells moved into the field, at the upper right, during the interval between the taking of figures 2 and 3.

Comparison of figures 3 and 4, sporangia "a" and "c," illustrates the occurrence of a most startling phenomenon. The endospore of each sporangium was suddenly and forcefully expelled from the sporangium. (The fact that endospore "a" is still partially within its sporangium is due to the resistance to its exit offered by the sporangium just below it.) That considerable force is exerted in this expulsion is evidenced by the fact that the expelled spores occasionally move several microns through the medium before coming to rest.

Search of the literature has revealed no previous mention of this type of spore release in the bacilli. Yet, this forceful expulsion is evidently a normal phenomenon since the same event was observed in many different preparations and since the expelled spores are viable.

In figure 5, sporangium "b" shows a marked change from its appearance in figure 4. Within a period of 17 minutes, the endospore has undergone a decided loss in refractility and appears to have swollen slightly. During the 65-minute interval between figures 5 and 6, further swelling of the endospore of sporangium "b" has occurred and the spore liberated from sporangium "a" has also begun to swell. In figure 7, spores "a" and "b" are obviously germinating and spore "c" has started to swell. Figures 8 and 9 show further growth of cells "a" and "b". (Cell "c" now lies just below the plane of focus of "a" and "b".) No further changes were observed in this field in the next 24 hours, presumably due to exhaustion of the nutrient medium or oxygen supply, or both.

The absence of cytoplasmic inclusions from the young cells is not surprising. Under more favorable conditions for growth, e.g., an agar slant, the inclusions seen in the sporulating cells usually appear within about 12 hours. That the conditions for growth of the cells in this particular preparation were somewhat less than ideal is indicated by the slow growth rate and the early cessation of growth.

This photographic sequence has shown that spores may germinate and the resulting cells grow whether the spore is forcefully expelled from the sporangium or remains within the sporangium. The process of germination, in each case, was accompanied by a loss of refractility and a swelling of the spore as described by Cook ('32) and Knaysi ('38, '48).

It should be mentioned that the phenomenon of spore germination within the sporangium is a rare event but has been reported in the literature as a personal observation of Knaysi ('38). It would seem that the field under observation was indeed a remarkable one for in it were observed the

forceful ejection of a spore from the sporangium, the germination of a spore within the sporangium, and the release of a spore by disintegration of the sporangium.

The granular cytoplasmic inclusions which may be seen in most of the cells appear to be principally lipoid in content as they stained readily by the Burdon ('46) technique. The granules moved about in the sporangia but failed to enter the sporogenous areas. These observations agree with those of Bayne-Jones and Petrilli ('33). As the above sequence of figures, and also figures 10 and 11 show, the granules persist in the medium after disintegration of the sporangium. (Note especially the granules of cell "a" in figures 2 to 9 and of cell "e" in figures 10 and 11.) This persistence is in accord with observations by Burdon ('46) of similarly staining granules and with the observations of granules pictured by Bayne-Jones and Petrilli ('33). The behavior is different from that described by Lewis ('34), wherein refractive granules in the cells of *Bacillus mycoides* disappeared during the ripening of the spore, and from that reported by Knaysi ('46), who found that the inclusions disintegrate. Of course, the granules of Lewis and Knaysi could have been of different composition.

Figures 10 and 11, in addition to illustrating the forceful ejection of the spore from the sporangium and the persistence of the granular inclusions after disintegration of the sporangium, show that, considering the frequently occurring two-cell pairs of sporangia, the endospores may lie at either end of the cells. Within a given sporangium, however, the endospore always lies subterminally and never has more than one endospore been observed in a single sporangium in any of our preparations. These two observations differ from those of Knaysi ('46), who reported that the endospore might be located anywhere in the sporangium and that two endospores might be found within a single sporangium — presumably due to a delay in a cross-wall formation.

In agreement with Knaysi ('46) and in disagreement with Lewis ('34), no movement of the spore along the sporangium axis was observed.

One other phenomenon observed is illustrated by cell "f" of figures 12 and 13. The time interval between these figures is $3\frac{1}{2}$ hours. During that time, the nearly mature endospore in cell "f" gradually lost its refractility and finally became indistinguishable. In effect, it appeared to have "dedifferentiated." The difference in appearance of cell "f" in figures 12 and 13 was not due to different focal planes but to a real change in optical properties of the cell. We have observed such "dedifferentiation" several times but no explanation for its cause can be given, especially since no more than one cell in a given field has exhibited the change.² The only similar observation previously reported is the one by Knaysi ('45, pp. 620-621), who states that "... in suspensions where there is no tendency for normal germination and growth ... a few endospores may very slowly become nonrefractive without a noticeable change in size." It would seem that this phenomenon may be physiologically related to but distinct as to developmental stage concerned from that described above. Apparently, the spores described by Knaysi were free spores, while, in the present instance, it is clearly a developing endospore which undergoes the loss of refractility. Incidentally, there was no tendency of the spores described herein to form groups — a tendency noted by Knaysi ('45). The different conditions of observation indicate that this finding is probably of no significance.

It is obvious from the accompanying figures that little can be said regarding the internal structure of these cells. (Should future studies, with particular reference to nuclear material and spore coats, be undertaken, the use of ultraviolet optics in conjunction with the television microscope should be especially valuable.) The image quality provided by the present system does, however, justify one further comment. The appearance of cell "e" in figure 10 suggests that the lipoid inclusions must occupy most of the non-sporogenous region of the sporangium. It is difficult to imagine how then there could be room for much nuclear material in this region, at

² The phenomenon may be associated with the death of the cell.

least in these cells at this stage of development. Additional work on this question is desirable as is seen from the recent work by Knaysi ('52, '55) on strain C₃ of *B. cereus*. The later work shows clearly that most or all of the nuclear material is concentrated in the developing forespore, with little or no nuclear staining material in the non-sporogenous zone. The earlier work showed that other nuclei that may be present in the sporangium migrate away from the sporogenous zone. It appears, therefore, that the rather indirect suggestion, provided by the present work, that all of the nuclear material of these sporulating cells is confined to the endospore is substantiated by the figures included in the 1955 report by Knaysi. It is, of course, also possible that the present figures and those of Knaysi ('55) represent stages of development which occur after the vegetative supportive nucleus has disappeared (DeLamater and Hunter, '52). The figures presented in all of the papers then become compatible.

SUMMARY

1. The use of the television microscope in the study of living bacteria has led to the observation of two heretofore undescribed phenomena: (a) the sudden and forceful expulsion of spores from sporangia, and (b) a "dedifferentiation" of nearly mature spores.

2. Prominent cytoplasmic inclusions, principally lipid in nature, have been observed. These inclusions did not become incorporated into the developing spore, and upon disintegration of the sporangium persisted independently in the medium.

3. Spores have been observed to occupy every possible combination of terminal positions in neighboring sporangia.

4. The method has been found to be particularly useful in long-term, continuous studies of living cells, especially in cases where contrast enhancement is desirable.

ACKNOWLEDGMENTS

The authors wish to thank Drs. Arthur K. Parpart and Frank H. Johnson for their assistance with various aspects of this work.

LITERATURE CITED

- BAYNE, JONES, S., AND A. PETRILLI 1933 Cytological changes during the formation of the endospore in *Bacillus megatherium*. *J. Bact.*, 25: 261-274.
- BURDON, K. L. 1946 Fatty material in bacteria and fungi revealed by staining dried, fixed slide preparations. *J. Bact.*, 52: 665-678.
- COOK, R. P. 1932 Bacterial spores. *Biol. Revs.*, 7: 1-23.
- DELAMATER, E. D., AND M. E. HUNTER 1952 The nuclear cytology of sporulation in *Bacillus megatherium*. *J. Bact.*, 63: 13-21.
- FLORY, L. E. 1951 The television microscope. Cold Spring Harbor Symp. on Quant. Biol., 16: 505-509.
- KNAYSI, G. 1938 Cytology of bacteria. *Bot. Rev.*, 4: 83-112.
- 1945 Investigation of the existence and nature of reserve material in the endospore of a strain of *Bacillus mycoides* by an indirect method. *J. Bact.*, 49: 617-622.
- 1946 On the process of sporulation in a strain of *Bacillus cereus*. *J. Bact.*, 51: 187-197.
- 1948 The endospore of bacteria. *Bact. Revs.*, 12: 19-77.
- 1952 The cytology of sporulation. *Bact. Revs.*, 16: 93-101.
- 1955 On the structure and nature of the endospore in strain C₃ of *Bacillus cereus*. *J. Bact.*, 69: 130-138.
- LEWIS, I. 1934 Cell inclusions and endospore formation in *Bacillus mycoides*. *J. Bact.*, 28: 133-144.
- PARPART, A. K. 1951 Televised microscopy in biological research. *Sci.*, 113: 483-484.
- WYCKOFF, R. W. G., AND A. TER LOUW 1931 Some ultraviolet photomicrographs of *Bacillus subtilis*. *J. Exptl. Med.*, 54: 449-451.
- ZWORYKIN, V. K., AND L. E. FLORY 1952 Television in medicine and biology. *Elec. Eng.*, 71: 40-45.

PLATES

All figures are of unstained living bacteria and have a final magnification of approximately 7,000 \times .

PLATE 1

EXPLANATION OF FIGURES

- 2 Time = "O". (Time "O" is the time the first image was photographed.)
Typical field of sporulating cells after 24 hours growth on Difco nutrient agar 1.5%.
- 3 Time = 25 mins. Cell "d" is disintegrating prior to the release of the spore. Two new cells appear at upper right of field.
- 4 Time = 33 mins. Cells "a" and "c" have expelled their spores.

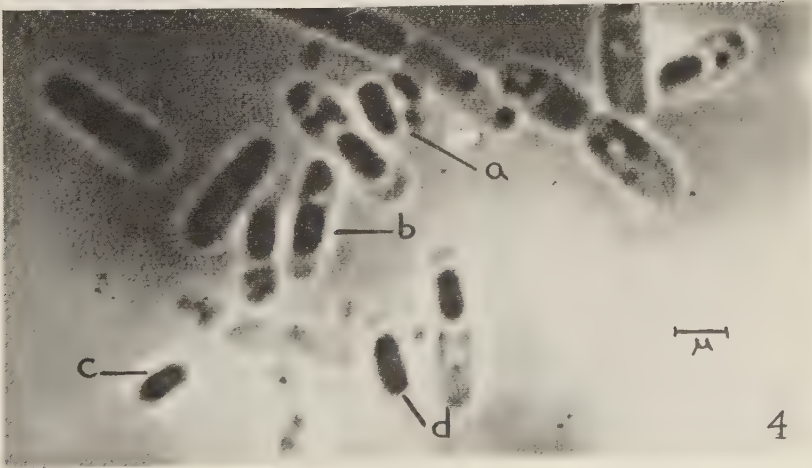
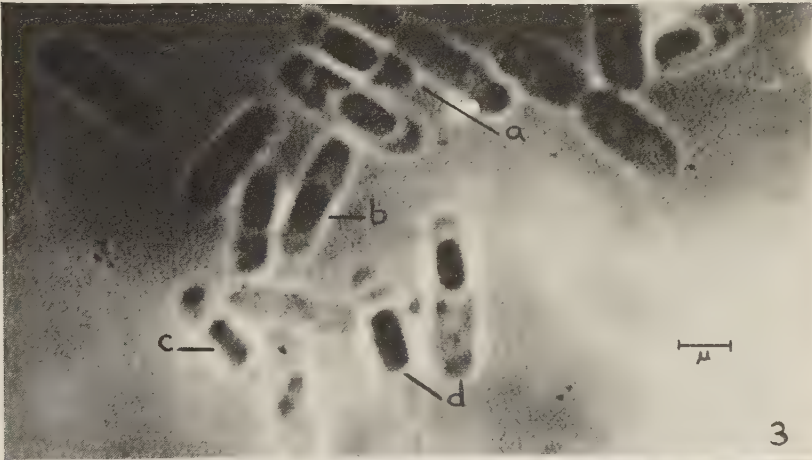
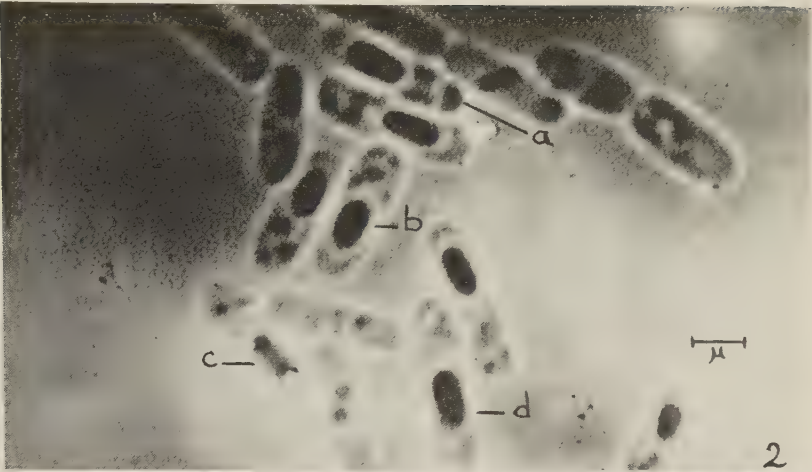


PLATE 2

EXPLANATION OF FIGURES

- 5 Time = 50 mins. Endospore "b" shows loss of refractility.
- 6 Time = 115 mins. Spore "a" is swelling. Endospore "b" is swelling.
- 7 Time = 210 mins. "a" and "b" can now be considered young vegetative cells. Spore "c" is swelling.

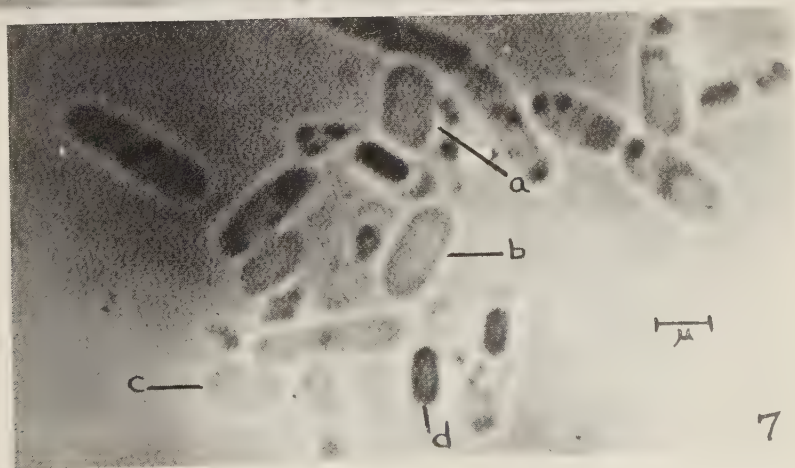
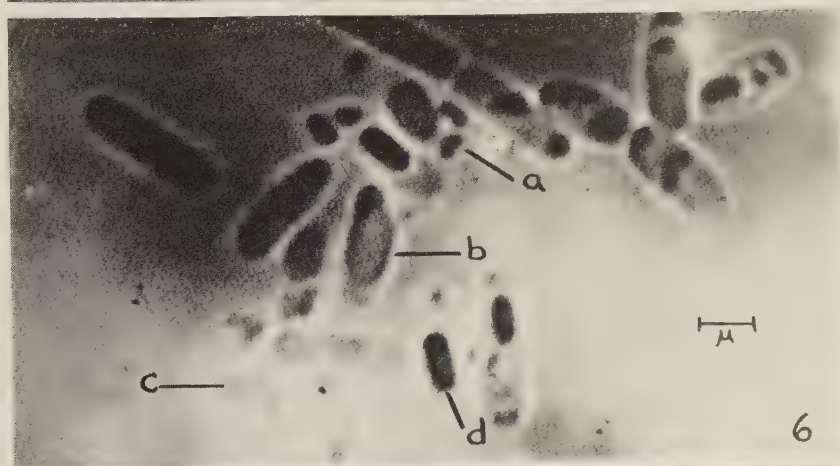
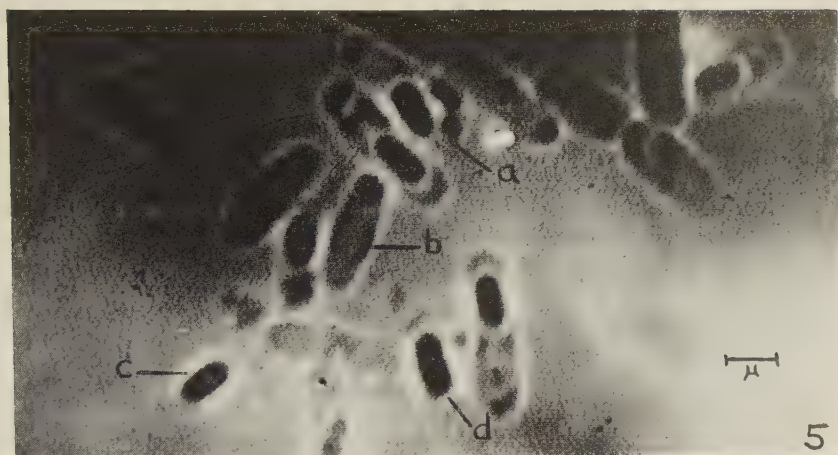
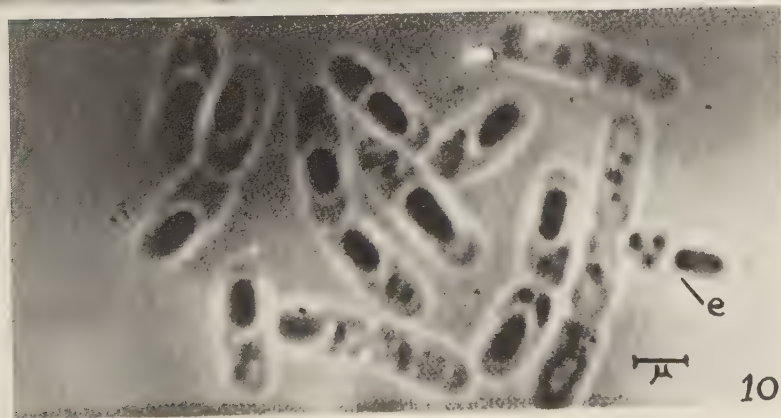
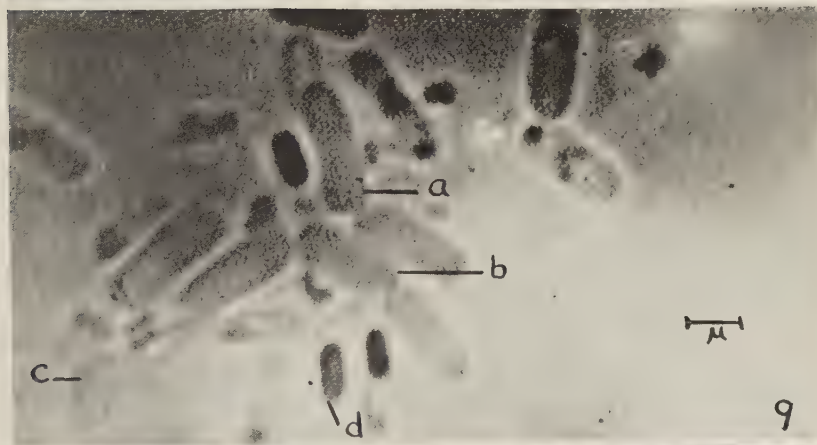
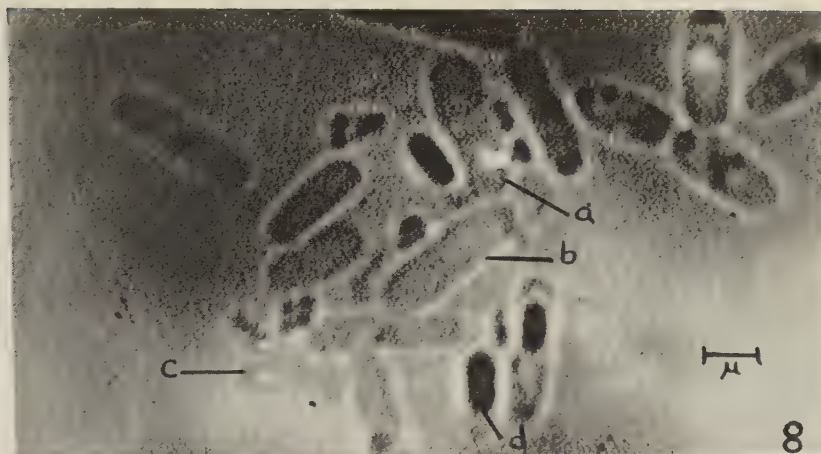
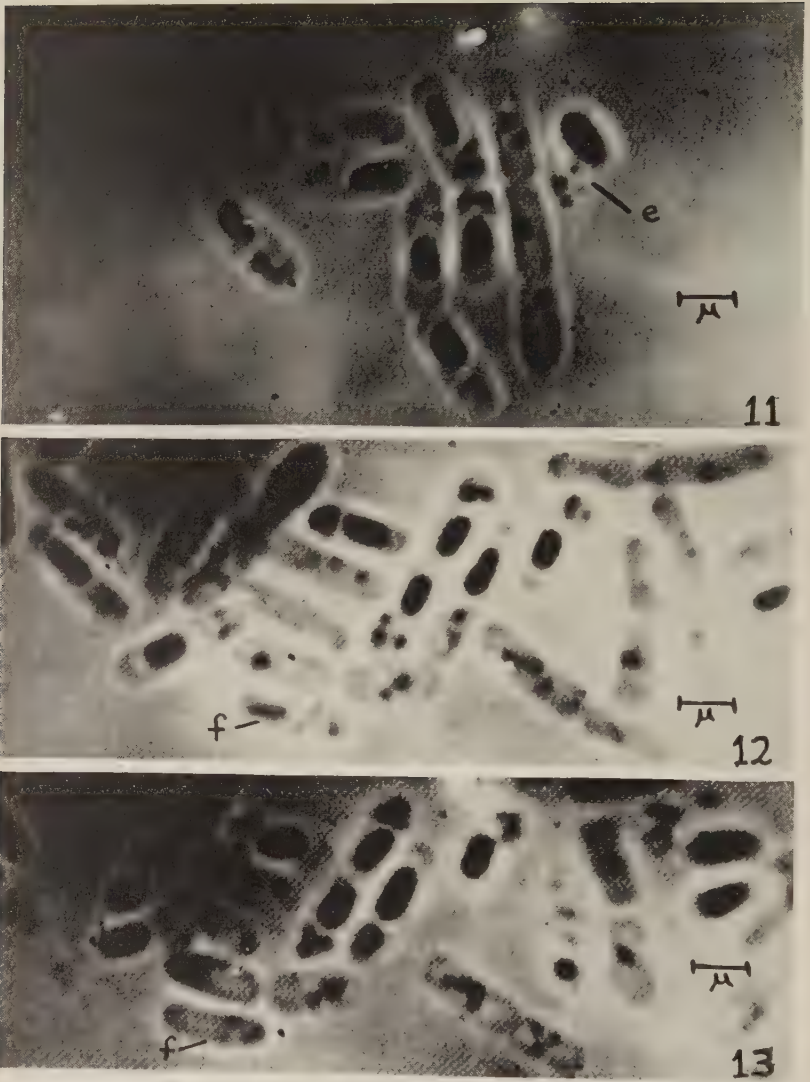


PLATE 3

EXPLANATION OF FIGURES

- 8 Time = 450 mins. Further vegetative growth of cells 'a' and 'b'. Cell 'c' is in a different plane of focus.
- 9 Time = 25½ hours. The field indicates continued vegetative growth.
- 10 Variability of endospore location in adjacent sporangia and the persistence of the granules after spore release, cell 'e'.





- 11 Variability of endospore location in adjacent sporangia and the persistence of the granules after spore release, cell "e".
- 12, 13 The time interval between these two photographs is $3\frac{1}{2}$ hours. The nearly mature endospore, "f," of figure 12 has "dedifferentiated" by the time of taking figure 13.

ANAEROBIC NUTRITION OF *SACCHAROMYCES CEREVISIAE*

III. AN UNIDENTIFIED GROWTH PROMOTING FACTOR AND ITS RELATIONSHIP TO THE ESSENTIAL LIPID REQUIREMENTS ¹

A. A. ANDREASEN ² AND T. J. B. STIER

*Department of Physiology, Indiana University
Bloomington, Indiana*

Strains of the yeast *Saccharomyces cerevisiae* proliferate only to a very limited extent under anaerobic conditions when cultured in media containing water soluble ingredients (Pasteur, 1879; A. Brown, '05; H. Brown, '14; Windisch, '32; White and Munns, '51). On the other hand, it has been found that a moderate amount of anaerobic growth can be obtained if relatively high concentrations of certain crude materials are employed in the medium. For example, a medium containing 5-7% yeast extract, phosphate and glucose produces *ca* 100 million cells/ml (Scalf and Stier, '50). Subsequent experimentation showed that the addition of unsaponifiable material from edible oils (e.g. wheat germ) increases the population to as much as 300 million cells/ml (Stier, Scalf and Peter, '50). These results prompted an investigation of anaerobic growth requirements using chemically defined media. The investigation resulted in the discovery that two lipids are required in the defined medium, otherwise growth under continuous anaerobic conditions will not occur. These lipids are ergosterol or certain other sterols (Andreasen and Stier, '53) and oleic acid or other long-chain unsaturated fatty acids (Andreasen and Stier, '54). Anaerobic

¹ This work was aided by a grant from Joseph E. Seagram & Sons, Inc.

² Seagram Research Associate at the Laboratory of Cell Physiology, Indiana University, assigned by Joseph E. Seagram & Sons, Inc., Louisville, Kentucky, February, 1950.

populations ranging from 200 to 250 million cells/ml can be consistently obtained in the defined basal-lipid medium (Andreasen and Stier, '54).

Since greater populations than these had been obtained in a medium containing yeast extract and unsaponifiable matter from edible oils, various crude materials were tested in defined media as sources of additional anaerobic growth promoting factors. The type of crude materials having growth promoting activity, the relationship between their activity and that of the essential lipids and some of the properties of the factor(s) are described below.

EXPERIMENTAL PROCEDURES

Yeast strain. All experiments were conducted with a distillery type yeast; a strain ³ of *Saccharomyces cerevisiae*, SC-1 (DCL), obtained from Joseph E. Seagram and Sons, Inc., Louisville, Kentucky.

Growth criterion. The number of yeast cells in a known dilution of culture was determined by direct count in a Neubauer chamber. All buds the size of the smallest independent cell were included in the count. The populations were expressed as million (M) cells/ml. The samples were preserved by acidification prior to counting.

Removal of oxygen. Anaerobic conditions were obtained by thoroughly flushing all experimental vessels and media with Linde "high-purity dry nitrogen." The manufacturer claims an oxygen content of less than 20 p.p.m. (or *ca* 0.01 mmHg). This oxygen concentration is insignificant if anaerobic growth is relatively good, but it is necessary to reduce the oxygen concentration of the nitrogen to *ca* 1 p.p.m. by chromous chloride absorption for crucial experiments when anaerobic growth is meager.

Inoculum. Inocula for the anaerobic shake cultures were taken from an anaerobic culture unit and were used in an amount to give an initial population of 0.5–0.7 M cells/ml.

³ The yeast employed was erroneously called a haploid strain in a previous publication (Andreasen and Stier, '54).

The anaerobic culture unit (Stier, Scalf and Brockmann, '50; Andreasen and Stier, '53), is an all-glass apparatus that provides a regular supply of inoculum having a continuous anaerobic history. Aerobic experiments were conducted with inocula which had been previously subcultured under aerobic conditions.

Management of shake cultures. Anaerobic shake culture tests were conducted in all-glass equipment in the manner described by Andreasen and Stier ('53). The aerobic shake flask procedure consisted of directing a stream of air onto the surface of 25 ml of medium at an air flow rate of *ca* 50 ml/minute.

Media. Three different basal media were employed during the course of this investigation. The initial experiments were performed with Difco Yeast Nitrogen Base medium, based on a formulation devised by Wickerham ('51). The remaining experiments were performed using two modifications of the commercial product and are designated Basal No. 2 and Basal No. 3. The compositions of these media are presented in a previous publication (Andreasen and Stier, '54). The Basal No. 2 medium contained for the most part only those ingredients which were found to be essential or stimulatory. The Basal No. 3 medium was devised for convenience and consisted of Yeast Nitrogen Base fortified with additional amounts of ingredients present in growth limiting concentration. These media were completed by adding 12% glucose and 16 volume per cent of 0.3 M sodium succinate buffer, pH 5. When crude materials were added it was necessary to increase the glucose concentration to 15%.

Approximately 20 μ g ergosterol and 140 μ g oleic acid (pure or as Tween 80) per milliliter of medium were required to obtain maximal anaerobic growth in the defined media. When crude materials were added to the media, the ergosterol concentration was increased to *ca* 50 μ g/ml for maximal growth. Details of the preparation of the lipid stock solutions are described by Andreasen and Stier ('54).

Aerobic experiments were conducted with Basal No. 2 or No. 3 media which were modified to contain only 4% glucose. No lipids were used. It was also necessary to supplement the Basal No. 2 medium with inositol, to the concentration found in the other media, because it is required for maximal aerobic growth.

When crude materials were employed, they were made up in concentrated aqueous solution and sterilized by boiling. A known amount was then combined with the basal medium constituents and the volume adjusted with water.

Extraction of lipids from crude material was accomplished by first mixing the dry material with a large volume of acetone and shaking overnight. The acetone was then decanted and petroleum ether added. After shaking for one hour, the ether mixture was boiled and decanted. Boiling in fresh ether was repeated three times.

EXPERIMENTAL RESULTS

Exploratory experiments. A number of compounds and commercial preparations were added to lipid-Yeast Nitrogen Base medium to determine their growth promoting activity. Nearly all of them were tested at more than one concentration in order to determine the approximate optimal concentration. The basal medium contained 1750 $\mu\text{g/ml}$ oleic acid (as Tween 80) and 70 $\mu\text{g/ml}$ ergosterol. The inocula were prepared in a similar basal medium. This lipid basal medium produced a population of 125 million (M) cells/ml, a population which was later found to be about 40% low due to vitamin deficiencies.

Two crude materials, Difco yeast extract and BBL myosate were the most potent materials tested. At the optimal concentration of 3% both products gave populations in the range of 450–530 M cells/ml. A second group of preparations gave less growth promotion. Populations in the range of 330–400 M cells/ml were obtained from the following: Bacto-peptone, 3%; Wilson liver-L, 3%; Armour biopar B, 6%; biopar A, 3%; biopar D, 2% BBL polypeptone, 3%; Viobin

whole liver, 6% ; fresh beef heart, 4% water soluble solids, and BBL phytone, 4%.

The following materials had little or no growth promoting activity in the lipid medium, giving populations in the range of 100–275 M cells/ml: BBL lactalysate, biopar E, Wilson liver-2, BBL gelysate, BBL milk protein, Bacto protone, BBL trypticase, biopar F, glycyl glycine, glutathione, carnosine, putrescine, aspartic acid, choline, casein hydrolysate-acid and enzymatic, Parenamine, a mixture of purines and pyrimidines, nucleic acid, nucleic acid hydrolyzed, adenylic acid-yeast and muscle, vitamin B₁₂ and Armour coenzyme concentrate.

TABLE 1

The effect of crude materials and essential lipids on anaerobic growth in a defined medium. Lipid concentrations were: ergosterol, 30 µg/ml (solubilized in 0.3% Triton), increased to 50 µg/ml for 400–500 M/ml populations; oleic acid, 141 µg/ml. The crude materials were acetone-petroleum ether extracted. The inoculum was prepared in Basal no. 2 medium with both lipids present in optimal concentration. The inoculum was washed twice in freshly autoclaved water, resuspending the cells by bubbling high-purity nitrogen through the suspension.

LIPID ADDED	BASAL NO. 2	BASAL + MYOSATE, 3 %	BASAL + YEAST EXTRACT, 3 %
	M cells/ml	M cells/ml	M cells/ml
None	5	14	41
Ergosterol only	26	187	193
Oleic acid only	12	23	37
Ergosterol + oleic acid	193	500	470

Experiments with acetone-ether extracted BBL myosate and Difco yeast extract. The two preparations having the greatest growth promoting activity in the basal-lipid medium were tested for activity in media of different lipid composition. The data are presented in table 1. Both the myosate, an enzymatic heart digest, and yeast extract were extracted with acetone and petroleum ether (cf. Experimental Procedures). The medium, Basal no. 2, was complete with respect to known water soluble growth substances so that any growth response was due either to unextractable lipids or to unidentified water soluble factor(s) in the crude material.

The following comments can be made in connection with the data of table 1. The first three figures in column 1 represent the poor growth obtained when the defined medium is incomplete with respect to essential lipids. Even these low populations are excessive, probably due to a carry-over of essential anaerobic growth substances with the inoculum and to the presence of a trace of oxygen in the high purity nitrogen used for flushing the shake flasks. Growth has been shown to be virtually absent on subcultivation in similar media when the experiments were performed in the anaerobic culture unit using nitrogen treated with chromous chloride (Andreasen, '53; Andreasen and Stier, '53). The 4th figure in column 1 represents an optimal population for a defined medium containing known anaerobic growth constituents.

Table 1, line 1, shows the populations obtained in a non-lipid medium to which lipid-extracted myosate and yeast extract have been added. Growth was comparatively poor in each case. The greater growth obtained with the crude materials might be ascribed to incomplete removal of lipid during extraction. When an optimal concentration of ergosterol was added to these media, line 2, the presence of the crude materials caused a considerable growth response. This increase may be attributed to the presence, in the crude materials, of difficultly extractable unsaturated fatty acid, or to the presence of an "oleate replacing factor." On the other hand, when oleic acid was the only lipid additive, line 3, the growth responses were again quite small, comparable to those of line 1. This indicates that the crude materials had very little "ergosterol activity."

The data of table 1, line 4, represent the populations obtained in the three media when the essential lipids were present in non-limiting concentrations. The addition of crude materials to the lipid basal medium caused a 2.5-fold increase in population. These populations are the greatest that have been obtained under anaerobic conditions at the present time.

Comparison of the effect of lipids and crude materials on aerobic and anaerobic growth. It has been demonstrated that

ergosterol and oleic acid are necessary for anaerobic growth and it has been shown above that an unidentified factor promotes additional growth provided these lipids are present. It was of interest, therefore, to determine the effect of these substances under aerobic culture conditions. The aerobic experiments were conducted in Basal no. 2 or no. 3 media modified to contain 4% glucose and, in the case of the Basal no. 2 medium, inositol. The lipids were tested at concentrations found to be optimal for anaerobic growth. BBL myosate and Difco yeast extract were used at 3% concentration with approximately equivalent results. The range of populations obtained from various experiments are given in table 2.

TABLE 2

Comparison of anaerobic and aerobic populations. Basal no. 2 and no. 3 media were employed; see text for composition when used under aerobic and anaerobic conditions. Lipids, when used, were employed at concentrations optimal for anaerobic growth. Aerobic test cultures were inoculated with aerobic yeast.

MEDIUM	POPULATION RANGE, M CELLS/ML	
	Anaerobic	Aerobic
(1) Basal	0-2	400-500
(2) Basal + myosate or yeast extract, 3%	10-40	400-500
(3) Basal + lipids	180-250	300-350
(4) Basal + lipids + myosate or yeast extract, 3%	450-500	400-500

The data of table 2 permit several observations. For example, in contrast to anaerobic results, the non-lipid basal media provide excellent aerobic growth whether crude material is added or absent (lines 1 and 2). Aerobic growth in the media containing crude material is equally good whether the lipids are added or absent (lines 2 and 4). The addition of lipids to the basal medium (line 3) results in a substantial reduction in aerobic growth. The presence of crude materials evidently neutralizes this depressive action (lines 3 and 4). Finally, the media containing lipids and crude material support equally great populations under both anaerobic and aerobic conditions (line 4). These data may be taken as

preliminary evidence that the essential lipids and the unidentified factor, or their biological counterparts, are biosynthesized by the aerobic cells. Anaerobic cells require an external supply of these substances for comparable growth promotion.

Biosynthesis of the anaerobic growth factor. To test the point of whether an anaerobic growth promoting substance is formed by cells grown anaerobically, anaerobic yeast grown in the Basal no. 3 lipid medium was assayed for activity. Aerobic yeast grown in lipid-free basal medium was also assayed for comparison. A crude extract was prepared from these cells by subjecting them to acetone-petroleum ether extraction followed by extraction in boiling water for 20 minutes. The cell debris was removed from the water extract by centrifugation. When 1% (w/v) of this "anaerobic yeast extract" was employed in an anaerobic Basal no. 3 culture containing optimal concentrations of oleic acid and ergosterol, the population was equivalent to that obtained by the use of 1% Difco yeast extract or 1% "aerobic yeast extract" prepared in the laboratory, i.e. *ca* 350 M cells/ml. These results show that anaerobic, and aerobic, cells biosynthesize a substance having anaerobic growth factor activity.

Nature and properties of the unidentified factor. The unidentified factor can be characterized at the present time only by certain observations made from the above experimental results and by a few fractionation experiments. The data in the section on Exploratory Experiments, for example, show that only tissue extracts, tissue digests, or certain fractions from these, are active. Enzymatic digests prepared from proteins are virtually inactive, as are the amino acid mixtures and the known compounds tested. Since the latter inactive materials represent a variety of nuclear constituents, amino acids and peptides it is unlikely that the activity results from nitrogenous "building units."

Although the active substance in crude materials has not been concentrated appreciably, several properties have been tentatively determined through fractionation experiments.

For example: (1) It is highly soluble in water. (2) It is soluble in ethanol-water mixtures, although losses to the insoluble fraction are high above 80% ethanol. (3) It is insoluble in acetone and ether. (4) The material is rapidly and apparently quantitatively dialyzable. (5) It is stable to prolonged boiling, and to autoclaving, in crude form. There is loss of activity, however, when water extracts prepared from laboratory yeast are stored in air at 8°C. for about one month. (6) Activity is apparently destroyed by heating for two hours in strong mineral acid, while partial enzymatic digestion of active crude material appears to enhance activity. (7) The active material is not precipitated by ammonium sulfate, phosphotungstic acid or trichloroacetic acid.

DISCUSSION

The experiments presented above demonstrate that yeast cells grown either aerobically or anaerobically contain a growth stimulating factor. Under aerobic conditions, a growth factor is biosynthesized from defined medium ingredients in sufficient quantity to produce populations of 400–500 M cells/ml. Under anaerobic conditions, however, populations of only *ca* 200 M cell/ml are produced, provided the essential lipids are present.

The limited anaerobic growth of 200 M cell/ml in the defined lipid medium might be attributed to a partial medium deficiency inasmuch as vitamin (Andreasen, '53) and lipid requirements also differ under aerobic and anaerobic conditions. However, aerobic cells are able to utilize defined medium ingredients for production of amounts of growth stimulating factor sufficient to give crops of 400–500 M cells/ml while anaerobic growth is limited to 200 M cells/ml even if the medium ingredients are present in supraoptimal amounts. This indicates an alteration in the biosynthetic mechanism which perhaps results in (1) limited anaerobic biosynthesis of the factor which is produced in "nonlimiting" amounts under aerobic conditions or, (2) the anaerobic production of

what would be nonlimiting amounts of the factor if it were *totally available to the cells*.

Two explanations have been considered in connection with the concept that nonlimiting amounts of factor may be produced by anaerobic cells but that it is only partially available because of some binding mechanism. 1. Just one factor is produced intracellularly and only a portion of it becomes "unbound" anaerobically, under the conditions of our experiments, and is then available for the production of anaerobic populations of *ca* 200 M cells/ml. 2. At least two types of intracellular growth stimulating substances are produced, but under anaerobic conditions one is held in a bound form and the other is free and available.

Quantitative experiments on the content of these growth factors in aerobic and anaerobic yeast and their purification and identification may reveal the controlling mechanism of aerobic and anaerobic cell division. It may also be of general interest to find out whether the growth promoting substance found in various active tissue preparations (enzymatic digests) is identical with the growth factor(s) of yeast and whether a similar growth regulating mechanism operates in the tissues of animals.

SUMMARY

A strain of *Saccharomyces cerevisiae* will not proliferate when subcultured under anaerobic conditions in the defined media usually employed for aerobic propagation. It was found, however, that anaerobic populations of 200–250 million cells/ml could be obtained when oleic acid *and* ergosterol were added to the defined medium, establishing these and related active lipids as essential anaerobic nutrilites. It has now been demonstrated that anaerobic populations up to 500 million cells/ml can be produced in the defined lipid medium if certain types of crude material are added, indicating the existence of an anaerobic growth promoting factor(s).

More than three dozen crude materials and known compounds were tested for activity but only 11 crude materials

gave a response. Difco yeast extract and BBL myosate had the greatest potency. Tissue and yeast extracts and tissue digests were active while protein digests and nuclear materials were inactive. High activity was also found in extracts prepared in the laboratory from yeast grown anaerobically in defined lipid medium and from yeast grown aerobically in defined medium. Some properties of the factor are given.

Data are presented showing that aerobic populations of 400–500 M cells/ml are obtained whether or not lipids and crude material having growth factor activity are added to the defined medium, while both must be present to obtain comparable anaerobic populations. Although the extraction experiments indicate that the unidentified factor is actually biosynthesized by anaerobic yeast in a medium without added growth factor, the material formed under these conditions does not have the same cell forming activity as that produced within aerobic cells from the same medium ingredients. Possible reasons for this phenomenon are briefly discussed.

LITERATURE CITED

- ANDREASEN, A. A. 1953 Anaerobic nutrition of *Saccharomyces cerevisiae*. Doctorate thesis, Indiana University.
- ANDREASEN, A. A., AND T. J. B. STIER 1953 Anaerobic nutrition of *Saccharomyces cerevisiae*. I. Ergosterol requirement for growth in a defined medium. *J. Cell. and Comp. Physiol.*, 41: 23.
- 1954 Anaerobic nutrition of *Saccharomyces cerevisiae*. II. Unsaturated fatty acid requirement for growth in a defined medium. *J. Cell. and Comp. Physiol.*, 43: 271.
- BROWN, A. J. 1905 The influences regulating the reproductive functions of *Saccharomyces cerevisiae*. *J. Chem. Soc. (London)*, 87: 1395.
- BROWN, H. T. 1914 Studies on yeast. II. The metabolism of the yeast cell, with special reference to the thermal phenomena of fermentation. *Ann. Bot.*, 28: 197.
- PASTEUR, L. 1879 Studies on Fermentation. Macmillan and Co., London.
- SCALF, R. E., AND T. J. B. STIER 1950 Effect of commercial malt sprouts on the anaerobic growth of distiller's yeast. *Trans. Ky. Acad. Sci.*, 13: 69.
- STIER, T. J. B., R. E. SCALF AND M. C. BROCKMANN 1950 An all glass apparatus for the continuous cultivation of yeast under anaerobic conditions. *J. Bact.*, 59: 45.

- STIER, T. J. B., R. E. SCALF AND C. J. PETER 1950 Edible oils as sources of lipid anaerobic growth factors for distiller's yeast. *J. Cell. and Comp. Physiol.*, *36*: 159.
- WHITE, J., AND D. J. MUNNS 1951 The effect of aeration and other factors on yeast growth and fermentation. *Wallerstein Lab. Comm.*, *14*: 199.
- WICKERHAM, L. J. 1951 Taxonomy of yeasts. *Tech. Bull. no. 1029, U.S.D.A.*, 56 pp.
- WINDISCH, FRITZ 1932 Die Bedeutung des Sauerstoffs für die Hefe und ihre biochemischen Wirkungen. *Biochem. Z.*, *246*: 332.

SUPPLEMENT

SOCIETY OF GENERAL PHYSIOLOGISTS

Abstracts of papers presented at the eleventh Annual Meeting,¹ held in conjunction with the meetings of the American Institute of Biological Sciences, at the University of Connecticut, Storrs, Connecticut, August 27-29, 1956.

¹ Abstracts or summaries of programs of previous meetings will be found in *Biol. Bull.*, 91: 236; 93: 222; 95: 281; 97: 267; 99: 308 (1946-50); *Science*, 114: 699; 118: 768; 121: 10; 122: 1098 (1951-55); *J. Nat. Cancer Inst.*, 13: 1379; (1953); and *J. Cell. and Comp. Physiol.*, 44: 327 (1954) and 46: 351 (1955).

SYMPOSIUM

THE INFLUENCE OF TEMPERATURE ON BIOLOGICAL SYSTEMS

(Organized by Frank H. Johnson, and dedicated to A. V. Hill),
Storrs, August 27 and 28

ABSTRACTS

Part I. DAVID F. WAUGH, presiding

1. A CRITICAL COMPLEX THEORY OF BIOSYNTHESIS.¹ Henry Eyring, University of Utah and Frank H. Johnson, Princeton University.

In biological systems reaction mechanisms may be conveniently classified as (a) organizational and (b) disorganizational. Typical of the first category are the many enzyme catalyzed syntheses, while denaturations exemplify disorganization. These ideas may be made precise by defining them with respect to the velocity of reaction,

$$-\frac{dc_1}{dt} = c_1 \dots c_n \frac{kT}{h} e^{-\frac{\Delta F^\ddagger}{RT}} = c_1 \dots c_n \frac{kT}{h} e^{-\frac{\Delta H^\ddagger}{RT}} \frac{\Delta S^\ddagger}{R}$$

If the entropy of activation ΔS^\ddagger is zero, as in the breaking of a single bond in the simplest unimolecular decompositions, we have the intermediate case of essentially no change in organization in passing from the normal to the activated state. In organizational reactions, ΔS^\ddagger tends to be negative, while ΔS^\ddagger is positive in disorganizational reactions. The rate equation describes the probable rate of reactions involved in the origin of life, as well as those encountered every day.

Back about a billion years ago, in pre-Cambrian time, the period of chemical evolution drew to a close and biological evolution evidently began. As we consider this transition with the best scientific evidence available, the conclusion seems inescapable that a single event lasting 10^{-13} seconds marked the close of the one era and the beginning of the next. A most compelling bit of evidence is the fact that the living world is optically active and configurationally related. If the entire world were reflected through a looking glass, it would be exactly as efficient as it now is. It follows that at some time in the past a critical event transpired, involving an optically active system, which has determined the subsequent history of the living world. This critical event was the formation of a critical complex which was autocatalytic. Before its emergence, chemical evolution had been going on for a long time. Many kinds of complex molecules had appeared and disappeared. At this turning point in biological history the final bond was formed,

yielding a template molecule larger and more perfect than the unfinished approximations to it which had appeared previously. This critical template had, for the first time, the property of reproducing itself using the enzymes it could form, and those present in the surrounding milieu, in a period shorter than its own lifetime. With the emergence of self duplication of this comparatively perfect template, the living world suddenly "went critical" in the same sense as an ordinary explosion, or as the atomic bomb does under critical conditions. Sudden nucleation of a supersaturated solution is an analogous phenomenon. It is natural to suppose that ribonucleic acid, with a configuration which selected and combined the levo amino acids, first reached the critical length and perfection of configuration which enabled it to become self duplicating in a shorter time than its own lifetime. Once this happened, the world quickly filled with templates and enzymes, and no subsequent template of independent origin could ever attain the complicated structure which could compete at this new tempo. Thus it is likely that all living things ultimately derive from a single template that attained critical length and perfection of structure long ago.

¹ Aided in part by a contract with the Office of Naval Research.

2. THE STUDY OF STRUCTURAL FACTORS INVOLVED IN PROTEIN STABILITY. Walter Kauzmann, Princeton University.

One of the principal factors determining the behavior of living organisms at high temperatures is the stability of their proteins, and any discussion of the effects of temperature on protein stability will usually invoke the word "denaturation." This word has long been used to describe the loss of activity and solubility that results from exposure to high temperature, but more recently it has been defined in more fundamental terms, involving reversible and irreversible structural changes peculiar to proteins. Both meanings of the word are useful, but confusion has resulted when the existence of two meanings was not recognized.

Two complementary types of experimental measurement are available for detecting the structural changes that accompany protein denaturation. One type of property is sensitive to the over-all shape of the molecule and is illustrated by the solution viscosity, the rotational diffusion rate and dissymmetry in the scattering of light. The other type of property is determined by short range interactions between different parts of the molecule and is illustrated by infra-red and ultra-violet spectra, optical rotatory power and the chemical reactivity of groups in the molecule. Studies of the structural changes that occur in proteins during denaturation should, if possible, be made using at least one property from each of these two groups in order to give a maximum amount of structural information with a given amount of experimental effort. The viscosity and the optical rotatory power are especially convenient for this purpose. Structural changes that lead to a change in viscosity are usually interpreted in terms of a model consisting of a rigid ellipsoid, but the random coil model is more suitable for some conditions and it is not hydrodynamically equivalent to any ellipsoid. The changes in optical rotation that occur on denaturation are often attributed vaguely to changes in the contributions of asymmetric carbon atoms present in the protein molecule. This terminology is inappropriate because the magnitude

of the optical rotation depends only very indirectly on the presence of asymmetrical carbon atoms in a molecule. The important factor is the vicinal actions of groups on each other. These interactions change whenever the relative spatial positions of groups are changed. Therefore the optical rotation of a protein will change whenever the polypeptide chain is twisted into a new conformation, even though no change may have taken place in the asymmetric carbon atoms themselves. Some interesting recent studies of the viscosity and optical rotation changes on denaturation are discussed.

3. EFFECTS OF TEMPERATURE, DIELECTRIC CONSTANT, AND DIFFUSION RATES ON THE FORMATION OF THE INTERMEDIATE COMPOUND OF CATALASE AND HYDROGEN PEROXIDE. E. Ackerman, G. K. Strother and R. L. Berger, The Pennsylvania State University.

The reactions of beef liver catalase with H_2O_2 were studied under conditions of varying temperature, dielectric constant, and viscosity of the suspending medium. These studies showed that the rate k_1 at which beef liver catalase combines with H_2O_2 to form the intermediate compound is temperature independent from 5°C. to 45°C. , not appreciably altered by the dielectric constant, but dependent on diffusion rates if these are lowered below $0.8 \times 10^{-6} \text{ cm}^2/\text{sec.}$ The constant k_4 , at which the intermediate complex reacts with a second molecule of hydrogen peroxide is also little altered by variations in the dielectric constant, but is dependent on temperature and diffusion rate. These results are in accord with the prediction of the entropy of activation from absolute rate theory. The results also indicate that any encounter with a portion of the molecular surface appreciably larger than an iron atom will be effective in producing a reaction in the diffusion controlled range.

4. THE EFFECT OF TEMPERATURE UPON THE COMBINATION OF PEROXIDASE AND PEROXIDE AND CYTOCHROME a_3 AND OXYGEN. Britton Chance, Johnson Research Foundation, University of Pennsylvania.

A simple equation for the calculation of the velocity constant (k_4) for the reaction of an enzyme-substrate complex with the second substrate or hydrogen donor has been used for some time (Chance, '43):

$$k_4 a = k_3 = x_0 / p_{\max} t_{\frac{1}{2} \text{ off}} \quad (1)$$

If this equation is now combined with the value of the velocity constant for the combination reaction (k_1) computed from the Michaelis constant, we get the second simple equation for enzyme-substrate kinetics

$$k_1 = \frac{1}{(e-p) t_{\frac{1}{2} \text{ off}}} \quad (2)$$

The quantity $k_4 a$ is easily made greater than the velocity constant for the dissociation of substrate (k_2). This equation allows the accurate computation of k_1 from three simple quantities: (1) the enzyme concentration, (2) the steady state concentration of the enzyme-substrate (Michaelis) complex, (3) the time between half formation and half decay of the steady-state concentration of the

enzyme-substrate complex values of k . Values of k_1 and k_4 measured by this method are in good agreement with the earlier data for peroxidase (Chance, '51) and show temperature effects corresponding to 3600 and 10,000 calories respectively. Equation (2) is approximately applicable to the cytochrome system when the oxygen concentration is large enough to give an appreciable steady state. The value of k_1 for the cytochrome a_3 -oxygen reaction of yeast cells reaches $10^6 \text{ M}^{-1} \times \text{sec}^{-1}$ at 47° (cf. Ludwig and Kuby, '55) and shows a temperature effect corresponding to about 9000 cal.

5. TEMPERATURE DEPENDENCE OF CHOLINESTERASE ACTIVITY. L. E. Chadwick, Army Chemical Center.

The literature on the response of cholinesterases (ChE's) to temperature change was reviewed. The available data were discussed under three headings.

1. Temperature and rate of hydrolysis.
2. Inactivation of ChE by heat.
3. Effect of temperature on the rate of reaction with inhibitors.

The temperature coefficient of ChE-catalyzed hydrolysis of acetylcholine (ACh) and other substrates is generally small. Q_{10} values from 1.3 to 1.5 are usual. With many preparations, activity is directly proportional to temperature over the range below 35°C ., but some experiments have given results consonant with the Arrhenius formulation. Other difficulties concerned in the calculation and interpretation of the standard thermodynamic constants are outlined; and it is concluded that with most preparations the temperature response is modified by complicating factors of an unknown nature.

Heat inactivation of ChE's is rapid at temperatures above 50°C . Fly head preparations are somewhat more sensitive than the ChE's of mammalian blood. Apparent energies of activation for the denaturation are of the order of 40 to 60 kcal./mole; however, the reaction fails to follow first order kinetics over longer exposures, and analysis of the data shows a rapid initial phase and a subsequent slower phase. Both processes appear to be first order. The reason for the biphasic course of denaturation is not known, although it obviously indicates that more than one reaction is involved in the denaturation process.

The ChE's of mammalian serum are in addition reversibly inhibited at temperatures above 40°C . In contrast, all the reduction in activity observed with fly head ChE is attributable to irreversible denaturation. None of the current hypotheses accounts satisfactorily for all of the anomalies in the temperature response.

The temperature dependence of the reaction with competitive inhibitors, whether reversible or "irreversible," is in general similar to the response of the enzyme-substrate system, insofar as the scanty data available permit one to judge. Similar complexities are indicated. Some noncompetitive inhibitors at low concentrations combine reversibly with the enzyme, in a process that has a small temperature coefficient. These same inhibitors, at high concentrations, denature the enzyme irreversibly. The energy requirement for such denaturations is of the order of 40 to 60 kcal./mole, as for denaturation by heat.

In all three areas considered, the need for further study is evident. Little has been done as yet from the point of view of comparative physiology, and there

have been no investigations of the temperature dependence of these reactions in the living organism. These gaps will have to be filled, and the anomalies that have come to light must be explained, before useful generalizations about the system will be possible.

Part II. WILLIAM D. McELROY, presiding

6. MECHANISM OF HEAT ACTIVATION OF ENZYMES. Morton N. Swartz, Nathan O. Kaplan and Mary E. Frech, The Massachusetts General Hospital and the McCollum-Pratt Institute of Johns Hopkins University.

In sonic extracts of bacteria of various species (e.g. *Mycobacterium butyricum*, *Proteus vulgaris*, *Bacillus subtilis*), nucleotide-splitting enzymes which are in the inhibited state have been found. These enzymes are extremely heat-stable and are "activated" on being heated to temperatures of 100°C. This activation is brought about by the destruction at these high temperatures of a relatively heat-labile inhibitor of these enzymes. These inhibitors are non-dialyzable and have been purified by some of the common protein fractionation procedures. The inhibitors do not appear to cross-react i.e. the inhibitor from *Mycobacterium* will not inhibit the *Proteus* enzyme or the enzyme from *B. subtilis*. The union of inhibitor with enzyme appears to be by a salt type linkage rather than through a strong chemical bond. In the case of the *Mycobacterium* system at an acid pH the inhibitor and enzyme dissociate and active enzyme can be demonstrated. Upon restoring the pH to neutrality the enzymatic activity is again inhibited. However, in the case of the *Proteus* system, acid treatment appears to destroy the inhibitor and upon neutralization the enzyme remains in the active state. It can be shown that the enzyme and inhibitor react at a measurable rate and that this complex is essentially undissociable at neutral pH.

These enzymes show the same type of reversible heat denaturation as does purified trypsin. The heat-stability of the *Proteus* enzyme depends on the presence of inorganic pyrophosphate or an unidentified naturally-occurring organic phosphate compound when the enzyme is subjected to high temperatures. This requirement for the protective factor exists as well for the purified enzyme as for the crude preparations. The mechanism of this protection is obscure.

Antibodies to the *Proteus* enzyme inhibit the enzyme. Heating the antibody-enzyme complex reactivates the enzyme. The relation of antibody to inhibitor is under study.

The role of these inhibited enzymes in the whole cell is not at all clear. Thus far, heat-activated enzymes have not been found in higher plant or animal tissues.

7. MYOSIN ATP-ASE ACTIVITY IN RELATION TO TEMPERATURE AND PRESSURE. Karl F. Guthe, University of Michigan.

The rate of splitting of adenosine triphosphate (ATP) by myosin at high substrate concentration is increased by temperature, by pressure, and by hydroxyl

ion, at pH above 7.4. The kinetic data show that these factors change the rate not only because they affect the breakdown of the enzyme-substrate complex, but also because they alter an equilibrium between native and reversibly denatured forms of the enzyme. Johnson and others have shown the presence of a similar reversible denaturation in bacterial luminescence.

The breakdown of the enzyme-substrate complex is favored by temperature and hydroxyl ion, but inhibited by pressure. It proceeds with a volume increase of 60 cm³/mole and a heat of activation of about 23,000 calories per mole. This process governs the over-all rate of splitting at pH 6.3, where pressure decreases the activity of myosin.

In the reversible denaturation of myosin, temperature and hydroxyl ion favor the denatured form while pressure favors the native form. When a native molecule (active site) is reversibly denatured, it loses a proton with a pK about 7 and it increases in volume by about 100 cm³/mole. The heat of reaction is about 10,000 calories per mole. Pressure increases the over-all splitting of ATP by myosin in alkaline solution, where this equilibrium becomes important.

Although the heat of reaction for the reversible denaturation of myosin is low, and only one hydrogen ion is involved, the large volume increase indicates that configurational changes in the protein, such as unfolding or dehydration, must accompany the loss of the proton.

In the present experiments, myosin was studied in the presence of sodium salts, in contrast to the potassium salts usually used by other investigators. Comparison of the available data suggests that the presence of potassium ion may decrease the susceptibility of myosin to reversible denaturation.

8. THE PRESSURE-TEMPERATURE RELATIONSHIP IN MUSCULAR CONTRACTION. D. E. S. Brown, University of Michigan.

The concept is developed that temperature and pressure relations in contraction may be interpreted in terms of the activation of actomyosin and those "steady state" reactions which establish the concentrations of phosphate donors and acceptors. In the glycerated psoas fiber, with ATP present, tension increases with pH beginning at pH 5.6 and reaches full tension at pH 6.6. The relation is described as: $\log_{10} \left(\frac{y}{1-y} \right) = \Delta H + \Delta V - 3(pH - pk)$ where y is the fractional tension, pk is the pH for half tension and $n = 3$, indicating that three active sites are involved per unit tension. The pk is increased by $[CP]$ and decreased by AMP. In respect to CP the pk is defined: $pk = 6.45 - 2 \log \frac{[CP]}{10}$ where 6.45 is the pH for 10 mM of CP and two phosphate ions are required per unit change in pk .

In glycerated fiber, tension is dependent on an activator, pH, and on the concentrations of phosphate donors. It is proposed that the same relation obtains in muscular contraction with an activator C substituted for pH. In both it is considered that temperature and pressure affect tension (a) through the volume and thermal changes involved in actomyosin-complex activation and (b) by affecting the rates of enzymatic reactions which act on phosphate donors.

The evidence is based on the value of ΔH and ΔV for tension $\left(\frac{y}{1-y}\right)$, under conditions where the activation of the actomyosin complex predominates and (b) where "steady state" tension exists. The evidence is the following:

Activation of AM complex and temperature: for $\left(\frac{y}{1-y}\right)$, ΔH $48,000 \div 3 = \Delta H$ 16,000 for pk. These values obtain for the 0.5 activated psoas fiber and for twitch tension in turtle auricle.

Activation and pressure: for $\left(\frac{y}{1-y}\right)$, $\Delta V = 350$ cc/mol. This value obtains for activation of the resting psoas fiber at pH 5.6, for tension increment in the pressure contracture, and for the tension increase of the resting treppe auricle. Since $m = 3$, ΔV for pk = -115 cc/mol.

The "steady state" of maximum tension and temperature: for $\left(\frac{y}{1-y}\right)$, $\Delta H = 36,000 \div 3 = \Delta H$ 12,000 for pk. These values exist in the psoas fiber for maximum tension above pH 6.6. Here the ΔH for pk is experimentally determined. For maximum tetanus tension similar values obtain although here the ΔH for pk is calculated.

"Steady state" of tension and pressure: for $\left(\frac{y}{1-y}\right)$ the ΔV is from + 50 to 60 cc/mol for both the glycerated psoas fiber and the tetanic contraction.

In myosin ATPase, the reversible denaturation yields $\Delta H = 10,000$ calories and $-\Delta V = 120$ cc while for the splitting of ATP, ΔH is 16,000 and ΔV is + 50 cc/mol. The similarity in values to those above suggests a basic role.

9. TEMPERATURE-PRESSURE STUDIES ON THE ROLE OF SOL-GEL REACTIONS IN CELL DIVISION.¹ Douglas A. Marsland, New York University.

A survey of the evidence bearing on the mechanism of cytokinesis in marine eggs provides firm support for the hypothesis that cleavage results from the contraction of the strongly gelled cortical cytoplasm (plasmagel layer), first in the equatorial region, and then in the walls of the deepening furrow. The strength of the furrowing reaction appears to be determined by the structural state of this plasmagel layer, as measured by the centrifugal method. Whenever the structural strength of the plasmagel is weakened to a critical degree, by high pressure or by low temperature, acting singly or in combination, furrowing is aborted and cleavage fails. Also, lesser degrees of weakening produce a proportionate retardation in the progress of the furrows.

Evidence is submitted which indicates that the splitting of the high potential phosphate bonds of adenosine triphosphate may contribute energy to the formation of the plasmagel structure—which is an endothermic process. In any event, the furrowing reaction and the plasmagel structure are both strengthened when additional ATP is provided via the surrounding sea water, and weakened when mersalyl acid (salyrgan), an inhibitor of ATP hydrolysis, is employed.

Generally speaking, the data indicate that the gelation process is causally related to the development of protoplasmic contractility and represents a mechanism by which the cell utilizes metabolic energy in the performance of mechanical work.

¹ Work supported by grant C807 and continuations from the National Cancer Institute.

Part III. C. STACY FRENCH, presiding

10. SYNCHRONIZATION OF CELL DIVISION BY CHANGES IN TEMPERATURE. Victor G. Bruce, Princeton University.

Recent work on the synchronization of the division cycle of bacteria and protozoa is reviewed and those systems in which synchronization has been effected by means of temperature changes are discussed in some detail. Recent ideas of the description of the division cycle, based on observations made principally on protozoa, are discussed. Attention is drawn to the existence of a period in the division cycle preceding division during which the cell is presumably reorganizing to divide. There is evidence to suggest that at some point during this period the cells enter more or less irreversibly into division and that there exists a sensitive step preceding this point which may be blocked by a variety of temperature effects. Experiments by O. Maaløe and the author, suggesting that the division cycle in bacteria is in some respects similar to that in protozoa, are briefly described.

The effects of sudden temperature changes on growth and cell division in the several synchronization systems described are considered. It is concluded that, at least in several of these systems, sudden temperature changes away from the optimum act in such a way as temporarily to prevent the completion of a specific step which is necessary to initiate division. On the other hand cells which have completed this step are not specifically inhibited by the temperature change.

11. TEMPERATURE ALTERATIONS OF THE RESPONSE OF CELL DIVISION TO URETHAN. Ivor Cornman, Hazleton Laboratories.

Carbamates, over a four-fold dose range, retarded the division of sea-urchin eggs without disrupting the ontogenetic process. *Echinarachnius* eggs at 20° C. were slightly retarded by 11 mM urethan and time to first cleavage was doubled at 22 mM. Carbamates of a great variety of alkyl and aryl substitutions also retarded cleavage in proportion to dose and, in general, the higher congeners were more effective than ethyl carbamate. In the two species most extensively studied, the effectiveness of carbamates varied with temperature. The first cleavage of *Arbacia* was retarded 6% at 21° C., 17% at 17° and was partially suppressed at 13° in one series using 55 mM urethan. In another, 44 mM retarded 2% at 21°, 7% at 25°, and 27% at 29°. Ethyl-N,N-diethyl carbamate also retarded minimally at 20–21°. It was always more effective than urethan, 7 mM retarding first cleavage 10% at 21°. *Echinarachnius* also showed these two separate trends in response to temperature, but the break in the curve came at 16°. It is proposed that the carbamate series are typical nonspecific hypnotics, held loosely in the cell by some physical mechanism. The carbamate molecules are less readily captured by the cell components at higher temperatures, but beyond a critical temperature, heat accelerates the process promoted by the carbamates. Denaturation of a single enzyme would fit this picture, but the system is too complex to yield a definitive answer.

12. CUMULATIVE EFFECTS OF OPTIMUM AND SUBOPTIMUM TEMPERATURES ON INSECT DEVELOPMENT. A. Glenn Richards, University of Minnesota.

Eggs of the Milkweed Bug, *Oncopeltus fasciatus*, incubated at constant temperatures, give the usual nearly hyperbolic time-temperature curve for development to hatching. The reciprocal of this curve, the rate-temperature curve, is sigmoid, and zero hatching is found experimentally at a considerably higher temperature (14° C.) than would be predicted from prolonging the rate-temperature curve to zero. Both direct examination and alternation between two or more temperatures show that embryonic development does occur at temperatures somewhat below the hatching threshold. If allowance is made for the rate of development at each temperature the time of hatching can be predicted with considerable precision, i.e., the necessary time for development can be calculated on a day-degree or calorie-counter basis.

In studies to determine the nature of the hatching threshold it was shown that the hatching process itself is not critical, and that there is no sensitive period during development when a vital process is blocked by threshold temperature. Arrhenius plots show that oxygen consumption of developing bugs is linear over the range 10–40° C., but that developmental rate is not. In the range 20–30° C. developmental rate gives a slope similar to that for oxygen consumption, but below 20° C. the developmental rate curve becomes much steeper. It follows that progressively more and more energy should be required to complete development as the temperature is lowered below 20°. This is confirmed by gross weight and fat determinations on bugs incubated at 25° and 17°, approximately 1.8 × as much energy being expended for development at the lower temperature. Calculation shows that the hatching threshold (14° C) is well correlated with the point at which complete exhaustion of the fat reserves in the egg would be expected.

But there is some change more vital than just developmental rate at incubation temperatures below 20° C because nymphs hatched at constant temperatures of 15–17° usually die even though placed under optimal conditions for growth. Also, nymphs hatched under optimal conditions (25° C, 75% R.H.) almost all eventually die if reared at 17°. Appropriate tests revealed no pathology even at the mitochondrial level, no significant difference in oxygen consumption, and no nutritional deficiency correctable by a fortified diet. However, the fatal debility can be prevented by brief daily exposure of eggs or nymphs to 25° even though the average temperature remains in the range that is fatal when maintained constantly. It is postulated that some factor needed for vitality requires temperatures above 20° for its synthesis, but available data do not exclude the alternative possibilities of an inhibitor or a physico-chemical change.

13. THEORETICAL IMPLICATIONS OF SOME EFFECTS OF TEMPERATURE ON PLANT PROCESSES. F. W. Went, California Institute of Technology.

Effects of temperature on plants are manifold. There are those in which temperature clearly influences the activation of a chemical process, and in which the Q_{10} ranges between 2 and 3. This is most clearly expressed in the effects of temperature on respiration. Above 35° C. the rate of respiration is decreased

with a pronounced time factor, suggesting a superimposed temperature effect on protein denaturation.

For many individual physiological processes such exponential relationships have been found. But for an even greater number of processes, especially of intact organisms, different and far more complicated temperature relationships exist.

Apparently simple is the effect of temperature on protoplasmic streaming. When the rate of streaming is plotted against temperature an almost straight line appears. This means that the Q_{10} steadily decreases from a high value to well below 2. Here an exponential plot obscures the real relationship. The same straight line temperature relationship exists for the effect of temperature on morphological differentiation in the growing point of peas, for instance.

For stem elongation and dry weight production in intact plants a very different temperature relationship exists. According to the species, variety, age and size of plant a different, but usually low, optimal temperature is found. In the tomato plant the optimal temperature in light is 23° C.; in darkness it is high (above 25° C.) in the seedling stage, and decreases gradually to 15–18° C. in mature plants, at least in full daylight. At lower light intensities this night optimal temperature drops to below 10° C. Greenhouse tomato varieties have lower optimal temperatures than outdoor varieties. Thus far, breeding has not extended the temperature range of tomato varieties, and they still require a relatively warm climate.

Again other processes have a temperature coefficient only slightly above 1. The growth in length of young pea plants is independent of temperature over the range of 13–23° C. The internal 24-hour rhythm of development of most plants is almost temperature independent.

At a Q_{10} of 2–3 it can be assumed that a chemical process controls plant growth. Below 17° C. it can be made reasonably certain that reactions involving auxin and other growth substances limit growth: only below 17° can tomato growth be accelerated by auxin or vitamins. Above this temperature physical processes involving all molecules, and not just the activated ones, become limiting for plant development.

Part IV. W. R. AMBERSON, presiding

14. THE USE OF LOW TEMPERATURE IN THE STUDY OF CERTAIN RESPONSES OF NERVE FIBERS. F. Crescitelli. University of California at Los Angeles.

The effects of low temperature on certain ion responses of the A and B fibers of the bullfrog sciatic nerve were examined with the view of showing the differences in behavior on the part of these two different fiber groups. The responses in the temperature range of 1° to 5° C were compared with the responses at 22° to 24° C. Cold was found to accelerate the rate of block by solutions containing high potassium. This was probably related to the increase in rate of depolarization by such solutions as the result of low temperature. The differential action of such high potassium solutions whereby the A fibers, as a group, blocked well ahead of the B fibers was found both at low and at

normal temperatures. The most notable effect of cold on the responses to sodium ions was the striking inhibition of recovery of the A fibers which were blocked as the result of treatment by solutions lacking sodium ions. Recovery following addition of a solution with a limiting concentration of NaCl (0.011M) was retarded or completely inhibited as the result of low temperature. In striking contrast to this behavior of the A fibers, the similarly blocked B fibers which, at 23° C., failed to respond to the limiting concentration of NaCl, were restored to significant activity by such a treatment at the low temperature. The differential action to sodium ions was thus radically altered by cold. These results are interpreted by assuming the existence of temperature sensitive systems in the A and B fibers. Each of these systems is assumed to have a temperature optimum for sodium action with a fall-off on either side of this optimum. The optimum for the B fibers is assumed to occur at lower temperature than the optimum for the A fibers. Differences in thermal responses on the part of different fiber groups is thus suggested as a characteristic of peripheral nerve fibers, thus confirming some of the ideas of the Swedish investigators in this area of research.

15. THE INFLUENCE OF CHANGES IN TEMPERATURE AND PRESSURE UPON THE ACTIVITY OF THE NERVE FIBER. Ichiji Tasaki and Constantine S. Spyropoulos, National Institutes of Health.

The effects of temperature and pressure changes upon the frog (or toad) single myelinated nerve fiber and the squid giant axon were reviewed. The material presented was obtained partly from observations published by other workers and partly from the authors' recent observations. Special emphasis was placed on the experiments made with internal stimulating and recording electrodes in the squid axon and on the observations carried out with single-node preparations of the toad. The first half of the discussion was devoted to the effects of temperature upon (1) the resting potential, (2) the capacity and resistance of the resting membrane, (3) the resistance of the axoplasm, (4) the size and shape of the action potential, (5) the time course of the action current, (6) the membrane resistance during activity, (7) thresholds, and (8) the conduction velocity. The second half of the discussion dealt with the effects of high hydrostatic pressures upon the squid giant axon and upon the toad nerve fiber. A reversible prolongation of the duration of the action potential (up to 4-fold increase at high pressures) was the main feature discussed. A short discussion was given of the temperature and pressure dependence of the effects of narcotics on the nerve fiber.

16. TEMPERATURE EFFECTS ON VISUAL PROCESSES. V. J. Wulff, Syracuse University.

The bleaching of illuminated rhodopsin is a thermo-labile process. At temperatures below 0° C., illuminated rhodopsin undergoes a slight change in color, forming transient orange, but bleaching occurs slowly or not at all (Broda and Goodeve, '41; Wald, et al., '50). Warming of a solution of transient orange results in bleaching of the pigment. The kinetics of the bleaching process

have recently been studied employing the technique of flash photolysis (Wulff, *et al.*, '56; Hagins, '56). Hagins employed isolated but intact eyes from previously dark adapted albino rabbits and demonstrated a transient bleaching of pigments in the retina following flash excitation. The bleaching was measured at 480 $m\mu$. The bleaching process followed an exponential time course having the following half-times: at 12° C., 20 msec.; at 26° C., 1 msec.; and an estimated $\frac{1}{2}$ time of 125 μ sec. at 37° C. The effect of temperature upon the behavior of cattle rhodopsin in solution was determined employing flash photolysis techniques. At room temperature rhodopsin excited by a 400 joule flash of 80 μ sec. duration exhibits the following transient changes: (1) a new absorption band appears during the flash, exists less than 200 μ sec and has a maximum at 600 $m\mu$; (2) a second new absorption band appears in the blue with a maximum at 425 $m\mu$; (3) bleaching with a maximum at 525 $m\mu$ begins late during the exciting flash and progresses in the dark, reaching a maximum about 5 msec. later at 28.5° C; (4) the maximum of the blue absorption band first moves toward the red, about 445 $m\mu$ and then declines; (5) as the bleaching process approaches completion a new broad absorption band appears with a maximum at 380 $m\mu$.

Cold rhodopsin (approximately 0° C.) excited as above, exhibits strong red and blue absorption bands as long as 500 μ sec. after excitation and, up to this time, no bleaching is apparent.

The latent period of the retinal action potential elicited by illuminating dark adapted photoreceptors with short light flashes increases in duration as the temperature is reduced (Fry, *et al.*, '55). The Q_{10} values obtained from experiments with grasshopper, *Limulus* and frog eyes range from 2.3 to 4.0. The magnitude of the retinal action potential is much less affected by temperature than is the latent period. Q_{10} values obtained range from 1.0 to 1.3. In grasshoppers one can select intensities and durations of illumination such that temperature in the range 10° C. to 30° C. has no effect on the magnitude. The effect of temperature upon both latent period and magnitude of the retinal action potential are discussed in terms of a kinetic model of two coupling processes: an electrochemical process which generates the retinal action potential and a timing process which controls the duration of the latent period (Wulff, *et al.*, '55).

17. THE INFLUENCE OF TEMPERATURE UPON RESISTANCE TO ASPHYXIA. J. A. Miller, Emory University. (Abstract not received.)

18. EFFECTS OF LOW BODY TEMPERATURES ON RESPIRATORY GAS EXCHANGE IN THE ANESTHETIZED DOG. Arthur B. Otis, University of Florida College of Medicine.

Lowering the body temperature of the anesthetized dog produces a relatively greater reduction in ventilation than in oxygen consumption and CO₂ production, with an accompanying hypoxia and respiratory acidosis. At a temperature of about 20–25°C., breathing ceases entirely and asphyxial death results. If ventilation is continued by artificial means the circulation may continue to be adequate for respiratory gas transport at temperatures down to 15° C. or lower, although ventricular fibrillation occurs rather frequently at temperatures below

25°C. Transfer of O₂ and CO₂ by diffusion probably remains adequate in both lung and tissues as long as ventilation and circulation are maintained, although there is a possibility that it may fail in localized regions of the body.

Contributed papers

Storrs, Connecticut, August 29

ABSTRACTS

19. THE ACCURACY OF THE ENDOGENOUS ACTIVITY RHYTHMS OF SMALL MAMMALS AND THEIR RESPONSE TO LOW BODY TEMPERATURES. Kenneth S. Rawson, Harvard University.

The time of onset of the major daily spontaneous activity of wood mice (*Peromyscus leucopus noveboracensis*) and bats (*Myotis l. lucifugus* and *Eptesicus f. fuscus*) is an accurate measure of their "24-hours" activity rhythms. In constant darkness each animal exhibited an endogenous rhythm which differed both from an exact 24-hour period and from the "24-hour" periods of other animals studied at the same time.

Analysis of a 39 day record of one of the most accurate *Peromyscus* in constant darkness showed a period of 23 hours 54 minutes \pm 1.62 minutes for the rhythm. The scatter of the daily measurements was described by 95% confidence limits of \pm 10 minutes. The periods of the rhythms of other mice ranged in value between slightly less than 23 hours and slightly more than 24 hours.

Bats recorded in constant darkness for several months exhibited endogenous activity rhythms with much shorter periods than the mice (about 21 hours). Experimentally lowering the body temperatures of both mice and bats increased the periods of the endogenous rhythms, but only slightly. The temperature relationships may be described by Q_{10} values ranging between 1.04 and 1.1.

20. THE PERMEABILITY OF RAT LIVER MITOCHONDRIA TO ELECTROLYTES.¹ Henry Tedeschi and Daniel L. Harris, The University of Chicago.

The uptake of ions has been studied by photometric methods in heart sarcosomes (Cleland, '52) and by radioactive tracer or analytical techniques in mitochondria of various tissues, in the presence or absence of substrates (Harman, '50; Bartley and Davies, '52; Spector, '53; MacFarlane and Spencer, '53; Stanbury and Mudge, '53; Mudge, '54; Robertson et al., '55). Although results of great interest have been obtained, few data appear to be available which would permit analysis of the underlying physico-chemical mechanisms.

In the present study the permeability of rat liver mitochondria to ions was studied in the absence of substrate using photometric techniques (see Tedeschi and Harris, '55) together with direct analytical estimation.

Mitochondria are probably bounded by a lipid semi-permeable membrane, since they obey osmotic laws and their permeability to non-electrolytes depends on the oil-water partition coefficient of the penetrants (Tedeschi and Harris, '55). Evi-

dence has now been obtained supporting the following interpretations which are in complete accord with those reached, on both theoretical and experimental grounds, in comparable systems, e.g., the erythrocyte:

1. The distribution of ions depends on the charge of the non-diffusible molecules within the mitochondrion (Donnan effect), anions tending to penetrate to balance a positive charge, cations a negative one.
2. The shifts in ionic content are reflected in osmotic volume changes.
3. Weakly ionized compounds exchange mainly in their non-ionized form.
4. The rate of exchange of charged particles is a function not only of the concentration gradient for the particular ion, but also of the charge of the ionic groups within the mitochondria.
5. In general, anions penetrate more readily than cations. There seem, also, to be changes with pH in the permeability properties of the membrane.

¹Supported in part by a grant-in-aid from the American Cancer Society upon recommendation of the Committee on Growth of the National Research Council and in part by the Wallace C. and Clara M. Abbott Memorial Fund.

21. FACTORS INFLUENCING THE SWELLING AND ELECTROLYTE CONCENTRATIONS OF MONKEY BRAIN SLICES. J. F. Manery and H. Husdan, University of Toronto.

When thin slices of cerebral cortex were incubated for three hours in mammalian Ringer's solution at 2° C. they swelled until the concentration of water reached an asymptotic level of 87% of the final wet weight; the gain of sodium exceeded the loss of potassium and the gain of chloride exceeded the net gain of measured cations ($\Delta \text{Na} - \Delta \text{K}$). The addition of 7% albumin to the medium reduced the water uptake without altering the electrolyte pattern appreciably.

Similarly cortex slices incubated for one hour at 37° C in mammalian Ringer's solution containing glucose and glutamate swelled and gained water to a value of 87%. Although less potassium was lost and less sodium gained than at 2° C., still the sodium gain exceeded the potassium loss and the chloride uptake was in excess of the net cation uptake. The addition of 7% albumin to this medium reduced the water uptake to the same extent as in the cold and also caused a reduction in the quantity of sodium and chloride gained by the tissue.

The influence of 4 factors (temperature, substrates, electrolyte changes and external colloid osmotic pressure) on water movement in brain slices will be discussed.

22. RESPIRATORY PATTERNS IN REGENERATING NUCLEATE AND ENUCLEATE FRAGMENTS OF *Stentor coeruleus*. Arthur H. Whiteley, University of Washington and the Carlsberg Laboratory, Copenhagen.

The respiratory rates of whole stentors, of stentors that have been cut in two but allowed to reform a whole, and of half stentors containing various nuclear and cytoplasmic proportions have been measured during 6 days following the operations. The animals were starved during this period. Both classes of whole stentors show a general decline in rate of respiration with time, reflecting starvation and diminution in size. Emaconucleate "halves," cut to include the

mouth, heal but regenerate only minimally and die within 6 days. The respiratory rate falls correspondingly, most quickly during the first two days. By contrast, nucleate "halves," containing all the macronuclear beads and two-thirds of the cytoplasm, but lacking the mouth and zone of junction of fine and coarse ciliated lines, regenerate completely in 24 hours. These show a sizeable absolute rise in respiratory rate which, relative to the controls, is considerable. After two days, the rate declines progressively until death. The rise is not a response to cutting. To distinguish between the possibilities (1) that the rise is a corollary of head regeneration *per se* and (2) that it is an over-compensation in the cytoplasm due to the abnormally high macronuclear/cytoplasmic ratio, respiratory patterns have been determined in fragments with normal macronuclear/cytoplasmic ratios, and with and without head regeneration. These and other results support the second alternative: that, when stimulated, the macronuclear complement of a whole stentor tends to form the respiratory machinery of a whole, even in a diminished amount of cytoplasm.

23. INDUCED BIOSYNTHESIS OF RESPIRATORY ENZYMES IN BAKER'S YEAST.
Aristid Lindenmayer, University of Pennsylvania.

Anaerobically grown yeast cells lack the enzymes of the respiratory chain, but will synthesize them upon exposure to oxygen. Previous workers (Ephrussi, Slonimski) found adaptation kinetics of the first order both for the increase in the rate in O_2 uptake and for cytochrome *c* formation, while we find a discrepancy between their developments. The study of this adaptive system has the advantage that most of the enzymes involved can be measured directly by spectrophotometric methods, and these might also be applicable to possible precursors and inducer complexes. Cells of *Saccharomyces cerevisiae*, strain LK2G12 were grown under strict anaerobiosis in a medium containing ergosterol and oleic acid, and harvested in the late logarithmic phase. Adaptation took place in a 3% glucose-M/15 KH_2PO_4 solution, and samples were taken at 20 minute intervals for three hours. Determinations were made of the O_2 uptake in the presence of several substrates with a polarized platinum electrode, and of the cytochrome difference spectra with a recording sensitive spectrophotometer. Both intact cells and cell-free extracts were used, and in the extracts the cytochrome *c* oxidase and the succinic- or DPNH-cytochrome *c* reductase activities were also measured. The adaptation kinetics for the rate of O_2 uptake was found to be linear with time, while the formation of the cytochromes *a*, *b* and *c* followed S-shaped kinetics. The QO_2 increased to 30% of its adapted value before any change appeared in the level of cytochromes, thus indicating that some other adapting member of the respiratory system was rate limiting during that period.

24. METABOLIC EFFECTS OF A DEFICIENCY IN CO_2 FIXATION IN NEUROSPORA.¹
Bernard S. Strauss, Syracuse University.

Conidia of *Neurospora crassa* incubated in sucrose and buffer incorporate $C^{14}O_2$ into an acid-soluble and a residual fraction. Addition of an ammonium salt causes a threefold increase of incorporation into both fractions. Conidia of a mutant

requiring a dicarboxylic acid for growth are unable to increase the amount of $C^{14}O_2$ fixed into the residual fraction on the addition of an ammonium salt although the amount fixed in the acid-soluble fraction increases. Asparagine increases CO_2 fixation into the mutant residual fraction in the presence of ammonium salts but inhibits wild-type CO_2 incorporation. Ammonium ion inhibits the incorporation of $CH_3C^{14}OOH$ into acid-soluble, alcohol-ether soluble and residual fractions of the mutant but stimulates acetate incorporation by the wild-type. Asparagine overcomes the ammonium inhibition of acetate incorporation by the mutant. Glutamic acid is present in both mutant and wild-type conidia but disappears from mutant conidia on incubation in sucrose-buffer plus ammonium ion. The mutant accumulates pyruvic acid and ketoisovaleric acid when incubated in sucrose-buffer only in the presence of ammonium ion. It is supposed that the mutation has blocked dicarboxylic acid synthesis by CO_2 fixation. Ammonium ion diverts the limited supply of dicarboxylic acid available from catalysis of the tricarboxylic acid cycle thereby inhibiting acetate incorporation and leading to keto acid accumulation. This hypothesis is supported by the finding that strains carrying the gene leading to a dicarboxylic acid requirement for growth are unable to incorporate $C^{14}O_2$ into pyruvic acid in contrast to the ability of acetate-requiring mutants.

¹ Supported in part by funds from the U. S. Atomic Energy Commission and the National Science Foundation.

25. ORIGIN OF THE ACTION POTENTIAL. Reinhard H. Beutner, Des Moines Still College.

The presently accepted ionic permeability theories postulate a purely physical process, *viz.* ion transfer according to the mobility of ions, but this postulate is at variance with many facts. While the action potential depends on the outside Na^+ concentration, this cannot be caused by Na^+ transfer, since ion mobility is never specific, but depends on ion size. The e. m. f.'s in tissue are likely to be generated at phaseboundaries by the contact of immiscible conductors, like lipoid with aqueous solution. These contact p. d.'s exist at the very boundary of immiscible conductors. There is nothing in between, no distance greater than molecule to molecule. In comparison, ion diffusion, like any diffusion, extends along some distance.

Two mutually opposing contact p.d.'s stand face to face, one at each membrane contact surface inside and outside. Moreover, the membranes are chemically variable and reactive. Stimulation elicits rapid chemical changes which are initiated when the stimulating current drives an enzyme activating ion into the nerve membrane. A most likely reaction to be elicited by such an enzyme action is the reversible splitting of the phospholipids, whereby the electrogenic choline or a cholinester is formed. This occurs at first only on one side of the membrane, rendering the membrane asymmetrical and producing an e. m. f. causing the upstroke of the spike. The splitting then extends across the membrane (transmembrane reaction), and on reaching the other contact surface, effects the downstroke. *A single chemical reaction progressing in one direction can thus account for both up- and down-stroke.* No Na^+ pump is needed.

26. ENZYME LOCALIZATION IN SPERMATOOA AT THE ELECTRON MICROSCOPE LEVEL. Leonard Nelson, University of Chicago.

Tissues prepared by freezing and drying may be expected to retain to a high degree their spectrum of native enzyme activity. Rat epididymal sperm were frozen in propane at -175°C. , and dried *in vacuo* in such a way as to avoid formation of ice crystals large enough to be visible with the electron microscope. Without further preliminary treatment, the sperm were infiltrated *in vacuo* in barbital buffer, pH 9.4, containing CaCl_2 and cysteine. After incubation in adenosinetriphosphate at room temperature for 2, 5, 10 and 30 minutes respectively, the specimens were washed with alcohol to terminate the reaction. Numerous controls were run. The specimens were embedded in methacrylate, sectioned and viewed in the electron microscope.

The phosphate liberated by enzymatic activity is precipitated as calcium salt which appeared in the microscope as electron dense regions. The nine radially disposed axial fibers running through the flagellum show markedly more contrast than those in the control specimens. It is concluded that adenosinetriphosphatase may be present in greater activity in these sites. The short incubation periods required of material prepared for electron microscopy, may very sharply limit the amount of diffusion of enzyme or enzyme reaction product. The relation of these observations to a mechanism of sperm motility will be discussed. Similar methods are being employed in distribution studies of additional enzyme systems in spermatozoa as well as other cell types.

PHOTORECEPTOR STRUCTURES¹

I. PIGMENT MONOLAYERS AND MOLECULAR WEIGHT

JEROME J. WOLKEN

*Biophysical Research, Laboratory Molecular Biology, Eye and Ear Hospital,
University of Pittsburgh Medical School, Pittsburgh, Pa.*

FOUR FIGURES

We are investigating the structure of photoreceptors, the chloroplasts and retinal rods in a variety of plant and animal material, and particularly the structural changes accompanying the synthesis and bleaching of the pigments during the light \rightleftharpoons dark reactions (Wolken and Palade, '52, '53; Wolken and Schwartz, '53, and Wolken and Mellon, '56).

Newer techniques in fixation and thin-sectioning for electron microscopy have shown that the chloroplasts from a variety of plant material (Steinman, '52, '55; Palade, '53) and the retinal rods of frog, guinea pig and perch are laminated discs whose thickness is the same order of magnitude (Sjostrand, '49, '53, and Fernández-Morán, '54).

Our studies by electron microscopy of osmium fixed algal flagellates showed that the chloroplasts are composed of piled-up discs or plates, approximately 42 for *Euglena* and 20 for *Poteriochromonas*. These plates consisted of dense bands approximately 250 Å in thickness with denser peripheries 60–100 Å in thickness with less dense interspaces 200–500 Å in thickness. This laminated chloroplast structure was formed only in photosynthesizing light-adapted organisms and not in chemosynthesizing dark-adapted organisms. This structural arrangement together with the pigment analysis permitted a

¹ Aided in part by grants-in-aid from U. S. Public Health Service, Institute Neurological Diseases and Blindness (B-397); the National Council to Combat Blindness, Inc. (158-C); and The McClintic Endowment.

schematic molecular model of the chloroplast in which the pigment (chlorophyll) molecules are oriented at the interfaces between protein and lipid layers. The interfacial area occupied by each chlorophyll molecule was calculated from the experimental data of the geometry of the chloroplast, the number of chlorophyll molecules per chloroplast, and the number of the dense laminae. These calculated values for *Euglena* and *Poteriochromonas* were found to be 226 Å and 246 Å squared respectively, which is in good agreement with known x-ray data of the "porphyrin head" of the chlorophyll molecule. In addition, the ratio of the number of chlorophyll to carotenoid molecules could be predicted (Wolken and Schwartz, '53).

In the present paper we have extended these studies to (1) the electron microscopy of the photoreceptors, the chloroplast, and the outer segments of the frog and cattle retinal rods, (2) the calculation of the pigment-macromolecule weight from geometric considerations, based on our schematic model, for both the chloroplast and retinal rod, and (3) the pigment-macromolecule molecular weight from analytical data, independent of the geometry, for algal chloroplastin and frog rhodopsin.

EXPERIMENTAL METHODS

Isolation of retinal rods. Dark-adapted cattle eyes were obtained from the slaughter house and frog eyes from dark-adapted frogs (*Rana pipiens*) in our laboratory. The retinas were dissected from 24 cattle and 60 frog eyes in red light. The dissected retinas were shaken and vigorously stirred in 1.32 molar sucrose using 15 ml sucrose per 24 retinas. The suspension was poured through several layers of cheese cloth. The resulting suspension was centrifuged at 1800 rpm for 15 minutes, and the sediment discarded, this was repeated several times for 5 minutes. The outer retinal rod segments remain in the supernatant. A fraction of these were fixed in osmium tetroxide for electron microscopy, the remainder was used for rhodopsin extraction.

Electron microscopy. The fixation, dehydration, embedding, and sectioning used have been described by Palade ('52) and by Wolken and Palade ('53). The chloroplast electron micrographs were obtained using a model EMU electron microscope. The frog and cattle retinal rod electron micrographs were obtained using Phillips 100 EM electron microscope. In neither case was the material shadow-cast or the plastic material removed from the specimens.

Chloroplastin was prepared from cultures in the log phase of growth from two algal flagellates (*Euglena gracilis* and *Poterochromonas stipitata*). The organisms were concentrated by centrifugation and the centrifuged pellets were ground with sand and 0.9% saline in the cold and recentrifuged twice at 3000 rpm. Each time the pelleted material was discarded. The green supernatant fluid was dried under vacuum. This dried supernatant was extracted either with 2% aqueous digitonin² or Nacconal NRSF² and the extracts diluted to 1.8% with buffer to pH's between 9.2–8.6. The *chlorophyll concentration* was determined according to the method of Arnon ('49) using the specific absorption coefficient for chlorophyll a and b as given by McKinney ('41). The method is given in Wolken and Schwertz ('53).

The pigment concentration, sedimentation constant, nitrogen, and dry weight of the chloroplastin-detergent extracts were determined on freshly prepared material, from three separate preparations.

Rhodopsin was prepared as outlined by Collins, Love and Morton ('52), which is essentially Saito's method. All work was carried out in red light. Prior to extraction of rhodopsin, the number of rods/ml were determined in a Levy blood counting chamber. The rhodopsin was extracted with 2% aqueous digitonin and the extracts diluted with buffer to 1.8% and to a pH of 9.2–8.6.

² Nacconal NRSF — anionic organic detergent-alkyl aryl sulfonate, National Aniline Division, Allied Chemical and Dye Corporation. Digitonin — (C⁵⁵H⁹⁰O²⁰) — anionic detergent, D-58, Fisher Scientific Company.

The purity of the rhodopsin was estimated using the criteria of Wald ('38 and '51) using $K_{\frac{400}{500}}$, the absorption ratio in millimicron. These values varied from 0.29–0.67 for separate extractions.

Rhodopsin concentration was determined by measuring the optical density at 500 mμ in a Beckman spectrophotometer and using the molar extinction value (40,600 cm²/mole) as determined by Wald and Brown ('53).

$$\log_{10} \frac{I_0}{I} = e \times c \times l$$

where I_0 is the incident light, I the absorbed light, e the molar extinction, c the concentration in moles/liter, and l the depth of the solution in centimeters.

The pigment concentration, sedimentation constant, nitrogen, and dry weight of the rhodopsin-digitonin extracts were determined on freshly prepared material from three separate preparations.

Ultracentrifuge measurements were performed with Spinco Model E. For determining the sedimentation constant (S_{20}), the density and viscosity of the medium at the temperature of the ultracentrifuge were measured by use of a calibrated pycnometer and Oswald viscosimeter, respectively.

The average value, S_{20} (in Svedburg units), for the rhodopsin-digitonin complex was 12.1×10^{-13} , for digitonin 7.1×10^{-13} , for chloroplastin-digitonin complex 13.5×10^{-13} , for chloroplastin-Nacconal complex 5.4×10^{-13} , and for Nacconal 2.9×10^{-13} . In figure 4 analytical ultracentrifuge patterns are shown. These show the rhodopsin-digitonin complex sediments as a single boundary and the complex is homogeneous.

The molecular weights were calculated from the equation

$$M = \frac{RTS_{20}}{D_{20} (1 - p \bar{V}_{20})}$$

where R the gas constant, is 8.32×10^7 dynes/cm, T , the absolute temperature, S_{20} , the experimentally determined sedimentation constant, D_{20} the diffusion constant, p the density, and \bar{V}_{20} the partial specific volume. The values for the dif-

fusion constant of the digitonin complex (D_{20}), 4×10^{-7} cm²/sec., and the partial specific volume (\bar{V}_{20}), 0.738, were obtained from Hubbard ('54). Similar values for Nacconal (in the calculation, $D_{20} = 10.3 \times 10^{-7}$ cm²/sec. and $\bar{V}_{20} = 0.75$) were obtained from the work of Miller and Anderson ('42).

Nitrogen was determined in the algal chloroplastin and frog rhodopsin by a micro Kjeldahl method using Nessler's reagent with standards.

EXPERIMENTAL RESULTS AND CALCULATIONS

The chloroplasts appear in the light microscope as elongated cylinders measuring $\sim 1 \mu \times 10 \mu$, the outer frog retinal rods $\sim 5 \times 50 \mu$, and the outer cattle retinal rods $\sim 1 \times 10 \mu$. In the phase contrast microscope (the chloroplasts) show a faint lamination and in the polarizing microscope they appear to be birefringent. Both these facts, particularly the latter, suggest the existence of an ordered structure below the limits of resolution of the light microscope (W. J. Schmidt, '34). The retinal rods of the frog appear laminated in the light microscope, but are not of the same order of magnitude observed in the electron microscope (Wald, '54).

The total thickness of the dense layers measured from the electron micrographs and their number were used for calculation, and not their apparent denser peripheries ~ 60 – 100 Å. The structural data for the photoreceptors are given in table 1, and are average values obtained from measurements of many electron micrographs. Wilmer ('55), in a critical review summarizes much of the recent information on the retinal structure.

CALCULATIONS OF MOLECULAR WEIGHTS

A. Molecular weight from geometry and schematic molecular model

The chloroplast and retinal rod photoreceptors have a lamellar structure comprising alternate layers of lipids and aqueous protein complexes as shown in figure 3, a schematic model for the retinal rod photoreceptor. (See Wolken and

Schwartz, '53 for schematic molecular model for the chloroplast.) According to the models there are monomolecular layers of pigments at the interfaces between these layers and each pigment molecule is bound to a single lipoprotein³ macromolecule.

On this view, the layer containing the lipids and lipoproteins consists of a double layer of *lipoprotein macromolecules* with the low molecular weight lipids occupying the interstitial spaces. This arrangement is shown in the enlarged portion of figure 3. The maximum cross-sectional area, A , associated with each macromolecule, and therefore with each pigment molecule, is

$$A = \frac{\pi D^2}{4P} \quad (1)$$

where D is the diameter of the photoreceptor and P is the number of pigment molecules in a single monomolecular layer. The *maximum* possible volume, V , associated with a macromolecule is then

$$V = \frac{\pi D^2 T}{8P} \quad (2)$$

where T is the average thickness of the lipid-lipoprotein layers. The maximum pigment-macromolecule molecular weight, M , is therefore

$$M = \frac{\pi D^2 T s L}{8P} \quad (3)$$

where s is the lipoprotein density and L is Avogadro's Number. If N is the pigment concentration expressed in molecules per photoreceptor and n is the number of lipid layers per photoreceptor,

$$P = \frac{N}{2n} \quad (4)$$

Equation (3) may therefore be written in a form containing only the experimental observables:

$$M = \frac{\pi D^2 T s L n}{4N} \quad (5)$$

³ *Lipoprotein* is used in preference to lipid layer, since it includes the lipids and other macromolecular material. As yet there is no chemical analysis of these layers, but the dense layers are referred to in the literature as either lipid or lipoprotein because of their affinity for osmium tetroxide used in fixation.

To calculate the molecular weight, we take $s = 1.3$ gm per cubic centimeter and $L = 6 \times 10^{23}$. The other quantities appearing in equation (5) are listed in table 1. The data relative to the two algae appearing in this table were taken from Wolken and Schwertz ('53). The experimental values for T and n of the frog and cattle retinal rod were obtained from our electron micrographs of fixed isolated preparations (see figure 1 c, d, e and figure 2 a, b, c, d). The molecular weights

TABLE 1
Structural data and calculated molecular weights

PHOTORECEPTOR	D, PHOTO- RECEPTOR DIAMETER, IN MICRONS	T, THICK- NESS OF LIPID LAYERS, IN ANGSTROMS	n, NUMBER LIPID LAYERS PER PHOTO- RECEPTOR	N, NUMBER PIGMENT MOLECULES PER PHOTO- RECEPTOR	M, MOLECULAR WEIGHT OF PIGMENT- MACRO- MOLECULE
Chloroplast of <i>Euglena gracilis</i>	8.27	242	21	1.02×10^6	21,000
Chloroplast of <i>Poterochromonas</i>	4.15	390	10	1.10×10^5	37,000
Retinal rod of frog	5.0	150	1000	$3.8 \times 10^{10*}$	60,000
Retinal rod of cow	1.0	200	180	$4.2 \times 10^{10+}$	40,000

* Hubbard ('54) uses 2.1×10^9 molecules to calculate a molecular weight $\sim 50,000$ for frog rhodopsin. Broda, Goodeve and Lythgoe ('40) determined value of 3.7×10^9 , this would give a molecular weight 61,000.

+ Value of Hubbard ('54).

calculated with the aid of these data are entered in the last column of table 1.

It is of interest to consider the calculation of the *maximum* cross sectional area, A , associated with each macromolecule and therefore with each pigment molecule. This can be derived from Equation (1) where P is replaced by $N/2n$:

$$A = \frac{\pi D^2 n}{2N} \quad (6)$$

The values calculated from this equation are listed in table 2 along with the values of macromolecular diameters, d_m , calcu-

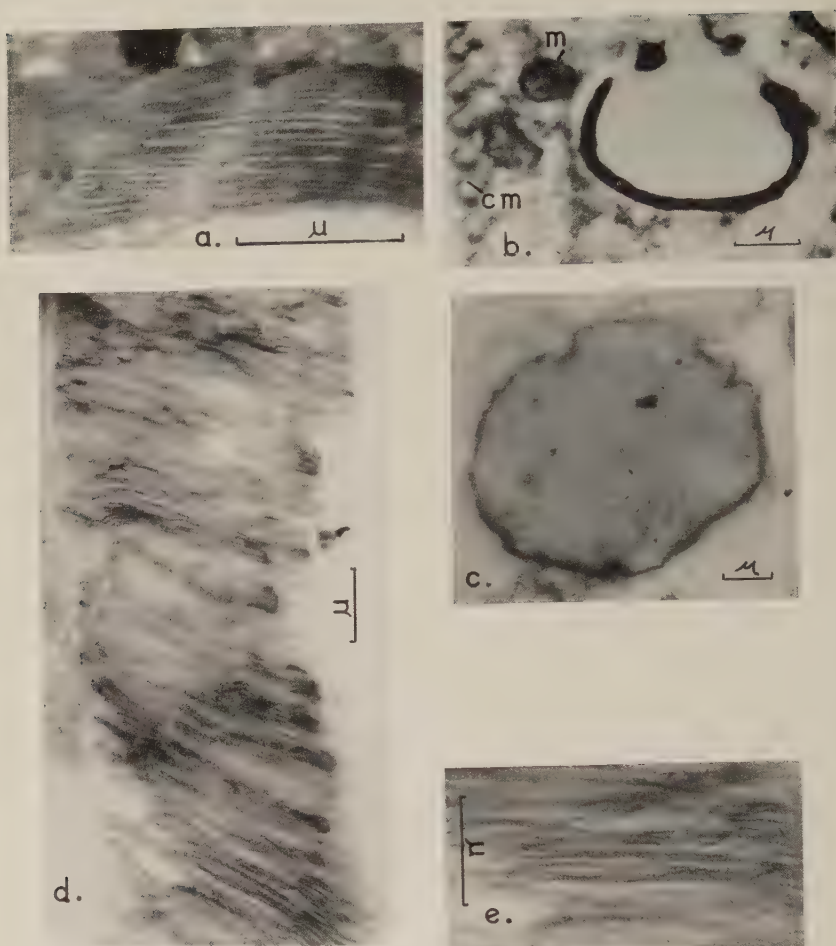


Figure 1

a. Electron micrograph thin-section *Euglena gracilis* showing chloroplast *in situ*, indicating lamella, dense and less dense layers. Magnification $\times 39,000$.

b. Electron micrograph thin-section *Euglena gracilis*, dark-adapted, showing collapsed chloroplast or "ghost structure." Also showing cm, cell membrane; m, mitochondria. Magnification $\times 15,000$.

c. Electron micrograph thin-section of isolated frog retinal rod, cross-section of a unit disc. Magnification $\times 11,500$.

d. Electron micrograph thin-section of isolated frog retinal rod outer segment, longitudinal section showing lamellar structure. Magnification $\times 17,200$.

e. Electron micrograph of part from d, enlarged to show apparent double membranes in lamellar structure. Magnification $\times 26,000$.

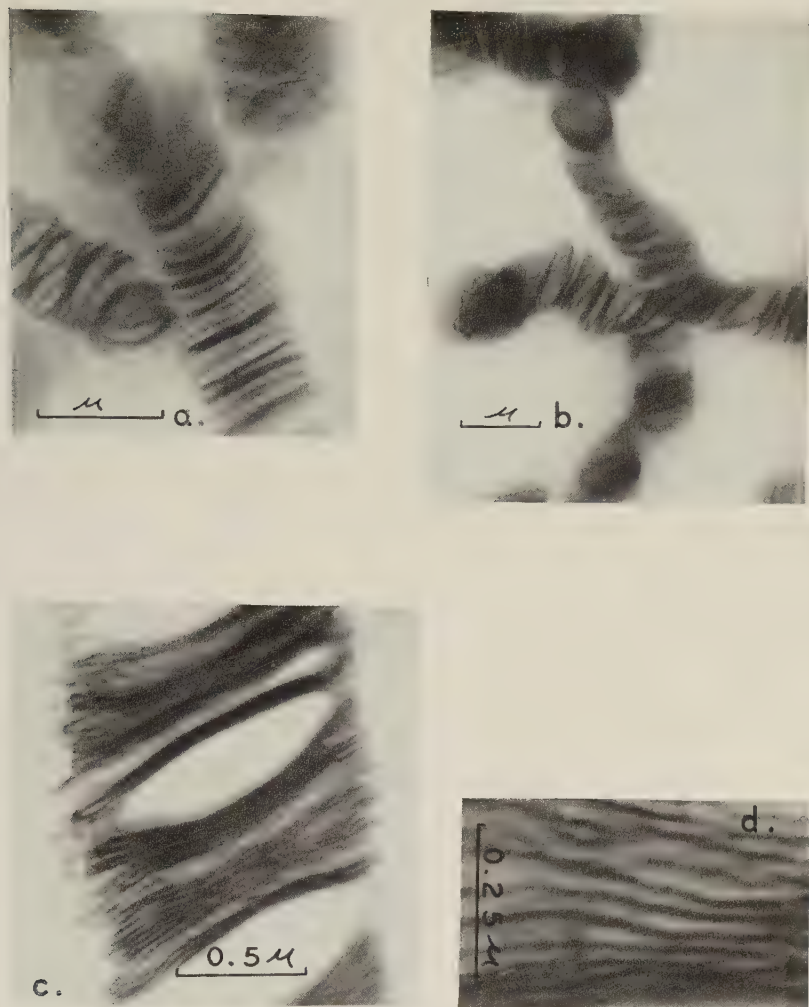


Figure 2

a. Electron micrograph thin-section of isolated cattle retinal rod, showing laminated structure and "pile-up of plates." Magnification $\times 27,800$.

b. Same as (a) above, at lower magnification to indicate length $\sim 10 \mu$ for retinal rod outer segment. Magnification $\times 18,500$.

c. An enlarged section of the retinal rod membranes indicating an apparent double layer. Magnification $\times 46,000$.

d. A greatly enlarged section of the retinal rod membranes. Magnification $\times 137,000$.

lated on the assumption that the molecules are cylindrical rods (Wolken and Schwertz, '53).

As in our earlier paper (Wolken and Schwertz, '53), the quantity A is associated with the area of the hydrophilic porphyrin head of the chlorophyll pigment. The porphyrin heads of the chlorophyll molecules in the algal flagellates are rather *tightly packed* together in the interfacial monolayers; however, the linear pigment molecules retinene in the retinal rod are *loosely packed*.

TABLE 2

Dimensions of pigment macromolecules calculated from the photoreceptor geometry

PHOTORECEPTOR	CROSS-SECTION AREA, A, OF MACROMOLECULES IN ANGSTROMS SQUARED	DIAMETER, d_m , OF MACRO- MOLECULES IN ANGSTROMS	LENGTH, $T/2$ OF MACROMOLECULES IN ANGSTROMS
<i>Euglena gracilis</i> chloroplastin	222	17	121
<i>Poteriochromonas</i> <i>stipitata</i> chloroplastin	246	18	195
Frog rhodopsin (<i>Rana pipiens</i>)	2620	51	100
Cattle rhodopsin	2500	50	100

B. Molecular weight from analytical data

In order to obtain an independent value for the molecular weights, the pigment-lipoprotein macromolecules were extracted from the photoreceptors with the aid of aqueous solutions of nitrogen-free detergents. From the extracts, chloroplastin and rhodopsin, it was possible to obtain 4 important quantities: (1) the pigment concentration by absorption spectroscopy; (2) the molecular weight of the pigment-lipoprotein detergent complex by analytical ultracentrifugation; (3) the dried weight of the extract from which the pigment-lipoprotein weight could be obtained by subtracting the known contribution of the detergent; and finally, (4) the nitrogen content of the dried extract.

The pigment-lipoprotein molecular weights may be calculated from these data by assuming that the nitrogen content is 15% by weight, and the pigment molecules are arranged in monolayers. Data from analytical ultracentrifugation permitted an estimation of the lipoprotein molecular weights. These were calculated from the weights obtained for the pigment-lipoprotein-detergent complexes and the detergent

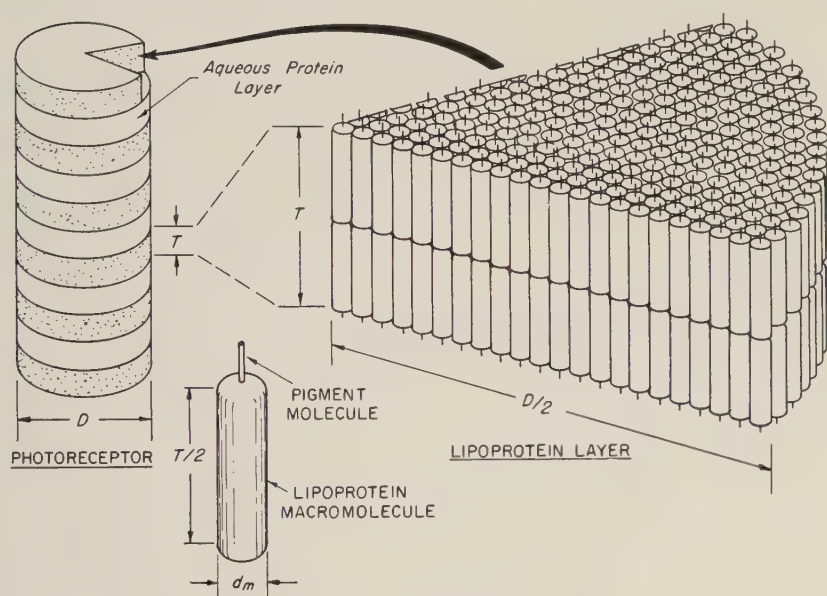


Fig. 3 Schematic molecular photoreceptor model for the outer segment of the retinal rod.

micelles alone. The detergents used in the experiments were Nacconal NRSF and digitonin. A discussion of detergents and detergent micelle molecular weights are reviewed by Putnam ('48). Nacconal forms micelles in water of minimal molecular weight equal to 12,500–15,000. Miller and Anderson ('42) and Smith and Pickels ('40) have similarly shown that digitonin forms micelles of minimal molecular weight equal to 75,000. Hubbard ('54) has demonstrated that three such micellar units of digitonin are probably associated with rho-

dopsin. Assuming that a similar situation holds for Nacconal, the lipoprotein molecular weights may be readily determined. The results are shown in 1 and 2 of table 3. From these published values, the quantity $3 \times 75,000 = 225,000$ for the digitonin-complex weight and $3 \times 12,500 = 37,500$ for the Nacconal-complex weight have been subtracted to give the molecular weights indicated in 3 and 4. The molecular weights appearing in 5 and 6 of the table were obtained using three-halves of the authors' experimental values for the detergent micelle weight for the following reasons: 1. The micellar groups are almost certainly symmetrical with respect to a certain position of symmetry. In this position the hydrocarbon, hydrophobic tails of the detergent molecules probably meet back-to-back, the hydrophilic heads being imbedded in the surrounding water. 2. When these micellar groups are shaken in the presence of the pigment-lipoprotein complexes, they cleave across the plane of symmetry, the segments reforming about the body of the pigment-lipoprotein macromolecule with the hydrocarbon, hydrophobic tails of the detergent molecule positioning back-to-back against the hydrocarbon portion of the lipoprotein macromolecule and the hydrophilic heads again projecting into the surrounding water. Only two "sides" and the "bottom" of the lipoprotein macromolecule will be so sheathed, the hydrophilic pigment being entirely compatible with the surrounding aqueous atmosphere. If such reasoning is sound, one should use three-halves of the micellar molecular weight in estimating the contribution of the detergent to the molecular weight values entered in 5 and 6 of table 2. The agreement between the values of table 1 and table 3 is reasonably good although the bases for the calculations are different.

From the analytical data in table 4 for the algal chloroplastin and frog rhodopsin, the molecular weight can be calculated from

$$M = \frac{w' (100)}{P (15)} \quad (7)$$

where M is the molecular weight of the pigment-lipoprotein

macromolecule, w' is the weight of nitrogen in milligrams associated with 1 ml of the extract, and P is the pigment concentration in moles per liter of extract. The calculated values of M are entered in table 4. The other experimental data

TABLE 3
Molecular weights of pigment-macromolecule complexes

PHOTORECEPTOR	<i>Euglena gracilis</i> CHLOROPLASTIN	<i>Potriochromonas</i> <i>stipitata</i> CHLOROPLASTIN	FROG RHODOPSIN
1. Complex weight with digitonin	290,000	275,000	300,000
2. Complex weight with naccenal	69,400	65,000	.. .
3. Molecular weight complex (minus digitonin micelle weight)	65,000	50,000	75,000
4. Molecular weight from naccenal complex (minus naccenal micelle weight)	31,900	27,500	.. .
5. Molecular weight from digitonin complex (minus digitonin ¹ micelle weight)	57,500	42,500	67,500
6. Molecular weight from naccenal complex (minus naccenal ¹ micelle weight)	31,150	26,750

¹ Experimental minimum digitonin micelle weight 155,000.

Experimental minimum naccenal micelle weight 25,000.

listed in table 4 are M' the molecular weight of the complex as determined by the analytical ultracentrifuge, w the total dry weight in milligrams associated with a milliliter of the extract, and w'' the contribution in milligrams of the detergent to the dry weight per milliliter of extract.

TABLE 4
Analytical data

ALGAL CHLOROPLASTIN (<i>Euglena gracilis</i>)	DIGITONIN COMPLEX			NAGCONAL COMPLEX		
	1	2	3	1	2	3
w mg/ml	29.0	27.3	29.6	44.3	42.5	23.0
w' mg/ml	0.37	0.36	0.35	3.1	3.8	0.67
w'' mg/ml	21.6	21.6	21.6	19.8	19.8	19.8
P moles/liter	4.2×10^{-5}	6.3×10^{-5}	7.7×10^{-5}	9×10^{-4}	9×10^{-4}	0.91×10^{-4}
M' gram/mole	290,000	290,000	290,000	69,400	69,499	69,400
M calculated molecular weight	59,000	38,000	30,000	23,000	28,000	50,000

FROG RHODOPSIN (<i>Rana pipiens</i>)	1	2	3
	1	2	3
w mg/ml	21.0	20.0	20.0
w' mg/ml	0.033	0.029	.026
w'' mg/ml	13.2	15.0	15.0
P moles/liter	3.2×10^{-5}	1.6×10^{-5}	2.2×10^{-5}
M' gram/mole	300,000	300,000	300,000
M calculated molecular weight	69,000	120,000	54,000

DISCUSSION

Molecular weights calculated from the geometrical considerations and independent methods for algal chloroplastin are in reasonably good agreement. No recent experimental data are available for the molecular weight of algal chloroplastin for comparative purposes. The data for chloroplastin has been previously obtained from leaf extracts (spinach and aspidistra) prepared, however, in a similar manner and analyzed in the ultracentrifuge. Smith ('41a, b, c) and Smith and Pickels ('40) found molecular weights of the order of 265,000;

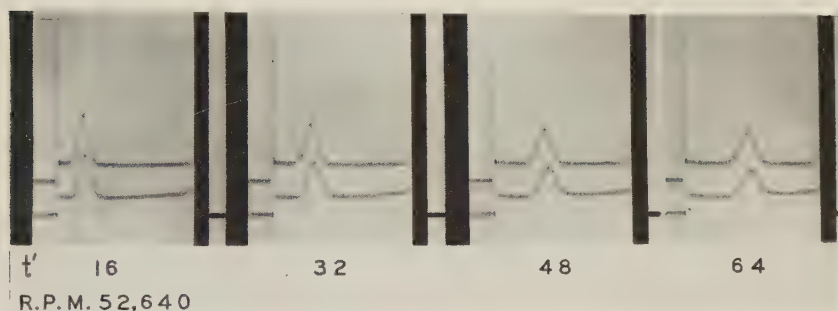


Fig. 4 Plate from Analytical ultracentrifuge showing sedimentation the rhodopsin-digitonin complex, for various time intervals to 64 minutes, run at 52,640 rpm.

this high estimate is in part due to the contribution of the digitonin micelle. Takashima ('52) crystallized a chlorophyll-lipoprotein complex from an α -picoline leaf extract at low temperature, and from diffusion studies found its molecular weight to be 19,200, and postulated a complex of two molecules of chlorophyll per molecule of lipoprotein.⁴

From the chloroplastin analytical data table 4 it is possible to show that one pigment molecule is associated with each macromolecule. This is done by demonstrating that the ex-

⁴Recently Smith and Kupke (*Nature*, 178: 751, 1956) isolated from bean seedlings (*Phaseolus vulgaris*) a chlorophyll-holochrome in glycine-KOH pH 9.6 and determined its S_{20} -15.3-16.2 which suggests a molecular weight 400,000. They did not determine the number of chlorophyll molecules or the chlorophyll to protein ratio in this complex.

perimentally determined chlorophyll concentration P is substantially the same as p' calculated from the formula

$$P' = \frac{w}{M'} \frac{\text{weight of dried residue}}{\text{molecular weight of complex from ultracentrifuge}} \quad (7)$$

(Wolken and Schwertz, '56).

With frog rhodopsin the situation is more difficult because of the questionable criteria of purity. Our values may be distorted by both low nitrogen values for rhodopsin and high values for dry weight (the weight is high with respect to the pigment concentration). It is felt, however, that the values for pigment concentration, the ultracentrifuge data, and the nitrogen determinations are reliable. Using this information we can evaluate a minimum molecular weight of rhodopsin. In the ultracentrifuge, we have obtained an average molecular weight for the frog rhodopsin-digitonin complex of 300,000 and that for the digitonin micelle of 155,000.

Now, to answer the question of how many rhodopsin molecules add up to this weight: if it is one, two, or three molecules, then one can calculate the expected nitrogen for a solution of known concentration, if one assumes a nitrogen content of 15%. Our solution in this case had a concentration of 3.18×10^{-6} moles per liter.

Concentration X assumed molecular weight $X .15 = N$ in grams per liter.

	145,000		.069
	or		or
$3.18 \times 10^{-6} \times$	72,000	$\times .15 =$.035
	or		or
	48,000		.023

If one uses either our nitrogen value of .033 or our minimum of .026, then the lower molecular weights are the most probable. It will be remembered that the geometrical model predicts a value of 60,000.

The molecular weight of the tightly bound lipoprotein macromolecules, from algal chloroplasts, frogs and cattle

retinal rods, have been calculated from the model assuming that each molecule is bound to a single pigment molecule. The contribution of the macromolecules to the total weight of the dried extract was then calculated from nitrogen analyses assuming that nitrogen comprises 15% of the protein weight. A knowledge of this weight together with the pigment concentration permitted the calculation of the lipoprotein macromolecular weight. In addition, the lipoprotein molecular weight was determined by an independent method which *did not* involve the assumption that each pigment molecule was attached to a single lipoprotein macromolecule. For this method the analytical ultracentrifuge was used to determine the molecular weight of the complexes comprising the pigment. The molecular weight was calculated on the assumption that the fractional weight of lipoprotein in the complex was the same as that in the dried extract. Here again, molecular weights were obtained which were in good agreement with values obtained by the previously described techniques.

It is of interest to include one other calculated value for the pigment-macromolecule weight associated in the chloroplast. Although these studies are only in its beginning, it was possible to calculate the mass associated for the chloroplast in *Euglena g. in vivo*. The Cooke-Dyson Interference microscope permits one to calculate the mass of the chloroplast from the wave path difference and having previously determined the area of the chloroplast and its pigment concentration, it was possible to calculate the pigment-macromolecule molecular weight as given by Davies et al. ('54) from the following equation

$$M = \frac{\phi A N}{X P} \quad (8)$$

Where M is the mass or the gram molecular weight associated with the pigment-macromolecule, ϕ is the optical path difference produced by the chloroplast, X is a constant associated with the medium, P is the average number of chlorophyll molecules per chloroplast, and N Avogadro's number. By sub-

stituting the experimental values ⁵ in equation (8) an average of 16,000 was calculated for the macromolecular weight. Although it sets a lower limit to the molecular weight of algal chloroplastin it is surprisingly similar to the molecular weight calculated from geometric considerations alone.

The experimental value for frog rhodopsin determined by Broda, Goodeve, and Lythgoe ('40) was 27,600. This was based on the assumption that there are 10 chromophores per molecule of rhodopsin. Weale ('49) has calculated a value of 45,600 from spectroscopic considerations. Hubbard ('54), from analytical methods, reported the molecular weight of cattle rhodopsin to be 40,000, and estimated that a similar value, $\sim 50,000$, would apply for frog rhodopsin. Our molecular weight data is in agreement with that of Hubbard, which indicates that the ratio of chromophore to lipoprotein molecules is within experimental error, one-to-one. Nevertheless, we cannot exclude the possibility that the lipoprotein macromolecules may span the width of the lipid layer with a pigment molecule at each interface, thus yielding a *two-to-one* ratio.

SUMMARY

A schematic molecular model for the photoreceptor is proposed on the basis that the plant and animal photoreceptors, chloroplasts and outer segment of the retinal rods, are probably composed of alternating layers of lipid and aqueous protein complexes separated by monomolecular layers of pigment molecules. The molecular weights of the pigment-macromolecule complex from two algal flagellates, frog rhodopsin, and cattle rhodopsin has been determined from: 1. the schematic model and geometry of the photoreceptors, values of 21,000 and 37,000 were obtained for the complex from the algal flagellates, *Euglena g.* and *Poteriochromonas* respectively;

$$^5 \phi = 1.1 \times 5460 \text{ \AA} \lambda \text{ green filter} \times 10^{-8} \text{ cm or } .73 \times 6600 \text{ \AA} \text{ red filter} \times 10^{-8} \text{ cm}$$

$$X = 0.18 \text{ constant}$$

$$A = \text{area of chloroplast } 8 \times 10^{-8} \text{ cm}^2$$

$$M = \text{gram molecular weight pigment-macromolecule}$$

$$P = \text{average number of molecules chlorophyll per chloroplast } 1 \times 10^9$$

$$N = \text{Avogadro's Number } 6 \times 10^{23}$$

60,000 and 40,000 for frog and cattle rhodopsin respectively, (2) the analytical ultracentrifuge values 57,000–65,000 for *Euglena* chloroplastin, 27,000–50,000 for *Poterochromonas* chloroplastin, and 67,000–75,000 for frog rhodopsin, (3) the nitrogen analysis, dry weight, and pigment concentration 30,000–59,000 for *Euglena* chloroplastin, 23,000–50,000 for *Poterochromonas* chloroplastin, and 54,000–120,000 for frog rhodopsin.

From calculations of the maximum cross-sectional area occupied by the pigment-macromolecule the chlorophyll molecule would be tightly packed at the interfaces in the chloroplast and the retinene molecules would be loosely packed at the interfaces in the retinal rod. The calculations also suggest that a single pigment molecule is associated with each lipoprotein macromolecule.⁶

ACKNOWLEDGMENTS

I should like to thank Dr. F. A. Schwartz for the many discussions and suggestions during the progress of this research.

LITERATURE CITED

- ARNON, D. I. 1949 Copper enzymes in isolated chloroplasts. *Plant Physiol.*, **24**: 1.
- BRODA, E. E., C. F. GOODEVE AND R. J. LYTHGOE 1940 The weight of the chromophore carrier in the visual purple molecule. *J. Physiol.*, **98**: 397.
- COLLINS, F. D., R. M. LOVE AND R. A. MORTON 1952 Studies on rhodopsin. 4. Preparation of rhodopsin. *Biochem. J.*, **51**: 292.
- DAVIES, H. G., AND M. H. F. WILKINS 1954 The use of the interference microscope to determine dry mass in living cells and as a quantitative cytochemical method. *Q. J. Micros. Sci.*, **95**, part 3: 271.

⁶ Since this paper was submitted, additional reviews have appeared on the chloroplast structure by K. Mühlethaler, *International Review Cytology*, **IV**, 1955; J. B. Thomas, *Progress in Biophysics and Biophysical Chemistry*, **V**, 1955; H. Leyon, *Svenk. Kem. Tidskr.*, **68**: 70, 1956; E. I. Rabinowitch, *Photosynthesis and Related Processes*, **II**, pt. 2, 1956. Additional electron microscopic studies have also appeared on the retinal structures by E. De Robertis, *J. Biophys. and Biochem. Cytol.*, **2**: 319, 1956, and H. Fernandez-Moran, *Nature*, **177**: 742, 1956. Our own work has been extended to include the "eye-spot" in *Euglena* (*J. Protozool.*, **3**, No. 4, 1956) and the insect visual structure, the rhabdomere (*J. Exp. Zool.*, in press, 1957).

- FERNÁNDEZ-MORÁN, H. 1954 The submicroscopic structure of nerve fibres. *Prog. Biophys. and Biophys. Chem.*, 4: 112.
- HUBBARD, R. 1954 The molecular weight of rhodopsin and the nature of the rhodopsin-digitonin complex. *J. Gen. Physiol.*, 37: 381.
- McKINNEY, G. 1941 Absorption of light by chlorophyll solutions. *J. Biol. Chem.*, 140: 315.
- MILLER, G. L., AND K. J. I. ANDERSON 1942 Ultracentrifuge and diffusion studies on native and reduced insulin in duponol solution. *J. Biol. Chem.*, 144: 475.
- PALADE, G. E. 1952 A study of fixation for electron microscopy. *J. Exp. Med.*, 95: 285.
- 1953 An electron microscope study of the mitochondrial structure. *J. Histochem. and Cytochem.*, 1: 188.
- PUTNAM, F. W. 1948 The interaction of proteins and synthetic detergents. *Advances in Protein Chemistry*, IV: 79.
- SCHMIDT, W. J. 1934 Doppelbrechung, Dichroismus und Feinbau Des Aus-sengleides Der Sehzellen Vom Frosch. *Z. Zellforsch. u. mikroskop. Anat.*, 22: 189.
- SJOSTRAND, F. S. 1949 An electron microscope study of the retinal rods of the guinea pig eye. *J. Cell. and Comp. Physiol.*, 33: 383.
- SJOSTRAND, F. S. 1953 The ultrastructure of the outer segments of rods and cones of the eye as revealed by the electron microscope. *J. Cell. and Comp. Physiol.*, 42: 15.
- SMITH, E. L. 1941 (a) The effect of detergents on the chlorophyll-protein compound of spinach as studied in the ultracentrifuge. *J. Gen. Physiol.*, 24: 753. (b) The chlorophyll-protein compound of the green leaf. 565. (c) The action of sodium dodecyl sulphate on the chlorophyll-protein compound of the spinach leaf. 583.
- SMITH, E. L., AND G. E. PICKELS 1940 Micelle formation in aqueous solutions of digitonin. *Proc. Nat. Acad. Sciences*, 26: 272.
- STEINMAN, E. 1952 An electron microscope study of the lamellar structure of chloroplasts. *Exp. Cell Res.*, 3: 367.
- STEINMAN, E., AND F. S. SJOSTRAND 1955 The ultrastructure of chloroplasts. *Exp. Cell Res.*, 8: 23.
- TAKASHIMA, S. 1952 Chlorophyll-lipoprotein obtained in crystals. *Nature*, 169: 182.
- WALD, G. 1938 On rhodopsin in solution. *J. Gen. Physiol.*, 21: 795.
- 1951 The chemistry of rod vision. *Science*, 113: 287.
- 1954 Mechanism of Vision. Nerve Impulse—Transactions 4th Conference Josiah Macy, Jr., Foundation, New York, N. Y.
- WALD, G., AND P. K. BROWN 1953 The molar extinction of rhodopsin. *J. Gen. Physiol.*, 37: 189.
- WEALE, R. 1949 Absorption spectra, molecular weights, and visual purple. *Nature*, 163: 916. *Nature*, 164: 959.
- WILLMER, E. N. 1955 Physiology of vision. *Annual Review Physiology*, 17: 339.
- WOLKEN, J. J., AND A. D. MELLON 1956 The relationship between chlorophyll and the carotenoids in the algal flagellate, *Euglena*. *J. Gen. Physiol.*, 39: 675.

- WOLKEN, J. J., AND G. E. PALADE 1952 Fine structure of chloroplasts in two flagellates. *Nature*, 170: 114.
- 1953 An electron microscope study of two flagellates. Chloroplast structure and variation. *Ann. New York Acad. Sci.*, 56: Art. 5, 373.
- WOLKEN, J. J., AND F. A. SCHWERTZ 1953 Chlorophyll monolayers in chloroplasts. *J. Gen. Physiol.*, 37: 111.
- 1956 The molecular weight of algal chloroplastin. *Nature*, 177: 136.

METABOLISM OF SOME CARBOHYDRATE AND PHOSPHATE COMPOUNDS DURING HIBERNATION IN THE GROUND SQUIRREL¹

MARILYN L. ZIMNY^{2,3,4}

*Department of Anatomy, Stritch School of Medicine,
Loyola University, Chicago, Illinois*

TWELVE FIGURES

INTRODUCTION

Recent trends in the field of research concerning metabolism have once again focused attention upon the phenomena of hibernation. Many phases of possible adjustment mechanisms in the hibernating mammal have been studied. This work has proposed various theories which have been reviewed by Rasmussen ('16), Johnson ('31), Suomalainen ('35), Benedict and Lee ('38), Kayser ('53) and Lyman and Chatfield ('55).

Although levels of blood glucose and tissue glycogen have been determined in hibernating animals (see above reviews), quantitative determinations of other compounds involved in the Meyerhoff-Krebs glycolysis cycle of muscle contraction have not been undertaken. The present study was designed to fill, at least partially, this rather serious gap in our knowledge of the physiology of the hibernating mammal. It includes in addition to biochemical and histochemical determinations of liver, skeletal muscle and cardiac muscle glycogen in hibernating ground squirrels, biochemical determinations

¹ Supported by a grant from the Chicago Heart Association issued to Dr. George Finlay Simmons.

² Standard Oil Research Fellow, 1953-54.

³ Partial fulfillment of the requirements for the degree of Doctor of Philosophy.

⁴ Present address: Louisiana State University, School of Medicine, New Orleans, Louisiana.

of skeletal and cardiac muscle lactate and phosphate fractions and histochemical determinations of phosphate deposition in these tissues. Considering the slow heart rate during hibernation phosphate determinations seemed particularly important since Wollenberger ('51), working with dogs, found that a marked decrease in heart rate resulted in a significant rise in cardiac phosphocreatine content and a corresponding decrease in free inorganic phosphate.

MATERIALS AND METHODS

Adult male ground squirrels, *Citellus tridecemlineatus*, captured in the field during the Spring and Summer of 1952 and 1953 were paired according to sex and age. The latter factor was based upon the date of capture and sexual condition at that time. These animals were nembutalized and the following values recorded: (1) body weight; (2) body temperature, using a Leeds-Northrup short-range potentiometer with an iron-constantan thermocouple which was inserted rectally to a depth of 5 cm; (3) heart rate, as determined by a Sanborn single-channel viso-cardiette; and (4) respiration rate, by means of a stop-watch. In recording the latter rate three counts were made during the hour preceding sacrifice and the average taken as the representative value. Following these measurements and after fully recovering from the anesthesia, one animal of each pair was placed in a control room (25° C.) and the other animal was placed in a cold room (3-5°C.). Both controls and experimentals received food and water ad libitum.

During the time the experimental animal in the cold room was in hibernation, the fore-mentioned physiological values were recorded, the animal sacrificed and tissue taken for biochemical and histochemical studies. In all instances skeletal muscle samples were obtained from the hind limbs. The same procedure was followed the same day for the control, non-hibernating animal. In sacrificing control animals, nembutal was injected intraperitoneally to anesthetize the animals. The thoracic cage was then opened and the heart frozen in

situ with an ether-dry ice mixture. Liver and skeletal muscle were also frozen in situ before removal. This same procedure was used for the experimental animals. However, before the injection was made the nembutal, syringe and needle were cooled to the temperature of the cold room. The anesthesia was not necessary for this group but was used to equalize the procedure.

The criteria for determining hibernation in the ground squirrel were as follows: (1) the hibernating position, as described by Johnson ('31); (2) coldness to touch; (3) spasticity of limbs, as demonstrated by the slow but definite recoil process which followed manual stretching of limb by experimenter; (4) a decrease in heart rate to 25 beats/min. or less; (5) a decrease in body temperature to within 1 to 1.5° above that of the environmental temperature; and (6) a decrease in respiration rate to 0.5 to 5 respirations/min.

In accord with the work of Foster, Foster and Meyer ('39) and Lyman ('43) the present work was based upon short-term hibernation. The animals that were used for the glycogen studies had hibernated two to three days while those used for the lactate and phosphate studies had hibernated 4 to 5 days.

Tissue removed for biochemical glycogen studies was frozen in an ether-dry ice mixture. The weights of the samples varied from 0.950 gm to 1.00 gm for liver, 0.890 gm to 1.00 gm for skeletal muscle and 0.810 gm to 1.00 gm for cardiac muscle. Liver and skeletal muscle tissue were digested in 5 ml of 30% potassium hydroxide while cardiac muscle was digested in 2.5 ml of 30% potassium hydroxide. Biochemical determinations were made in duplicate according to Pfluger's method as modified by Good, Kramer and Somogyi ('33) for glycogen and Somogyi's method as modified by Nelson ('44) for glucose hydrolyzed from glycogen.

Samples of liver, skeletal muscle and cardiac muscle taken for histochemical study were immediately fixed in Rossman's fluid (9 parts saturated solution of picric acid in absolute alcohol, one part neutral formalin) refrigerated over night,

dehydrated and imbedded in paraffin the next day. Sections were cut at 6μ and stained by the periodic acid-Schiff's technique. In order to confirm the fact that glycogen was responsible for the staining reaction, the glycogen was removed from control sections by digestion in 0.5% malt diastase (Pfanstiehl) for 20 min. at 37°C .

Due to the small size of the heart, sufficient tissue was not available in a single animal to enable one to make all determinations on each individual of one series of animals. Therefore, the animals of one series were used for the glycogen studies only and the animals of a second series were used for both lactate and phosphate studies. In the animals of the latter series the same tissue sample was analyzed in obtaining these values. The biochemical determination of lactate followed that of Miller and Muntz ('38) and that of the phosphate fractions was based upon the Fiske-Subbarow reaction ('29) as used by Wollenberger ('47).

For histochemical localization of phosphate in cardiac and skeletal muscle, tissues were fixed in absolute alcohol, dehydrated and imbedded in paraffin. Sections were cut at 7μ , hydrated and hydrolyzed for 5 to 10 min. in a molybdate solution (a mixture of equal parts of 5% ammonium molybdate and 1% nitric acid). This was a modification of the procedure of Serra and Queiroz Lopes ('45) whereby the phosphate is liberated from organic combinations in the tissue before it can be detected. Following a wash in tap water, the slides were immersed in 10% silver nitrate solution and irradiated with ultra-violet light for one hour. The silver nitrate precipitation and consequent silver reduction represent a modification of the procedures of Gersh ('38) and von Kossa ('01). The sections were then washed again, dehydrated, cleared in xylene and mounted in picolyte.

RESULTS

The physiological measurements in this investigation pertain to body weight, rectal temperature, respiration rate and heart rate. These values along with the observations of the

hibernating position (Johnson, '31), spasticity of limbs, as previously described and coldness to touch are indicators as to whether or not the animals are truly hibernating. The decreases in all of these values were significant and correspond favorably with the measurements reported in the literature, especially the work done on the same species (Johnson, '31). An analysis of this data is given in figure 1. From this evidence it can be said that the experimental animals in this

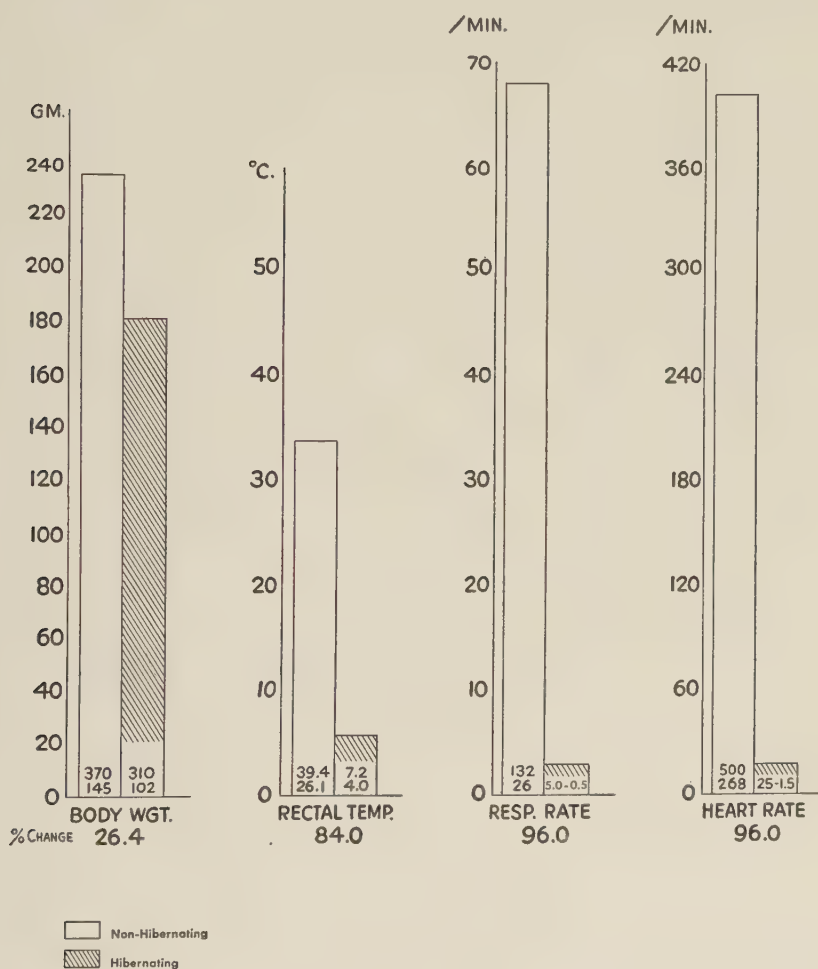


Fig. 1 Analysis of physiological measurements.

investigation were hibernating when tissue samples were taken for analysis. These results also indicate a decreased oxygen intake along with lowered metabolism.

As to be expected in animals fed ad libitum there was a great variation in the glycogen values between individuals of both the control, non-hibernating, and the experimental, hibernating, ground squirrels. It was also notable that after two to three days of hibernating 60% of the experimental animals showed markedly decreased levels, while 40% maintained control levels. In comparing the results for the hibernating animals, the data was broken down into three categories. First, taking the groups as a whole (table 2, animals nos. 1542-1551 and 1564-1568) the average values were as follows: cardiac muscle, 221 mg %; skeletal muscle, 219 mg %; and liver, 675 mg %. Secondly, considering those animals that showed a marked depletion of glycogen (table 2, animals nos. 1542, -43, -44, -45, -47, -51, -64, -65, and -68) the average values were the following: cardiac muscle, 101 mg %; skeletal muscle, 129 mg %; and liver, 50 mg %. Thirdly, the average values for those animals that maintained normal levels during hibernation (table 2, animals nos. 1546, -48, -49, -50, -66, and -67) were as follows: cardiac muscle, 400 mg %; skeletal muscle, 535 mg %; and liver, 1593 mg %. Whether one considers the group as a whole or in the preceding segregated arrangement, it is evident that in depletion of glycogen during hibernation liver, skeletal muscle and cardiac muscle decrease in that order, respectively. When comparing the experimental animals that showed a marked depletion of glycogen with the controls the following percentage decreases took place during hibernation: cardiac muscle, 72.9%; skeletal muscle, 79.8%; and liver, 98.5%. In comparing the individuals within the experimental group of the series used for the glycogen studies it became evident that the experimental animals maintaining control levels had respiration rates during hibernation of 3 to 5 respirations/min. as opposed to the other experimental animals showing marked glycogen depletion that had respiration rates of 0.5 to 2/min.

The fact that cardiac muscle appears to be the last to undergo glycogenolysis during glycogen depletion in the intact animal agrees with work cited by Soskin and Levine ('52). The results obtained from those animals which did not show depletion of glycogen during hibernation essentially agree with the work of Lyman and LeDuc ('53) on the hamster.

A significant decrease in both cardiac ($P < .05$) and skeletal muscle ($P = .05$) lactate levels was found after 4 to 5 days of hibernation. In both cardiac and skeletal muscle increases and decreases after 4 to 5 days of hibernation pertain to the same phosphate compounds. The decrease in inorganic phosphate during hibernation was not great (cardiac muscle a 1% decrease and skeletal muscle a 23% decrease) thus attention is given to the significant changes which occurred in regards to adenosine polyphosphate ($P < .01$) and phosphocreatine ($P < .01$). Adenosine polyphosphate decreased while phosphocreatine was the only compound in this investigation which showed a persistent significant increase. It may also be of interest to note that the percentage decrease in adenosine polyphosphate and the percentage increase in phosphocreatine were approximately the same. This applies to both cardiac and skeletal muscle.

An analysis of the lactate and phosphate biochemical data is given in figure 2. Due to the variations in the biochemical glycogen data it is not included in this scheme. Composite records of the data for control and experimental animals appear in table 1 and table 2, respectively.

Tissue glycogen in cardiac muscle, skeletal muscle and liver was demonstrated by the periodic acid-Schiff procedure (figs. 3 to 8). Uniform distribution of glycogen throughout the lobule was noted in the liver. In skeletal muscle glycogen was usually found in close proximity to the Z-membrane. However, it was also scattered in varying amounts throughout the muscle fiber. Cardiac muscle glycogen being reported as extremely labile (Illingworth and Russell, '51) showed no

definite arrangement histologically, but did provide visual support for the biochemical values. These results are in accord with similar studies on the hamster (Lyman and Le-Duc, '53).

Those animals that showed marked decreases in biochemical glycogen levels during hibernation likewise showed depletion histochemically. The same degree of correlation applies to those animals that maintained normal glycogen levels during hibernation. The tissue from these animals gave a control, non-hibernating picture. Thus in all cases the histochemical localization of glycogen coincided with the quantitative biochemical determinations.

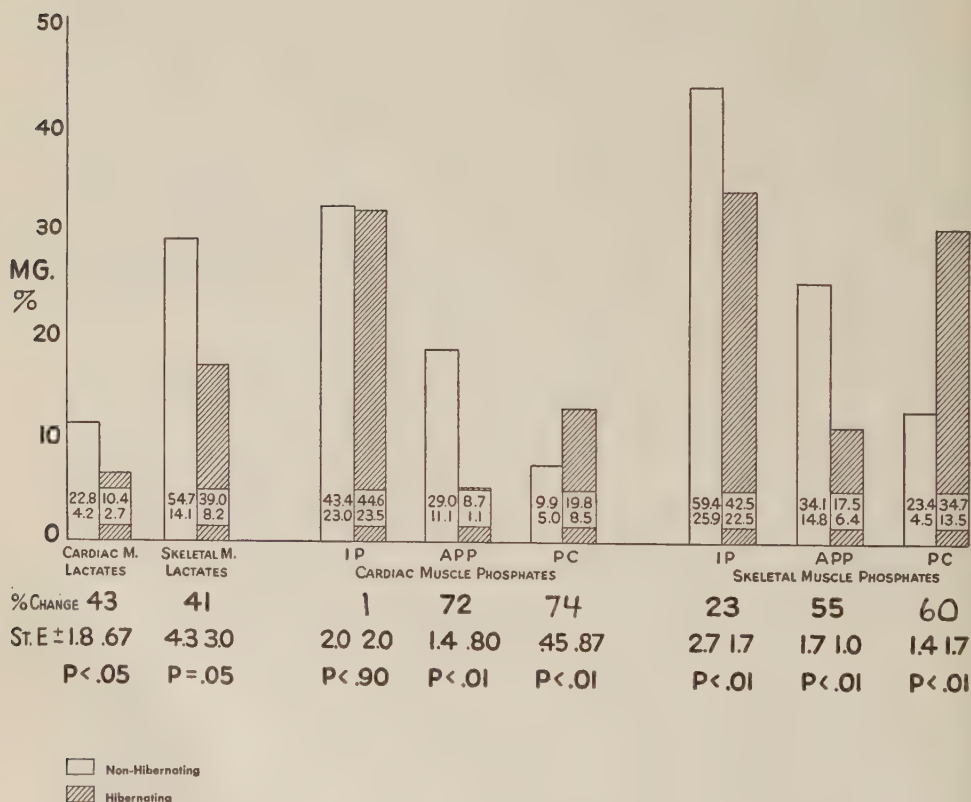


Fig. 2 Analysis of biochemical data.

TABLE 1

Composite record of data for control ground squirrels

ANIMAL	BODY WT. IN GM.	RECTAL TEMP. °C.	RESP. RATE /MIN.	HEART RATE /MIN.	CARDIAC GLYCOGEN	SKELETAL M.	LIVER GLYCOGEN	CARDIAC LACTATE	SKELETAL M. LACTATE	CARDIAC I.P.	M. A.P.P.	CARDIAC P.O.	SKELETAL I.P.	SKELETAL M. A.P.P.	SKELETAL P.O.
					mg %	mg %	mg %	mg %	mg %	mg %	mg %	mg %	mg %	mg %	mg %
1520	146	30.1	43.3	327	376	398	1381								
1521	186	28.1	47.1	340	307	636	1302								
1522	178	30.9	80.0	295	384	436	1696								
1523	177	34.0	99.0	467	207	312	1408								
1524	213	34.4	132.0	500	219	537	1724								
1525	222	32.7	103.0	500	341	427	1733								
1526	156	29.8	52.3	375	352	664	1564								
1527	180	33.1	34.0	417	770	1724	1711								
1528	190	32.7	45.1	389	369	744	1711								
1529	200	36.0	41.0	389	256	506	1724								
1530	257	38.7	44.0	375											
1531	240	37.9	48.0	402											
1532	237	35.4	75.0	402											
1533	322	39.0	84.0	429											
1534	179	35.8	56.0	465											
1535	262	33.0	81.0	375											
1536	238	34.2	50.0	351											
1537	315	33.6	50.0	402											
1538	263	36.5	85.0	402											
1539	232	37.2	54.0	268											
1540	339	35.0	101.0	375											
1541	230	32.4	111.0	429											
Average	226	33.7	68.9	394	358	595	1597	11.3	29.0	32.1	18.4	7.4	43.4	24.6	12.5

Localization of phosphate in cardiac and skeletal muscle was accomplished through molybdate hydrolysis and silver nitrate precipitation (figs. 9 to 12). Both types of muscle showed scattered phosphate deposits whether from non-hibernating or hibernating animals. In no way could the histochemical studies be correlated with the biochemical determinations. The only conclusion that could be made was that phosphate was present in cardiac and skeletal muscle in both non-hibernating and hibernating ground squirrels.

DISCUSSION AND CONCLUSIONS

In order to obtain some new information with regard to the factors involved in the initiation of, maintenance of and awakening from hibernation it is important to study further the biological fluctuations which take place during this period. A number of theories had been postulated but as yet a cause and effect relationship had not been established.

In this investigation it was observed that body temperature, heart rate, respiration rate and body weight decreased significantly during hibernation in the 13-striped ground squirrel. Of these measurements the change in body weight was the least. These facts are in agreement with the work of Johnson ('31) who worked with the same species. He found that the weight loss during hibernation was small in comparison to the weight loss in starvation. The animals used in the present work had food in their cages at all times so the factor of starvation is not important since the duration of hibernation before sacrifice was small. Kayser ('50) suggested that the loss of weight during hibernation was due to a loss of water which resulted from the combustion of lipids. It is possible that loss of fat deposits could account for some of the weight loss in this present study since subcutaneous fat deposits were found to be scant, if any, during hibernation.

The electrocardiograms taken during the hibernating phase of the present experiment showed a decrease in heart rate. A decrease in peripheral blood flow was also noted, as evi-

denced by a relatively bloodless operative field while removing tissue as well as lack of blood upon puncturing the tail or any of the feet. This corresponds with the findings of Johnson ('31). During the course of experimentation it was observed that in many instances the rectal temperature of an animal would drop to 1 to 1.5° above environmental temperature and maintain this level for a period of time while heart and respiration rates were well above those of hibernating animals. This suggests the possibility that one of the first physiological values to decrease was that of body temperature. Conceivably, a decrease in body temperature could result in the subsequent decline of respiration and heart rates.

The next factors to be considered are related to the metabolic state of the animals during hibernation. Biochemical levels of certain metabolic compounds were determined. These may aid in determining the chemical anatomy of the hibernating 13-striped ground squirrel.

Carbohydrate metabolism in hibernation. Although many authors agree that during hibernation the blood sugar content is lower than in non-hibernating animals (Dubois, 1894; Endres and von Frey, '30; Dische, Fleischmann and Trevani, '31; Feinschmidt and Ferdman, '32; and Suomalainen, '38) there has been little agreement concerning the amounts of glycogen present in the hibernating as compared to the non-hibernating animal.

The findings from this present investigation indicate a tendency toward a decrease in tissue glycogen levels during hibernation. It is interesting to note that 40% of the animals showed levels within the non-hibernating range. In considering the data as a whole one finds a correlation between the glycogen levels and the respiration rates. In all cases, the animals maintaining high glycogen levels during hibernation had slightly higher respiration rates. It is possible that this relatively higher rate of oxygen intake, than is needed at lowered body temperatures, is maintaining the glycogen storage by not calling upon anaerobic glycolysis as much as in animals with lower rates of respiration.

Also of importance in the cyclic events of carbohydrate metabolism is the lactate content of corresponding tissues. Cardiac and skeletal muscle lactate levels decreased during hibernation. The percentage decrease was essentially the same. Since the lactate determinations were not made on the same group of animals as the glycogen determinations, correlation is not possible. However, the decrease in lactate content may be due to the fact that during the relatively anaerobic state of hibernation glycogen breakdown is likely to occur at a much slower rate. This in turn could account for a lactate decrease whether glycogen levels remained within the non-hibernating range or were relatively depleted during hibernation.

High-energy metabolism in hibernation. The breakdown of adenosine polyphosphate to adenosine monophosphate provides energy for (1) synthesis within the body, (2) metabolic work, (3) phosphorylations and (4) mechanical work. The formation of adenosine polyphosphate from adenosine monophosphate is mainly dependent upon (1) glycolysis, (2) biological oxidations and (3) phosphocreatine. However, the role of phosphocreatine in this process is reversible. From consideration of the above statements and corresponding literature it can be said that adenosine polyphosphate is the immediate source of energy for physiological processes utilizing chemical energy, while phosphocreatine is the emergency storage form of high-energy phosphates, and the transfer of energy from both compounds is freely reversible (Potter, '44; and Soskin and Levine, '52).

Adenosine polyphosphate ($P < .01$) and phosphocreatine ($P < .01$) showed the significant changes during hibernation. During hibernation the animal is stationary, consequently skeletal muscular movement was not observed. The decrease in cardiac muscle activity was evidenced by the decrease in the heart rate. Therefore, it can be seen that the need for adenosine polyphosphate breakdown is greatly decreased during hibernation. At the same time the rate of synthesis is probably decreased. The low adenosine polyphosphate

level may therefore suggest that synthesis does not keep pace with utilization. However, another factor which may be closely involved in the lowered adenosine polyphosphate level is the rise in the phosphocreatine level. Since adenosine polyphosphate and phosphocreatine are considered to be in equilibrium at body temperature, the basis for this change is difficult to explain. However, once again it should be pointed out that what is lost by adenosine polyphosphate is gained by phosphocreatine in approximately the same percentage ratio.

An increase in phosphocreatine while slowing the heart rate of dogs was reported by Wollenberger ('51). Although the decline in work in his experiment was around 28%, he stated that it was unlikely that the increase was due to a sparing effect on the utilization of the energy-rich phosphate bond. Considerable changes in the work performance of the mammalian heart brought about variations in cardiac output which were shown to have no effect on the adenosine triphosphate and phosphocreatine content (Wollenberger, '49). Therefore, he concluded that it was likely that the slow heart rate was responsible for the increased phosphate content, which in turn would be in accord with the present work on the hibernating 13-striped ground squirrel. The combined results of Wollenberger ('49 and '51), and the data obtained in the present investigation appear to suggest that when energy is not used, it tends to be stored in the form of phosphocreatine in increased amounts. Conceivably, this storage could play an important role in the arousal mechanism. To test this hypothesis, it would be interesting to determine what occurs in the phosphocreatine level during the awakening process.

SUMMARY

1. A decline in body temperature, heart rate, respiration rate and body weight occurred during hibernation.
2. There was a tendency toward decreased glycogen levels for liver, cardiac muscle and skeletal muscle. However, interestingly enough 40% stayed within the normal range.

These variations may be related to fluctuations in oxygen intake at lowered body temperatures.

3. The lactate content of cardiac and skeletal muscle decreased significantly during hibernation. Considering the relatively anaerobic state which exists at this time, it is likely that glycolysis occurs at a slower rate, thus producing lower lactate levels.

4. Inorganic phosphate and adenosine polyphosphate both decreased during hibernation, the latter significantly. However, phosphocreatine increased significantly. This high energy compound is the only one that shows a persistently higher level during hibernation.

5. Histochemically, glycogen loss occurred uniformly throughout liver, cardiac muscle and skeletal muscle. In all cases these studies provided visual confirmation of the biochemical determinations.

6. Histochemically, phosphate appeared scattered throughout cardiac and skeletal muscle in both non-hibernating and hibernating tissue samples.

LITERATURE CITED

- BENEDICT, F. G., AND R. C. LEE 1938 Hibernation and Marmot Physiology. Carnegie Institution of Washington Publication, 497.
- DISCHE, Z., W. FLEISCHMANN AND E. TREVANI 1931 Zur Frage des Zusammenhanges zwischen Winterschlaf und Hypoglykämie. *Pflüger's Arch. f. d. ges. Physiol.*, 227: 235-238.
- DUBOIS, M. RAPHAEL 1894 Variations du Glycogene du Foie et du Sucre du Sang et du Foie Dans L'Etat de Torpeur, Chez la Marmotte et de L'Influence des Nerfs Pneumogastriques et Sympathiques sur le Sucre du Sang et du Foie Pendant le Passage de la Torpeur a L'Etat de Veille. *Comp. rend. Soc. biol.*, 46: 219-220.
- ENDRES, G., AND W. VON FREY 1930 Über Schlaftiefe und Schlafmenge. *Ztschr. f. Biol.*, 90: 70-80.
- FEINSCHMIDT, O., AND D. FERDMANN 1932 Beiträge zur Biochemie des Winterschlafs; Über die chemischen Bestandteile des Blutes Winterschlafhaltender Tiere. *Biochem. Ztschr.*, 248: 107-114.
- FISKE, CYRUS H., AND YELLAPROGADA SUBBAROW 1929 Phosphocreatine. *J. Biol. Chem.*, 81: 629-679.
- FOSTER, MARK A., R. C. FOSTER AND R. K. MEYER 1939 Hibernation and the endocrines. *Endoc.*, 24: 603-611.

- GERSCH, I. 1938 Improved histochemical methods for chloride, phosphate-carbonate and potassium applied to skeletal muscle. *Anat. Rec.*, 70: 311-329.
- GOOD, C. A., R. KRAMER AND MICHAEL SOMOGYI 1933 The determination of glycogen. *J. Biol. Chem.*, 100: 485-491.
- ILLINGWORTH, B. A., AND J. A. RUSSELL 1951 The effects of growth hormone on glycogen in tissues of the rat. *Endocrinol.*, 48: 423-434.
- JOHNSON, GEORGE EDWIN 1931 Hibernation in mammals. *Quart. Rev. Biol.*, 6: 439-461.
- KAYSER, CH. 1950 Le Sommeil Hibernial. *Biol. Rev.*, 25: 255-282.
- KAYSER, CHARLES 1953 L'Hibernation des Mammiferes. *Année Biol.*, 29: 109-150.
- KOSSA, J. VON 1901 Ueber die in Organismus Kunstlich erzeugbaren Verkümmungen. *Beitr. Path. Anat. U. Allgem. Path.*, 29: 163-202.
- LYMAN, CHARLES P., AND ELIZABETH H. LEDUC 1953 Changes in blood sugar and tissue glycogen in the hamster during arousal from hibernation. *J. Cell. and Comp. Physiol.*, 41: 471-492.
- LYMAN, CHARLES P., AND PAUL O. CHATFIELD 1955 Physiology of hibernation in mammals. *Physiol. Rev.*, 35: 403-425.
- LYMAN, RUFUS A. 1943 The blood sugar concentration in active and hibernating ground squirrels. *Journ. Mamm.*, 24: 467-474.
- MILLER, BENJAMIN F., AND JOHN A. MUNTZ 1938 A method for the estimation of ultramicro-quantities of lactic acid. *J. Biol. Chem.*, 126: 413-421.
- NELSON, NORTON 1944 A photometric adaptation of the Somogyi method for the determination of glucose. *J. Biol. Chem.*, 153: 375-380.
- POTTER, V. R. 1944 Biological energy transformations and the cancer problem. *Advances in Enzymology*, 4: 201-256.
- RASMUSSEN, ANDREW T. 1916 Theories of hibernation. *Am. Nat.*, 50: 609-625.
- SERRA, J. A., AND A. QUEIROZ LOPES 1945 Une methode pour la demonstration histochemique du phosphore des acides nucleiques. *Portugaliae Acta Biol.*, 1: 111-122.
- SOSKIN, SAMUEL, AND RACHMIEL LEVINE 1952 *Carbohydrate Metabolism*. University of Chicago Press, Chicago.
- SUOMALAINEN, P. 1935 Über den Winterschlaf des Ingels. *Ann. Academia Scientiarum Fennicae, Ser. A, Tom. XLV*, 2: 1-115.
- 1938 Production of artificial hibernation. *Nature*, 142: 1157.
- WOLLENBERGER, ALBERT 1947 On the energy-rich phosphate supply of the failing heart. *Am. J. Physiol.*, 150: 733-745.
- 1949 The energy metabolism of the failing heart and the metabolic action of the cardiac glycosides. *Pharm. Rev.*, 1: 311-352.
- 1951 Metabolic action of the cardiac glycosides. II. Effect of Ouabain and Digoxin on the energy-rich phosphate content of the heart. *J. Pharm. and Exp. Therapy*, 103: 123-135.

PLATES

PLATE 1

EXPLANATION OF FIGURES

Photomicrographs of 6μ sections fixed in Rossman's fluid and stained with periodic acid-Schiff's reagent for the demonstration of glycogen. A Wratten B green filter was used to accentuate the fuchsin color.

- 3 Liver of a non-hibernating 13-striped ground squirrel. A large amount of glycogen is uniformly distributed throughout the lobule. Chemical determination of glycogen content: 1733 mg %. $\times 200$. Animal no. 1525.
- 4 Liver of a hibernating 13-striped ground squirrel showing glycogen depletion. Chemical determination of glycogen content: 12 mg %. $\times 200$. Animal no. 1547.
- 5 Skeletal muscle of a non-hibernating 13-striped ground squirrel. Glycogen can be seen primarily in close proximity to the Z-membrane. Chemical determination of glycogen content: 436 mg %. $\times 300$. Animal no. 1522.
- 6 Skeletal muscle of a hibernating 13-striped ground squirrel showing glycogen depletion. Chemical determination of glycogen content: 19 mg %. $\times 300$. Animal no. 1544.
- 7 Cardiac muscle of a non-hibernating 13-striped ground squirrel. Glycogen distribution shows no constant pattern. Chemical determination of glycogen: 384 mg %. $\times 300$. Animal no. 1522.
- 8 Cardiac muscle of a hibernating 13-striped ground squirrel showing glycogen depletion. Chemical determination of glycogen: 108 mg %. $\times 300$. Animal no. 1547.

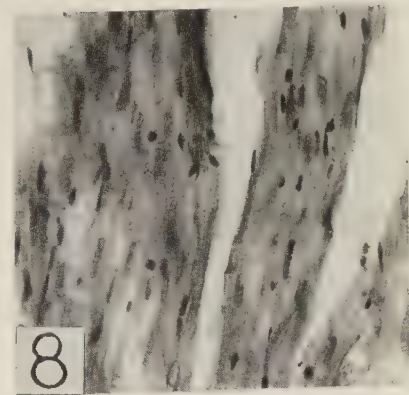
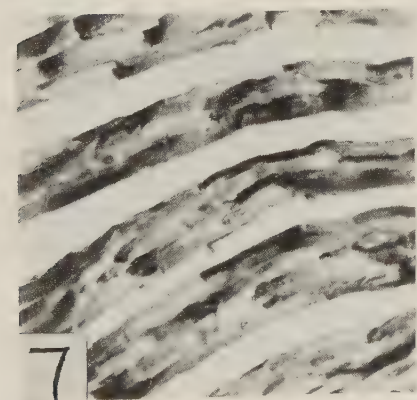
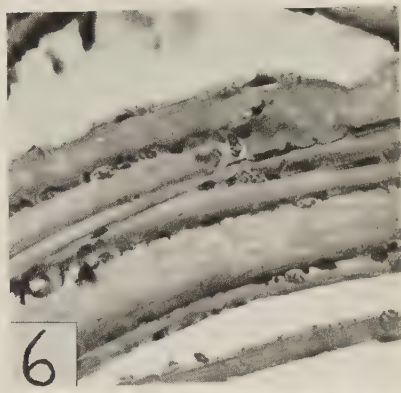
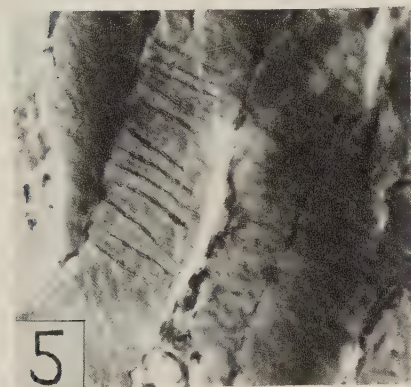
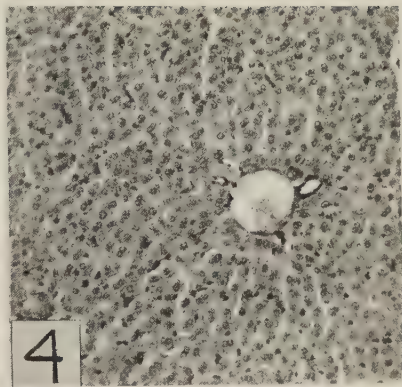
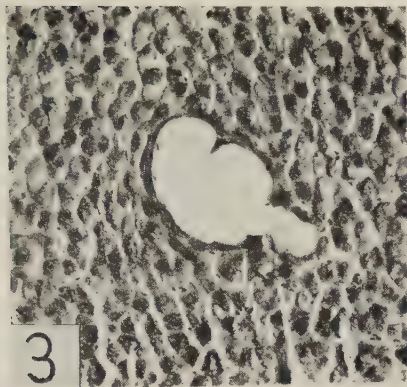
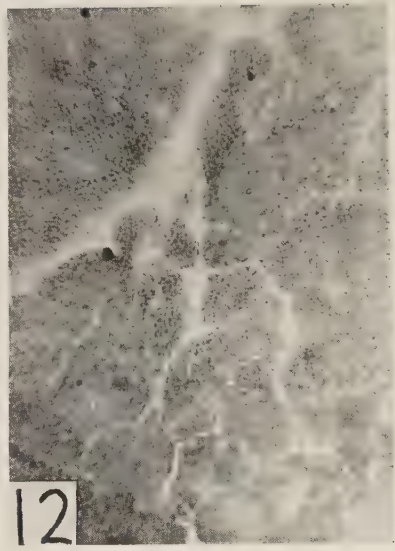
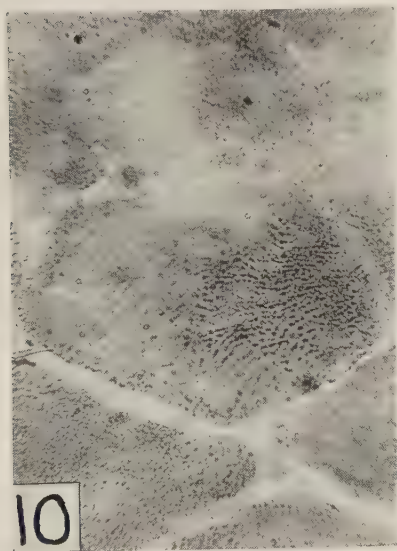
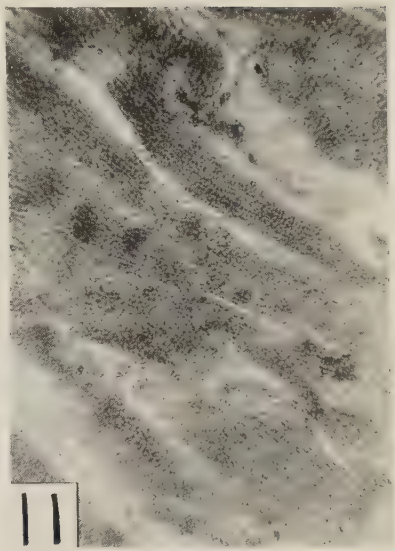
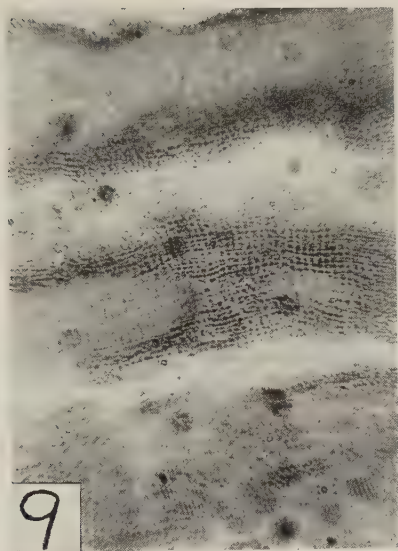


PLATE 2

EXPLANATION OF FIGURES

Photomicrographs of 7μ sections fixed in absolute alcohol and stained by a modification of Von Kossa's silver nitrate procedure following molybdate hydrolysis for the demonstration of phosphate.

- 9 Longitudinal section of skeletal muscle showing scattered precipitation of phosphate. $\times 850$.
- 10 Cross-section of skeletal muscle showing scattered precipitation of phosphate. $\times 850$.
- 11 Longitudinal section of cardiac muscle showing scattered precipitation of phosphate. $\times 850$.
- 12 Cross-section of cardiac muscle showing scattered precipitation of phosphate. $\times 850$.



SOME ASPECTS OF THYROID PHYSIOLOGY IN RAINBOW TROUT ¹

PAUL O. FROMM AND E. P. REINEKE

*Department of Physiology and Pharmacology, Michigan
State University, East Lansing, Michigan*

THREE FIGURES

A compact thyroid gland has been described in the swordfish (*Xiphias*) by Addison and Richter ('32) and in the Bermuda parrot fish (*Sparisoma* sp.) by Smith and Matthews ('48). However, in most teleosts the thyroid consists of follicles scattered in the connective tissue along the ventral aorta and afferent branchial arteries as described by Guder-natsch ('11) and Hoar ('39) and for this reason surgical thyroidectomy is impossible.

Matthews and Smith ('48) have shown that the parrot fish thyroid gland concentrates I^{131} and similar results have been obtained on other teleost and elasmobranch fish. Gorbman et al. ('52) have reported that thyroxine synthesis by the shark (*Scyliorhinus canicula*) appears to follow the same route as in mammals. Similar results were found with Platyfish (Berg and Gorbman, '53).

La Roche and Leblond ('54) noted that every thyroid follicle in the Atlantic salmon accumulates injected radioiodine and successive monthly injections of 100, 50, 40 and 30 μ c of I^{131} caused complete destruction of thyroid follicles in the experimental animals.

This approach to thyroidectomy affords an ideal way to study the effect of the thyroid on oxygen consumption in fish. Previous literature, for the most part, has demonstrated in

¹ Published with the approval of the director, Michigan Agricultural Experiment Station, as journal series no. 1828.

fish no response of oxygen consumption to thyroidal hormone stimulation (Root and Etkin, '37; Etkin et al., '40; Hasler and Meyer, '42; Smith and Everett, '43). These experiments were carried out using mammalian thyroid preparations. Smith and Matthews ('48) injected white grunts (*Bathystoma*) with extracts of the thyroid gland of the Bermuda parrot fish and reported significant increases in the oxygen consumption of fish weighing 15 gm or more but smaller fish failed to respond in a similar way.

Inhibition of the thyroid of *Fundulus heteroclitus* by thiourea (Matthews and Smith, '47) did not decrease the oxygen consumption below that of controls nor did thyroxine administration cause any increase.

Experiments on lampreys (Horton, '34; Leach, '46) have shown that the oxygen consumption and metamorphosis in this species is unaffected by administration of thyroid substances or by abdominal injection of thiourea.

The species specificity of fish thyroid extract has been tested by Smith and Brown ('52). They found that an extract of the Parrot fish thyroid has the same effect on the respiratory metabolism of rats as that of mammalian thyroid extract or synthetic thyroxine.

The present work was undertaken to test the effect of radio-thyroidectomy on the oxygen consumption of Rainbow trout and to devise a method of estimating the accumulation of I^{131} by the thyroid of intact fish and to determine the output rate of this accumulated radioiodine over a period of several days.

MATERIALS AND METHODS

Rainbow trout (*Salmo gairdnerii*) obtained from the Wolf Lake fish hatchery were maintained in tap water at 15°–17° C. for two weeks prior to use. They were fed twice weekly a diet consisting of a mixture of approximately two parts ground cereal grains and one part ground fish meal. The food contained 2% iodized salt. This is an experimental diet used by the Michigan Department of Conservation. None of the experimental or control animals died during the course of the

investigation with the exception of those few which flopped out of the aquarium. Injections of carrier-free I^{131} as NaI were given intraperitoneally and the volume per injection never exceeded 0.2 cc.

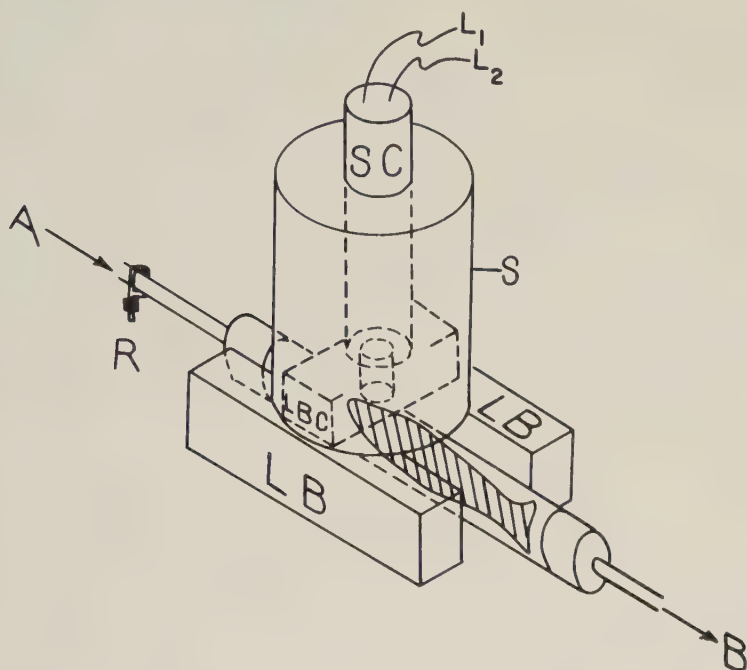


Fig. 1 Apparatus for measuring radioactivity in the head region of fish. Scintillation counter (SC) projects down into a cylindrical lead shield (S) which is recessed allowing lead collimator (LBC) to be put in place. The cylindrical shield rests on two lead blocks (LB) allowing space for the fish chamber which is placed in a holder (not shown). A, indicates inflow of water from reservoir and B, outflow to a collecting vessel. The rate of flow through the chamber can be regulated by an adjustable stopcock (R). The scintillation counter is connected to a count rate meter by two leads, L_1 and L_2 .

Records of the thyroïdal accumulation and output by Rainbow trout were made at constant geometry using the apparatus shown in figure 1. The fish were inserted into the counting chamber and always oriented "upstream." They remained quiescent and it was an easy matter to get constant counts over a period of 30 seconds to 1½ minutes. The radioactivity

of the head region as far posterior as the pectoral fins was determined using a scintillation counter (Nuclear Instrument and Chemical Corp., Model DS-1) and recorded by use of a count rate meter (Nuclear Instrument and Chemical Corp., Model 1620) and an Esterline-Angus Graphic Ammeter. At the end of a series of experiments the lower jaws of I^{131} treated fish were removed and counted at constant geometry. It was found that counts made on the live fish about one hour prior to the lower jaw counts differed from the jaw counts by less than 1%. It is thus believed that the method employed is valid for measuring the accumulation and output of I^{131} by the head region of intact fish. Accumulation of injected I^{131} is expressed in terms of per cent of initial dose given. The output rate is presented as output half-time which is the time in days required for the thyroid follicles to release one-half of the accumulated I^{131} . The latter figure was calculated using the method of least squares.

A continuous flow type apparatus similar to that described by Keys ('30) was used for the determination of oxygen consumption. Analysis for dissolved oxygen was made by the sodium azide modification of the Winkler method. All measurements were made at 15.5°–16.5° C. and data are given in ml/gm/hr. The weight refers to the wet or live weight of the fish.

RESULTS

Thyroidectomy and oxygen consumption

Eight fish (Group 2) were given graded doses of I^{131} ; two each received 1000, 750, 500 and 250 μ c. One fish that received 1000 μ c flopped out of the aquarium and was lost. All others survived. Thirty two days after injection of graded doses of I^{131} the lower jaws of these animals were removed, fixed in Bouin's fluid and then stained with Ehrlich's hematoxylin.

The location of thyroid follicles in Rainbow trout as described by Gudernatsch ('11) was confirmed. A representative section from a control animal (fig. 2, A) shows well developed follicles with most cells being of the columnar type. The

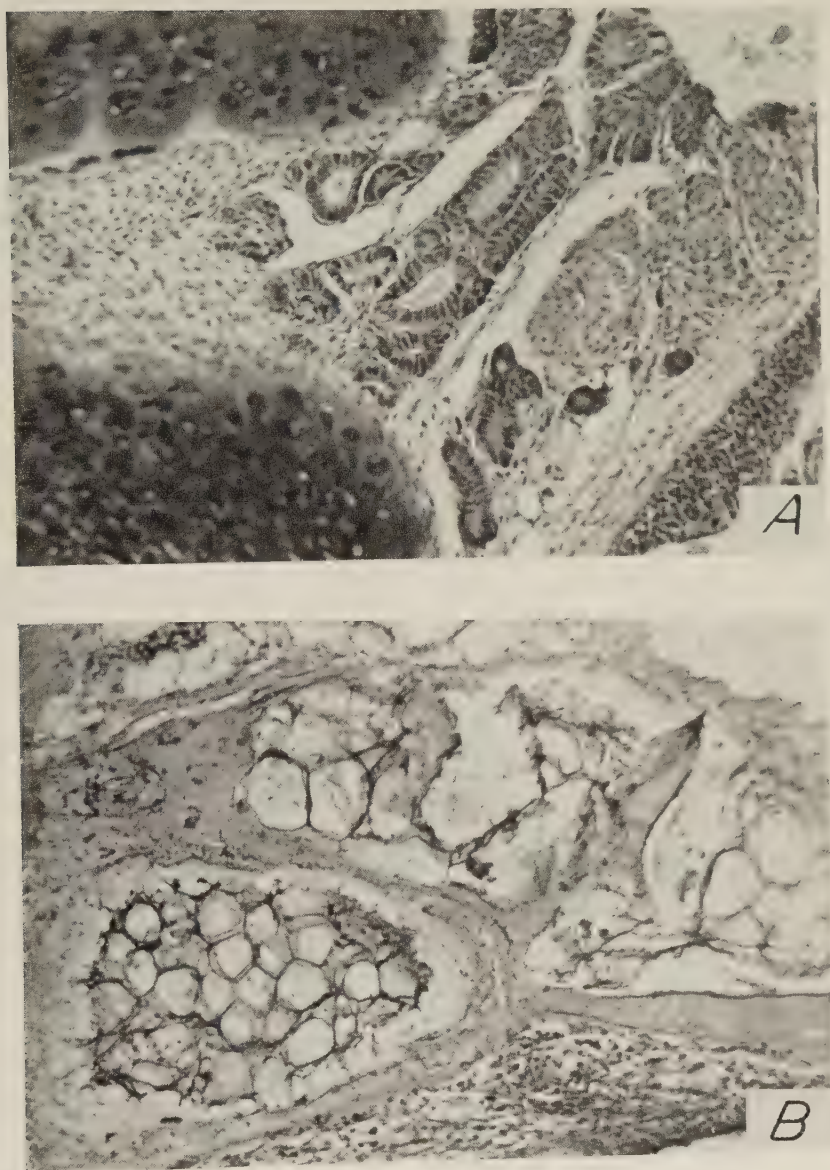


Fig. 2 Histological sections (15μ) of lower jaws of Rainbow trout. The tissue was fixed in Bouin's fluid and stained with Ehrlich's hematoxylin. A, normal control. B, section from animal 33 days after single injection of $250\mu\text{c}$ of radioiodine. See text for further description.

follicles are quite widely scattered in the connective tissue. Sections from fish which received 1000 and 750 μc of I^{131} show a complete absence of any thyroid epithelium or colloidal material. In lower jaw sections of fish that received 500 μc of I^{131} the thyroid epithelium was completely destroyed and some retention of colloidal material occurred. Figure 2, B is a section from the lower jaw of a fish that received 250 μc of I^{131} . It shows complete destruction of the follicular cells and only a small retention of colloid in the "follicular skeletons."

TABLE 1

Oxygen consumption of normal and radiothyroidectomized Rainbow trout fingerlings measured at 15.5°–16.5°C. Data are expressed in milliliters oxygen consumed per gram (wet weight) per hour.

	NUMBER OF VALUES	OXYGEN CONSUMPTION
Controls	34	0.20–0.005 ¹
Thyroidectomized	29	0.21–0.007 ¹

¹ Standard error.

Calculations of data obtained 11 to 15 days after injection resulted in a mean output half-time of 4.6 days and on the basis of a low overall output half-time and histological examination it was concluded that a single injection of 250 μc of I^{131} was sufficient to completely thyroidectomize young Rainbow trout under the conditions employed.

Ten Rainbow trout fingerlings ranging in weight from 3.8 to 6.0 gm were radiothyroidectomized by giving intraperitoneal injections of 250 μc of I^{131} . Another group of fish from the same lot and kept under identical conditions served as controls. The thyroidectomized fish showed a mean oxygen consumption of 0.21 ml/gm/hr. compared to 0.20 ml/gm/hr. for controls when measured at 15.5°–16.5° C. The difference is not significant (based on the Fisher "t" test).

Uptake and output of I^{131} by Rainbow trout

Eleven fish (Group 1) were injected with 10 μc of I^{131} and the radioactivity of the head region determined daily for

7 days. Similar treatment was given the radiothyroidectomized fish (Group 2) 26 days after injection of graded doses of I^{131} . The results are shown in figure 3. The animals in Group 1 (solid line in fig. 3) show a peak accumulation of 60% of the initial dose 48 hours after injection. The thyroidectomized fish had a peak accumulation of 40% of the injected dose 24 hours after injection (broken line in fig. 3). The mean

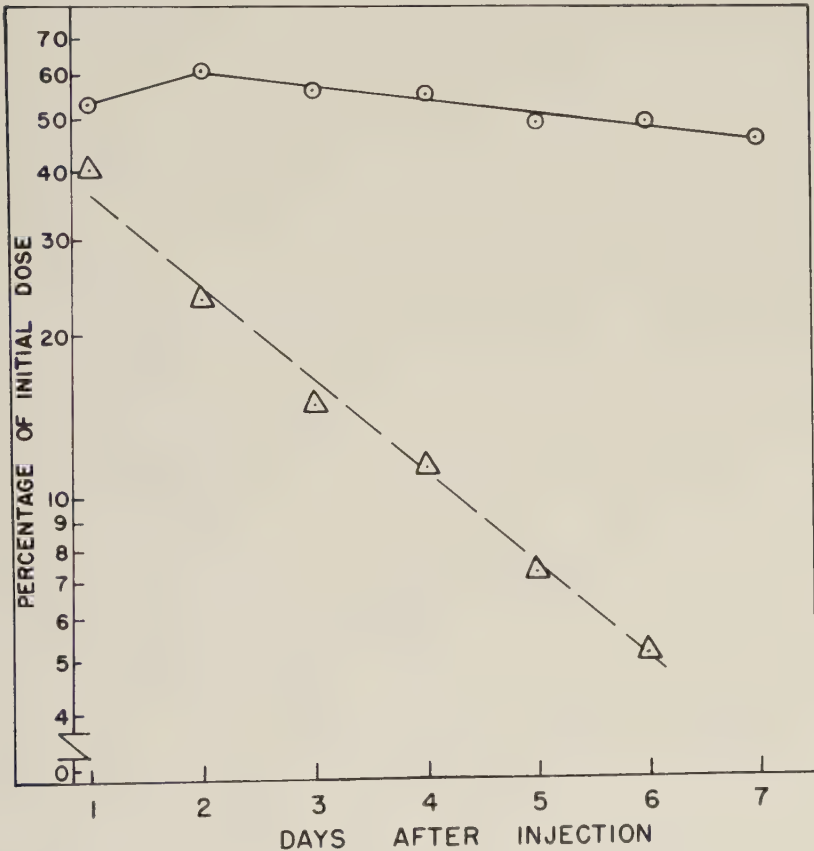


Fig. 3 Semi-log plot of radioiodine accumulation in the head region and loss over a period of one week in normal (solid line) and radiothyroidectomized (broken line) Rainbow trout. Fish were maintained in 20 liters of aerated tap water at 15° – 17° C, which was changed 3 times during the week.

overall output half-time for the intact fish was 15.5 ± 4.0 ² days compared to 1.8 ± 0.1 days for the thyroidectomized fish.

DISCUSSION

Radiothyroidectomy did not decrease the oxygen consumption of Rainbow trout fingerlings below that of control animals which is consistent with most results for other species of fish. The results presented here are probably most comparable to those of Matthews and Smith ('47) on *Fundulus* whose thyroids had been inhibited by thiourea. The present work eliminated the possibility of partial inhibition of the thyroid, however, and offers evidence that the Rainbow trout thyroid is not involved in the overall regulation of energy metabolism. It must be noted that these data were obtained on trout fingerlings and on the basis of results by Smith and Matthews ('48) it may be possible that larger fish would react differently.

The accumulation of I^{131} in the head region of Rainbow trout was found to be quite high. The counts on intact fish include both thyroidal and non-thyroidal accumulation of I^{131} whereas counts on radiothyroidectomized fish must indicate non-thyroidal accumulation only. The level of non-thyroidal I^{131} is probably lower in intact than in thyroidectomized fish because of uptake by the thyroid in the former. Subtraction of the values for the thyroidectomized from those for intact fish at a given time period would, therefore, give a maximal correction. If this is done the peak *thyroidal* accumulation is 44% of the injected dose and occurs 4 days after injection. The non-thyroidal I^{131} in the head region amounts to a considerable percentage of the total count during the first few days after injection. The output half-time of this fraction of the radioactivity was found to be 1.8 days and thus by some 8 days after injection the amount remaining in the head region is negligible. It has been noted above that counts on intact fish and isolated lower jaws taken 8 days after injection of I^{131} differed by less than 1%.

² Standard error.

The biological half-life or output half-time calculated from data on intact fish (15.5 days) is not a true figure for the turnover rate of iodine by the thyroid of Rainbow trout. This calculated rate is based on values that are influenced by both the thyroidal and non-thyroidal I^{131} output rates. Since the output half-time for the non-thyroidal I^{131} is 1.8 days it is evident that the actual output half-time of the thyroid follicles is longer than 15.5 days. Values for the output half-time or thyroidal iodine turnover rates in fish have not been found in the literature. Previous measurements of thyroidal accumulation and output of radioiodine in fish usually have been made starting with a relatively large number of animals, injecting tracer doses of I^{131} and sacrificing a few animals at appropriate times after injection. The radioactivity of hydrolyzed samples (usually pooled samples) of these fish was then measured. The experiments rarely lasted more than 7 days. From the results presented here it is suggested that true thyroidal iodine turnover rates for Rainbow trout (probably other fish also) must be determined by data collected subsequent to the 8th day after injection of I^{131} .

The value for thyroidal I^{131} accumulation in Rainbow trout reported here (44%) is somewhat higher than those found for other species of fish (literature summarized by Berg and Gorbman, '53). This difference may be due in part to the use of different counting techniques. Also the amount of iodine available to fish has been shown to influence the uptake of injected I^{131} . Berg and Gorbman ('53) have shown that Platyfish conditioned to water containing 60 parts per million KI for one week accumulated only 3% of the injected dose of I^{131} whereas fish in normal stock water accumulated 29%. In general, marine fish accumulate only a small percentage of injected radioiodine in the thyroid although Gorbman et al. ('52) reported a peak uptake of 34% of the injected dose by the marine shark (*Scyliorhinus canicula*) 6 hours after injection accompanied by a very rapid loss. Similarly, Platyfish (Berg and Gorbman, '53) in iodine enriched water lost nearly all of the injected I^{131} within two days whereas fish

in normal stock water retained about 40% of the injected dose as long as 6 days after injection. The latter results appear contradictory in that the maximum accumulation of I^{131} reported for Platyfish by these authors is 29% of the injected dose. *Fundulus heteroclitus* and *Fundulus majalis* have slow output rates which are somewhat similar in both fresh and sea water (Gorbman and Berg, '55). That the high uptake of I^{131} in the head region of Rainbow trout may indicate the animals were "iodine starved" seems unlikely because their diet contained 2% iodized salt.

CONCLUSIONS

1. Total destruction of thyroids in Rainbow trout (*Salmo gairdnerii*) was accomplished by a single injection of 250 μ c of I^{131} as well as by higher doses.

2. Radiothyroidectomy of Rainbow trout fingerlings did not significantly alter their rate of oxygen consumption from that of normal controls.

3. A method is described whereby the thyroïdal accumulation and output rate of injected I^{131} may be estimated on intact fish.

4. Hatchery raised Rainbow trout maintained in tap water at 15°–17°C. and injected with 10 μ c of I^{131} accumulated in the head region some 60% of the injected dose within 48 hours after injection. The amount of non-thyroidal accumulation of I^{131} in the head region of trout was determined and subtraction of this amount of radioactivity from the values for non-thyroidectomized fish has shown that maximal *thyroidal* accumulation of I^{131} by Rainbow trout was some 44% of the injected dose. Peak thyroïdal accumulation occurred 4 days after injection.

5. Non-thyroidal I^{131} in the head region of Rainbow trout is lost quite rapidly (output half-time 1.8 days) so that by 8 days after injection a negligible amount still remains in the thyroïdal area.

6. An overall output half-time for I^{131} by the thyroïdal region of Rainbow trout was found to be 15.5 ± 4.0 days. The

output half-time was significantly decreased by injections of from 250 to 1000 μc of I^{131} .

ACKNOWLEDGMENT

The authors wish to express their appreciation to Dr. Ellen St. John Monkus for her aid during this investigation and to Mr. E. F. Grassl, nutritionist for the Michigan Department of Conservation for his cooperation in acquiring the experimental animals. Photomicrographs were done by Mr. P. G. Coleman, photographic assistant for the Agricultural Experiment Station.

LITERATURE CITED

- ADDISON, W. H. F., AND M. N. RICHTER 1932 A note on the thyroid gland of the swordfish (*Xiphias gladius*, L.). Biol. Bull., 63: 472-476.
- BERG, O., AND A. GORBMAN 1953 Utilization of iodine by the thyroid of the Platyfish, *Xiphophorus (Platyopocilus) maculatus*. Proc. Soc. Exp. Biol. and Med., 83: 751-756.
- ETKIN, W., R. W. ROOT AND B. P. MOFSHIN 1940 The effect of thyroid feeding on oxygen consumption of goldfish. Physiol. Zool., 13: 415-429.
- FISHER, R. A., 1946 Statistical methods for research workers. Oliver and Boyd, London.
- GORBMAN, A., S. LISSITZKY, R. MICHEL AND J. ROCHE 1952 Thyroidal metabolism of iodine in the shark *Scyliorhinus (Scyllium) canicula*. Endocrinology, 51: 311-321.
- GORBMAN, A., AND O. BERG 1955 Thyroidal function in the fishes *Fundulus heteroclitus*, *F. majalis* and *F. diaphanus*. Endocrinology, 56: 86-92.
- GUDERNATSCH, F. J. 1911 The thyroid gland of the teleosts. J. Morph., 21: 709-782.
- HASLER, A. D., AND R. K. MEYER 1942 Respiratory responses of normal and castrated goldfish to teleost and mammalian hormones. J. Exp. Zool., 91: 391-404.
- HOAR, W. S. 1939 The thyroid gland of the Atlantic salmon. J. Morph., 65: 257-295.
- HORTON, F. M. 1934 On the relation of thyroid to metamorphosis in the lamprey. J. Exp. Biol., 11: 257-261.
- KEYS, A. 1930 The measurement of the respiratory exchange of aquatic animals. Biol. Bull., 59: 187-198.
- LA ROCHE, G., AND C. P. LEBLOND 1954 Destruction of thyroid gland of Atlantic salmon (*Salmo salar* L.) by means of radio-iodine. Proc. Soc. Exp. Biol. and Med., 87: 273-276.
- LEACH, W. J. 1946 Oxygen consumption of lampreys, with special reference to metamorphosis and phylogenetic position. Physiol. Zool., 19: 365-374.

- MATTHEWS, S. A., AND D. C. SMITH 1947 The effect of thiourea^a on the oxygen consumption of *Fundulus*. *Physiol. Zool.*, 20: 161-164.
- 1948 Concentration of radioactive iodine by the thyroid gland of the parrot fish, *Sparisoma* sp. *Am. J. Physiol.*, 153: 222-225.
- ROOT, R. W., AND W. ETKIN 1937 Effect of thyroxine on oxygen consumption of the toadfish. *Proc. Soc. Exp. Biol. and Med.*, 37: 174-175.
- SMITH, D. C., AND G. M. EVERETT 1943 The effect of thyroid hormone on growth rate, time of sexual differentiation and oxygen consumption in the fish, *Lebistes reticulatus*. *J. Exp. Zool.*, 94: 229-240.
- SMITH, D. C., AND S. A. MATTHEWS 1948 Parrot fish thyroid extract and its effect upon oxygen consumption in the fish, *Bathystoma*. *Am. J. Physiol.*, 153: 215-221.
- SMITH, D. C., AND F. C. BROWN 1952 The effect of parrot fish thyroid extract on the respiratory metabolism of the white rat. *Biol. Bull.*, 278: 278-286.

GROWTH, WORK OUTPUT AND SENSITIVITY TO INCREASED GRAVITATIONAL FORCES IN WHEAT COLEOPTILES ¹

BETTY F. EDWARDS AND STEPHEN W. GRAY

*Department of Anatomy, Division of Basic Sciences,
Emory University, Emory University, Georgia*

FOUR FIGURES

INTRODUCTION

Increased gravitational attraction has been shown to decrease the height which the wheat seedling coleoptile may attain (Gray and Edwards, '55), when forces from 10 to 500 times normal gravity are applied for the entire growth period of the coleoptile. We suggested that this decrease in height results in part from the increase in physical work required to raise a given mass of tissue to a given height.

Certain of the data indicate that the gravitational influence does not operate equally over the whole growth period of 96 hours. More specifically, it seems possible that there is a stimulatory response masked by the more obvious inhibition, and that the inhibition may be greatest during periods of maximum physical work output.

In this paper, the effects of supranormal gravitational forces applied during selected hours of the growth period have been studied, with the hope of determining the relative sensitivity of the different phases of growth to such forces.

METHOD

Sanford winter wheat seeds were grown in the dark at 26° C. on sterile Ottawa sand in 50 ml centrifuge tubes, as

¹This investigation was supported in part by a research grant from the Division of Research Grants and Fellowships of the National Institutes of Health, U. S. Public Health Service, and in part by a grant-in-aid from the Carnegie Foundation.

described in our earlier paper ('55). They had no nutriment other than that inherent in the seed and in boiled tap water.

The growing period was counted from the time of soaking the seeds, and was subdivided into 24-hour periods for the 4 days during which the coleoptile achieves its growth. Planted seeds were centrifuged at various forces and for various periods during these 4 days. Growing coleoptiles were measured at intervals, and then coleoptile height, diameters, weight, and root length were measured on uprooted plants. Cell measurements were made at the base of the coleoptile on approximate mid-sagittal sections of fixed and sectioned plants.

TABLE 1

Effects of centrifugation at $50 \times G$ during wheat coleoptile growth

PERIOD CENTRIFUGED	FINAL HEIGHT	INHIBITION (DIFFERENCE FROM CONTROL)
	<i>mm</i>	<i>mm</i>
Control	41.17	
0-24 hrs.	42.15	+ 0.98
24-48 hrs.	37.34	— 3.83
48-72 hrs.	34.28	— 6.89
72-96 hrs.	39.22	— 1.95
	Total	— 11.69
0-96 hrs. (whole time)	32.39	— 8.78

DATA

Height. Seedlings centrifuged continuously at forces from 10 to $500 \times G$ for 4 days are shorter than control seedlings. To determine when this inhibition of growth occurs, plants were centrifuged for each of the 24-hour periods separately. The results of such centrifugation at $50 \times G$ appear in table 1.

The sum of the effects produced by each of four 24-hour periods of centrifugation is 11.69 mm, which exceeds by 33% the 8.78 mm inhibition of plants centrifuged continuously at $50 \times G$ for 96 hours. Higher ($150 \times G$) and lower ($25 \times G$) forces produce similar results.

The total inhibition produced at $50 \times G$ amounts to 12.67 mm, but this total is reduced by the fact that centrifugation

during the first 24 hours results in stimulation and not in inhibition of growth. More detailed analysis of this growth-stimulating effect shows that it is present at all forces up to $500 \times G$, although at this higher force it is not statistically significant.

TABLE 2

Height of coleoptiles in millimeters centrifuged for the first 24 hours only

HOURS	CONTROL	10 \times G	25 \times G	50 \times G	150 \times G	200 \times G	500 \times G
	4.47		5.61				
29	± 1.79 ¹		± 1.49				
	(63) ²		(49)				
	9.26	11.94	10.82	10.84	11.87	7.66	
48	± 2.12	± 1.24	± 4.01	± 2.47	± 2.07	± 1.92	
	(135)	(19)	(76)	(33)	(41)	(15)	
	14.37	19.43	16.85	16.76	16.97	14.80	14.81
55	± 2.86	± 1.42	± 3.94	± 2.82	± 2.96	± 3.37	± 3.23
	(577)	(19)	(173)	(115)	(95)	(19)	(34)
	18.76	24.43	20.42	22.40	21.70	20.16	18.82
60	± 3.80	± 1.73	± 4.61	± 2.99	± 3.11	± 3.65	± 2.24
	(716)	(19)	(195)	(115)	(95)	(19)	(34)
	23.92	28.38	25.40	27.45	25.73	25.94	22.25
65	± 4.00	± 2.23	± 4.87	± 3.33	± 4.13	± 3.57	± 3.42
	(808)	(19)	(262)	(92)	(150)	(19)	(114)
	31.14	32.76	31.84	35.00	32.19	33.92	27.60
72	± 4.70	± 2.47	± 4.97	± 3.20	± 4.62	± 3.50	± 3.34
	(949)	(19)	(262)	(92)	(150)	(19)	(114)
	37.71	33.38	37.87	38.79	39.41	39.39	33.46
80	± 4.32	± 2.60	± 4.65	± 3.64	± 4.08	± 3.01	± 3.11
	(646)	(19)	(231)	(121)	(149)	(19)	(113)
	40.46		41.82	40.08	42.63	40.82	36.71
96	± 4.20		± 5.28	± 3.94	± 5.18	± 2.85	± 3.86
	(658)		(194)	(121)	(154)	(19)	(113)

¹ Standard deviation.

² (\times) Number of plants.

In table 2 are shown the heights attained at different hours by plants centrifuged for the first 24 hours at various forces.

Final height attained is not, however, the adequate measure of the stimulation, because the subsequent slower rate of growth cancels out much of the earlier increase. Indeed, at $500 \times G$ the stimulation is extremely slight and transitory;

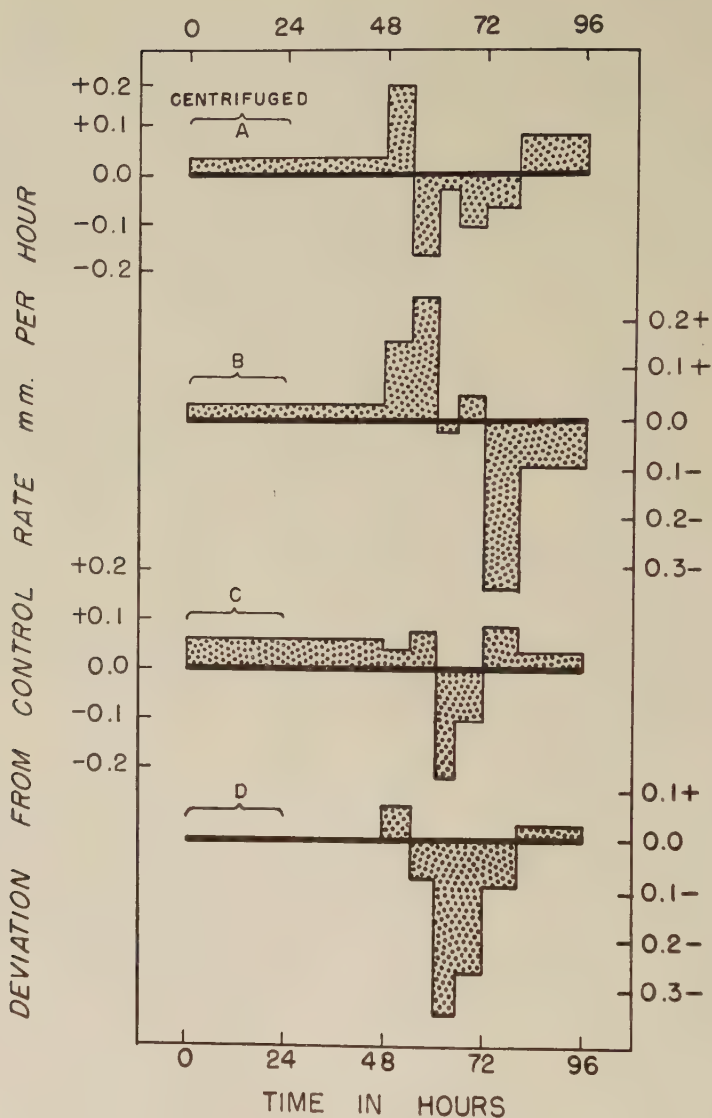


Fig. 1 Growth rates of coleoptiles centrifuged during the first 24 hours expressed as deviation from growth rate of control plants. A. at $25 \times G$, B. at $50 \times G$, C. at $150 \times G$, D. at $500 \times G$.

the end result is a markedly shorter plant. Thus it becomes important to compare *rate* of growth rather than attained height. Figure 1 shows the growth rates of plants centrifuged at various forces for the first day only. Growth rate is indicated as being greater or less than the control rate at the same period.

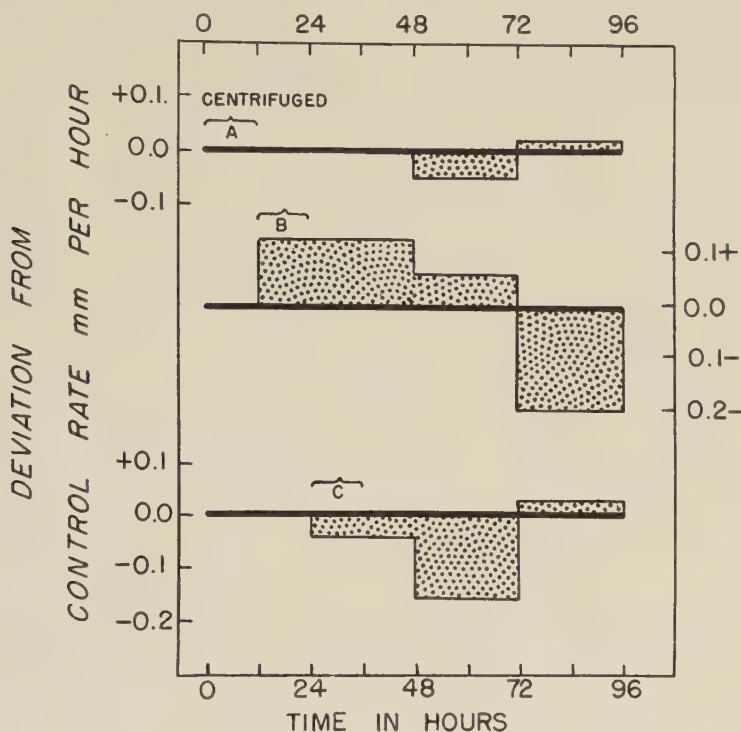


Fig. 2 Growth rates of coleoptiles centrifuged for three different 12 hour periods (indicated by horizontal brackets) expressed as deviation from rate of control plants.

An increase in the growth rate appears within the first 48 hours (except at the two highest forces used). During the next 12 hours, the rate further increases and then begins to fall off, becoming lower than the control rate. At $10 \times G$ and $50 \times G$ this pattern varies as there is a subsequent increase in growth rate again at the end of the growing period.

Thus there is a lag or latent period in the recovery response during which the growth rate remains depressed even though the disturbing force has been removed. It is the accumulation of 4 such latent periods which makes the sum of the effects

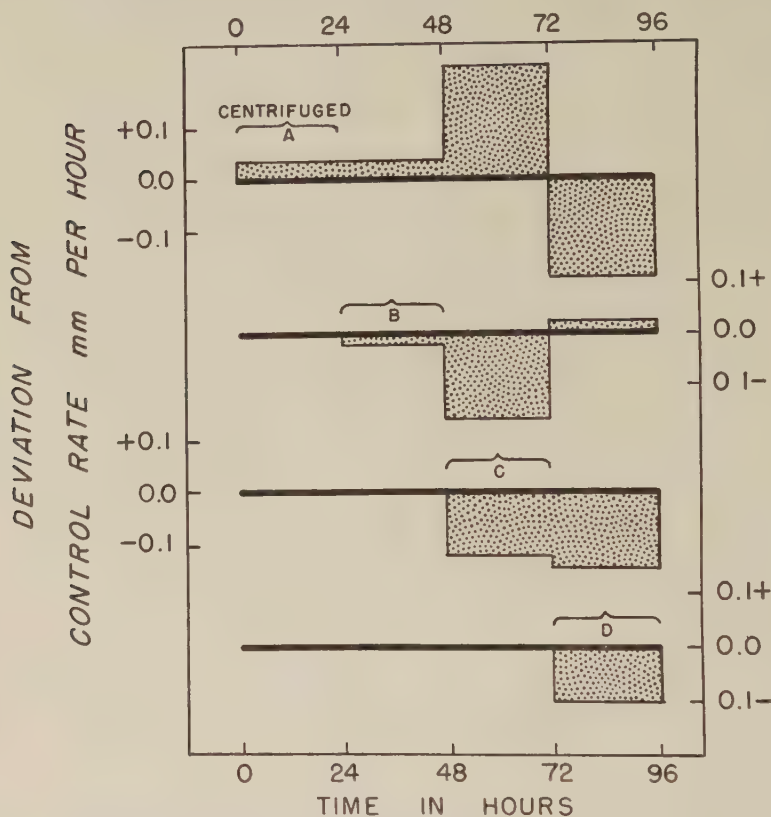


Fig. 3 Growth rates of coleoptiles centrifuged on different days of the growth period. Rates are expressed as deviation from rate of control plants.

of 4 short exposures exceed the effect of continuous exposure (see table 1).

Subdivision of the first day of growth into 0-12 hour and 12-24 hour periods of centrifugation at $25 \times G$ indicates that centrifugation for the first 12 hours only produced no significant change in growth rates. The second 12-hour period produced marked stimulation of growth for the first three

days, followed by a depression on the fourth day greater than if the centrifugation had been applied for the whole of the first 24 hours. This depression was not followed by the recovery which the 24-hour exposure produced. Centrifugation during the 24–36 hour period produced no stimulatory effect, and the results were similar to those resulting from 24–48 hour exposure. These effects are illustrated in figure 2, which should be compared with figure 1, A.

Centrifugation during the second, third and fourth days of life produces inhibition of growth during the period of

TABLE 3

Changes in cross sectional area of coleoptiles centrifuged 150 × G at different hours

PERIOD CENTRIFUGED	AREA OF X-SECTION	DIFF. FROM CONTROL
	<i>mm²</i>	
Control	1.580 ± 0.186	
0–24	1.627 ± 0.096	2.97% increase
24–48	1.792 ± 0.183*	13.42% increase
48–96	1.814 ± 0.124*	14.81% increase
		Total 31.20% increase
0–96	2.376 ± 0.273*	50.38% increase

* Difference from control is significant.

exposure and the succeeding 24 hours. For example, the rate of growth returns to normal on the fourth day, when the plant is centrifuged on the second day. Figure 3 shows these responses and illustrates the lag in response mentioned above.

Diameters and cross sectional area. It has been previously shown that *continuous* centrifugation produces an increase in both diameters of the wheat coleoptile. Further experiments show that centrifugation during *any* day of the life of the coleoptile produces an increase in both large and small diameters, with a resulting increase in the cross-sectional area. Unlike the inhibition of vertical growth, the sum of the effects of 4 single day's centrifugation upon cross-sectional

area fails to equal the effect of continuous centrifugation for 4 days (see table 3).

Only a small effect on cross-sectional area is produced by centrifugation for the first day. Applied on the second day

TABLE 4
Changes in diameters and cross sectional area
Coleoptiles centrifuged 0-24 hours only

	CONTROL (443)	10 × G (22)	25 × G (236)	50 × G (74)	150 × G (93)	500 × G (134)
Small diameter (mm)	1.140	1.178	1.159	1.198	1.193	1.239
Large diameter (mm)	1.578	1.591	1.605	1.643	1.625	1.659
Difference ¹ (mm)	0.438	0.413	0.446	0.445	0.432	0.420
Area of X-section (mm ²)	1.412	1.472	1.462	1.547	1.522	1.608
% of control x-s area	100.0	104.3	103.5	109.6	107.8	113.9

¹ Average difference in diameters = 0.432 mm.

TABLE 5
Ninety-six hour weight and volume of coleoptile and shoot
Centrifuged 0-24 hours only

	CONTROL (118)	25 × G (28)	50 × G (27)	150 × G (56)	500 × G
Wet weight in mg	47.26	44.71	40.20	53.629	
Wet wt./mm ht.	1.167	1.069	1.003	1.129	
Dry wt./mm ht.	0.109	0.096	0.086	0.119	
Dry wt. % of wet wt.	9.34	8.98	8.57	10.54	
Volume of coleoptile (mm ³)	42.23	43.58	43.33	45.66	40.75
Volume of total shoot (mm ³) ¹	57.13	61.14	62.00	64.88	59.03

¹ Shoot volume was computed as:

$$v_{\text{shoot}} = \frac{D_1}{2} \frac{D_2}{2} \pi H$$

$$v_{\text{coleoptile}} = \left(\frac{D_1}{2} \frac{D_2}{2} - \frac{d_1}{2} \frac{d_2}{2} \right) \pi H$$

where D = diameter of coleoptile and d = diameter of the central lumen.

it produces about a 13% increase and a similar amount of enlargement is produced during the last two days.

Table 4 shows the diameters and areas of cross section produced by various forces applied during the first 24 hours.

Volume. As a result of these enlarged diameters, the total shoot volume increases for forces up to 150 × G applied

for the first day. The volume at $500 \times G$ is understandably less, for in spite of larger diameters, plants are significantly shorter. Computed volumes on control and experimental plants are shown in table 5.

Weight. Seedling weight, both wet and dry, decreases in plants centrifuged at $25 \times G$ and $50 \times G$ during the first 24 hours only, but rises again at $150 \times G$. The per cent dry weight also declines with lower forces, but exceeds that of control plants if $150 \times G$ forces are applied during the first day (see table 5). A similar rise in per cent dry weight was produced with continuous centrifugation at $150 \times G$ and

TABLE 6
Parenchyma cell size
98 hour coleoptiles

PERIOD CENTRIFUGED $150 \times G$	AGE	HEIGHT	CELL LENGTH	CELL WIDTH
	<i>hrs.</i>	<i>mm</i>	μ	μ
Control	98	40	217.21 ± 29.97	22.38 ± 2.59
0-24	98	40	198.94 ± 25.13	23.11 ± 3.26
24-48	98	40	201.41 ± 33.41	24.64 ± 3.06
48-96	98	25	194.98 ± 33.13^1	29.59 ± 4.05^1
24-96	98	25	184.90 ± 29.45^1	32.00 ± 3.04^1
0-96	98	25	190.67 ± 22.02^1	38.97 ± 3.26^1
Control	70	25	125.90 ± 15.65	23.41 ± 2.58

¹ Difference from 25 mm control is significant.

$500 \times G$. Lower forces did not evoke the rise even when applied for the entire growing period, nor did $150 \times G$ produce a further increase with exposures longer than 24 hours.

Cell size. On no day of the growth period did a force of $150 \times G$ produce an alteration in the length of the parenchyma cells at the base of the coleoptile. Previously ('55) we had found that even $500 \times G$ for the entire period affected neither the final length of these cells nor the rate at which it was attained.

Parenchyma cell width, on the other hand, is increased by centrifugation on any but the first day. Table 6 shows cell size in plants centrifuged at $150 \times G$ for various periods of time.

Roots. Continuous centrifugation delays the appearance of the roots of the wheat seedling, but does not affect their subsequent rate of growth relative to coleoptile height. Forces applied during the first 24 hours, up to $500 \times G$, had no detectable effect upon the roots, which have normally grown no more than 5 mm at the end of the first day. However, centrifugation during the second day (24–48 hours) at $150 \times G$, for instance, produced roots averaging about 30% shorter than those of control plants. Similar centrifugal force applied continuously for 4 days produced 50% inhibition.

Specifically, normal control plants 30–34 mm tall have three roots with an average total length of 103 mm. The average for 30–34 mm plants centrifuged at $150 \times G$ for the first day is 107 mm, which is not significantly different; for those centrifuged for the second day only, the average root length is 73 mm. Plants of similar size centrifuged during the third and fourth days had approximately 58 mm of roots, while the roots of those continuously centrifuged averaged 44 mm. Thus, exposure during the third and fourth days was almost as inhibitory as exposure for the entire time.

This is in agreement with Keeble, Nelson and Snow ('31) who found that horizontally growing roots of peas and maize grew faster than downward growing ones. More recently, however, Larsen ('53) found that reduction of gravity to zero along the root axis of *Artemesia* by means of a Klinostat did not result in longer roots but in shorter ones. He chose to interpret this as inhibition due to gravity acting horizontally rather than as the absence of gravity acting vertically.

DISCUSSION

If the course of the 96-hour life of the average normal wheat coleoptile be broken into four 24-hour periods, growth and percentage growth for each period will be as shown in table 7.

Calculation of the work accomplished by the growing shoot during each of the 4 days of growth is also shown in table 7. Since both wet and dry weights are proportional to height

over most of the growth period the amount of mechanical work done in vertical growth increases arithmetically with height. The work accomplished by upward growth in any given time period may be expressed as follows:

$$\text{Work} = \frac{(\Delta H + H) (\Delta F)}{2}$$

where H = height at the beginning of the period and F = weight at the same time.

It will be noted that 95% of the work is done on the third and fourth days, while only 77% of the growth is being accomplished. In addition, on these days transport of transpired water also involves the most mechanical work.

TABLE 7

Comparison of growth and work accomplished during maturation of the normal wheat coleoptile

PERIOD	GROWTH	GROWTH	WORK DONE	WORK
<i>hours</i>	<i>mm</i>	<i>%</i>	<i>mg/mm</i>	<i>%</i>
0-24	3.5	8.65	7.15	0.75
24-48	5.76	14.24	42.94	4.49
48-72	21.88	54.08	516.31	53.97
72-96	9.32	23.03	389.86	40.79
	40.46	100.00	956.26	100.00

Now, whatever other physiological changes may be taking place in the centrifuged coleoptiles, the physical task of raising the materials necessary for growth has been greatly increased. Table 8 shows how a force of $50 \times G$ will affect the work requirement for *normal* growth. Applied during the first day, centrifugal force equivalent to 50 times gravity increases the first day's work from 7.15 mg mm to 357.5 mg mm; but this is not greater than 516.31 mg mm that will normally be put out during a single day later in life.

Applied for the second day, however, the work required for normal growth during that day would be 4 times as great as that normally required on the hardest working day. The same force applied on either the third or fourth day increases

the work required to 50 and 38 times the normal maximum day's work. Similarly, even $150 \times G$ applied during the first 24 hours will put no greater work load on the plant than will $25 \times G$ on the second day, or $2 \times G$ on the third.

Comparison of these figures in table 8 with growth rates in figure 3 shows that the greatest growth inhibition takes place when centrifugation is applied on the third or fourth day. There is a smaller response to centrifugation on the second day, and, as we have seen, no depression of growth at all with centrifugation on the first day, the only day during which the added strain of centrifugation remains within normal limits.

TABLE 8

Calculated work in milligram millimeters if normal coleoptile growth were maintained when centrifuged at $50 \times G$

GROWTH PERIOD	CONTROL	TIME OF EXPOSURE TO $50 \times G$			
		0-24	24-48	48-72	72-96
0-24	7.15	<i>357.50</i>	7.15	7.15	7.15
24-48	42.94	42.94	<i>2147.00</i>	42.94	42.94
48-72	516.31	516.31	516.31	<i>25815.50</i>	516.31
72-96	389.86	389.86	389.86	389.86	<i>19493.00</i>
Total (mg mm)	956.26	1306.61	3060.32	26255.45	20059.40

Italic figures indicate the changed work load resulting from centrifugation during the indicated hours.

It seems reasonable to conclude that the increase in work load resulting from centrifugation places no strain on the plant during the first day when the work load is small, but during the later days when more work is normally accomplished, the increase becomes intolerable and decreased growth rates result.

How this increase in work load operates to slow the processes of growth can only be surmised. Probably, the effect is exerted principally upon the water which makes up most of coleoptile bulk. Turgor pressure, which Burström ('51) has defined as the difference in diffusion pressure of the water outside and inside the cell, must increase over the external pressure if the tissues are to increase in size. The external

pressure which Burström considered as the elastic tension of the cell wall, is greatly increased with centrifugation because to this wall pressure must be added the increased static pressure from the overlying cells. The resulting smaller *effective* pressure difference between the cells and their environment, and slower uptake of water could only be overcome by an increase in soluble substances and a higher osmotic pressure within the cells. It is possible that the increased per cent dry weight in shoots found at $150 \times G$ and $500 \times G$ represents just such an increase in soluble substance.

Not only is there no inhibition resulting from first-day centrifugation, but there is a stimulation of growth following this treatment. We can, at this time, only consider this an example of homeostatic overcompensation. The coleoptile, having adjusted at the very beginning to supranormal gravitational attraction then existing, does not immediately readjust when this attraction is reduced. The seedling continues to expend energy at the previously established rate for many more hours and thus grows faster and taller than control plants which started life under normal gravitational force. The subsequent decline in growth to less than the control rate during the fourth day may mean that, having reached its normal height a little sooner, the coleoptile ceases to grow as rapidly as the control which still must achieve its full growth.

It appears that centrifugation for even short periods of time causes an increase in the cross-sectional area of the coleoptile (table 3) and that the width of the individual parenchyma cells is also increased by the same forces (table 6).

If the cell area be compared with coleoptile area, as in figure 4, it will be seen that the relationship is linear. The line, prolonged, will intercept the ordinate at about 1.19 mm^2 , if parenchyma cell size is zero. Thus there remains a constant number of parenchyma cells assuming that the 1.19 mm^2 represents the area occupied by the central canal (about 0.48 mm^2 , roughly 30.4% of the total area enclosed by the outer wall) and the non-parenchymal cellular elements which *may*

not increase with centrifugation. Then, taking cell areas to be hexagons and the measured cell width to be a random diameter, cell area may be determined as:

$$\text{Area}_{\text{hexagon}} = 2.598 \frac{(\frac{1}{2} \text{ diameter})^2}{0.933}$$

Average shrinkage of the cell diameter during fixing and sectioning was determined to be 20%. If this adjusted cell

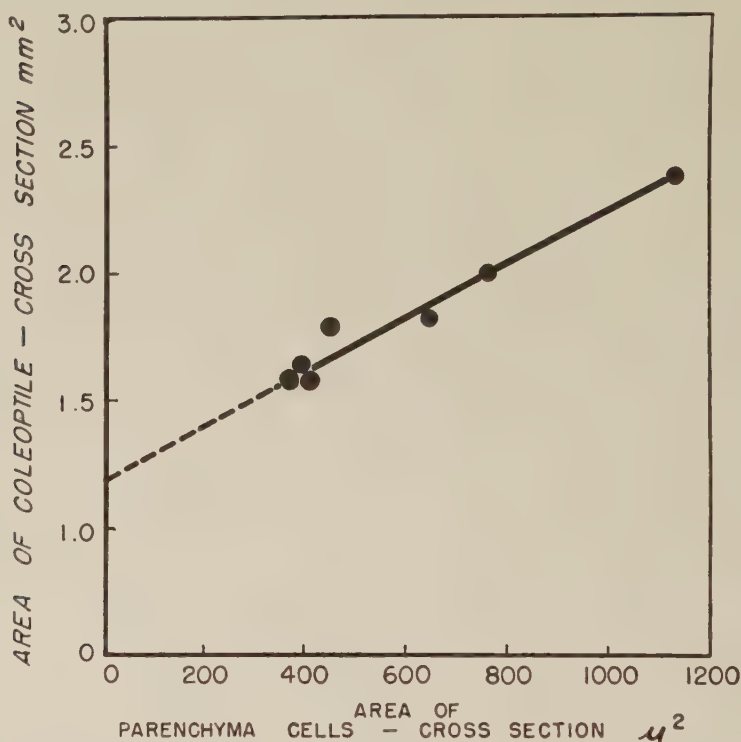


Fig. 4 Relation of parenchyma cell cross section area to coleoptile cross section area. $150 \times G$ for varying lengths of time.

area is divided into the coleoptile area (minus the 1.19 mm^2 discussed above), the result is an approximately constant parenchyma cell number of 668 cells for control and experimental plants. This, when adjusted for comparison, is slightly higher than the number found by Avery *et al.* ('45) in *Avena*

coleoptiles. If, on the contrary, it is not assumed that the size of the non-parenchymatous elements is constant, one is forced to conclude that centrifuged cells become fewer as they become larger. While it is possible that fewer than a normal number of cells might be produced when centrifugation is applied during the early part of the growing period, it is less likely that cell number could be reduced when the coleoptile is subjected to centrifugation after the 48th hour. Few new cells are formed after that time, and cells already formed could hardly vanish from their position in the coleoptile without leaving a trace.

While cell diameter is not significantly altered by centrifugation at $150 \times G$ during the first or the second day only, exposure during both of them produces enlargement. Exposure during the last two days, however, produces the greatest effect on diameter, possibly because then the weight of the overlying tissues is greater, and hence its absolute increase with supranormal gravitational forces is tremendously greater.

We are not prepared to say if the effect on diameters is reversible. Perhaps the enlargement noted in mature coleoptiles centrifuged during the first day of life would have been greater had the plants been sacrificed immediately following the period of centrifugation.

SUMMARY AND CONCLUSIONS

1. Wheat coleoptiles grown in the dark were centrifuged at various forces between $10 \times G$ and $500 \times G$ for various periods during their 4 day life.

2. Centrifugation during the first 24 hours produces an early increase in growth rate, while centrifugation during the second, third, or fourth day of life produces a depression in the growth rate which persists for 24 hours after cessation of centrifugation.

3. Depression of growth rate is roughly proportional to the milligram-millimeters of work done by the coleoptile in growing upward against gravity. It is suggested that the

inhibition is the result of increasing the work requirement beyond the physiological limits of the tissues.

4. Cross-sectional areas of both the coleoptile and the parenchyma cells at the coleoptile base increase with application of centrifugal forces, and these areas are more affected toward the end of the growing period when the weight of the overlying structures is greatest.

5. As in previous experiments, basal cell length varies only with age and not with final height of coleoptile.

6. Root growth is increasingly inhibited as the growth period progresses.

LITERATURE CITED

- EVERY, G. S. JR., M. PIPER AND P. SMITH 1945 Cell number in successive segments of *Avena* coleoptiles of different ages. *Am. J. Bot.*, 32: 575-579.
- BURSTRÖM, H. 1951 Plant growth substances. Ed. by Folke Skoog, University of Wisconsin Press. Mechanisms of cell elongation, 43-55.
- GRAY, S. W., AND B. F. EDWARDS 1955 Effects of centrifugal forces on growth and form of coleoptile of wheat. *J. Cell. and Comp. Physiol.*, 46: 97-126.
- KEEBLE, F. M., M. G. NELSON AND R. SNOW 1931 The integration of plant behavior. III. The effect of gravity on the growth of roots. *Proc. R. Soc. London, series B*, 108: 360-365.
- LARSEN, P. 1953 Influence of gravity on rate of elongation and on geotropic and autotropic reactions in roots. *Physiol. Plantarum*, 6: 735-774

RELATIONSHIP BETWEEN ELECTRICAL AND MECHANICAL CHANGES IN MUSCLE CAUSED BY COOLING¹

RITA GUTTMAN AND MILTON M. GROSS

*Department of Biology, Brooklyn College; State University of New York,
College of Medicine at New York City, and the Marine
Biological Laboratory, Woods Hole*

SIX FIGURES

INTRODUCTION

A number of studies have been made on the effect of cold upon the electrical properties of living cells. In attempting to prove that the membrane potential is essentially a diffusion potential, Bernstein ('02) showed that the resting potential of frog nerve and muscle is proportional to the absolute temperature. The Q₁₀ for frog sartorius muscle was established as 1.4 by Buchtal and Lindhard ('36) and as 1.1 by Ling and Woodbury ('49)

That rapid cooling can result in an action potential in the plant cell, *Nitella*, was shown by Hill ('35). Perkins et al. ('50) found that rapid cooling is effective as a stimulus for mammalian smooth muscle contraction, but recorded no potential changes. Ercoli and Guzzon ('52) showed that rapid cooling induces a contraction in isolated guinea pig intestine, though not in rabbit intestine. They recorded no potentials, but suggested that sudden temperature changes may stimulate by liberating a histamine-like mediator.

In the experiments here reported, rapid cooling was used merely as a device in an attempt to correlate the electrical

¹ This investigation was supported in part by a research grant (B-343) from the National Institutes of Health, Public Health Service, and in part by an Office of Naval Research Contract Nonr-09703 with the Marine Biological Laboratory, Woods Hole, made to one of us (R.G.).

and mechanical changes occurring in muscle on contraction, and not primarily because it was of interest in itself as a stimulus for contraction.

MATERIAL AND METHODS

Electrical potentials and either isometric or isotonic contractions were simultaneously recorded for the anterior byssus retractor muscle of *Mytilus edulis*. This is an invertebrate smooth muscle, the fibers of which are parallel and run the full length of the muscle (Fletcher, '36).

Large specimens of *Mytilus edulis* (about 10 cm in long diameter of the shell) were used. The anterior byssus retractor muscle which is about 4 cm long when relaxed, was dissected out, usually the night before, and suspended by means of a 10 gm weight in running aerated sea water overnight. The muscle was mounted in the chamber in the morning and usually remained excitable for as long as 7 hours.

In mounting, the muscle was threaded through holes in two rubber diaphragms, which divided a lucite chamber into three compartments (fig. 1). The portion of the muscle in one compartment was bathed in 0.26 M KCl (which contains 20 times as much potassium as is found in sea water), which served to depolarize that end (Curtis and Cole, '42). The other end of the muscle lay in a compartment filled with sea water or experimental solution. The middle inter-electrode region was bathed in paraffin oil (Twarog, '54). Agar bridges led to beakers of sea water and 0.26 M KCl respectively, each containing a silver-silver chloride electrode.

Control experiments indicated that the electrodes were affected by temperature changes and the use of the agar bridges eliminated this factor.

In the preliminary experiments (Guttman and Katz, '52), potentials were measured by means of a D.C. amplifier and recorded on a Grass ink writer.² In the main bulk of the experiments a galvanometer, used as a null point instru-

² We wish to thank Dr. John F. Perkins, Jr., for his kindness in lending us the apparatus used in the preliminary experiments.

ment, and a student potentiometer were substituted for the ink writer and amplifier since the contractions studied were extremely slow; 4 minutes or longer for contraction and relaxation, depending upon the initial tension exerted on the muscle. Contractions were recorded either isometrically or isotonically on a slow moving kymograph (2.5 cm per minute).

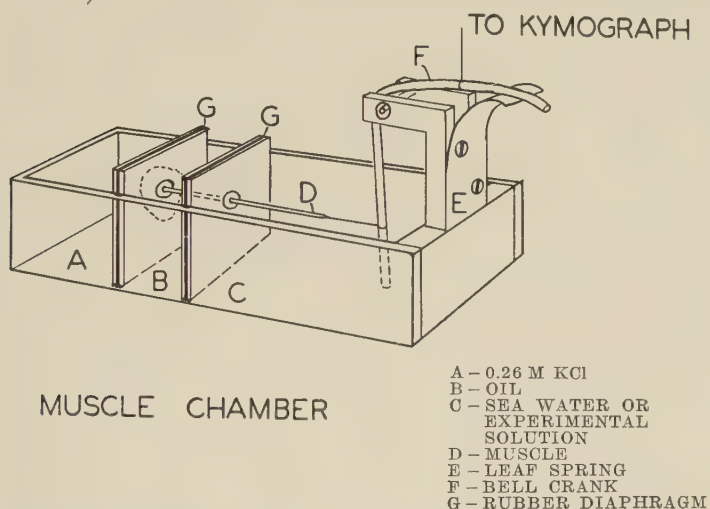


Fig. 1 Mounting chamber for measuring electrical potentials of *Mytilus* muscle.

Fresh solutions were made up daily. Where necessary, osmotic pressure was adjusted by adding distilled water sufficient to make up a 3% salt solution.

Experiments were done on 27 muscles.

RESULTS

Muscles were first placed in sea water containing excess potassium (from 3 to 7 times the amount of KCl found in sea water, .026 M to .078 M KCl added to sea water) for 4 minutes. These solutions did not contain sufficient excess potassium to cause contraction although they did cause the potentials to drop³ slightly. Then the muscles were rapidly cooled

³ By "drop," a numerical decrease in potential is meant.

(within a few seconds) from about 22°C. to 2°C. by rinsing the chamber three times with the cold sea water solution containing the excess potassium. Upon this rapid cooling the potentials dropped markedly and a contraction occurred

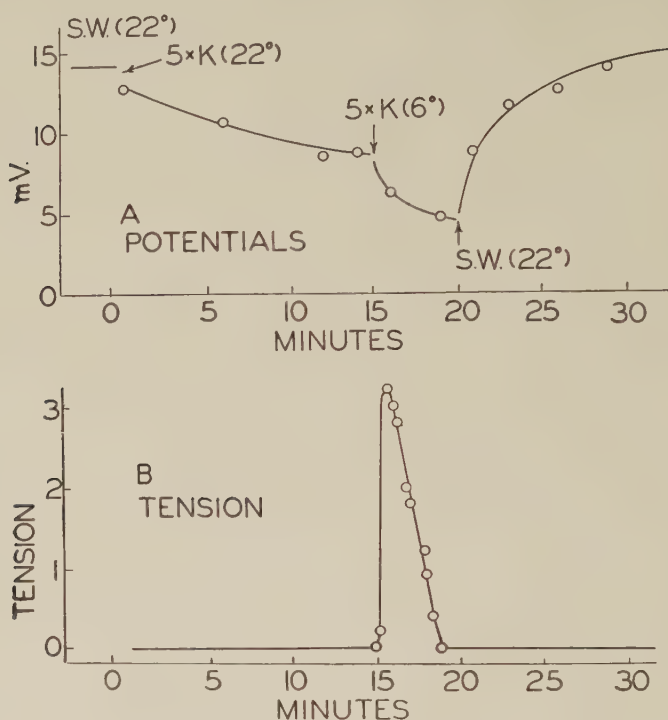


Fig. 2 Time course in minutes of potential changes (A), in millivolts as recorded on a Grass ink writer, and tension developed (B), in arbitrary units as simultaneously recorded on a kymograph, upon application of sea water solutions containing 5 times normal amount of potassium, at 22°C. and at 6°C. Effect is reversible on treatment with sea water at 22°C.

(fig. 2). Rapid cooling over as much as 22.5°C. does not result in contraction unless extra potassium is present.

The effect of varying the magnitude of the rapid temperature drop. If rapid temperature drops ($\Delta T.$) less than 20°C. were tried, the potential changes ($\Delta P.D.$) were correspondingly less. Below a certain magnitude of $\Delta T.$ and $\Delta P.D.$, no

contractions occurred. In figure 3, where 9 different ΔT 's and $\Delta P.D.$'s were recorded over a period of 7 hours on the same muscle, the threshold seems to occur at a ΔT . of about 14°C . and a corresponding $\Delta P.D.$ of about 3 mV. The ΔT . threshold varied considerably from muscle to muscle, however, i.e. from about 6° to 15°C .

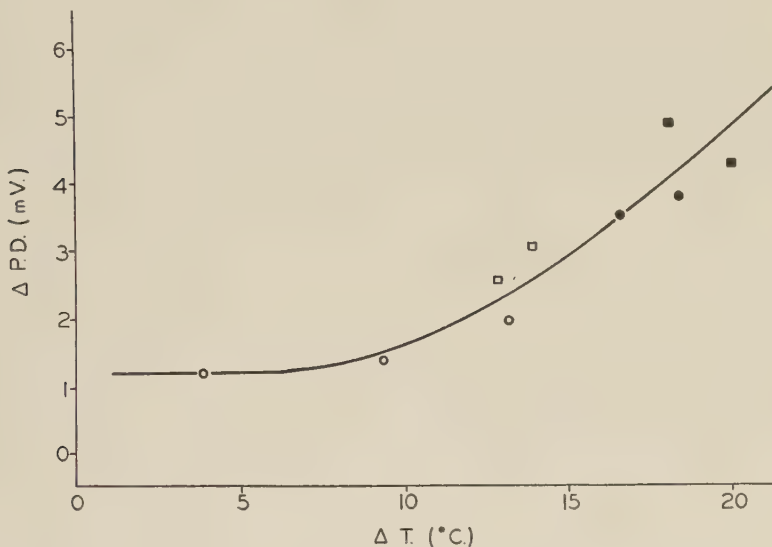


Fig. 3 Amount of potential change ($\Delta P.D.$) obtained on rapidly cooling *Mytilus* smooth muscle various amounts (ΔT). All readings obtained on same muscle over a 7 hour period. Circles indicate first run and squares indicate second run. Contraction occurred in solid squares and circles, not in open squares and circles. Threshold for this muscle occurred at about 3 mV, corresponding to a temperature change of about 4°C .

Gradual cooling vs. rapid cooling. The rate of cooling was also studied. When the cooling was accomplished in a fraction of a minute by rinsing the chamber three times with the cold solution, contraction occurred. If the cooling was accomplished over a $5\frac{1}{2}$ minute period by cooling in steps of 4° , then contraction occurred during the last two steps. If the cooling was still more gradual, i.e. over an 8 minute period, no contraction occurred (figs. 4, 5, and 6). Thus a threshold for rate of cooling exists between approximately $5\frac{1}{2}$ and 8 minutes.

The same amount of potential change occurred whether cooling was rapid (where contraction occurred) or gradual (where no contraction occurred) (figs. 4 and 5). In no case was what might be described as an action current spike ob-

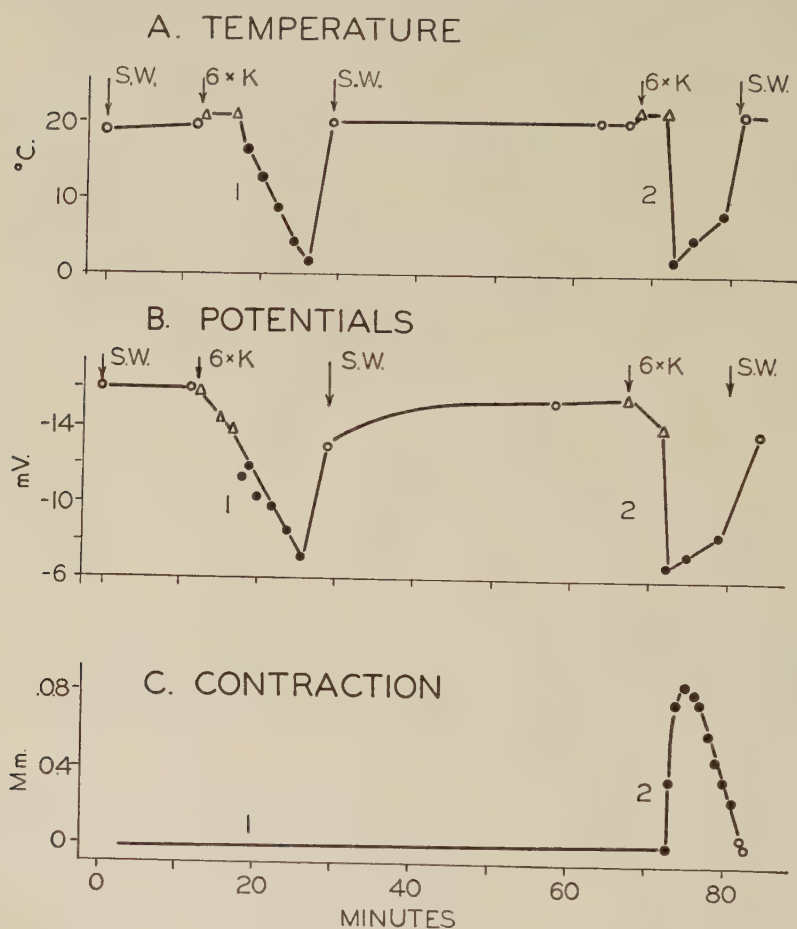


Fig. 4 Effect of sea water containing excess KCl (6 times the amount found in sea water) and of gradual and rapid cooling upon potentials in mV (B) and mechanical changes in millimeters of shortening (C) in *Mytilus* smooth muscle. Temperature of bathing solution is recorded in degrees Centigrade in A. Equal amounts of potential change occur on gradual and rapid cooling but mechanical shortening occurs only on rapid cooling. Recovery in sea water occurs in two stages, the first rapid and the second more gradual. All data obtained from same muscle.

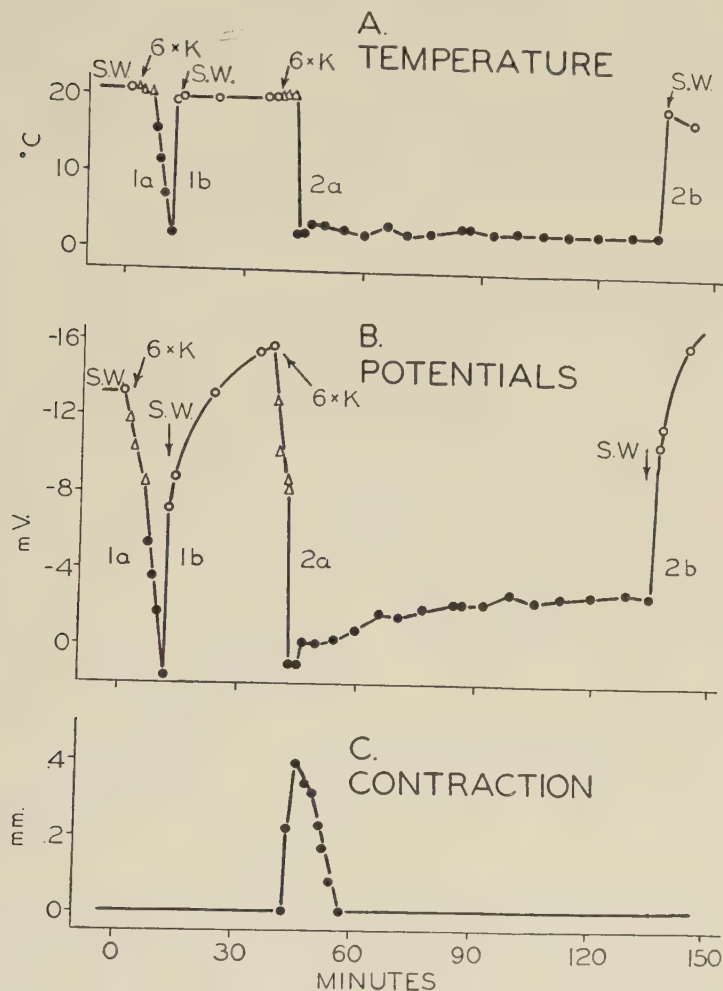


Fig. 5 Effect of sea water containing excess KCl (6 times the amount found in sea water) and of rapid (1b) and gradual (1a) cooling upon potentials in mV(B) and mechanical changes in millimeters of shortening (C) in *Mytilus* smooth muscle. Temperature of bathing solutions is recorded in degrees Centigrade in A. Equal amounts of potential change occur on rapid and gradual cooling but mechanical shortening occurs only on rapid cooling. When the bathing solution is kept cold for about 90 minutes the muscle relaxes but the potential gradually rises somewhat. Recovery in sea water (1b and 2b) occurs in two stages, the first rapid and the second more gradual. All data obtained from same muscle.

served, possibly due to the slowness of the galvanometer. The galvanometer had a period of 12 seconds.

Maintenance of cold temperature. In certain experiments the muscle was rapidly cooled (after treatment with extra potassium) and then the cold temperature was maintained

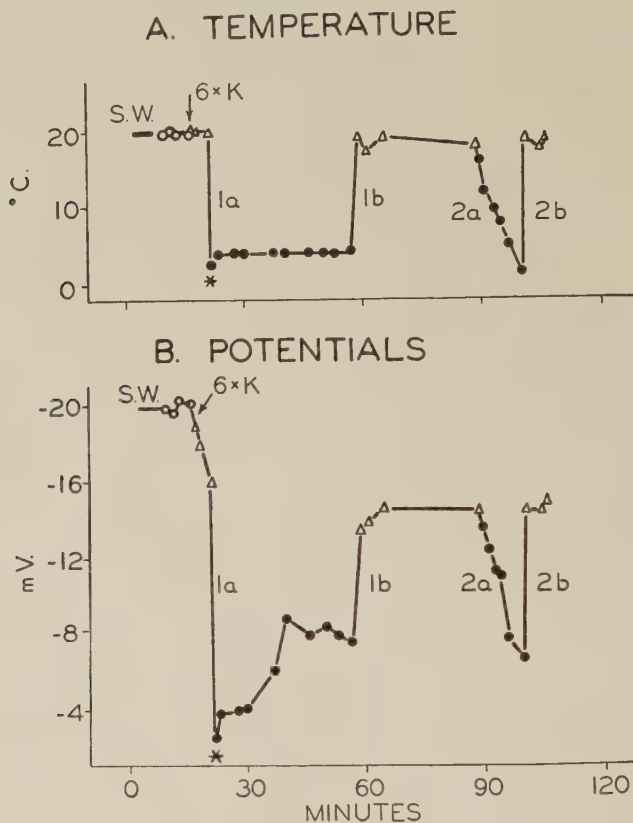


Fig. 6 Effect of sea water containing excess KCl (6 times the amount found in sea water) and of rapid (1a) and gradual (2a) cooling upon potentials in mV(B) and mechanical change in *Mytilus* smooth muscle. Contraction is indicated by the asterisk. Temperature of bathing solutions is recorded in degrees Centigrade in A. Recovery (1b and 2b) occurs in sea water containing 6 times the amount of KCl normally found in sea water. Note that the recovery potential in $6 \times$ KCl is lower than in sea water and that contraction occurs on rapid (1a) but not on gradual (2a) cooling. Since recovery has taken place in a solution containing excess potassium (1b), gradual and sudden cooling do not result in equal amounts of potential change. All data obtained from same muscle.

over a considerable period of time (2 and 2a, fig. 5). When the cold was maintained the potential rose only slightly (only from about $+1$ mV to about -3 mV in one hour, 2a, fig. 5). However, the contraction occurred only at the onset of the treatment with cold. After 14 minutes the muscle relaxed.

Throughout, the term "contraction" has been used in a general sense, i.e. not in the sense of a mechanical change such as a twitch or a tetanus accompanied by an action potential. Indeed, some aspects of the phenomenon here described resemble contracture in a phasic muscle such as frog Sartorius which has been subjected to a high potassium solution, where the mechanical change occurs only at the onset of the treatment and does not persist throughout the treatment, although the potential change produced is maintained (cf. fig. 5 and also Kuffler and Vaughan Williams, '53).

Contractures may be defined as contractile responses that are prolonged, reversible and non-propagated (Gasser, '30). While the first two properties are characteristic of the responses here reported, the last has not been exhaustively investigated as yet and so we prefer to use the general term "contractions," rather than "contractures," for the time-being. "Contraction" may be employed to describe any mechanical change involving shortening or tension changes and does not imply propagation.

Recovery after cooling. If the cold is not maintained but instead the muscle is returned to room temperature sea water, the return of the potential takes place invariably in two stages: an initial rapid stage (2 minutes in 1b, fig. 5) followed by a prolonged second stage (16 minutes in 1b, fig. 5). If, instead, the muscle is returned to room temperature sea water containing extra potassium, the return of the potential occurs in only one stage (2b, fig. 6). The fact that recovery here occurs in only one stage suggests that the second stage obtained on warming in sea water may be due to the time that is taken for the potassium in the muscle to diffuse out, while the first stage is probably a thermal effect.

It should be noted that the return of the potential when recovery takes place in the solution containing extra potassium is to the potassium level (about -15 mV in fig. 6) and not to the sea water level (-20 mV).

DISCUSSION

As mentioned previously, the authors were not primarily interested in establishing that rapid cooling is an effective stimulus for *Mytilus* smooth muscle which has been previously treated with extra potassium. Rather, they used potassium and rapid cooling as devices whereby they attempted to investigate the relationship between potential changes and the mechanical aspects of contraction.

The potential changes resulting from rapid and from gradual cooling are identical in magnitude, yet rapid cooling results in contraction and gradual cooling does not. An accommodation mechanism may be involved here.

The role of potassium is not clear. Rapid cooling over as much as 22.5°C . does not result in contraction unless extra potassium is present. (It is hoped to investigate the possibility of the substitution of other ions for potassium, i.e. sodium, calcium, rubidium, etc., in future experiments.) In some experiments, cooling was not introduced until the potential had first reached an equilibrium value in the high potassium solutions and yet the result was the same, i.e. cooling caused the potentials to drop markedly. Thus it cannot be argued that the change in potential on cooling represents merely an acceleration of the attainment of a new equilibrium value connected with ion shifts.

Why rapid cooling should trigger the contraction is not clear although there are a number of hypotheses which might be put forward.

1. Perhaps rapid cooling causes rupture of a non-aqueous layer (the fiber membrane) which has a different coefficient of contraction from the surrounding aqueous portions.⁴

⁴ Bartlett, J. H. Personal communication.

2. Or perhaps cooling adversely affects the metabolic processes which normally prevent potassium leakage across the membrane, and so contraction is brought about.

3. Or perhaps cold directly affects the myosin molecule, causing the chain to shorten. (However, with regard to this third hypothesis, no contractions were observed when artificial muscle fibers were rapidly cooled (Weber and Weber, '51; Ulbrecht and Ulbrecht, '52).

Further work along the line of the experiments here reported may possibly offer a basis for choice among these hypotheses.

A possible application of this work to the physiopathology of "immersion foot" (Montgomery, '54) is suggested.

The authors are deeply grateful to Dr. James H. Bartlett of the University of Illinois for his many valuable suggestions throughout this work.

SUMMARY

1. Electrical potentials and mechanical changes obtained on rapid cooling were simultaneously recorded for the anterior byssus retractor muscle of *Mytilus edulis* (an invertebrate smooth muscle) one end of which had previously been treated with a sea water solution containing from 3 to 7 times the amount of KCl normally present in sea water. This amount of extra KCl does not in itself cause contraction, although it does result in the potential dropping slightly. When pretreatment with extra KCl is followed by rapid cooling, potentials drop markedly and contraction occurs. However, cooling alone without treatment with extra potassium does not cause contraction.

2. With abrupt cooling, the ΔT . threshold for contraction varied from about 6° to 15°C.

3. When cooling was more gradual, the threshold for the rate of cooling necessary to achieve contraction varied from 5½ to 8 minutes.

4. Rapid cooling and gradual cooling resulted in identical magnitudes of potential change, yet rapid cooling resulted in contraction while slow cooling did not. An accommodation mechanism may be involved here.

5. When the low temperature is maintained after rapid cooling, contraction occurs only at the onset of the treatment with cold. During the course of the treatment with cold, the potential rises slightly, finally achieving a new equilibrium value.

6. When, after cooling, the muscle is returned to sea water at room temperature, the return of the potential to its original value occurs in two stages. The first stage is rapid (probably a thermal effect) and the second one is slower (probably due to an adjustment of the diffusion layer).

If, after cooling, the muscle is returned to a room temperature solution containing excess KCl, the potential change is correspondingly less and occurs in only one stage (presumably a thermal effect only).

LITERATURE CITED

- BERNSTEIN, J. 1902 Untersuchungen zur Kenntnis der bioelektrischen Ströme. Erste Theil. Arch. f. d. ges. Physiol., 92: 521-562.
- BUCHTAL, J., AND J. LINDHARD 1936 Ueber den Einfluss der Temperature auf Potentialdifferenzen der Muskelfaser und im System motorische Endplattmuskelfaser. Skand. Arch. f. Physiol., 74: 223-238.
- CURTIS, H. J., AND K. S. COLE 1942 Membrane resting and action potentials from the squid giant axon. J. Cell. and Comp. Physiol., 19: 135-144.
- ERCOLI, N., AND V. GUZZON 1952 Thermal stimulation of isolated organs and its inhibition by pharmacological agents. Science, 115: 672-674.
- FLETCHER, C. M. 1936 Action potentials recorded from an unstriated muscle of simple structure. J. Physiol., 90: 233-253.
- GASSER, H. S. 1930 Contractures of skeletal muscle. Physiol. Rev., 10: 35-109.
- GUTTMAN, R., AND A. M. KATZ 1953 Potential and mechanical changes in muscle on rapid cooling. XIX Internat. Physiol. Congress, 424.
- HILL, S. E. 1935 Stimulation by cold in Nitella. J. Gen. Physiol., 18: 357-367.
- KUFFLER, S. W., AND E. M. VAUGHAN WILLIAMS 1953 Properties of 'slow' skeletal muscle fibers of the frog. J. Physiol., 121: 318-340.
- LING, G., AND J. W. WOODBURY 1949 Effect of temperature on the membrane potential of frog muscle fibers. J. Cell. and Comp. Physiol., 34: 407-412.
- MONTGOMERY, H. 1954 Experimental immersion foot. Review of the physiopathology. Physiol. Rev., 34: 127-137.

- PERKINS, J. F., JR., M. LI, C. H. NICHOLAS, W. H. LASSEN AND P. E. GERTLER
1950 Cooling as a stimulus to smooth muscles. *Am. J. Physiol.*, *163*:
14-26.
- TWAROG, B. M. 1954 Responses of a molluscan smooth muscle to acetylcholine.
J. Cell. and Comp. Physiol., *44*: 141-164.
- ULBRECHT, O., AND M. ULBRECHT 1952 Der isolierte Arbeitszyklus glatter
Muskelatur. *Z. f. Naturforsch.*, *7b*: 434-443.
- WEBER, A., AND H. H. WEBER 1951 Zur Thermodynamik der Kontraktion des
Fasermodells. *Bioch. et Biophys. Acta*, *7*: 339-348.

EFFECTS OF HIGH INTENSITY SOUND ON ELECTRICAL CONDUCTION IN MUSCLE¹

WALTER WELKOWITZ² AND WILLIAM J. FRY
Bioacoustics Laboratory, University of Illinois, Urbana, Illinois

TWELVE FIGURES

INTRODUCTION

In recent years there has been considerable experimentation on the biological and medical applications of ultrasound. Pertinent literature can be located by reference to bibliographies (Naimark et al., '51; Curry et al., '51) and symposium publications (Matthes and Rech, '49; Giacommi, '50; Fry et al., '53). Some of this research has dealt with effects on muscle tissue (Gersten, '53 and '54; Gary and Gerendas, '49; Harvey, '29). In much of the reported work there is no adequate description of the characteristics of the sound field so that quantitative physical interpretations are difficult.

In this paper, the results of a study of the effect of intense acoustic radiation on the propagation of the action potential in muscle tissue are presented. Temperature measurements in the muscle were accomplished during irradiation, and the effect of pure heating on the electrical conduction process was investigated. The results indicate that irreversible suppression of the propagated action potential by the sound can be accomplished in the absence of a damaging temperature level. Although no experimental work was performed under a hydrostatic pressure sufficiently high to insure that no tension forces existed in the muscle, it is possible to conclude

¹Supported by Contract AF33(038)-20922 with the Aero-Medical Laboratory of the Wright Air Development Center, Ohio.

²Submitted in partial fulfillment of the requirements for the degree of Doctor of Philosophy at the University of Illinois, 1954. Present address: Gulton Mfg. Corp., Metuchen, New Jersey.

on the basis of indirect observations that no extensive cavitation occurred in the muscle tissue.

EXPERIMENTAL METHODS

1. Ultrasonic generation

A travelling wave sound field, frequency 991 kc/sec., was used for most of the experimental work. This field was pro-

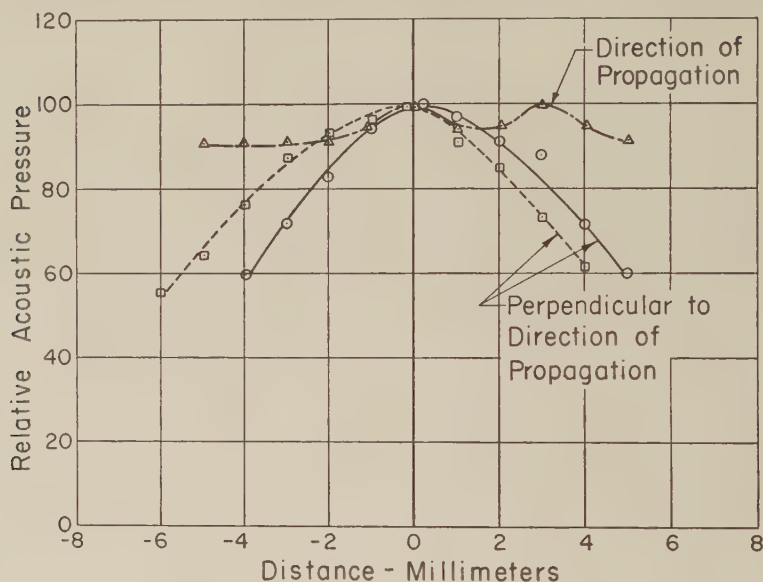


Fig. 1 Acoustic pressure distribution in the sound field. The zero of the coordinate system is the point at which the muscles were centered in the field. The value of the relative pressure amplitude at this point is arbitrarily taken equal to 100.

duced in degassed Ringer's solution by a flat, one inch diameter x-cut quartz crystal mounted as previously described (Fry, '50). The sound field distribution produced by the crystal system and measured at the muscle location is shown graphically in figure 1. The system was calibrated with a thermocouple probe described by Fry and Fry ('54). The intensity and acoustic pressure amplitude, as determined from measurements made with this device at the spatial peak

of the field, are given in table 1 as a function of the voltage applied to the crystal. The biological preparations were subjected to single pulses (square wave envelope) of radiation. The temperature of the solution in which the muscles were immersed could be adjusted to any desired value.

TABLE 1
Calibration data for the crystal systems

SYSTEM	CRYSTAL VOLTAGE	PRESSURE AMPLITUDE	INTENSITY
	<i>volts</i>	<i>atmospheres</i>	<i>watts/cm²</i>
1	8000	19.0	123
	7000	16.6	94
	6000	14.2	69
2	8000	22.2	168
	7000	19.4	128
	6000	16.6	94

2. *Biological preparation*

Excised hind leg biceps muscles from *Rana pipiens* were utilized in these studies. They were mounted in the holder as shown in figure 2. Irradiation was carried out with the muscle immersed in Ringer's solution. To eliminate cavitation during irradiation, the solution was degassed by boiling for 10 minutes and then cooled rapidly. The preparation was positioned, transverse to the direction of propagation, at the peak of the sound field by means of a probe and pointer system. The positioning procedure was found to give the same location repeatedly within one millimeter. Any nerve or nerve-muscle endplate effects were eliminated by curarizing the preparation to block nerve-muscle stimulation. The muscle fibers were excited directly by a square wave electrical pulse. The curarization was carried out by introducing d-tubocurarine chloride into the Ringer's solution at a concentration of 6 mg per liter. This concentration is about 5 times the dosage found by Kuffler ('42) to be necessary to completely block the nerve-muscle excitation path for single muscle fibers. For complete curarization, checked by electrical

test, the muscle was permitted to remain in the solution for 20 minutes before irradiation.

The experimental procedure followed was to excite the muscle with a pair of electrodes at one end, record the propa-

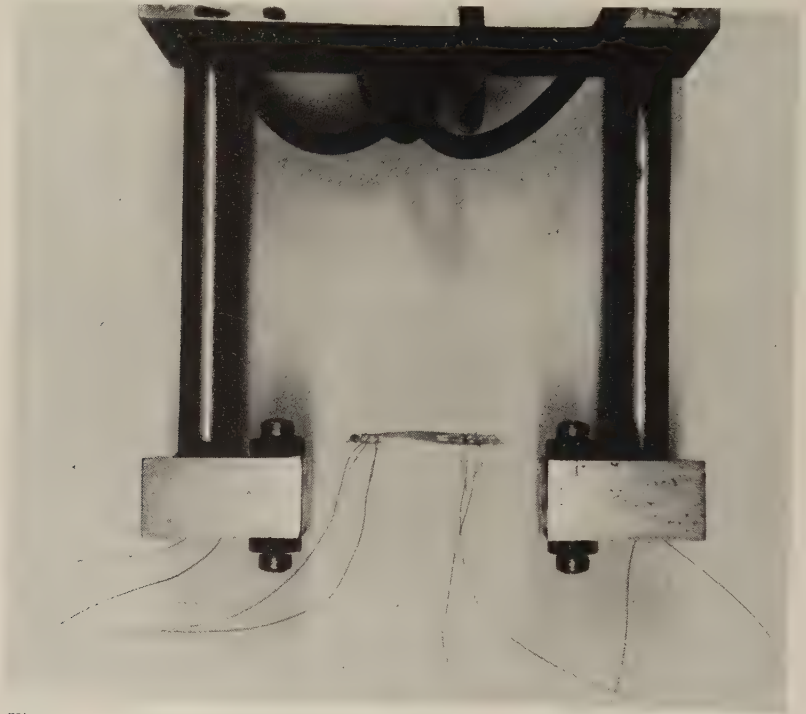


Fig. 2 Muscle mounted in holder. The electrical leads to both ends are shown.

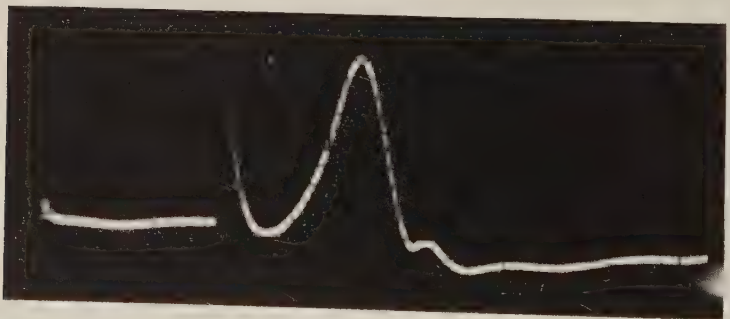


Fig. 3 Propagated muscle action potential obtained with the arrangement illustrated in figure 2.

gated action potential with a pair of electrodes at the opposite end and irradiate with sound between the pairs of electrodes. A propagated muscle action potential obtained under the experimental conditions outlined is shown in figure 3. No special attempt was made to obtain monophasic responses since this would have complicated the experimental procedure. The amplitude of such an action potential was the quantitative measure used throughout the experiments.

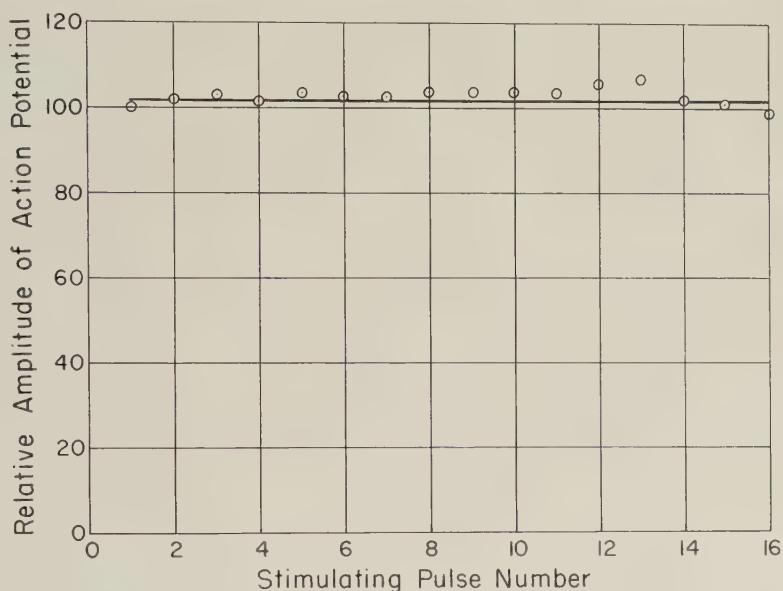


Fig. 4 Variation in the amplitude of the action potential of a muscle stimulated once every five seconds.

EXPERIMENTAL RESULTS

1. *Effects of acoustic irradiation*

Before proceeding to the irradiation studies, electrical control measurements were carried out on a number of muscle preparations. A typical graph of the relative amplitude of the action potential as observed on a muscle stimulated approximately once every 5 seconds for a minute and a half is shown in figure 4. This set of measurements and others

like it demonstrate that deviations from an average value of less than about 5% can be obtained by this technique. The stability of the preparation using the experimental procedure described is therefore quite good.

The most pronounced effect obtained from irradiation was a large permanent suppression, even complete block, of the action potential after exposure to a single pulse of sound.

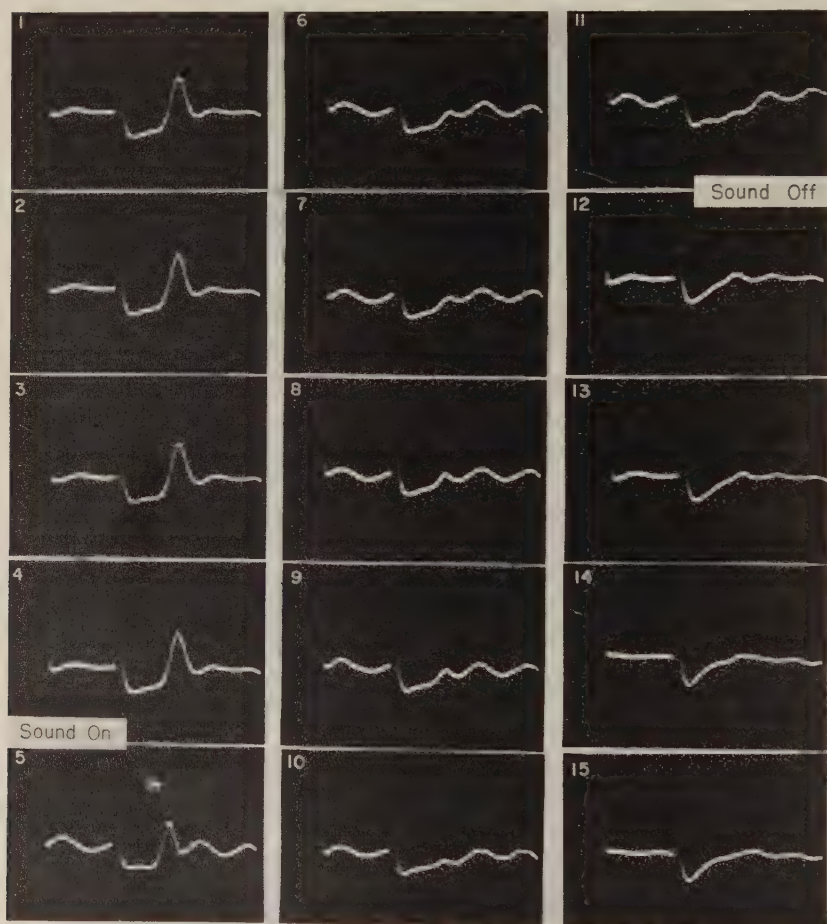


Fig. 5 Effect of acoustic radiation on the action potential of muscle. The propagated electrical responses to successive stimuli are ordered in columns. See figure 6 for a plot of relative amplitude.

This effect was established by measurements made on about 30 muscles. A typical run of data taken at 20°C. with a peak acoustic pressure amplitude of 19 atmospheres and a 40 second pulse of sound is shown in figure 5. The relative amplitude as a function of time is presented graphically in figure 6. Monotonically decreasing curves have been obtained

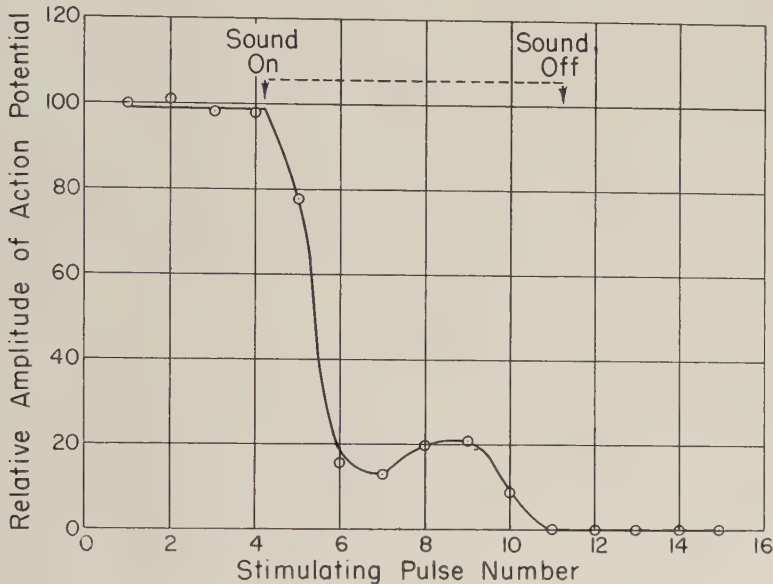


Fig. 6 Relative amplitude of the action potential of muscle as affected by acoustic irradiation. Values obtained from the records of figure 5. A length of the muscle between stimulating and receiving electrodes was subjected to the sound. Acoustic pressure amplitude, 19 atm.; period of irradiation, 40 sec.; bath temperatures, 20°C.

in addition to the type illustrated which shows a small rise during the period of suppression by the sound. No fundamental significance is attached to this small rise. The muscle was stimulated to twitch about once every 5 seconds. Four control measurements were taken before the sound was turned on and 4 more after the sound was turned off. From the figure and the graph it is apparent that propagation of the action potential was completely blocked by the sound. This effect

is obtainable under various dosage conditions. Figure 7 shows a graph of results using a peak pressure amplitude of 16.6 atmospheres with a 100 second pulse. Similar effects can be obtained at lower temperatures. Figure 8 shows a run taken at 15°C. The amplitude of the action potential is presented graphically in figure 9. In this case about 75% suppression was obtained. A 60 second pulse of sound at 19

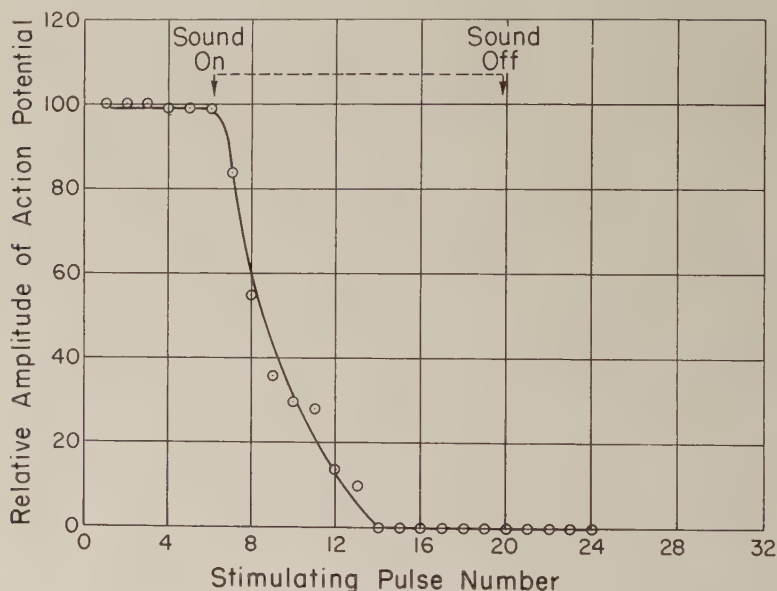


Fig. 7 Relative amplitude of the action potential of muscle as affected by acoustic irradiation. A length of the muscle between the stimulating and receiving electrodes was irradiated. Pressure amplitude, 16.6 atm.; period of irradiation, 100 sec.; bath temperature, 20°C.

atmospheres was used in obtaining this result. This run, in conjunction with others made at lower temperatures, indicates that the dosage conditions required to produce the observed effect on muscle are temperature dependent.

In order to derive more quantitative information from the experiments than that provided by a single dosage condition, data were obtained for a curve of minimum dosage required to produce a prescribed change in the electrical conduction

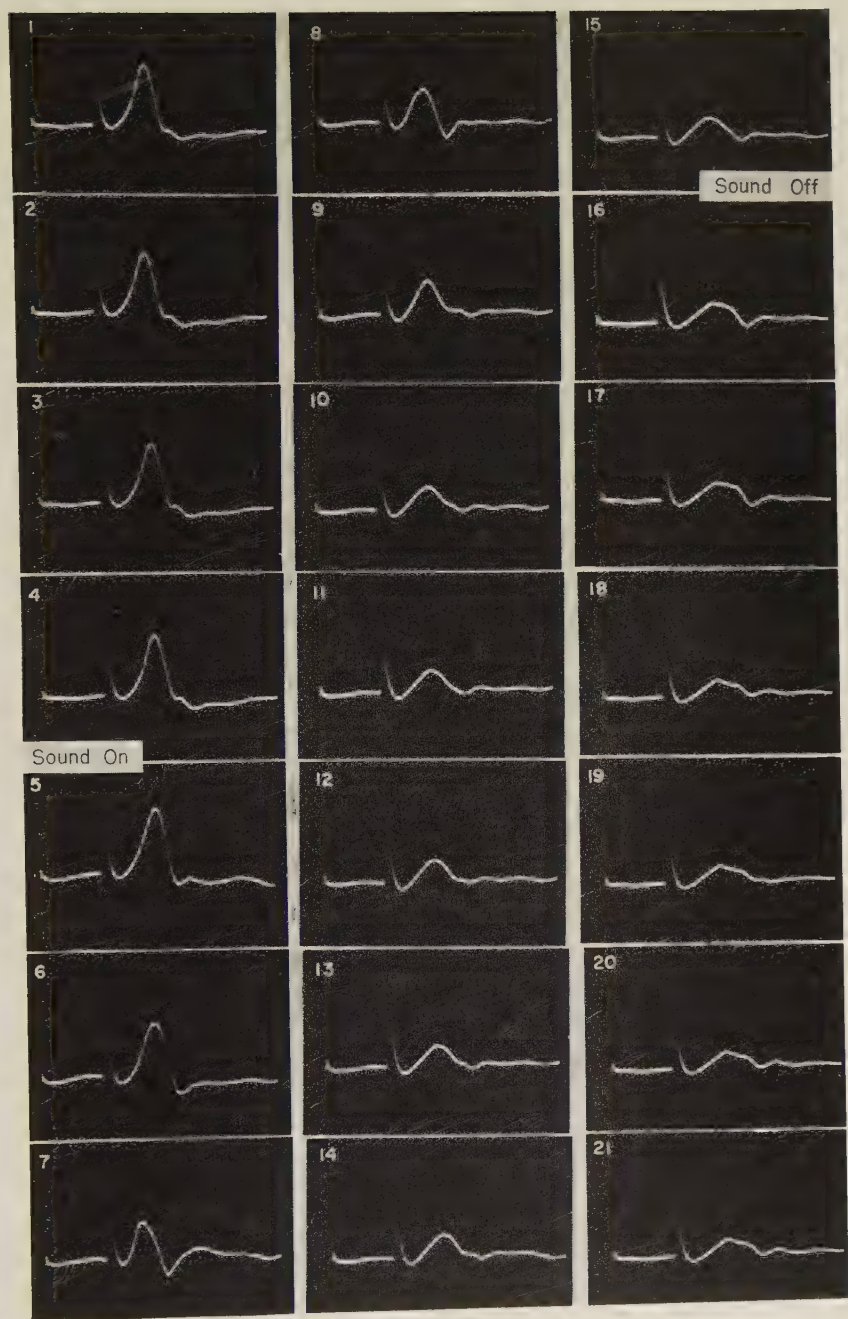


Fig. 8 Effect of acoustic radiation on the action potential of muscle. The propagated electrical responses to successive stimuli are ordered in columns.

characteristic of the biceps muscle. Minimum dosage was defined in the following manner. For each irradiation time, three muscles were subjected to the sound at each of several driving voltages across the crystal. These were spaced 250 volts apart, this increment representing less than 5% of the total driving voltage. The pressure amplitude of minimum

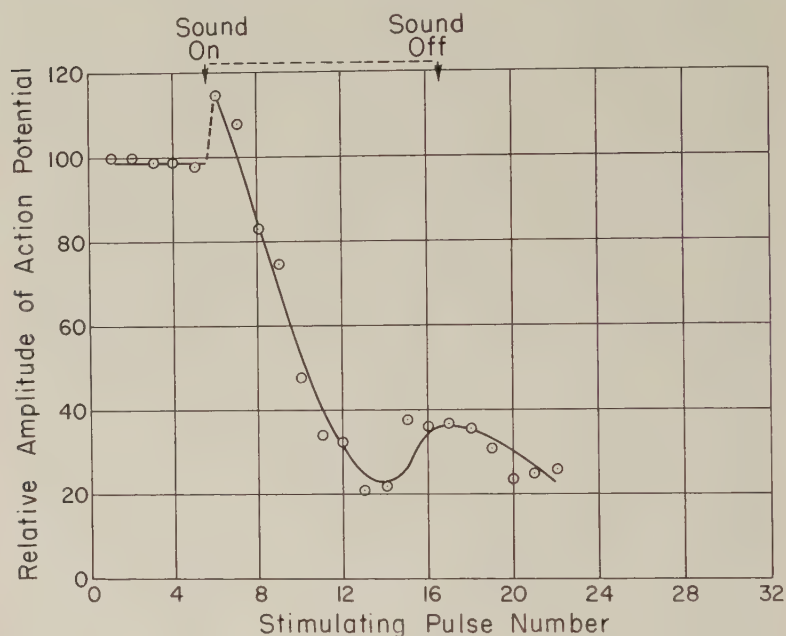


Fig. 9 Relative amplitude of the action potential of muscle as affected by acoustic irradiation. Values obtained from the records of figure 8. Acoustic pressure amplitude, 19 atm.; period of irradiation, 60 sec.; bath temperature, 15°C.

dosage for a specific duration of irradiation was defined to lie between the pressure amplitude corresponding to the voltage at which at least two of the three muscles experienced a reduction of more than 10% in action potential amplitude and that pressure amplitude at which no more than one muscle was so affected. A further proviso was required that at higher pressure amplitudes than the first, a greater reduction in action potential must be observed, and at pres-

sure amplitudes below the second, the observed effects must be smaller. The reciprocal of the irradiation time was plotted against the sound pressure amplitude of minimum dosage to yield the curve of figure 10. The temperature range over which all these data were obtained was between 18 and 20°C.

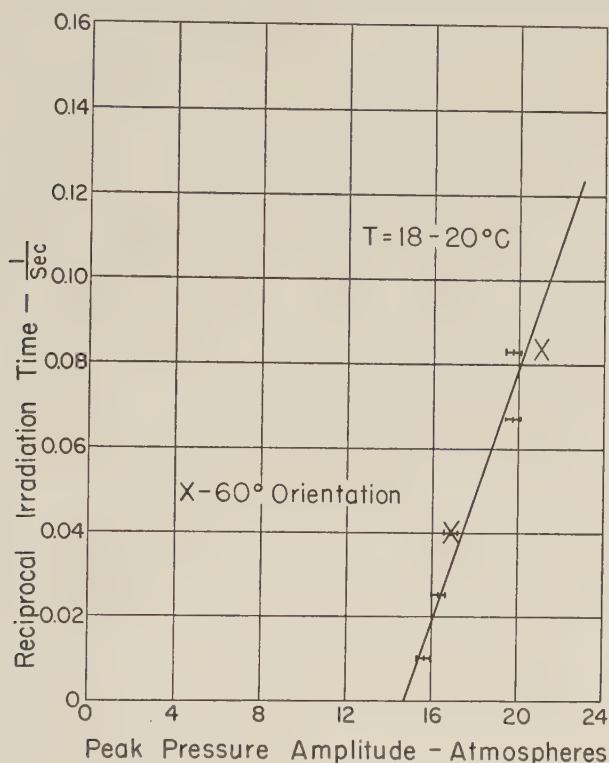


Fig. 10 Reciprocal of the minimum duration of irradiation to obtain a permanent reduction of the muscle action potential as a function of the acoustic pressure amplitude. See text for a precise definition of minimum dosage.

Over 120 frogs were used in obtaining the measurements on minimum dosage. The straight line relationship of the data is similar to the curve obtained by Fry ('51) from data on the paralysis of frogs irradiated in the lumbar enlargement region of the spinal cord. It is of interest to note here that the induction by ultrasound (lower in pressure amplitude than the levels used in the experiments reported in this paper)

of reversible changes in muscle which can be ascribed to a non-temperature mechanism have been previously reported (Busnel et al., '53).

It was observed in the course of the experimentation that no difference in effects occurred by switching the muscle end for end. The possible dependence of the observed effects on the geometrical orientation of the muscle with respect to the direction of propagation of the sound was considered. Consequently, experiments were performed at two of the pulse durations used in obtaining the data for figure 10 with the muscle oriented at 60 degrees with respect to the direction of propagation rather than perpendicular to it. These results, plotted in figure 10, indicate that there is no major difference for the orientations tested.

Histological studies were carried out on irradiated muscles stained with hematoxylin-eosin. The tissue was fixed in formalin immediately after irradiation. No differences were observed microscopically between the irradiated and normal tissue. Examination of sections of irradiated tissue indicate no tissue tearing or vacuolization.

Preliminary work on the acoustic irradiation of striated muscle with the vascular system intact (gastrocnemius muscle of *Hyla*) indicates that results similar to those described in this paper are obtained.

Irradiation of excised sciatic nerve of *Rana pipiens* at the highest sound level used in the studies reported herein, exposed for much longer periods of time than that required to permanently block muscle action potentials, produces no observable suppression in the nerve action potential.

2. Temperature changes in muscle produced by irradiation

Temperature changes were measured in muscles during irradiation by means of imbedded thermocouples. These thermocouples were made of three mil copper and constantan wires joined with a soldered lap junction. The thermocouple was threaded through the excised mounted muscle. Equi-

librium temperature measurements were made. Practical equilibrium was established in less than 10 seconds after the sound was turned on. The thermocouple was placed in the muscle as close to the center line as possible. As indicated previously the muscle was located at the peak of the sound field by means of a probe and pointer. The thermocouple emf was observed for various sound levels so that a curve

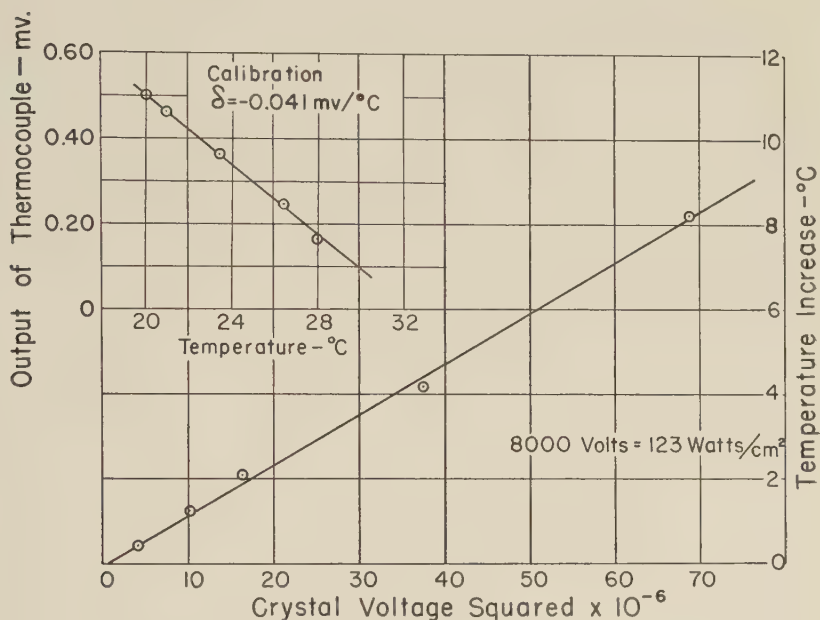


Fig. 11 Equilibrium temperature rise in a muscle at various sound levels determined by measuring the emf generated by an imbedded thermocouple.

could be obtained of temperature change versus acoustic intensity. The thermocouple was calibrated for each muscle while imbedded in the muscle. The holder with muscle and imbedded thermocouple was placed in baths of Ringer's solution at various temperatures and emf readings were taken. The temperatures of the baths were measured with a mercury thermometer and a calibration curve of thermocouple emf as a function of temperature was plotted.

Data of the type described were taken on 10 muscles. A typical thermocouple calibration curve and temperature measurement curve for a muscle are shown in figure 11. In all but one of these instances, a plot of temperature rise as a function of the square of the crystal voltage demonstrated a linear relationship. The one set of non-linear data was therefore disregarded as representing an atypical situation, possibly caused by cavitation at the thermocouple-muscle interface. Table 2 shows values of the equilibrium temperature rises in muscles for peak sound intensities of 123 and 94 watts/cm². At the higher acoustic level it is possible to block completely

TABLE 2

Measured temperature changes in excised biceps muscle under acoustic irradiation

MUSCLE NUMBER	TEMPERATURE CHANGE AT 94 WATTS/CM ²	TEMPERATURE CHANGE AT 123 WATTS/CM ²
	°C.	°C.
1	5.5	7.1
2	5.9	7.8
3	4.5	5.8
4	4.3	5.6
5	3.2	4.2
6	3.4	4.4
7	4.6	6.0
8	5.3	6.9
9	9.6	12.5

the muscle response in about 40 seconds. At the lower level about 100 seconds are required. It is apparent from table 2 that quite a wide range of values for the equilibrium temperature rise is obtained in various muscles. The reasons for this are readily understood on the basis of the following discussion.

In the problem being considered, the muscle is roughly the shape of a long cylinder and is imbedded in a large bath of Ringer's solution which is maintained at essentially constant temperature. Transverse to the axis of the muscle, the sound intensity varies less than 10% over the muscle. In the axial direction the beam is about 7 mm wide at the half power points. The muscle is generally quite a bit longer than this.

Two simple geometries for the mathematical solution of the problem suggest themselves for the physical conditions. One is an infinitely long, solid, circular cylinder with a constant amount of heat per unit volume generated throughout and with the surface kept at a constant temperature. Since the sound beam is finite and small, the other suggested geometry is a solid sphere with a constant amount of heat per unit volume generated throughout and with the surface kept at a constant temperature. The cylindrical model leads to predicted temperature values in the muscle which are high, since heat is not actually supplied all along the cylinder but only in a small region. The second geometry probably leads to low values of predicted temperature rise, since part of the boundary is then not Ringer's solution but is muscle and does not remain at the fixed temperature of the Ringer's solution.

For the cylindrical situation, under equilibrium conditions, the solution to the general heat flow equation is (see for example Carslaw and Jaeger, '47)

$$T - T_1 = A(a^2 - r^2)/4k \quad (1)$$

while for the spherical case

$$T - T_1 = A(a^3 - r^3)/6k \quad (2)$$

In equations (1) and (2), T_1 is the constant temperature of the Ringer's solution and T designates the temperature in the muscle. The symbol r represents the radial coordinate and a is the radius of the muscle. The symbol k designates the heat conductivity coefficient of the muscle and A is the heat generated per second per unit volume resulting from absorption of acoustic energy. These equations demonstrate that the solutions for the temperature distribution as a function of radial coordinate are identical in form and differ for any value of r by only 33% in magnitude. Since these are extreme situations with the physical case falling somewhere between, it seems reasonable to use these solutions to describe approximately the actual condition in the muscle. Comparison of the temperature changes predicted by the equations

with the measured values can be made by inserting appropriate values of the constants into equations (1) and (2).

The value of A , the heat generated per unit volume per second, is given by

$$A = I \mu \quad (3)$$

where I designates the sound intensity and μ the intensity absorption coefficient per unit path length. In order to calculate values corresponding to the measured results given in table 2, intensities of 123 and 94 watts/cm² were used. The value of μ for striated frog muscle was found by Fry et al. ('50) to be about 0.2. For lack of more complete information, the value of the thermal conductivity coefficient of water ($k=0.0060$ watts/cm²/°C. at 20°C.) was used in

TABLE 3

Computed temperature changes along the axis of a model of a muscle under sound irradiation

SOUND INTENSITY	TEMPERATURE RISE CYLINDRICAL GEOMETRY	TEMPERATURE RISE SPHERICAL GEOMETRY
watts/cm ²	°C.	°C.
123	10.3	6.9
94	7.9	5.3

the calculations. Measurements of the diameters of 50 muscles indicated an average value of $a=0.1$ cm. Table 3 shows the computed values of peak temperature rise ($r=0$) for the two geometries at the two sound intensities chosen.

A comparison of tables 2 and 3 demonstrates that the agreement between calculation and measurement is good. An examination of equations (1) and (2) helps explain the variation in the measured values. Part of the variation may be accounted for by inaccurate positioning of the thermocouple. For example, if the thermocouple is positioned at half the radial distance away from the axis of the muscle, then the temperature rise will be only three quarters of the peak value ($r=0$). Much of the variation can be accounted for by differences in muscle size. Since the equilibrium temperature rise is proportional to the square of the muscle radius,

an increase in this value of only 25% leads to a change in the value of the temperature rise of more than 50%.

A pertinent point to note from the equations is that the temperature rise at any radial distance is proportional to the quantity (a^2-r^2) , therefore half the muscle fibers undergo a temperature rise of less than half the peak value.

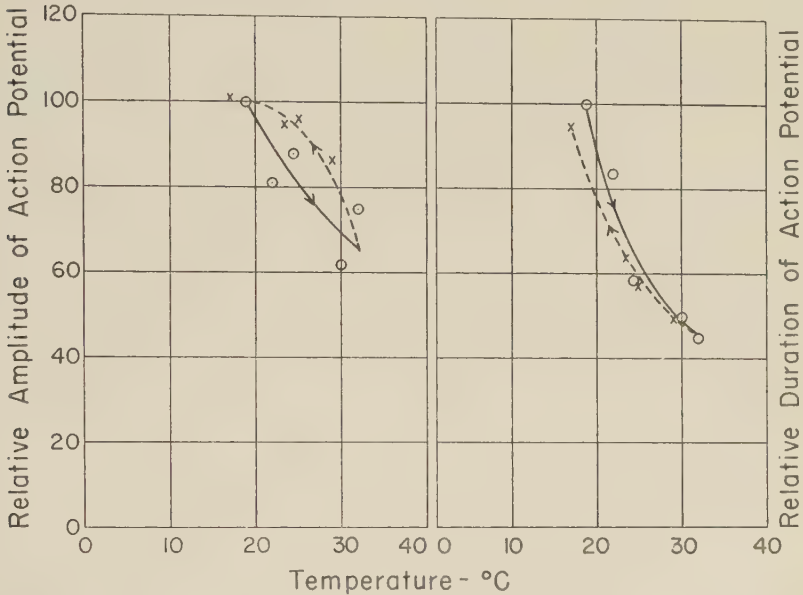


Fig. 12 Relative amplitude and duration of the action potential of frog biceps muscle as a function of the temperature.

3. *Effects of temperature changes on muscle action potential*

Study of some of the literature in the field (Doi, '20; Walker, '49) yielded little conclusive information on the effects of temperature changes on the action potential of muscle. Experiments were therefore undertaken to determine the effects of temperature changes on the frog muscle action potential under conditions similar to those established for the acoustic irradiation experiments. Measurements were carried out on 7 muscles under the following conditions. A number of saline-

tubocurarie baths were kept at various fixed temperatures and each muscle was run through the different baths. The muscle was kept in each bath for two minutes to bring about equilibrium conditions before electrical measurements were made. This procedure yielded consistent results. In 6 of the 7 muscles, almost complete reversibility in height and duration of the action potential was measured as the muscle was carried through a temperature cycle from about 20°C. to about 35°C. then back to 20°C. In no case was the amplitude of the action potential reduced to zero. A graph of the relative changes in amplitude and duration of the action potential as a function of temperature is shown in figure 12 for a typical muscle. These measurements of the effects of temperature change on the action potential demonstrate that if acoustic absorption in the muscle does not result in a temperature greater than 35°C. throughout the muscle, permanent reduction or irreversible block of the action potential cannot be attributed to the temperature change.

DISCUSSION OF RESULTS

Before considering the physical mechanism of the action of sound on muscle tissue, it is necessary to eliminate possible artifacts. Hydrodynamical flow, which is present in intense sound fields in fluids, might cause mechanical difficulties at the connection of the electrodes to the muscle. In addition, direct mechanical forces on the electrodes, such as radiation pressure, might contribute to the observed effects.

In investigating the hydrodynamic flow artifact possibility, experiments were carried out with flows produced by ejecting fluid from a jet immersed in the coupling liquid and directing it at the muscle. The effects on the observed action potential, caused by flow velocities 6 to 10 times those present during acoustic irradiation, are slight and indicate that the results obtained during ultrasonic irradiation (large reduction or complete block of the action potential) are not caused by a flow artifact.

Two types of experiments were carried out to eliminate the possibility of direct electrode artifacts. When a balsa wood fixture was mounted on the muscle holder for the purpose of shielding the electrodes from the sound field, large reductions of the height of the action potential were still attainable under ultrasonic irradiation. When a pair of electrodes was placed at the peak of the acoustic field and irradiated with a sound level equivalent to that normally incident on the electrodes for the customary geometry only slight changes in the observed response were evident. Therefore electrode artifacts do not account for the observed ultrasonic effects.

Besides these artifacts, it is always possible that the observed effects can be caused by heating or cavitation in the muscle tissue. Finally, the mechanical forces which are inherent in a sound field travelling through a medium can be involved in the mechanism. These forces can be unidirectional, such as radiation pressure or Oseen type, or sinusoidally varying with time such as the oscillatory viscous force associated with the relative motion between a fluid medium and imbedded particles.

The possibility that the observed irreversible suppression of the action potential is caused by excessive muscle heating has been eliminated. An examination of the irradiation data indicates that it is possible to block permanently or greatly reduce the amplitude of the action potential with the muscles at initial temperatures of 20°C. and 15°C. by irradiating at a peak sound pressure amplitude of 19 atmospheres (123 watts/cm²). The measured values of the temperature rise in the muscle under the same irradiation conditions show that the temperature in the tissue does not exceed approximately 30°C. for an initial temperature of 20°C., and for an initial temperature of 15°C. the maximum temperature does not exceed 25°C. An examination of the effects on the muscle action potential of a temperature cycle reaching a maximum value of 35°C. proves that blocking does not occur and that the amplitude changes are essentially reversible. The experimentally measured values of the temperature rise in the muscle

during irradiation are in agreement with calculated values, and the analysis further indicates that half the fibers in the muscle undergo temperature changes of less than half the maximum value.

In discussing the possible role of cavitation in the mechanism of the observed effects produced in muscle, it is noted that as yet no direct attempt has been made to completely eliminate the cavitation possibility by carrying out the experiments under a hydrostatic pressure sufficiently high to insure that no tension forces exist in the tissue. Such experiments are currently in the planning stage. However, there are a number of indications that cavitation was not present, at least to any appreciable extent, under the experimental conditions which prevailed. The first evidence comes from an examination of the thermocouple measurements of temperature rise in the muscle under sonic irradiation. These measurements indicate that for peak sound pressure amplitudes up to about 20 atmospheres the temperature change is proportional to the square of the crystal voltage. Marked deviation from this linear relationship would be expected in the presence of cavitation. Many investigators have demonstrated that sound level measurements, in a medium in which cavitation is present, become erratic. A second piece of evidence against excessive cavitation in the tissue under irradiation results from an examination of the stained sections of irradiated muscle. Microscopic study shows no vacuole formation or fiber tearing. Another argument against the possibility that cavitation is involved in the mechanism of the effect produced in these experiments is brought out by the work of Esche (52) in which he found no evidence of cavitation at a hydrostatic pressure of one atmosphere and a frequency of 500 kc/sec, in beef muscle up to sound intensities in the tissue of about 400 watts/cm².

It appears that neither tissue heating nor cavitation is the primary physical factor involved in producing irreversible block of the action potential in striated muscle under the experimental conditions described in this paper. The effect of

the high intensity acoustic irradiation of the muscle may therefore be a result of mechanical forces acting on submicroscopic elements of the tissue. From the experimentally observed form of the minimum dosage curve, it is reasonable to expect the mechanism to take a mathematical form approximating that proposed by Fry et al. ('51). If the threshold value is chosen as unity for the scale along the horizontal axis for the muscle dosage curve and for the frog paralysis dosage relation (Fry et al., '51) then the two relations appear almost identical. This suggests that the mechanism may well be the same in the two cases. Knowledge of the apparent lack of a dependence of the effect on the angle between the direction of the muscle fibers and the direction of propagation of the sound, should be useful in any attempt to establish a mechanical force mechanism.

SUMMARY

The studies presented in this paper demonstrate that under appropriate ultrasonic dosage conditions, the propagated action potential of an excised striated muscle can be permanently reduced or completely blocked. This can be accomplished in the absence of a temperature level sufficient in itself to cause permanent suppression. A quantitative determination of the minimum dosage relation (duration of exposure as a function of sound level) for a 10% permanent reduction of the muscle action potential has been accomplished. The form of this relation is the same as that given by Fry et al. ('51) for the relation between the minimum exposure time for paralysis of the hind legs of frogs, irradiated in the lumbar enlargement region of the spinal cord, and the sound level. Histological examination of stained tissue sections shows no gross tearing or vacuolization which might be expected if cavitation were present. Measurements made during irradiation with an acoustic probe imbedded within the muscle provide supporting evidence that cavitation is absent.

Results similar to those obtained on excised muscles were obtained on muscles with intact vascular systems.

No permanent suppression of the nerve action potential was produced on excised sciatic nerves under irradiation conditions similar to those used on excised muscles.

ACKNOWLEDGMENT

J. W. Barnard, F. J. Fry, and L. Dreyer also contributed to this study.

LITERATURE CITED

- BUSNEL, R. G., J. GLIGORJEVIC, P. CHAUCHARD AND H. MAZOUÉ 1953 Contribution à l'étude des effets et des mécanismes d'action des ultrasons sur le système neuro-musculaire. *Der Ultraschall in der Medizin*, 6: 1-25.
- CARSLAW, H. S., AND J. C. JAEGER 1947 Conduction of heat in solids, Oxford University Press, Oxford, England.
- CURRY, B., E. HSI, J. S. AMBROSE AND F. W. WILCOX 1951 Bibliography — Supersonics or Ultrasonics, Research Foundation, Oklahoma A. and M. College.
- DOI, Y. 1920 Studies on muscular contraction. I. The influence of temperature on mechanical performance of skeletal and heart muscle. *J. Physiol.*, 54: 218-226.
- ESCHE, R. 1952 Untersuchung der Schwingungskavitation in Flüssigkeiten. *Akustische Beihefte*, 4: 208.
- FRY, F. J. 1950 An ultrasonic projector design for a wide range of research applications. *Rev. Sci. Inst.*, 21: 940-941.
- FRY, W. J., V. J. WULFF, D. TUCKER AND F. J. FRY 1950 Physical factors involved in ultrasonically induced changes in living systems. I. Identification of non-temperature effects. *J. Acoust. Soc. Am.*, 22: 867-876.
- FRY, W. J., D. TUCKER, F. J. FRY AND V. J. WULFF 1951 Physical factors involved in ultrasonically induced changes in living systems. II. Amplitude duration relations and the effect of hydrostatic pressure for nerve tissue. *J. Acoust. Soc. Am.*, 23: 364-368.
- FRY, W. J., J. F. HERRICK, J. F. LEHMANN, J. J. WILD, ET AL. 1952 Symposium on ultrasound in biology and medicine. University of Illinois. *J. Acoust. Soc. Am.*, 25: 1-25 and 270-285.
- FRY, W. J., AND R. B. FRY 1954 Determination of absolute sound levels and acoustic absorption coefficients by thermocouple probes — Experiment. *J. Acoust. Soc. Am.*, 26: 311-317.
- GARAY, K., AND M. GERENDAS 1949 Effect of ultrasonic vibration on muscle fibres in vitro. *Experientia*, 5: 410-411.
- GIACOMINI, A. Editor of *Atti del Convegno Internazionale di Ultracoustica* 1950 Supplement Vol. VII, Ser. IX Nuovo Cimento, Rome, Italy.
- GERSTEN, J. W. 1953 Thermal and non-thermal changes in isometric tension, contractile protein, and injury potential, produced in frog muscle by ultrasonic energy. *Archives Phys. Med.*, 34: 675-685.

- GERSTEN, J. W. 1954 Ultrasonics and muscle disease. *Am. J. Phys. Med.*, *33*: 68-74.
- HARVEY, E. N. 1929 The effect of high frequency sound waves on heart muscle and other irritable tissues. *Am. J. Physiol.*, *91*: 284-290.
- KUFFLER, S. W. 1942 Electric potential changes at an isolated nerve-muscle junction. *J. Neurophysiol.*, *5*: 18-26.
- MATTHES, K., AND W. RECH Editors of *Der Ultraschall in der Medizin* 1949 S. Hirzel, Zürich, Switzerland.
- NAIMARK, G. M., J. KLAIR AND W. A. MOSHER 1951 A bibliography on sonic and ultrasonic vibration; biological, biochemical, and biophysical applications. *J. Franklin Institute*, *251*: 279-299 and 402-408.
- WALKER, S. M. 1949 Potentiation of twitch tension and prolongation of action potential induced by reduction of temperature in rat and frog muscle. *Am. J. Physiol.*, *157*: 429-435.

A NOTE ON THE PORPHYRINS EXCRETED
BY THE BLUE-GREEN MUTANT OF
RHODOPSEUDOMONAS
SPHEROIDES ¹

W. R. SISTROM,² MARY GRIFFITHS AND R. Y. STANIER
Department of Bacteriology, University of California, Berkeley

SEVEN FIGURES

In the accompanying paper (Sistrom, Griffiths and Stanier, '56) it has been mentioned that the excretion of green, water-soluble pigments with a mixed spectrum characteristic of porphyrins invariably accompanies chlorophyll synthesis by the blue-green mutant of *Rhodopseudomonas spheroides*. We have attempted to separate and characterize these compounds; and although the characterizations are by no means complete, the information obtained appears of sufficient interest to merit brief presentation.

METHODS

Separations of pigments by partition between hydrochloric acid and either benzene or ether were performed as described by Fischer and Stern ('40). In partitions which involved use of concentrated acid solutions, all the liquids were chilled beforehand.

For chromatographic separations, three solvent mixtures were employed. Solvent A consisted of benzene saturated with water (100 ml) and glacial acetic acid (0.4 ml). Solvent B consisted of A, with addition of ethyl acetate (5 ml). Solvent

¹ This work was supported by grants from the National Science Foundation, and from the American Cancer Society upon recommendation of the Committee on Growth of the National Research Council.

² Present address: Institut Pasteur, Paris 15, France.

C consisted of benzene saturated with water (100 ml), glacial acetic acid (3.5 ml) and ethyl acetate (15 ml). All runs were made on paper, either by ascending chromatography on sheets of Whatman paper, or by column chromatography on Whatman powdered cellulose.

Fractionation procedure

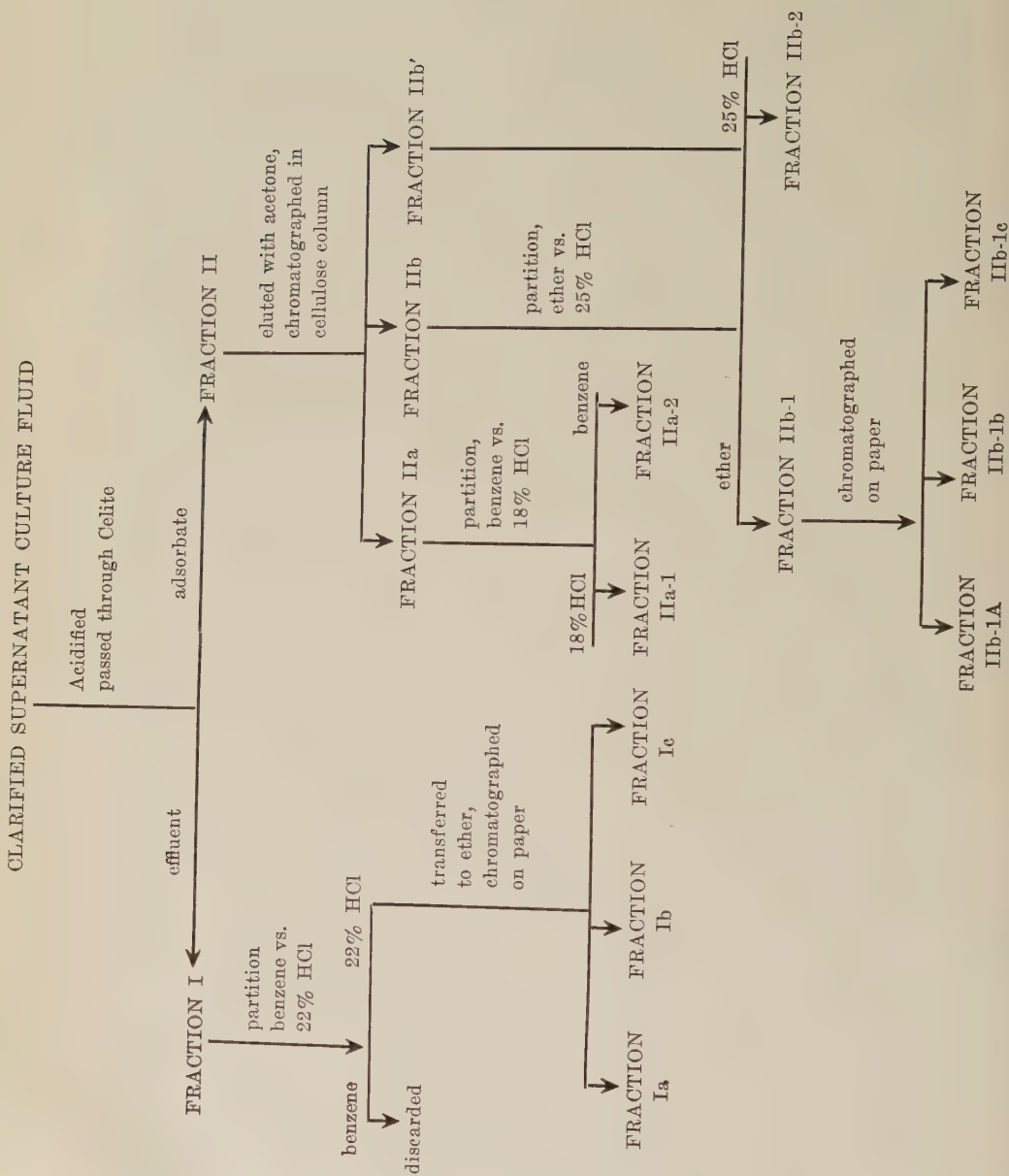
The starting material consisted of approximately 6 l of fluid, derived from 6 separate cultures of the blue-green mutant, grown anaerobically in the light and harvested just before the end of the exponential phase of growth. The bulk of the cells was removed by centrifugation, and the supernate was further clarified by passage through a thin layer of Celite. The clear, green filtrate was then acidified with 0.025 vol. of concentrated HCl, and again filtered through Celite, which was thoroughly washed with 1% HCl. This treatment separates the pigments into two main groups: fraction I, those not absorbed on Celite; and fraction II, those retained on Celite.

The filtrate containing the pigments of fraction I was extracted with ethyl acetate. The ethyl acetate extract was dried and evaporated *in vacuo*. The pigments were redissolved in benzene and partitioned with 22% HCl. Only a small amount of color remained in the benzene layer, which was discarded. After a benzene wash, the acid extract was diluted and the pigments were transferred into ether, extracted with 22% HCl, and transferred back into ether. They were then placed on paper, and chromatographed with Solvent B. Three bands appeared: two small ones with Rf values of 0.55 and 0.1 (fractions Ia and Ic, respectively); and a large one with Rf 0.26 (fraction Ib). These bands were eluted with ethyl acetate, and Ib and Ic were separately rechromatographed with solvent C. The former contained traces of two minor colored constituents, which were discarded. The latter was chromatographically homogeneous.

The pigments retained on Celite (fraction II) were eluted with acetone, transferred to benzene, and placed on a powdered cellulose column (60×250 mm), which was developed with solvent A until a front-running yellow-green band (fraction IIa) had been eluted. The column was then extruded, and the two main colored regions (blue-green and yellow-green) were eluted separately with ethyl acetate, yielding fractions IIb and IIb' respectively. The extracts were evaporated to dryness, and the pigments taken up separately in ether.

Fraction IIa contained two main pigments, which were separated from one another by repeated partition between benzene and 18% HCl; the aqueous layer was a brilliant green, and the benzene layer pink. The green pigment in the aqueous layer (fraction IIa-1) was transferred to ether. The benzene layer containing the pink pigment was washed with 22% HCl, dried and evaporated, and the residue was dissolved in ether and extracted several times with 25% HCl. The pink pigment passed into the acid layer, leaving a very small amount of a pale green pigment in the ether layer, which was discarded. The pink pigment was transferred to ether, washed and dried (fractions IIa-2). Further purification by paper chromatography was attempted, but the pigment appeared to decompose on the chromatograms with the formation of a pale green, strongly fluorescent material. The characterization was therefore later performed on the unchromatographed material, although this was evidently not pure. The small amounts available precluded attempts to purify it by other methods.

Fractions IIb and IIb', ethereal solutions containing the pigments eluted from the extruded cellulose column, were separately treated with 25% HCl. The ethereal layer of IIb' was discarded, since it contained almost no pigment. Examination showed that both HCl layers contained the same pigments, so they were combined and washed with ether. The ether wash was added to the ethereal layer of fraction IIb, to compose fraction IIb-1. The pigment in combined acid layers (fraction II-2) was transferred to ether.



The pigments in fraction IIb-1 were subjected to paper chromatography using solvent C, and yielded three bands, fractions IIb-1a, IIb-1b and IIb-1c, with R_f values of 1.0, 0.8 and 0.7, respectively. Additional chromatograms performed on the three isolated substances showed only traces of colored impurities.

The complete fractionation procedure is outlined in figure 1.

Characterization of the isolated pigments

As the fractionation procedure suggests, the pigment mixture proved to be an exceedingly complex one. None of the components was obtained in large quantities, and some of the isolated fractions contained only just enough pigment for the determination of absorption spectra. Consequently, we were unable to make definitive characterizations by standard chemical analyses, and had to depend largely on spectral properties, supplemented by information on solubility and in some cases also phase tests.³ Fortunately all compounds isolated proved to be closely related to chlorophyll, and for substances of this kind the absorption spectrum is the most valuable single means of identification. Thanks to the extensive data obtained by Stern and his collaborators (Stern and Pruckner, '39; Stern and Wenderlein, '35, '36), it is almost always possible to make a class assignment of an unknown chlorophyll derivative, if not a specific identification, on the basis of its spectrum. In order to simplify the discussion, we shall start by describing briefly the chemistry and terminology of chlorophyll derivatives.

The structures of chlorophyll *a* and of bacteriochlorophyll are shown in figure 2. They differ in only two respects: the nature of the substituent on ring I at position 2 (vinyl in chlorophyll *a*, and acetyl in bacteriochlorophyll); and the level of oxidation of ring II (more reduced by two H-atoms in bacteriochlorophyll). From each kind of chlorophyll, there

³ The phase test was performed as described by Fischer and Stern ('40). It is a color test for the presence of the pentanone ring in chlorophylls and their derivatives.

stem parallel series of related compounds, whose derivations are indicated by a prefix or affix. Compounds of the bacteriochlorophyll series carry the prefix bacterio-, compounds of the chlorophyll *a* series the affix *a*. Thus pheophytin derived from chlorophyll *a* is pheophytin *a*, that derived from bacteriochlorophyll is bacteriopheophytin. The most important of these derivatives for purposes of the present discussion are: *pheophytins*, chlorophylls without magnesium; *pheophorbides*, pheophytins without phytol; *chlorins*, pheophorbides with the pentanone ring (the isocyclic ring attached to pyrrole ring III) opened; and *chlorophyllides*, chlorophylls without the phytol sidechain.

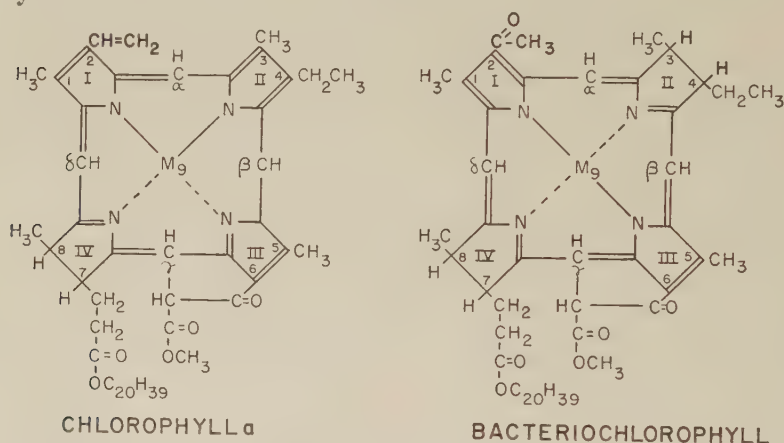


Fig. 2 The structural formulae of chlorophyll *a* (left) and bacteriochlorophyll (right).

The spectral properties in each series are principally governed by two factors: the presence or absence of magnesium (or other metals); and the presence or absence of the pentanone ring. Esterification has little or no influence on the spectrum. Thus chlorophylls, chlorophyllides and similar chelates with metals other than magnesium all have spectra of one configuration; pheophorbides and pheophytins have spectra of a second configuration; and chlorins have spectra of a third configuration. Furthermore, the spectra of chlorophyll *a* and all its derivatives of the *a* series are very different

TABLE 1

Positions and relative extinctions¹ of the absorption maxima of the excreted porphyrins of the blue-green mutant, and of some known substances

CLASS	FRACTION OR COMPOUND		WAVELENGTH (M μ) AND RELATIVE EXTINCTION								
			1	2	3	4	5	6	7	8	9
1	IIa-2	λ	750	675	(620) ²		525	495	455	384	357
		R.E.	100	18.2	(7.6)		43.4	10.8	6.3	113	203
	Bacteriopheophytin ³	λ	750	682	625		525	492	460	384	356
		R.E.	100	15.5	6.6		43	8.7	4	95	172
	IIa-1	λ		670	612	560	535	505	470	409	
		R.E.		100	15.7	5.8	19.5	23.9	8.4	2.2	
2	Ethyl pheophorbide a ⁴	λ		670	610	560	534	505	470	408	
		R.E.		100	15.4	5.7	19.4	22.4	8.2	210	
	Ia	λ		667	607	(560) ²	532	505	465	408	
		R.E.		100	18.6	(9.0)	21.6	27.3	12.9	242	
	Ib	λ		660	602	555	532	502	470	405	
		R.E.		100	21.4	9.2	26.9	27.7	10.6	276	
3	Ic	λ		662	602	552	530	500	465	400	
		R.E.		100	15.5	6.5	15.3	23.1	9.2	216	
	IIb-2	λ		662	605	555	530	500		405	
		R.E.		100	20.5	10.8	19.5	25.7		234	
	Chlorin e ₈ dimethyl ester ⁵	λ		663	607	555	530	502			
		R.E.		100	10.2	4.4	10.5	26.8			
	2-acetyl methyl pheophorbide a ⁶	λ		681	620	570	544	511	476		
		R.E.		100	9.6	3.6	18.6	22.3	6.4		
	IIb-1a	λ		650	602	550		505		422	(395) ²
		R.E.		100	27.2	12		14.5		175	(148)
4	IIb-1b	λ		645	597	547		502		419	397
		R.E.		100	21.9	9.9		9.4		159	125
	IIb-1c	λ		642	597	545		500		419	395
		R.E.		100	22.4	8.9		8.5		156	118
	Ethyl chlorophyllide a ⁷	λ		660	614	574	530			428	410
		R.E.		100	15.4	8.3	4.2			134	83

¹ Based on an extinction of 100 for the peak of longest wavelength.

² Figures in parentheses refer to shoulders.

³ Obtained from Professor C. B. van Niel.

⁴ Obtained from Dr. A. S. Holt.

⁵ Data of Stern and Wenderlein ('35).

⁶ Data of Stern and Pruckner ('39).

⁷ Data of Holt and Jacobs ('54).

from the spectra of the analogous substances in the bacterio-series, since the difference in the oxidation level of ring II profoundly modifies the resonance pattern.

Table 1 lists the positions and relative extinctions of the absorption maxima for all the isolated substances, and also includes similar data for a few reference compounds. Ex-

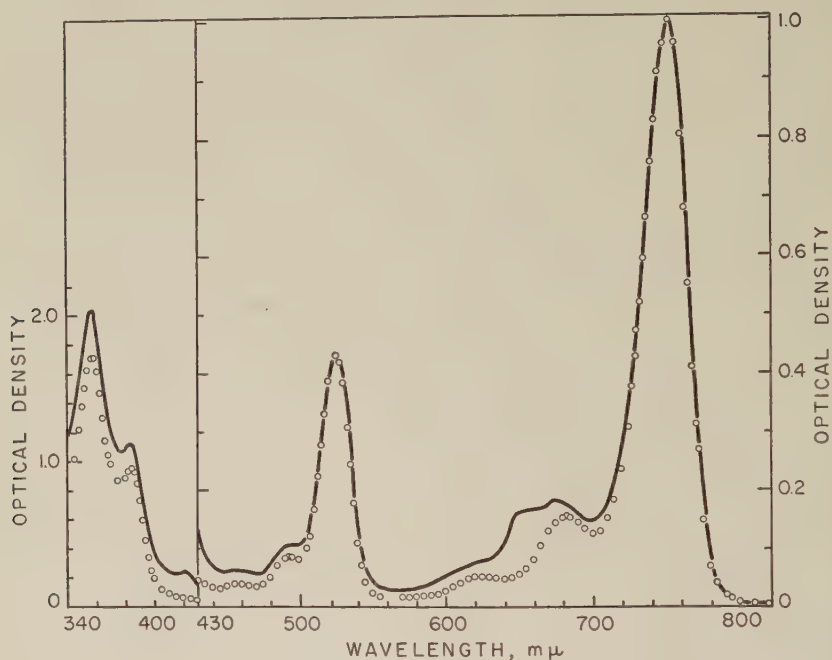


Fig. 3 The absorption spectrum of fraction IIa-2 compared with that of pure bacteriopheophytin. Both measured in ether, and adjusted to an optical density of 1.000 at 750 mμ. The solid line is the curve for fraction IIa-2; the points indicate the curve for bacteriopheophytin.

amination shows that the substances isolated fall into 4 main spectral classes. The first class, with a long wavelength absorption maximum at 750 mμ, contains only fraction IIa-2. As we have already mentioned, this pigment is certainly not pure; but its salient spectral characters show that it is a member of the bacteriochlorophyll series, with a spectrum which very strongly resembles that of bacteriopheophytin

(fig. 3). None of the isolated compounds can be pheophytins, since they are all soluble in water, whereas the pheophytins are not. Furthermore, IIa-2 is readily extracted from ether by 22% HCl, whereas bacteriopheophytin is not. IIa-2 gives a positive phase test, and therefore still contains the pentanone ring. Consequently it is most likely bacteriopheophorbide.

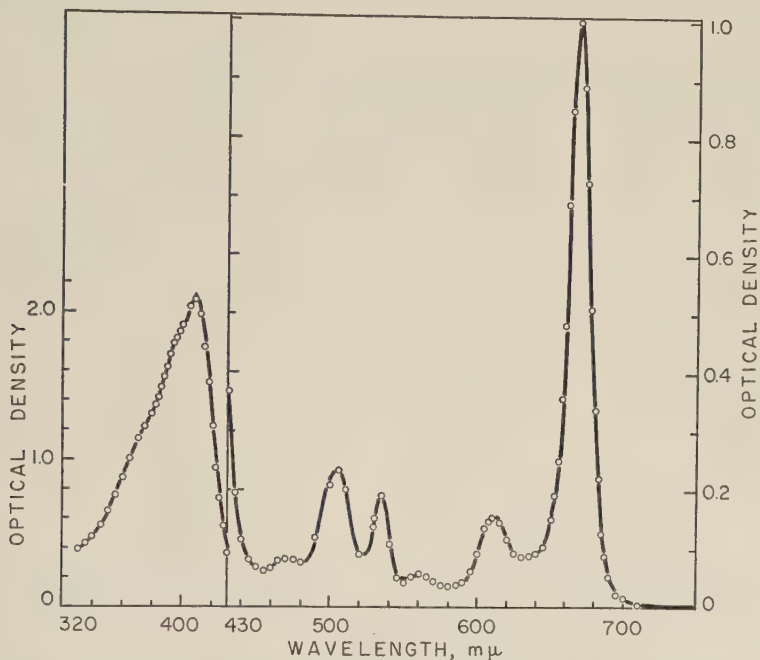


Fig. 4 The absorption spectrum of fraction IIa-1 compared with that of pure ethyl pheophorbide *a*. Both measured in ether and adjusted to an optical density of 1.000 at 670 μ . The solid line is the curve for fraction IIa-1, and the points indicate the superimposable curve for ethyl pheophorbide *a*.

The second class, characterized by a long wavelength absorption maximum near 670 mμ, contains two fractions, Ia and IIa-1. The spectrum is that characteristic of pheophytin *a* and pheophorbide *a*; in fact, IIa-1 is spectrally indistinguishable from ethyl pheophorbide *a* (fig. 4). Fraction IIa-1 also gives a positive phase test. On account of its solubility it cannot be a pheophytin, and therefore we conclude that it is

pheophorbide *a*. A phase test could not be performed on Ia, since there was too little material. However, its spectral near-identity with IIa-1 and ethyl pheophorbide *a* show that it must be a very closely related substance.

The third class, characterized by a long wavelength absorption maximum at 660–662 $m\mu$, includes fractions Ib, Ic

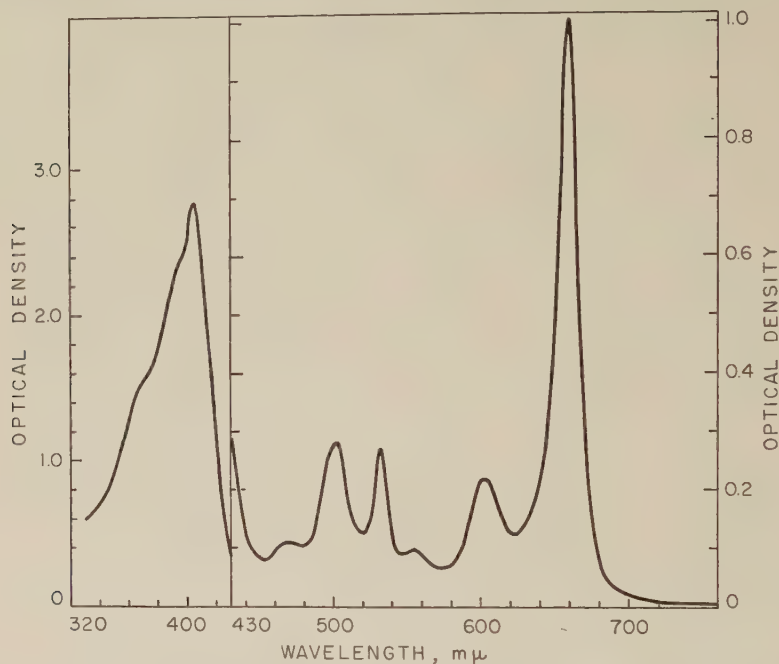


Fig. 5 The absorption spectrum of fraction Ib, measured in ether and adjusted to an optical density of 1.000 at 660 $m\mu$. Note the near-identity of this curve in shape to the curves for fraction IIa-1 and ethyl pheophorbide *a*.

and IIb-2. The spectrum (fig. 5) is unmistakably similar in shape to that of pheophytin *a* and pheophorbide *a*, but the maxima are systematically shifted to somewhat shorter wavelengths. Fraction Ib gave a positive phase test; the other two could not be tested. Thus fraction Ib is certainly a pheophytin or a pheophorbide, and its solubility properties indicate that it is of the latter class. It shows marked spectral differences from 2-acethyl methyl pheophorbide, the only other known

pheophorbide with the ring system on the oxidation level of chlorophylls *a* and *b* which has a spectrum of the *a* shape. Therefore its identity cannot be further established at present. However, the spectral difference from pheophorbide *a*, which is entirely positional, suggests a relatively minor chemical difference, probably involving a substituent group.

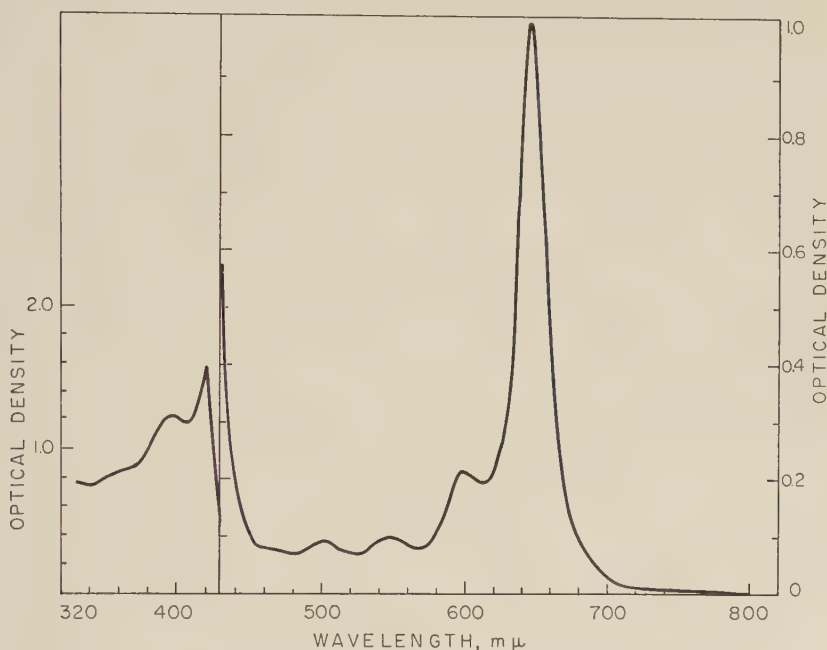


Fig. 6 The absorption spectrum of fraction IIb-1b, measured in ether and adjusted to an optical density of 1.000 at 650 mμ. This substance is presumed to be a copper chelate of an unidentified chlorophyll derivative.

Since the quantities of Ic and IIb-2 were too small for the performance of phase tests, it is not certain that they contain the pentanone ring; but the structure of their spectra (especially in the regions of peaks 5 and 6) resembles that of pheophorbide *a* much more than that of chlorin *a* (see table 1), and hence they are also probably phorbides related to the *a* series.

The fourth class consists of fractions I Ib-1a, I Ib-1b (fig. 6) and I Ib-1c, with long wavelength absorption maxima between 640 and 650 $m\mu$. It is likely that all three are copper chelates, artefacts produced during the growth of the cultures

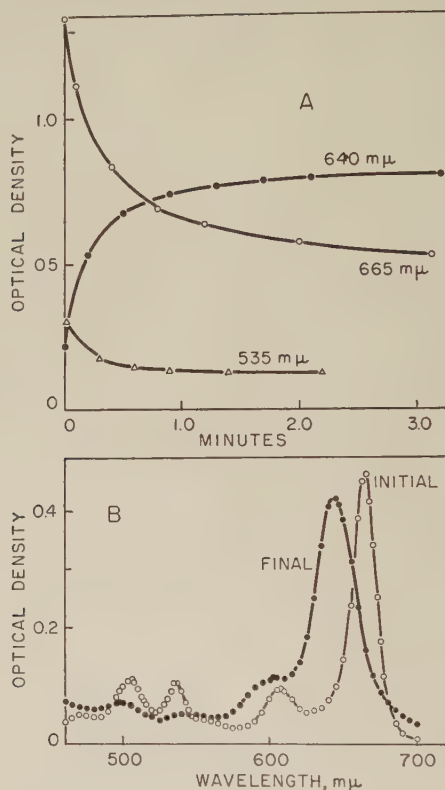


Fig. 7 Formation of a copper chelate from fraction Ic, by addition of methanolic cupric acetate to a solution of the porphyrin in chloroform. A. Changes in optical densities at various wavelengths with time, illustrating the rapidity of the chelation at room temperature. B. Initial and final spectra. Note the similarity on shape of the final spectrum to that of fraction I Ib-1b, presumed to be a copper chelate formed in the culture medium.

owing to the fact that the medium contained, along with other trace metals, small amounts of added copper. Copper will chelate chlorophyll derivatives with great avidity under extremely mild conditions (see fig. 7), and the similarity in shape

of the spectra of these three fractions to the spectrum of methyl chlorophyllide *a* (table 1) indicates their chelated state. Most metal chelates of chlorophyll and its derivatives are dissociated by treatment with 25% HCl, but the copper chelates are not. The fact that these fractions were unchanged by treatment with 25% HCl is accordingly a strong indication that copper is the chelating metal. In an attempt to characterize them further, we prepared copper chelates from several other fractions and compared their spectra with those of the various IIb fractions. Although similar in spectrum (fig. 7), none of them could be identified with the IIb fractions. The relation of the IIb fractions to the other porphyrins isolated therefore remains obscure.

SUMMARY AND CONCLUSIONS

The characterization of the individual porphyrins excreted by the blue-green mutant during photosynthetic growth leaves much to be desired; but the data so far obtained provide a sufficiently clear picture of their general nature, which was the primary goal. With the possible exception of the compounds in group 4, they are derivatives either of bacteriochlorophyll or of chlorophylls of the *a* type. Surprisingly, the one bacteriochlorophyll derivative (IIa-2) is a minor constituent of the mixture. The two principal substances isolated are IIa-1, which is spectrally identical with pheophorbide *a*, and Ib, another pheophorbide of unknown structure, but with a spectrum closely similar in shape to that of pheophorbide *a*.

Since bacteriochlorophyll is known to be relatively labile, it is necessary to consider the possibility that the preponderance of compounds related to the *a* series among the isolated porphyrins might have resulted from the oxidation of compounds belonging to the bacterio-series during the fractionation of the mixture. The spectrum of the crude culture fluid before fractionation (Sistrom, Griffiths and Stanier, '56; fig. 3) does not provide any support for this interpretation:

its main light absorption in the visible region is between 650 and 680 m μ , and absorption between 700 and 800 m μ (where compounds of the bacterio-series should absorb strongly) is negligible by comparison. The fact that the major isolated compounds, IIa-1 and Ib, have their main visible absorption maxima at 670 and 660 m μ , respectively, encourages the belief that they were the main components of the original mixture. It therefore appears that the chlorophyll derivatives excreted by the blue-green mutant are principally dihydroporphins. These substances may constitute intermediates (or derivatives of intermediates) in the biosynthesis of bacteriochlorophyll; however, there is no evidence at present to exclude the alternative interpretation that they are products of an intracellular degradation of bacteriochlorophyll.

LITERATURE CITED

- FISCHER, H., AND A. STERN 1940 Die Chemie des Pyrrols, Leipzig, Akademische Verlagsgesellschaft.
- HOLT, A. S., AND E. E. JACOBS 1954 Amer. J. Botany, 41: 710.
- SISTROM, W. R., M. GRIFFITHS AND R. Y. STANIER 1956 The biology of a photosynthetic bacterium which lacks colored carotenoids. J. Cell. and Comp. Physiol., 48: 473.
- STERN, A., AND F. PRUCKNER 1939 Physik Chem. A, 185: 140.
- STERN, A., AND H. WENDERLEIN 1935. Z. Physik. Chem. A, 174: 81.
- 1936 Z. Physik. Chem. A, 176: 81.

THE BIOLOGY OF A PHOTOSYNTHETIC BACTERIUM WHICH LACKS COLORED CAROTENOIDS¹

W. R. SISTROM,² MARY GRIFFITHS AND R. Y. STANIER

Department of Bacteriology, University of California, Berkeley

ELEVEN FIGURES

During the course of studies on the photosynthetic bacterium *Rhodopseudomonas spheroides*, we have isolated several classes of mutants that differ from the wild type in the nature of their pigment systems. Strains of one class, the so-called *blue-green* phenotype, proved to be completely devoid of colored carotenoids, and to contain in their place a colorless C₄₀ polyene, phytoene (Griffiths and Stanier, '56). As the phenotypic designation suggests, these mutants still contain bacteriochlorophyll and they can also develop under photosynthetic conditions. In nature, carotenoid pigments invariably accompany chlorophyll as constituents of the photosynthetic apparatus (Strain, '49), and to the best of our knowledge the blue-green mutant of *R. spheroides* is the unique example of an organism which lacks these pigments, but is nonetheless capable of photosynthetic development. The very universality of the association of carotenoids with the photosynthetic apparatus has in the past set limits on the experimental analysis of the physiological role that these pigments play in phototrophic organisms, and hence it seemed possible that a careful study of the blue-green mutant might help to elucidate the wider problem of carotenoid function. The first results of such a study are reported in this paper. A preliminary

¹ This work was supported by grants from the National Science Foundation, and from the American Cancer Society upon recommendation of the Committee on Growth of the National Research Council.

² Present address: Institut Pasteur, Paris 15, France.

account of some of our findings has already appeared (Griffiths, Sistrom, Cohen-Bazire and Stanier, '55).

The biological material

All the experiments on the blue-green mutant described in the following pages have been carried out with a single strain, UV-33, obtained by ultraviolet irradiation of the wild type (Griffiths and Stanier, '56). Our collection contains several other independent isolates of this phenotype, but UV-33 is exceptionally favorable experimental material on account of its genetic stability; most blue-green stocks revert very rapidly to wild type when cultivated under conditions of obligatory photosynthesis. On original isolation UV-33 also had a tendency to revert under these conditions, albeit less frequently than other stocks, but with the passage of time it has acquired an increased stability, and can now often be transferred several times in succession under photosynthetic growth conditions without reverting.

The maintenance of blue-green stocks requires a special cycle of transfers. The danger of reversion precludes the usual method of maintenance for *R. spheroides*, as stab cultures incubated in the light; but experience has shown that steady maintenance on slants incubated in the dark, although it prevents reversion to the wild type, sometimes leads to a loss of photosynthetic ability. We have therefore adopted the procedure of making three or four successive transfers on slants incubated in the dark, followed by transfer to a completely filled Florence flask of liquid medium, which is incubated in the light; the resulting photosynthetic culture is plated, and a typical, well-pigmented colony of the blue-green phenotype is picked and transferred to a slant, which provides the starting material for the repetition of the cycle.

The wild type used in comparative experiments was strain 2.4.1 of *R. spheroides*, from which UV-33 was originally derived.

The semisynthetic medium described by Cohen-Bazire, Sistrom and Stanier ('57) was used in all experiments. The

solid medium for maintenance of stocks and for making plates consisted of: Difco yeast extract, 0.3 g, Difco casamino acids 0.2 g, and agar 1.5 g, all dissolved in 100 ml of tap water.

Methods used in growth experiments

Our general procedures for studying the growth of non-sulfur purple bacteria under a variety of conditions are described elsewhere (Cohen-Bazire, Sistrom and Stanier, '57). A few minor modifications used in the present work merit description. The light source consisted of two 300 W flood lamps, mounted at an angle to one another in such a fashion as to give even illumination over a fairly wide area. In order to reduce stray light, all surfaces of the glass water bath except the entrance window were painted black. The light intensity at the entrance window was measured with a Weston photoelectric light meter. At the start of an experiment, the relative positions of the two lamps were adjusted to obtain even intensity over the entrance window, and their distance from the window was fixed so as to give the desired incident light intensity. From time to time during an experiment the light intensity was measured, and the distance of the light source changed, if necessary, to maintain the intensity at the original value. The culture flasks were always placed in the water bath at the same distance (0.5 cm) from the entrance window.

The procedures described above ensure satisfactorily reproducible light conditions, but the measurements of light intensity do not permit even a rough calculation of the effective flux actually entering the cultures. As a matter of convenience, we have made all measurements at the surface of the entrance window, rather than in the culture flasks. Even if a correction were to be made for this, however, the absolute values would still be of little significance, since the most effective region of the spectrum for photosynthesis by purple bacteria lies in the near infrared between 800 and 950 m μ , and is hence not recorded in the light meter reading. Consequently in

experiments where numerical values in foot-candles (f.-c.) for light intensity are reported, this has been done exclusively for comparative purposes.

Turbidimetric measurements of growth and spectrophotometric measurements of chlorophyll and carotenoids were made as described by Cohen-Bazire, Sistrom and Stanier ('57).

Growth and pigment synthesis in anaerobiosis and light

Under strictly anaerobic conditions, the nonsulfur purple bacteria cannot grow unless illuminated. This fact demonstrates that photosynthesis is their only source of energy for growth in the absence of oxygen, and permits one to use the growth rates of cultures in anaerobiosis and light as a measurement of photosynthetic capacity. Preliminary growth experiments established that the blue-green mutant could still photosynthesize; but they suggested at the same time that its photosynthetic function was somewhat impaired by comparison with that of the wild type, and that after growth at a comparable light intensity, its chlorophyll content was less than that of the wild type. It may be recalled that in the wild type of *R. spheroides* under conditions of photosynthetic growth, the differential rates of chlorophyll and carotenoid synthesis³ are inversely related to light intensity (Cohen-Bazire, Sistrom and Stanier, '57). Hence, a thorough comparison of the two strains necessitated a series of parallel experiments at different light intensities. The two were grown side by side at 4 light intensities in the range between 100 and 1000 f.-c., and after steady state conditions of pigment synthesis had been attained, the growth rates and pigment contents were determined. The results are shown in fig. 1. Some extra values, which had been obtained in experiments on the wild type alone, are also included. Since our measurements of light intensity have relative, but not absolute significance, these data can serve only to reveal the general type

³ That is, their rates of synthesis relative to the total rate of synthesis of cell material.

of response by the two strains to varying light intensity. Both strains appear to be approaching maximal growth rates at the top of the intensity range used, but isolated experiments with the wild type suggest that at still higher light intensities the growth rate continues to rise slowly. Unfortunately, even illumination could not be obtained with the available light source at intensities much above 1000 f.c., which precluded systematic extension of the experiments to a higher range. It

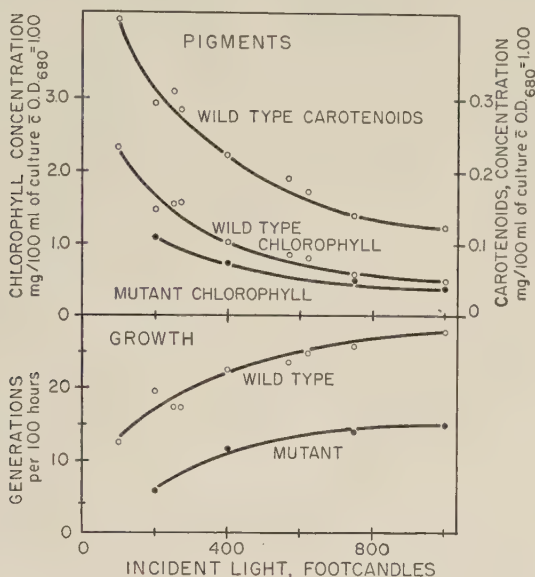


Fig. 1 The dependence of photosynthetic growth rate and pigment content on light intensity: a comparison of the blue-green mutant with the wild type of *E. spheroides*. Atmosphere: 95% N_2 -5% CO_2 . Temperature 30°C.

can be seen that at any given light intensity within the experimental range the growth rate of the blue-green mutant is about half that of the wild type. Since the two strains have identical growth rates at 30° C. under aerobic conditions in the dark (31 generations per 100 hours), the greatly reduced capacity of the blue-green mutant for photosynthetic growth must be ascribed specifically to a weakness of its photosynthetic metabolism, and not to any more general derangement of metabolism.

The concentrations of photosynthetic pigments in the cells of the two strains appear to be approaching minima at a light intensity of 1000 f.-c.; but in one experiment with the wild type at a very high light intensity (approx. 6000 f.-c.) the steady state concentration of pigment was about half that in the cells grown at 1000 f.-c. At any given light intensity, the concentration of chlorophyll in the cells of the blue-green mutant is some 70–80% of that in the cells of the wild type. Since for both strains light intensity is limiting at the points of comparison, this difference in chlorophyll content provides a partial explanation for the difference in growth rate. Indeed, it is possible that the low growth rate of the mutant is caused *solely* by the reduction of its total photosynthetic pigment content, since the absence of colored carotenoids might also affect the growth rate in a complete spectrum. Several lines of evidence (Thomas, '50; Duysens, '52; Clayton, '53) show that in other species of purple bacteria, the light absorbed by some of the carotenoid pigments can be used for photosynthesis, and the measurements by Duysens ('52) on chlorophyll fluorescence show that quanta absorbed by carotenoids can give excitations with yields about 40% of those with quanta absorbed by the bacteriochlorophyll itself. If a similar situation obtains in *R. spheroides*, the total content of photosynthetically functional pigment in the wild type will be greater by an unknown factor than its chlorophyll content, whereas in the blue-green mutant it will be equal to the chlorophyll content, since the absorption bands of phytoene lie far outside the range of possible energy transfer to chlorophyll. Hence, the low growth rate of the blue-green mutant may well reflect relatively weak light absorption, and not an impairment of intrinsic photosynthetic efficiency.

Figure 1 also shows that the response of the mutant to different light intensities is qualitatively similar to that of the wild type, with respect both to growth rate and to pigment concentration; in each case, the curves for the two strains relating these properties to light intensity essentially parallel one another.

The response to light intensity can be tested in another way, by examining the behavior of cells in the exponential phase of photosynthetic growth when they are suddenly exposed to a sharp change of light intensity. Cells of the wild type growing in dim light, and consequently well stocked with pigment, cease to synthesize chlorophyll and carotenoids at an appreciable rate when placed in bright light, although growth continues at the same or an even higher rate. When, as a consequence of growth, the pigment concentration of the cells has fallen to a level which approaches that characteristic for the new light intensity, pigment synthesis is resumed (Cohen-Bazire, Sistrom and Stanier, '57). A similar experiment was accordingly undertaken with the blue-green mutant. A photosynthetic culture was grown in dim light (about 200 f.-c.), harvested in the exponential phase of growth, and resuspended in a fresh medium of the same composition which was illuminated at an intensity of 1800 f.-c. As shown in figure 2, growth was exponential from the start, but the chlorophyll content of the culture remained stationary for almost five hours. Thereafter chlorophyll synthesis was resumed and attained a rate identical with the growth rate 10 hours after the start of the experiment. It is therefore evident that the mutant responds to a sudden change of light intensity in exactly the same qualitative fashion as does the wild type.

Early in our studies on the blue-green mutant, it was observed that the supernatant culture fluid after the centrifugation of fully-grown photosynthetic cultures has a distinct green color. Since green, water soluble pigments are never excreted by the wild type or by other classes of photosynthetic mutants, the phenomenon appeared to merit study. Figure 3 shows the absorption spectrum of such a green supernatant culture fluid, concentrated tenfold by lyophilization and subsequent reconstitution in a smaller volume. The general shape of this spectrum, particularly the peak in the Soret region around 400 m μ , is virtually diagnostic of porphyrins. As shown in an accompanying note (Sistrom, Griffiths and Sta-

nier, '56), the mixture in fact consists mainly, if not exclusively of phorbides, i.e., of chlorophyll derivatives which lack the phytol side chain and magnesium. From figure 3, it can be seen that a rough estimate of the total quantity of excreted porphyrins may be made by optical density determinations on clarified samples of culture fluid at 395 m μ , the absorption

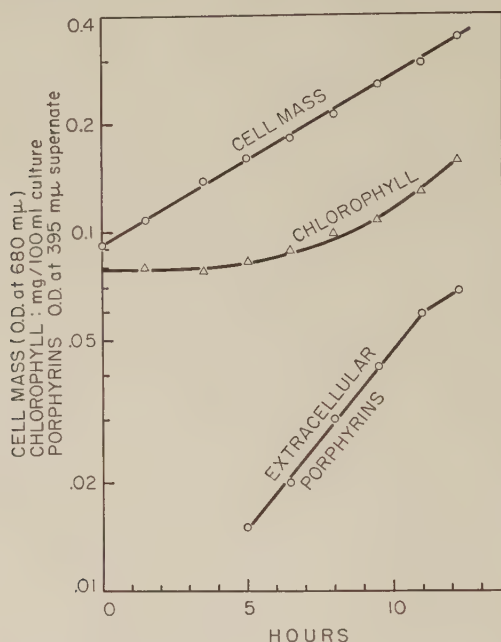


Fig. 2 The differential effect of a sudden increase of light intensity on growth and chlorophyll synthesis by the blue-green mutant. At zero time, cells growing exponentially in very dim light (*ca.* 200 f.c.) were transferred to a light intensity of 1800 f.c. Also shown is a curve illustrating the excretion of porphyrins. Atmosphere: 95% N₂-5% CO₂. Temperature: 30°C.

maximum in the Soret region of the mixed substances. We have used such measurements to determine the kinetics of porphyrin excretion in a number of growth experiments, and figure 2 includes illustrative data. These and similar data show that excretion is an invariable concomitant of chlorophyll synthesis. When a culture is in the steady state of chlorophyll synthesis, the rate of porphyrin excretion parallels, within

the limits of error of the measurements, the rates of growth and pigment synthesis, and declines with them as the culture enters the stationary phase. The experiment shown in figure 2 was terminated too soon to provide a clear indication of this parallelism. The wild type can also excrete porphyrins, but they are not chlorophyll derivatives, and they are never

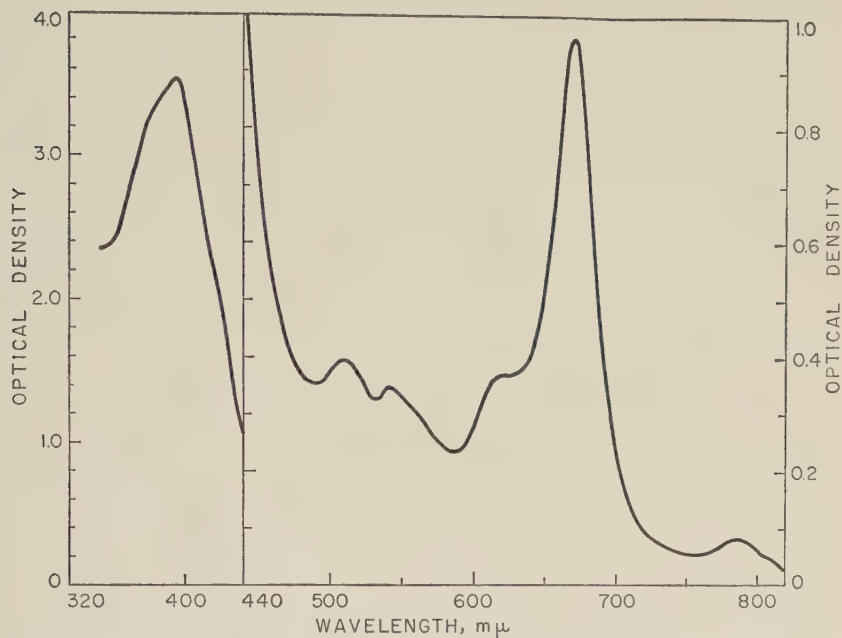


Fig. 3 The absorption spectrum of the supernatant medium concentrated tenfold, from a culture of the blue-green mutant in the late exponential phase of photosynthetic growth.

excreted during exponential growth at a time of active chlorophyll synthesis, instead making their appearance in the culture medium just as photosynthetic cultures are entering the stationary phase. Hence, the wild type can evidently incorporate all the chlorophyll that it makes during exponential growth. Under comparable conditions of light intensity, cells of the blue-green mutant contain from 70-80% as much chlorophyll as do cells of the wild type, but these values

measure only the incorporated chlorophyll. Since the blue-green mutant is at the same time excreting phorbides into the medium, whereas the wild type is not, it is entirely conceivable that the total rates of *synthesis*, as contrasted with *incorporation*, are identical in the two strains.

To summarize the experiments so far reported, we can say that the behavior of the blue-green mutant under conditions of obligatory photosynthetic growth is relatively orthodox, and does not suggest that any major physiological catastrophe has resulted from the disappearance of colored carotenoids from its cells: chlorophyll incorporation is somewhat reduced, and this, possibly coupled with the absence of carotenoid pigments, prevents it from absorbing as much photosynthetically effective light as the wild type can under comparable conditions. However, the intrinsic effectiveness of its chlorophyll as a photosynthetic pigment is probably only slightly, if at all, impaired.

The effect of air and light on the blue-green mutant

In studies on the wild type, Cohen-Bazire, Sistrom and Stanier ('57) have found that air almost completely suppresses the synthesis of chlorophyll and carotenoids, both in the presence and absence of light. The pigments already formed are not, however, destroyed. Consequently aerobic growth leads to a bleaching of the cells by simple dilution of their pigments, so that, even in the presence of light, there is a progressive shift from photosynthetic to respiratory metabolism. Such cells show a lag in growth upon return to conditions of obligatory photosynthesis (i.e., anaerobiosis and light), the duration and severity of the lag being governed by the extent of the bleaching that has taken place. During this lag in growth, synthesis of the photosynthetic pigments resumes at a very high differential rate, which begins to decline only as the anaerobic steady state concentration is approached. Hence an examination of the effects of air on chlorophyll synthesis afforded another means of testing the

physiological behavior of the blue-green mutant. In the first of such experiments, parallel cultures of the blue-green mutant and the wild type were grown anaerobically in the light until steady state conditions of pigment synthesis had been attained, at which point the anaerobic gas mixture (95% N_2 -5% CO_2) being used for aeration was replaced by a mixture of 95% air and 5% CO_2 , illumination being maintained at a constant level. The wild type responded in its usual fashion;

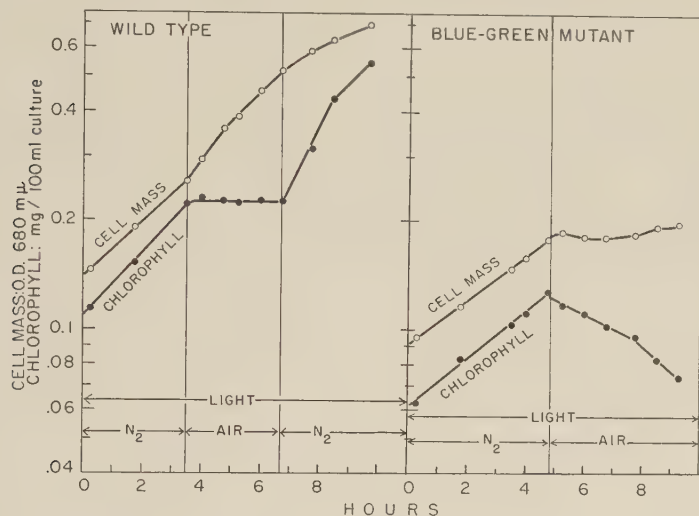


Fig. 4 The effect of air in the presence of light on growth and pigment synthesis by the blue-green mutant and the wild type of *R. spheroides*. Atmosphere: 95% N_2 -5% CO_2 , or 95% air- 5% CO_2 as indicated on graphs. Temperature: 30° C.

after several hours of aerobic growth, the culture was returned to anaerobiosis, and again showed the customary response (fig. 4). The response of the blue-green mutant to the introduction of air was totally different and wholly unexpected: growth ceased abruptly and the chlorophyll content of the culture, far from remaining stationary, underwent a steady decline which continued for many hours (fig. 4).

A more detailed experiment to elucidate the effects observed with the blue-green mutant was then undertaken. Four iden-

tical cultures of it were prepared, and grown anaerobically in the light until steady state conditions of pigment synthesis had been reached. At this point, three of the cultures were exposed to air, the fourth one being maintained under the initial growth conditions to serve as a control. One of the cultures exposed to air was also shielded from light with a screen of aluminum foil at the moment when the gas mixture was changed, while the other two remained illuminated.

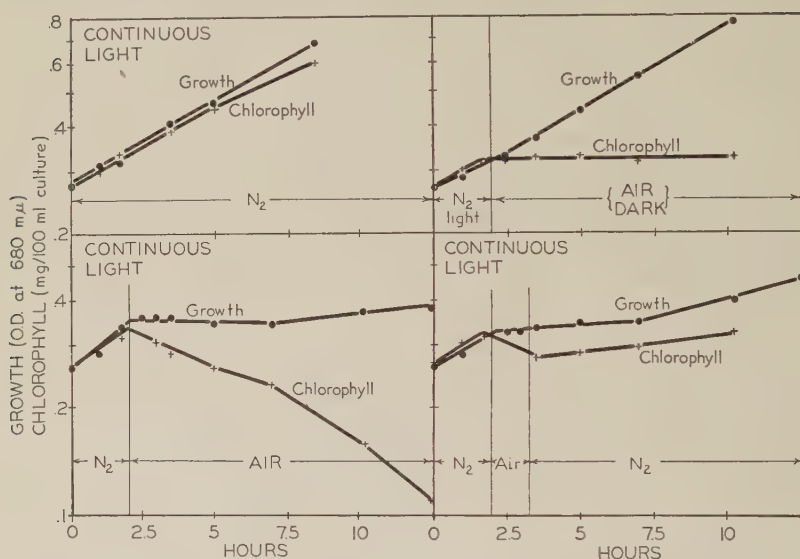


Fig. 5 The effect of air and light on the growth rate and chlorophyll content of the blue-green mutant. All 4 cultures were initially growing anaerobically in the light, the environmental conditions being changed as indicated for each culture on the graph. Both gas mixtures contained 5% CO_2 . Temperature: 30°C .

After exposure to light and air for 90 minutes, one of the two last mentioned cultures was returned to anaerobiosis. Periodic determinations of turbidity and chlorophyll content were made on all 4 cultures throughout the experiment. The results are shown in figure 5. A comparison of the changes in cultures exposed to air in the presence and in the absence of light shows conclusively that the abnormal response observed in the first experiment is not a response to air alone, but to

air in conjunction with light; the shielded culture continued to grow at a steady exponential rate, and its total chlorophyll content remained at the level which had been attained during previous photosynthetic growth. Thus if shielded from light, the blue-green mutant shows the same response to air as does the wild type. The behavior of the culture which was continuously illuminated but returned to anaerobic conditions after a relatively brief exposure to air is also noteworthy. The re-establishment of anaerobiosis brought chlorophyll destruction to a halt, but did not appreciably restore the capacity for chlorophyll synthesis: the increase in the chlorophyll content of the culture during the ensuing 7 hours was very small. It should be recalled that the return of an illuminated culture of the wild type to anaerobic conditions after a short exposure to air causes an immediate resumption of chlorophyll synthesis at a high rate (see fig. 4). Furthermore, the increase in turbidity following the return to anaerobiosis was extremely slow, whereas exposure of the wild type to air in the presence of light for so short a period as 90 minutes has a relatively slight effect on its subsequent photosynthetic growth rate. These facts suggested that in addition to arresting growth and causing destruction of chlorophyll, the combined action of light and air had actually killed a large proportion of the cells.

Accordingly, the experiment on the combined effects of air and light was repeated with the inclusion of viable counts. All dilutions and platings were made as rapidly as possible in dim light, and the plates were incubated in the dark under aerobic conditions at 30° C. Spread plates, rather than the customary poured plates, were prepared. Since all the colonies on a spread plate develop under reasonably uniform environmental conditions, variations of size or structure are significant, whereas such variations in a poured plate may simply reflect non-uniformity of the environment. The changes in viable numbers, turbidity, and chlorophyll content which followed the introduction of air are shown in figure 6. It can be seen that death was rapid and massive: after two

hours, 98% of the original population was no longer viable. The surviving population then resumed growth at a rate roughly comparable with the rate of aerobic growth in the dark (approximately 30 generations per 100 hours).

On the plates prepared from the culture before the introduction of air, the colonies that developed were of uniform size. In contrast, plates prepared from the culture after the introduction of air bore many abnormally small colonies when first examined, 72 hours after inoculation. With continued

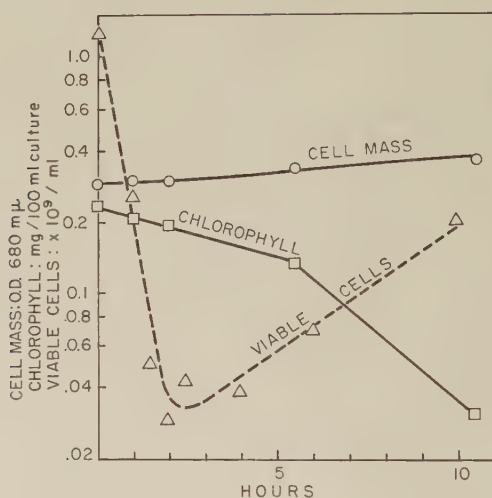


Fig. 6 The effect of air and light on the turbidity, viable count, and chlorophyll content of a culture of the blue-green mutant previously growing anaerobically in the light. Air was introduced at zero time.

incubation of the plates, most of these colonies eventually attained a normal size. On samples removed from the culture during the early stages of aeration, 30% of the population give rise to such small colonies. These colonies evidently constitute the progeny of cells that initiate growth only after a considerable delay. Hence the combined action of light and air produces a substantial number of sublethal casualties, in addition to the high percentage of actual deaths.

As yet, we have not made a detailed study of the processes of death and eventual recovery. Preliminary observations

suggest, however, that the surviving members of the population do not owe their good fortune to a genetic difference that enables them to resist the effects of light and air better than the majority of their fellows: several clones isolated from exposed populations after recovery had started were still of the gross blue-green phenotype, and still sensitive to the combined action of light and air after a period of anaerobic growth.

The blue-green mutant is sensitive to light and air only after a period of photosynthetic growth. If a culture has been growing for many generations under aerobic conditions in the dark, so that the cells have become almost completely bleached, exposure even to a high light intensity has no detectable effect on its growth rate.

The identity of the photosensitizer

In his book on photodynamic action, Blum ('41) defines this phenomenon as: "the sensitization of a biological system to light by a substance which serves as a light absorber for photochemical reactions in which oxygen takes part." The demonstration that the combined action of light and oxygen kills the blue-green mutant, neither factor alone being capable of doing so, created a very strong presumption that we were dealing with a case of photodynamic action as defined above by Blum. In order to make this presumption a certainty, it remained to identify the photosensitizing pigment. In photosynthetic cultures of the blue-green mutant, there are only two promising candidates for the rôle of photosensitizers: the excreted porphyrins, and bacteriochlorophyll itself. Consequently we adopted the working hypothesis that one of them was the responsible substance, and devised experiments that would either implicate or exclude these compounds. Two kinds of experiment with this aim were performed, and their results lead inescapably to the conclusion that bacteriochlorophyll is the photosensitizer. Since viable counts are tedious to perform, we depended on measurements of chlorophyll destruction for the quantitative evaluation of the photodynamic effect.

Experiment 1

Principle. If the photodynamic effect is caused by one or more of the excreted porphyrins, its magnitude should be a function of the concentration of these substances in the system.

Procedure. A culture of the blue-green mutant was harvested during exponential photosynthetic growth and divided into two aliquots, which were centrifuged. The sedimented cells were washed twice by centrifugation with fresh medium. One aliquot was then resuspended in fresh medium, and the

TABLE 1

Photodynamic destruction of intracellular bacteriochlorophyll in parallel cell suspensions exposed to different concentrations of excreted porphyrins

Two equal quantities of well washed cells from a photosynthetic culture of the blue-green mutant were resuspended, one in the supernatant medium that contained extracellular porphyrins as a result of previous photosynthetic growth by cells, and the other in fresh medium. They were then exposed to light (intensity 600 f.-c.) and aerated with 95% air-5% CO₂ at 30°C.

DURATION OF EX- POSURE TO LIGHT AND AIR, HR.	OPTICAL DENSITY OF SUPERNATE AT 395 M μ		CHLOROPHYLL, MG PER 100 ML OF CULTURE	
	Old medium	Fresh medium	Old medium	Fresh medium
0	0.144	0.012	1.06	1.11
1	0.180	0.017	0.98	1.01
2.75	0.180	0.026	0.92	0.92
6.5	0.165	0.035	0.72	0.71

other in the original supernatant medium, which contained the porphyrins excreted by the cells during their previous photosynthetic growth. The two suspensions were placed in a water bath and exposed to light and air in the usual fashion; the changes in chlorophyll content and extracellular porphyrin concentration that occurred during the exposure were measured at intervals.

Results. The results are shown in table 1. Both suspensions excreted some porphyrins during the course of the experiment, as indicated by the increase in the optical density of the suspending medium at 395 m μ . Throughout, however, the extracellular porphyrin concentrations remained markedly

different. Initially the ratio of these concentrations in the two suspensions was 10:1, and it always remained 5:1 or greater. Despite this, the rates of chlorophyll destruction were identical, within the limits of error of the measurements. These observations appear to eliminate the excreted porphyrins as the major photosensitizers in the system, but do not afford any direct evidence that bacteriochlorophyll itself can play this rôle.

Experiment 2

Principle. In the bacterial cell, the major absorption band of bacteriochlorophyll lies in the near infrared region, between 800 and 950 m μ . No other known cell constituents absorb appreciably in the near infrared, and it is also well outside the main region of light absorption by the excreted porphyrins (see fig. 3). Hence the occurrence of photodynamic effects in a culture exposed simultaneously to air and to light exclusively of wavelengths greater than 800 m μ would constitute very strong evidence that bacteriochlorophyll is a photosensitizer.

Procedure. Two cultures of the blue-green mutant were prepared and placed in separate water baths, one of which was illuminated with unfiltered light, and one with light passed through a filter (Eastman Kodak Wratten 87C) that is completely opaque to all wavelengths less than 800 m μ . The transmission spectrum of this filter is shown in figure 7. After being mounted between panes of Lucite and masked by a frame of aluminum foil, it was placed immediately in front of the entrance window. All other surfaces of the bath were shielded as completely as possible with black paint and black cloth covers. Visual inspection showed that the interior was free from any stray white light. When all adjustments had been made, aeration of the inoculated cultures with 95% N₂-5% CO₂ was started and, after a suitable delay to ensure the establishment of complete anaerobiosis, the lights were turned on. As photosynthetic growth proceeded, the light intensities were adjusted, by changing the distances of the two light

sources, until both cultures had been brought to the same growth rate. When, after several hours of photosynthetic growth, both cultures had reached steady state conditions of pigment synthesis, the aeration mixture was changed to 95% air-5% CO₂. Determinations of turbidity and chlorophyll content were performed in parallel on both cultures during the period of anaerobic growth and after the introduction of air.

Results. As shown in figure 8, the introduction of air stops growth immediately and initiates chlorophyll destruction in both cultures. This demonstrates that the photodynamic ef-

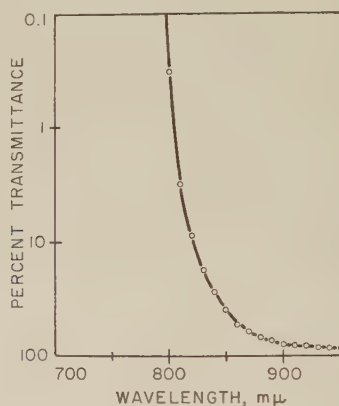


Fig. 7 The transmission of light by the Eastman Kodak Wratten filter 87C used in the experiment on infrared photosensitivity of the blue-green mutant.

fects previously observed with unfiltered light can be reproduced with infrared light alone, and provides very powerful evidence in favor of the conclusion that bacteriochlorophyll is the major photosensitizer in the system.

Additional conclusions can be drawn for a consideration of the quantitative aspects of the experiment. After the introduction of air, the rates of chlorophyll destruction in the two cultures were virtually identical for three hours. From the Reciprocity Law, which states that the product of the duration, t , and the intensity, I , of light flux that will produce a given quantity of a given chemical reaction is constant, it follows that I (PDA), the photodynamically effective intensity

of light flux for chlorophyll destruction, was identical in the two cultures. What is the explanation of this striking coincidence? Before the introduction of air, the two cultures were growing photosynthetically at the same rate. Since the light intensities were in the growth-limiting range, this system can also be treated as a photochemical one, in which the newly-synthesized cell material constitutes the gross reaction product. Again from the Reciprocity Law, it follows that I (Ph), the photosynthetically effective intensity of light flux, was

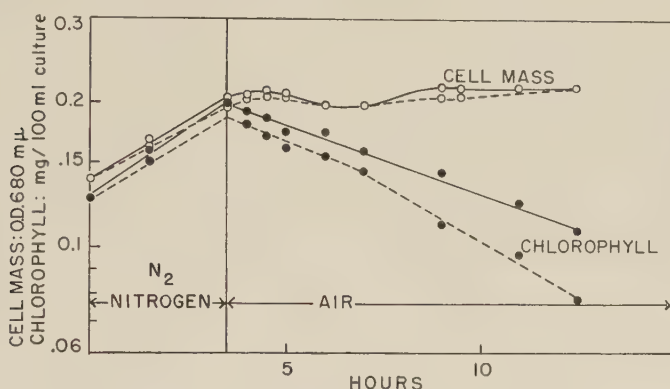


Fig. 8 The effect of air on growth and pigment synthesis by the blue-green mutant in infrared light and in a complete spectrum. During the initial period of anaerobic growth, the light intensities were adjusted until the two cultures were growing photosynthetically at identical rates. At the time indicated by the vertical line, air was introduced. Dotted lines: cell mass and chlorophyll content in a complete spectrum. Solid lines: cell mass and chlorophyll content in infrared light.

identical in the two cultures. In the blue-green mutant, the only wavelengths of light that are effective for photosynthesis are those absorbed by bacteriochlorophyll, and hence for this organism I (Ph) is identical with I (Chl), the flux of light into bacteriochlorophyll. In other words, the light intensities had been so adjusted, prior to the introduction of air, that the bacteriochlorophyll in both cultures was absorbing the same total quantity of photons per unit time, in the one case confined to the infrared portion of the spectrum, and in the other case distributed throughout the visible and infrared regions.

Under these circumstances, the identity of the values for I (PDA) in the two cultures therefore must mean that the photosensitizer has the same ratio of light absorption in the infrared to total light absorption as does bacteriochlorophyll. Since bacteriochlorophyll is unique among cell constituents by virtue of its extremely high absorption in the near infrared region, the equivalence of the values for I (PDA) and I (Chl) in the two cultures permits the unequivocal conclusion that bacteriochlorophyll, and bacteriochlorophyll alone, is responsible for the observed photodynamic effect during the first three hours of aeration.

As shown in figure 8, the rates of destruction of chlorophyll in the two cultures begin to diverge after three hours, in a manner which suggests that I (PDA) in the complete spectrum has become somewhat greater than I (PDA) in infrared light. This fact is most reasonably interpreted by the assumption that additional photosensitizers, active only in the visible region of the spectrum, have been produced as a consequence of the photodecomposition of bacteriochlorophyll. Some evidence for this can be found by comparing the absorption spectrum of the cells after 9 hours of aeration with their spectrum before aeration (fig. 9). After aeration, absorption at both the main chlorophyll peaks (375 and 875 $m\mu$) has greatly decreased, but the relative decreases are not the same, the loss of absorption at 875 $m\mu$ being much more substantial than that at 375 $m\mu$. Among porphyrins, absorption in the near infrared region is confined to tetrahydroporphyrins such as bacteriochlorophyll, whereas absorption in the violet and near ultraviolet is a general property of the entire chemical class. Further evidence for a qualitative change in the pigments of the cells after aeration can be found in the marked distortion of the ultraviolet peak, and in the appearance of new minor peaks in the visible region around 525, 650 and 745 $m\mu$. Although the nature of these spectral changes suggests an intracellular accumulation of porphyrins, the quantities concerned are evidently so small that their characterization would be a very difficult task.

All the experiments illustrating the photodynamic effect show apparent minor changes of cell density during the first few hours after the introduction of air. At first, these fluctuations puzzled us; but the spectra shown in figure 9 suggest their cause. Our method of determining cell density, by the measurement of optical density at 680 $m\mu$, is based on the assumption of negligible light absorption by the cells at this point in the spectrum, which may no longer be true during the

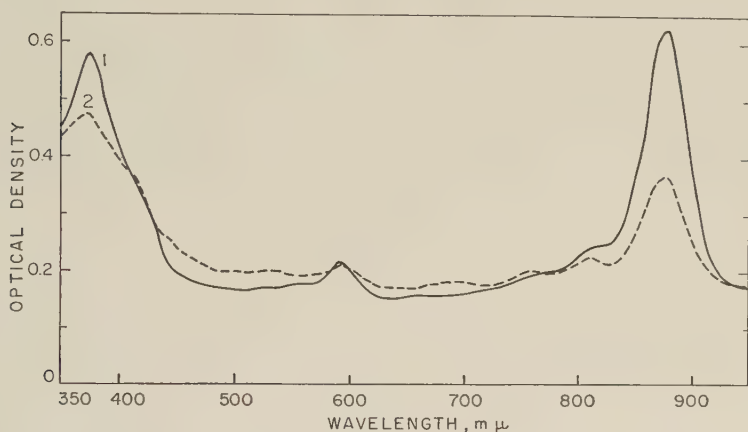


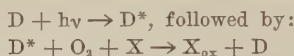
Fig. 9 The effect of air and light on the spectrum of whole cells of the blue-green mutant. Data from the experiment shown in figure 8. The spectra were measured in a special cuvette holder equipped with a pane of opal glass between cuvettes and photocell in order to minimize the effects of light scattering. Both spectra were adjusted to the same optical density at 1000 $m\mu$. Curve 1: spectrum before admission of air. Curve 2: spectrum after aeration with air for 9 hours in infrared light.

intracellular photodecomposition of bacteriochlorophyll. Consequently, the apparent fluctuations of cell density during the early stages of aeration, when viable counts show a high rate of killing, probably reflect absorptive changes in the system.

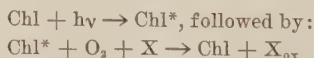
We may now summarize the direct conclusions to be drawn from the experiments concerned with the effect of light and air on the blue-green mutant. This mutant is rendered photosensitive by its own bacteriochlorophyll, but the photosensitization is not apparent under the normal conditions of

photosynthetic growth, owing to the fact that bacterial photosynthesis does not result in the evolution of free oxygen, and is hence a strictly anaerobic process. However, the introduction of air into a photosynthesizing culture produces immediate and catastrophic consequences. Photosensitization has at least three experimentally observable effects: severe but sublethal damage to the cell; death; and the destruction of bacteriochlorophyll. The death rate is much higher than the rate of chlorophyll destruction.

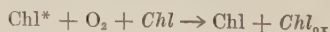
A tentative formulation of the course of events, based on what is known of photosensitized oxidations in model systems, will now be attempted. In the first place, there is very good evidence that the dye molecule in a photosensitized oxidation performs primarily a catalytic rôle, which can be formulated as:



where D is the dye molecule in its ground state, D^* the dye molecule in its excited state, X the oxidizable substrate and X_{ox} the product formed from the oxidizable substrate after reaction with O_2 . In the present case, we can write Chl and Chl^* in place of D and D^* , where Chl and Chl^* represent the ground state and the excited state, respectively, of bacteriochlorophyll in the cell. X , the oxidizable substrate, may be any suitable molecule of cell material adjacent to the excited chlorophyll molecule, and it seems reasonable to assume that in fact a number of different cell materials undergo oxidation. Thus the general formulation of the events that follow the introduction of air becomes:



One of the intracellular substrates that undergoes oxidation is clearly bacteriochlorophyll itself. Model systems also show that, in the absence of any other suitable substrate, the dye molecule itself may serve as the oxidizable substrate. Therefore we can formulate one of the intracellular photo-oxidations more precisely as:



using italics to distinguish the chlorophyll molecule that undergoes oxidation from the one that undergoes excitation. It is possible, though not very probable, that the oxidation of bacteriochlorophyll is the only photochemical oxidation occurring in the system; on this view, death would result from secondary effects produced by *Chl*_{ox}. More likely, death of the cell occurs when some vital cell constituent becomes the direct substrate.

The mechanism which permits some cells to survive is obscure. As already mentioned, the existence in the population of a small fraction resistant for genetic reasons to photodynamic death appears to be excluded, since clones isolated from the surviving population are still sensitive to the combined action of light and air after a period of photosynthetic growth. Hence a phenomic mechanism of survival must be sought. If all cells in the population are inherently susceptible, the prime requirement for survival is clearly a low content of photosensitizer. Any cell which manages to accomplish this will be able to grow in air and light by making use of its capacity for oxidative metabolism; and since air suppresses chlorophyll synthesis, the endogenous generation of more photosensitizer is prevented. Thus the real question is how the chlorophyll content of an occasional cell in the population becomes low enough for survival. One obvious answer, the destruction of bacteriochlorophyll by photodynamic action, does not appear to be satisfactory, for the following reasons. From the data in figure 6, it is evident that the surviving cells resume growth in the presence of light and air at a time when the chlorophyll content of the whole culture has fallen only to some 80% of its initial level. Hence it is highly improbable that the survivors could have achieved desensitization solely through the photodynamic destruction of their chlorophyll. The only plausible explanation for survival that has occurred to us is that the distribution of chlorophyll in the initial population is far from uniform, a few cells containing so little as to be more or less immune to photodynamic killing.

Peculiarities of the blue-green mutant: a recapitulation

In the foregoing pages we have described certain properties of the blue-green mutant that distinguish it sharply from the wild type of *R. spheroides*, and others are reported elsewhere (Griffiths and Stanier, '56). Although there are numerous phenotypic differences between them, the blue-green mutant and the wild type are probably separated by only a single mutational step, since reversions—very frequent in most blue-green stocks—yield a phenotype in all respects like that of the wild type. It is, consequently, tempting to look for a primary functional disorder in the blue-green mutant which might explain all the phenotypic peculiarities that characterize it. As a preliminary to this essay in interpretation, we shall summarize briefly the respects in which it differs from the wild type.

1. *Carotenoids*. The two colored carotenoids of the wild type have been replaced in the mutant by a single colorless polyene, phytoene, in amounts roughly equivalent on a weight basis to the carotenoids of the wild type. No phytoene is detectable in cells of the wild type. The carotenoids of the wild type are exclusively localized in submicroscopic cytoplasmic particles, the chromatophores, which also contain all the bacteriochlorophyll of the cell, and are evidently the site of the primary photosynthetic process. All the chlorophyll and at least 90% of the phytoene in the mutant are in its chromatophores; a small fraction of the phytoene is probably located elsewhere in the cell (Griffiths and Stanier, '56).

The structure of phytoene as given by Goodwin ('55) is shown in figure 10, together with that of lycopene, a representative aliphatic carotene.

2. *Chlorophyll*. Both wild type and mutant contain the same chemical species of chlorophyll, bacteriochlorophyll (Griffiths and Stanier, '56). However, under comparable steady state conditions of pigment synthesis, there is less chlorophyll in the mutant than in the wild type. The manufacture of chlorophyll by the mutant is always accompanied

by excretion of chlorophyll derivatives, but this phenomenon is never encountered in the wild type. Since the actual chlorophyll content of the mutant is 70–80% of the chlorophyll content of the wild type, the combined rate of synthesis of chlorophyll and its derivatives by the mutant is probably very close to the rate of chlorophyll synthesis by the wild type.

3. *Absorption spectrum.* The absorption spectra of whole cells of the two strains differ in the expected fashion between 450 and 550 $m\mu$, the region of light absorption by the carotenoids of the wild type. In addition, however, they have completely different absorption spectra in the near infra-red region, despite the fact that both contain the same chemical species of chlorophyll. The cells of the wild type have a major

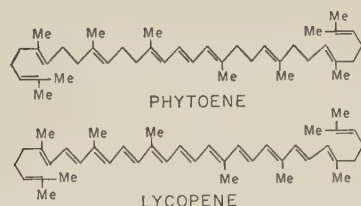


Fig. 10 The structural formulae of phytoene and lycopene.

peak at 855 $m\mu$, a minor one at 805 $m\mu$, and a shoulder at about 880 $m\mu$. The cells of the mutant have a single, symmetrical peak at 875 $m\mu$, and a broad, low shoulder around 810 $m\mu$ (Griffiths and Stanier, '56).

4. *Photosensitivity.* The mutant is photosensitized by its bacteriochlorophyll, whereas the wild type is not.

One other relevant fact should be mentioned. We have also studied in some detail (Cohen-Bazire, Sistrom and Stanier, '57; Griffiths and Stanier, '56) a *green* mutant that is qualitatively different from the wild type in its carotenoid constitution, containing two new yellow carotenoid pigments. The spectrum of the cells is correspondingly modified between 450 and 550 $m\mu$; but in all its remaining properties the green mutant is indistinguishable from the wild type.

The blue-green mutant: an interpretation

Let us examine first the loss of carotenoid pigments that has taken place in the blue-green mutant. Considered by itself, this effect of the mutation can be rather simply interpreted on the biochemical level, as resulting from a total block at one point in the chain of biosynthesis, with a concomitant accumulation of the immediate precursor:



Furthermore, such a formulation receives considerable support from findings with other biological systems, which indicate that the relatively saturated C_{40} polyenes, including phytoene, may be the biosynthetic precursors of colored carotenoids. This concept received its first expression in the scheme of carotenogenesis proposed by Porter and Lincoln ('50) as a result of their extensive analyses of carotenoid distribution in the fruits of tomatoes. Phytoene is one of the postulated early intermediates in the Porter-Lincoln scheme. Claes ('54) found that induced mutants of the green alga *Chlorella* with derangements of normal carotenogenesis accumulate large amounts of saturated polyenes, including phytoene. Most of these mutants are characterized by complex patterns of accumulation; however, one of them parallels perfectly the blue-green mutant of *R. spheroides*, since it contains no colored carotenoids and accumulates exclusively phytoene. Interestingly enough, these mutants of *Chlorella* show a marked simultaneous reduction of chlorophyll content, evidently far greater than the reduction of chlorophyll content in the blue-green mutant. This fact even led Claes to question whether the primary blocks in her mutants might not lie rather in chlorophyll synthesis than in the synthesis of carotenoids; but in the case of the blue-green mutant of *R. spheroides* such a possibility seems to be fairly excluded. Most of the *Chlorella* mutants are sensitive to visible light, although no details concerning this phenomenon have been published so far. Thus in *Chlorella* and in *R. spheroides*, early blocks

in normal carotenogenesis are accompanied by other parallel phenotypic changes.

As a simple working hypothesis, we may assume that the primary biochemical lesion in the blue-green mutant lies in the chain of carotenogenesis. In *R. spheroides*, as in other photosynthetic bacteria, the carotenoid pigments are exclusively incorporated, either during or after their synthesis, in submicroscopic intracellular structures, the chromatophores. The chromatophores contain in addition all the chlorophyll of the cell, protein, lipids, and a small amount of ribonucleic acid (Pardee, Schachman and Stanier, '52; unpublished observations). Since the chromatophore is the exclusive site of the primary photochemical reaction in bacterial photosynthesis, the spatial arrangement of its various chemical constituents must be ordered by its functional rôle. One constituent of this ordered system, the carotenoid pigments, has been completely replaced in the blue-green mutant by a substance of similar molecular *size* but very different *shape*. With only three conjugated double bonds in the center of the molecule, phytoene lacks in large measure the molecular rigidity that is conferred on the colored carotenoids by their extensive conjugation system (fig. 10). For purely geometrical reasons, then, the positions of the other molecular constituents of the chromatophore may either be modified, or else somewhat strained by the introduction of phytoene. Given such a situation, the subnormal chlorophyll content becomes readily understandable: only 70–80% of the usual number of molecules can make a correct fit in such a malformed chromatophore. Since the primary genetic block lies, according to our hypothesis, in the chain of carotenogenesis, the biosynthesis of chlorophyll will nevertheless proceed normally, subject to control by light intensity in exactly the same fashion, both qualitative and quantitative, as in the wild type. The consequence will therefore be an unincorporated surplus, which is degraded and excreted into the medium as a mixture of phorbides. The far more severe reduction of chlorophyll content that occurs in *Chlorella* when carotenoid pigments are

replaced by phytoene may be caused by the greater complexity of its photosynthetic apparatus, which renders accomodation to a structural change of this kind more difficult. Indeed, when one takes into account the structural complications that are bound to arise in this class of biochemical mutants, the fact that a functional photosynthetic apparatus can survive at all is remarkable.

The changes in the infrared absorption spectrum

We are now confronted with the problem of explaining the changes in the infrared spectrum of the cells; but paradoxically enough, it is the infrared spectrum in the wild type, rather than in the blue-green mutant, that it is difficult to understand. Since the first extensive studies on the infrared spectra of purple bacteria by Katz and Wassink ('39) and Wassink Katz and Dorrestein ('39), it has been known that some species (e.g., *Rhodospirillum rubrum*) show a single main symmetrical band in the infrared region that corresponds in structure (though not in position) to the long wavelength band of bacteriochlorophyll in organic solvents, while other species (e.g., *Chromatium*) show a multiplicity of bands in the infrared region (usually 3, counting a more or less pronounced shoulder) that have no obvious counterparts in the spectrum of pure bacteriochlorophyll. The long wavelength peak of bacteriochlorophyll in organic solvents lies at about 775 mμ. The very large positional shift towards longer wavelengths that characterizes the absorption of bacteriochlorophyll *in vivo* has been generally interpreted as reflecting conjugation with protein, although the existence of a bacteriochlorophyll-protein conjugate has not yet been established directly by isolation. This interpretation of the *positional* shift was extended by Wassink, Katz and Dorrestein ('39) to explain also the supernumerary infrared peaks which they discovered in certain species: they suggested that in these cases there exist two or more different bacteriochlorophyll-protein conjugates in the cell, each characterized by a distinct infrared peak. Wassink, Katz and Dorrestein also observed that the relative

heights of the infrared peaks in *Chromatium* can be varied to a considerable extent by the light intensity employed during cultivation of the bacteria; the same phenomenon has been found subsequently in *R. spheroides* (Cohen-Bazire, Sistrom and Stanier, '57). The Dutch workers interpreted such variations as reflecting shifts in the ratios of the various conjugating proteins.

Duysens ('52) has offered a similar but more general interpretation of the complex infrared spectra of some purple bacteria, primarily to explain his observations on fluorescence emission spectra. He found that during excitation of the photosynthetic pigment system, the fluorescence emission spectrum always mirrors in shape and position the infrared maximum at the longest wavelength. The result obtained with *Chromatium* were particularly striking. Despite a highly asymmetrical infrared absorption spectrum, with peaks of almost equal height at 800 and 850 m μ and a slight shoulder at 890 m μ , this species has a fluorescence emission spectrum with an almost perfectly symmetrical and well-isolated main peak, which can be correlated with the shoulder in the absorption spectrum at 890 m μ . Duysens assumed that the bacteriochlorophyll in the cell is conjugated with three different "bearer molecules," and designated these three conjugates as B 800, B 850 and B 890. Since monochromatic light of wavelengths absorbed by the carotenoids or by any of the three hypothetical conjugates of bacteriochlorophyll always gives rise to the same fluorescence emission spectrum, Duysens concluded that energy transfer takes place successively from the carotenoids through the three conjugates, B 800, B 850 and B 890, and that only B 890 actually participates in fluorescence and in the primary chemical reaction of photosynthesis.

Duysens also observed that when an autolysate of *Chromatium* cells was heated to 100°C. for one minute, B 890 disappeared while the relative intensities of B 850 and B 800 increased; these changes were accompanied by a migration of the fluorescence peak to a shorter wavelength. When the same

experiment was performed with an autolysate of *Rhodospirillum rubrum*, which has a single symmetrical infrared peak at 880 $m\mu$, there was a general fall in absorption beyond 800 $m\mu$, and a new peak arose at 785 $m\mu$, indicative of the formation of free bacteriochlorophyll in the cell. The fluorescence peak did not change appreciably in position. Duysens ('52) interpreted these facts as follows:

"The foregoing observations suggest the following picture of the bacteriochlorophyll types in *Chromatium* and *Rhodospirillum rubrum*: a molecule of a given type consists of a bacteriochlorophyll molecule connected to a specific bearer molecule. In *Chromatium* three different kinds of bearer molecules are present, which, being connected to a bacteriochlorophyll molecule, give rise to three bacteriochlorophyll types. A short heating destroys the bearers of B 890 and liberates the bacteriochlorophyll molecules, which become attached to free bearer molecules of another type. In *Rhodospirillum* only one type of bearer molecule is present. If this type is destroyed by heating, the liberated bacteriochlorophyll is not attached to a bearer and therefore it becomes colloidal."

From this summary, it is evident that a number of distinct and very complex phenomena in purple bacteria have been explained on the assumption that the bacteriochlorophyll of certain species is carried by several different "bearer molecules" (Duysens) or proteins (Wassink, Katz and Dorrestein), an assumption introduced in the first place to explain the occurrence of supernumerary bands in the infrared spectrum of the cells.

The wild type of *R. spheroides* has an infrared spectrum of the *Chromatium* type (fig. 11); according to the assumptions outlined above, this may be taken to imply the presence of three different conjugates of bacteriochlorophyll with bearer molecules. Following the terminology of Duysens, we may designate them as B 805, B 855 and B 880. The blue-green mutant has a spectrum of the *Rhodospirillum* type (fig. 11); again, according to the above assumptions, this should imply that only one kind of conjugate is present, B 875, which we

may equate with the B 880 of the wild type, whose exact position is subject to some uncertainty since it lies on the shoulder of B 855. The concept of specific bearer molecules therefore necessarily leads to the conclusion that the muta-

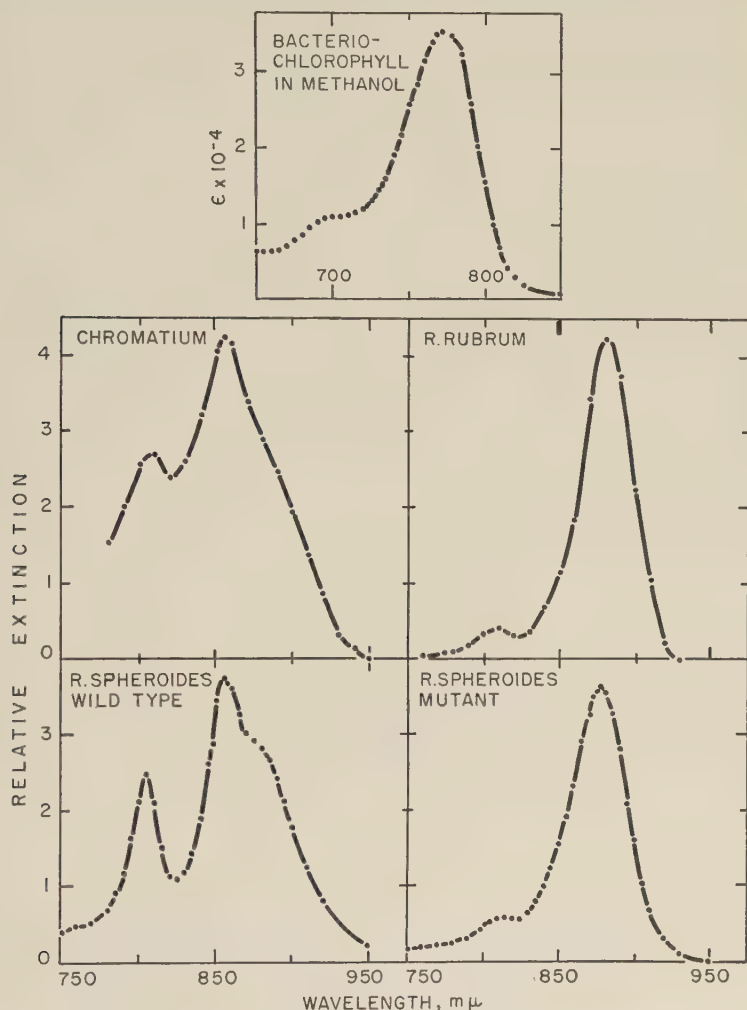


Fig. 11 Infrared light absorption by pure bacteriochlorophyll and by cells of various purple bacteria. Top pair: the prototypes, *Chromatium* (left) and *Rhodospirillum rubrum* (right). Bottom pair: *Rhodopseudomonas sphaeroides*, wild type (left) and blue-green mutant (right). Spectrum of *Chromatium* copied from Duyssens ('52).

tional step from wild type to blue-green has resulted in the disappearance from the chromatophore of two bearers for bacteriochlorophyll, this substance being exclusively attached in the mutant chromatophore to the third kind of bearer. Furthermore, since the B 880 peak in the chromatophore of the wild type is relatively low, accounting at most for some 20–30% of the total infrared absorption, it follows that in the mutant the burden carried by B 880 has greatly increased, since at any given light intensity the mutant chromatophore has some 70–80% of the normal bacteriochlorophyll content of a wild type chromatophore.

If our working hypothesis concerning the nature of the primary biochemical lesion in the blue-green mutant is correct, the spectral change in the infrared region must be regarded as a consequence of the replacement of colored carotenoids by phytoene. It must be admitted, however, that a simple explanation for this effect cannot at present be offered; instead, we shall outline two alternative possibilities, one of which would be in accord with the concept of specific bearer molecules, and the other of which would necessitate its abandonment.

In terms of the concept of specific bearer molecules, B 805 and B 855 could be regarded as bearer systems for bacteriochlorophyll which are also linked to colored carotenoids, and whose formation is dependent upon the simultaneous formation of carotenoid pigments; hence the suppression of carotogenesis results in the simultaneous suppression of the synthesis of these bearers. A slightly more elegant version of this hypothesis can be achieved by assuming that the non-pigmented components of B 805, B 855 and B 880 are identical, but that the linkages of B 805 and B 855 to carotenoids modify in some fashion their ability to conjugate with bacteriochlorophyll; it might be imagined that the resonance of these conjugates is less than that of the B 880 conjugate, since their absorption maxima lie at shorter wavelengths. On this view, the elimination of the colored carotenoids would automatically transform the non-pigmented

components of the B 805 and B 855 systems into that of the B 880 system, thus obviating the necessity to assume a specific suppression of the synthesis of two bearers, and explaining at the same time the apparent increase in the B 880 system in the chromatophores of the blue-green mutant.

The alternative possibility, already suggested by Calvin ('55) is to assume that the complex infrared spectrum of the wild type reflects not the presence of three different chlorophyll-bearer conjugates, but rather the coupling of the resonance systems of bacteriochlorophyll and carotenoids through a pi-complex. As he has pointed out, Scheibe ('48) has described model systems which show qualitative spectral changes resulting from intermolecular electronic coupling. Since only three central double bonds of phytoene are in conjugation, an effective electronic coupling with bacteriochlorophyll of the kind that could be envisaged for a colored carotenoid would be impossible in the blue-green mutant. This hypothesis necessitates, of course, new interpretations for a large body of earlier data, and implies that two different molecular arrangements of bacteriochlorophyll and carotenoids occur in the chromatophores of purple bacteria. In organisms of the *Rhodospirillum* type (also represented by the blue-green mutant), there is no electronic coupling between the two classes of pigments, and hence the general shape of the infrared spectrum approximates to that of bacteriochlorophyll in organic solvents, although a great positional shift, no doubt reflecting conjugation to some sort of bearer, exists. In organisms of the *Chromatium* type (also represented by the wild type of *R. sphaeroides*) coupling between the pigments is responsible for the supernumerary peaks; since the general positional shift exists here, too, conjugation of the coupled pigment systems to a bearer must also be envisaged.

Photosensitization and its implications

Lastly, we come to the problem of photosensitization in the blue-green mutant. Since this is caused by its bacterio-

chlorophyll, which is chemically identical with that of the wild type and likewise located exclusively in the chromatophores (Griffiths and Stanier, '56), it seems evident that photosensitization occurs because the structure of the chromatophore has been modified. There is evidence that the photosynthetic efficiency of the blue-green mutant has been only slightly, if at all, impaired, since its lowered photosynthetic growth rate can be explained in considerable part by reduced absorption of photosynthetically effective light. Hence under anaerobic conditions its bacteriochlorophyll still operates in a fashion that is normal, or nearly so; the system falls apart only when air is introduced. Under these circumstances, the bacteriochlorophyll catalyzes photo-oxidations (including its own oxidation) which result, either directly or indirectly, in the death of the cell. Photosensitivity is not manifested when the normal colored carotenoids of the wild type are replaced by other, qualitatively different, colored carotenoids, as shown by the example of the green mutant. It is also not correlated with an *in vivo* infrared spectrum of the *Rhodospirillum* type, since *R. rubrum* itself is not sensitive. We therefore suggest that photosensitization is a specific consequence of the replacement of carotenoid pigments by a *colorless* polyene. This contention is supported by the parallel observation of Claes ('54) that *Chlorella* mutants with blocks in carotenogenesis causing the accumulation of colorless polyenes are killed by exposure to visible light. Before a detailed explanation of this positive correlation is attempted, it is necessary to review some of the work on photosensitization by chlorophyll in other biological systems.

“Photodynamic effects” and “photoautooxidations”

The photosensitization of a biological system may be either endogenous or exogenous. In animals, the classic instance of endogenous photosensitization is that which sometimes accompanies congenital porphyria; the individual is sensitized to light by the abnormal accumulation of porphyrins which

results from the primary metabolic defect. Exogenous photosensitizations may also occur in nature; the disease of domestic animals known as hypericemia, which follows the ingestion of certain *Hypericum* species, is a case in point. However, by far the largest number of observed exogenous photosensitizations have been experimentally induced, either by injection of a suitable fluorescent dye, or by immersion of tissues in a solution of the dye.

In his treatise on photodynamic action, Blum ('41) describes a number of exogenous photosensitizations that have been experimentally induced in plants, but does not mention the existence of endogenous photosensitization in plants. One might thus be led to conclude that photosynthetic organisms are immune to endogenous "photodynamic effects." This would indeed be an extraordinary situation, since in a photosynthetic plant tissue the stage is perfectly set for the occurrence of photosensitization. There is an extremely high concentration of fluorescent pigments (chlorophylls, and phycobilins as well in certain algae), and upon exposure to light, oxygen is evolved as a result of photosynthesis. In actual fact, however, endogenous "photodynamic effects" are well known in algae and higher plants; but they masquerade under a different name in botanical circles, being termed "photoautooxidations." This highly confused area of plant physiology has been ably and critically reviewed by Rabinowitch ('45), and in the following account we shall draw heavily on his summary. The occurrence of photoautooxidation in photosynthetic plant tissues is marked by a reversal of gas exchange, oxygen liberation giving place in the presence of light to oxygen consumption, which proceeds at a rate substantially higher than the normal rate of respiration in the dark. This change can be induced by several different means, the effectiveness of which depends either on the preliminary inhibition of photosynthesis (e.g., by narcotization or removal of carbon dioxide); or on the direct enhancement of autooxidation (e.g., by increasing light intensity or the partial pressure of oxygen). It has been assumed that

the substrates for photoautooxidation are cellular reserve materials, since no obvious damage is caused during the period of rapid oxygen consumption. Only after the process has continued for some time is bleaching of the pigments apparent; the onset of bleaching is correlated with a decline in the rate of oxygen uptake. The photosensitizing rôle or chlorophyll in photoautooxidations is suggested by the effectiveness of red light, but no careful measurements of the action spectrum appear to have been made.

Sensitivity to damage caused by light intensity alone appears to vary widely among higher plants, the so-called "shade plants" being injured by exposure to far lower light intensities than those required to damage "sun plants." Other factors may play a rôle in causing damage at high light intensities, but Rabinowitch ('45) concludes that photoautooxidation is nonetheless involved in many cases.

A careful study of the effect of light intensity was carried out on *Chlorella* by Myers and Burr ('40), who examined the kinetics of oxygen evolution at a series of light intensities. They found that the net production of oxygen gives place to a net consumption at a light intensity of about 13,000 foot-candles; but even at much higher light intensities, oxygen consumption does not begin immediately at a steady rate upon exposure to light. Instead, there is a pronounced lag, presumably caused by the initial occurrence of photosynthesis. At a light intensity of 27,700 foot-candles the steady rate of oxygen consumption established after the initial lag was more than twice as great as the rate of dark respiration. As long as oxygen consumption proceeded at a steady rate, no irreversible injury was apparent, but when the rate of photoautooxidation started to decline, bleaching could be observed.

The various facts concerning photoautooxidation which are summarized above show that plants are not wholly immune to endogenous photosensitization, although the conditions required to produce lasting damage by this means are often very drastic, as shown by the work of Myers and Burr. Since chlorophyll is an excellent exogenous photosensitizer in animal

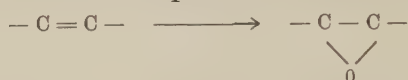
tissues, as shown by the experiments of Hausmann ('09) and Eisler and von Portheim ('22), it is evident that in normal photosynthetic tissues there must exist an effective buffering mechanism for the prevention of photodynamic effects. The mere fact that in such tissues the chlorophyll is mainly engaged in transferring its activation energy into photosynthesis is insufficient to account for their relative immunity, since the fluorescence of chlorophyll *in vivo* shows that part of the absorbed energy gets drained off in other ways; consequently it is certain that in the presence of oxygen some excited chlorophyll molecules will catalyze photooxidations. Curiously enough, many students of photosynthesis do not seem to have been clearly aware that a problem exists, and the one completely explicit statement of it that we have encountered (admittedly during an unsystematic perusal of the vast literature on photosynthesis), is by Franck ('49):

“Indeed, it is one of the miracles of photosynthesis that the plant can use a dye able to fluoresce in the presence of oxygen predominantly for the purpose of reduction, and is able to hold the process of photooxidation in check so that damage is prevented or minimized even under severe conditions.”

*A general function for carotenoids
in photosynthetic organisms*

Does the behavior of the blue-green mutant in the presence of light and air provide a clue to the solution of this problem? Taking into consideration the facts about photoautooxidation in plants, we can describe its behavior in a slightly different way: *the buffering mechanism which prevents endogenous photosensitization by chlorophyll in the wild type and the green mutant has been lost in the blue-green mutant, and its threshold for light damage in the presence of air is consequently much lower.* But the principal chemical difference which separates the blue-green mutant from both the green mutant and the wild type is precisely the absence of colored carotenoids, and this suggests that the colored carotenoids may be able to act as chemical buffers against light damage.

A chemical mechanism that would provide such buffering action, not only in *R. spheroides* but in all photosynthetic organisms, is not difficult to envisage. If the chlorophyll and carotenoid molecules are arranged in the photosynthetic unit in such a fashion that an excited chlorophyll molecule has an extremely high probability of photooxidizing an adjacent carotenoid chain, rather than some other cell-constituent, lethal damage would be minimized as long as the carotenoids could continue to be oxidized. Their photooxidation might occur by the formation of epoxides across the double bonds:



Such a formulation is suggested by the fact that 5:6- and 5:8-carotenoid epoxides have been demonstrated to occur in leaves (Karrer and Krause-Voith, '48; Karrer, Krause-Voith and Steinling, '48). Furthermore, Meyer ('33) has shown that chlorophyll readily photooxidizes ethylenic double bonds *in vitro*. If such a buffering mechanism is to be effective, an enzymatic mechanism for the reduction of the epoxide to the normal carotenoid must also be postulated.

According to this hypothesis, permanent photooxidative damage in normal photosynthetic tissues would become manifest only when the rate of photooxidation of the carotenoid pigments exceeded the rate at which they could be reduced again. To the best of our knowledge, no studies of the effects of photoautooxidation in plants have included a careful and systematic search for *qualitative* changes in the carotenoid pigments. Such a study provides an obvious means of testing the general validity of the hypothesis.

From what has already been said, it is evident that a replacement of colored carotenoids by phytoene could be expected to result in a lowering of the threshold of light intensity for permanent damage, since the number of double bonds available for oxidation is greatly reduced. The hypothesis therefore predicts that any photosynthetic organism

in which colored carotenoids have been replaced by phytoene or other highly saturated polyenes will show dramatic increase of susceptibility to light damage. This prediction is already fulfilled in two cases: *Chlorella* and *R. spheroides*. Indeed, even if chlorophyll incorporation in the photosynthetic apparatus were to continue, a mutational change of this kind in organisms whose photosynthesis results in oxygen evolution should always prevent the occurrence of normal photosynthesis. Its failure to do so in the blue-green mutant of *R. spheroides* is dependent on the fact that bacterial photosyntheses are strictly anaerobic processes.

The general function of carotenoids in photosynthetic organisms which is postulated above can also be extended to explain the presence of carotenoid pigments in heterotrophic microorganisms such as bacteria and fungi, where they occur widely. Since most of these organisms also contain porphyrins, although in relatively low concentrations, they are potentially liable to endogenous photosensitization, and a buffering mechanism would consequently possess adaptive value. Indeed, many of the previously isolated facts about carotenoid distribution and carotenoid behavior in heterotrophic microorganisms fall into a pattern and begin to assume adaptive significance when considered from this standpoint. Two of these facts which now become meaningful are the high concentration of carotenoids in reproductive cells liable to intense light exposure (e.g., the conidia of *Neurospora* and other fungi), and the stimulation of carotenoid production by light, a well-known phenomenon both in bacteria (*Mycobacterium* spp.) and in fungi (*Neurospora*, *Phycomyces*). Visible radiations are not commonly supposed to have deleterious effects upon heterotrophic microorganisms, but Beam and Elkind (personal communication) have found during careful photobiological studies on *Saccharomyces cerevisiae* that exposure of this yeast to high intensities of visible light under conditions where temperature effects are excluded causes a slight but significant and reproducible drop in the viable count. Since it

was irrelevant to the subject of enquiry, they did not mention it explicitly in their published work (Beam and Elkind, '55).

Lastly, our interpretation of the function of carotenoids in photosynthesis fits the evolutionary proposal advanced some years ago by van Niel ('49); namely, that photosyntheses of the bacterial type preceded green plant photosynthesis in time. Since carotenoids have never been shown to function directly in the photosynthetic process, and appear to serve only by transfer of absorbed energy to chlorophyll, a chlorophyll-catalyzed photosynthesis could conceivably have developed in organisms devoid of carotenoids; but this would have been possible only if external hydrogen donors could be used in the disposal of the oxidized moiety resulting from the photochemical split of water, thus permitting the maintenance of an anaerobic mode of life. The development of carotenoids to serve as ancillary light-gathering pigments might then have occurred, since pigments serving this function have an obvious adaptive value in all photosynthetic organisms. But at the same time, this evolutionary development would have constituted an essential preadaptive step in the emergence of green plant photosynthesis, since the disposal of the oxidized moiety from the photochemical split of water as molecular oxygen is possible only if the system is already buffered against photooxidations.

SUMMARY

A mutant of the photosynthetic bacterium *Rhodopseudomonas spheroides* that contains no colored carotenoids has been subjected to physiological study. This mutant can still grow photosynthetically under anaerobic conditions in the light, its growth rate at any given light intensity being about half that of the wild type. In both strains, the chlorophyll content of the cells is inversely related to light intensity; and at any given light intensity the chlorophyll content of the mutant is about 70-80% of that of the wild type. This reduction of chlorophyll content is correlated with the excretion of water-soluble chlorophyll derivatives into the me-

dium during photosynthetic growth and chlorophyll synthesis, a phenomenon never manifested by the wild type.

The metabolic derangements of this mutant when grown under anaerobic conditions in the light can be simply interpreted. Chlorophyll incorporation in the photosynthetic unit is somewhat reduced, the synthetic surplus being excreted in the form of several chlorophyll derivatives; as a consequence of the reduction in chlorophyll content, possibly coupled with the absence of effective light absorption in the normal region of carotenoid absorption, the growth rate under conditions of limiting light intensity is lower than that of the wild type. However, an additional and much more severe physiological derangement manifests itself when a culture of the mutant which has been grown under anaerobic conditions in the light is exposed simultaneously to air and light. Most of the cells are rapidly killed, and there is at the same time a net destruction of the intracellular chlorophyll. Under comparable conditions, the wild type continues to grow at an unchanged, or even slightly increased rate, and although chlorophyll synthesis stops, no reduction in the total chlorophyll content of the population occurs. The death of the blue-green mutant and the destruction of its chlorophyll require the simultaneous presence of air and light; if shielded from light at the same time that it is exposed to air, it behaves exactly as does the wild type. This photosensitization was shown to be attributable exclusively to the intracellular bacteriochlorophyll.

The multiple phenotypic derangements of this mutant can be interpreted satisfactorily as stemming either directly or indirectly from the replacement of normal carotenoids by a colorless polyene, phytoene. The relative immunity of photosynthetic organisms to photodynamic damage is discussed, and a new hypothesis concerning carotenoid function in photosynthetic organisms, suggested by the observations on the mutant of *R. spheroides*, is presented. This hypothesis assumes that the primary function of carotenoid pigments in phototrophs is to act as chemical buffers against photooxida-

tion of other cell constituents by chlorophyll, thus conferring a high degree of immunity to endogenous photosensitization. The same general hypothesis is extended to account for the wide-spread occurrence of carotenoid pigments in heterotrophic microorganisms that contain other potential endogenous photosensitizers.

It is a pleasure to acknowledge the assistance of Dr. Germaine Cohen-Bazire, who collaborated with us in the first kinetic experiments with the blue-green mutant, and of Mrs. Ruth Harold, who gave us valuable aid at a later stage. We are also most grateful to Professor C. B. van Niel for providing us with space during the summer of 1954 in his laboratory at the Hopkins Marine Station, where this work, like many other studies on the photosynthetic bacteria, was begun.

LITERATURE CITED

- BEAM, C. A., AND M. ELKIND 1955 *Radiation Res.*, **3**: 89.
BLUM, H. 1941 *Photodynamic Action and Diseases Caused by Light*, New York, Reinhold.
CALVIN, M. 1955 *Nature*, **176**: 1214.
CLAES, H. 1954 *Z. Naturforsch.*, **9b**: 401.
CLAYTON, R. 1953 *Arch. Mikrobiol.*, **19**: 107.
COHEN-BAZIRE, G., W. R. SISTROM AND R. Y. STANIER 1957 *J. Cell. and Comp. Physiol.*, in press.
DUYSENS, L. N. M. 1952 *Transfer of Excitation Energy in Photosynthesis*, Thesis, Utrecht.
EISLER, M., AND L. VON PORTHEIM 1922 *Biochem. Z.*, **130**: 497.
FRANCK, J. 1949 *In: Photosynthesis in Plants* (J. Franck and W. E. Loomis, editors). Ames: Iowa State College Press, 308.
GOODWIN, T. W. 1955 *Ann. Rev. Biochem.*, **24**: 496.
GRIFFITHS, M., W. R. SISTROM, G. COHEN-BAZIRE AND R. Y. STANIER 1955 *Nature*, **176**: 1211.
GRIFFITHS, M., AND R. Y. STANIER 1956 *J. Gen. Microbiol.*, **14**: 698.
HAUSMANN, W. 1909 *Biochem. Z.*, **16**: 294.
KARRER, P., AND E. KRAUSE-VOITH 1948 *Helv. Chim. Acta*, **31**: 802.
KARRER, P., E. KRAUSE-VOITH AND K. STEINLIN 1948 *Helv. Chim. Acta*, **31**: 113.
KATZ, E., AND E. C. WASSINK 1939 *Enzymologia*, **7**: 97.
MEYER, K. 1933 *J. Biol. Chem.*, **103**: 597.
MYERS, J., AND G. O. BURR 1940 *J. Gen. Physiol.*, **24**: 45.
VAN NIEL, C. B. 1949 *in Photosynthesis in Plants* (J. Franck and W. E. Loomis, Editors). Ames: Iowa State College Press, 437.

- PARDEE, A. B., H. K. SCHACHMAN AND R. Y. STANIER 1952 *Nature*, 169: 282.
- PORTER, J. W., AND R. E. LINCOLN 1950 *Arch. Biochem.*, 27: 390.
- RABINOWITCH, E. I. 1945 *Photosynthesis and Related Processes*. I. New York, Interscience Publishers.
- SISTROM, W. R., M. GRIFFITHS AND R. Y. STANIER 1956 A note on the porphyrins excreted by the blue-green mutant of *Rhodospirillum rubrum*. *J. Cell. and Comp. Physiol.*, 48: 459.
- STRAIN, H. H. 1949 *in* *Photosynthesis in Plants* (J. Franck and W. E. Loomis, editors), Ames, Iowa State College Press, 133.
- THOMAS, J. B. 1950 *Biochim. Biophys. Acta*, 5: 186.
- WASSINK, E. C., E. KATZ AND R. DORRESTEIN 1939 *Enzymologia*, 7: 113.

THE SOURCE OF OXYGEN SECRETED INTO THE SWIMBLADDER OF COD ¹

P. F. SCHOLANDER, L. VAN DAM AND THEODORE ENNS

*Woods Hole Oceanographic Institution, and Department
of Medicine, Johns Hopkins University*

ONE FIGURE

In vitro studies of blood from several species of deep sea fish revealed that neither a high CO₂ tension nor a low pH could unload the oxygen from the hemoglobin against such high oxygen pressures (100–200 atmospheres) as are known to exist in the swimbladder (Scholander and van Dam, '54). This cast serious doubt on the theory that either the Bohr or the Root effect is the cause of the high oxygen pressures produced in live fish, and made it desirable to endeavor to find out what exactly is the source of the oxygen secreted into the swimbladder. We describe tracer experiments below, where codfish were induced to secrete oxygen while breathing oxygen¹⁸ dissolved in ordinary sea water. These experiments were designed to show whether the oxygen was derived directly from the molecular oxygen dissolved in the water, or whether it came from other sources.

APPARATUS AND MATERIAL

An experimental fish chamber was made from a 100 l metal container fitted with a window and coated on the inside with beeswax. Synthetic air could be recirculated through the chamber by means of a gear pump, which drove the air through a CO₂ absorber and down into a 15 cm long cloth hose which

¹Contribution No. 881 from the Woods Hole Oceanographic Institution. This investigation was supported by a grant from the National Science Foundation.

acted as a bubbler for the fish tank. The gas returned to a 40 l spirometer, and from there back to the pump (fig. 1). By introducing some oxygen into the system while recirculating, it was established by gas analysis that a complete equilibration with the water phase took place within 20 minutes. Water containing > 1.4 atom per cent O^{18} was obtained on allocation by the U. S. Atomic Energy Commission from the Stuart Oxygen Company, San Francisco. Oxygen¹⁸ labeled oxygen was produced by electrolysis of the water on platinum electrodes, with sulfuric acid added.

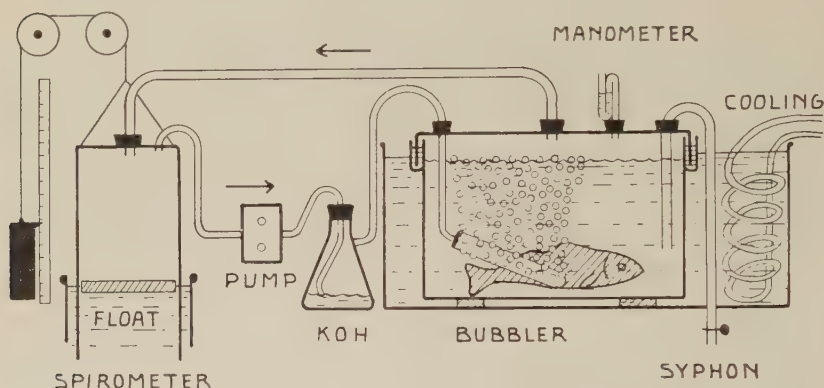


Fig. 1 Fish chamber and closed circuit arrangement for circulating oxygen¹⁸.

Codfish (*Gadus callarias*) were used in these experiments, since they secrete oxygen relatively quickly. They were obtained through the courtesy of Mr. David F. Ryder, of Chatham, Massachusetts. In order to make them secrete while confined in the relatively cramped space of the fish chamber, it was necessary to administer yohimbine (Fänge, '53), in addition to deflating the swimbladder. In the course of 10 hours after a complete deflation they would then fill their swimbladders to almost normal buoyancy.

EXPERIMENTAL PROCEDURE

The spirometer was filled with 9.5 l of electrolyzed tagged oxygen and 30 l tank nitrogen. The fish tank was filled to

the top with sea water, the apparatus closed, and recirculation continued for an hour, after which the circulation was stopped, all hoses were clamped, and the lid was opened.

Meanwhile the swimbladder gas had been removed from the codfish by puncture, and the traces of oxygen left were washed out with nitrogen, all of which was drawn out. Analysis of this gas showed that no more than 0.2–0.4 cm³ of air oxygen remained in the bladder. Yohimbine was given intramuscularly (about 0.8 mg/kg), and the fish was slipped into the fish tank. All handling was done with the fish submerged or with its gills irrigated. Additional fish were prepared in the same way. The tank was closed and connected with the spirometer. Twenty liters of water were siphoned out of the tank to keep foam from spreading, and recirculation was started. The gas phase maintained an oxygen concentration between 20 and 21%, with CO₂ less than 0.1%. After a run of 10 hours, the now buoyant fishes were taken out. Gas was withdrawn from their swimbladders and stored in 20 cm³ syringes, which had been lubricated with concentrated lithium chloride. Checks showed that the system was completely air tight, and that the dilution of the introduced O¹⁸ enriched oxygen checked exactly with the dilution calculated from the amount of normal oxygen which was added to the system by introducing the fish.

The isotope determinations were performed on a mass spectrometer at the Johns Hopkins University School of Medicine (Chinard and Enns, '54).

RESULTS

Table 1 shows the results of two experiments with deflated codfish treated with yohimbine. The amount of gas secreted by each fish was between 40 and 50 cm³. Both carbon dioxide and oxygen concentrations are high, and correspond well with the composition of the gas which the gland itself secretes (Scholander, '56).

It will be seen from the almost identical figures for the oxygen¹⁸ concentration in the gas phase of the water and in

the swimbladder that the fish deposits only the molecular oxygen dissolved in the sea water into the swimbladder. No other source of any significance is involved. Consequently, we know now that the oxygen is picked up through the gills, and is transported by the hemoglobin to the *rete*-gland system of the swimbladder. It is then deposited into the swimbladder, sometimes against pressures of 100 atmospheres or more. There is no knowledge as to how such high pressures are attained. At the very low partial pressures of oxygen prevailing in our tracer experiments (less than one atmosphere) a Root effect, caused by 10–14% CO₂, would undoubtedly liberate oxygen from the red cells. But whether enough of

TABLE 1

Oxygen secretion in deflated codfish treated with yohimbine
Water temperature, 5°C. O¹⁸ in air found as 0.204 atom %. Time, 10 hours

EXP. NO.	FISH NO.	CHAMBER GAS		SWIMBLADDER GAS			
		O ₂	O ¹⁸	O ₂	O ¹⁸	CO ₂	CO ₂
		vol. %	atom %	vol. %	atom %	vol. %	atom % O ¹⁸
I	1	21.0	1.13	78.0	1.12	10.0	
II	1	20.0	1.11; 1.10	44.8	1.15	14.2	0.44
	2			68.8	1.13	11.5	0.44
	3			69.3	1.14	11.3	0.37

this excess tension of CO₂ could be transmitted to the proximal end of the *rete* to effect an oxygen secretion is a question which must await experimental evidence (cp. Scholander, '54).

Spectro photometry of the blood of several deep sea fishes indicated that the limiting dissociation pressure via excessive acidification of oxyhemoglobin was often less than 40–50 atmospheres, falling short by 2–5 times of the oxygen pressure which the gland produces. One is therefore led to assume that some additional process must be responsible for the ultimate step-up of the pressure. One may wonder whether the secreting cells covering the capillary loops of the gas gland can actively take molecular oxygen from the plasma and secrete

it into the swimbladder. Some such arrangement may be responsible for the nitrogen and argon deposition (cp. Scholander, van Dam, and Enns, '56). Or it may be that some as yet undiscovered means exists for dissociating off oxygen from the hemoglobin to yield the very high pressures required, in which case the nitrogen secretion must be an entirely different process.

In the codfish oxygen secretion takes place accompanied by high CO_2 tensions (table 1). In many fishes this apparently is not so (cp. Scholander, '54). It can be seen from table 1 that the O^{18} atom fraction of CO_2 in the swimbladder was only about 0.4%, against 0.2% in air and 1.1% in the oxygen dissolved in the chamber water, i.e. only about one quarter of the CO_2 was labeled. The respiratory CO_2 formed in the fish during the experiment would be O^{18} labelled and would exchange with the large unlabeled bicarbonate pool in the fish and sea water. The accumulation of CO_2 in the swimbladder would therefore always involve both labeled and unlabeled CO_2 and it would be very difficult from the isotope ratio to conclude how the CO_2 was formed. Copeland ('52) and Fänge ('53) found that glycogen disappears from the gland during secretion and Ball, Strittmatter and Cooper ('55) found that gland tissue *in vitro* produces a rapid breakdown of glucose to lactic acid. It is therefore possible that the high CO_2 tension found in the swimbladder during secretion is caused by lactic acid production in the gland, but if so it must be very slight, inasmuch as Fänge ('53) failed to find it.

SUMMARY

Codfish treated with yohimbine after complete deflation were kept in ordinary sea water containing dissolved O^{18} labeled oxygen. In 10 hours the swimbladder filled with oxygen, all of which was labeled and was hence derived from the dissolved oxygen in the water. The *rete*-gland system accordingly transfers molecular oxygen from the blood into the swimbladder. There is at the present time no known mechanism which can account for the resultant extremely

high pressures. Of the 10–14% CO₂ deposited with the oxygen, only one quarter was labeled. Possible causes of the elevated CO₂ tension are discussed.

We are greatly indebted to Dr. V. T. Bowen, of the Woods Hole Oceanographic Institution, for his help and advice.

LITERATURE CITED

- BALL, E. G., C. F. STRITTMATTER AND O. COOPER 1955 Metabolic studies on the gas gland of the swimbladder. *Biol. Bull.*, 108: 1–17.
- CHINARD, F. P., AND T. ENNS 1954 Relative rates of passage of deuterium and tritium oxides across capillary walls in the dog. *Amer. Jour. Physiol.*, 178: 203–205.
- COPELAND, D. E. 1952 The histophysiology of the teleostean physoclistous swimbladder. *J. Cell. and Comp. Physiol.*, 40: 317–334.
- FÄNGE, R. 1953 The mechanisms of gas transport in the euphysoclist swimbladder. *Acta Physiol. Scandinavica*, vol. 30, suppl. 110, 133 pp.
- SCHOLANDER, P. F. 1954 Secretion of gases against high pressures in the swimbladder of deep sea fishes. II. The *rete mirabile*. *Biol. Bull.*, 107: 260–277.
- 1956 Observations on the gas gland in living fish. *J. Cell. and Comp. Physiol.*, 48: 523–528.
- SCHOLANDER, P. F., AND L. VAN DAM 1954 Secretion of gases against high pressures in the swimbladder of deep sea fishes. I. Oxygen dissociation in blood. *Biol. Bull.*, 107: 247–259.
- SCHOLANDER, P. F., L. VAN DAM AND T. ENNS 1956 Nitrogen secretion in the swimbladder of whitefish. *Science*, 123: 59–60.

OBSERVATIONS ON THE GAS GLAND IN LIVING FISH ¹

P. F. SCHOLANDER

*Woods Hole Oceanographic Institution and
Lerner Marine Laboratory, Bimini*

In spite of all the information available regarding the function of the gas gland in fishes, one may safely say that none of the three cardinal feats of the gland can as yet be explained; namely, the production of 100–200 atmospheres of oxygen, of 10–20 atmospheres of nitrogen, and of 0.1–0.2 atmospheres of argon. It is believed that some advance towards solving these problems can be gained by studying the secretion more closely on the intact gland itself.

This paper presents some observations on the gas gland in living fish, giving analyses of the gas bubbles secreted by the gland of cod and of the oxygen content and capacity of the blood leaving the active gland in barracuda. In these two species it is relatively easy to expose the swimbladder gland and to induce gas secretion for studies *in situ*. After deflation, about half the number of barracudas examined continued to secrete gas on the operating table, and deflated codfish, when treated with yohimbine (Fänge, '53), would do the same.

The barracudas (*Sphyræna barracuda*) were obtained at the Lerner Marine Laboratory, Bimini, Bahamas, in January, 1955, and the codfish (*Gadus callarias*) were procured through the courtesy of Mr. David F. Ryder, of Chatham, Massachusetts. The cod were kept in live cars near the laboratory in Woods Hole.

¹Contribution No. 880 from the Woods Hole Oceanographic Institution. This investigation was supported by a grant from the National Science Foundation.

*Composition of the gas bubbles secreted
by the gland of cod*

The codfish was deflated by puncture and given 5–10 mg yohimbine per kilogram. After one or two hours the fish was lifted onto a V board, lashed in place, and provided with a rubber tube and mask, through which the water passed into its mouth and out under the gill covers. A rubber collar behind the gills prevented the water from flowing back over the body. The tail end of the fish was covered with a plastic apron and was kept irrigated with cold water. The swimbladder was exposed and opened along one side, so as not to sever the gland. Part of the gland was exposed by turning over the ventral swimbladder wall. The bubble foam which usually covered the gland was wiped off with a fine glass rod, or if necessary rinsed off with 0.17 M saline. A small square of household Saran wrapping film was placed on the gland, without trapping any air bubbles. In a few minutes an active gland would produce masses of bubbles under the Saran, which slowly coalesced into larger ones. Under the binocular microscope small bubbles could be removed from beneath the Saran film, by means of a mercury pipette with a hair-fine tip bent at an angle. They were handled and analyzed according to a micro gasometric technique described by Scholander and Evans ('47).

The composition of the gas bubbles secreted under the Saran film is given in table 1. There is a considerable variability. The carbon dioxide averages some 9% and the oxygen some 63%. These figures, including the spread, agree well with the gas composition found in the swimbladder of fish treated with yohimbine, where the bladder had been completely emptied (cp. Scholander, van Dam, and Enns, '56).

These analyses are significant in that the composition of the gas has not been modified by a differential elimination of gas by the oval, but represents what is actually being secreted. In the codfish the oxygen secretion is accompanied by a carbon dioxide tension which seems exceptionally high. A

great variety of fishes have been found to secrete oxygen with a much lower CO_2 concentration, sometimes only a small fraction of 1%. This should, however, be verified by analyses of bubbles taken directly from the gland.

It is an interesting fact that the bubbles secreted into the mucus covering the gland or into crevices between the cells are formed only on the outside of the gland cells; i.e., towards the swimbladder lumen. As the gas pressure in a bubble, due to surface tension, is inversely proportional to the diameter, considerable pressures are necessary for the formation of

TABLE 1

Composition of gas bubbles secreted under Saran film by the gas gland of codfish treated with yohimbine; sample 0.5 mm³

FISH NO.	SAMPLE	% CO_2	% O_2	% N_2
I	1	8.6	81.1	10.3
	2	5.0	70.3	24.7
II	1	15.8	76.6	7.6
III	1	6.9	49.5	43.6
	2	6.8	61.1	32.1
	3	5.9	66.5	27.6
	4	13.9	30.1	56.0
IV	1	7.2	69.2	23.6
Average		8.8	63.1	28.1

bubbles *de novo*. If the primary tension build-up were in the blood of the capillary loops one might ask why the bubbles do not form there, rather than on the outer side of the large gland cells. Unfortunately, because of the complexity of bubble formation, this cannot be taken as an indication of how the tension gradients run in relation to the epithelium.

Blood analyses in barracuda

A living barracuda was lashed to a V board and irrigated with water. The swimbladder was exposed, as described for the cod. Part of the gland was covered with a piece of

Saran film, through which the gas secretion could be clearly observed. Blood samples were taken directly from the gland vein with a fine, heparinized glass pipette, and were at once analyzed for oxygen content. In one large secreting barracuda enough blood could be collected from the gland vein to determine both oxygen content and capacity. For the latter the blood was rotated with air in a 5 cm³ vial, shielded against evaporation loss. Normal oxygen capacity was determined in blood obtained by heart puncture. Three independent series (IIIa, b, and c in table 2) were performed on this fish at

TABLE 2

Oxygen in blood from heart and secreting gas gland in three barracudas. Oxygen saturation is calculated by taking air-equilibrated heart blood as 100%

FISH NO.	GLAND BLOOD				HEART BLOOD			
	Content		Capacity		Content		Capacity	
	Vol. %	Sat.	Vol. %	Sat.	Vol. %	Sat.	Vol. %	Sat.
I	9.7	98%					9.9	100%
IIa	9.3	88%					10.6	100%
IIb	10.0	94%					10.6	100%
IIIa	11.9	92%	13.2	102%	5.9	46%	12.9	100%
IIIb	11.7	91%	13.2	102%	5.0	39%	12.9	100%
IIIc	10.9	89%	12.7	104%	5.0	41%	12.2	100%

With fishes II and III the set of determinations was repeated at intervals of approximately one hour, as long as the fish secreted. There is evidence of a slight anemia in IIIc.

intervals of about one hour. All samples were analyzed by a micro gasometric method (Scholander and van Dam, '56).

The oxygen capacity of the barracuda blood was usually between 10 and 13 volume per cent. In table 2 the capacity of the heart blood has been set at 100%. Relative to this the blood leaving the secreting gland had an oxygen content averaging 92%. This is a very high figure, considering that the normal arterial saturation could hardly be expected to be more than perhaps 95%. The oxygen capacity of the blood leaving the gland was not lower than that of heart blood, but possibly slightly higher. The oxygen saturation

of the heart blood was low, as would be expected, averaging 42%.

There are two striking points in these results: (1) that oxygen secretion took place with a hardly measurable A-V difference in the gland blood, and (2) that the blood leaving the gland had apparently lost none of its oxygen carrying capacity.

We know from oxygen¹⁸ experiments on codfish that the oxygen secreted by the gland is derived directly from the dissolved oxygen in the sea water, and is hence transported to the gland via the blood stream (Scholander, van Dam, and Enns, '56). We would therefore feel safe in making the generalization that whenever oxygen is being secreted the gas gland must have a positive A-V difference. That this difference may be surprisingly low was evident from mere inspection of the *retes* in the barracuda. They are multiple in this species, and can readily be observed under a binocular. While secreting, they are hyperemic and of bright arterial color, but when there is no secretion they are poorly circulated and cyanotic. If CO₂ and fixed acids poured into the *rete* blood during secretion, the concentration in barracuda must have been quite low, since it did not visibly reduce the blood. Again, if fixed acid were the cause of oxygen secretion via the Bohr or Root effect, it would show up as a diminished oxygen capacity in the leaving blood, which however was not indicated by our analyses. Even in the codfish, with its high CO₂ tension in the secreted gas, it has not been conclusively demonstrated so far that there is a rise in lactic acid associated with the secretion (Fänge, '53). One might also mention here, for whatever it may be worth, that indicator paper placed on the mucus of the secreting gland in codfish gave a pH of 7 ± 0.2 , and the same very trifling acidity was also found in a wreckfish caught near Bimini at a depth of 600 meters.

From theoretical considerations of the *rete* as a counter current exchange system, one may calculate that a very minute primary increment in the CO₂ tension at the glandular

pole of the *rete* could easily be multiplied to tensions of such magnitude as are commonly found at this site. The swim-bladder gas secreted by 4 deflated barracudas contained 3.6 to 5.2% CO₂, but nevertheless the blood which left the secreting gland had almost full arterial oxygen saturation. This strongly indicates a low CO₂ tension in the leaving blood. Such a tension drop along the *rete* is in accordance, of course, with the assumed function of this structure.

SUMMARY

Gas bubbles secreted under a Saran film by the intact gas gland of cod contained 5–16% CO₂ and 30–81% oxygen. The blood leaving the secreting gland of barracuda had an average oxygen saturation of 92%, i.e.; nearly arterial. Secretion in barracuda can therefore take place with a very low A-V difference. The *retes*, while secreting, were hyperemic and of bright arterial color, but cyanotic and poorly circulated when there was no secretion. There was no measurable loss in oxygen combining capacity of the blood leaving the active gland.

I wish to express my gratitude to Dr. C. M. Breder, Jr., of the American Museum of Natural History, for arranging my stay at Bimini, and to Mr. and Mrs. Michael Lerner for their help in getting barracuda alive. For assistance in the studies on barracuda, I am much indebted to Dr. L. A. Krumholz, of the Lerner Marine Laboratory, and to Mrs. Susan I. Scholander.

LITERATURE CITED

- FÄNGE, R. 1953 The mechanisms of gas transport in the euphysoelist swim-bladder. *Acta Physiol. Scandinavica*, vol. 30, suppl. 110, 133 pp.
- SCHOLANDER, P. F., AND L. VAN DAM 1956 Micro gasometric determination of oxygen in fish blood. *J. Cell. and Comp. Physiol.*, 48: 529–532.
- SCHOLANDER, P. F., L. VAN DAM, AND T. ENNS 1956 The source of oxygen secreted into the swimbladder of cod. *J. Cell. and Comp. Physiol.*, 48: 517–522.
- SCHOLANDER, P. F., AND H. J. EVANS 1947 Microanalysis of fractions of a cubic millimeter of gas. *J. Biol. Chem.*, 169: 551–560.

MICRO GASOMETRIC DETERMINATION OF OXYGEN IN FISH BLOOD¹

P. F. SCHOLANDER AND L. VAN DAM

Woods Hole Oceanographic Institution

ONE FIGURE

The micro gasometric method for oxygen determination in blood by Roughton and Scholander ('43) works well with the blood from humans, dogs, rabbits, and rats, but may be difficult, sometimes impossible, to use on the blood of cats, birds, or fishes, where the reagents do not properly break up the blood proteins into a flocculate precipitate, but produce a viscid foam. By increasing the acidity of the final blood mixture, with due changes in technique, this difficulty has been overcome. With the present method we believe determinations can be made on a much wider range of animal material than was possible before. For details in procedure and equipment the basic papers by Scholander and Roughton ('42) and Roughton and Scholander ('43) should be consulted.

APPARATUS

The syringe analyzer and the calibrated blood pipette, with a capacity of about 40 mm³, are described by Scholander and Roughton ('42). The strong acid used in the present modification of the method produces a rapid CO₂ evolution, which makes it necessary to close the analyzer with a special wire clip, instead of with the finger (fig. 1). The clip has a polyethylene tip made by pressing a piece of polyethylene tubing into the lumen of a piece of drawn out warm glass tubing. The plug is self-holding, and closes the capillary gas tight.

¹Contribution no. 879 from the Woods Hole Oceanographic Institution. This work was supported by a grant from the National Science Foundation.

REAGENTS

1. Distilled water.
2. Isotonic saline. Dissolve 11.7 gm NaCl in 1 liter of water ($= 0.20\text{ M}$).
3. Caprylic alcohol.
4. Ferricyanide solution. Dissolve 12.5 gm $\text{K}_3\text{Fe}(\text{CN})_6$, 3 gm KHCO_3 , and 0.5 gm saponin in 50 ml water.
5. Acid sulfate solution. Dissolve 30 gm Na_2SO_4 anhydrous in 100 ml water and add 5 ml concentrated H_2SO_4 .
6. NaOH solution. Dissolve 10 gm NaOH in 50 ml H_2O and add 5 gm Na_2SO_4 anhydrous.

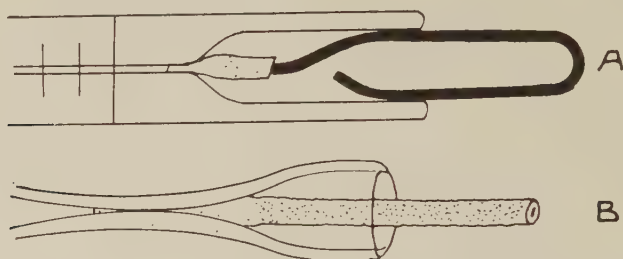


Fig. 1 A. Wire clip with polyethylene tip sealing the capillary of the analyzer. B. Method of forming the polyethylene tip in warm glass tubing.

7. Pyrogallol solution. Add 15 gm pyrogallol to 100 ml of 20% NaOH and cover with a layer of oil 2 cm thick. Dissolve under the oil by stirring with a glass rod.

Store the above solutions in 2–5 ml syringes provided with drawn out glass tips.

PROCEDURE

Clean the analyzer and blood pipette with dichromate H_2SO_4 cleaning solution, and rinse them thoroughly with water. Dry the warm pipette by suction. Rinse the capillary and barrel of the analyzer twice with ferricyanide solution. Fill the cup with the solution to the mark and draw it down into the capillary. Rinse the cup with saline, and empty. Place a drop of

caprylic alcohol in the bottom of the cup. Expel any trapped air bubbles.

Fill the blood pipette with the blood to be analyzed and transfer the sample into the analyzer in the usual way. Discharge the air bubble that is on top of the blood through the caprylic alcohol. Draw in the caprylic alcohol to the zero mark, and remove the rest by suction. Fill the cup with acid sulfate solution to the mark.

Place the metal plug in position in the bottom of the cup, so that the plastic tip almost closes the capillary. Draw the acid sulfate solution into the barrel, and close the capillary by immediately seating the plug. Shake the analyzer horizontally for two minutes. At short intervals loosen the plunger arresting clip to equalize the pressure.

Adjust the gas pressure to atmospheric with the plunger. Remove the plug carefully, while manipulating the plunger so as to maintain the liquid seal in the capillary. Attach the NaOH cup and fill it with NaOH solution. Eject the air trapped in the capillary, and draw some NaOH into the barrel, letting the plunger up during the absorption. Towards the end of the absorption move the bubble up into the capillary, where it is protected against reabsorption.

Remove the NaOH cup, and empty the analyzer cup by suction. Clean the upper part of the capillary where the readings will be taken by twirling a fine stainless steel wire. Temperature equilibrate the analyzer in a beaker containing water of room temperature for half a minute. Dry the analyzer by wiping it lightly with cheesecloth, and read the volume of the bubble (V_1).

Fill the glass cup with pyrogallol solution. Draw it down slowly over the bubble in the barrel. Read the volume of the bubble (V_2).

The oxygen content in volume per cent equals $(V_1 - V_2 - c) \times f$, where c is the blank correction for oxygen in the reagents (about 0.9 vol. %), and f is the STP correction.

ACCURACY

Duplicate analyses in a variety of fishes usually agreed within 0.2 to 0.3 volume per cent. The gasometric method checks linearly with an optical method (Scholander and van Dam, '54), and when samples of tautog blood of different oxygen contents were mixed anaerobically in syringes the results agreed well with the calculated value.

LITERATURE CITED

- ROUGHTON, F. J. W., AND P. F. SCHOLANDER 1943 Micro gasometric estimation of the blood gases. I. Oxygen. *J. Biol. Chem.*, 148: 541-550.
- SCHOLANDER, P. F., AND L. VAN DAM 1954 Secretion of gases against high pressures in the swimbladder of deep sea fishes. I. Oxygen dissociation in blood. *Biol. Bull.*, 107: 247-259.
- SCHOLANDER, P. F., AND F. J. W. ROUGHTON 1942 A simple microgasometric method of estimating carbon monoxide in blood. *J. Industrial Hygiene Toxicology*, 24: 218-221.

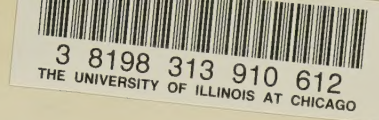
INDEX

- A**CTIVITY of mitochondria from myxomycete plasmodia succinoxidase 243
- ADELMAN, J. WILLIAM. The relation of accommodation to current distribution in single muscle fibers 181
- Anodal effects during the refractory period of cardiac muscle 237
- Anaerobically, occurrence of respiration deficient mutants in baker's yeast cultivated 95
- ANDREASEN, A. A., AND T. J. B. STIER. Anaerobic nutrition of *Saccharomyces cerevisiae*. III. An unidentified growth promoting factor and its relationship to the essential lipid requirements 317
- Anoxic anoxia and apnea on renal function in the harbor seal (*Phoca vitulina* L.), comparison of the effect of 35
- Antihistaminic on growth, contractility and plasmocrine activity in cultures of embryonic chick heart, studies on the individual and joint effects of histamine and an 147
- Apnea on renal function in the harbor seal (*Phoca vitulina* L.), comparison of the effect of anoxic and anoxia and 35
- Arbacia gametes, comparative effect of methylated xanthines on the fertilization capacity and life span of 253
- Arthropod, chemoreception, electrophysiological studies of. I. General properties of the labellar chemoreceptors of diptera 51
- Aspects of thyroid physiology in Rainbow trout, some 393
- Avena* coleoptile respiration, several factors which influence the rate of 77
- AIRD, B. ROBERT, AND BILL GAROUTTE. Diffusion from brain slices in vitro 167
- B**ACILLUS *cereus*, television microscopy of sporulation and spore germination of 301
- Bacterium which lacks colored carotenoids, the biology of a photosynthetic 473
- Baker's yeast cultivated anaerobically, occurrence of respiration deficient mutants in 95
- Biology of a photosynthetic bacterium which lacks colored carotenoids, the 473
- BISHOP, P. O., AND W. R. LEVICK. Saltatory conduction in single isolated and non-isolated myelinated nerve fibers 1
- Blue-green mutant of *Rhodospseudomonas spheroides*, a note on the porphyrins excreted by the 459
- BRADEY, STANLEY E. See Lowrance, Preston B., James F. Nickel and Cheves McC. Smythe 35
- Brain, the entry of $P^{32}O_4$ into rat 139
- Brain, slices in vitro, diffusion from 167
- BROOKS, MCC. CHANDLER, PAUL F. CRANEFIELD, BRIAN F. HOFFMAN AND ARTHUR A. SIEBENS. Anodal effects during the refractory period of cardiac muscle 237
- BRONSWIEG, D. RUTH, AND JAMES H. GREGG 293
- BURGEN, A. S. V. The secretion of non-electrolytes in the parotid saliva 113
- C**APACITY and life span of Arbacia, comparative effect of methylated xanthines on the fertilization 253
- Carbohydrate and phosphate compounds during hibernation in ground squirrel, metabolism of some 371
- Cardiac muscle, anodal effects during the refractory period of 237
- Carotenoids, the biology of a photosynthetic bacterium which lacks colored 473
- CHAPMAN, B. GEORGE, AND KATHERINE A. ZWORYKIN 301
- Changes in muscle caused by cooling, relationship between electrical and mechanical 421
- Chemoreception, I. General properties of the labellar chemoreceptors of diptera; electrophysiological studies of arthropod 51
- CHENEY, HOLT RALPH. Comparative effect of methylated xanthines on the fertilization capacity and life span of Arbacia gametes 253
- Chick heart, studies on the individual and joint effects of histamine and an antihistaminic on growth, contractility and plasmocrine activity in cultures of embryonic 147
- Cholinesterase, from insects, the properties of 215
- Cod, the source of oxygen secreted into the swimbladder of 517
- Coleoptile respiration, several factors which influence the rate of *Avena* 77
- Coleoptiles, growth, work output and sensitivity to increased gravitational forces in wheat 405
- Cholinesterase, in insects, soluble and particulate 197
- Colored carotenoids, the biology of a photosynthetic bacterium which lacks 473
- Comparison of the effect of anoxic anoxia and apnea on renal function in the harbor seal (*Phoca vitulina* L.) 35
- Competence, in *Escherichia coli*, sexual 271
- Conduction in muscle, effects of high intensity sound on electrical 435
- Conduction in single isolated and non-isolated myelinated nerve fibers, saltatory 1
- Current distribution in single muscle fibers, the relation of accommodation to 181

- Cooling, relationship between electrical and mechanical changes in muscle caused by 421
- CRANEFIELD, F. PAUL. See Brooks, Chandler McC., Brian F. Hoffman and Arthur A. Siebens 237
- Cultures of embryonic chick heart, studies on the individual and joint effects of histamine and an antihistaminic on growth, contractility and plasmocrinine activity in 147
- D**ICTYOSTELIUM *discoideum*, biochemical events accompanying stalk formation in the slime mold 293
- Distribution in single muscle fibers, the relation of accommodation to current 181
- E**ASTON, DEXTER M. Some tensile properties of nerve 87
- EDWARDS, BETTY F., AND STEPHEN W. GRAY. Growth, work output and sensitivity to increased gravitational forces in wheat coleoptiles 405
- Electrical conduction in muscle, effects of high intensity sound on 435
- Electrical and mechanical changes in muscle caused by cooling, relationship between 421
- Electrophysiological studies of arthropod chemoreception. I. General properties of the labellar chemoreceptors of diptera 51
- ENNS, THEODORE. See Scholander, P. F. 517
- Embryonic chick heart, studies on the individual and joint effects of histamine and an antihistaminic on growth, contractility and plasmocrinine activity in cultures of 147
- Entry of $P^{32}O_4$ into rat brain, the 139
- Escherichia coli*, sexual competence in 271
- F**ACTORS which influence the rate of *Avena* coleoptile respiration, several 77
- Fertilization capacity and life span of *Arbacia* gametes, comparative effect of methylated xanthines on the 253
- Fibers, the relation of accommodation to current distribution in single muscle 181
- Fish blood, micro geometric determination of oxygen in 529
- Fish, observations on the gas gland in living 523
- FROMM, PAUL O., AND E. P. REINEKE. Some aspects of thyroid physiology in Rainbow trout 393
- FRY, WILLIAM J. See Welkowitz, Walter 435
- G**AROUTTE, BILL, AND ROBERT B. AIRD. Diffusion from brain slices in vitro 167
- Gas gland in living fish, observations on the 523
- Gasometric determination of oxygen in fish blood, micro 529
- Germination of *Bacillus cereus*, television microscopy of sporulation and spore 301
- Gland in living fish, observations on the gas 523
- GRAY, STEPHEN W. See Edwards, Betty F. 405
- Gravitational forces in wheat coleoptiles, growth, work output and sensitivity to increased 405
- GREGG, H. JAMES, AND RUTH D. BRONSWIG. Biochemical events accompanying stalk formation in the slime mold, *Dictyostelium discoideum* 293
- GRIFFITHS, MARY. See Sistrom, W. R. 459, 473
- GROSS, MILTON. See Guttman, Rita 421
- Growth, contractility and plasmocrinine activity in cultures of embryonic chick heart, studies on individual and joint effects of histamine and an antihistaminic on 147
- Growth, work output and sensitivity to increased gravitational forces in wheat coleoptiles 405
- GUTTMAN, RITA, AND MILTON M. GROSS. Relationship between electrical and mechanical changes in muscle caused by cooling 421
- H**ARRIS, MORGAN. Occurrence of respiration deficient mutants in baker's yeast cultivated anaerobically 95
- Heart, studies on the individual and joint effects of histamine and an antihistaminic on growth, contractility and plasmocrinine activity in cultures of embryonic chick 147
- Hibernation in the ground squirrel, metabolism of some carbohydrate and phosphate compounds during 371
- Histamine and an antististaminic on growth, contractility and plasmocrinine activity in cultures of embryonic chick heart, studies on the individual and joint effects of 147
- HODGSON, EDWARD S., AND KENNETH D. ROEDER. Electrophysiological studies of arthropod chemoreception. I. General properties of the labellar chemoreceptors of diptera 51
- HOFFMAN, F. BRIAN. See Brooks, Chandler McC., Paul F. Craneffeld and Arthur A. Siebens 237
- I**NDIVIDUAL and joint effects of histamine and an antihistaminic on growth, contractility and plasmocrinine activity in cultures of embryonic chick heart, studies on 147
- Intensity sound on electrical conduction in muscle, effects of high 435
- Insects, the properties of cholinesterase from 215
- Insects, soluble and particulate cholinesterase in 197
- In vitro, diffusion from brain slices 167
- Isolated and non-isolated myelinated nerve fibers, saltatory conduction in single 1
- J**OINT effects of histamine and an antihistaminic on growth contractility and plasmocrinine activity in cultures of embryonic chick heart 147
- JOHNSON, GEORGE T., AND CARL MOOS. Succinoxidase activity of mitochondria from myxomycete plasmodia 243

- L**EVICK, W. R. See Bishop, P. O. 1
- Life span of *Arbacia* gametes, comparative effect of methylated xanthines on the fertilization capacity and . . . 253
- LOWRANCE, PRESTON B., JAMES F. NICKEL, CHEVES MCC. SMYTHE AND STANLEY E. BRADLEY. Comparison of the effect of anoxic anoxia and apnea on renal function in the harbor seal (*Phoca vitulina* L.) . . . 35
- M**ECHANICAL changes in muscle caused by cooling, relationship between electrical and . . . 421
- Metabolism of some carbohydrate and phosphate compounds during hibernation in the ground squirrel . . . 371
- Micro gasometric determination of oxygen in fish blood . . . 529
- Microscopy of sporulation and spore germination of *Bacillus cereus*, television . . . 301
- Mold, *Dictyostelium discoideum*, biochemical events accompanying stalk formation in the slime . . . 293
- Molecular weight, I. Pigment monolayers and Photoreceptor structures . . . 349
- Monolayers and molecular weight, I. Pigment. Photoreceptor structures . . . 349
- MOOS, CARL. See Johnson, George T. . . 243
- Muscle, caused by cooling, relationship between electrical and mechanical changes in . . . 421
- Muscle, effects of high intensity sound on electrical conduction in . . . 435
- Mutant of *Rhodopsudomonas spheroides*, a note on the porphyrins excreted by the blue-green . . . 459
- Mutants in baker's yeast cultivated anaerobically, occurrence of respiration deficient . . . 95
- Myelinated nerve fibers, saltatory conduction in single isolated and non-isolated . . . 1
- Muscle, anodal effects during the refractory period of cardiac . . . 237
- Muscle fibers, the relation of accommodation to current distribution in single . . . 181
- Myxomycete plasmodia, succinoxidase activity of mitochondria from . . . 243
- N**ELSON, T. C. Sexual competence in *Escherichia coli* . . . 271
- Nerve fibers, saltatory conduction in single isolated and non-isolated myelinated . . . 1
- Nerve, some tensile properties of . . . 87
- NICKEL, JAMES F. See Lowrance, Preston B., Cheves McC. Smythe and Stanley E. Bradley . . . 35
- Non-electrolytes in the parotid saliva, the secretion of . . . 113
- Non-isolated myelinated nerve fibers, saltatory conduction in single isolated and . . . 1
- Note on the porphyrins excreted by the blue-green mutant of *Rhodopsudomonas spheroides*, a . . . 459
- Nutrition of *Saccharomyces cerevisiae*, anaerobic. III. An unidentified growth promoting factor and its relationship to the essential lipid requirements . . . 317
- O**BSERVATIONS on the gas gland in living fish . . . 523
- Occurrence of respiration deficient mutants in baker's yeast cultivated anaerobically . . . 95
- Oxygen in fish blood, micro gasometric determination of . . . 529
- Oxygen secreted into the swimbladder of cod, the source of . . . 517
- P**AROTID saliva, the secretion of non-electrolytes in the . . . 113
- (*Phoca vitulina* L.). Comparison of the effect of anoxic anoxia and apnea on renal function in the harbor seal . . . 35
- Phosphate compounds during hibernation in the ground squirrel, metabolism of some carbohydrate and . . . 371
- Photoreceptor structures. I. Pigment monolayers and molecular weight . . . 349
- Photosynthetic bacterium which lacks colored carotenoids, the biology of a . . . 473
- Physiology in Rainbow trout, some aspects of thyroid . . . 393
- Pigment monolayers and molecular weight. I. Photoreceptor structures . . . 349
- Plasmodia, succinoxidase activity of mitochondria from myxomycete . . . 243
- P³²O₄ into rat brain, the entry of . . . 139
- Porphyrins excreted by the blue-green mutant of *Rhodopsudomonas spheroides*, a note on the . . . 459
- Properties of nerve, some tensile . . . 87
- R**AINBOW trout, some aspects of thyroid physiology in . . . 393
- Rat brain, the entry of P³²O₄ into . . . 139
- Refractory period of cardiac muscle, anodal effects during the . . . 237
- REINEKE, E. P. See Fromm, Paul O. . . 393
- Relationship between electrical and mechanical changes in muscle caused by cooling . . . 421
- Renal function in the harbor seal (*Phoca vitulina* L.), comparison of the effect of anoxic anoxia and apnea on . . . 35
- Respiration deficient mutants in baker's yeast cultivated anaerobically, occurrence of . . . 95
- Respiration, several factors which influence the rate of *Avena* coleoptile respiration . . . 77
- Rhodopsudomonas spheroides*, a note on the porphyrins excreted by the blue-green mutant of . . . 459
- RICHTER, KENNETH M. Studies on the individual and joint effects of histamine and an antihistaminic on growth, contractility and plasmocrine activity in cultures of embryonic chick heart . . . 147
- ROEDER, KENNETH D. See Hodgson, Edward S. . . 51
- S**ACCHAROMYCES *cerevisiae*, anaerobic nutrition of. III. An unidentified growth promoting factor and its relationship to the essential lipid requirements . . . 317
- Saliva, the secretion of non-electrolytes in the parotid . . . 113
- Saltatory conduction in single isolated and non-isolated myelinated nerve fibers . . . 1

- SCHOLANDER, P. F. Observations on the gas gland in living fish 523
- SCHOLANDER, P. F., AND L. VAN DAM. Micro gasometric determination of oxygen in fish blood 529
- SCHOLANDER, P. F., L. VAN DAM AND THEODORE ENNS. The source of oxygen secreted into the swim-bladder of cod 517
- SCHERANK, A. R. Several factors which influence the rate of *Avena* coleoptile respiration 77
- Seal (*Phoca vitulina* L.), comparison of the effect of anoxic anoxia and apnea on renal function in the harbor 35
- Sensitivity to increased gravitational forces in wheat coleoptiles, growth, work output and 405
- Several factors which influence the rate of *Avena* coleoptile respiration 77
- Single isolated and non-isolated myelinated nerve fibers, saltatory conduction in 1
- SISTROM, W. R., MARY GRIFFITHS AND R. Y. STANIER. A note on the porphyrins excreted by the blue-green mutant of *Rhodospseudomonas spheroides* 459
- SISTROM, W. R., MARY GRIFFITHS AND R. Y. STANIER. The biology of a photosynthetic bacterium which lacks colored carotenoids 473
- Slices in vitro, diffusion from brain 167
- Slime mold, *Dictyostelium discoideum*, biochemical events accompanying stalk formation in the 293
- SMYTHE, CHEVES MCC. See Lowrance, Preston B., James F. Nickel and Stanley E. Bradley 35
- SIEBENS, A. ARTHUR. See Brooks, Chandler McC., Paul F. Cranefield and Brian F. Hoffman 237
- Single muscle fibers, the relation of accommodation to current distribution in 181
- SOCIETY OF GENERAL PHYSIOLOGISTS. Abstracts of papers presented at the eleventh Annual Meeting, held in conjunction with the meetings of the American Institute of Biological Sciences at the University of Connecticut, Storrs, Connecticut, August 27-29, 1956 329
- Some tensile properties of nerve 87
- Sound on electrical conduction in muscle, effects of high intensity 435
- Source of oxygen secreted into the swimbladder of cod, the 517
- SMALLMAN, B. N., AND L. S. WOLFE. Soluble and particulate cholinesterase in insects 197
- SMALLMAN, B. N., AND L. S. WOLFE. The properties of cholinesterase from insects 215
- Sporulation and spore germination of *Bacillus cereus*, television microscopy of 301
- Squirrel, metabolism of some carbohydrate and phosphate compounds during hibernation in the ground 371
- STANIER, R. Y. See Sistrom, W. R. 459, 473
- STIER, T. J. B. See Andreassen, A. A. 317
- STREICHER, E. The entry of $P^{32}O_4$ into rat brain 139
- Studies on the individual and joint effects of histamine and an antihistaminic on growth, contractility and plasmocrine activity in cultures of embryonic chick heart 147
- Structures, photoreceptor. I. Pigment monolayers and molecular weight 349
- Swimbladder of cod, the source of oxygen secreted into the 517
- T**ENSILE properties of nerve, some 87
- The secretion of non-electrolytes in the parotid saliva 113
- Thyroid physiology in Rainbow trout, some aspects of 393
- Trout, some aspects of thyroid physiology in Rainbow 393
- V**AN DAM, L. See Scholander, P. F. 517, 529
- W**ELKOWITZ, WALTER, AND WILLIAM J. FRY. Effects of high intensity sound on electrical conduction in muscle 435
- Wheat coleoptiles, growth, work output and sensitivity to increased gravitational forces 405
- WOLFE, L. S., AND B. N. SMALLMAN. Soluble and particulate cholinesterase in insects 197
- WOLFE, L. S., AND B. N. SMALLMAN. The properties of cholinesterase from insects 215
- WOLKEN, JEROME J. Photoreceptor structures. I. Pigment monolayers and molecular weight 349
- Work output and sensitivity to increased gravitational forces in wheat coleoptiles, growth 405
- X**ANTHINES, on the fertilization capacity and life span of *Arbacia* gametes, comparative effect of methylated 253
- Z**IMNY, MARILYN L. Metabolism of some carbohydrate and phosphate compounds during hibernation in the ground squirrel 371
- ZWORYKIN, A. KATHERINE, AND GEORGE B. CHAPMAN. Television microscopy of sporulation and spore germination of *Bacillus cereus* 301



REFERENCE
FOR READING ROOM
USE ONLY

